

**This PDF was created from the British Library's microfilm copy of the original thesis. As such the images are greyscale and no colour was captured.**

**Due to the scanning process, an area greater than the page area is recorded and extraneous details can be captured.**

**This is the best available copy**

D48820 84

Attention is drawn to the fact that the copyright of this thesis rests with its author.

This copy of the thesis has been supplied on condition that anyone who consults it is understood to recognise that its copyright rests with its author and that no quotation from the thesis and no information derived from it may be published without the author's prior written consent.

**IV**

415

D 48820/84

ROCA PEREZ R.

415.

INTERACTION OF PHENOL-FORMALDEHYDE  
CONDENSATES WITH ISOPRENE RUBBER

A thesis submitted to the  
Council for National Academic Awards  
for the degree of  
Doctor of Philosophy

by

Rafael Roca Perez, M.Sc., Grad. PPI

London School of Polymer Technology,  
The Polytechnic of North London,  
Holloway Road,  
London N7 8DB.

Collaborating establishment

The Malaysian Rubber Producer's Research Association  
Brickendonbury  
Hertford

July 1983

Interaction of phenol-formaldehyde condensates with isoprene rubber

Thesis submitted for Ph.D.(C.N.A.A.) by R. Roca, July 1983

Abstract

The study is concerned with the interaction between p-tertiary butyl phenol-formaldehyde condensates and isoprene rubber under conditions resembling those used in industrial vulcanization processes, and involves investigations of reaction rates, mechanisms of reactions and structures produced. The work is an extension of an earlier study (A. Fitch, Thesis for Ph.D.(C.N.A.A.), 1978).

'Model' phenol-formaldehyde condensates (2-methylol 4-tert.butyl 6-methyl phenol and the ether derived from it by thermal condensation) are shown to interact with isoprene rubber (cis-1,4-polyisoprene) to form adducts containing chroman structures. The ether reacts somewhat more quickly and more efficiently than the methylol compound. 'Lewis acid' catalysts will greatly accelerate the reaction, but cause concurrent structural isomerization of the isoprene rubber, to an extent depending on the nature of the catalyst.

In separate experiments involving only rubber and catalyst, it is found that, of the three catalysts examined, tin(II) chloride dihydrate causes extensive isomerization, tin(II) chloride (anhydrous) causes little isomerization and zinc(II) chloride (anhydrous) causes negligible isomerization under the appropriate reaction conditions. The structural changes are evaluated, and involve cis-trans interconversions double-bond shifts, cyclization and crosslinking.

Using zinc(II) chloride as catalyst, a study is made of the effectiveness of five different polyfunctional phenol-formaldehyde condensates as vulcanizing agents for isoprene rubber. The condensates consist of 2,6-dimethylol 4-tert. butyl phenol and four of its derivatives containing different molar proportions of methylol, dibenzyl ether and diaryl methane groups. One of the derivatives is a commercially-available vulcanizing agent. Measurements of rubber-combined phenolic material and of crosslink concentrations are made at different times of reaction, and results show that the condensates containing high proportions of dibenzyl ether links are the most efficient vulcanizing agents. Efficiency may be further improved by the addition of a formaldehyde donor to suppress side-reactions. The results indicate that, in all cases, combination with the rubber occurs through chroman linkages and the crosslinks contain at least two phenolic nuclei joined by dimethylene ether or methylene links.

### ACKNOWLEDGEMENTS

The author wishes to express his sincere thanks to Dr. D. Aubrey (Director of Studies) for his unfailing guidance and encouragement. I also wish to express my deep gratitude to Dr. M. Porter (External Supervisor) for his constant interest, encouragement and many helpful suggestions.

I am grateful to the Central University of Venezuela for granting my study leave and for the provision of a Research Studentship.

Finally, it is also a pleasure to express my gratitude to Dr. A.C. Haynes for his generous help at all times and also to Miss. Jayanti Kotiyan for helping in the preparation of this thesis.

To Maricarmen,  
Isabella,  
and Rafael Alejandro

## CONTENTS

	<u>Page</u>
ABSTRACT	ii
ACKNOWLEDGEMENTS	iii
CONTENTS	iv
CHAPTER 1 INTRODUCTION	1
1.1 Background	1
1.2 Previous studies	4
(a) Theories for the phenol-formaldehyde vulcanization mechanism	4
(b) O-quinone methides and other postulated reactive intermediates	5
(c) Formation of chroman linkages with rubbers	11
(d) Formation of adducts linked via methylene groups	26
(e) Crosslink formation by both chroman and methylene linkages	30
(f) Views of mode of action and side- effects of catalysts and inhibitors	32
(g) Halogen-containing organic activators and 'self reactive resins'	42
(h) Other views	44
1.3 Aim of this project	45
1.4 Glossary and nomenclature	46

## CONTENTS

	<u>Page</u>
CHAPTER 2 INTERACTION OF TIN(II) CHLORIDE, TIN(II) CHLORIDE DIHYDRATE AND ZINC CHLORIDE WITH SYNTHETIC POLYISOPRENE RUBBER	52
2.1 Purpose of this study	52
2.2 Reagents	53
2.3 Reaction conditions and procedure	53
2.4 Characterisation of products	54
(a) Total unsaturation	55
(b) Types of unsaturation	55
(c) Glass-transition temperature	56
(d) Molecular weight changes and gel content	57
2.5 Possible structures and types of unsaturation	57
2.6 Total unsaturation	61
(a) Measurement of total unsaturation	61
(b) Present study	62
2.7 Infra-red spectroscopy	64
(a) Earlier ir studies	64
(b) Present work	66
(c) Quantitative analysis of ir spectra	71
2.8 Nuclear magnetic resonance(nmr) spectroscopy	73
(a) Earlier nmr studies	73

	<u>Page</u>
(b) Present work	75
(c) Quantitative analysis of nmr spectra	81
2.9 Glass transition temperature	86
2.10 Molecular weight changes and gel content	88
2.11 Discussion	89
(a) Total unsaturation	89
(b) Cis/trans isomerization	91
(c) Double-bond shifts	92
(d) Cyclization	95
(e) Overall mechanistic scheme	98
 CHAPTER 3	
INTERACTION OF PHENOL-FORMALDEHYDE "MODELS" CONDENSATES WITH SYNTHETIC POLYISOPRENE RUBBER	107
3.1 Purpose of this study	107
3.2 Reagents	107
3.3 Reaction conditions and procedure	109
3.4 Characterisation of products	110
(a) Bound phenolic material	110
(b) Structure of the adduct	112
(c) Isomerization of polyisoprene during reaction	113
(d) Molecular weight changes and gel content	113
3.5 Bound phenolic material	114
(a) Earlier studies	114
(b) Results in the present study	117

## CONTENTS

	<u>Page</u>
3.6 Nature of the linkage between rubber and phenolic material	127
(a) Earlier studies	129
(b) Results of the present study	134
3.7 Hydroxyl concentration	159
3.8 Total unsaturation	164
3.9 Isomerization	171
3.10 Glass-transition temperature	174
3.11 Molecular weight changes and gel content	179
3.12 Discussion	183
(a) Kinetics of adduct formation	183
(i) Bound phenolic material	183
(ii) Relationship to Fitch's model study	184
(iii) Unbound unextractable material	186
(b) Isomerization and other side reactions	188
(i) Cis-trans isomerization and double bond shifts	188
(ii) Cyclization	190
(iii) Crosslinking and gel content	194

## CONTENTS

	<u>Page</u>
(c) Nature of the adduct	195
(i) Evidence from residual phenolic hydroxyl	196
(ii) Evidence from unsaturation	198
(iii) Other spectroscopic evidence	200
(d) Mechanism and catalysis of adduct formation	201
(i) Overall scheme	201
(ii) Uncatalysed mechanism of adduct formation	201
(iii) Catalysed mechanism involving $\text{SnCl}_2 \cdot 2\text{H}_2\text{O}$	203
(iv) Mechanism for catalysts other than $\text{SnCl}_2 \cdot 2\text{H}_2\text{O}$	206
(v), Relative activity of metal halides	213
CHAPTER 4      BIFUNCTIONAL PHENOL-FORMALDEHYDE CONDENSATES AS VULCANIZING AGENTS FOR IR	219
4.1 Introduction	219
(a) Objective of this study	219

## CONTENTS

	<u>Page</u>
(b) Reagents	220
(c) Reaction conditions and procedure	222
(d) Characterisation of products of vulcanization	223
(i) Bound phenolic material	223
(ii) Crosslink concentration	223
(iii) Phase separation	224
(iv) Efficiency	225
4.2 Characterization methods and results	226
(a) Characterization of the vulcanizing agents used	226
(i) Earlier studies	226
(ii) Results in the present study	228
(b) Bound phenolic material	230
(c) Crosslink concentration	233
(i) Measurement of crosslink concentration	233
(ii) Results in the present study	240
(d) Efficiency	256
4.3 Discussion	257
(a) Vulcanization with bifunctional methylol derivatives	257
(i) Structure, functionality and expected efficiency of reaction	257

## CONTENTS

	<u>Page</u>
(ii) Results and discussion	265
(b) Vulcanization with products of polyetherification of the bifunctional methylol derivatives	276
(i) Structure and characterization	276
(ii) Functionality and reactivity	278
(iii) Results and discussion	282
(iv) Nature of the crosslinks	292
(c) Vulcanization with the commercial resin	297
(i) Analysis	297
(ii) Results and discussion	301
(d) Discussion of technological implications	308
(i) Requirements for high efficiency	308
(ii) Structural requirements of vulcanizing condensate	308
(iii) Addition of ancillary materials	309
(iv) Comparison of rates and efficiencies with conventional systems	311

## CONTENTS

	<u>Page</u>
(v) Cure safety	313
(vi) Properties of vulcanizates	314
CHAPTER 5 CONCLUSIONS	316
CHAPTER 6 EXPERIMENTAL	319
6.1 Reagents	319
6.2 Interaction of phenolic condensates and/or catalysts with IR	326
6.3 Analysis and characterization methods	328
6.4 Tables	369
REFERENCES	391

## 1. INTRODUCTION

### 1.1 Background

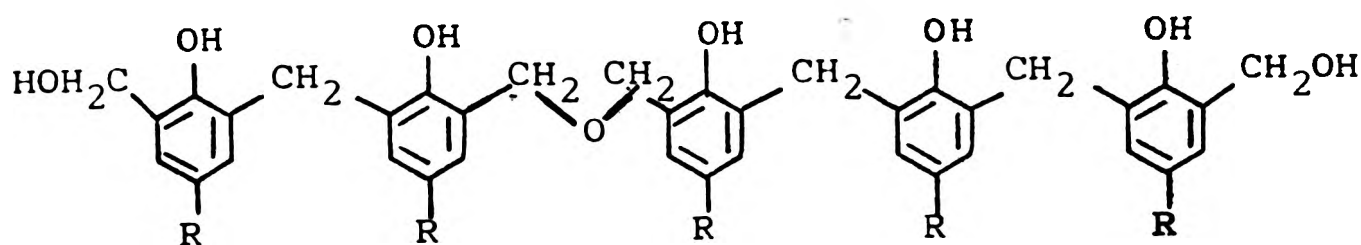
The reaction between unsaturated rubbers and resinous alkylphenol-formaldehyde condensates to produce vulcanizates has been known for nearly forty years. Although these "resin cures" have not been developed commercially to any great extent (except for butyl rubber), there has been continued interest in their possibilities.<sup>1</sup> These reactions are not only of academic interest but have considerable technological potential in such fields as the rubber, adhesives and coating industries.<sup>2</sup>

Today, alkylphenol-formaldehyde condensates are increasing in importance as vulcanizing agents for alkenically-unsaturated elastomers such as natural rubber,<sup>1</sup> butyl rubber<sup>3</sup> and nitrile rubber; they are extensively used for their reactions with chloroprene rubber in adhesives, and also are employed for their reactions with drying oils to produce varnishes.<sup>4</sup> Thus, their interaction with unsaturated materials generally is of widespread interest.

The reactive alkylphenol-formaldehyde condensates used ("resols") are formed by electrophilic substitution of the phenol nucleus with formaldehyde in alkaline medium; the "phenol alcohols" or "methylol phenols" produced may retain their free methylol ( $-\text{CH}_2\text{OH}$ ) groups or may undergo some further condensation to form dimethylene ether ( $-\text{CH}_2\text{OCH}_2-$ ) or methylene ( $-\text{CH}_2-$ ) bridges between nuclei. The more

reactive resins have a preponderance of methylol and dimethylene ether groups, which react with olefinic double bonds. Methylene links are inactive but are often considered necessary to obtain crosslinking as will be discussed later.

A typical molecular formula for a reactive condensate might therefore be:



I

although the number of phenolic nuclei present may range between about 2 and 10.

The rate of vulcanization of butyl rubber with the methylol resin systems is considerably slower than with a typical sulphur accelerator system but the "resin" vulcanizate has much greater stability toward prolonged heating.<sup>5</sup> A marked improvement in rate of cure can be obtained through the catalysing action of metallic halides such as  $\text{SnCl}_2$ ,  $\text{SnCl}_2 \cdot 2\text{H}_2\text{O}$ ,  $\text{ZnCl}_2$  and  $\text{FeCl}_3 \cdot 6\text{H}_2\text{O}$ . These may give extremely fast, scorchy cures.<sup>5,6</sup> The resin concentration used is in the range 5-12 parts per hundred rubber (phr) and the vulcanizing temperature is 150-180°C. The resulting vulcanizates exhibit heat- and air-ageing characteristics superior to those of sulphur-cured stocks, providing for practical utility at temperatures up to 240°C.

A number of patents have been filed showing the catalytic activation of the resin cure of rubbers by means of halogenated additives such as polychloroprene,<sup>7</sup> chlorosulphonated polyethylene ("hypalon"),<sup>8</sup> chlorinated waxes<sup>9</sup> and halogenated butyl rubbers.<sup>10</sup> Halogenated derivatives (containing halomethyl groups) of the methylol resins are self-activating in curing butyl rubbers; thus, a resin obtained by substitution of the hydroxyl of the methylol group with bromine (marketed as SP1055, Schenectady Chemical Co.) requires no additional halogen donor.

The controversy as to whether the resin combines with unsaturated rubbers at activated methylene groups or at double bonds, the mechanism of the reaction involved and the structure of the resulting vulcanizates are still not fully resolved. Many of the investigations made in the past have been of a very brief and superficial nature, being designed mainly for technological ends. However, in a recent study by Fitch<sup>11</sup> the interaction between a 'model' phenol-formaldehyde condensate (2-methyl-4-tert-butyl 6-methyl phenol) and a 'model' for polyisoprene rubber (2-methyl-2-pentene) was studied in detail. The study gives information of technological relevance relating to the chemistry of the interaction and the structure of the adduct formed. Furthermore, it shows ways in which the yield of adduct can be optimised.

In Fitch's study reaction conditions were kept as close as possible to those used in resin vulcanization, so that the

results should have relevance to technological vulcanization processes and vulcanizate structures. This present study is based on Fitch's findings, and represents an attempt to examine the mechanisms, kinetics and structures using real (i.e., not model) rubbers and resins. Particular attention will be given to conditions suitable for use in industrial vulcanization processes.

## 1.2 Previous Studies

### (a) Theories for the phenol-formaldehyde vulcanization mechanism

There are two points of view regarding the chemical structures produced in the vulcanization of unsaturated rubbers by alkylphenol-formaldehyde (p/f) derivatives. One school considers the linkage to be via a chroman ring structure, whereas the second views the linkage as a simple methylene bridge. Other workers have propounded the view that both types of adduct are present.

There is a large measure of agreement between most investigators that the reactive intermediate species is most probably the ortho (o)-quinone methide (see Section (b) below).

The basis of the 'chroman theory', which is also its strongest supporting evidence, is the fact that simple methylol-phenols, in their reactions with simple unsaturated

compounds, have been shown to form chroman derivatives. Although such "model" reactions may provide information about the reactive sites in the unsaturated molecule and about the possible type of linkage, their findings cannot be transformed unreservedly to real vulcanization reactions. "Model" compounds have been extensively used because of the difficulties of characterisation and analysis imposed by working with crosslinked polymers. However, even with the "models" used (and consequently therefore with unsaturated elastomers) there is relatively sparse evidence for the mechanism and structures proposed. Recent studies of p/f condensates have been directed mainly towards the applications of them as binders and adhesives for wood, rubber and metals, but few attempts have been made to elucidate the mechanism, structures or kinetics involved in such applications and only the physical properties of the final product have normally been reported. The various views are now discussed in more detail.

(b) O-quinone methides and other postulated reactive intermediates

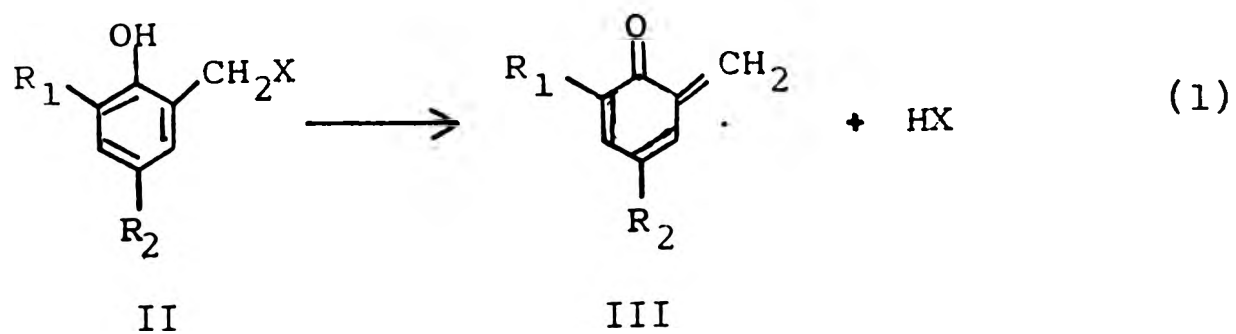
It has been suggested by Van der Meer in a number of studies<sup>12-15</sup> that in the interaction of unsaturated rubbers with o-methylolphenols (II where X=OH) the latter first dehydrates to a quinone methide intermediate (Formula III) which then adds to the rubber. This intermediate has also been proposed in the reaction of o-methylolphenols with simple unsaturated compounds.<sup>16-18</sup> In general such

structures have been surmised as transient entities in a number of chemical processes.<sup>19</sup> Their formation is commonly represented as in reaction (1).

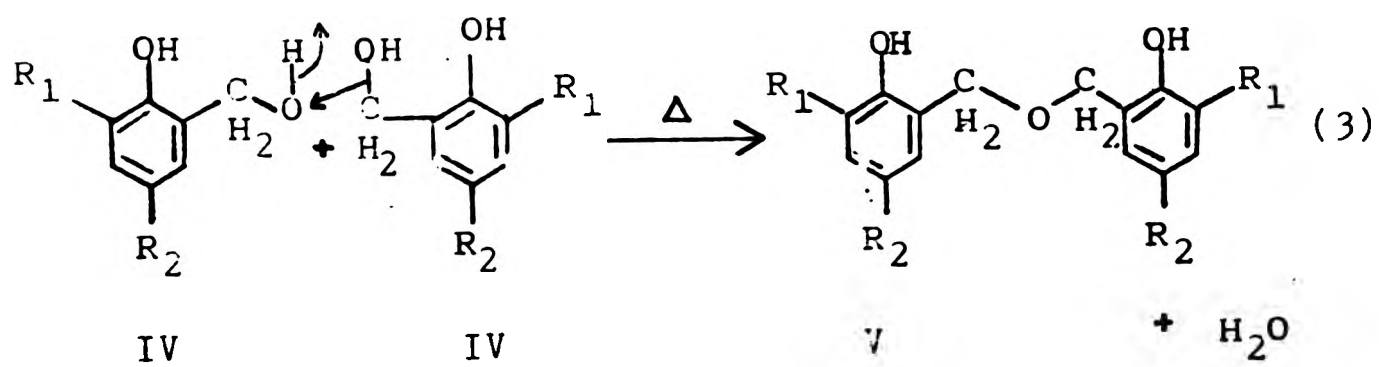
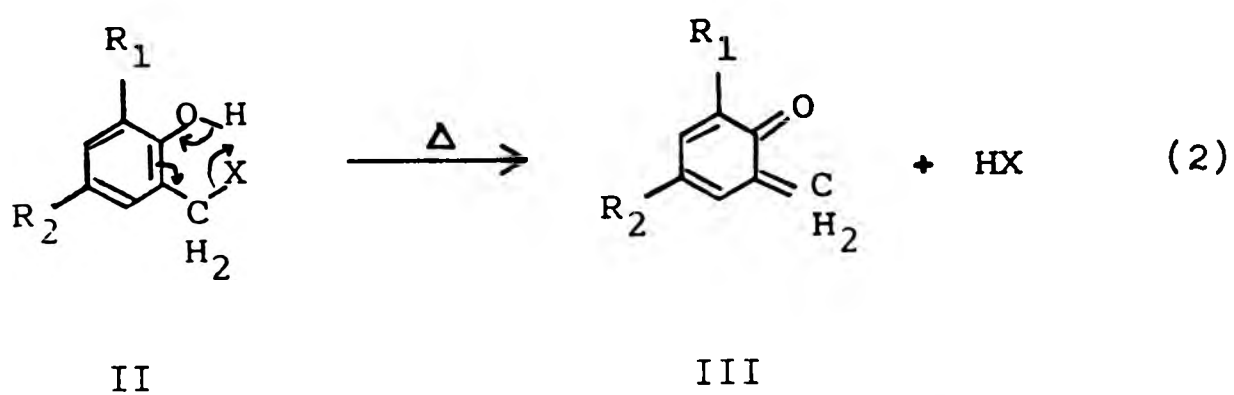
For thermal elimination, reaction (1) may be envisaged as occurring via a six-membered intramolecular transition state (Mechanism (2)).

It is well-known that methylolphenols may undergo self-condensation at the temperatures used during vulcanization. It was proposed by Van der Meer<sup>12-15</sup> and by Wildschut<sup>20</sup> that in the vulcanization of unsaturated rubber with methylolphenol-containing condensates the o-quinone methide intermediate was formed by dehydration of the methylolphenol. Fitch's study<sup>11</sup> demonstrated that formation of a dibenzyl ether derivative (V) readily occurs on heating a methylolphenol derivative (IV) (o-methylolphenol) at 150°C as in (3). An alternative route for the quinone methide (III) therefore involves the formation and decomposition of the dibenzyl ether derivative (V)<sup>11</sup> (Reactions (3) and (4)).

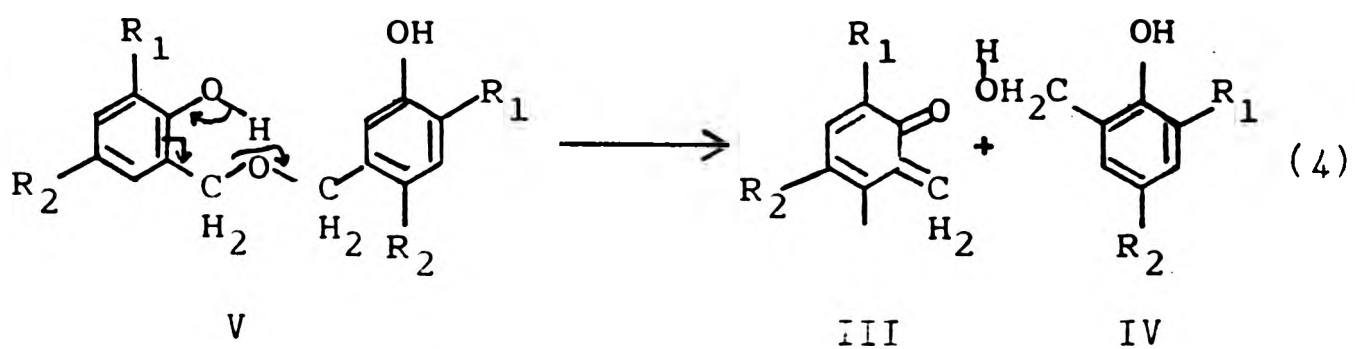
In this latter sequence, (3) and (4), mechanism (4) is the same as (2), and produces more methylolphenol enabling the cycle to be repeated. This hypothesis is supported by the fact that p/f resins with a high (18%) content of dimethylene-ether bridges have reputedly greater vulcanizing activity than resins of lower ether content based on p-tert-butylphenol (8.3% ether) and p-tert octylphenol (0% ether).<sup>21</sup> In addition, it has been shown that the crosslinking rate of



Where X = H, OH, OR, N(CH<sub>3</sub>)<sub>2</sub> or halogen

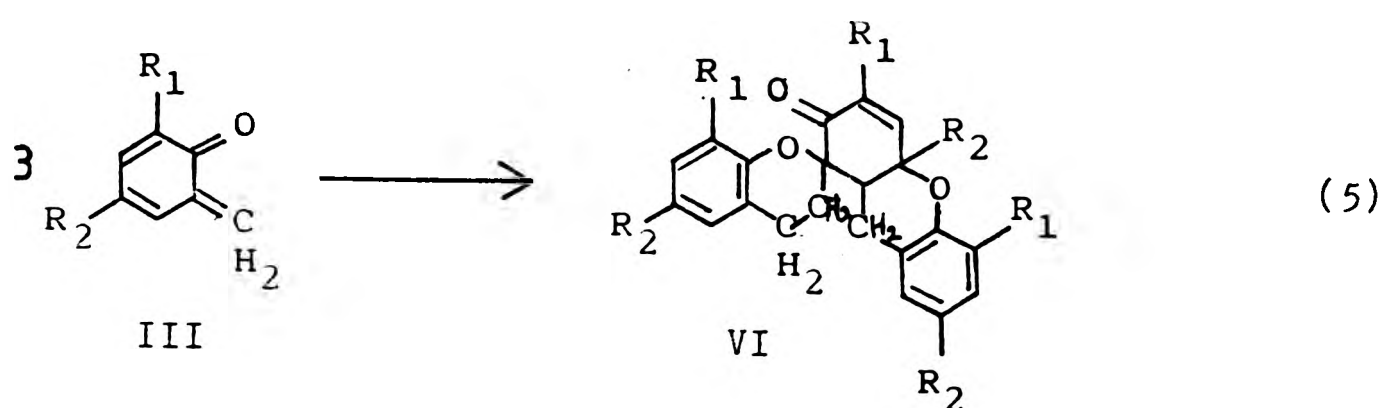


where R<sub>1</sub> = CH<sub>3</sub>, R<sub>2</sub> = C(CH<sub>3</sub>)<sub>3</sub>

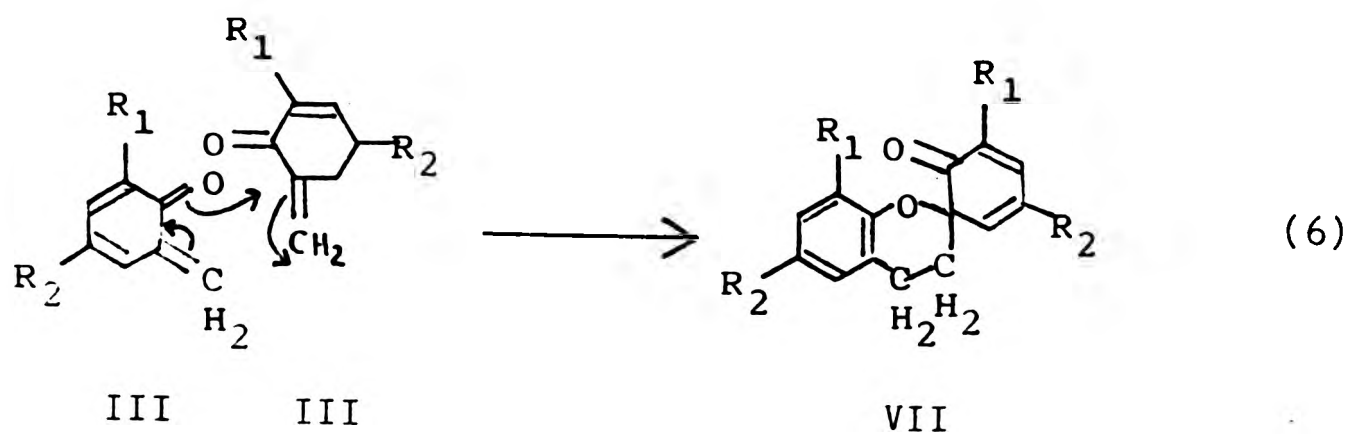


butyl rubber with a dimethylolphenol (IV where  $R_1 = \text{CH}_2\text{OH}$  and  $R_2 = \text{C}(\text{CH}_3)_3$ ) depends on such ether formation.<sup>22</sup>

O-quinone methides are very unstable molecules and have never been isolated with the possible exception of the parent compound of the ortho series, o-benzoquinone methide (III where  $R_1 = R_2 = \text{H}$ ).<sup>23</sup> They polymerise spontaneously in the absence of a suitable addendum, but may be trapped by reactive dienophiles and nucleophilic agents and the evidence for their existence and identity is largely based on the nature of the final products obtained.<sup>24</sup> They readily undergo trimerization, which can be represented as follows:



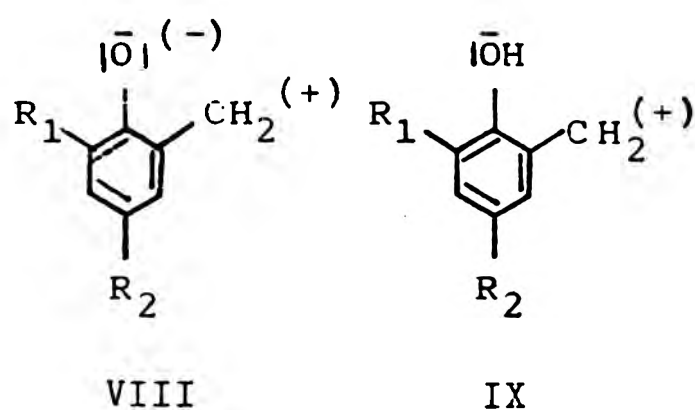
The structure (VI) has been fully characterised.<sup>23-25</sup> A two stage mechanism for its formation has been proposed.<sup>23,26</sup> The first, relatively slow, step envisages the formation, via a Diels-Alder-type addition, of the quinone methide dimer (VII):



This dimer (VII), in the subsequent faster step, then undergoes a further cyclo-addition reaction yielding the trimer (VI).

In trimerization and trapping experiments of simple o-quinone methides, no dimeric species have been obtained. Fitch<sup>11</sup> reported a trimer, not a dimer, as end-product. However, mixtures of quinone methide oligomers including dimers have been reported.<sup>26</sup>

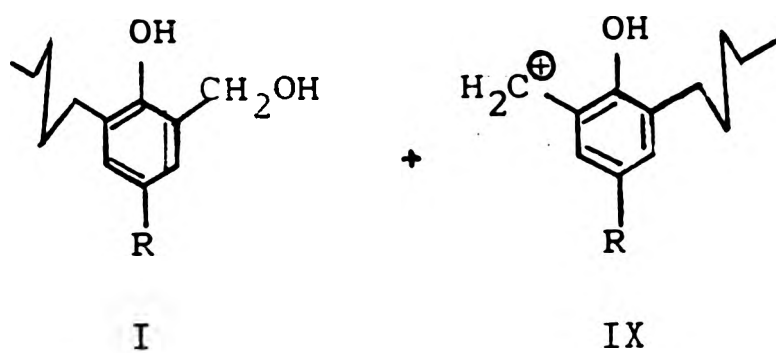
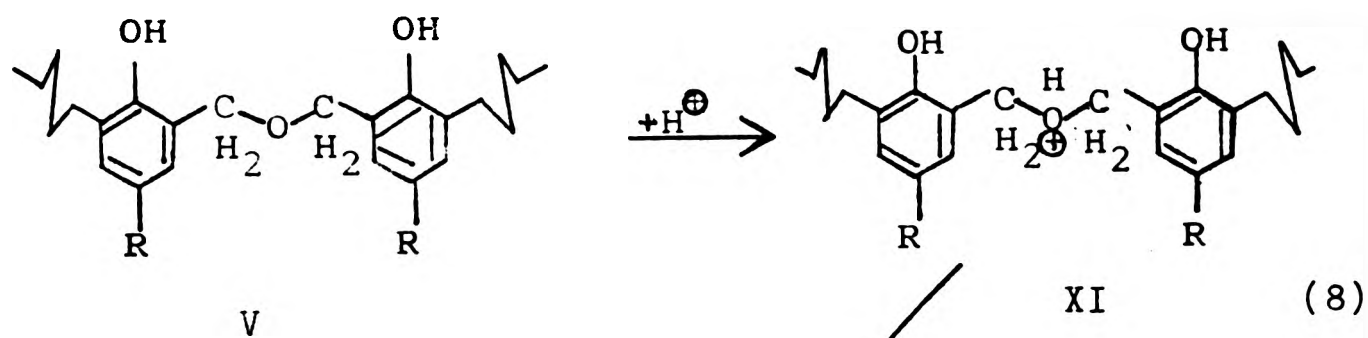
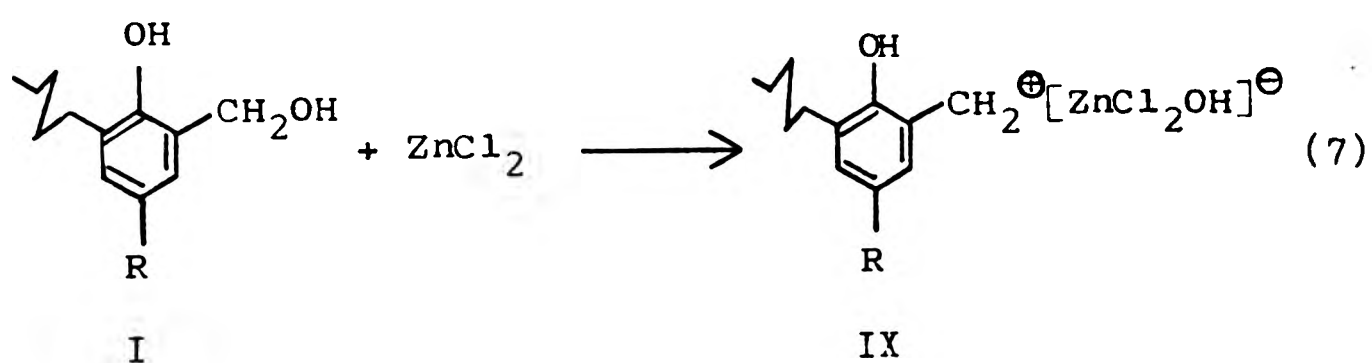
The very specific orientation encountered in quinone methide adducts,<sup>27</sup> and the facility with which certain reagents add<sup>28</sup> suggested polar influences to direct the addition. To explain these observations a Lewis structure (VIII) was proposed. Other workers, however, have postulated



a carbonium ion (IX) as reactive intermediate.<sup>29,30</sup>

The benzylic cation (IX) can be regarded as the protonated form of the quinone methide (III), obtained by interaction of the methylol compounds with activators or catalysts employed.<sup>31,32</sup> These catalysts are normally Lewis

acids such as zinc (II) chloride or tin (II) chloride. The formation of the carbonium ion (IX) has been represented by two different mechanisms. The activator employed may complex directly with the methylol group of (I) as in (7). Alternatively, (IX) or some other protonating species ( $H^+$ ) may protonate a methylene ether unit as in (8). In each case,



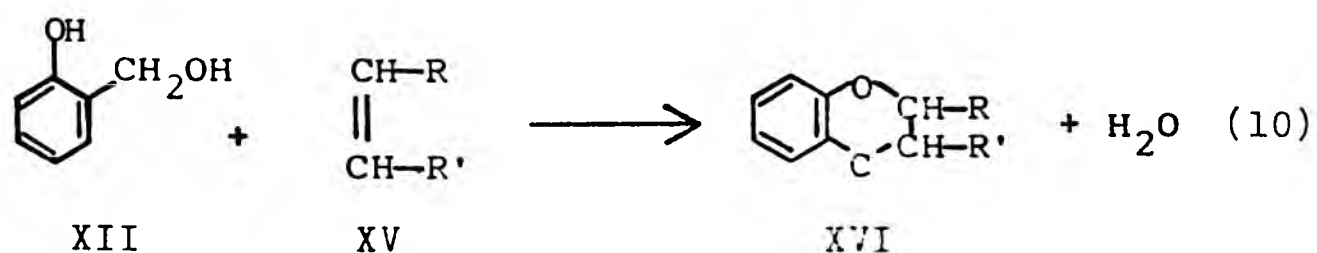
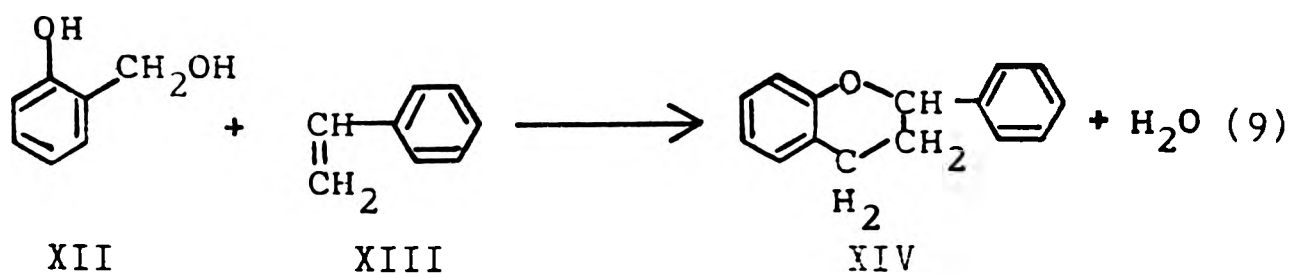
(7) and (8), a carbonium ion (IX) is produced. Fitch's study showed that tin (II) chloride dihydrate readily decomposes an

ether, (V, where  $R_1=CH_3$  and  $R_2=C(CH_3)_3$ ) and he suggested that the reaction (8) may be the more likely to produce such intermediate.

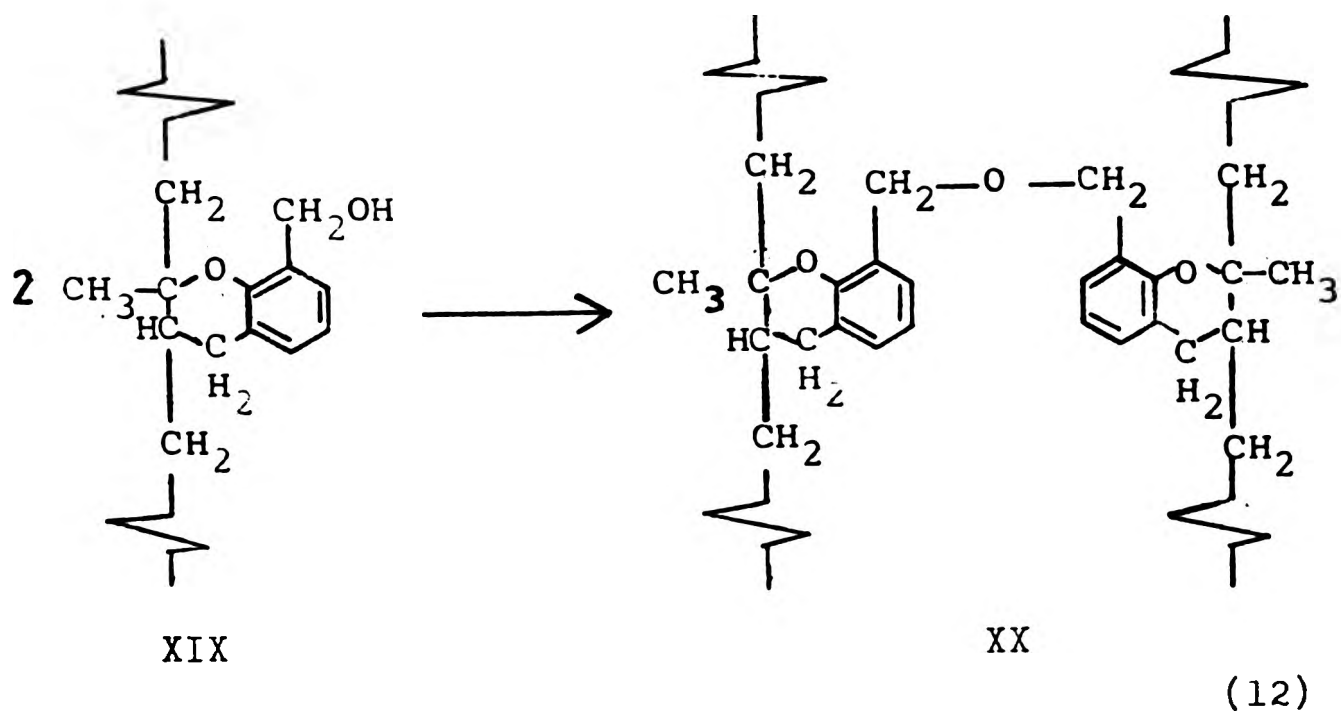
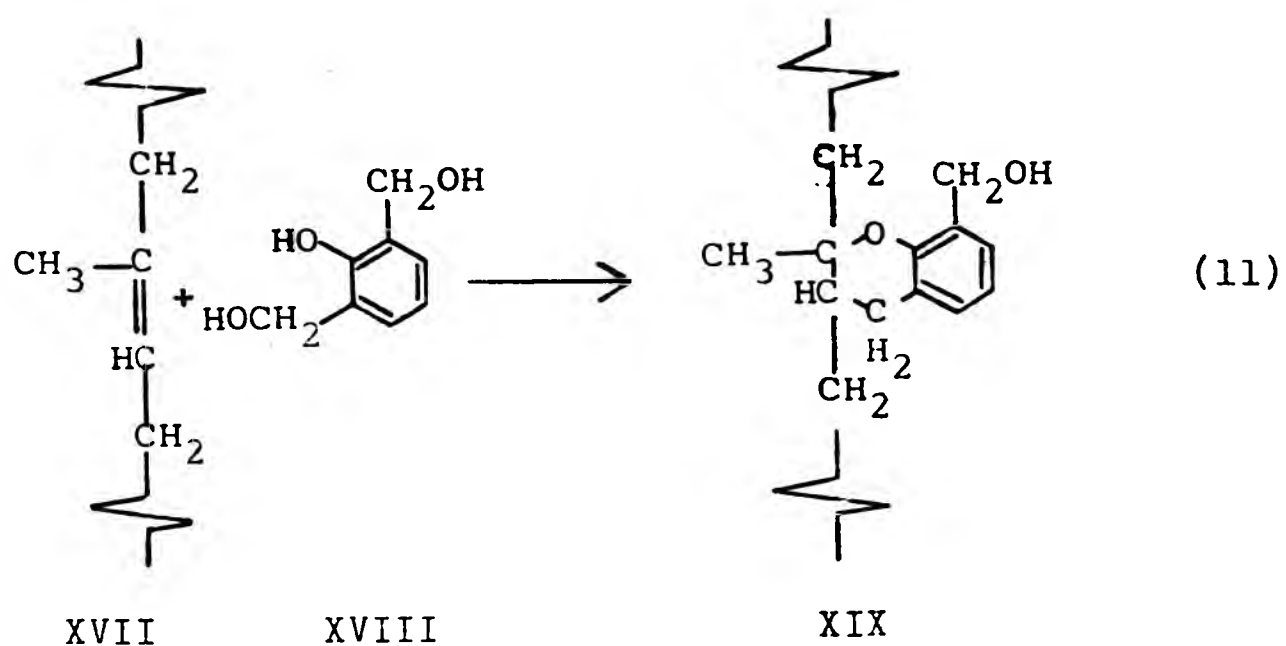
A recent (1974) review discusses the synthesis and chemistry of quinone methides in more detail.<sup>33</sup>

(c) Formation of chroman linkages with rubbers

The "chroman theory" was first formulated by Hultzs<sup>46</sup> following a study of the reaction between 2-methylolphenol (XII) (IV where  $R_1=R_2=H$ ) and styrene (XIII). He showed that this reaction yielded 2-phenyl chroman (XIV) as in (9). A quinone methide intermediate was postulated by Hultzs<sup>34</sup> for reaction (9) and for other reactions of 'phenol alcohols' with simple unsaturated reagents that he had studied. The 'chroman theory' was supported by Greth<sup>35</sup> who showed that 2-methylolphenol (XII) adds to the olefinic double bond of alkyl compounds (XV) producing chroman derivatives (XIV) as in (10).

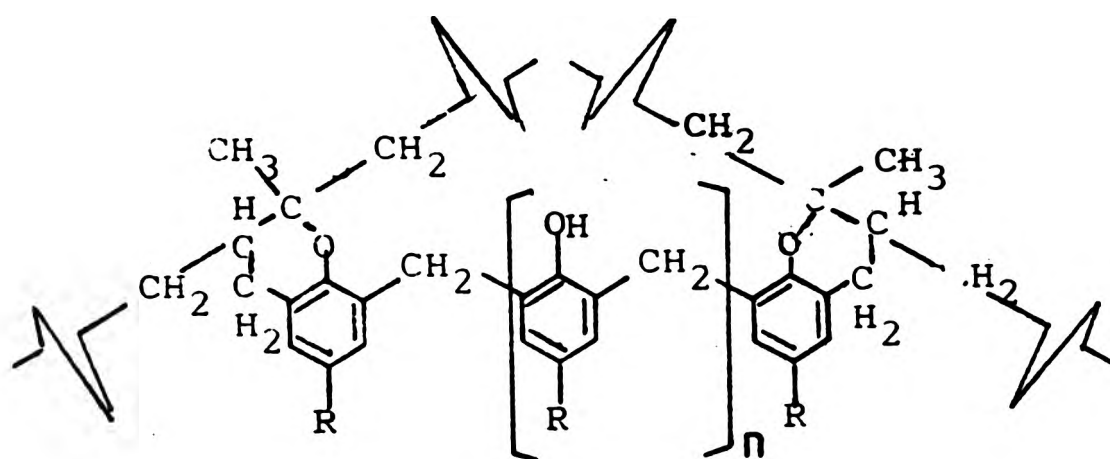


Greth<sup>35</sup> proposed a mechanism leading to the formation of a crosslinked structure containing chroman nuclei for vulcanization of natural rubber (XVII) (cis 1,4 polyisoprene) by 2,6 dimethylolphenol (XVIII) (IV where  $R_1 = \text{CH}_2\text{OH}$ ,  $R_2 = \text{H}$ ) (reactions (11) and (12)). However, reaction (12) seems improbable, involving as it does the condensation of 2 simple primary benzylic alcohols.



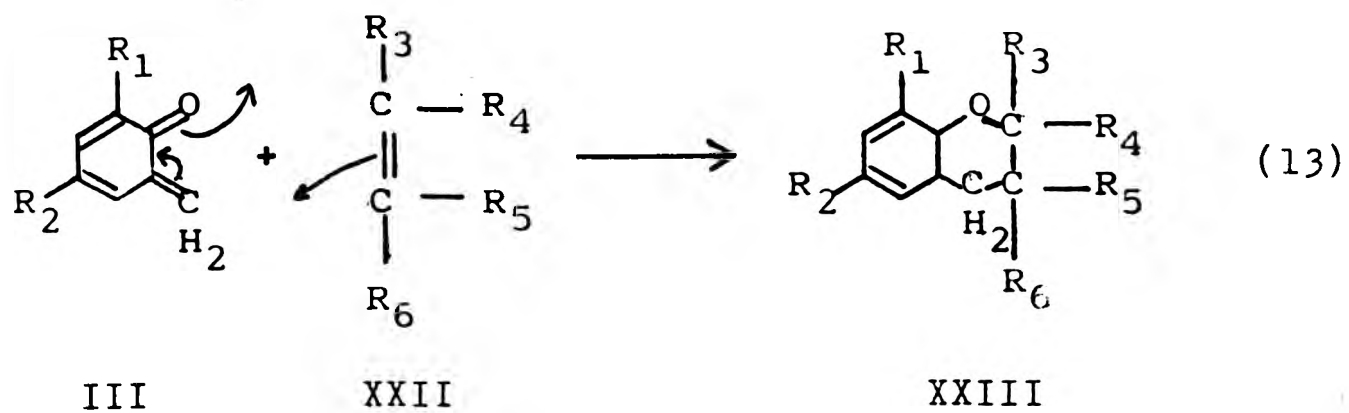
Evidence supporting the formation of a chroman structure such as (XIX) was obtained when *o*-methylolphenol (IV where  $R_1=R_2=H$ ) was treated with two simple analogues of natural rubber, 1-methylcyclohex-1-ene and 2,6-dimethylocta-2,6-diene, at 180°C. In each case chroman derivatives were produced as shown by ultra-violet absorption spectra,<sup>17</sup> and the transient polarised *o*-quinone methide intermediate (IX) was suggested to be the more likely.

Tawey et al.<sup>5</sup> discussed the vulcanization of butyl rubber with *p/f* condensates, giving a structure similar to (I) as a simplified polymeric vulcanizing agent. The authors suggest crosslinking involving reaction through the isoprene double bond, via the intermediate *o*-quinone methide (III) (see 1 earlier), to yield chroman derivatives represented as follows:

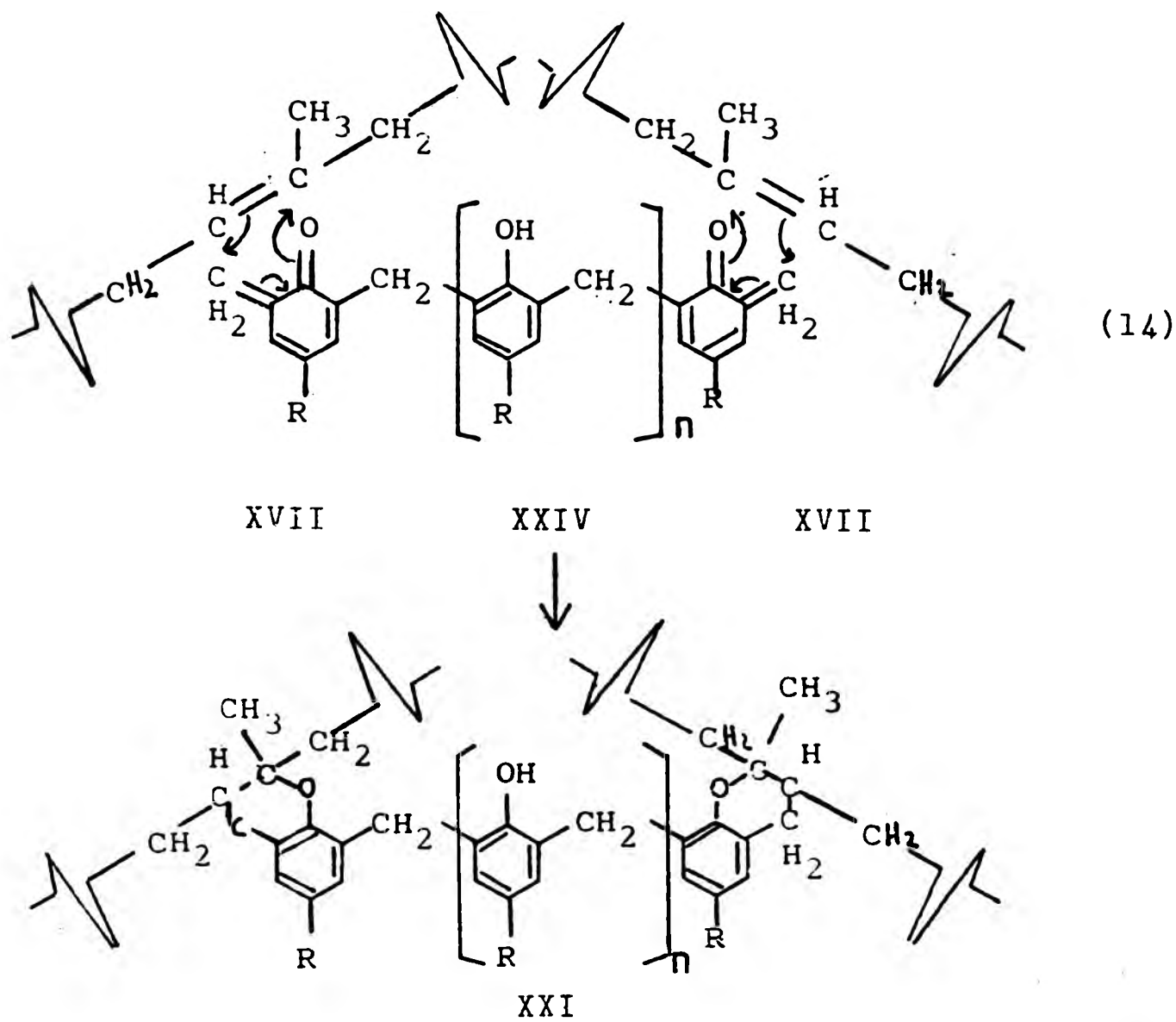


XXI

Reaction (9) has been regarded as a Diels-Alder-type addition<sup>36</sup> between a diene (III) and a dienophile (XXII):



The crosslinked structure (XXI) can be envisaged as being formed similarly; both methylol groups of an idealised alkylphenol-formaldehyde condensate (XXIV) (diene), react with different rubber chains (dienophile), to produce a crosslink (reaction (14)).



The "chroman theory" for the mechanism of vulcanization of unsaturated elastomers with p/f resins, as illustrated in (19), postulates that, as the reaction proceeds, the double bonds of the unsaturated units are consumed, i.e., chemical unsaturation should decrease. This has been supported by Zapp and Perry.<sup>37</sup> They found that use of a phenolic resin instead of a sulphur curing system to vulcanize a butyl rubber compound, greatly improved the ozone resistance of the vulcanizate. Since ozone attack occurs at double bonds, these authors suggested that unsaturation is being reduced during phenolic resin vulcanization and therefore structures XXI are more likely to form. A number of studies have been made of the reaction between methylolphenol materials and a variety of simple alkenes<sup>26-29</sup> and drying oils;<sup>38</sup> in each case formation of a substituted chroman was proposed.

In Fitch's work<sup>11</sup> the decomposition of a p/f "model" condensate and its interaction with a simple alkene was studied, both in the presence and in the absence of catalyst (stannous chloride dihydrate). His experiments were all carried out in sealed glass tubes, mainly with a vapour space of 3/4 of the tube volume (i.e., a free:occupied volume ratio of 1.5:1). A methylolphenol (IV) (where  $R_1=CH_3$ ,  $R_2=C(CH_3)_3$ ) and its dibenzyl ether derivative (V) (where  $R_1=CH_3$ ,  $R_2=C(CH_3)_3$ ) were used as resin 'models', and the alkene 2-methyl-pent-2-ene, was used as a model for natural rubber. Irrespective of whether the methylolphenol (IV) or dibenzyl ether (V) were used, the products observed during thermal decomposition at 150°C were: methylolphenol (IV) dibenzyl

ether (V), original phenol (XXVI), diphenylmethane (XXVII), trimer (XXXI), benzaldehyde (XXVIII) and dimethylolphenol (XXIX) (see Fig. 3 for the proposed decomposition scheme and for the meaning of these abbreviated names). The first three are intermediate products capable of further reaction to produce a transient alkene-reactive entity believed to be quinone-methide or related structure. The observed kinetics of catalysed decomposition of methylol-phenol and dibenzyl ether are shown in Figs. 1 and respectively. The relative induction times, rates of formation and concentration maxima of the products are given in Table 1, together with the corresponding values for uncatalysed and catalysed sealed tube experiments. The measured half times ( $t$ ) for decomposition of methylolphenol and dibenzyl ether are shown in Table 2. In the interaction of both p/f resin 'models' with excess (1:10 w:w) alkene, the products of decomposition again appeared to be similar in nature, but in this case adduct formation between the presumed quinone methide and alk-2-ene also occurred. The adduct was a chroman (XXXII) (see Fig. 4) formed by an apparently regiospecific (i.e., specific in orientation) interaction. With the methylolphenol as starting material, the dibenzyl ether derivative (IV), formed by condensation on heating at 150°C, was considered to be the probable alkene-reactive entity rather than the methylolphenol itself (see Fig. 3 for proposed reaction scheme for the interaction of dibenzyl ether (V) with alk-2-ene (XXXI). However, the efficiency (E) (defined in Section 3.5(b)) of chroman formation was found to be similar with both phenolic materials. The efficiency (E)

did not change appreciably with extent of reaction in either the methylolphenol or dibenzyl ether interaction with alk-2-ene. However, (E) was lower than theoretical because of side-reactions resulting in the formation of inactive by-products (original phenol, diphenylmethane and trimer). Since the decomposition of methylolphenol into original phenol was found reversible (see Fig. 3), addition of formaldehyde and retention of volatiles were found to improve the efficiency (E) by suppressing these side reactions. The observed kinetics of interaction of methylolphenol (IV) and dibenzyl ether (V) with alk-2-ene (XXXI) are shown in Figs. 5 and 6 respectively and the corresponding kinetics with added formaldehyde in Figs. 7 and 8. Kinetic data for the products of reaction of methylolphenol and dibenzyl ether with alk-2-ene under various conditions are shown in Table 3.

In studies<sup>11,26-29,38</sup> of the reaction between methylolphenol materials and simple alkene and drying oils, the addition was stereospecific and regiospecific, in agreement with the stereochemistry of the Diels-Alder reaction,<sup>39</sup> the mechanism of which is still not fully elucidated.<sup>40</sup> The two possible mechanisms proposed are the one-step synchronous process (13) with a cyclic six-centred transition state, and a two-step process involving either a di-radical (reaction 15) or a di-ion (reaction 16) transition state. Fitch suggested that the most feasible mechanism is a synchronous Diels-Alder addition (13) process between uncharged species, although strong polar influences are present. In the case of

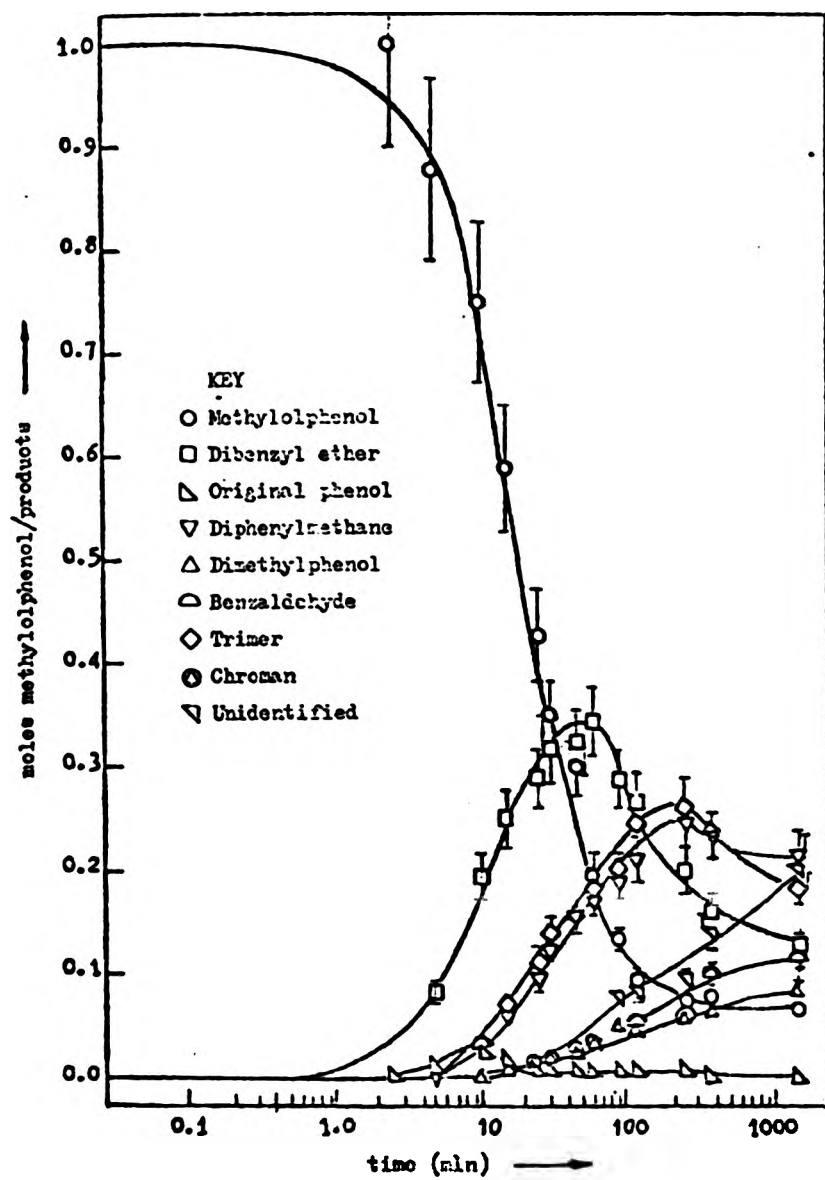
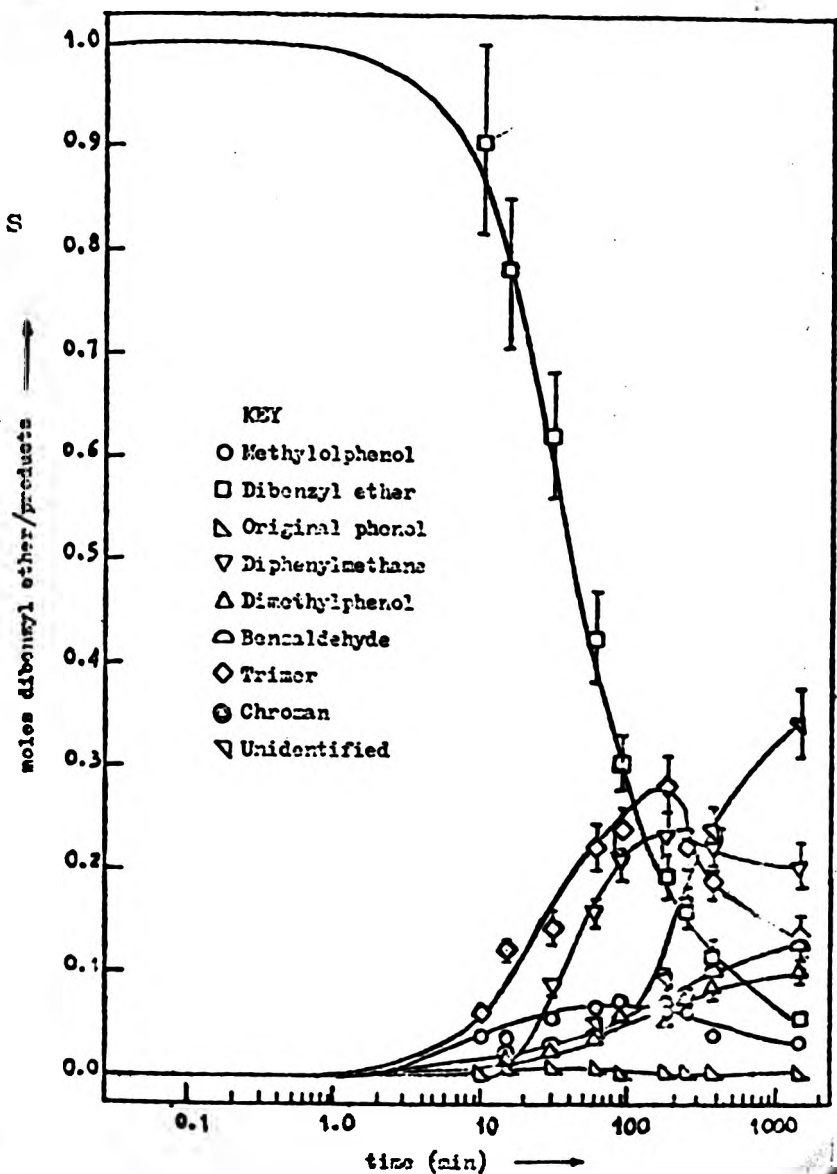


Fig. 1 : Changing concentrations of reactant and products, with time, for the decomposition at 150°C (catalysed, sealed tube) of methylolphenol.<sup>11</sup>

Fig. 2 : Changing concentrations of reactant and products, with time, for the decomposition at 150°C (catalysed, sealed tube) of dibenzyl ether.<sup>11</sup>



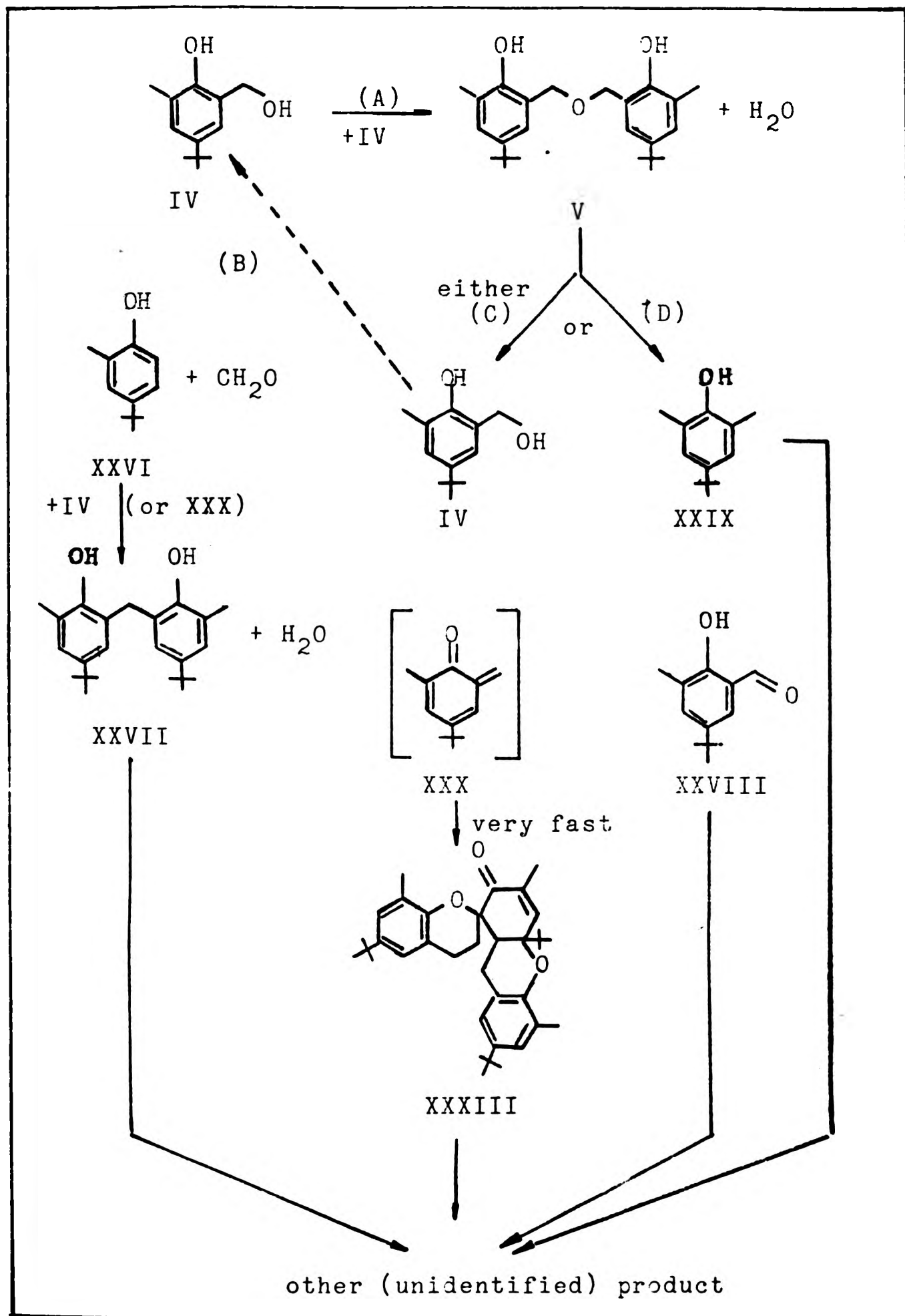


Fig. 3 Proposed reaction scheme for the thermal decomposition at 150°C of the methylolphenol (IV)/dibenzyl ether (V).<sup>11</sup>

Table 1: Induction times, rates of formation and concentration maxima of the various products of decomposition of the methylolphenol (IV) and the dibenzyl ether (V) at 150°C.<sup>11</sup>

PRODUCT	INDUCTION TIME (minutes)		RATE (time in mins. to reach 0.1 moles)		PEAK VALUE (moles)	
	a	b	c	d	e	f
Dibenzyl ether V	a	5		19		0.44
	b	2		5		0.34
	c	0.3		1		0.16
Original phenol XXVI	a	10	15	11*	50*	0.05
	b	4	10	5*	12+	0.02
	c	0.3	-	1	-	0.01
Diphenyl methane XXVII	a	15	25	135	479	0.13 <sup>u</sup>
	b	6	15	23	35	0.24
	c	0.3	0.3	0.9	1.4	0.38
Trimer XXXI	a	15	10	55	36	0.22 <sup>u</sup>
	b	6	4	21	14	0.26
	c	0.3	0.3	0.7	0.6	0.38
Benzaldehyde XXVIII	a	15	10	120*	40*	0.05 <sup>u</sup>
	b	6	4	22*	13	0.12 <sup>u</sup>
	c	0.3	0.3	2	0.6	0.11
Dimethylphenol XXVIII	a	15	10	120*	40*	0.04 <sup>u</sup>
	b	6	4	22*	13	0.03 <sup>u</sup>
	c	0.3	0.3	2	0.6	0.08
Methylolphenol IV	a		10		13*	0.15 <sup>u</sup>
	b		4		7	0.07
	c		0.3		0.7	0.03

Note: a = uncatalysed, vacuum-sealed tube; b = catalysed, vacuum-sealed tube; c = catalysed, in vacuo; \* = rate is time in minutes to reach 0.01 moles; + = rate is time in minutes to reach 0.001 moles; u = where peak value is also ultimate concentration, i.e. when time (t) for a = 24 hours and b = 256 minutes.

Table 2: The half lives ( $\tau$ ) of methylolphenol and dibenzyl ether.<sup>11</sup>

Compound	Experiment	(mins)
Methylolphenol	uncatalysed; sealed tube	70
	catalysed; sealed tube	20
Dibenzyl ether	uncatalysed; sealed tube	240
	catalysed; sealed tube	40
	catalysed; in vacuo	1

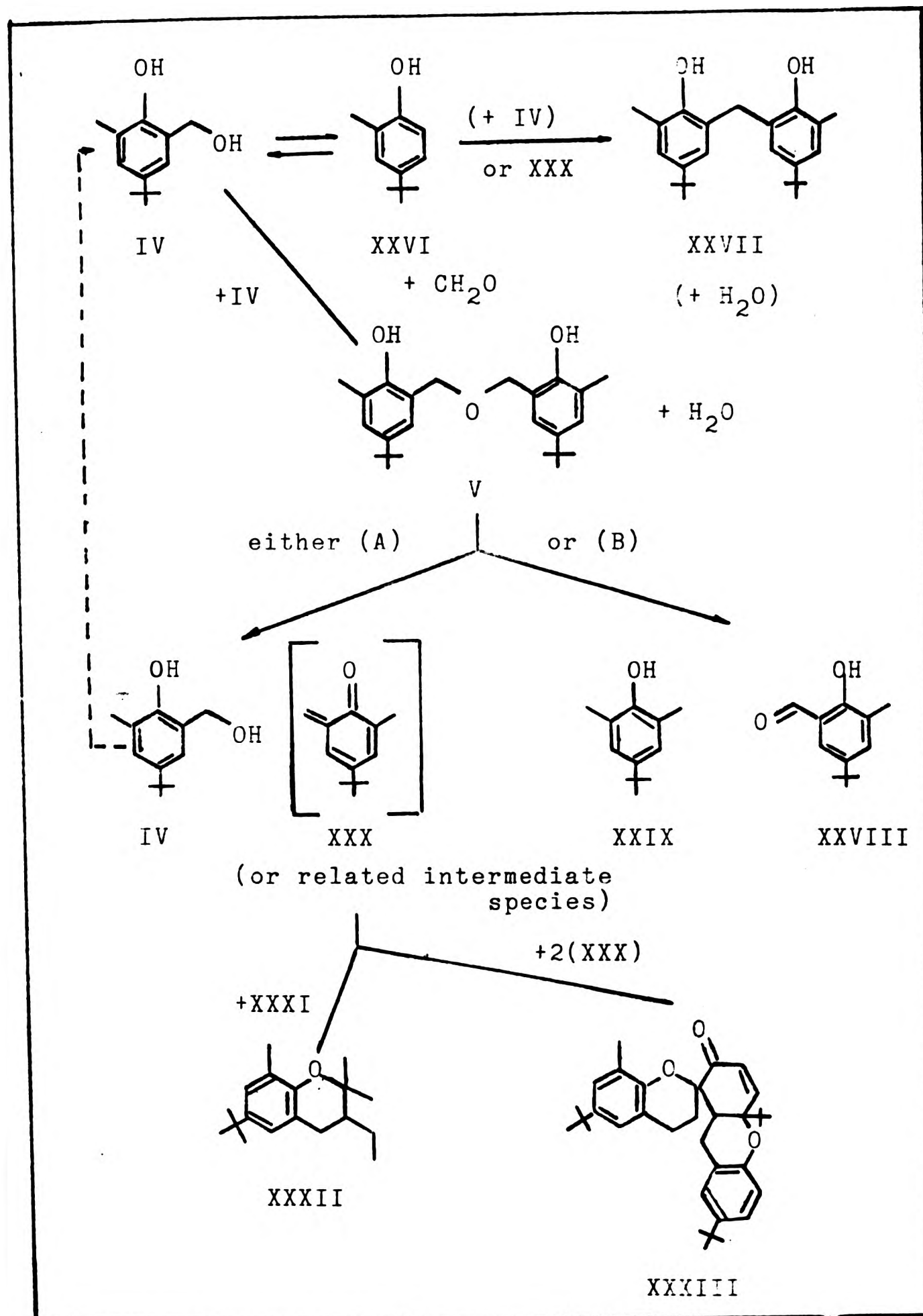


Fig. 4 Proposed reaction scheme for the interaction of the methylolphenol (IV)/dibenzyl ether (V) with alk-2-ene (XXXI).<sup>11</sup>

Table 3: Kinetic data for the products of reaction of the methylolphenol(IV) (1) in hexane, (2) with alk-1-ene, (3) with alk-2-ene, and (4) the dibenzyl ether with (V) alk-2-ene, under various conditions, 11 at 150°C.

		INDUCTION TIME				RATE				PEAK VALUE			
		(minutes)				(time to 0.1 moles)				(moles)			
		(1)	(2)	(3)	(4)	(1)	(2)	(3)	(4)	(1)	(2)	(3)	(4)
Dibenzyl ether	a	8	8	8		22	22	17		0.46	0.43	0.42	
	b	3	3	3		8	6	5		0.31	0.30	0.34	
	c			4				14				0.28	
	d			2				5				0.35	
Original phenol	a	13	12	13	30	22*	20*	14†	35*	0.01	0.01	0.01	0.01
	b	6	5	6	11	10*	12*	9*	30*	0.01	0.01	0.01	0.01
	c			22	45				50*			0.02	0.01
	d			-	-				-			-	-
Diphenyl methane	a	25	25	22	40	42*	44*	50*	145*	0.04 <sup>u</sup>	0.05 <sup>u</sup>	0.04 <sup>u</sup>	0.04 <sup>u</sup>
	b	12	8	8	15	17*	11*	10*	24*	0.13	0.12 <sup>u</sup>	0.11 <sup>u</sup>	0.10 <sup>u</sup>
	c			30	60				49*			0.03 <sup>u</sup>	0.03 <sup>u</sup>
	d			-	-				-			-	-
Trimer	a	25	25	22	8	91	110	1440	427	0.34 <sup>u</sup>	0.31 <sup>u</sup>	0.10 <sup>u</sup>	0.14 <sup>u</sup>
	b	12	8	8	3	40	63	71	36	0.31	0.29 <sup>u</sup>	0.28 <sup>u</sup>	0.29 <sup>u</sup>
	c			-	-				-			-	-
	d			-	-				-			-	-
Chroman	a	-	-	22	8	-	-	100	40	-	-	0.32 <sup>u</sup>	0.40 <sup>u</sup>
	b	-	8	8	3	-	33	26	16	-	0.41 <sup>u</sup>	0.42 <sup>u</sup>	0.45 <sup>u</sup>
	c			15	6			30	14			0.63 <sup>u</sup>	0.19 <sup>u</sup>
	d			6	3			16	10			0.76 <sup>u</sup>	0.83 <sup>u</sup>
Benzaldehyde	a	25	25	22	8	72*	63*	60*	35*	0.05 <sup>u</sup>	0.05 <sup>u</sup>	0.04 <sup>u</sup>	0.06 <sup>u</sup>
	b	12	8	8	3	30*	25*	30*	11*	0.13	0.06 <sup>u</sup>	0.06 <sup>u</sup>	0.07 <sup>u</sup>
	c			-	-				-			-	-
	d			6	3				20*			0.09 <sup>u</sup>	0.09 <sup>u</sup>
Dimethyl phenol	a	25	25	22	8	72*	63*	60*	35*	0.04 <sup>u</sup>	0.04 <sup>u</sup>	0.04 <sup>u</sup>	0.05 <sup>u</sup>
	b	12	8	8	3	30*	25*	30*	11*	0.09	0.05 <sup>u</sup>	0.06 <sup>u</sup>	0.07 <sup>u</sup>
	c			-	-				-			-	-
	d			6	3				20*			0.08 <sup>u</sup>	0.09 <sup>u</sup>
Methylol phenol	a				8				10*				0.15
	b				3				6*				0.09
	c				6				8*				0.09
	d				3				4*				0.13

Note: a = uncatalysed (free:occupied volume of vacuum-sealed tube of ca. 1.5:1.0); b = catalysed (ca. 1.5:1.0); c = catalysed (ca. 0.25:1); d = catalysed and added methanal (ca. 1.5:1.0); \* = rate is time in minutes to reach 0.01 moles; † = rate is time in minutes to reach 0.001 moles; u = where peak value is also ultimate concentration, i.e., when time(t) = 24 hours.

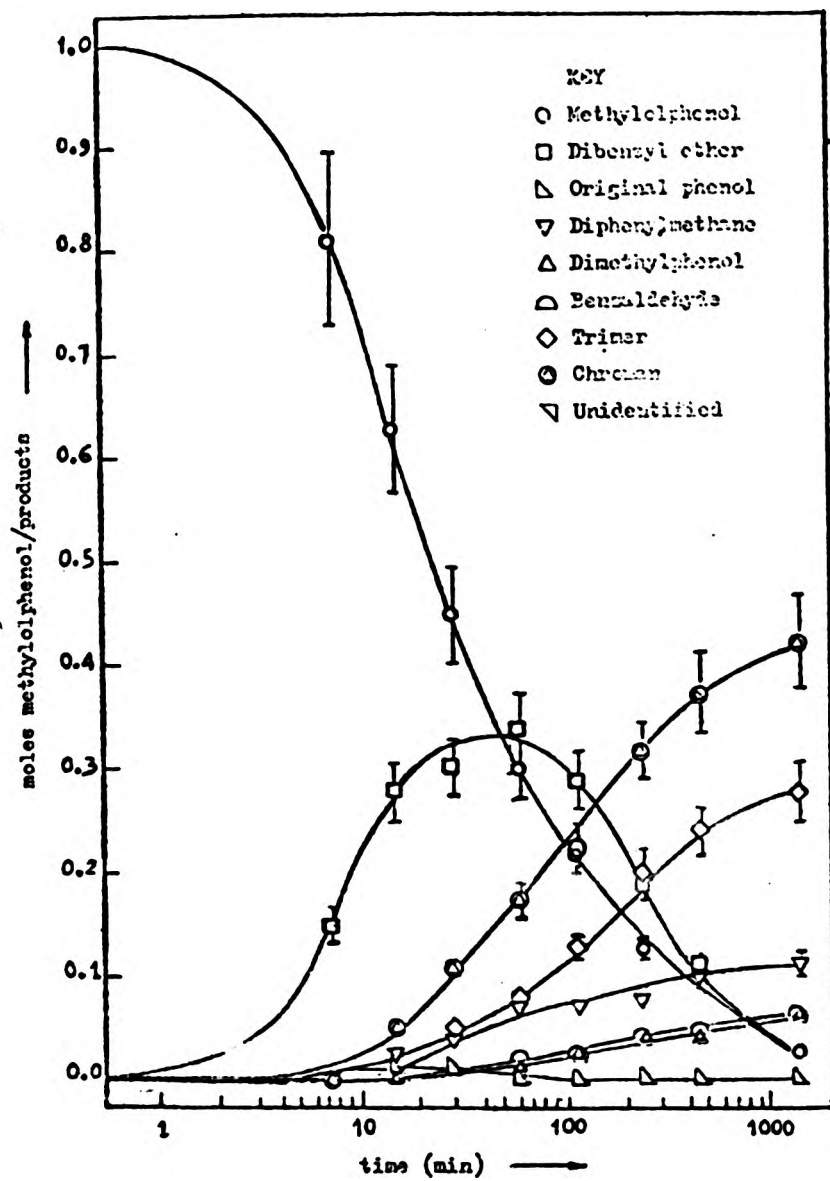
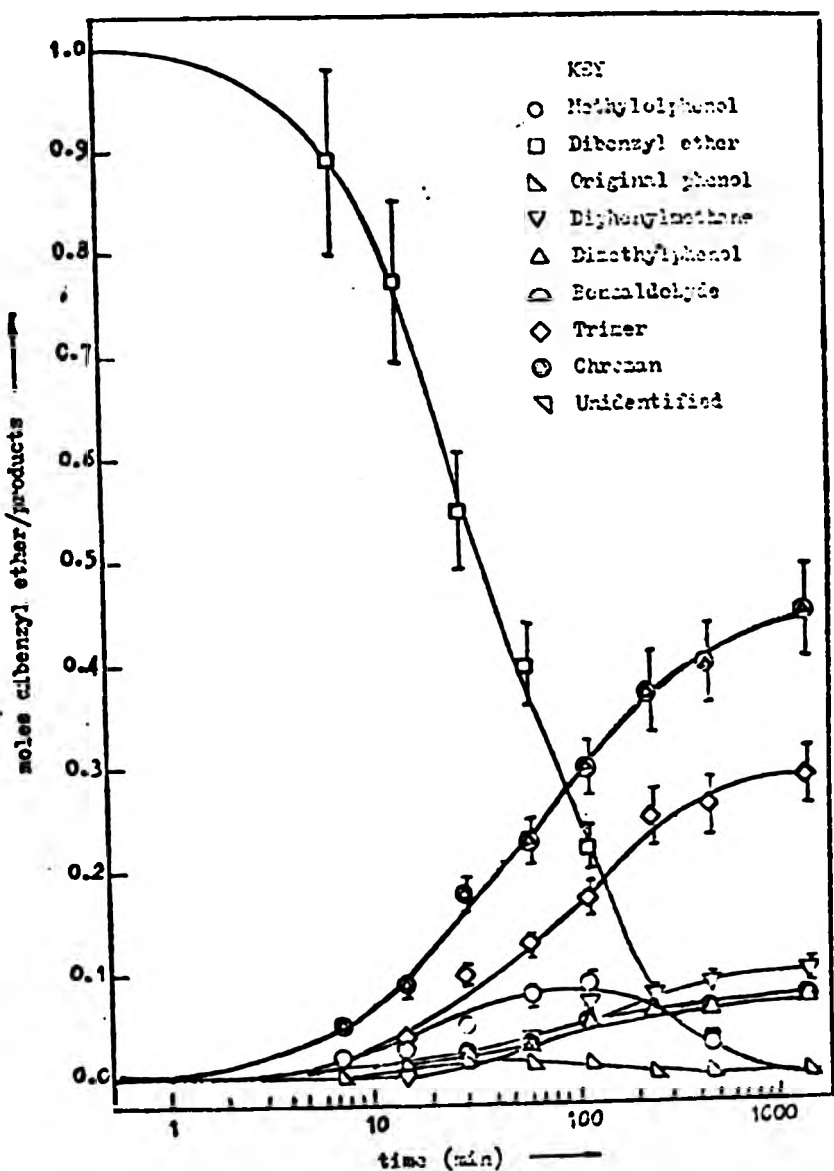


Fig. 5 : Changing concentrations of reactant and products, with time, on reaction with methylolphenol at 150°C in the presence of alk-2-ene (catalysed, sealed tube).<sup>11</sup>

Fig. 6 : Changing concentrations of reactant and products, with time, on reaction of dibenzyl ether at 150°C in the presence of alk-2-ene (catalysed sealed tube).<sup>11</sup>



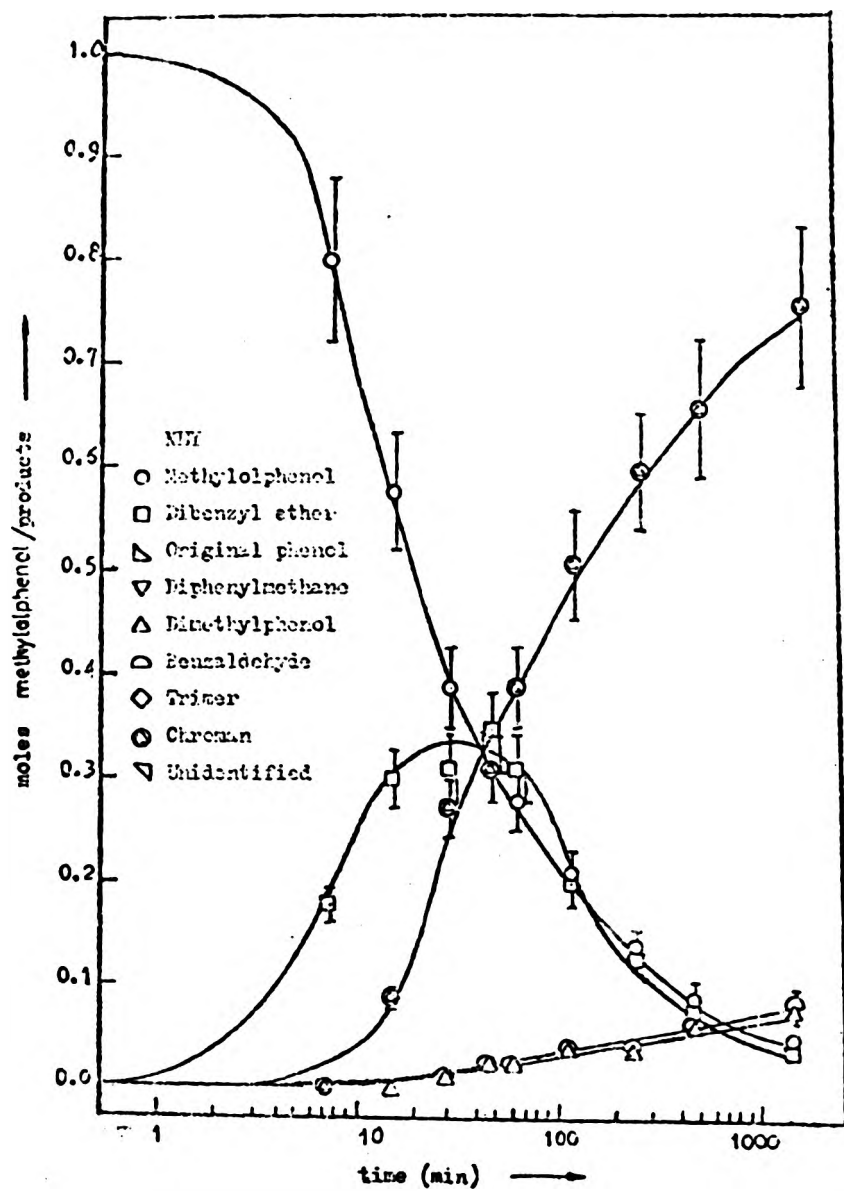
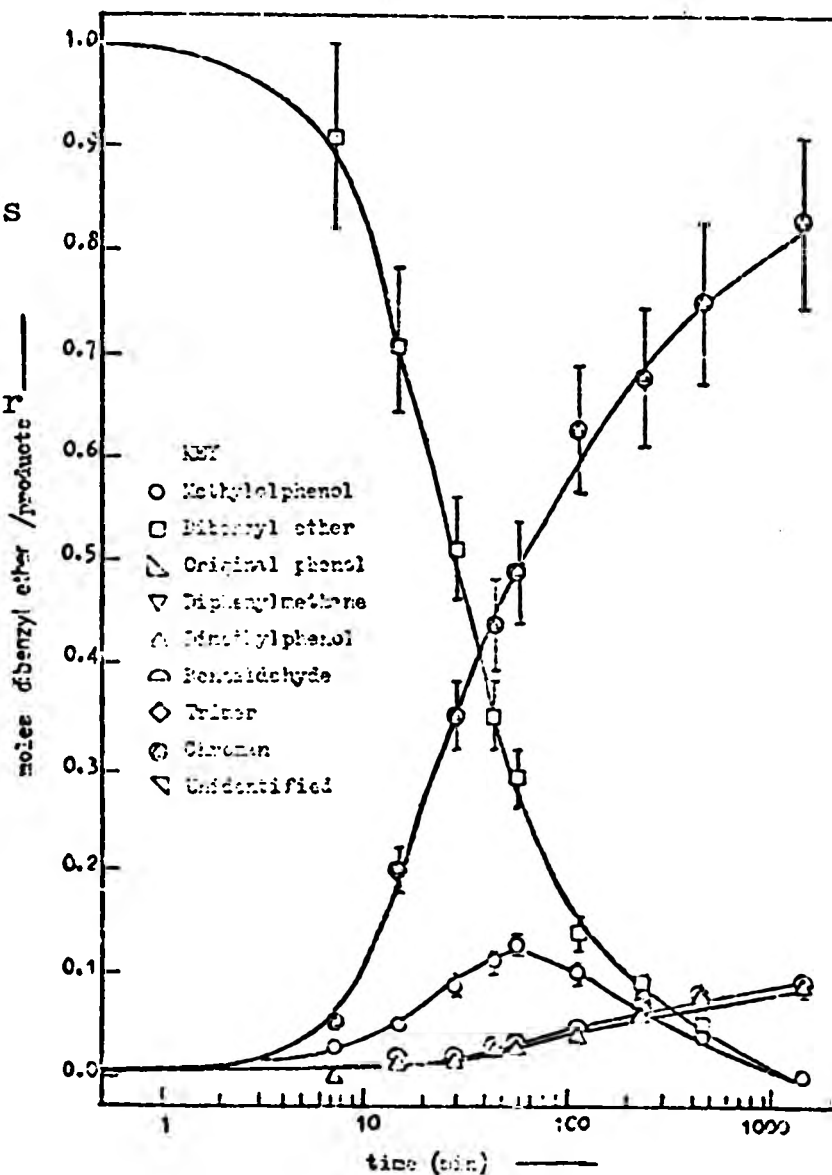
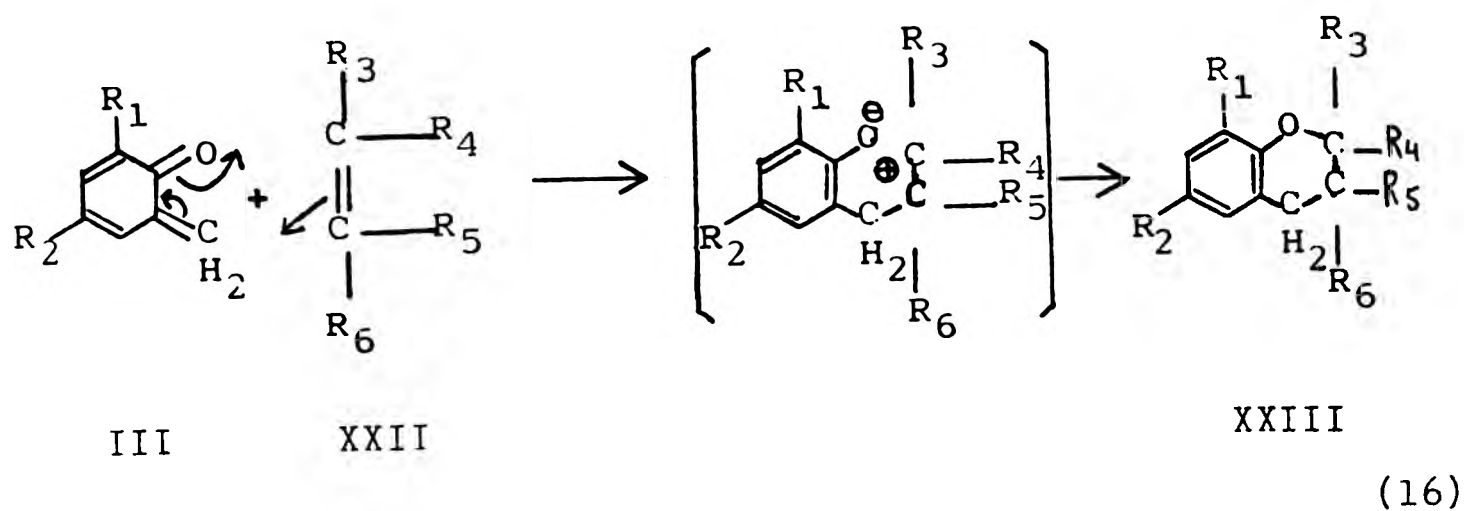
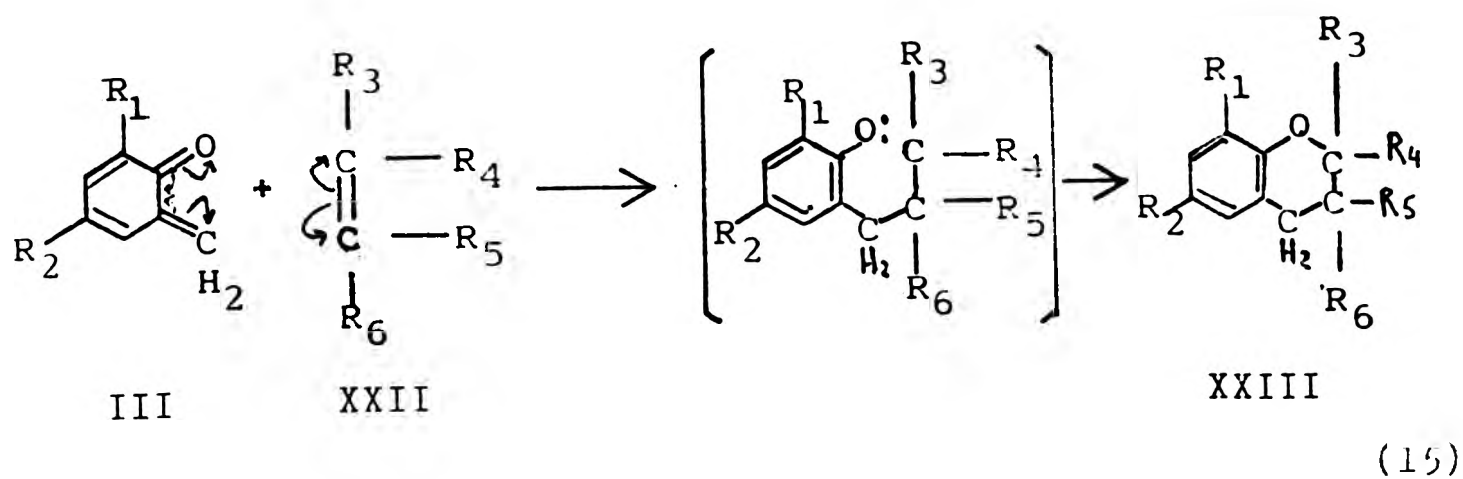


Fig. 7: Changing concentrations of reactant and products, with time, on reaction of methylolphenol at 150°C in the presence of alk-2-ene and added methanal (catalysed, sealed tube).<sup>11</sup>

Fig. 8: Changing concentrations of reactant and products, with time, on reaction of dibenzyl ether at 150°C in the presence of alk-2-ene and added methanal (catalysed, sealed tube).<sup>11</sup>

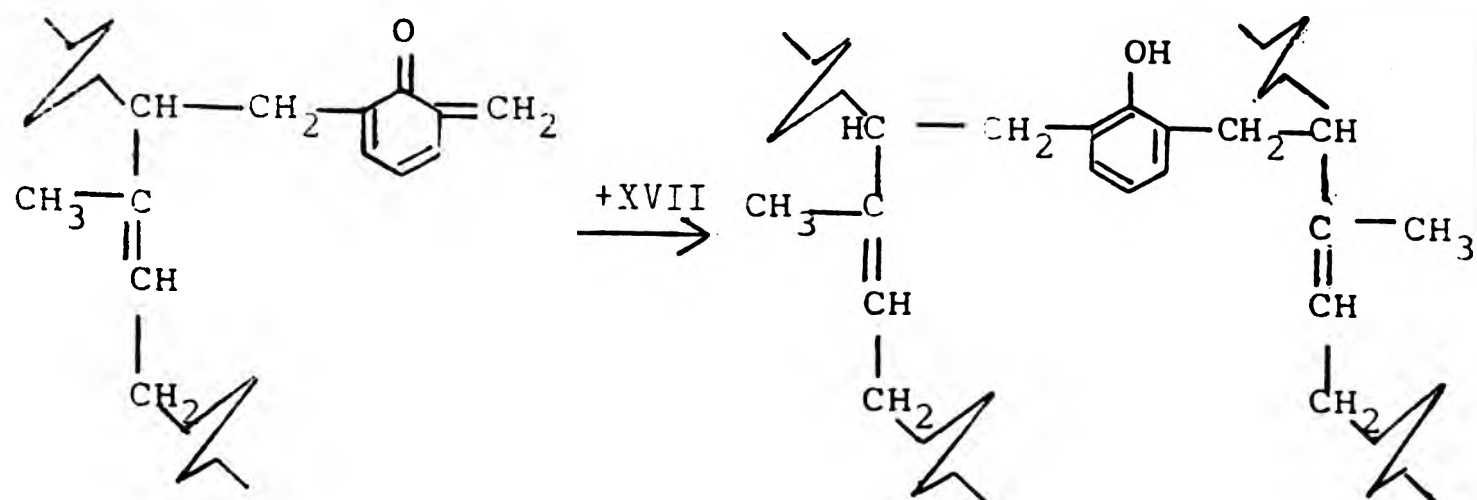
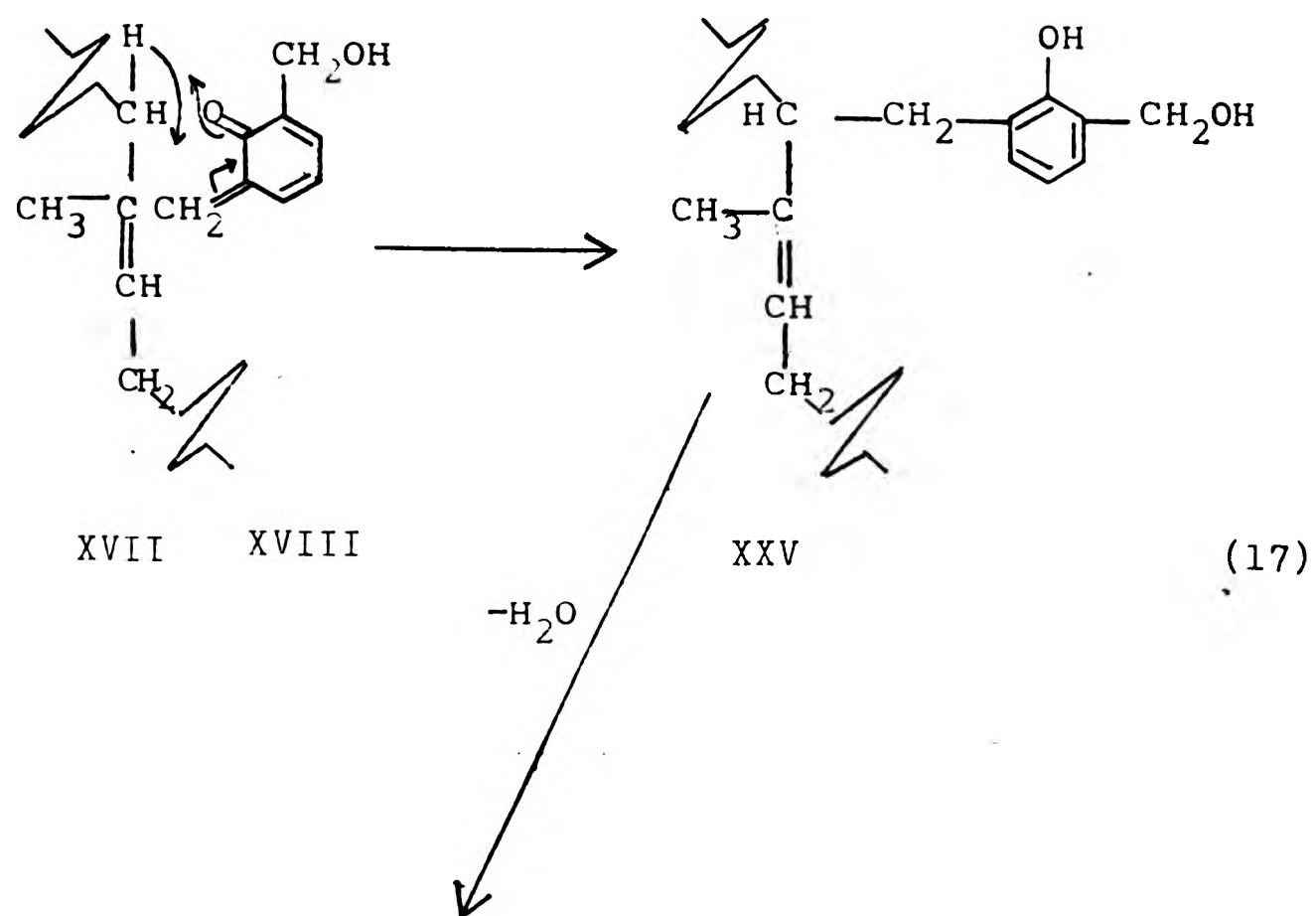




unsymmetrical alkenes, quinone methides yield only one adduct and the two-step ionic mechanism (16) is favoured,<sup>27</sup> while in dimer formation (see (5) earlier) the free-radical mechanism (15) explains the specific orientation obtained since dimerisation of an ionic species, such as VIII, is implausible.<sup>19,21</sup> It has been shown that the high temperature required for cycloadditions involving chroman is only necessary for the formation of the quinoid species, and not for their subsequent reaction with alkenes<sup>29</sup> (see Section (g) later).

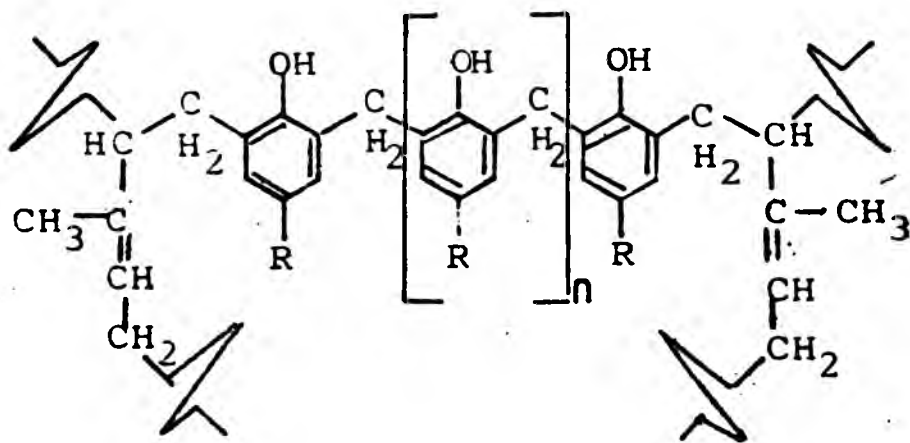
(d) Formation of adducts linked via methylene groups

One of the earliest proposals not involving chroman formation for the interaction between 2,6 dimethylolphenol (XVIII) and natural rubber came from Van der Meer.<sup>15</sup> He



suggested that, during natural rubber vulcanization, the two methylol groups of (XVIII) reacted with different rubber chains. This occurred through o-quinone methide intermediates, which attacked an "active" hydrogen present in an alpha-methylene group of the rubber molecule (XVII). Reaction (17) differs from the Diels-Alder-type addition (14) in that addition now occurs across a simple (C-H) bond instead of a double (C=C) bond. Later, Van der Meer examined the vulcanizing action of numerous phenol-formaldehyde condensates including the halomethyl phenols.<sup>13</sup> In each case he postulated adduct formation by a mechanism analogous to that shown in (17).

With the typical p/f condensate (I) the crosslinking would be envisaged as a reaction similar to (17) to produce XXXIV:

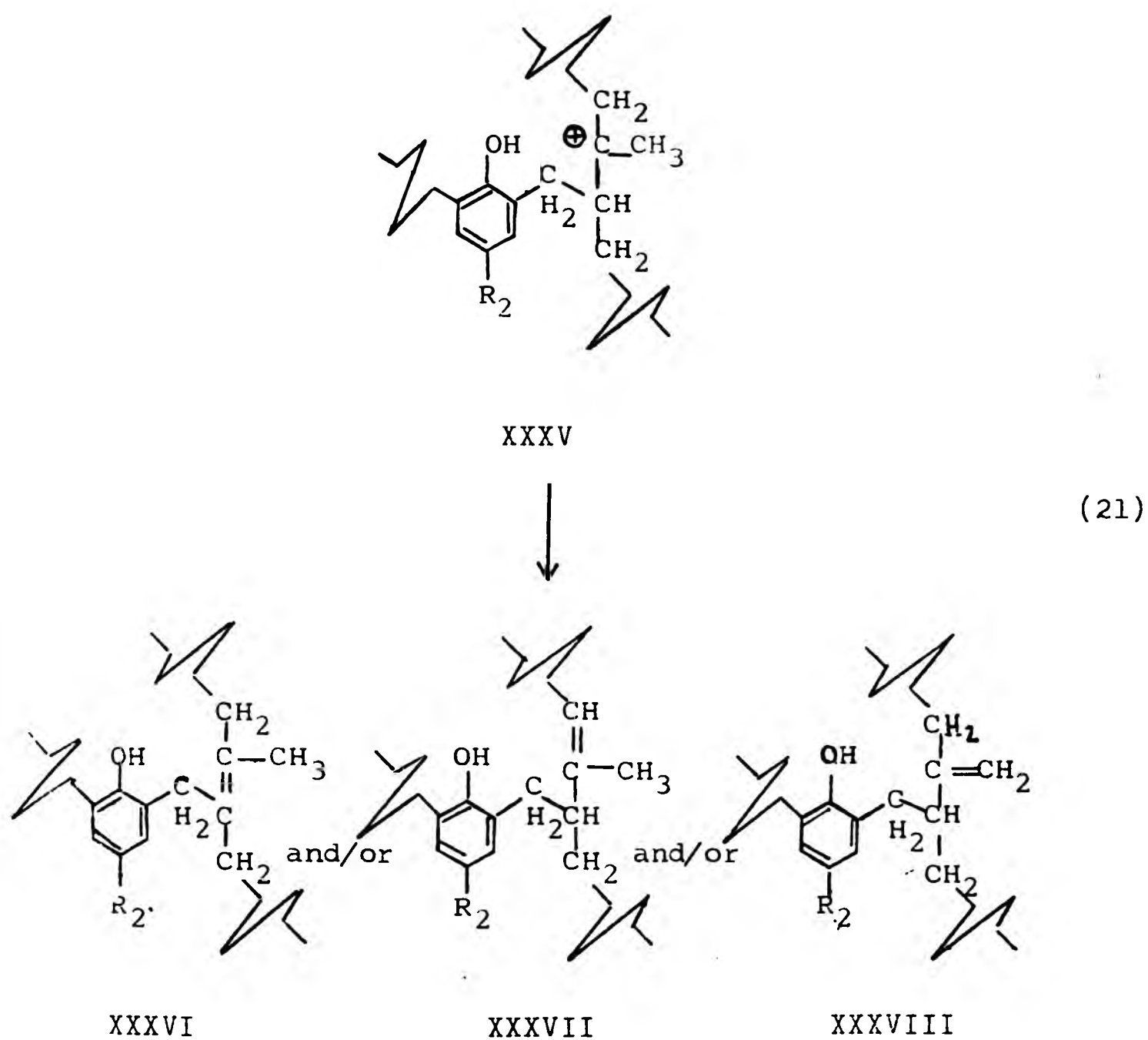


XXXIV

Van der Meer's mechanism (17) is pictured as a synchronous one, i.e., not involving any ionic or free-radical species. However, in view of the highly polarised state of the o-quinone methide (VIII) and the position of the hydrogen, Fitch<sup>11</sup> has suggested an ionic mechanism for the reaction



Subsequently, XXXV, in order to stabilise itself, will expel a proton to produce one or more compounds in which the position of the original double bond may have shifted:



Hofman<sup>31</sup> favoured XXXVI, whereas Elmer<sup>32</sup> considered XXXVII as the product. Fitch<sup>11</sup> postulated that if mechanism (21) is operating then all three (XXXVI-XXXVIII) are possible, although as the alkylphenol XXXVI is the most thermodynamically stable, it should be present in the highest proportion.

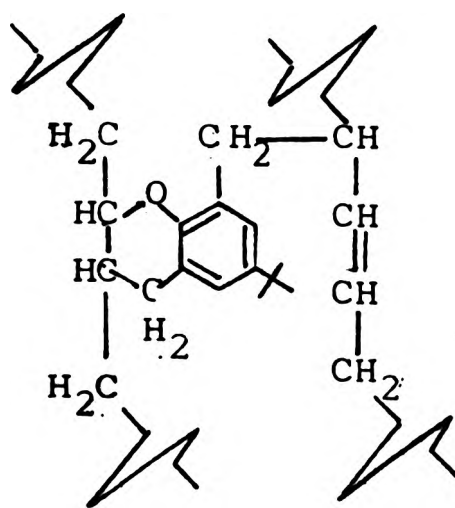
No reduction in unsaturation (infra-red method) was observed after NR vulcanization at 150°C and 130°C/60 min. with 30 phr of p-ter, butyl phenol-formaldehyde resin (commercial source), either catalysed  $\text{SnCl}_2 \cdot 2\text{H}_2\text{O}$  (2phr) or  $\text{ZnCl}_2$  (5phr) or uncatalysed.<sup>41</sup> From these observations the authors suggested the formation of crosslinks of the type (XXXVI-XXXVIII), i.e., where double bonds are not consumed in the reaction. However, irrespective of the mechanism of vulcanization operating in the curing of natural rubber in presence of Lewis acid catalysts, some cyclisation of the rubber might be expected (see Section (f) later) which would reduce rubber unsaturation. Furthermore, the reduction in unsaturation to be expected after vulcanization involving double bond consumption is small, and could be difficult to measure with sufficient precision. Also, the tetra-alkyl ethylene XXXVI would not be infrared-active.

Thus, some doubt is cast on the conclusions drawn from this previous work.

(e) Crosslink formation by both chroman and methylene linkages.

The hypothesis that both types of linkage were formed has been supported by Ginzburg.<sup>42</sup> In his work, vulcanization of butyl rubber and SKD rubber (93% cis-1,4 polyisoprene) with 6phr of 2,6-dimethylol 4-p-tert.butyl phenol (IV where  $\text{R}_1 = \text{CH}_2\text{OH}$ ,  $\text{R}_2 = \text{C}(\text{CH}_3)_3$ ) and 3phr of tin (II) chloride dihydrate was carried out. Infra-red spectra of the vulcanizates

indicated that the phenolic hydroxyl concentration was reduced to approximately 50% of its original value. Thus, he concluded that both chromanic structures (whose formation (11) results in a loss of phenolic hydroxyl) and methylene linkages (whose formation (17) involves no such loss) were present; and gave a structure XXXIX:-



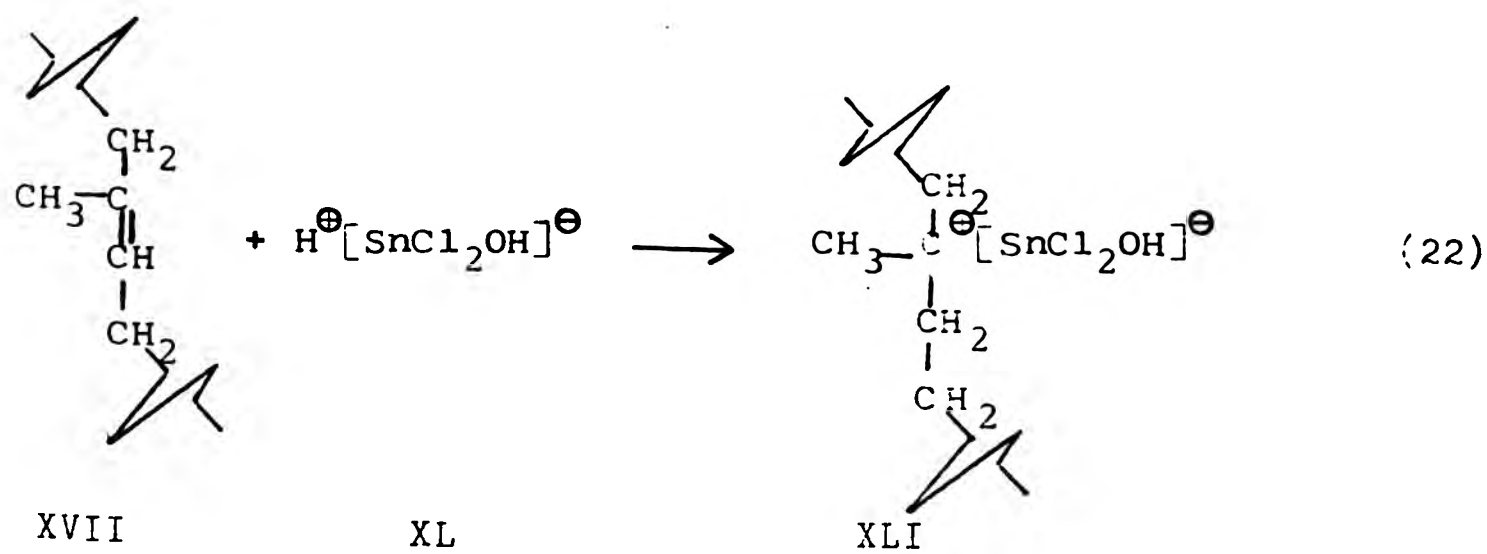
Ginzburg obtained similar results with bromomethyl-phenol derivatives.<sup>43</sup> However, Ginzburg apparently did not extract his vulcanizates; thus the presence of phenolic hydroxyl detected may be due to methylolphenol reaction products not necessarily attached directly to the elastomer.<sup>11</sup> In any case infra-red spectroscopy is not a sensitive enough method to use for hydroxyl determination, since it is well known that the phenolic hydroxyl absorption band is variable in position and intensity, and is strongly affected by the hydrogen-bonding capacity of its environment.

(f) Views of mode of action and side-effects of catalysts and inhibitors

Two of the deficiencies of the phenolic resin vulcanization system for unsaturated rubbers are the slow rate of reaction and the fact that some rubber compounding ingredients markedly decrease the rate and the state of cure. It was not until metal halides were introduced as accelerators or catalysts into the vulcanization system that significant progress was made in the field of resin vulcanization. These accelerators are similar to those Lewis acid catalysts used in the Friedel-Crafts reactions. Typical examples are the halides of group III-VIII transition metals (e.g.,  $\text{SnCl}_2$ ,  $\text{SnCl}_2 \cdot 2\text{H}_2\text{O}$ ,  $\text{ZnCl}_2$  and  $\text{FeCl}_3 \cdot 6\text{H}_2\text{O}$ ).

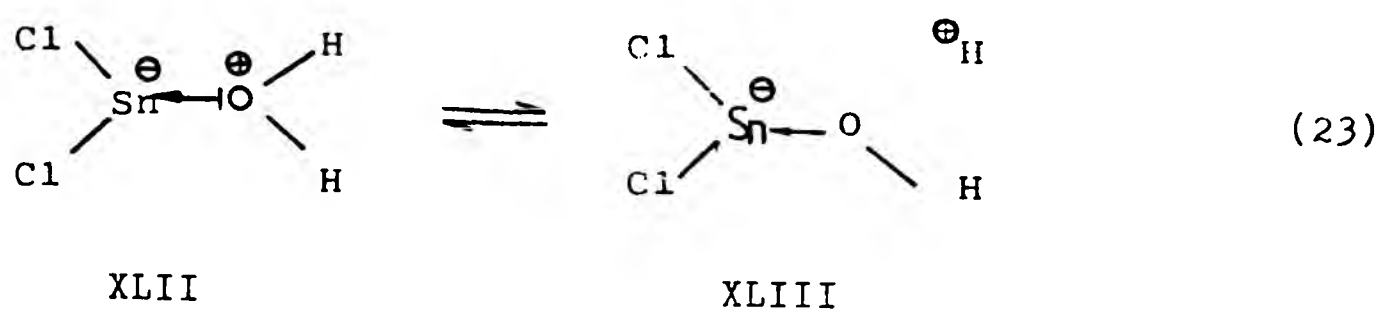
It is very difficult to study the mode of action of these catalysts, since they induce cationic chain reactions of very high rates, even in the most minute quantities.

A number of investigators have envisaged the catalyst complexing with the reactive condensate<sup>29-32,44</sup> to produce



for example, carbonium ions (see (7) and (8) earlier) and/or with the rubber,<sup>42,45</sup> for example according to reaction 22. The subsequent reactions of such complexes as (XLI) have been suggested to form chroman and/or methylene linkages.

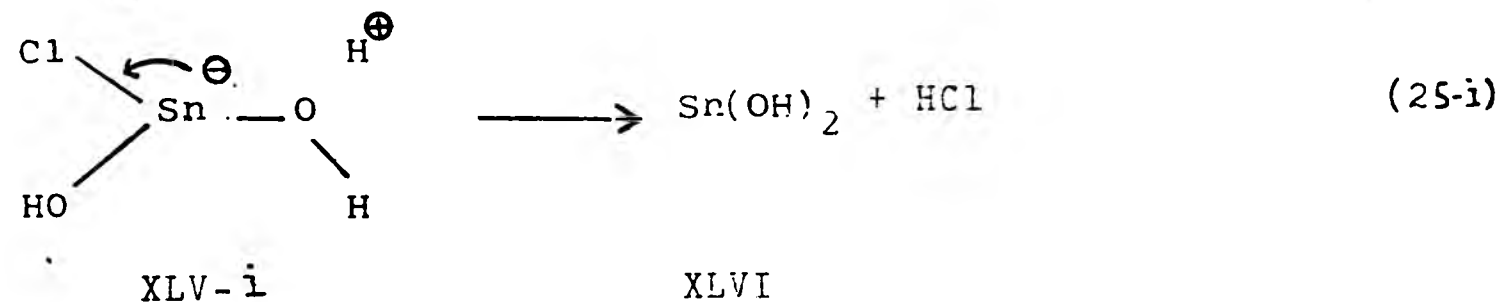
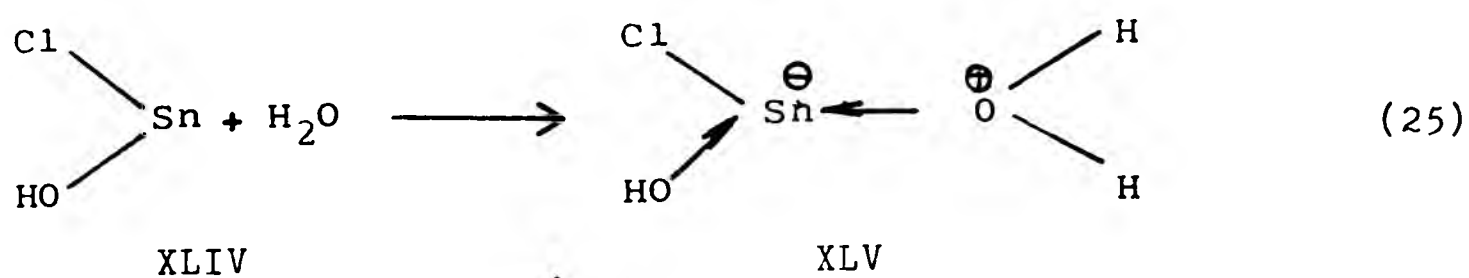
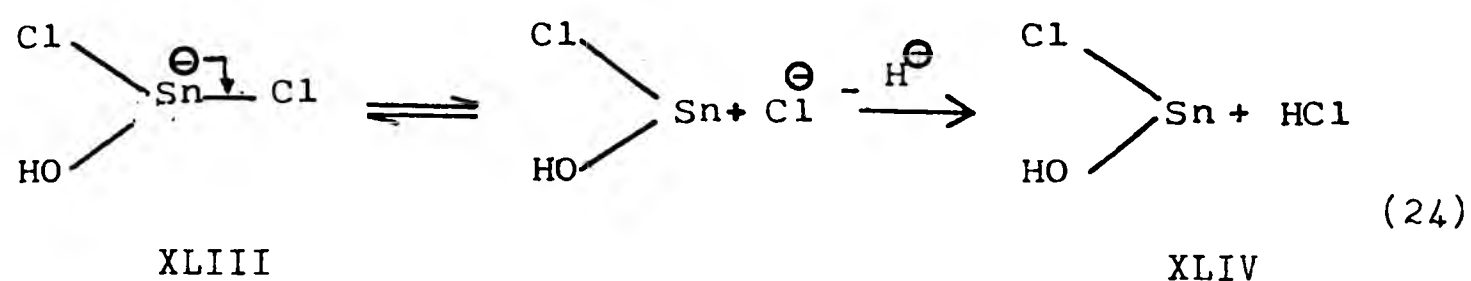
The nature and action of the tin (II) chloride dihydrate catalyst in the reaction between the p/f resin 'models' (the methylolphenol (IV) and its dibenzyl ether derivative (V)) and the models for natural rubber (2-methylpen-2-ene and 2-methylpent-1-ene- see glossary for structures) have been studied and discussed by Fitch.<sup>11</sup> Since one water molecule of the catalyst tin (II) chloride dihydrate, has been reported<sup>46</sup> to be lattice water, whilst the other is coordinated to the tin, the active catalyst complex is represented as the monohydrate (XLII). This complex acts as a source of free protons through a charge transfer (reaction 23). The proton may then initiate a cationic reaction



sequence involving an "ion-pair" mechanism where the counter-ion, (XLIII), is  $(\text{SnCl}_2\text{OH})^{\ominus}$ .

The gradual destruction of the catalyst with the

eventual formation of a hydrated tin (II) oxide and hydrogen chloride is considered by Fitch<sup>11</sup> to occur through the reaction sequence (24), (25) and (25-i) Clearly for catalytic

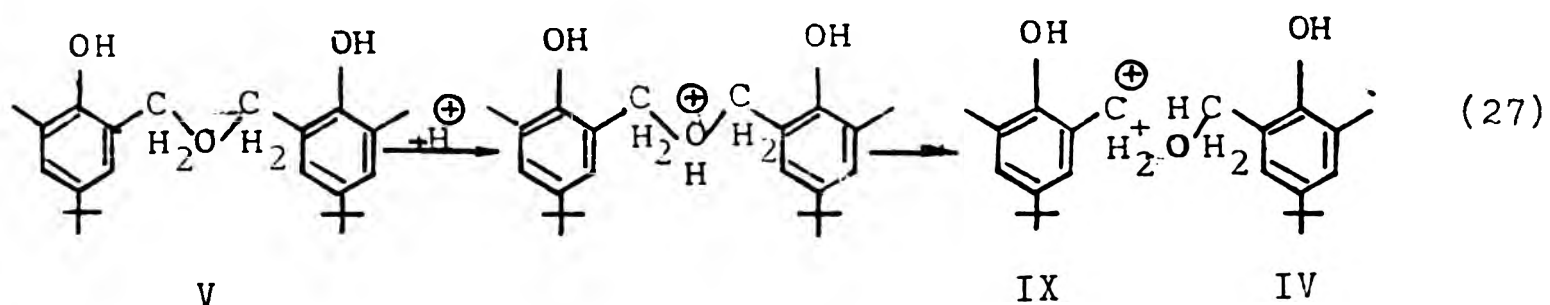
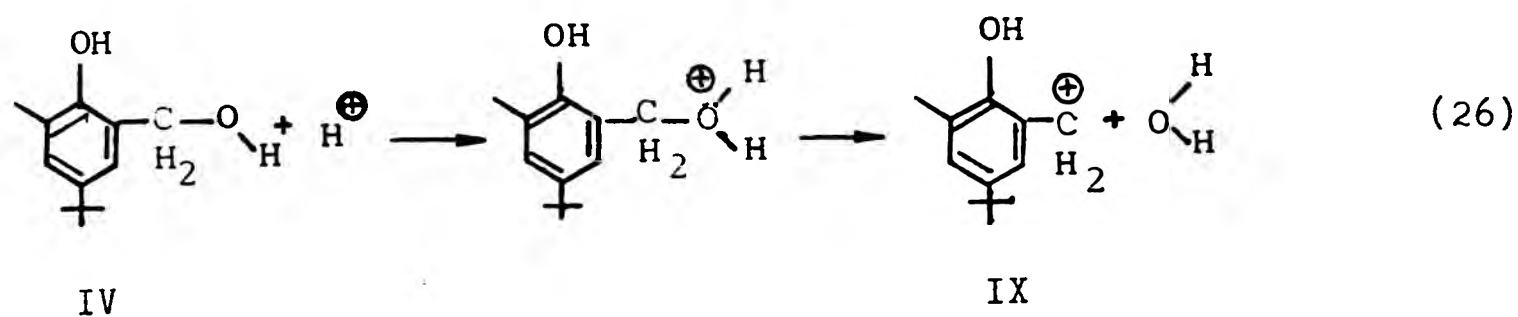


activity to be observed this reaction sequence must be slow enough to allow reasonable lifetimes of the ionised species (XLIII) and (XLV-i).

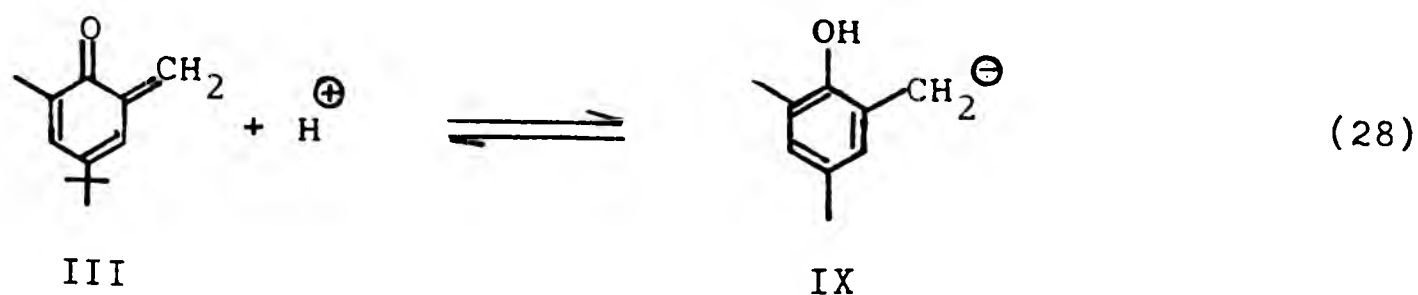
The rate of reaction of the "model" compounds used by Fitch in the presence of tin (II) chloride dihydrate was increased in the initial stages, but the rate in the final stages was similar to that the uncatalysed reaction. This

behaviour was attributed to the destruction of the catalyst by water (sequence (25)) as the reaction proceeds.

The mechanism of interaction of the 'ion-pair' (XLIII) with the phenolic materials used was represented by Fitch to yield structures such as (IX) as in reactions (26) and (27) (where the counter-ion is omitted in the interests of clarity).

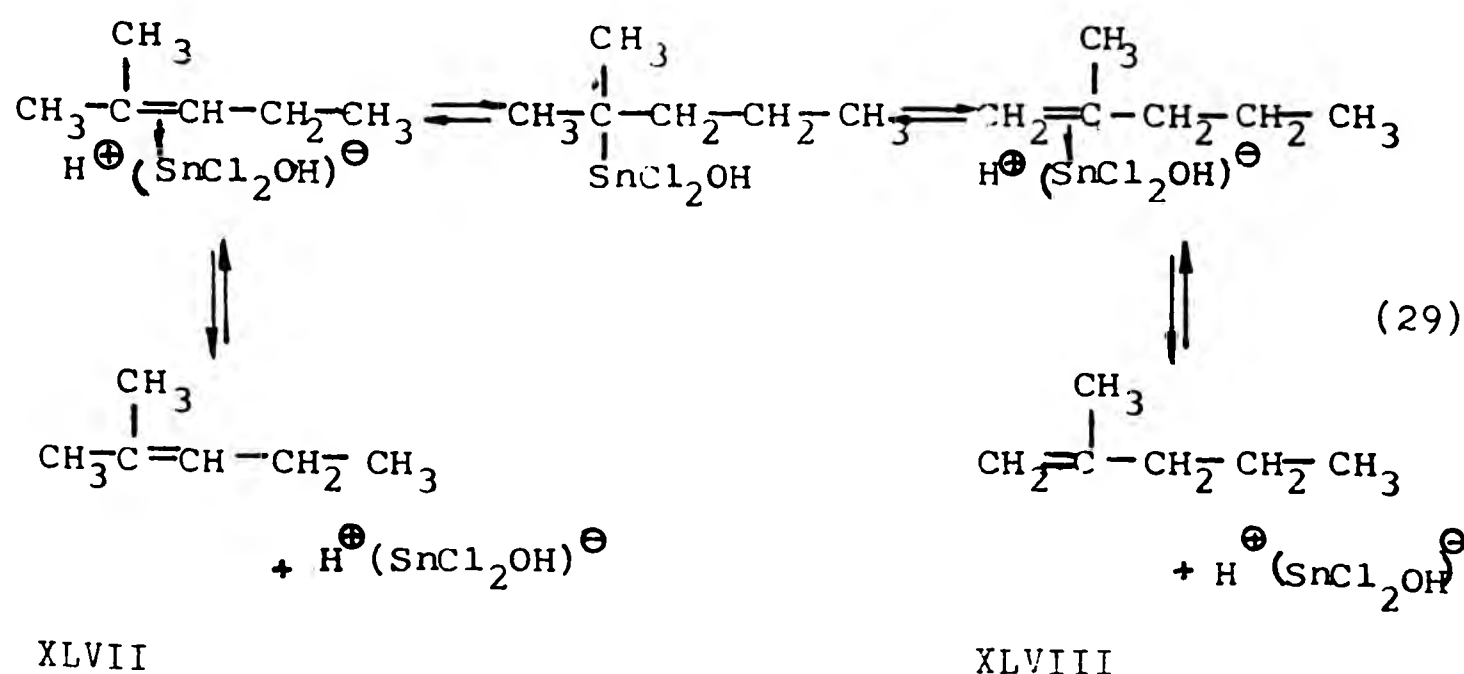


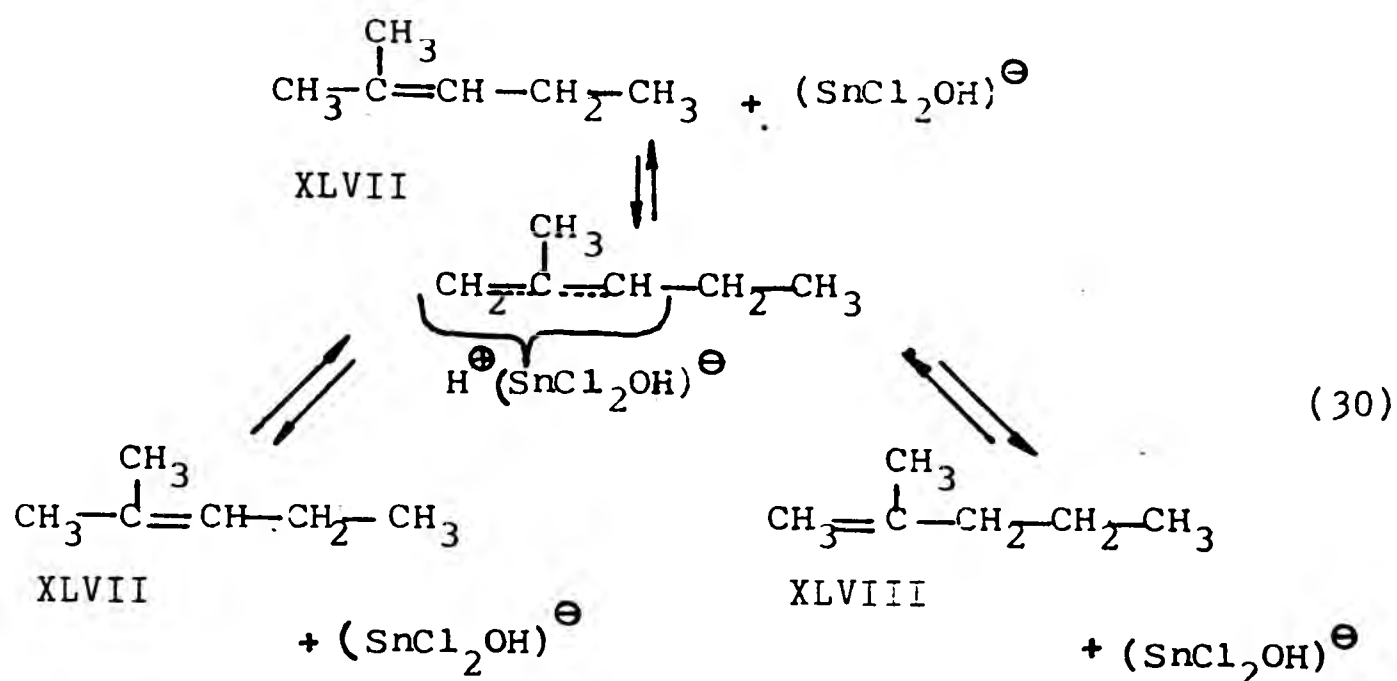
Also, it was suggested that structure (IX) can be formed by direct addition of a proton to the quinone methide (III) (equilibrium 28).



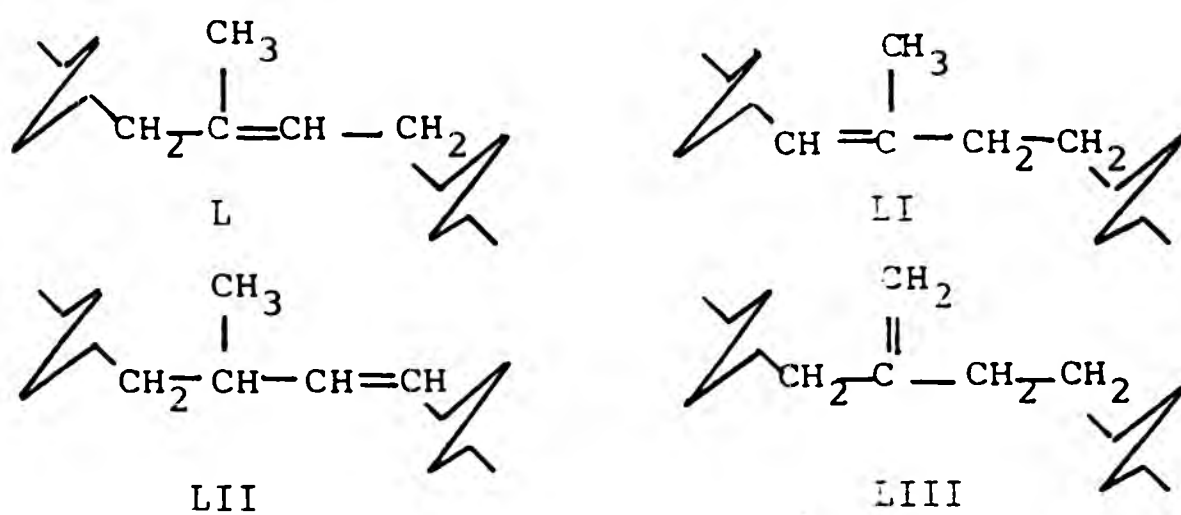
Thus, Fitch considered that the most likely ionic reactive species to be produced from any of the phenolic materials used is IX. It acts as a source of quinone methide through the equilibrium (28).

The catalyst may alternatively or additionally exert its effect at the double bonds of the unsaturated rubber (22). Transition metal compounds have been reported to cause isomerization of simple alkenes, and two possible mechanisms involving intermediate complexes have been suggested.<sup>47,48</sup> Isomerization of the mono-alkene, 2-methyl pent-2-ene (XXXIX) to an equimolar mixture of the alk-2-ene and the alk-1-ene (XIX) by a Lewis acid ( $\text{SnCl}_2 \cdot 2\text{H}_2\text{O}$ ) has been demonstrated.<sup>11</sup> According to the first proposed mechanism,<sup>47</sup> the alkene forms a complex with the tin and migration of the double bond proceeds by the addition-elimination sequence (29). The other mechanism proposed<sup>48</sup> again visualises a H-complex between the alkene and metal complex. In this case a three-





carbon delocalised allylic structure ( $\text{H}_2\text{C}=\text{C}=\text{CH}-$ ) can act in a "half-sandwich" bonding system with tin. It is proposed that fast intramolecular hydrogen shifts, via the allyl H-complex, then take place, as in (30). In the view of these isomerizations, it might be expected that vulcanization using Lewis acids would cause analogous double bond shifts in natural rubber. The possible structures are:

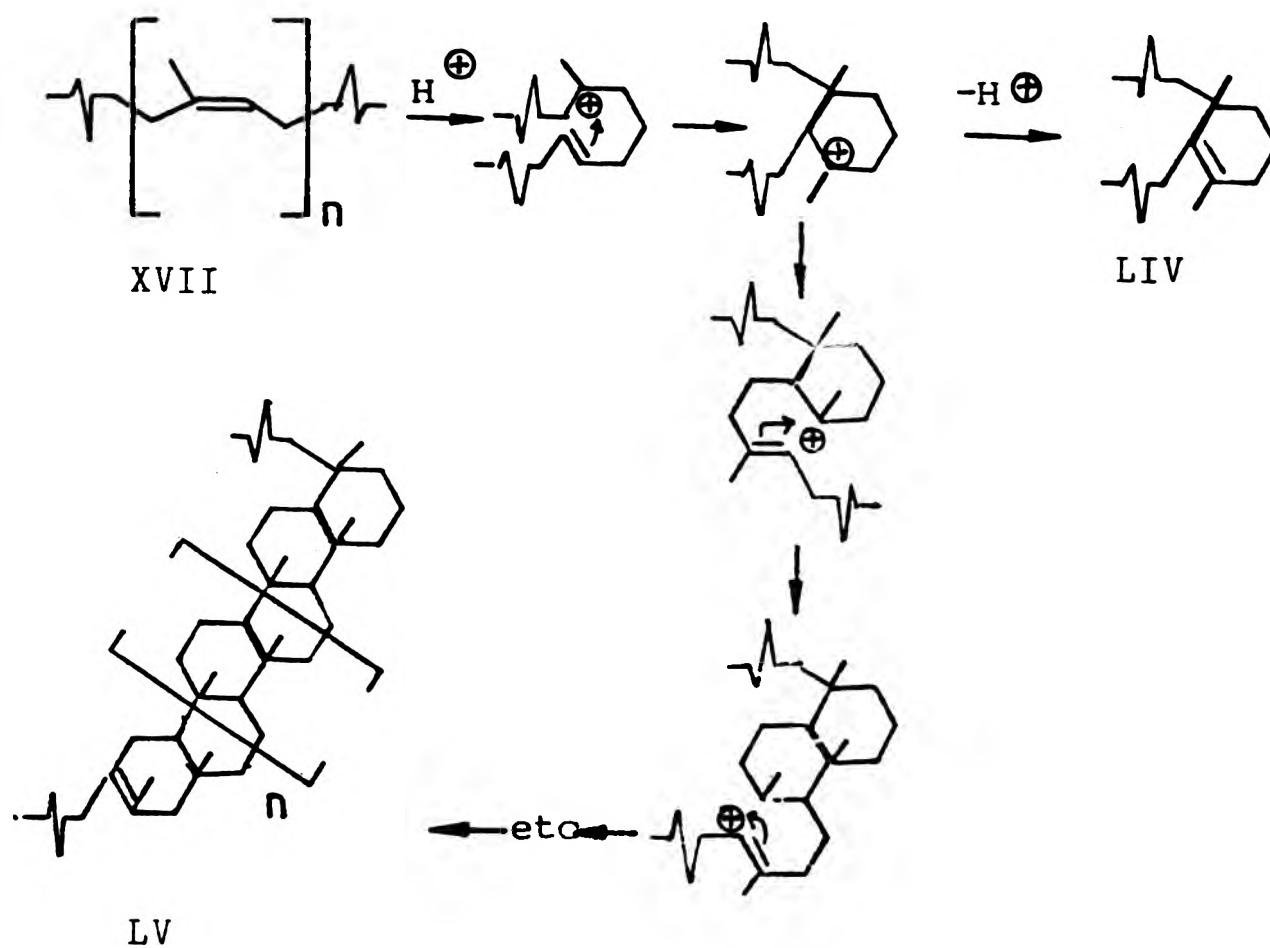


Structure (LII) can be visualised as anti-Markowininkof protonation of the double bonds, and this and structure LIII would have less-reactive double bonds than L and LI. Cis/trans isomerization is also possible for all these structures except LIII. Juxtaposition of structures L with LI or LII would give conjugated double bonds.

In addition to these double-bond shifts, another expected side-effect of interaction of the Lewis acid catalyst with natural rubber is geometric isomerism about double bonds. Various catalyst have been reported to cause cis/trans isomerization of unsaturated rubbers. Golub<sup>49,50,51</sup> converted the cis-1,4 units in polybutadiene into the corresponding trans units, by irradiation of the cis-polymer with ultra-violet light in the presence of various organic bromides and sulphur compounds. Cunneen<sup>52,53</sup> interconverted cis-1,4 polyisoprene units of natural rubber and trans 1,4 polyisoprene units by treatment of thin sheets of the unvulcanized rubber with thiol acids, sulphur dioxide and other sulphur compounds at 140°C. The changes in geometric configuration were readily followed by infra-red spectroscopy and by nuclear magnetic resonance spectroscopy, the latter offering a more accurate and absolute method.<sup>51</sup> The mechanism proposed was a reversible free-radical addition at the double bond involving formation of a freely rotating adduct.<sup>51</sup>

However, although cis/trans isomerization has been reported to result from Lewis acid treatment (hexachlorostannic (IV) acid, titanium (IV) chloride, phosphorus

trichloride oxide, and others), the products are also believed to be extensively cyclized.<sup>11</sup> It seems therefore, that cis/trans isomerization without cyclization is unlikely to occur with such Lewis acids as:  $\text{SnCl}_2 \cdot 2\text{H}_2\text{O}$ ,  $\text{SnCl}_2$ ,  $\text{ZnCl}_2$  or  $\text{FeCl}_3 \cdot 6\text{H}_2\text{O}$ . The mechanism of formation of cyclized structures, giving either monocyclic (LIV) and/or polycyclic (LV) structures is usually illustrated as follows:



In both types of structures, LIV and LV reduction in the number of double bonds (i.e., reduction of unsaturation) take place. D'Ianni et al.<sup>54</sup> have favoured monocyclic structures (LIV) as the main product on the basis of density and refractive index measurements and the observed loss of about 1/2 of the original unsaturation. Clearly, the

maximum loss of unsaturation possible for monocyclic structures (LIV) is 50%, but polycyclic structures (LV) would enable even greater loss of unsaturation to occur.

Several authors<sup>55,56,57</sup> have supported D'Ianni structure LIV mainly using theoretical statistical arguments. The polycyclic structure LV was proposed by Van Veersen on the basis of unsaturation values as low as 10% for cyclized rubber samples. Shelton and Lee<sup>59</sup> also obtained a low degree of unsaturation for 1,4 polybutadiene cyclized in solution by acid and therefore also favoured a polycyclic structure corresponding to (LV). The major difficulty with these studies is lack of reliability of the methods used to determine unsaturation. Lee et al.<sup>60</sup> made a comprehensive study of the unsaturation remaining in natural rubber after cyclization with stannic chloride. Perbenzoic acid oxidation enabled the best estimate of unsaturation to be obtained. The unsaturation in some samples was found to be below 20% of that in the original rubber. Thus, the authors concluded that polycyclic structures (LV) must be formed. In this latter study the "cyclicty" (i.e., average number of rings per cyclized sequence) obtained by treatment of natural rubber with stannic chloride in benzene solution for 65-72h was showed to be independent of both natural rubber and catalyst concentrations but to be markedly dependent on the temperature. The cyclicty varied from 1.5 at 110° to 6 at 60°C (i.e., the higher the temperature the lower the "cyclicty"). The rate of the reaction was first order with respect to the rubber and second order with respect to the catalyst.

The distinctive strain-induced crystallization behaviour, responsible for the high 'gum' tensile strength of natural rubber, is associated with the molecular orientations permitted by the cis configuration at the double bonds. Modification of the regular structure of natural rubber by partial conversion of cis to trans double bonds, as well as double-bond shifts, interferes with the orientation of the rubber chains and hence with the crystallization. This results in a marked retardation in rate of crystallization or, if isomerization is extensive, to a complete loss of ability to crystallize. Thus, "gum" tensile strength is adversely affected. Cyclization similarly disrupts structural regularity, and inhibits crystallization. Unlike cis/trans isomerization, however, cyclization dramatically raises the glass transition temperature ( $T_g$ ) and causes a loss in rubber elasticity. It is therefore an important part of the present study to ascertain the extent to which cis/trans isomerization, double bond shifts, and cyclization are caused by the catalysts used. Although the lack of strain crystallinity resulting from cis/trans irregularity and double bond shifts will not be very important in black-reinforced rubbers, the occurrence of cyclization would be a more serious problem, causing a large increase in rigidity in all compounds.

It has been established<sup>61,63</sup> that some rubber compounding ingredients, such as tetramethyl-thiuram disulphide and certain antioxidants (derivatives of p-phenylene diamine), markedly decrease the rate and extent of cure of rubber by

p/f resins even in such small amounts as 0.0002 moles. The retardation effect of the amino compounds has been found to depend on the electron density at the nitrogen atom and on the number of hydrogen atoms linked to it.<sup>61</sup> It was also found<sup>61</sup> that phenolic-type antioxidants have practically no effect on the vulcanization. Other compounding ingredients, such as silica filler, retard vulcanization by reacting preferentially with the Lewis acids catalyst.<sup>62</sup>

(g) Halogen-containing organic activators and 'self-reactive' resins

The patent literature describes methods to raise the rate of vulcanization of unsaturated elastomers by p/f resins by adding chlorinated polymers such as polychloroprene,<sup>7</sup> chlorosulphonated polyethylene ("hypalon"),<sup>8</sup> chlorinated waxes<sup>9</sup> and halogenated butyl rubbers.<sup>10</sup>

Fitch<sup>11</sup> suggested that the halogen-containing organic accelerators function by halomethylation of the methylol-phenol groups or by easier ether formation and/or reaction with zinc oxide present to form a Lewis acid catalyst. At vulcanization temperature these chlorinated polymers evolve small amounts of hydrogen chloride which may react with the resin and/or the zinc oxide. This idea has been taken a step further and the p/f condensates employed as vulcanizing agents have been halomethylated to a certain degree before sale. They are termed 'self-reactive' resins. The bromine derivative of a phenol-formaldehyde resin is commercially



(h) Other views

Different views of the reaction, involving free radical intermediates, have been postulated by several authors. Fel'dshtein<sup>67</sup> found from electron paramagnetic resonance (EPR) studies that free radicals are present when a p-tert butyl-phenol-formaldehyde resin was heated with stannous chloride dihydrate (10:1). The radiospectrometric data were obtained from samples heated at different times (30 sec to 11 min) at 130°C and 140°C. From this evidence the author concluded that the free radicals formed at vulcanization temperatures may be of basic importance in the structure-forming action of p/f resins. Ginzburg<sup>42</sup> studied the reaction of dimethylphenol (IV where  $R_1 = \text{CH}_2\text{OH}$ ,  $R_2 = \text{C}(\text{CH}_3)_3$ ) with butyl rubber (12 pphr) in the absence of accelerator at 180°C. He concluded from infrared analysis that the dimethylphenol first condensed to form the benzyl ether (V where  $R_1 = \text{CH}_2\text{OH}$ ,  $R_2 = \text{C}(\text{CH}_3)_3$ ); this was then believed to dissociate into radical fragments which caused crosslinking of the rubber by a free radical mechanism.

A radical mechanism of vulcanization of unsaturated rubbers by p/f resins was postulated by Boguslowski et al.<sup>68</sup> from the observation that when cis-1,4 polyisoprene rubber and a p-alkylphenol-formaldehyde resin (Amberol ST-137) were heated in an inert atmosphere (helium) either with or without activator (the ethyl ester of  $\alpha$ - $\beta$ -dibromophenyl propionic acid) no reduction in the intensity of the bands at 1065  $\text{cm}^{-1}$  and at 3400  $\text{cm}^{-1}$  in the ir spectra was observed. Intensity

reductions of these absorption bands did occur, however, during heating in air, and were taken by the authors as evidence of rubber-p/f resin interaction. It was therefore concluded that oxygen had an activating effect on the reaction and crosslinking involved an autooxidative free-radical reaction. Furthermore, these authors found that a free-radical acceptor inhibited the aerobic reaction.<sup>69</sup>

### 1.3 Aim of This Project

The object of the present work is to investigate the kinetics and mechanisms of reactions between alkyl phenol-formaldehyde resins and unsaturated elastomers, with particular attention to the conditions used in industrial vulcanization processes. The work is necessary in order to establish optimum conditions for efficient vulcanization. For this purpose adduct formation between p/f condensates of various functionalities and unsaturated elastomers (mainly cis-1,4-polyisoprene) are studied. In the initial stages of the work adduct formation between monofunctional p/f models (IV and V where  $R_1=CH_3$ ,  $R_2C(CH_3)_3$ ) and the polyisoprene rubber IR (synthetic cis-1,4 polyisoprene) are investigated. It was expected that the reaction products of this initial study would be uncrosslinked and soluble and, therefore, readily amenable to structural characterisation using methods such as nmr and ir spectroscopy. In addition to characterising the nature of the adduct, the possible occurrence of side reactions involving rubber isomerization or degradation by the catalyst used is also examined. The aim of this part of

the work is to optimise conditions for high yield of adduct accompanied by minimal degradation or otherwise undesirable side-effects.

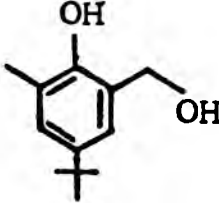
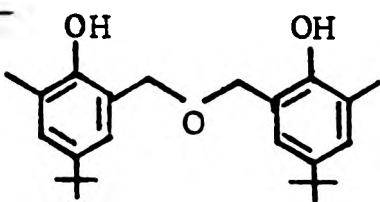
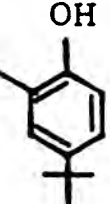
In the later stages of the study, the monofunctional p/f model is replaced by bi-functional compounds, so that the reaction product is a crosslinked network (i.e., a vulcanizate). The extent of crosslinking, measured by physical methods, is compared with that expected on the basis of the earlier kinetic and mechanistic studies. The possible occurrence of phase separation of resinous components is investigated in relation to its influence on the vulcanization process, and on the physical properties of the vulcanizate. The general aims of this later part of the work is to establish p/f structural requirements and reaction conditions for efficient vulcanization, whilst providing information enabling concurrent side reactions or phase separation processes to be understood and, possibly, controlled.

#### 1.4 Glossary and Nomenclature

For the various compounds, both the IUPAC\* nomenclature and the commonly-used name for each (as appears in most of the literature referred to) are presented in the following glossary. However, since even the "common" names are rather cumbersome and difficult to follow, each substance has been designated a concise abbreviated name, and this designation is used in the remainder of the text.

\*International Union of Pure and Applied Chemistry.

In addition, a condensed version of the structural formulae is given and this representation is used throughout.

NUMBER	STRUCTURAL FORMULA	NOMENCLATURE
IV		(a) I.U.P.A.C. (b) Common (c) Abbreviated  (a) (5-(1,1-dimethylethyl)-2-hydroxy-3-methylphenyl) methanol (b) 2-hydroxy-3-methyl-5-tert-butyl-benzyl alcohol (c) The methylolphenol
V		(a) 4,4'-Bis(1,1-dimethylethyl)-6,6'-dimethyl-2,2'-(oxydimethylene) diphenol (b) Di-(2-hydroxy-3-methyl-5-tert-butyl-benzyl)-ether (c) The dibenzyl ether
XXVI		(a) 4-(1,1-dimethylethyl)-2-methyl-phenol (b) 2-methyl-4-tert-butyl-phenol (c) The original phenol

NUMBER

STRUCTURAL  
FORMULA

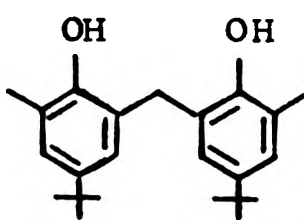
NOMENCLATURE

(a) I.U.P.A.C.

(b) Common

(c) Abbreviated

XXVII

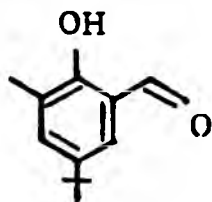


(a) 4,4'-Bis(1,1-dimethyl-ethyl)-6,6'-dimethyl-2,2'-methylene-diphenol

(b) Di-(2-hydroxy-3-methyl-5-tert-butyl-phenyl)-methane

(c) The diphenylmethene

XXVIII

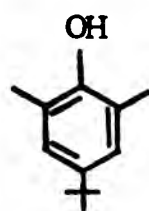


(a) 5-(1,1-dimethylethyl)-2-hydroxy-3-methyl-benzenecarbaldehyde

(b) 2-hydroxy-3-methyl-5-tert-butyl-benzaldehyde

(c) The benzaldehyde

XXIX

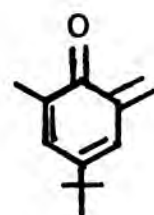


(a) 4-(1,1-dimethyl ethyl)-2,6-dimethyl-phenol

(b) 2:6-dimethyl-4-tert-butylphenol

(c) The dimethylphenol

XXX



(a) 4-(1,1-dimethyl ethyl)-2-methyl-6-methylene-cyclohexa-2,4-dienone

(b) 3-methyl-5-tert-butyl-quinone-(2)-methide

(c) The quinone methide

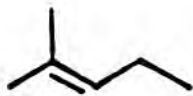
NUMBER

STRUCTURAL  
FORMULA

NOMENCLATURE

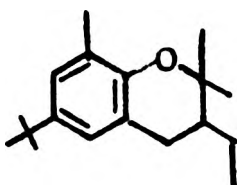
- (a) I.U.P.A.C.  
(b) Common  
(c) Abbreviated

XXXI



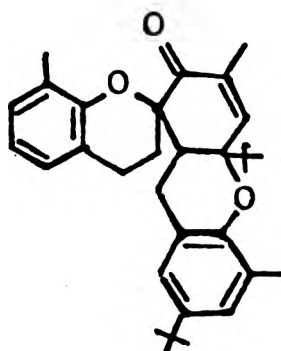
- (a) 2-methylpent-2-ene  
(b) As (a)  
(c) The alk-2-ene

XXXII



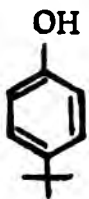
- (a) 6-(1,1-dimethyl ethyl)-  
3-ethyl-2,2,8-trimethyl-  
chroman  
(b) Not reported in the  
literature  
(c) The chroman

XXXIII



- (a) 4a,6'7-tris(1,1-dimethyl-  
ethyl)-3,5,8'-trimethyl-  
1,2,4a,9a-tetrahydro-  
xanthen-2-one-1-spiro-  
2'-chroman  
(b) Trimeric 3-methyl-5-  
tert-butylquinone-(2)-  
methide  
(c) The trimer

LVIII



- (a) 4-(1,1-dimethylethyl)  
phenol  
(b) 4-tertiary butyl phenol  
(c) tert-butyl phenol

NUMBER

STRUCTURAL  
FORMULA

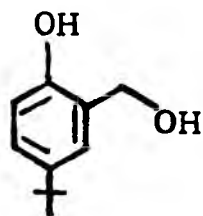
NOMENCLATURE

(a) I.U.P.A.C.

(b) Common

(c) Abbreviated

LIX

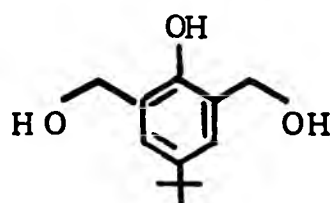


(a) 2-methylol-4(1,1-dimethyl-ethyl)phenol

(b) 2-methylol-4-tert-butyl phenol

(c) The monomethylolphenol

LX

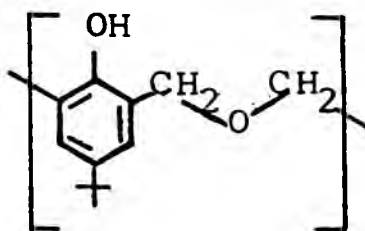


(a) 2,6-dimethylol-4(1,1-dimethylethyl)phenol

(b) 2,6-dimethylol-4-tert-butyl phenol

(c) The dimethylolphenol

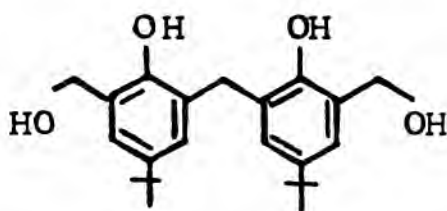
LXI



(c) The polybenzylether

(a) 6,6-bis dimethylol 4,4-bis(1,1-dimethylethyl)-2,2'-methylene diphenol

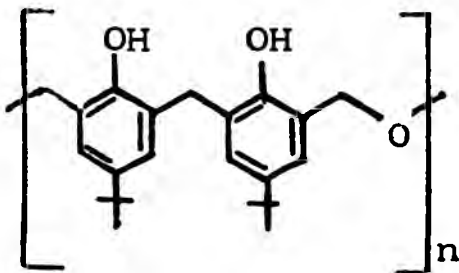
LXII



(b) D'-(2-hydroxy-4-tert-butyl-6-methylol-phenyl) methane

(c) The dimethylol diphenyl methane

LXIII



(c) Ether derivative of the dimethylol diphenyl methane

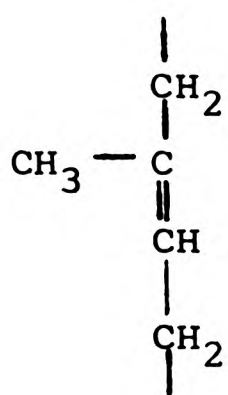
NUMBER

STRUCTURAL  
FORMULA

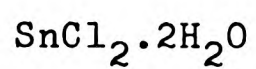
NOMENCLATURE

- (a) I.U.P.A.C.  
(b) Common  
(c) Abbreviated

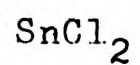
LXIV



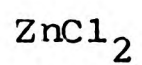
- (a) Cis-1,4 polyisoprene  
(b) Cis-1,4-polyisoprene  
(c) Isoprene rubber



- (a) Tin(II) chloride-2-water  
(b) Stannous chloride  
dihydrate



- (a) Tin(II) chloride  
(b) Stannous chloride



- (a) Zinc(II) chloride  
(b) Zinc chloride

2. INTERACTION OF TIN(II) CHLORIDE. TIN(II) CHLORIDE  
DIHYDRATE AND ZINC CHLORIDE WITH SYNTHETIC POLYISOPRENE  
RUBBER

2.1 Purpose of This Study

The purpose of this study was to investigate whether the catalyst itself is able to induce any chemical changes in the rubber, before using it to catalyse the phenol-formaldehyde-rubber reaction.

It is well known that natural rubber (NR), when treated at 60 to 80°C with strong acids such as  $H_2SO_4$ , Lewis acids such as  $SnCl_4$ ,  $BF_3$ ,  $TiCl_4$ ,  $FeCl_3$ , or by irradiation with uv light at 25-110°C undergoes progressive resinification with the formation of so-called cyclized rubber.<sup>76</sup> Synthetic polyisoprenes (IR) also undergo cyclization quite readily.<sup>54</sup> Cis/trans isomerization of polyisoprenes has been reported to result from Lewis acid treatment (hexachlorostannic(IV) acid, titanium(IV) chloride, phosphorus oxychloride and others). Isomerization of the alk-2-ene(XLVII) by  $SnCl_2 \cdot 2H_2O$ , to an equimolar mixture of alk-2-ene and alk-1-ene(XLVIII) has been reported.<sup>11</sup>

Therefore, the possible occurrence of these reactions and/or other chemical changes induced by the Lewis acid catalysts to be used in the later parts of this study was investigated.

## 2.2 Reagents

Although NR is of greater industrial interest, it was decided to use synthetic high-cis-1,4 polyisoprene because of its higher chemical purity, lack of gel content and reproducibility. The rubber selected was grade IP60 (Europren, Italy), stated to be 97% cis 1,4-polyisoprene, with Mooney viscosity (ML4 100°C) of 60, and 0.25 phr of a phenolic antioxidant (2,6-di-tert-butyl-4-methyl phenol) as the only additive.

The Lewis acids tin(II) chloride,  $\text{SnCl}_2$ , tin(II) chloride dihydrate,  $\text{SnCl}_2 \cdot 2\text{H}_2\text{O}$  and zinc(II) chloride,  $\text{ZnCl}_2$ , were examined as catalysts because of their industrial interest and their use in other studies with which comparison may be necessary.

## 2.3 Reaction Conditions and Procedure

The amount of tin(II) chloride catalyst employed was 1 part by weight per hundred parts of rubber (1.0 phr). Tin(II) chloride dihydrate was used in greater weight ratio (1.19 phr), so as to contain the same weight of tin. Thus, the results reveal the effects of the same amount of transition metal but in different coordination states (discussed fully later in 2.11e). The amount of zinc(II) chloride used (0.73 phr) was so as to contain the same atomic proportion of zinc as that of tin, again to enable comparisons to be made on a molar basis. This proportion of catalyst is lower

than that (2-4 phr) used in vulcanization of unsaturated rubbers with p/f condensates and was selected to resemble those to be used later for studies of the catalysed interaction of polyisoprenes with p/f condensate "models".

The interaction between the synthetic polyisoprene(IR) and each catalyst was examined in bulk, after first mixing the materials on a two-roll mill. Samples were placed between two thin (0.1 mm) sheets of an inert film of fluoroethylene-propylene copolymer (FEP) (a tetrafluoroethylene-hexafluoropropylene copolymer) and pressed between metal plates for various times at 160°C (detailed in the Experimental Section). The conditions and method were chosen for their similarity to those used in industry in catalysed vulcanization of unsaturated rubbers with p/f condensates. The IR was not extracted before reaction with catalyst, since the phenolic antioxidant was considered unlikely to react with the catalysts in a way which might interfere with subsequent reaction with methylol phenol compounds.

#### 2.4 Characterisation of Products

The products of interaction between IR and each catalyst were acetone extracted and stored in the dark in vacuo. They are referred to below as products IR/SnCl<sub>2</sub>, IR/SnCl<sub>2</sub>·2H<sub>2</sub>O and IR/ZnCl<sub>2</sub>, respectively. Solubility tests in toluene showed that whereas gel content is hardly detectable in product IR/SnCl<sub>2</sub>, and is absent in product IR/ZnCl<sub>2</sub>, it is present in appreciable amount in IR/SnCl<sub>2</sub>·2H<sub>2</sub>O

after about 45 min. of reaction time. Since spectroscopy(ir) showed that the sol is very similar to the gel, it was assumed that the chemical micro-structure of the sol and gel fractions were substantially the same. The gel was therefore discarded for characterisation purposes, but this does of course limit the value of viscosity measurements on the sol.

Each product was examined at various reaction times in respect of the following characteristics:

(a) Total unsaturation

A number of methods for determination of overall unsaturation in rubbers have been used by different workers (see later discussion). In this work the Wijs-Kemp method using iodine chloride (detailed in the Experimental Chapter) was used.

In the absence of extensive crosslinking, a loss of total unsaturation can be interpreted only in terms of cyclization.

(b) Types of unsaturation

The possible occurrence of cyclization, cis/trans isomerization and double bond shifts was examined by infra-red(ir) and by nuclear magnetic resonance(nmr) spectroscopy.

Infra-red spectra were obtained of films cast from

toluene solution on sodium chloride discs. The progress of reaction was monitored by measuring the intensity of bands attributable to double bonds relative to one due to methyl groups (at 7.3  $\mu\text{m}$ ).

Nuclear magnetic resonance spectroscopy(nmr) was used to monitor the progress of reaction by measuring total tri-alkyl ethylenic unsaturation, relative proportions of cis-trisubstituted and trans-trisubstituted double bonds, and 1,1 dialkyl ethylenic unsaturation.

The nmr spectra of IR/SnCl<sub>2</sub> and IR/ZnCl<sub>2</sub> products were obtained using 5% w/v solution in C<sub>6</sub>D<sub>6</sub> (98%). However, satisfactory spectra could not be obtained from IR/SnCl<sub>2</sub>·2H<sub>2</sub>O products after 45 min. of reaction time, because of the gel content.

(c) Glass-transition temperature

Differential scanning calorimetry(dsc) was used for determining the glass transition temperature(T<sub>g</sub>)(detailed in the Experimental Chapter). Although cis/trans inter-conversion and double-bond shifts are not expected to produce appreciable T<sub>g</sub> change, large changes are anticipated from cyclization, so that T<sub>g</sub> should be a sensitive measure of the occurrence of cyclization.

(d) Molecular weight changes and gel content

The possible occurrence of molecular weight changes in the interaction products IR/SnCl<sub>2</sub>, IR/SnCl<sub>2</sub>·2H<sub>2</sub>O and IR/ZnCl<sub>2</sub> was examined by measuring the intrinsic viscosity  $[\eta]_{c=0}$  in a 'suspended level dilution viscometer' (detailed in the Experimental Chapter) previously discarding the gel where present. Viscosity measurements were not carried out in products IR/SnCl<sub>2</sub>·2H<sub>2</sub>O after 45 min. of reaction time because of the large gel content (~60%).

The sol/gel ratio was measured in all products IR/SnCl<sub>2</sub> and IR/SnCl<sub>2</sub>·2H<sub>2</sub>O (detailed in the Experimental Chapter). Degree of swelling was not determined since the amount of swelling was very high and samples could not be handled.

An increase in viscosity and/or presence of gel content can be interpreted in terms of branching or crosslinking, whereas a decrease in viscosity would indicate degradation, i.e., chain scission.

Each of the above methods are considered in detail in Sections 2.6-2.10, below.

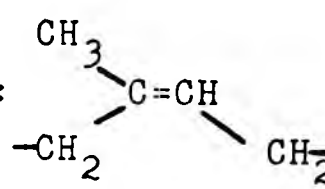
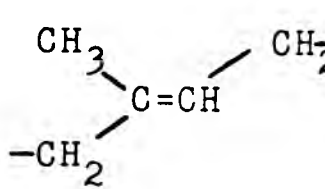
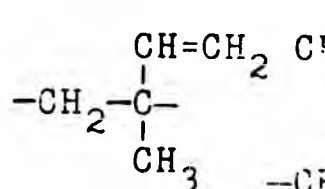
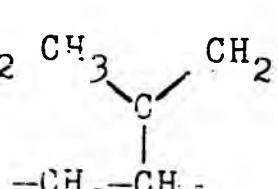
## 2.5 Possible Structures and Types of Unsaturation

Although the mechanisms for the various possible reactions have not yet been discussed, it is necessary at this stage to present some possible structures arising

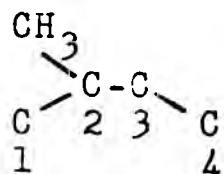
(a) in the original rubber, (b) in acyclic products of isomerization of the rubber and (c) in cyclic products of isomerization ("cyclization"). It is emphasised that the structures presented are not an exhaustive list, and further possibilities will be presented later. However, it is necessary to present these structures now for the purpose of interpreting ir and nmr results, below.

(a) Structures present in the original IR

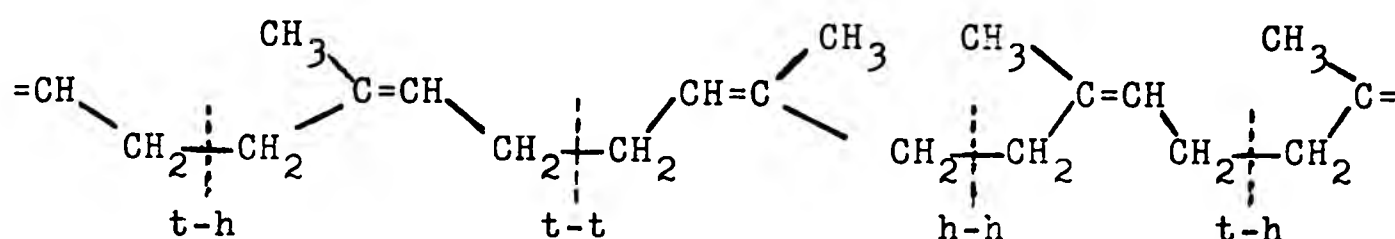
Although the rubber is stated to be 97% cis 1,4 (structure LXIV), no information is given by the manufacturer about the remaining 3%. It is assumed, however, that this consists of the other possible isomers (structures LXV, LXVI and LXVII).

Structure:				
No:	LXIV	LXV	LXVI	LXVII
Type of addition:	cis 1,4	trans 1,4	1,2	3,4
Position of un-saturation:	Δ-2,3 cis	Δ-2,3 trans	Δ-3,4	Δ-1,2
Type of un-saturation:	trialkyl ethylene	trialkyl ethylene	vinyl	1,1-dialkyl ethylene

The system of numbering is based on the 'isoprene' unit



The above units are probably linked mainly in a head-to-tail fashion. However, head-head and tail,tail enchainments are also possible, and will almost certainly be present where 1,4 addition has occurred (e.g., structure LXVIII).



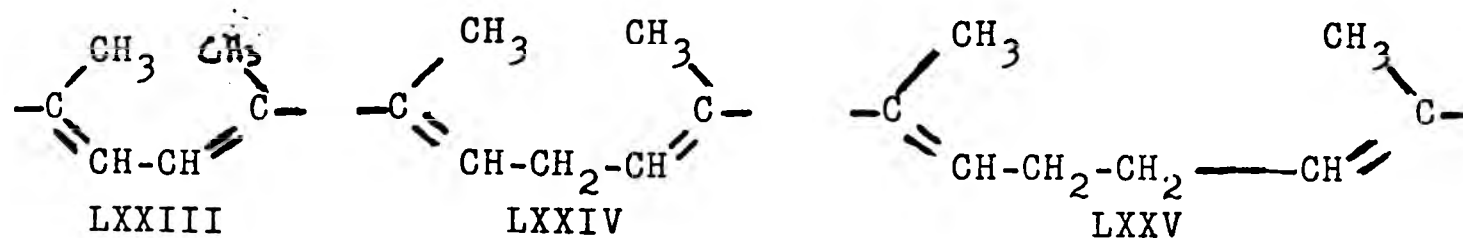
LXVIII

(b) Possible acyclic new structures arising by isomerization of cis-1,4 units

Structures LXIX-LXXI arise from double bond shifting about the 2-carbon atoms. Structure LXXII is referred to later in the text.

Structure:	$\begin{array}{c} \text{CH}_3 \\ \diagdown \\ \text{CH}=\text{C} \\ \diagup \\ \text{CH}_2-\text{CH}_2 \end{array}$	$\begin{array}{c} \text{CH}_2-\text{CH}_2 \\ \diagdown \\ \text{CH}=\text{C} \\ \diagup \\ \text{CH}_3 \end{array}$	$\begin{array}{c} \text{CH}_2 \\ \diagdown \\ \text{C}=\text{CH} \\ \diagup \\ \text{CH}_2-\text{CH}_2 \end{array}$	$\begin{array}{c} \text{CH}_2 \\    \\ \text{CH} \\   \\ \text{CH} \end{array}$
No:	LXIX	LXX	LXXI	LXXII
Unsaturation position:	$\Delta$ -1,2 cis	$\Delta$ -1,2 trans	$\Delta$ -2(exo)	
Unsaturation type:	trialkyl ethylene	trialkyl ethylene	1,1-dialkyl ethylene	vinyl

Double-bond shifting around head-head units, head-tail units and tail-tail units would be expected to produce some 1,3-diene (conjugation)(LXXIII), 1,4 diene (LXXIV) and 1,5 diene (LXXV), respectively.



(c) Possible cyclic new structures arising by intramolecular double-bond addition (cyclization) of the head-tail linked cis-1,4 structure LXIV.

(Condensed formulae are used for clarity of presentation)

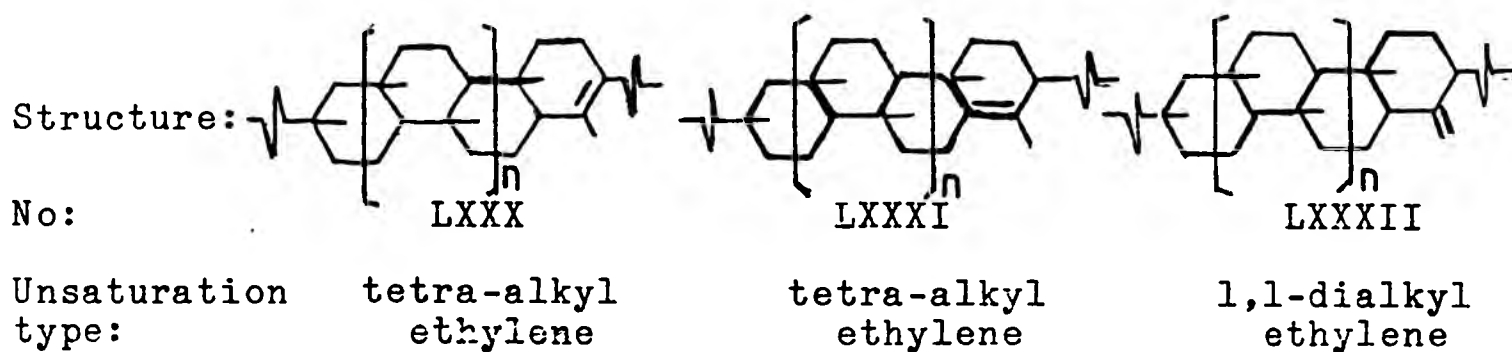
(i) Monocyclic

Cyclization involving 2 adjacent isoprene units can give structures LXXVI-LXXVIII. Structure LXXIX is referred to in the following sections.

Structure:				
No:	LXXVI	LXXVII	LXXVIII	LXXIX
Unsaturation position:	$\Delta$ -6,7	$\Delta$ -5,6	$\Delta$ -6(exo)	
Unsaturation type:	tetra-alkyl ethylene	trialkyl ethylene	1,1-dialkyl ethylene	(1-alkyl 2-dialkyl cyclopropane)

(ii) Polycyclic

Cyclization involving >2 consecutive isoprene units can give the structures LXXX-LXXXII, which have terminating double-bond types not including trialkylethylene. In these structures, the bicyclic case is given by  $n=0$ , tricyclic  $n=1.5$ , tetracyclic  $n=1$ , etc.



Although there is a theoretical possibility of cis-trans isomerism in structures LXXVI, LXXVII, LXXX and LXXI, it seems unlikely that more than one geometric isomer will be present.

## 2.6 Total Unsaturation

### (a) Measurement of total unsaturation

A number of methods have been used for the determination of total unsaturation, and hence estimate the degree of cyclization in cyclized rubber. Some of the reagents used were iodine chloride, ozone, perbenzoic acid and hydrogen chloride. Whilst the residual unsaturation of the cyclized rubber may be used as an accurate measure of the degree of cyclization, there has not been agreement amongst the various earlier workers on a reliable chemical method to measure it.

Some authors<sup>60</sup> have considered perbenzoic acid to be the most satisfactory reagent in determination of residual unsaturation at high degrees of cyclization, whereas others favour the hydrochlorination of double bonds.<sup>90</sup> These authors all claimed that with cyclized rubber iodine chloride reacts via a substitution as well as an addition process, probably associated with the existence of labile tertiary hydrogens atoms in cyclized rubber. Other authors<sup>91</sup> point out that although the perbenzoic acid method works well on cyclized dihydromyrcene, it remains to be established whether or not it is quantitative for a cyclized high molecular weight compound. They used iodine chloride and reported good agreement between the results and those obtained by nmr spectroscopy.<sup>77</sup> Under the aerobic conditions used in the present study no completely cyclized rubber could be obtained (supported by the persistence of the 12  $\mu\text{m}$  band in ir and 4.65  $\tau$  in nmr) and prolonged (>6 h) heating at 160°C led to oxidized products. Nevertheless the determination of residual unsaturation (iodine monochloride) showed that some disappearance of trisubstituted ethylenic double bonds must have occurred. The iodine monochloride method was considered best in the present work since it mainly involves low degrees of cyclization.

(b) Present study

Results obtained in this present study using the Wijs-Kemp method are detailed in the Experimental Chapter. They are summarised in Fig. 9 in graphical form, showing changes in total unsaturation as reaction proceeds.

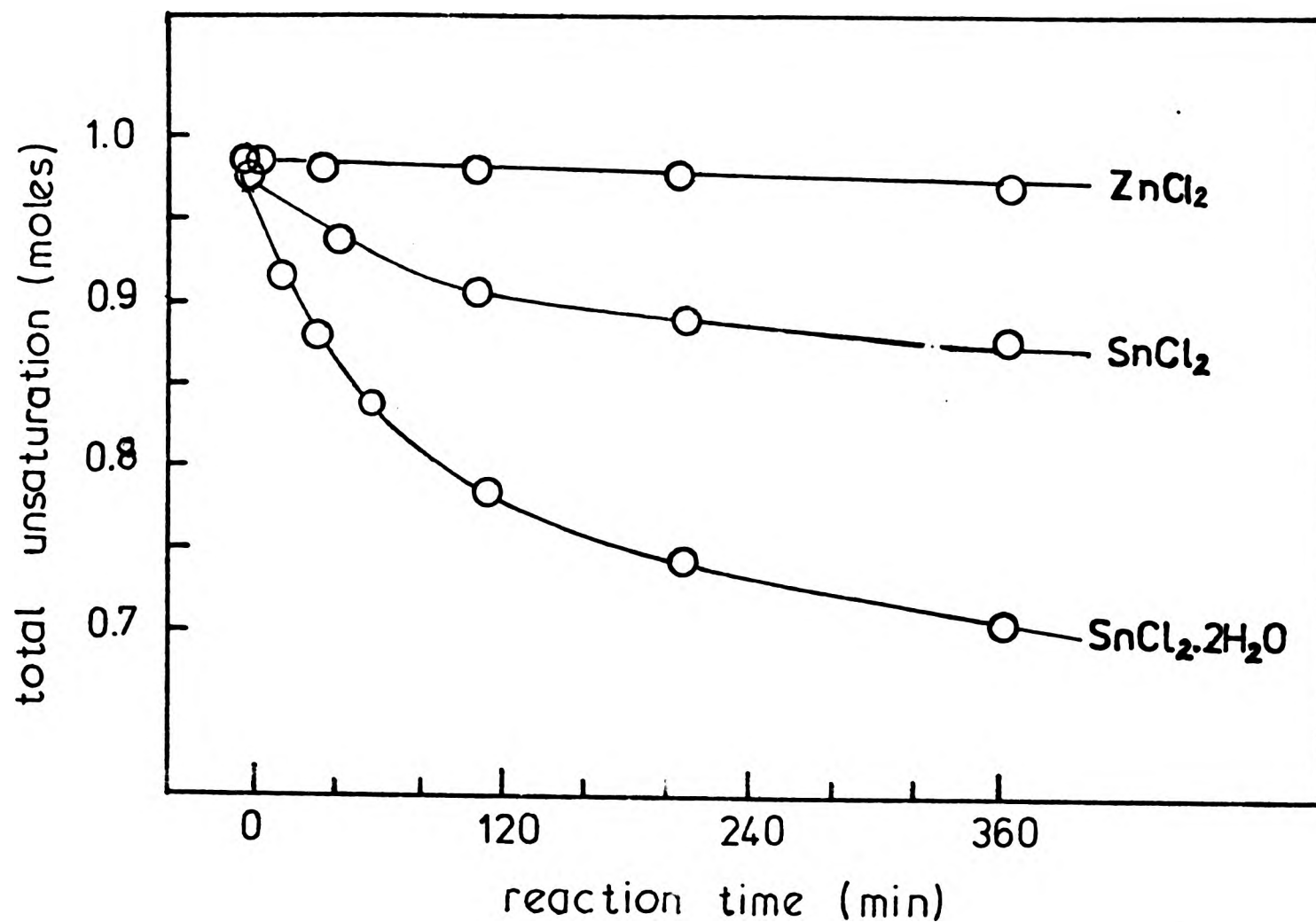


Fig. 9 Changes in total unsaturation with reaction time for IR heated at 160°C with different catalysts.

These results would appear to indicate that cyclization is occurring at a faster rate with  $\text{SnCl}_2 \cdot 2\text{H}_2\text{O}$  than with  $\text{SnCl}_2$ , and to a negligible extent with  $\text{ZnCl}_2$ . As an example, values taken from the graph after 300 min (5 hrs) heating suggest that approx. 29% of the original isoprene units are involved in cyclization using  $\text{SnCl}_2 \cdot 2\text{H}_2\text{O}$ , compared with only 13% in the case of  $\text{SnCl}_2$ .

## 2.7 Infra-red Spectroscopy

### (a) Earlier ir studies

Cis/trans isomerization of polyisoprenes under the influence of agents which can reversibly add to or complex with double bonds such as sulphur dioxide, thiol acids<sup>52,53</sup> or selenium<sup>81</sup> has been studied by ir spectroscopy. Spectral changes are, however, minimal since the main trialkyl ethylenic unsaturation LXIV and/or LXV is not affected. Evidence for cis/trans isomerization in these studies is based on the fact that NR and Balata (trans 1,4 polyisoprene, unit structure LXV) yield products with the same ir spectra after treatment with those agents. However, the evidence for cis/trans isomerization after treatment of NR or Balata by Lewis acids such as titanium tetrachloride,  $TiCl_4$ , or organometallic compounds is inconclusive. Isomerization of NR by these agents ( $TiCl_4$  or organometallic compounds) has been concluded<sup>32-34</sup> from changes in the 12  $\mu m$  band (associated with the cis or trans-1,4 units LXIV and LXV). However, other authors<sup>77</sup> have seriously questioned these studies and they pointed out that although a decrease in this band could indicate cis/trans isomerization (the extinction coefficient of the trans 1,4 unit LXV is approximately 60% of that of the corresponding cis 1,4 unit LXIV), it could also signify loss of the original double bonds through cyclization.<sup>77</sup> On the contrary, they report cyclization but no cis/trans isomerization in the reaction of NR and Balata with  $TiCl_4$  in benzene at 80°C. An additional feature of the ir spectrum of the fully cyclized

polyisoprenes was the occurrence of bands at 6.1 and 11.3  $\mu\text{m}$ . The band at 6.1  $\mu\text{m}$  was tentatively assigned to a C=C stretching vibration and the 11.3  $\mu\text{m}$  band to a skeletal vibration in an external double bond such as an exomethylene group. In that work the ir spectrum of Balata showed that the latter band develops, whereas it decreases somewhat in the spectrum of IR. Also, it is reported that this band was found in cyclized NR. On these grounds, the presence of some cyclized structures such as LXXVIII were suggested.

Cis/trans isomerization accompanied by cyclization giving rise to cyclopropyl groups (e.g., structure LXXIX) was reported,<sup>30</sup> when cis- and trans-polyisoprenes (natural or synthetic) were irradiated with uv light. The changes observed in ir were (i) a decrease in intensity of the 12  $\mu\text{m}$  band (cis or trans trialkyl ethylene), (ii) the development of a strong band at 11.3  $\mu\text{m}$  (1,1-dialkyl ethylene) and another band at 11.0  $\mu\text{m}$  (vinyl units), and (iii) an accompanying decrease in the 6.0  $\mu\text{m}$  band and growth of the 6.1  $\mu\text{m}$  band (C=C stretching vibration of internal and external double bonds respectively). In addition to the occurrence of cis/trans isomerization (confirmed by nmr), these observations suggested that some of the trialkyl-ethylene unsaturation was becoming involved in isomerization reactions in which it was replaced by vinylidene ( $\text{RR}'\text{C}=\text{CH}_2$ ) and Vinyl ( $\text{RCH}=\text{CH}_2$ ) unsaturation. Free radical mechanisms were proposed for this and for the cyclopropyl group formation.

Other studies of cyclization<sup>54,60,78</sup> also report a decrease in intensity and ultimate disappearance of the 12  $\mu\text{m}$  band (trialkylethylene), and a reduction in intensity of the 6.0  $\mu\text{m}$  band (C=C), 11.3  $\mu\text{m}$  band (1,1 dialkylethylene) and various bands in the 7.5-10.0  $\mu\text{m}$  region which change slightly with different isomeric forms. Complete elimination of the 11.3  $\mu\text{m}$  band and the associated band at 6.1  $\mu\text{m}$  has been reported in cyclization of 3,4 polyisoprenes.<sup>77-79</sup>

(b) Results in the present study

(i)  $\text{SnCl}_2$  as catalyst

Infrared spectra of IR before and after heating at 160°C for various times with  $\text{SnCl}_2$  are presented in Fig. 10. The more important changes in the spectrum as reaction proceeds are (1) a partial reduction of the 12  $\mu\text{m}$  band assigned to trialkylethylene unsaturation  $\text{RC}(\text{CH}_3)=\text{CHR}'$ , (2) an increase in intensity of the 11.3  $\mu\text{m}$  band assigned to 1,1 dialkylethylenes  $\text{RRC}=\text{CH}_2$ , (3) the development of a band at 6.1  $\mu\text{m}$  assigned to C=C stretching vibrations mainly of 1,1 dialkylethylenic double bonds, (4) alteration of the intensity and shape to the 7.5-9.0  $\mu\text{m}$  bands associated with various isomeric forms of polyisoprene and (5) a very slight reduction in intensity of the 6.0  $\mu\text{m}$  band assigned to C=C stretching vibration in 1,2-dialkyl and trialkyl substituted double bonds. These observations would appear to indicate that the major processes involved in the IR/ $\text{SnCl}_2$  interaction for up to 6 h of heating are cis/trans isomerization (for which there

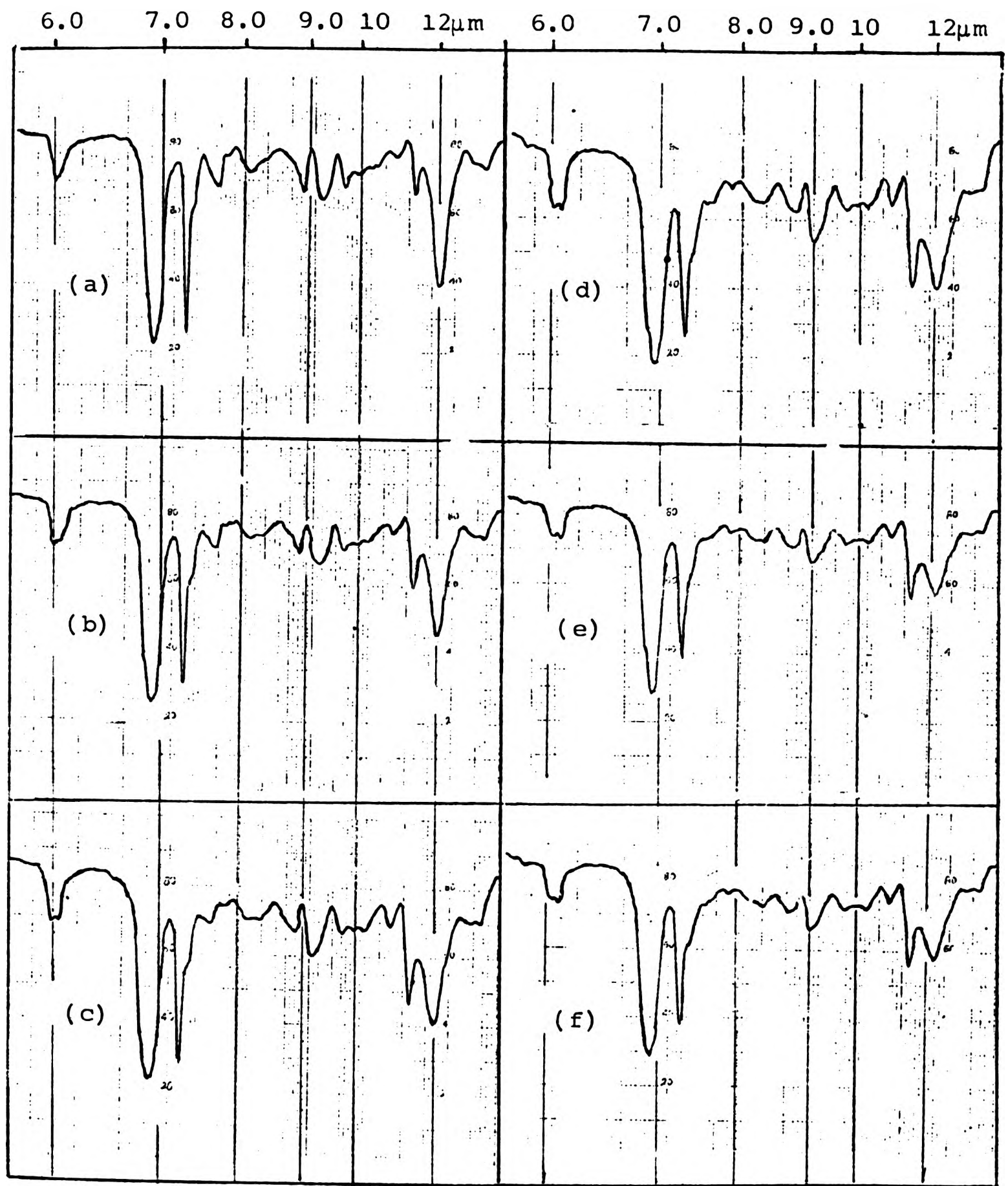


Fig. 10 Infra-red spectra of  $\text{IR/SnCl}_2$  products heated at  $160^\circ\text{C}$  for various times. (a) 0 min; (b) 15 min; (c) 45 min; (d) 120 min; (e) 210 min; (f) 360 min.

is ample nmr confirmation) and additional isomerization involving double bond shifts from trialkyl- to 1,1-dialkyl-substituted. Cyclization would appear to be unimportant since the overall unsaturation remains high. Some reduction in intensity of the 12  $\mu\text{m}$  band is to be expected due to the fact that the absorption coefficient of the trans 1,4 units (e.g., structure LXV) is only 0.625 times that of the corresponding cis unit (e.g., structure LXIV)<sup>81</sup> and also due to replacement of the 1,4 units (cis or trans) in fact, by 1,1-dialkylethylene double bonds. It may be noted that some 1,1-dialkylethylene unsaturation (3,4 addition, structure LXVII) is present in the original polymer, as seen by absorptions at 11.3  $\mu\text{m}$  and (slight) at 6.1  $\mu\text{m}$ . The reaction causes an increase in intensity of both peaks. The new 1,1-alkylethylene double bonds resulting from IR/ $\text{SnCl}_2$  interaction are, however, more likely to be in the form of structure LXXI which arises by double bond shift from the original trialkylethylene double bonds through a cationic mechanism in the Markownikof sense (see the Discussion Section). It is also possible that the new unsaturation is present in cyclized structures such as LXXXII<sup>77</sup> or in terminal double bonds (e.g., structure LXXII formed by a cationic mechanism.<sup>80</sup> Since the degree of cyclization must be very low (later evidence will confirm this) and a radical mechanism is unlikely with  $\text{SnCl}_2$ , such structures are considered much less likely than structure LXXI.

(ii)  $\text{SnCl}_2 \cdot 2\text{H}_2\text{O}$  as catalyst

Infra-red spectra of products IR/ $\text{SnCl}_2 \cdot 2\text{H}_2\text{O}$  after heating at  $160^\circ\text{C}$  for various times are presented in Fig. 11. The most pronounced changes in the ir spectrum are (1) a sharp decrease in the  $12 \mu\text{m}$  band (2) an accompanying decrease in the  $6.0 \mu\text{m}$  band and (3) the nearly total disappearance of the  $7.6$  and  $8.9 \mu\text{m}$  bands. An increase in intensity of the  $11.3$  and  $6.1 \mu\text{m}$  bands is observed in the early stages of reaction (up to 15 min), but these bands then remain approximately constant during the remaining time of reaction. These facts might signify that cyclization, cis/trans isomerization (for which again there is ample nmr confirmation) and probably double bond shifts are all present in this interaction. For the reason given earlier some of the decrease in the  $12 \mu\text{m}$  band is probably associated with cis/trans isomerization. However, in this interaction the decrease of the  $12 \mu\text{m}$  absorption is much more pronounced. This and the decrease of the band at  $6.0 \mu\text{m}$  and gradual disappearance of the  $7.6$  and  $8.9 \mu\text{m}$  bands strongly suggest that cyclization is occurring. The increase in intensity of  $11.3 \mu\text{m}$  and  $6.1 \mu\text{m}$  bands in the early stages of reaction, together with changes in the bands in the region  $8-10 \mu\text{m}$ , are very similar to the changes noted under (i) above for the IR/ $\text{SnCl}_2$  reaction. That is, in the early stages of reaction, cis/trans changes and double bond shifts to form structures of type LXXI occur. The 'vinylidene' absorption at  $11.3 \mu\text{m}$  cannot be due to exocyclic groups present in structures LXXVIII or LXXXII because very little cyclization has occurred at this stage. Furthermore, it does not increase further as cyclization proceeds.

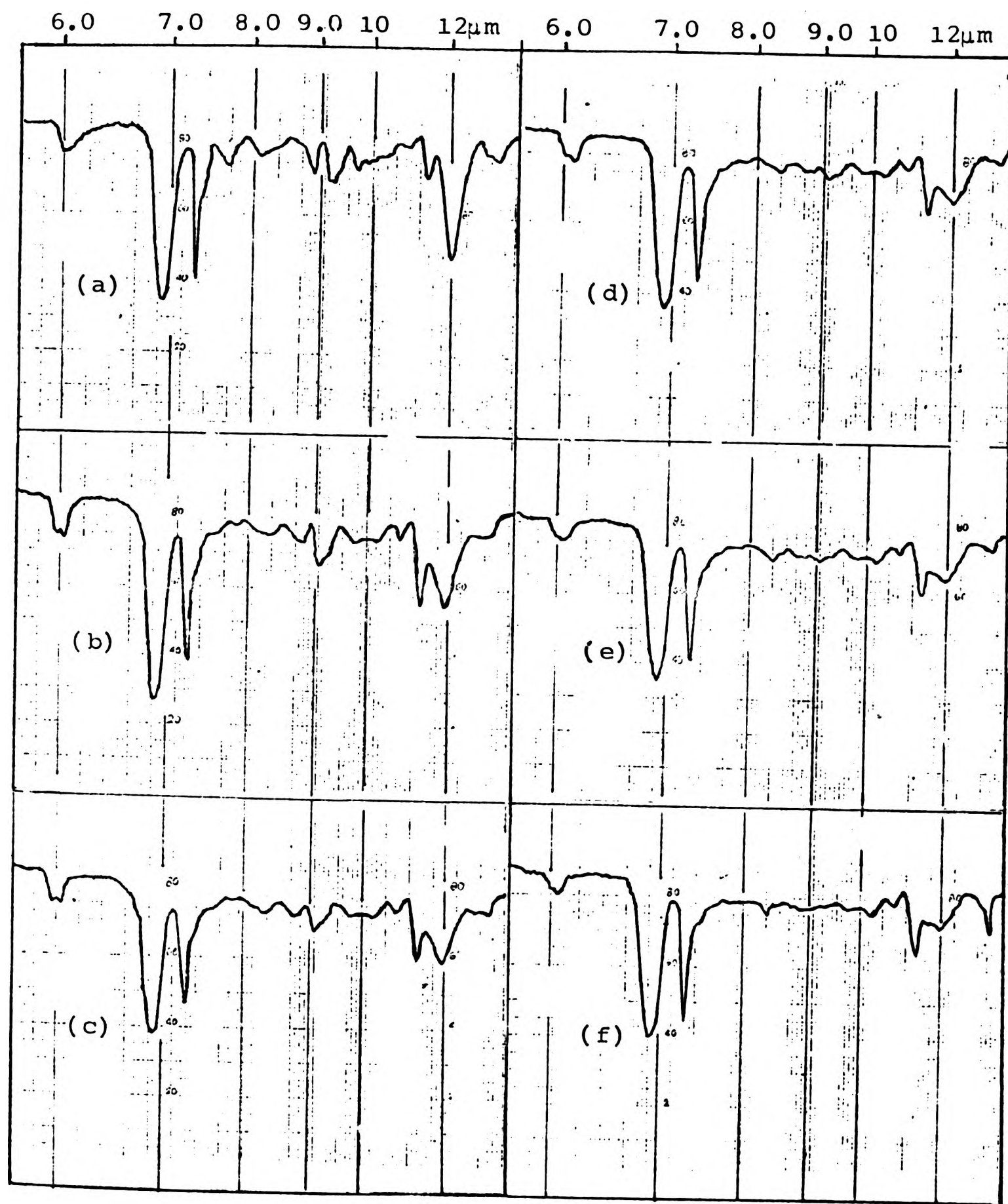


Fig. 11 Infra-red spectra of  $\text{IR/SnCl}_2 \cdot 2\text{H}_2\text{O}$  products heated at  $160^\circ\text{C}$  for various times, (a) 0 min; (b) 15 min; (c) 45 min; (d) 120 min; (e) 210 min; (f) 360 min.

(iii) Interaction of IR with  $\text{ZnCl}_2$

Infra-red spectra of IR/ $\text{ZnCl}_2$  interaction products after heating at  $160^\circ\text{C}$  for various times are presented in Fig. 12. In these spectra no change suggesting cis/trans isomerization, double bond shifts or cyclization could be observed and, indeed, no difference is detectable between these spectra and that of the original IR. Therefore, these results would appear to indicate that there is no reaction between IR and  $\text{ZnCl}_2$  under the conditions used.

(c) Quantitative analysis of ir spectra

It is not possible to derive absolute values for double-bond concentrations in the absence of reference samples, preferably polymers of known cis-1,4, trans-1,4, 1,2- and 3,4 unit contents. Since absolute values can be obtained from nmr spectra more accurately and without such a limitation, it was decided to concentrate on nmr for measurement of double-bond concentrations.

Nevertheless, it is possible to illustrate the loss of trialkylethylenic unsaturation by a plot of absorbance(A) ratio  $A_{12.0}/A_{7.3}$  (i.e., trialkylethylenic absorbance/methyl absorbance) against reaction time (Fig. 13).

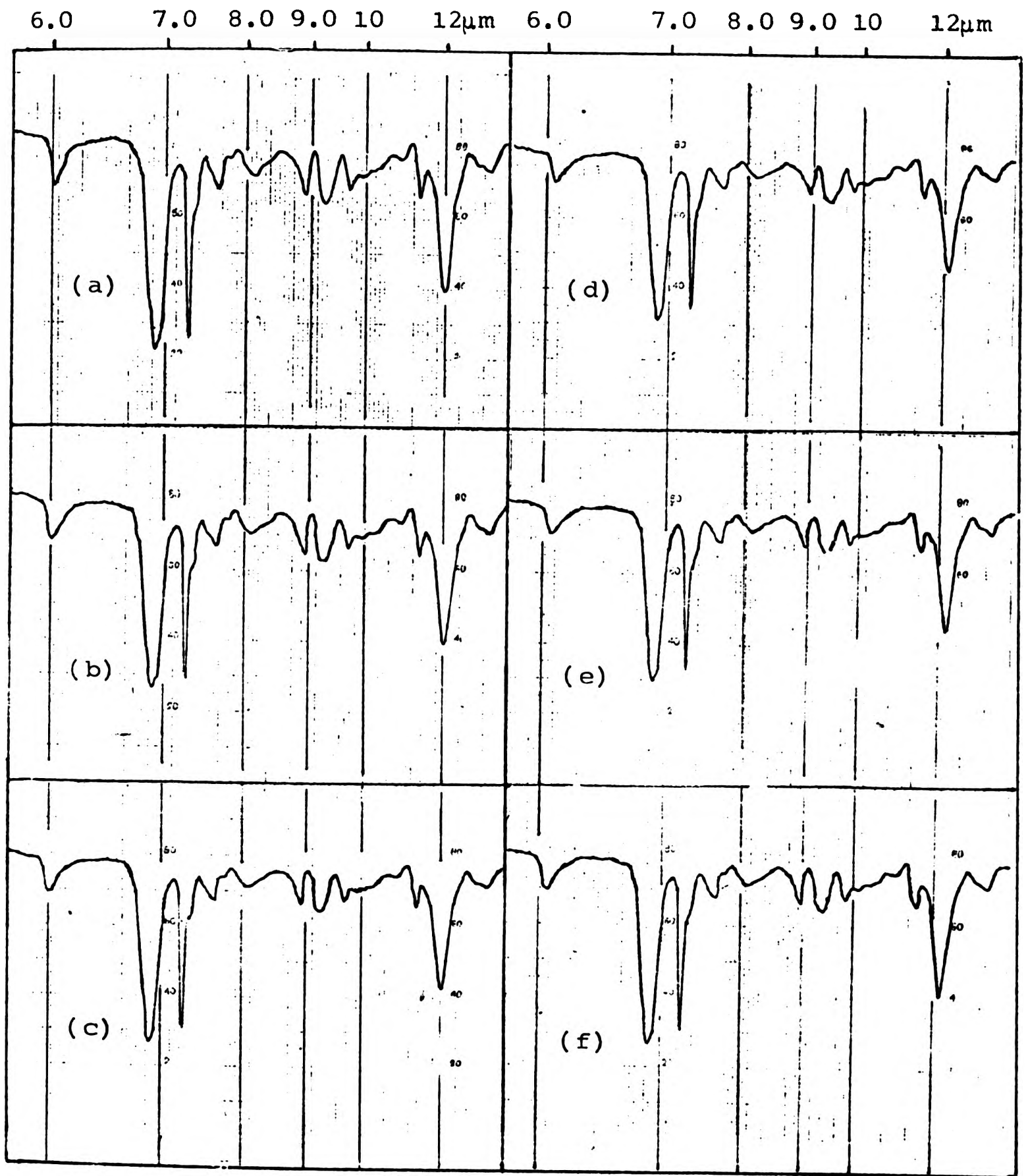


Fig. 12 Infra-red spectra of IR/ZnCl<sub>2</sub> products heated at 160°C for various times: (a) 0 min; (b) 15 min; (c) 45 min; (d) 120 min; (e) 210 min; (f) 360 min.

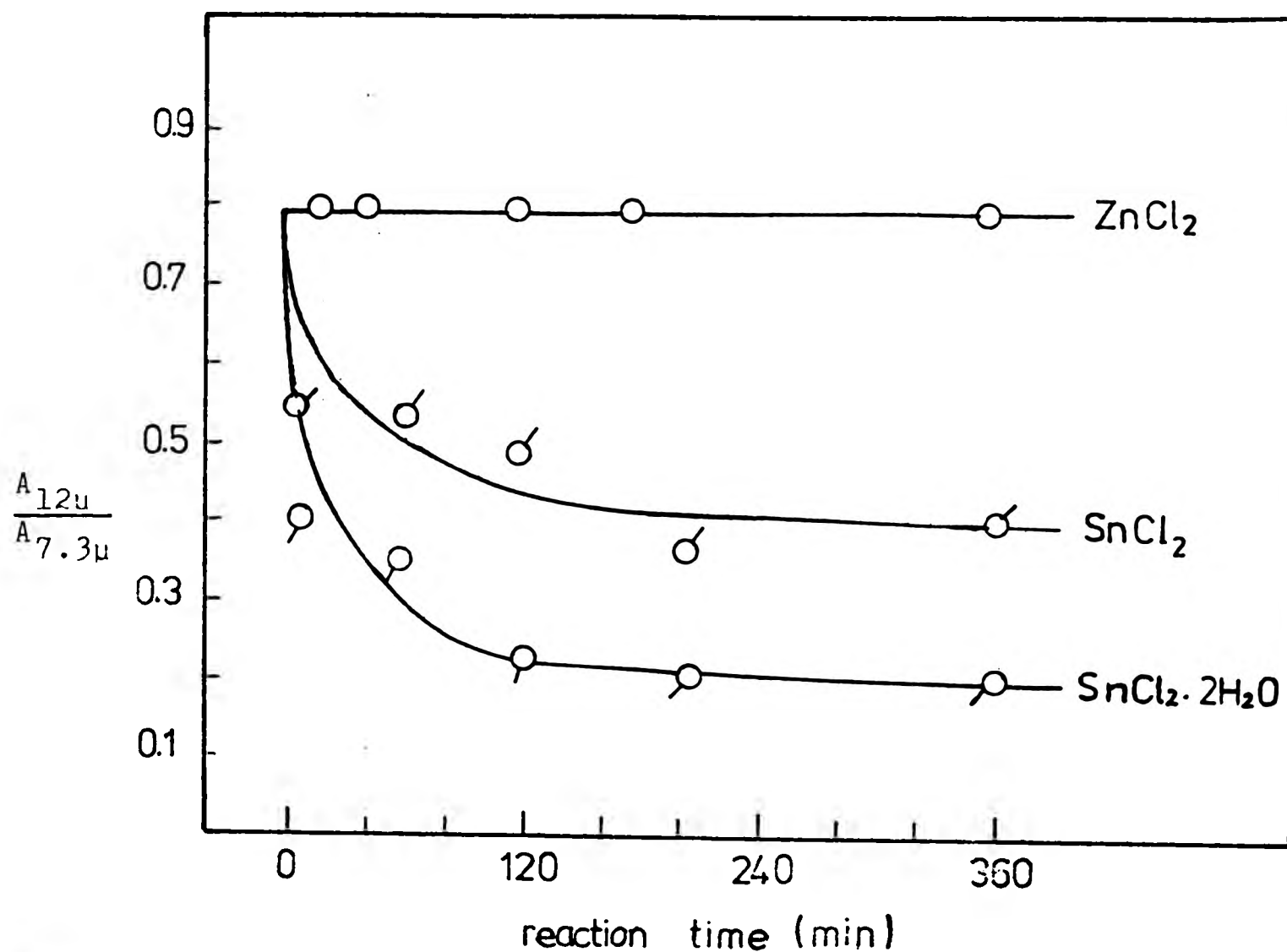


Fig. 13 Illustration of loss of trialkylethylenic unsaturation with time, using ratio of absorbance (A) of infra-red bands at 12.0 and 7.3  $\mu$ .

## 2.8 Nuclear Magnetic Resonance (nmr) Spectroscopy

### (a) Earlier nmr studies

Resonances due to methyl protons in cis- and trans-1,4 polyisoprenes (structures LXIV and LXV) are well separated in the nmr spectrum, especially in benzene solution when they occur at 8.21 and 8.35 $\tau$ , respectively. The positions of the methylene and vinylene proton resonances are insensitive to geometric isomerism about the double bond and appear at 7.90-7.97 and 4.80 $\tau$  respectively.<sup>86</sup> Measurements of cis/trans ratio by measuring the relative area of the cis and trans

methyl resonances is complicated by the resonance of the methyl protons of the 3,4 polyisoprene structure LXVII (if present) which is coincident with that of the trans-1,4 (LXV) methyl protons. This difficulty can be resolved by analysis of the resonances in the  $5\tau$  region;<sup>87</sup> the resonance at  $5.25\tau$ , due to vinylene protons in 3,4-units (LXVII), is well separated from the other isomeric structures (vinyl protons in 1,2 units appear at  $5.05\tau$ ) and is therefore well suited to the determination of the 3,4 isomer content. When the 3,4 content has been determined in this way, it is then possible to determine the trans-1,4- content from the methyl resonance at  $8.35\tau$ .

Several authors have employed nmr to demonstrate the occurrence of cyclization and/or cis/trans isomerization of NR and Balata,<sup>77,80</sup> synthetic cis-1,4 polyisoprene<sup>77,78,88</sup> and synthetic 3,4 polyisoprene.<sup>77,88</sup> An outstanding feature of the nmr spectra of all highly cyclized polyisoprenes is the extensive overlapping of resonance peaks throughout the 7 to  $10\tau$  region. This has been attributed to the presence in the cyclic structure of a variety of non-equivalent methylene groups with different chemical shifts. Despite the obvious complexity of these spectra two prominent peaks stand out at about  $8.4$  and  $9.1\tau$ , corresponding to protons on methyl groups attached to olefinic and saturated carbon atoms, respectively.<sup>77</sup> The nmr spectrum of the partially-cyclized product of photolysis of NR, in which cis/trans isomerization is also present, shows resonances at  $5.35$ ,  $8.75$  and  $9.04\tau$  in addition to those characteristic of cis and trans polyisoprenes

(at 8.21 and 8.35 $\tau$  respectively).<sup>80</sup> These resonances were assigned to  $\text{>C=CH}_2$ ,  $-\text{CH}_2-\overset{|}{\underset{|}{\text{C}}}-$  and  $\text{CH}_3-\overset{|}{\underset{|}{\text{C}}}-$  protons respectively. Two high field peaks observed at 9.60 and 10.03 $\tau$  (using benzene as internal standard) were assigned to the substituted cyclopropane structure LXXIX. In these spectra no extensive overlapping was observed, since cyclization was only partially completed. Nmr spectroscopy has been used to study cis/trans isomerization and partial cyclization in the interaction of cis-polyisoprene 3-d with sulphur dioxide.<sup>89</sup> The changes observed in the nmr spectra included the development of small peaks at 8.75 and 9.0 $\tau$  which were assigned to endocyclic methylene and methyl protons, respectively. In all of these studies, when cyclization is present, a decrease of the peak at 4.8 $\tau$  was reported, as expected due to loss of trisubstituted ethylene double bonds of the 1,4 structure (LXIV and/or LXV).

(b) Results in the present study

(i)  $\text{SnCl}_2$  as catalyst

Nmr spectra of IR/ $\text{SnCl}_2$  products after various times of reaction at 150°C are presented in Fig. 14.

In these spectra, resonances occurring in the original rubber, and persisting throughout the reaction, are seen at 4.65 $\tau$  ( $-\text{CH}=\$ ), 7.857 $\tau$  ( $-\text{CH}_2-\overset{|}{\underset{|}{\text{C}}}=\$ ), 8.25 $\tau$  (cis  $\text{CH}_3-\overset{|}{\underset{|}{\text{C}}}=\$ ) and (very weak peaks) at 8.70-9.30 $\tau$ , the latter probably being attributable to the presence of small amounts of 1,2 and 3,4

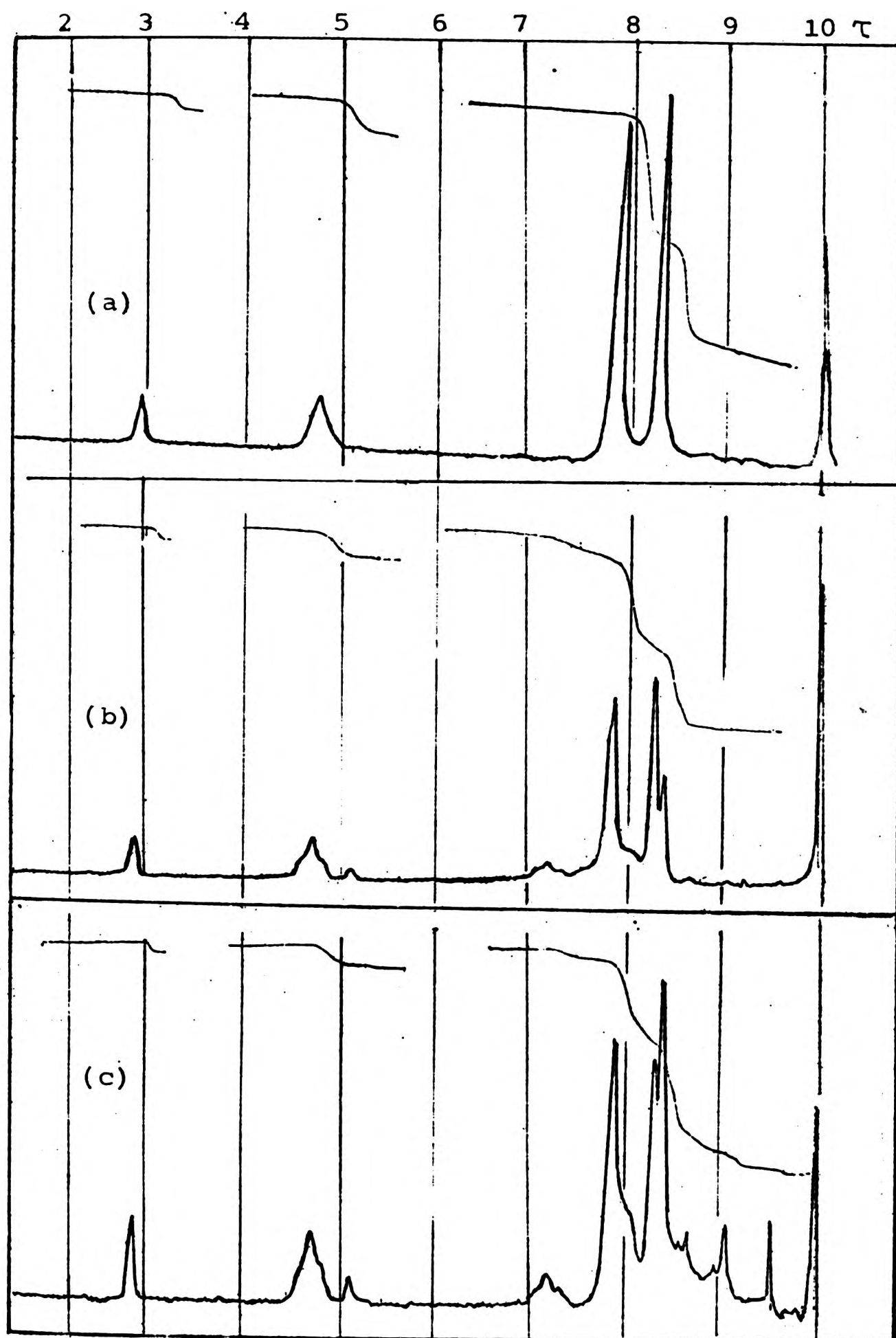


Fig. 14 Nuclear magnetic resonance spectra of IR/SnCl<sub>2</sub> products heated at 160°C for various times: (a) 0 min; (b) 45 min; (c) 360 min.

units (e.g., structures LXVI and LXVII respectively). The most pronounced change in the spectrum as reaction proceeds is the development of a new peak at 8.35 $\tau$  (which may be assigned to trans  $\text{CH}_3-\overset{|}{\text{C}}=$ ). Accompanying this change, new peaks also appear at 5.10 $\tau$ , 7.15 $\tau$ , 8.10 $\tau$  and, at later stages of reaction, at 8.65 $\tau$  and about 9.0 $\tau$ . These changes are accompanied by a slight decrease of the peak at 4.65 $\tau$  ( $-\text{CH}=\$ ). Vinyl protons in 1,2 polyisoprene units and vinylidene protons in 3,4 polyisoprene units (structures LXVI and LXVII) are reported to appear at 5.05 $\tau$  and 5.25 $\tau$ , respectively.<sup>86</sup> The peak at 5.10 $\tau$  in this work might reasonably be assigned to the vinylidene protons in 1,1 disubstituted ethylenes (e.g., structure LXXI) since the chemical environment of such protons would be expected to differ slightly from that of the vinyl and vinylidene protons in 3,4 or 1,2 polyisoprene units (structures LXVII and LXVI). Peaks at 8.10, 8.65 and 9.00 $\tau$  could be assigned to  $\text{CH}_3-\overset{||}{\text{C}}-$ ,  $-\text{CH}_2-\overset{|}{\text{C}}-$  and  $\text{CH}_3-\overset{|}{\text{C}}-$  protons, respectively, present in cyclized structures such as LXXVI where all these protons are represented. However, the small area of these latter peaks and that at 5.10 $\tau$ , together with the fact that only a slight decrease of the peak at 4.65 $\tau$  (assigned to original 1,4 double bonds) is observed, suggest that cyclization is not a prominent process in this interaction. The main processes operating would therefore appear to be cis/trans isomerization and some double-bond shifting to 1,1 disubstituted ethylene form (e.g., structure LXXI). It is important to note, however, that nmr will not distinguish between

structures LXIV and LXIX, or between LXV and LXX. Thus, much more double-bond shifting than is apparent may be occurring. Indeed, the resonance at 7.15 $\tau$ , assigned to methylene protons in structure LXXIV, supports the occurrence of such shifting, and is discussed more fully later.

(ii)  $\text{SnCl}_2 \cdot 2\text{H}_2\text{O}$  as catalyst

In general, the changes in the nmr spectra (Fig. 15) are the same as those described under (i) above for the IR/ $\text{SnCl}_2$  interaction, but they occur over a much shorter time scale. The spectra show new peaks at 5.10, 7.15, 8.35, 8.60 and 9.10 $\tau$  and overlapping of resonance peaks near 8 $\tau$  at heating times >15 min. Accompanying these changes is a marked reduction in the area of the peak at 4.7 $\tau$ . All these changes are consistent with the occurrence of (1) cis/trans isomerization (8.35 $\tau$ ), (2) cyclization (8.00, 8.60 and 9.1 $\tau$ ) accompanied by loss of 1,4 (cis or trans) double bonds (4.7 $\tau$ ) and (3) double bond shifts (5.10 $\tau$ ) yielding 1,1 disubstituted ethylene (e.g., structure LXXI). It should be noted that whereas this latter peak (5.1 $\tau$ ) remains nearly constant in the early stages of reaction it decreases slowly with extended reaction times (analogous to the changes noted by ir spectroscopy, above). The peak at 7.15 $\tau$  is observed to follow the same trend as that described in (i) above (see (c) in the Discussion Section). The much higher rates involved in the IR/ $\text{SnCl}_2 \cdot 2\text{H}_2\text{O}$  interaction, compared with the IR/ $\text{SnCl}_2$  interaction may be illustrated by the onset of cis/trans isomerization after

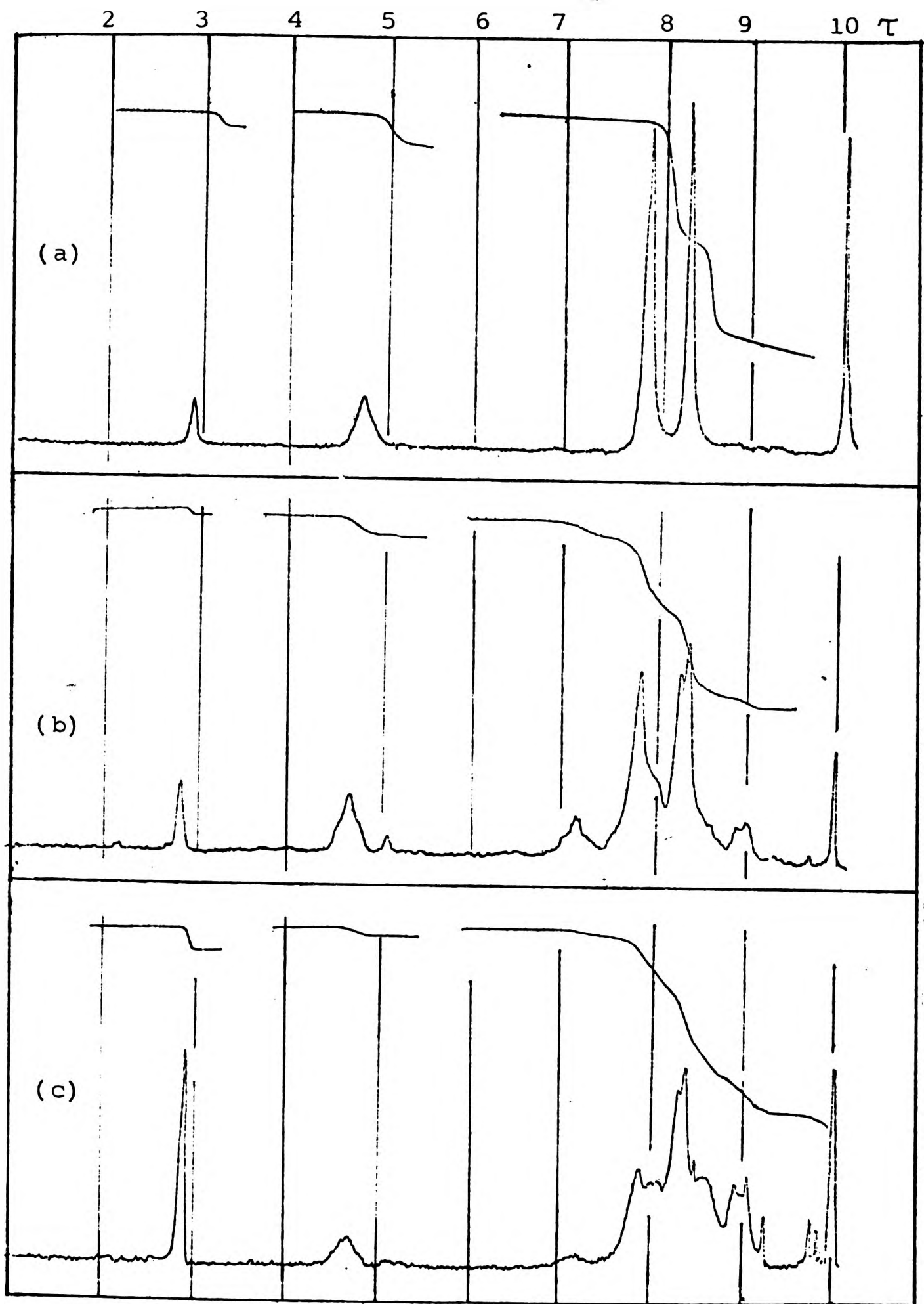


Fig. 15 Nuclear magnetic resonance spectra of  $\text{IR/SnCl}_2 \cdot 2\text{H}_2\text{O}$  products heated at  $160^\circ\text{C}$  for various times: (a) 0 min; (b) 45 min; (c) 360 min.

only ~4 min of heating. These observations would support the view that  $\text{SnCl}_2 \cdot 2\text{H}_2\text{O}$  is merely acting as a much more powerful catalyst than  $\text{SnCl}_2$ , i.e., the same changes occur with each but over a different time scale.

(iii)  $\text{ZnCl}_2$  as catalyst

Nmr spectra of IR/ $\text{ZnCl}_2$  products after heating at  $160^\circ\text{C}$  were identical after up to 360 min reaction time. Spectra of the original rubber and the 360 min product are illustrated in Fig. 16.

From this it is concluded that no isomerization of any kind is occurring.

(c) Quantitative analysis of nmr spectra

The concentration of double bonds of different types in the IR/ $\text{SnCl}_2$  and IR/ $\text{SnCl}_2 \cdot 2\text{H}_2\text{O}$  interactions were determined by nmr spectroscopy. The concentration of the residual overall trialkylethylenic unsaturation, and the 1,1 disubstituted ethylenic double bonds formed by double bond shifts were measured from the areas of the peaks at  $4.70\tau$  ( $-\text{CH}=\text{}$ ) and  $5.1\tau$  ( $\text{>C}=\text{CH}_2$ ), respectively. The concentration of the  $-\overset{|}{\text{C}}=\text{C}-\text{CH}_2-\overset{|}{\text{C}}=\text{C}-$  methylene protons was measured by the area of the peak at  $7.15\tau$ . This area should be directly proportional to the concentration of contributing protons and thus may be used to obtain the molar proportion of the corresponding structure.

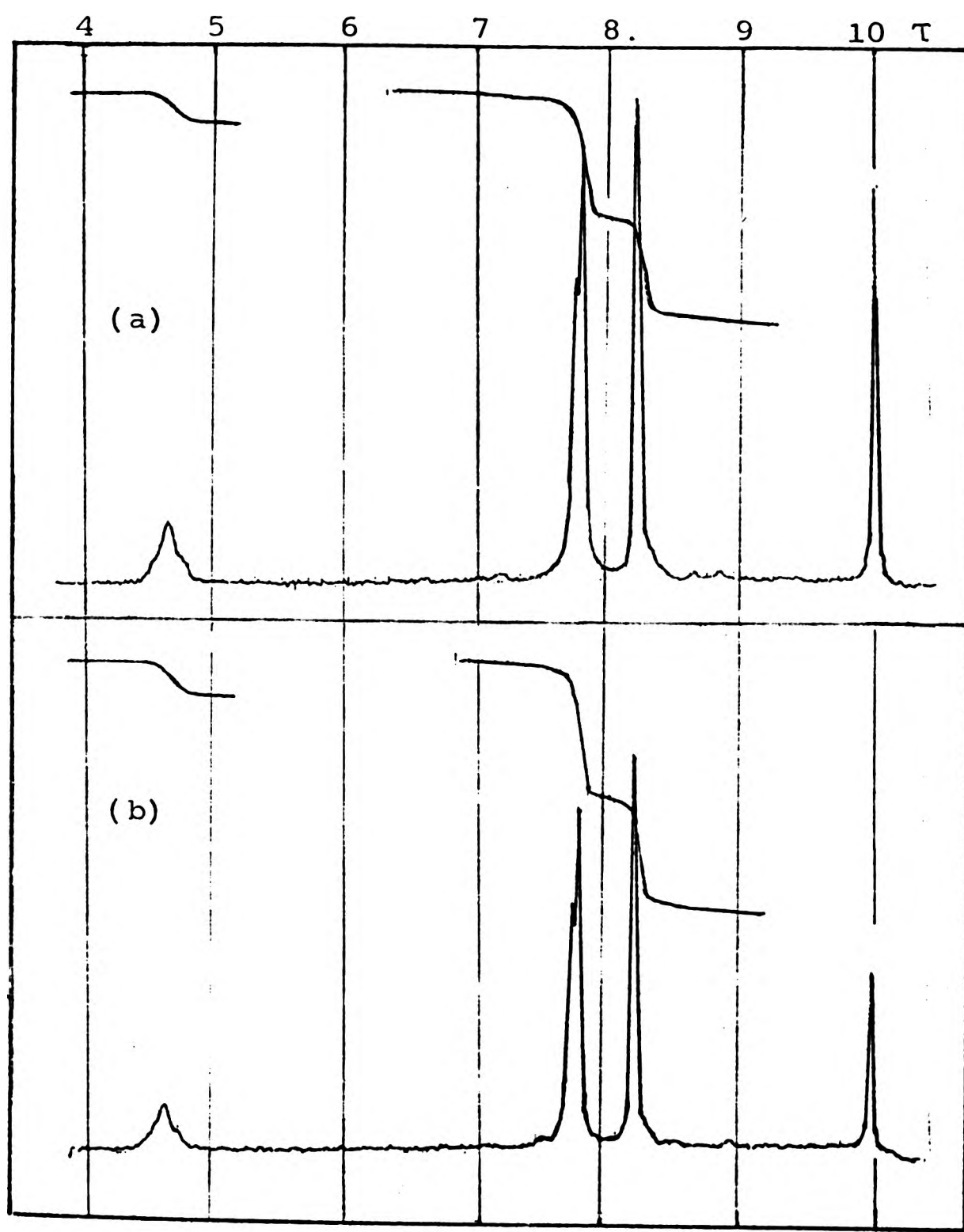


Fig. 16 Nmr spectra of IR/ZnCl<sub>2</sub> interaction products (a) unheated and (b) heated at 160°C for 360 min.

The concentration of unsaturation consumed by cyclization was obtained indirectly by the difference between the original (unreacted IR) trialkylethylenic double bond concentration and the sum of residual trialkylethylenic + 1,1 dialkylethylenic double bond concentration. From the analysis method used in this study, it seems that it is not possible to determine accurately the 'cyclicality' (see further Discussion below). Otherwise, from the protons contributing to the peak at 9.00 $\tau$  ( $\text{CH}_3-\overset{|}{\underset{|}{\text{C}}}$ ) it would be possible to determine the relative concentration of cyclized rubber and from this the molar proportion of double bonds involved in cyclization.

The cis/trans ratio was obtained from the ratio of the areas of the 8.25 and 8.35 $\tau$  peaks (cis and trans  $\text{CH}_3-\overset{|}{\text{C}}=$  respectively). In the IR/ $\text{SnCl}_2 \cdot 2\text{H}_2\text{O}$  interaction, the cis/trans ratio after 210 min of reaction time could no longer be measured because of the extensive overlapping of resonance peaks. The nmr spectrum of the unreacted IR shows very small peaks at 5.10-5.25 $\tau$  which cannot be quantitatively treated. Thus, it was not possible to make a correction for the  $\text{CH}_3-\overset{|}{\text{C}}=$  protons of 3,4 polyisoprene units present in the original IR, when the cis/trans content was determined. The cis and trans 1,4 methyl peaks are reasonably clearly resolved, but some overlapping occurs with this small 3,4-methyl resonance. Thus, in order to calculate the corresponding areas the overlapping portions of the peaks were separated by visual judgement. The area under each peak was measured both by cutting out peak areas from the chart

and weighing with an analytical balance to 0.1 mg, and by the integral curve, the height of which is a measure of the peak area.

Double bond concentrations derived from nmr are expressed as molar fractions of the total original IR unsaturation. Thus, for example, the value for trans-2,3 unsaturation (Formula LXV), originally obtained in the form of a cis/trans ratio (see Experimental Chapter and Fig. 21) from measurement of peak areas, was recalculated as a fraction of the total original (not residual) concentration and, as such, is shown in Fig. 17, and in the Experimental Chapter. This expression of results is satisfactory for the IR/SnCl<sub>2</sub> interaction mainly for products up to 45 min. of reaction time, where the amount of gel can be practically neglected. Thus, the nmr spectra are considered as reliably representing the concentration of polymer as made up. The same can be said for the IR/SnCl<sub>2</sub>.2H<sub>2</sub>O products up to 45 min. of reaction time (i.e., the amount of gel up to 45 min. of reaction time can be neglected), but not for those products after this time where >5% gel was observed. Therefore, the results expressed in this way for those products after 45 min. would be lower than the real ones, since the true solution concentration would be lower than that weighed out. However, since it is expected that the later vulcanization work will involve times of <45 min., the results as expressed in Fig. 17 are considered sufficiently reliable.

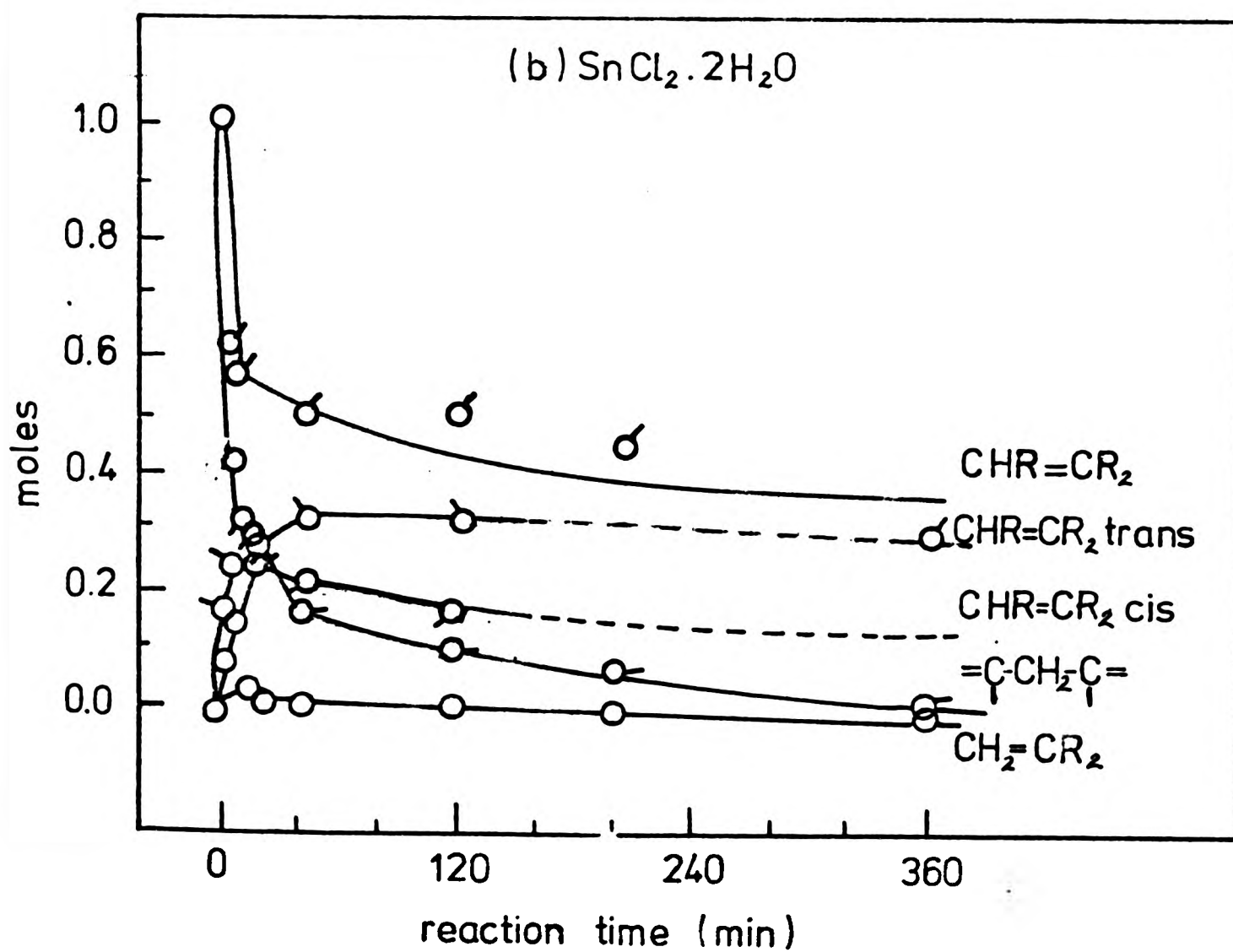
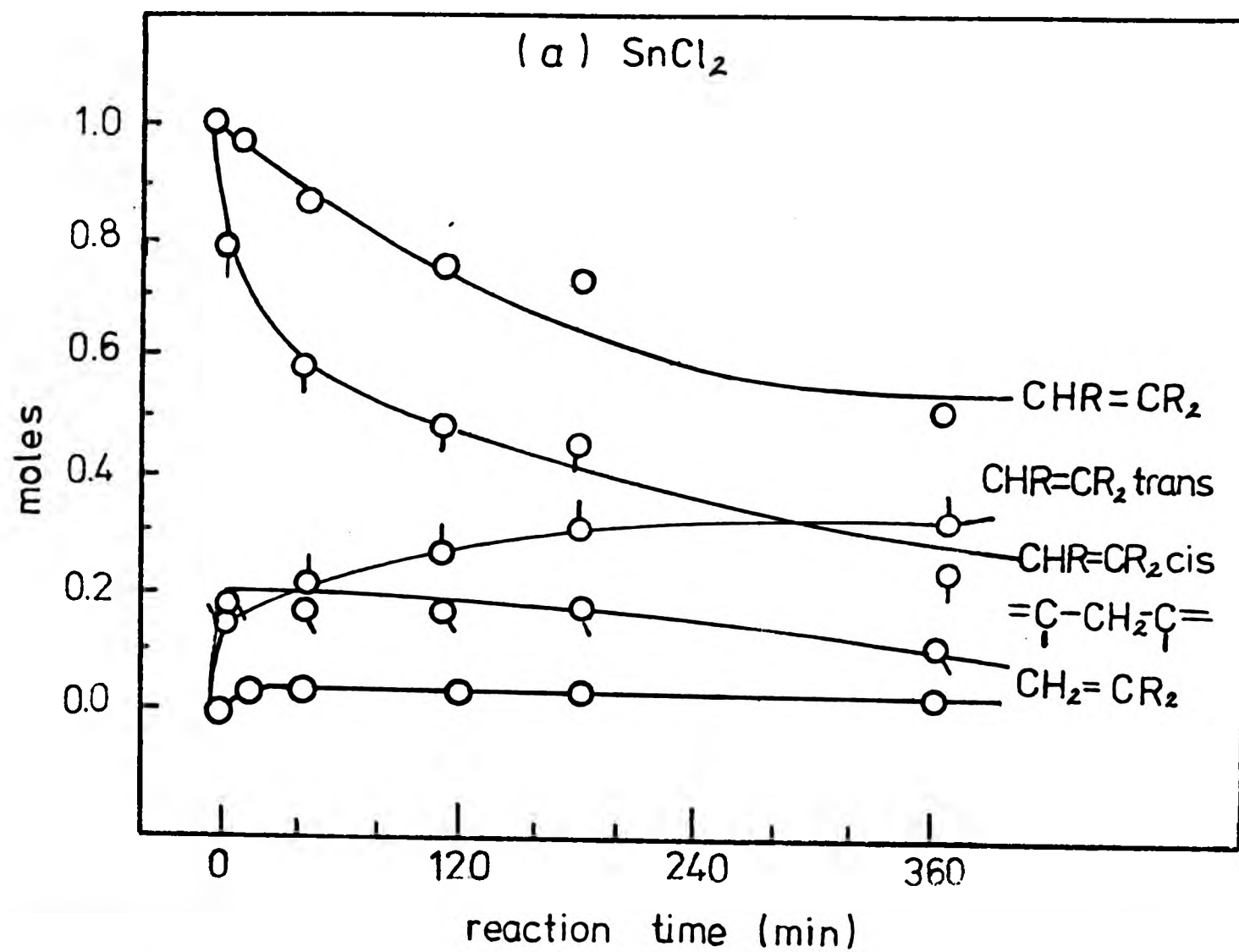


Fig. 17 Changes in type and amount of unsaturation with reaction time, as determined from nmr spectra (a) IR/ $\text{SnCl}_2$ , (b) IR/ $\text{SnCl}_2 \cdot 2\text{H}_2\text{O}$ .

## 2.9 Glass-transition Temperature

When a polymer is heated at a constant slow rate, it passes through a glass transition temperature,  $T_g$ , covering a few degrees over which there is a discontinuity in the specific volume-temperature relationship and a softening from a 'glassy' to a leathery state. This phenomenon is interpreted on a molecular basis in terms of the ability of short chain segments to obtain a greater rotational degree of freedom as they gain kinetic energy. Segmental rotations are inhibited by the presence of strong inter-chain attractions (i.e., by strongly polar groups) and by steric hindrance to rotation (i.e., by bulky groups). Thus, the main structural features determining  $T_g$  are the polarity and bulkiness of the chain structure. Features such as molecular weight (MW) and molecular weight distribution (MWD) exert negligible effect in high MW rubbers. Crosslinks may be regarded as points where there is steric hindrance to rotation and therefore produce a rise in  $T_g$ . However, the concentration of crosslinks in normal vulcanized rubbers is normally so low that this effect can be neglected.

It would be expected, therefore, that isomeric structural changes such as cis/trans interconversions and double-bond shifts would have only minor effects on  $T_g$ . Cis and trans polyisoprenes have been reported to have  $T_g$  values of 200 and 213°K respectively,<sup>92</sup> a difference which has been attributed to interference between methyl groups. However, cyclization would be expected to have a dramatic

(steric) effect and, indeed, highly cyclized rubber is glassy at room temperature. In view of these considerations, therefore, changes in  $T_g$  are likely to reflect mainly the degree of cyclization of the rubber.

Glass transition temperature ( $T_g$ ) values, as measured by differential scanning calorimetry, for the IR/SnCl<sub>2</sub>, IR/SnCl<sub>2</sub>.2H<sub>2</sub>O and IR/ZnCl<sub>2</sub> products after heating at 160°C for various times are presented in the Experimental Chapter and these values are plotted v. time in Fig. 18.  $T_g$  values follow the same general trend as was observed with the other methods of analysis used, i.e., values remain constant at 198°K (i.e., at  $T_g$  of the original IR) in the IR/ZnCl<sub>2</sub> interaction and increase faster in the IR/SnCl<sub>2</sub>.2H<sub>2</sub>O than in the IR/SnCl<sub>2</sub> interaction. These results clearly support the view that whereas cyclization is not operating in the ZnCl<sub>2</sub> case, extensive cyclization is occurring in the IR/SnCl<sub>2</sub>.2H<sub>2</sub>O interaction where a  $T_g$  increase of some 63° has occurred after 210 min. of reaction time. For the IR/SnCl<sub>2</sub> interaction,  $T_g$  increases by only 17° after 360 min. of reaction time. However, even this is believed too high to be accounted for by acyclic isomerization processes, and supports the occurrence of some cyclization, as was also concluded from the unsaturation results, discussed earlier.

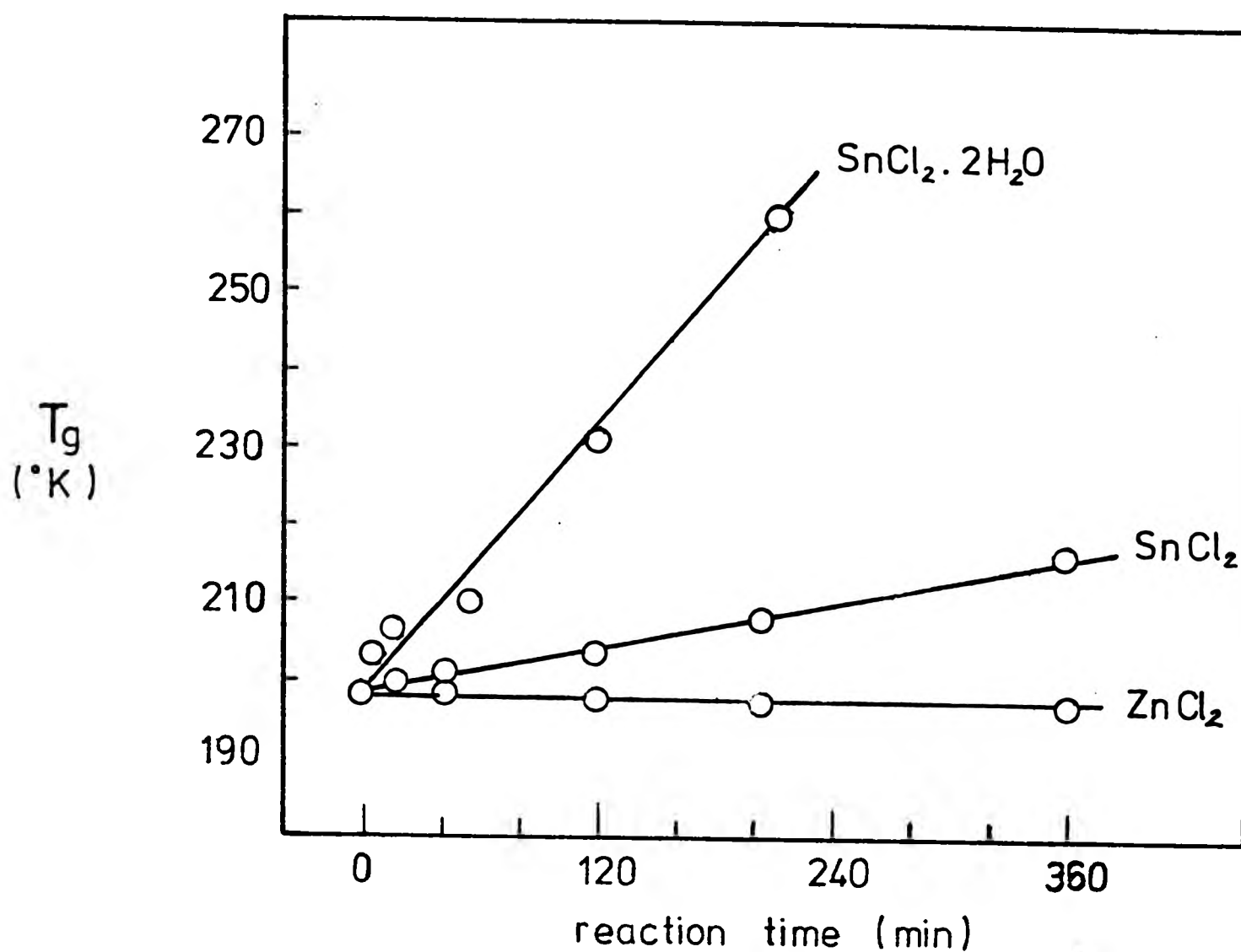


Fig. 18 Glass transition temperature,  $T_g$ , of IR heated at  $160^\circ\text{C}$  for various times with different catalysts.

#### 2.10 Molecular Weight Changes and Gel Content

Intrinsic viscosity  $(\eta)_{c=0}$  values for the IR/SnCl<sub>2</sub>, IR/SnCl<sub>2</sub>.2H<sub>2</sub>O and IR/ZnCl<sub>2</sub> products and gel contents for the IR/SnCl<sub>2</sub> and IR/SnCl<sub>2</sub>.2H<sub>2</sub>O products, after heating at  $160^\circ\text{C}$  for various times, are presented in the Experimental Chapter and plotted against reaction time in Fig. 19. These results show that, whereas the viscosity decreases somewhat in the IR/ZnCl<sub>2</sub> interaction, there is a increase in viscosity in the IR/SnCl<sub>2</sub> and IR/SnCl<sub>2</sub>.2H<sub>2</sub>O interactions. Gel content was absent in the IR/ZnCl<sub>2</sub> interaction, but was present in a small proportion (2-7%) in the IR/SnCl<sub>2</sub> interaction and in an appreciable amount

(5-70%) in the IR/SnCl<sub>2</sub>·2H<sub>2</sub>O interaction, increasing in the two latter cases with reaction time. The small decrease in viscosity in the IR/ZnCl<sub>2</sub> interaction may be attributable to the heat treatment rather than to the ZnCl<sub>2</sub> itself since the previous evidence (T<sub>g</sub> values, unsaturation, ir and nmr spectroscopy) appear to indicate that there is no reaction between IR and ZnCl<sub>2</sub>. The increase in viscosity and presence of gel content in IR/SnCl<sub>2</sub> and IR/SnCl<sub>2</sub>·2H<sub>2</sub>O indicate the formation of crosslinks, which clearly form at much higher rates in the IR/SnCl<sub>2</sub>·2H<sub>2</sub>O than in the IR/SnCl<sub>2</sub> interaction. However, despite the considerable proportion of gel observed in the IR/SnCl<sub>2</sub>·2H<sub>2</sub>O products the degree of swelling observed in both cases for those samples heated for times corresponding to normal vulcanization times was very high, and the swollen gels were very difficult to handle without breaking. This suggests that the number of crosslinks present are probably not very significant when compared with the degree of crosslinking produced in vulcanization of IR by p/f resins. A possible crosslinking mechanism will be suggested in later discussion.

## 2.11 Discussion

### (a) Total unsaturation

Total residual unsaturation, as calculated from Iodine values and from nmr measurements, was expressed as a molar fraction of the total original unsaturation. From nmr spectroscopy values for total residual unsaturation were

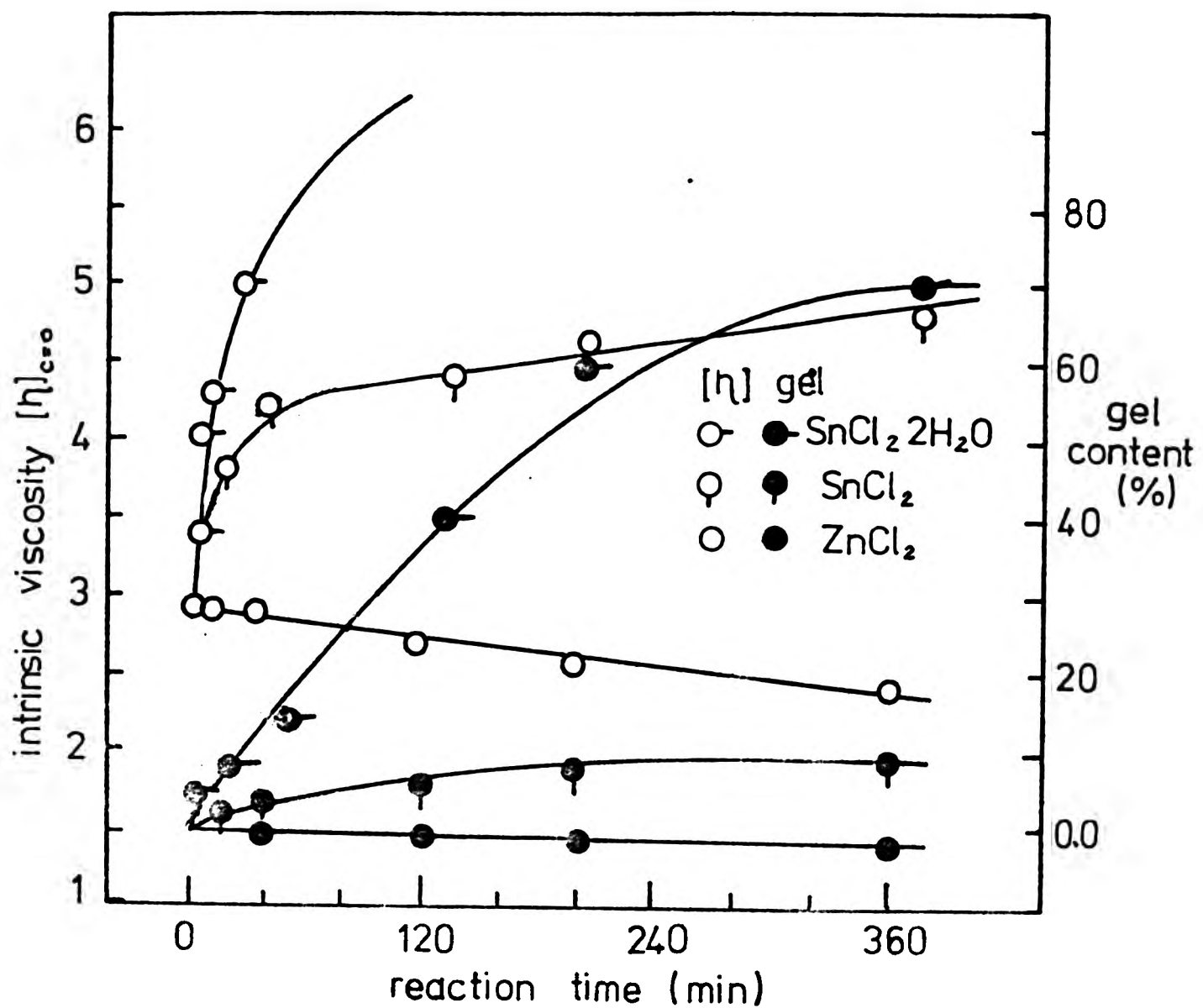


Fig. 19 Intrinsic viscosity (O) and gel content (●) for the IR/ $\text{SnCl}_2$ ; IR/ $\text{SnCl}_2 \cdot 2\text{H}_2\text{O}$  and IR/ $\text{ZnCl}_2$  interaction products.

calculated assuming the cyclicity to be one (i.e., monocyclic structures). There is some nmr evidence (see Discussion below) to support this assumption. Furthermore, it is assumed that the one double bond left after the formation of each ring is a tetraalkylethylene, a not unreasonable assumption since trialkylethylenic unsaturation eventually disappears completely with cyclization. The molar fraction of total residual unsaturation as measured by nmr is therefore taken to be equal to the sum of the

molar fractions of residual trisubstituted ethylene, 1,1 disubstituted ethylene and one half of the unsaturation consumed by cyclization.

A comparison of 'total unsaturation' as given by the Iodine monochloride and nmr methods is illustrated in Fig.20. Agreement is reasonable considering the reservations which have been expressed about both methods. Loss of unsaturation is approx. seven times more rapid in the  $\text{SnCl}_2 \cdot 2\text{H}_2\text{O}$  case than in the  $\text{SnCl}_2$  case.

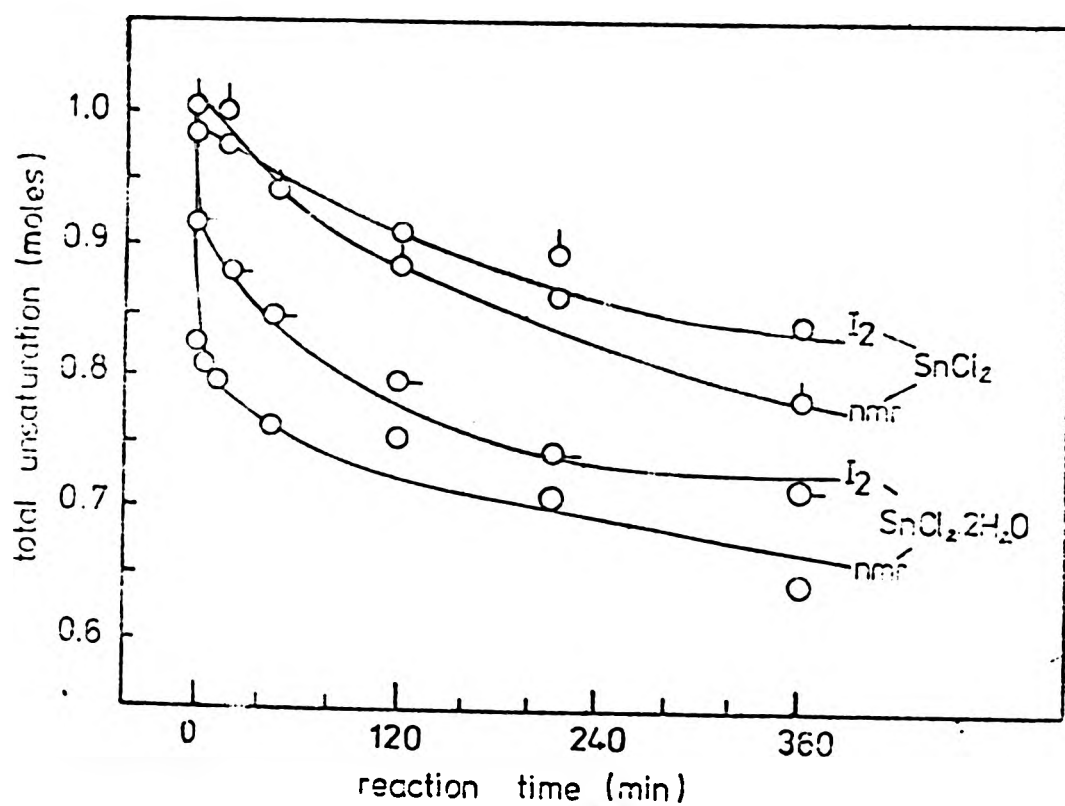


Fig. 20 Comparison of Iodine method and nmr method for total unsaturation.

(b) Cis/trans isomerization

From the nmr spectroscopy results (see Fig. 17) obtained in the present work it has been established that cis/trans isomerization is occurring in the interaction of IR with the Lewis acids catalysts,  $\text{SnCl}_2$  and  $\text{SnCl}_2 \cdot 2\text{H}_2\text{O}$ , but it

does not occur in the interaction of IR with  $\text{ZnCl}_2$  catalyst. The results show that cis/trans isomerization occurs some 7 times more rapidly with  $\text{SnCl}_2 \cdot 2\text{H}_2\text{O}$  catalyst than with  $\text{SnCl}_2$ .

In both interactions cis/trans isomerization is clearly a much faster process than cyclization. The rate of isomerization observed with both Lewis acids (see Fig. 17) is unexpectedly high when compared with work previously reported using other cis/trans isomerization agents. In the cis/trans isomerization of polyisoprenes under the influence of such agents as sulphur dioxide or thiol acids in anaerobic conditions at  $140-160^\circ\text{C}$ <sup>52,53,89</sup> or with ultraviolet light,<sup>80</sup> cis/trans ratios of 43/57 after 24 hr<sup>52,53</sup> of reaction (measured by ir spectroscopy), 53/47 in 5-8 hr<sup>89</sup> (measured by nmr spectroscopy) and 80/20 in 50 hr<sup>80</sup> (measured by nmr spectroscopy) have been reported. In the present study ratios of 76/24 and 47/53 after 45 min of reaction were obtained in IR/ $\text{SnCl}_2$  and IR/ $\text{SnCl}_2 \cdot 2\text{H}_2\text{O}$ , respectively and from the curves of Fig. 21 an extrapolated 'equilibrium' ratio of 45/55 was apparently reached in  $\sim 120$  min of reaction in the IR/ $\text{SnCl}_2 \cdot 2\text{H}_2\text{O}$  interaction, and a value of 41/59 in  $\sim 6$  hr in the IR/ $\text{SnCl}_2$  interaction. These results agree reasonably well with those which are probably the most reliable of the earlier studies.

(c) Double-bond shifts

In the IR/ $\text{SnCl}_2$  and IR/ $\text{SnCl}_2 \cdot 2\text{H}_2\text{O}$  interaction the occurrence of double bond shifts yielding structures such

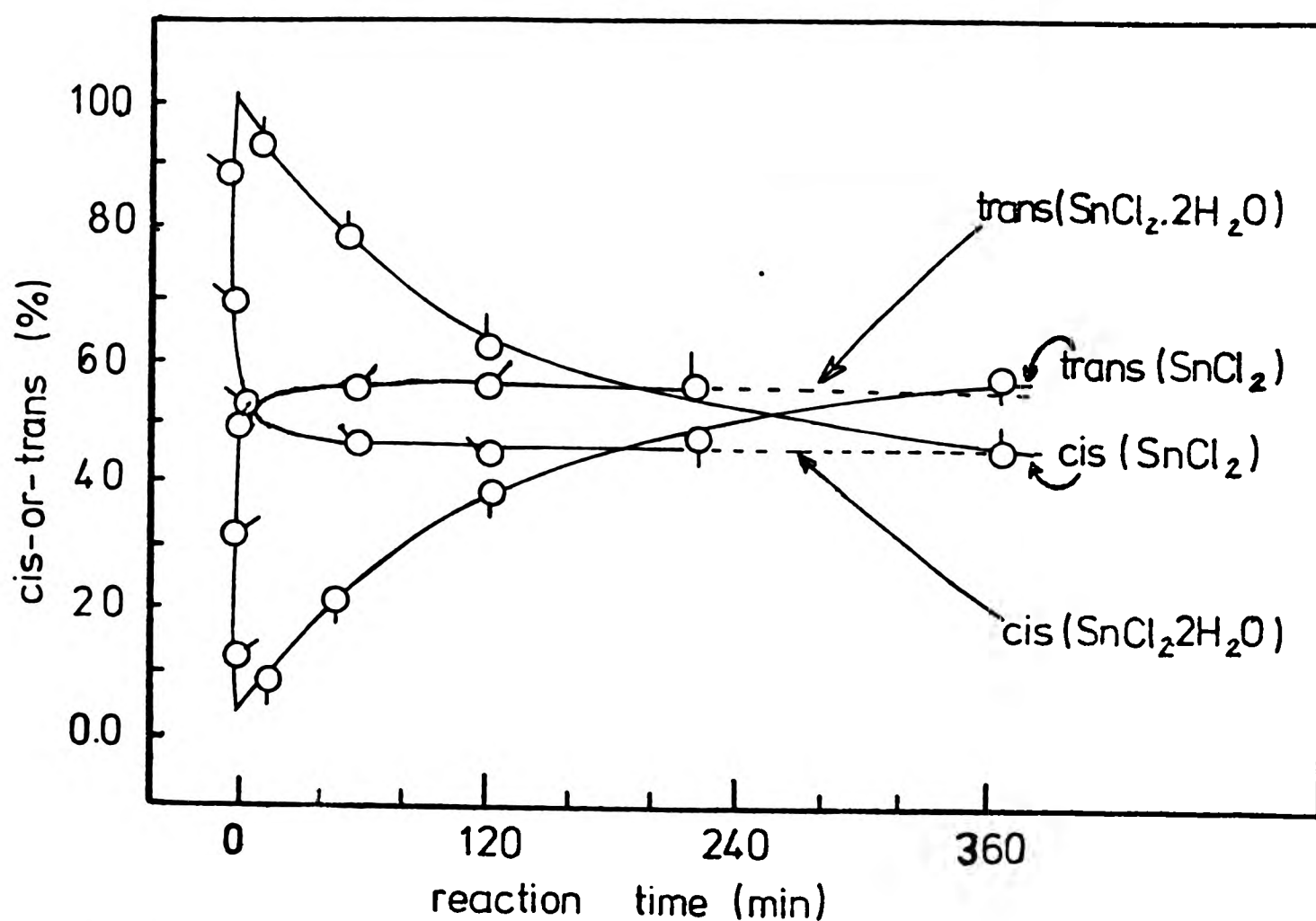


Fig. 21 Cis/trans ratios for the IR/SnCl<sub>2</sub> and IR/SnCl<sub>2</sub>.2H<sub>2</sub>O interactions.

as LXXI is suggested by ir and nmr spectroscopy (see Figs. 10-11 and 14-15 respectively), whereas it does not occur in the IR/ZnCl<sub>2</sub> interaction. In the IR/SnCl<sub>2</sub> interaction, where there is practically no cyclization (see Discussion below), the molar fraction (measured by nmr, Fig. 17a) of this double-bond type is very low (<0.07), and may be considered of negligible importance. In the IR/SnCl<sub>2</sub>.2H<sub>2</sub>O case this shift appears to be of more importance, but it seems that the 1,1 disubstituted double bonds initially formed may be consumed by cyclization in the later stages of reaction (both ir peak intensities and nmr molar fraction are maximum at 15 min. reaction time). In both interactions the 1,1 disubstituted double bonds may undergo cationic polymerisation

yielding crosslinking structures (see further discussion below).

Whether or not double bond shifts yielding cis and/or trans-1,2 trisubstituted ethylene double bonds (e.g., structures LXIX and LXX) are occurring is difficult if not impossible to ascertain directly by the methods of analysis used. A study of the interaction of the catalysts with polyisoprene-3d by ir and nmr spectroscopy would probably prove beneficial, since a similar study has been done for cis/trans isomerization by sulphur dioxide,<sup>88</sup> with useful results. In this study indirect evidence for cis and/or trans trisubstituted ethylene double bonds of the  $\Delta$ -1,2 type is afforded by the peak at 7.15 $\tau$  in the nmr spectra. Juxta-position of one of these units with the unrearranged cis and/or trans 1,4 units would yield  $\begin{array}{c} | \\ -C=CH-CH_2-HC=C- \\ | \end{array}$  which contains methylene protons in a different environment. These protons have been reported in 1,4-hexadiene and 1,4 penta-diene to resonate at 7.1 and 7.16 $\tau$ , respectively,<sup>44</sup> and in methyl linoleate at 7.15 $\tau$ .<sup>95</sup> Therefore, the peak at 7.15 $\tau$  arising in the IR/SnCl<sub>2</sub> and IR/SnCl<sub>2</sub>·2H<sub>2</sub>O interaction might reasonably be assigned to these methylene protons, thus supporting the occurrence of double bond shifts yielding isoprene units with 1,2 unsaturation. In these interactions the peaks at 7.15 $\tau$  are maximum at 120 and 15 min reaction time, respectively, so it appears that these groups may be consumed by cyclization.

Methyl protons in cis- and trans-1,2-unsaturated isoprene

units would have the same chemical shift in the nmr spectrum as those in cis- or trans-2,3-unsaturated isoprene units (i.e., normal 1,4 addition). It might reasonably be assumed that equal proportions of  $\Delta$ -1,2 and  $\Delta$ -2,3 structures will eventually arise since there appears to be no obvious difference in thermodynamic stability between them. Thus, the cis/trans ratios measured by nmr spectroscopy would represent the sum of equal amounts of both isomeric structures. Conjugate protons in 2,5-dimethylhexadiene-2,4 ( $\text{CH}_3-\overset{\text{CH}_3}{\text{C}}=\text{CH}-\text{CH}=\overset{\text{CH}_3}{\text{C}}-\text{CH}_3$ ) have been reported<sup>96</sup> to resonate at 4.19 $\tau$  in nmr spectroscopy. The absence of peaks at 4-4.4 $\tau$  in the nmr spectra of IR/SnCl<sub>2</sub> and IR/SnCl<sub>2</sub>·2H<sub>2</sub>O therefore suggests that the occurrence of conjugate double bonds arising from double bond shifts of t-t units in IR (structure LXXIII) is not likely, although there is a possibility that these structures are rapidly consumed by Diels-Alder addition or polymerization reactions.

(d) Cyclization

The nmr spectroscopy,  $T_g$  values and total unsaturation (Iodine values) results show the occurrence of cyclization in the IR/SnCl<sub>2</sub> and IR/SnCl<sub>2</sub>·2H<sub>2</sub>O interactions, whereas it does not occur in the IR/ZnCl<sub>2</sub> interaction. The rate and extent of this process in the IR/SnCl<sub>2</sub>·2H<sub>2</sub>O interaction are higher than in the IR/SnCl<sub>2</sub> case, cyclization being of negligible importance for up to 2 h of reaction time in the IR/SnCl<sub>2</sub> interaction, but occurring extensively in the IR/SnCl<sub>2</sub>·2H<sub>2</sub>O interaction after only 15 min of reaction

time (see Fig. 17).

The nmr spectra of the IR/SnCl<sub>2</sub>·2H<sub>2</sub>O interaction products (Fig. 15) show that the relative areas of the two peaks at 8.00 and 9.10τ which were assigned to CH<sub>3</sub>-C<sup>|</sup>= and CH<sub>3</sub>-C<sup>|</sup>- protons present in cyclized units (e.g., structures LXXVI and LXXVII) is nearly 1:1, suggesting that the cyclized structure consists mainly of monocyclic units. In fact the controversy as to whether the cyclized structure consist of monocyclic<sup>54-57</sup> or polycyclic ring structures<sup>58-60</sup> has not been fully resolved. It has been reported<sup>60-99</sup> that cyclicity is markedly dependent on reaction temperature, varying from as low as 1.5 at 110°C to 6 at 60°C and even in excess of 10 at reaction temperatures below 30°C. Thus, monocyclic rings might be expected under the present conditions at 160°C.

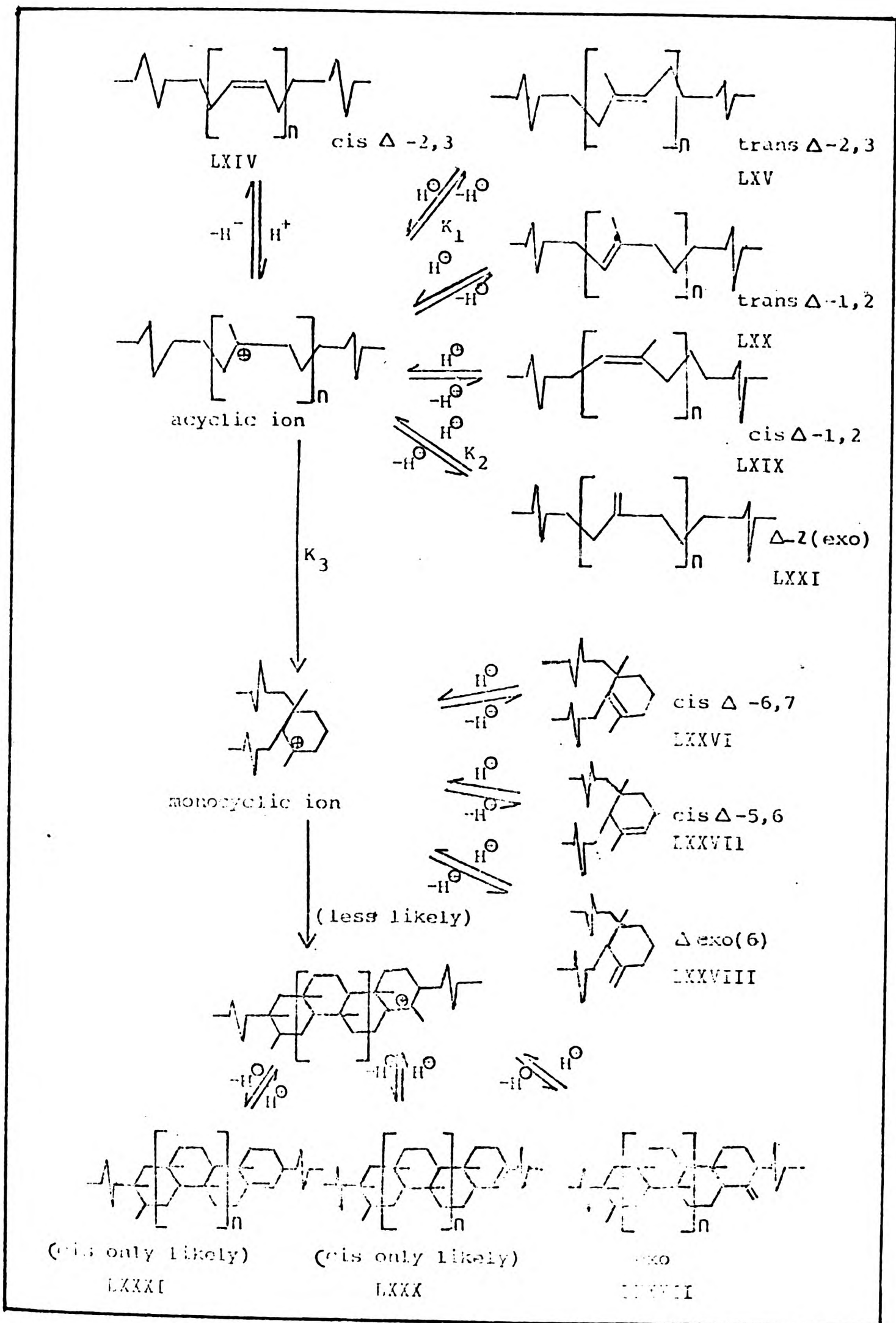
For the IR/SnCl<sub>2</sub> interaction products, where there is practically no cyclization, the total unsaturation measured by Iodine values is rather similar to that measured by nmr spectroscopy (Fig. 20). Similarly, there is not a big difference between those values in the early stages of the IR/SnCl<sub>2</sub>·2H<sub>2</sub>O interaction. Where extensive cyclization is occurring, however, Iodine values become larger than the nmr values. This might suggest that iodine chloride does not produce extensive substitutive or other side reactions as long as structures remain largely acyclic and this method might therefore be considered reliable in determination of unsaturation in this study.

The data obtained (Figs. 17 and 18) show that both  $T_g$  and cis/trans isomerization reach high values in the IR/SnCl<sub>2</sub>.2H<sub>2</sub>O interaction after only short times of reaction. Thus, the structural rearrangements in the vulcanization of polyisoprenes with p/f resins might be expected to affect the ability of the rubber to strain-crystallise, with corresponding detrimental effects on tensile strength and other mechanical properties of the final vulcanizate (later work will show that this is indeed the case). The raised  $T_g$  due to cyclization might also be detrimental in most applications. The increase of  $T_g$  can be neglected in the IR/SnCl<sub>2</sub> interaction, but since cis/trans isomerization occurs to an appreciable extent, it might be expected that the crystallizability and hence tensile strength of the rubber would be affected (later work will show that such an expectation is not, in fact, realised because of the insignificance of cis/trans isomerization).

From the kinetics of these isomerizations and from the fact that (apparently) there is no interaction between IR and ZnCl<sub>2</sub>, it might be expected that the vulcanization of IR with p/f condensates catalysed by SnCl<sub>2</sub>, would be at a lower rate than that catalysed by SnCl<sub>2</sub>.2H<sub>2</sub>O, and that there would be no catalytic effect with ZnCl<sub>2</sub>. However, at this stage it must be appreciated that absence of cationic activity with rubber alone does not preclude the possibility of activity in the presence of phenolic compounds (later work will show that p/f-rubber interaction is indeed catalysed by ZnCl<sub>2</sub>). These observations do, however, suggest that the catalyst exerts its action primarily by interacting with the p/f condensate rather than with the rubber.

(e) Overall mechanistic scheme

The mechanisms for cyclization, cis/trans isomerization and double bond shifts may be envisaged (Scheme 1) as involving carbonium ion intermediates. These would be produced from an active catalyst species such as  $\text{H}^+(\text{SnCl}_2 \cdot \text{OH})^-$  which initially protonates a double bond in the Markownikoff sense. The carbonium ion thus formed could expel a proton, resulting in either cis/trans isomerization of the original 2,3 double bond of the isoprene unit and/or a double bond shift yielding 2(exo) and 1,2 (cis and trans) double bonds. Thus, structures LXV, LXIX, LXX and LXXI are readily accounted for. Intra-molecular attack by the carbonium ion and an adjacent double bond results in cyclization, being followed by a deprotonation re-establishing the catalyst and leaving 3 possible types of double bond, i.e., 6.7, 5.6 and 6 (exo), corresponding to structures LXXVI, LXXVII and LXXVIII. In LXXVI and LXXVII the trans isomers are unlikely from thermodynamic considerations. Although monocyclic ring structures are considered more likely from the evidence given above, further intramolecular addition to give polycyclic rings is possible, with structures LXXX, LXXXI and LXXXII, analogous to those of the monocyclic products. It is emphasised that the structures shown are those resulting from intramolecular addition of the acyclic or cyclic cation to an unrearranged cis-1,4 unit LXIV. However, addition to the rearranged structures LXV-LXXI is also possible and may give a different product. Thus, the structure of the cyclized products is almost certainly not



Scheme 1 Possible mechanistic scheme involving protonated intermediate species.

as regular as that shown in Scheme 1.

The curves of the kinetics of total unsaturation (measured by Iodine values and/or nmr spectroscopy) and residual trisubstituted ethylene unsaturation (measured by nmr spectroscopy) for both IR/SnCl<sub>2</sub> and IR/SnCl<sub>2</sub>·2H<sub>2</sub>O interactions (Figs. 20 and 17) follow the same general shape as those found for total and trisubstituted ethylene unsaturation in the cyclization of NR with SnCl<sub>4</sub>, which was shown to be entirely consistent with a statistical theoretical treatment assuming a carbonium ion mechanism.<sup>60</sup> This lends support to the above mechanism proposed for cyclization. Similar mechanisms have been proposed<sup>54-60</sup> for cyclization of polyisoprenes by treatment of the rubber with several other agents. Since cyclization apparently proceeds at a much lower rate than the various acyclic rearrangements (Scheme 1), it seems reasonable to assume that the intermediate carbonium ion concentration is not significantly affected by them. Cyclization might therefore be expected to conform to the kinetics reported by other workers where no cis/trans isomerization or double bond shifting was reported. On these grounds the rate constants for cyclization were found to be  $12.7 \times 10^{-3}$  and  $35.1 \times 10^{-3} \text{ h}^{-1}$  for the IR/SnCl<sub>2</sub> and the IR/SnCl<sub>2</sub>·2H<sub>2</sub>O interactions, respectively.

The kinetics of cis/trans isomerization of NR and gutta-percha (as measured by the cis/trans ratio) by SO<sub>2</sub>, has been reported<sup>52</sup> to be expressible by the relationship:

$$\ln\left(\frac{b_e}{b_e - b}\right) = \frac{Ka}{b_e} t \quad (1)$$

where  $a$  is the initial concentration of cis or trans double bonds,  $b$  is the concentration of the other isomers formed by time  $t$ , and  $b_e$  is its equilibrium concentration. The relationship (1) is the general rate expression for a reversible reaction dependent on the concentration of one reactant. It may be derived for the  $\text{SO}_2$  isomerization mechanism assuming that the  $\text{SO}_2$  concentration and rate of radical generation are constant.<sup>52</sup> The cis/trans kinetics of the IR/ $\text{SnCl}_2$  interaction (cis/trans ratio) (Fig. 21) fit with relation (1) up to 120 min of reaction, after which a negative deviation is observed (Fig. 22). Thus, isomerization by  $\text{SnCl}_2$  presumably occurs via an "on-off" reaction at the double bond similar to that with  $\text{SO}_2$ , although the nature of the intermediates in this latter case is uncertain. Free radicals are not involved since the rate of isomerization appears to be insensitive to free radical catalysts and inhibitors. The negative deviations of Fig. 22 might be accounted for by the fact that loss of double bonds by cyclization becomes of importance from 120 min of reaction time and thus the equilibrium is disturbed. Alternatively or additionally, the catalyst may not remain constant in concentration like  $\text{SO}_2$ , and may be gradually hydrolysing. Even greater deviations in cis/trans kinetics of the IR/ $\text{SnCl}_2 \cdot 2\text{H}_2\text{O}$  interaction (Fig. 22) are observed when compared with that of the  $\text{SO}_2$ -isomerization, which might be accounted

for by a faster rate on loss of double bonds by cyclization (For which there is ample nmr and Iodine values evidence) and again a gradual destruction of the active catalyst species  $\text{H}^+(\text{SnCl}_2 \text{ OH})^-$  with increasing reaction time, which also has been reported.<sup>11</sup> According to this mechanism the rate constants for cis/trans isomerization were 10.8 and 142.8  $\text{h}^{-1}$  for the IR/ $\text{SnCl}_2$  and IR/ $\text{SnCl}_2 \cdot 2\text{H}_2\text{O}$  interactions, respectively.

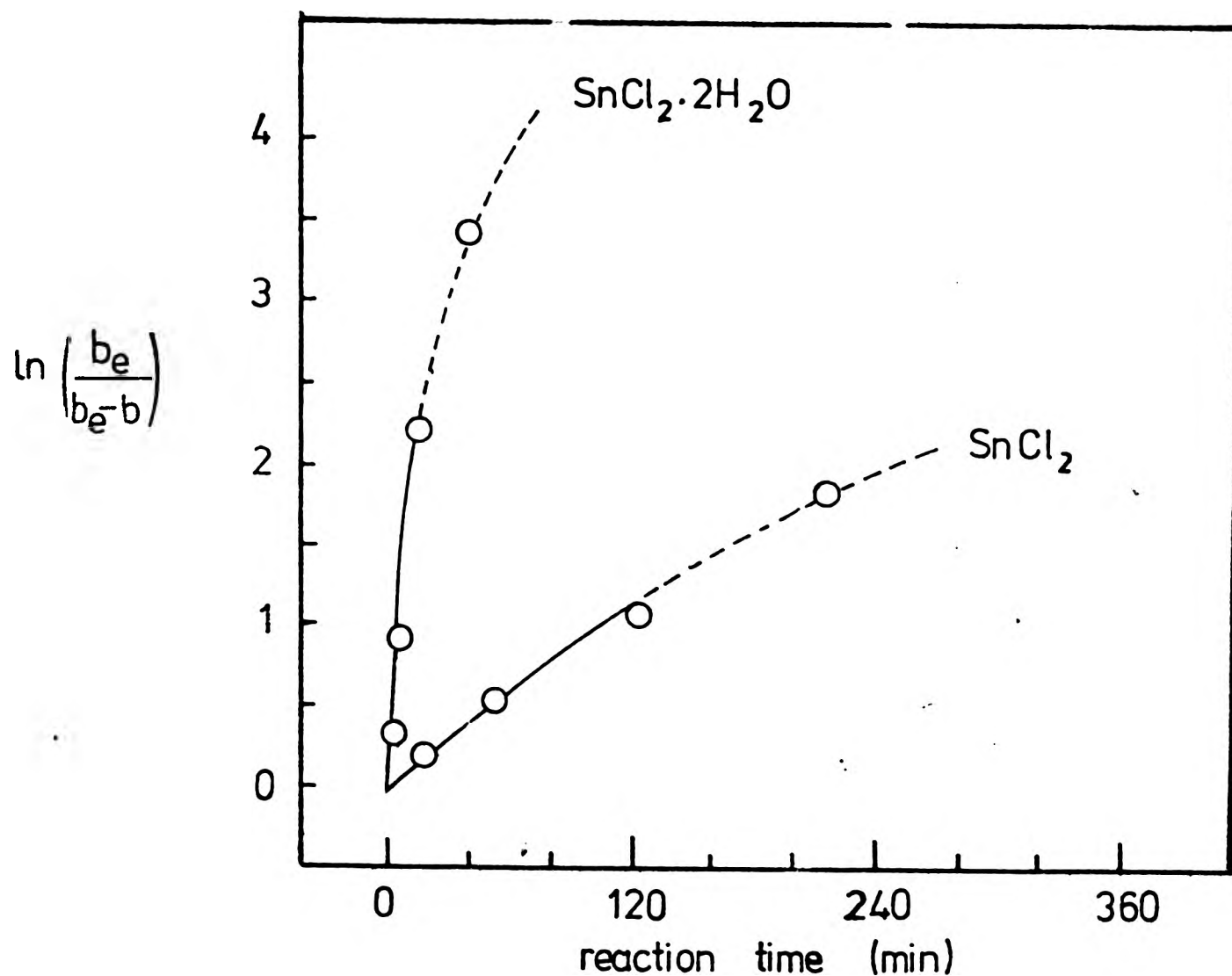


Fig.22 Plot of results according to equation (1) showing deviations.

The differences in kinetics between the IR/ $\text{SnCl}_2 \cdot 2\text{H}_2\text{O}$  and the IR/ $\text{SnCl}_2$  interactions may be interpreted in terms

of different active catalyst concentrations rather than different mechanisms. In the IR/SnCl<sub>2</sub> interaction, the active catalyst species such as H<sup>⊕</sup> {SnCl<sub>2</sub>·OH}<sup>⊖</sup> may need to be generated in situ from reaction of SnCl<sub>2</sub> and adventitious traces of water. Thus the concentration of this active species generated may be very low and may change with time.

The fact that interaction of IR with ZnCl<sub>2</sub> apparently does not occur, might suggest further evidence for H<sup>⊕</sup> {SnCl<sub>2</sub>·OH}<sup>⊖</sup> catalyst species to be the more likely in the IR/SnCl<sub>2</sub> interaction because, whereas ZnCl<sub>2</sub> hydrates with different molecules of water (1-4) per ZnCl<sub>2</sub> molecule are known, above 28°C only anhydrous ZnCl<sub>2</sub> is in equilibrium with the solution.<sup>97</sup> Therefore, from the results obtained in the present work, it might be concluded that neither the ZnCl<sub>2</sub> or SnCl<sub>2</sub> in anhydrous form possesses enough Lewis acid strength in order to induce cationic reactions in IR under the conditions used. In the IR/SnCl<sub>2</sub> interaction, however, the very likely possibility of SnCl<sub>2</sub> reacting in situ with traces of water yielding the complex active catalyst species H<sup>⊕</sup> {SnCl<sub>2</sub>·OH}<sup>⊖</sup> would account for the reactions observed. No such difficulty exists with SnCl<sub>2</sub>·2H<sub>2</sub>O, where one molecule of water is already in the form of this coordination complex, the other being water of crystallization.

In the cyclization of polyisoprenes by TiCl<sub>4</sub> where practically no cis/trans isomerization has been reported,<sup>77</sup> a TiCl<sub>4</sub>-induced carbonium ion mechanism was suggested, involving a coordination complex intermediate between TiCl<sub>4</sub>

and the trialkylethylenic double bonds of IR. Thus, the  $\text{TiCl}_4$  itself was considered the active catalyst species.  $\text{TiCl}_4$  has been reported<sup>98</sup> to be a powerful Lewis acid and in general forms a very extensive series of addition compounds. It would be expected to be more likely than  $\text{SnCl}_2$  to react with double bonds in IR. In that study<sup>97</sup> the absence of cis/trans isomerization was explained in terms of the absence of any reversibility to the attachment of  $\text{TiCl}_4$  onto the isoprenic double bonds, whereas reversibility in attack of these double bonds by  $\text{H}^+(\text{SnCl}_2 \cdot \text{OH})^-$  is suggested in the present study and would account for the extensive cis/trans isomerization observed.

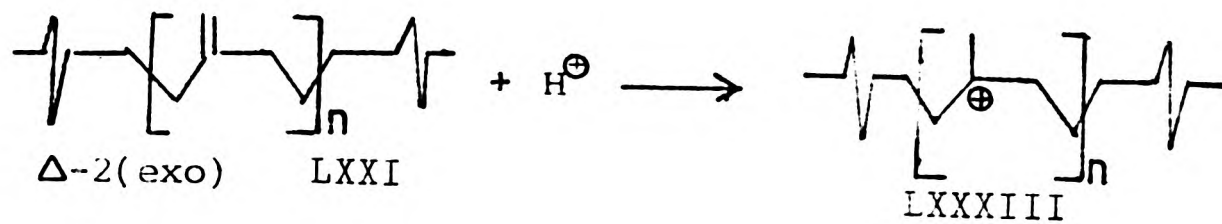
By analogy with the polymerization of isobutylene by the Lewis acid catalyst  $\text{BF}_3$  when a trace amount of water (co-catalyst) is added<sup>98</sup> (and in general with the Lewis acid-catalysed polymerization of double bonds with electron-releasing substituents), the crosslink formation in the IR/ $\text{SnCl}_2$  and IR/ $\text{SnCl}_2 \cdot 2\text{H}_2\text{O}$  interactions (revealed by the gel content) may be envisaged as involving a cationic addition of the 1,1 disubstituted double bonds (structure LXXI) formed by double bond shifts. Propagation of this addition (Scheme 2) yields crosslink structures, termination may be envisaged as a proton expulsion giving terminal unsaturation. Since cationic polymerization at high temperatures yield oligomeric products, the value 'm' in Scheme 2 is likely to be very low, possibly one.

An alternative or additional mechanism of crosslinking

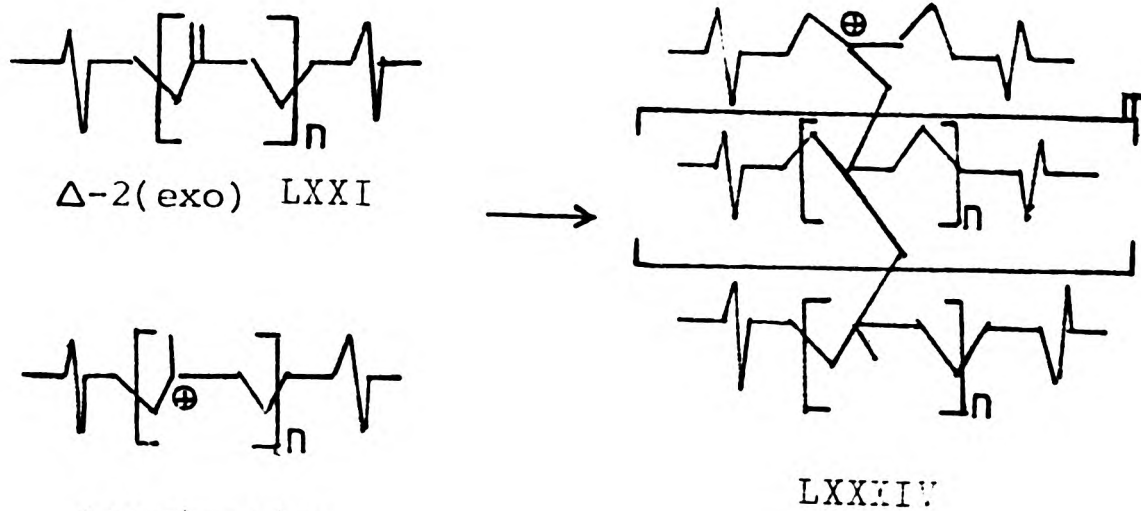
may be envisaged, involving conjugated double bonds (structure LXXIII). Such double bonds, if formed, would be expected rapidly to undergo Diels-Alder type addition to isolated single bonds, producing a cyclic crosslink (Scheme 2). Further, it is possible that conjugated double bonds could participate in cationic polymerization similar to that discussed above.

It is considered that the Diels-Alder mechanism is the more likely, since the temperatures used are well above the ceiling temperatures commonly observed for cationic polymerization processes. Whichever crosslinking mechanism applies, the smaller gel content, and the slower kinetics of gel formation for the IR/SnCl<sub>2</sub> interaction than for the IR/SnCl<sub>2</sub>·2H<sub>2</sub>O interaction (Fig. 19) is readily accounted for by the smaller concentration of active catalyst species, eg.,  $\text{H}^{\oplus} (\text{SnCl}_2 \cdot \text{OH})^{\ominus}$ , in the former case.

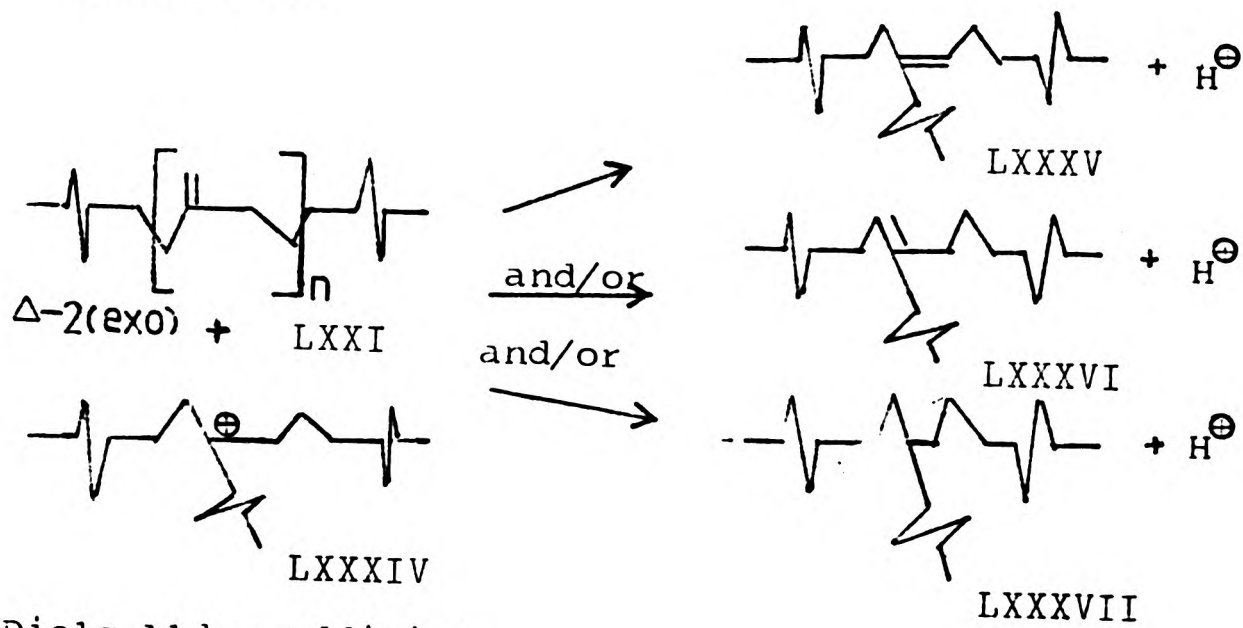
(1) Cationic Mechanism initiation



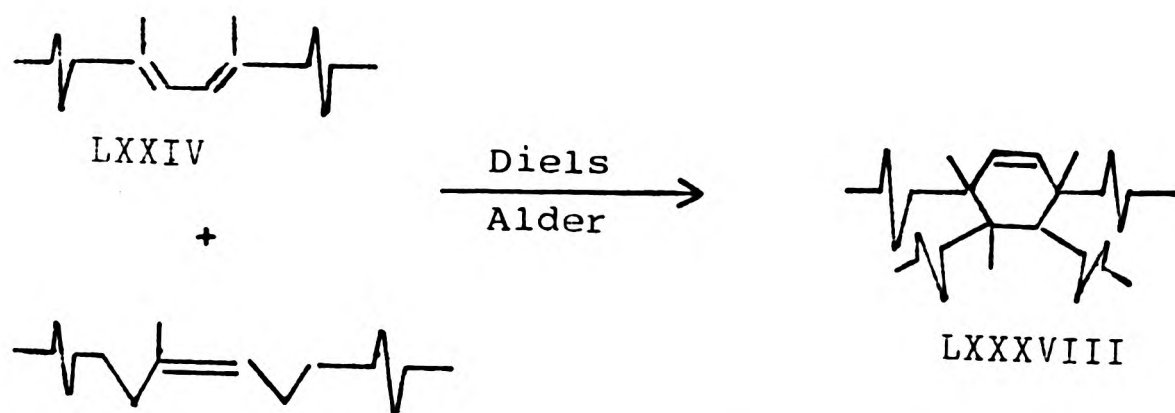
propagation



termination



(2) Diels Alder Addition



Scheme 2, Possible crosslinking mechanisms

### 3 INTERACTION OF 'MODEL' PHENOL-FORMALDEHYDE CONDENSATES WITH SYNTHETIC POLYISOPRENE RUBBER

#### 3.1 Purpose of This Study

The purpose of this study was to investigate adduct formation between monofunctional 'model' p/f condensates and IR. In view of the mono-functionality of the "models" used, they were expected to react with the rubber to form addition products rather than crosslinks, and therefore to produce soluble products which should be readily amenable to structural characterization. In addition, the possible occurrence of isomerization side reactions by the catalysts used (see previous chapter) may be expected to influence the progress of the reaction.

The establishment of optimum conditions for high yield of adduct accompanied by minimal degradation or otherwise undesirable side-effects was a primary aim of this part of the work. Such conditions should enable the number of crosslinks to be maximised when the monofunctional p/f models are replaced by bi-functional compounds in a later stage of this work (Chapter 4).

#### 3.2 Reagents

The rubber and catalysts examined were the same as those described in Chapter 2. The p/f condensate "models" used were the methylol phenol(IV), and its corresponding

dibenzyl ether derivative (V) which were previously synthesised (details in the Experimental Section). The main difference between the methylol phenol and the p/f condensates used in industry (e.g. I) is the low functionality of the former. The methylol phenol is mono-functional with respect to methylol, or bi-functional if the phenolic hydroxyl is taken into consideration. If, however, the two groups act in unison to produce a quinone methide moiety (XXX), then a chroman structure (XXXII) the functionality may for present purposes be regarded as unity. This concept assumes no reaction at the free ring positions or the substituent alkyl groups. The latter may react under oxidative conditions, but in the present study where the interaction of p/f condensates with rubber were carried out in a full enclosed mould, the reactions may be regarded as taking place under substantially anaerobic conditions. The ring positions meta- to the phenolic hydroxyl are unresponsive to electrophilic attack, and reactions at these sites would require much more vigorous conditions than were used in the present work.

The dibenzyl ether cannot be regarded as bifunctional, despite the fact that it is derived from a condensation of 2 molecules of methylol phenol. Its decomposition produces 1 molecule each of quinone methide and methylol phenol, and in all important respects its functionality may therefore be regarded as the same that of the methylol phenol. However, a different yield of adduct formation and solubility in rubber might be expected compared with those for the methylol phenol (by analogy with the results of Fitch), and these possibilities will be investigated.

### 3.3 Reaction Conditions and Procedure

The amount of methylol phenol employed was 25.0phr (i.e., 20% by weight of the total). The reasons for the use of such a high concentration of methylol phenol, which is 2-3 times the concentration used in industrial vulcanization, were (a) to ensure a high yield of any addition products so that any small variation would be more easily detected, and (b) because this condition is similar to that used by Fitch in his model compound kinetic studies<sup>11</sup>, thus enabling direct comparison to be made. The weight of dibenzyl ether used, 23.8 phr was slightly less than that of the methylol phenol, so as to contain the same number of "active moles", again enabling results to be directly compared. Since we are interested only in the fate of those substances which contain phenolic nuclei, we may define the "mole" as the average relative mass per formula unit of the natural nuclidic composition (i.e., molecular weight) in grams divided by the number of nuclei present. Thus, 1 gram-molecule of dibenzyl ether would constitute 2 moles, in accordance with the discussion concerning functionality above.

The amounts of catalyst used ( $\text{SnCl}_2$  1.0phr,  $\text{SnCl}_2 \cdot 2\text{H}_2\text{O}$  1.19phr and  $\text{ZnCl}_2$  0.73phr) were chosen to be the same as those employed for the study of the interaction of IR with catalysts only (Chapter 2).

The catalysed reactions with both p/f models were studied at 160°C. In order to speed up the uncatalysed

interactions, these were carried out at 180°C. In all cases the reactions were conducted in bulk in a vulcanization press, in the same way as described for the IR/catalyst interactions (Chapter 2).

### 3.4 Characterisation of Products

The products of interaction between IR and the p/f condensate models, both catalysed and uncatalysed, were acetone-extracted then stored in the dark in vacuo. They are referred to below as products IR/MP, IR/E, IR/MP/ZnCl<sub>2</sub>, IR/MP/SnCl<sub>2</sub>, IR/MP/SnCl<sub>2</sub>.2H<sub>2</sub>O, IR/E/ZnCl<sub>2</sub>, IR/E/SnCl<sub>2</sub> and IR/E/SnCl<sub>2</sub>.2H<sub>2</sub>O, where MP and E refer to methylol phenol (IV) and dibenzyl ether (V).

Each product was examined at various reaction times in respect of the following characteristics:

(a) Bound phenolic material

The total concentration of phenolic material combined was determined by: (i) acetone extraction, (ii) nmr spectroscopy and (iii) ir spectroscopy.

(i) Acetone extraction

Each product of interaction was thoroughly extracted with acetone in a Soxhlet apparatus, and the % weight extractable matter determined. Sample of the IR only and of the

unheated mixes were also extracted so as to allow the amount of phenolic material combined after each period of heating to be calculated (details in the Experimental Section).

It was suspected that some uncombined decomposition products of the p/f models and/or of the catalysts used might not be completely extractable with acetone. A series of experiments were therefore undertaken for comparison using a saturated ethylene-propylene rubber (EPR) ('Intolan 36', Shell Co., UK) which is not expected to react with the phenolic materials, catalysts, or their decomposition products. The EPR was mixed with the methylol phenol and the ether with and without catalysts, using the same proportions and reacting under the same conditions as those used for the IR interactions. Acetone extraction of these products after various reaction times, and of the EPR and the unheated mixes, allowed the amount of unextractable yet (presumably) uncombined matter to be calculated. These results were used to correct those obtained in the various interactions with IR.

(ii) Nmr spectroscopy

The nmr spectrum of the extracted polymer was used for determination of the concentration of combined phenolic material by comparing the area of a resonance band attributable to phenolic material with one due to IR.

(iii) Ir spectroscopy

Ir spectroscopy was used to monitor the combination of material by comparing the intensity of a band attributable to phenolic material with one due to IR. This gave a relative, not absolute, phenolic concentration, but was convenient for following the progress of reaction.

(b) Structure of the adduct

The above considerations relate to the total amount of adduct formed, but give no information about its structure. In order to distinguish between structures linked by chroman groups and those by methylene bridges (see Introduction), the following were examined:

(i) nmr and ir spectra were examined for evidence of chroman groups and other structures;

(ii) phenolic hydroxyl concentration (characteristic of the methylene-bridge-linked adduct) was determined using ir spectroscopy, a known phenol being used for calibration purposes;

(iii) total unsaturation (which, on a molar basis, should diminish only with chroman formation) was determined using iodine monochloride (Wijs-Kemp method) and perbenzoic acid reagents. In order to assess the reliability of the results, both methods were tested using model compounds

containing tertiary hydrogens, tetrasubstituted double bonds and phenolic nuclei.

(c) Isomerization of polyisoprene during reaction

As discussed in Chapter 2, cis-trans conversions and double-bond shifts may be revealed by ir and nmr spectroscopy, and these spectra were therefore obtained of each product. Cyclization is clearly revealed in the glass transition temperature,  $T_g$ , but in this case there is the complication that adduct formation itself is expected to raise the  $T_g$ . The discrimination between these two  $T_g$ -raising effects is discussed later.

(d) Molecular weight changes and gel content

Solubility tests in toluene showed that whereas gel is absent in products IR/MP, IR/E, IR/MP/ $ZnCl_2$  and IR/E/ $ZnCl_2$ , it is present in considerable amount in products IR/MP/ $SnCl_2$ , IR/MP/ $SnCl_2 \cdot 2H_2O$ , IR/E/ $SnCl_2$  and IR/E/ $SnCl_2 \cdot 2H_2O$  after about 15 min. of reaction time. Gel formation appears to occur concurrently with cyclization. Quantitative measurements of gel content in these cases were obtained as described in the Experimental Section. Despite the fact that ir spectroscopy showed that the sol is very similar to the gel it might be possible that the chemical micro-structure of the sol and gel fractions are not precisely the same. Thus, in these cases the results of nmr spectroscopy (above), which necessarily was carried out on the sol, may not be precisely representative of the product as a whole.

Since gel formation is expected to be preceded by a MW increase due to crosslinking, intrinsic viscosity values were determined on each of the soluble products. These were carried out in toluene solution, as described in the Experimental Chapter.

Each of the above methods are considered in more detail, and results in the present work are presented in Sections 3.5-3.11; below.

### 3.5 Bound Phenolic Material

#### (a) Earlier studies

In Fitch's work<sup>11</sup> the interaction of alk-2-ene XXXI and alk-1-ene XXXII with methylolphenol and dibenzyl ether (24 and 23 parts by weight per hundred parts of alkene respectively) was investigated both uncatalysed and catalysed ( $\text{SnCl}_2 \cdot 2\text{H}_2\text{O}$ , 0.24 parts weight per hundred of alkene) at  $150^\circ\text{C}$  and under various reaction conditions. Products were identified and monitored using a refined thin-layer chromatographic technique. In that study no methylene bridge type adducts were observed. Concentration of chroman, expressed as moles per mole of the starting phenolic material, are plotted against reaction time in Figs. 23 and 24 for various reaction conditions. The induction times, rates and concentration maxima for chroman formation and for the decomposition products of the methylolphenol and ether under the various conditions of Fitch's study are given in Table 3, Chapter 1. These results show that in both

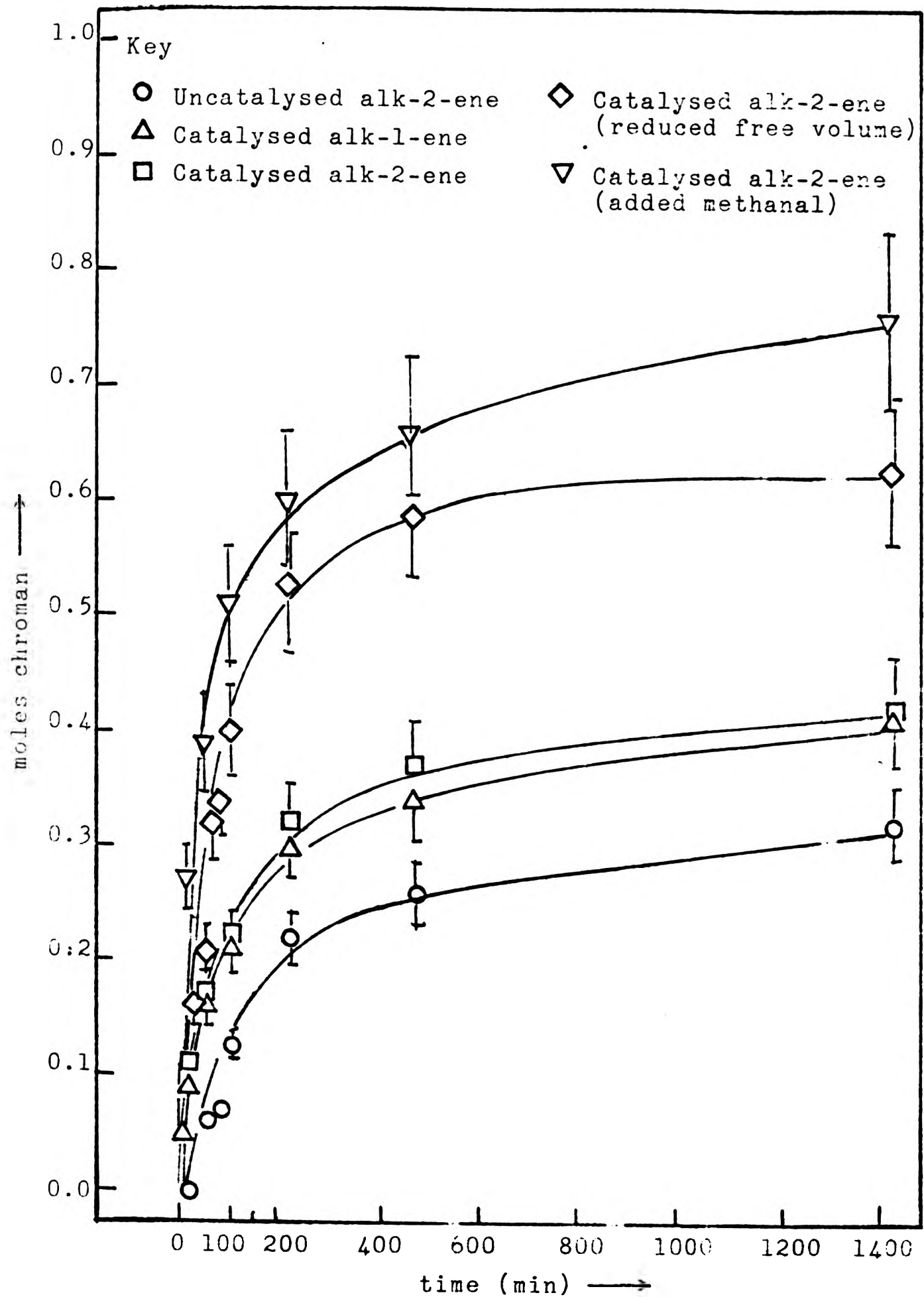


Fig. 23<sup>11</sup> Concentration of chroman, with time, on interaction of methylolphenol at 150°C with alk-2-ene/alk-1-ene under various conditions.

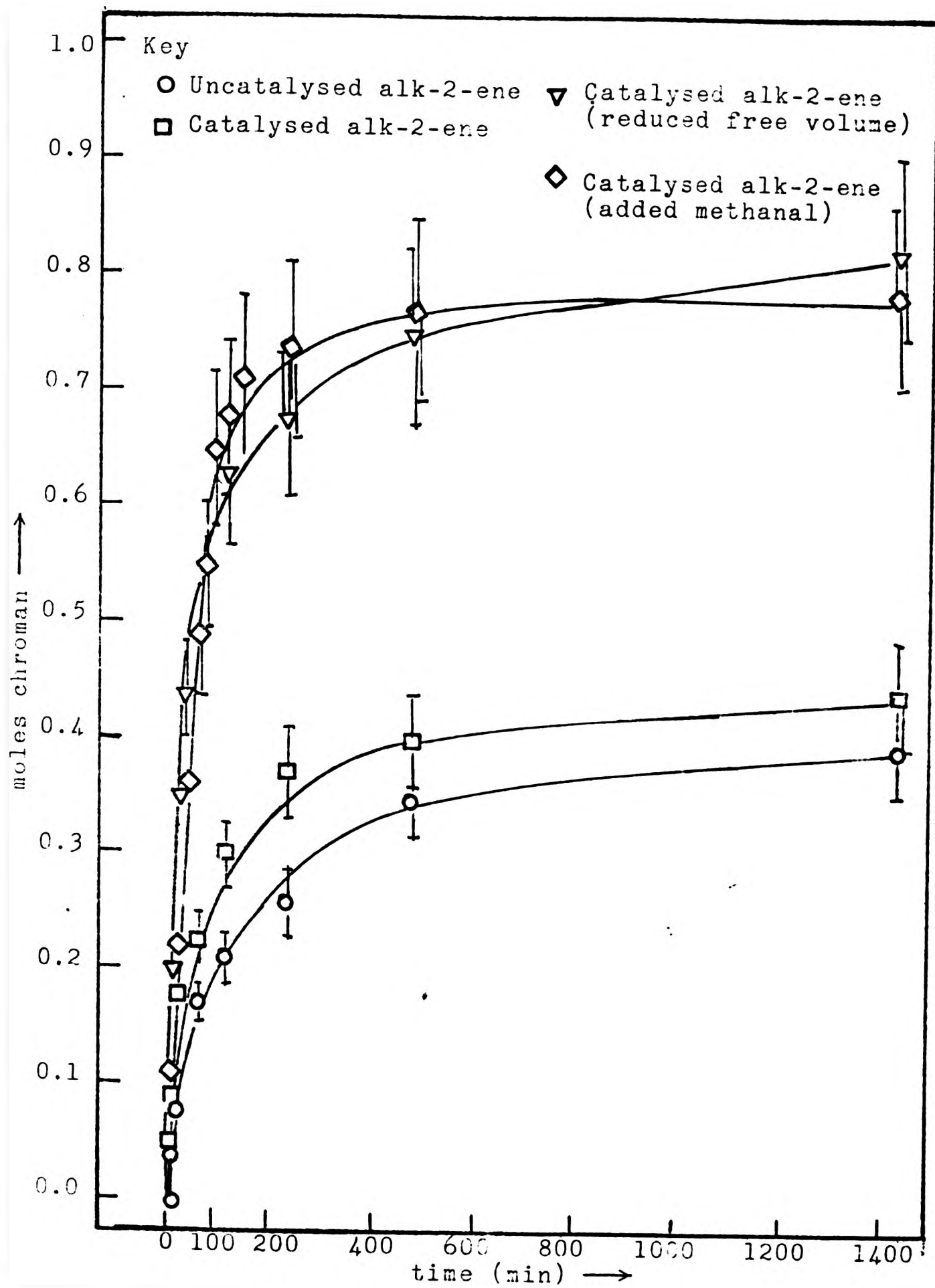


Fig. 24<sup>11</sup> Concentration of chroman, with time, on interaction of dibenzyl ether at 150°C with alk-2-ene under various conditions.

uncatalysed and catalysed interactions the rates of chroman formation were faster with the ether than with the methylolphenol. The rate and extent of chroman formation in the catalysed interactions with both methylolphenol and ether, where the free:occupied volume ratio (p 16) was high (1.5:1), were quite similar to those of the uncatalysed case. This unexpected similarity was attributed to isomerization of the alk-2-ene to an equimolar mixture of alk-2-ene and alk-1-ene, the latter being unreactive to chroman formation and no chroman was formed from this under uncatalysed conditions. Chroman concentration for both catalysed and uncatalysed interactions were slightly higher with the ether than with the methylolphenol. Substantial increases in reaction rates and chroman concentrations for both phenolic materials were observed in the catalysed interactions by addition of methanal and decreasing the free volume in the reaction vessel. These served to inhibit the formation of diphenyl methane by-product by increasing the partial presence of methanal and thereby inhibiting the formation of free phenol (see Fig. 4).

(b) Results in the present study

(i) Acetone extraction

Bound phenolic material was obtained by weighing the acetone extracts. The loss of material as volatile decomposition products (methanal and water) was considered to be negligible. As a check, combined material was also calculated

from increasing weight of the extracted rubber rather than from the weight of the extract. Surprisingly, however, these values resulted in slightly higher combined phenol values than those obtained from the weight of extract; this possibly arises from retention of acetone by the rubber even after drying samples in vacuo at 60°C for up to 7 hrs. The extent of the difference is illustrated for a typical set of values obtained by the 2 methods in Fig. 25. The analysis based on the weight of extract, corrected for the weight of extractable matter from the original rubber and the weight of acetone-insoluble uncombined phenolic matter, was considered the more reliable and was used in this study. Results were expressed as moles of phenolic material combined per mole of rubber and as the molar fraction of the starting phenolic material which had combined (the moles of bound phenolic material were obtained by dividing the weight in grams, obtained from the acetone extraction, by the MW (176) of the quinone methide unit XXX).

Detailed results showing corrections made are presented in the Experimental Chapter. Results are summarised in graphical form in Fig. 26, which shows moles of phenolic material combined per mole of rubber as well as molar fraction of the starting phenolic material combined as reactions proceed. The rates of combination (time 0.01 moles), maximum combined phenolic concentration achieved and concentration of phenolic material combined at 35 min. (a reasonable time for vulcanization) are given in Table 4. These results show that, in general, for the catalysed interactions rates of combination were faster and concentration maxima higher

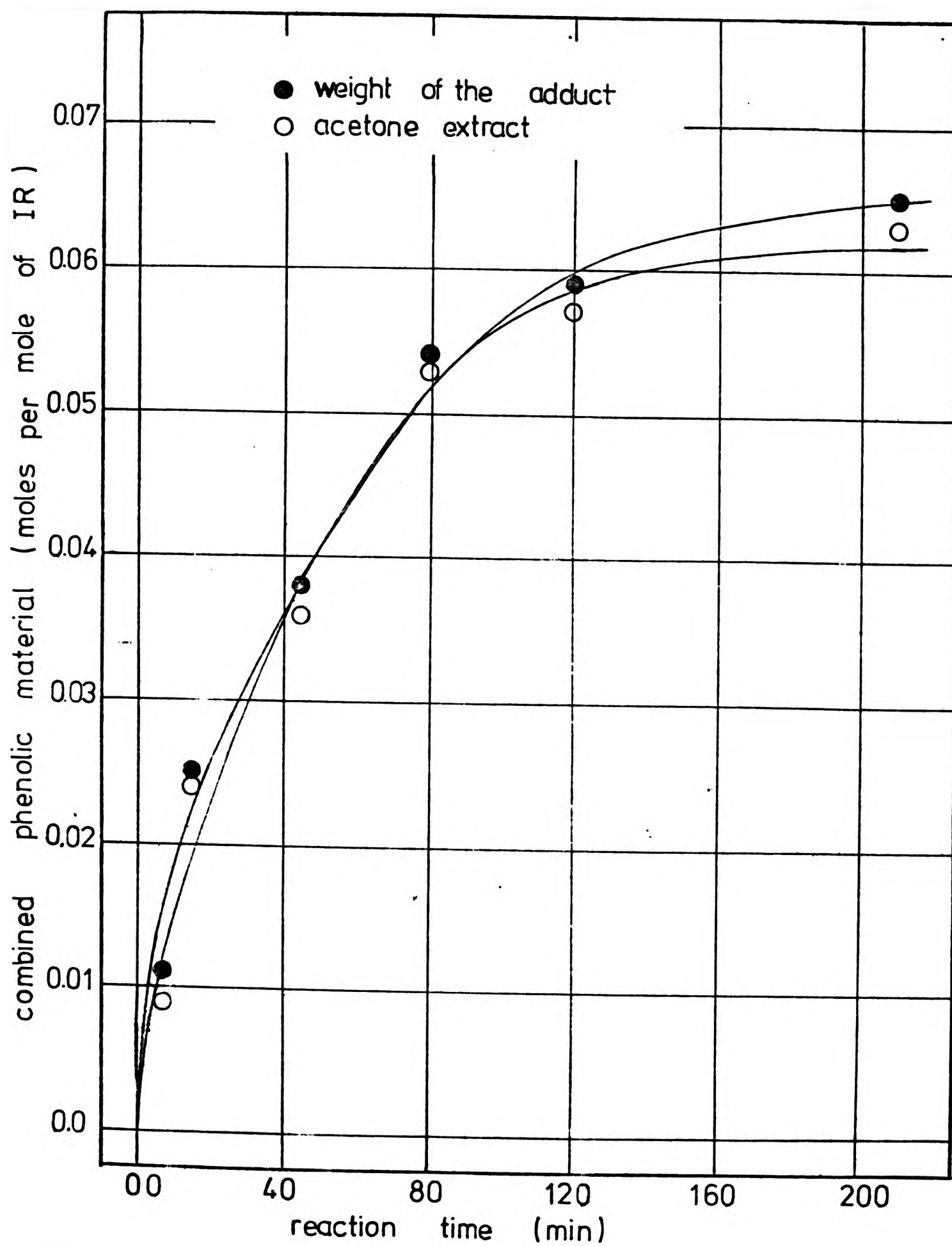


Fig. 25 Comparison of kinetics of combination of phenolic material for the IR/E/ZnCl<sub>2</sub> interaction as calculated from the amount of acetone extract and from the weight of the adduct.

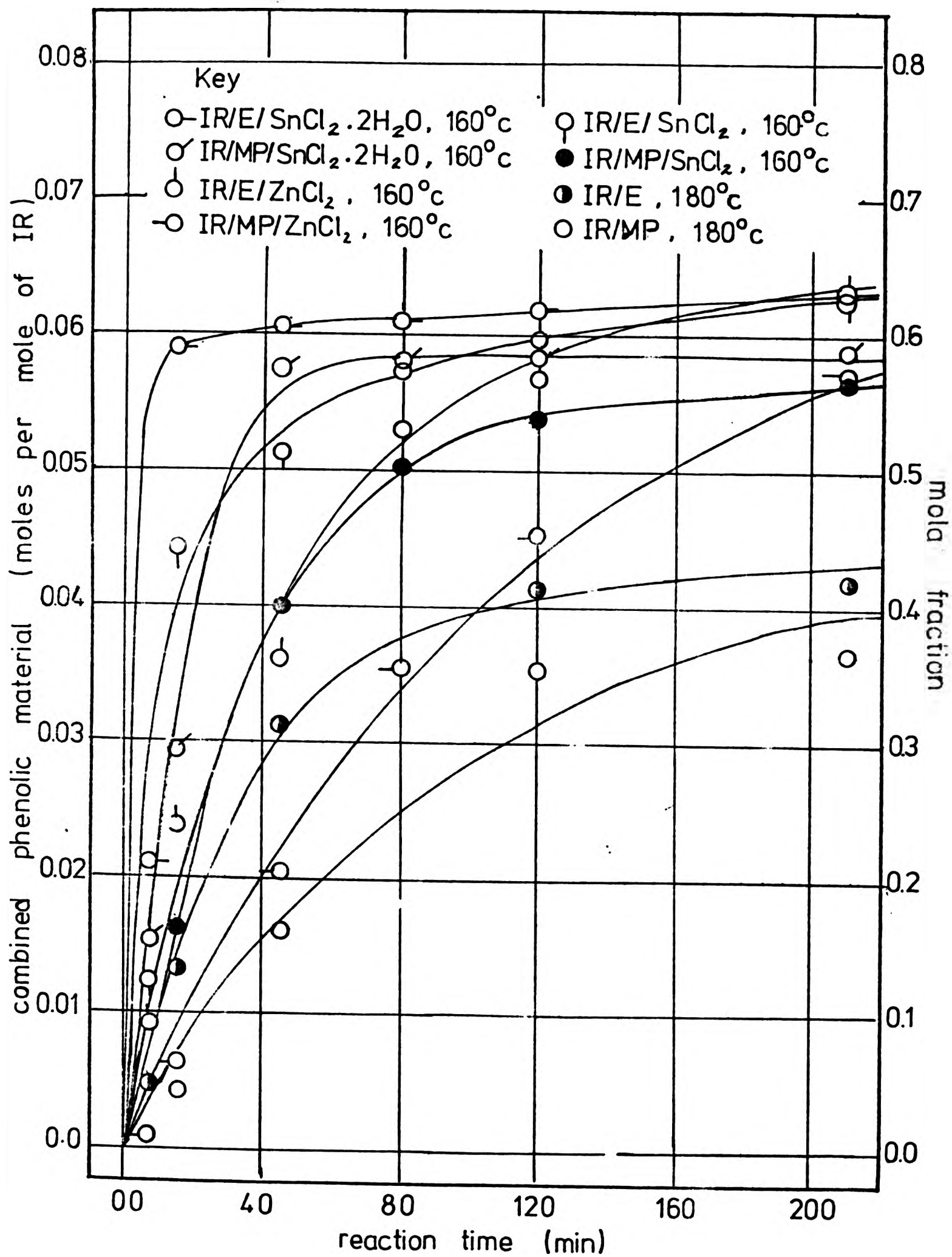


Fig. 26 Kinetics of combination of phenolic material as calculated from the amount of acetone extract.

Table 4 : Kinetic data for phenolic material combined in the various interactions, as calculated from the corrected amount of acetone extract.

Interaction	Rate (time in mins. to reach 0.01 mole)	Concentrations up to 35 mins (moles /mole of rubber) $\times 10^2$	Ultimate concentration (moles/mole of rubber) $\times 10^2$
IR/MP	22	1,45	3,90
IR/E	9	2.60	4.30
IR/MP/ZnCl <sub>2</sub>	18	1.80	5.90
IR/MP/SnCl <sub>2</sub>	5	3.35	5.15
IR/MP/SnCl <sub>2</sub> 2H <sub>2</sub> O	5	5.25	5.85
IR/E/ZnCl <sub>2</sub>	3	3.50	6.30
IR/E/SnCl <sub>2</sub>	5	4.75	6.40
IR/E/SnCl <sub>2</sub> 2H <sub>2</sub> O	2.5	6.00	6.22

Table 5 : Kinetic data for phenolic material combined for the various interactions as determined by nmr spectroscopy.

Interaction	Rate (time to 0.01 moles)	Concentration up to 35 min. (moles/mole of rubber) $\times 10^2$	Ultimate concentration (moles/mole of rubber) $\times 10^2$
IR/MP	30	0.90	3.60
IR/E	11	1.90	4.60
IR/MP/ZnCl <sub>2</sub>	17	1.50	5.60
IR/MP/SnCl <sub>2</sub>	8	2.65	5.60
IR/MP/SnCl <sub>2</sub> 2H <sub>2</sub> O	1	-	-
IR/E/ZnCl <sub>2</sub>	6	3.70	6.60
IR/E/SnCl <sub>2</sub>	2	4.50	7.30
IR/E/SnCl <sub>2</sub> 2H <sub>2</sub> O	1	-	-

than for the uncatalysed ones. In all cases the rates with the dibenzyl ether were considerably higher than with the methylolphenol, and the eventual concentration maxima for the former were slightly higher than for the latter. Comparison of results for the various catalysts used show that rates were highest with  $\text{SnCl}_2 \cdot 2\text{H}_2\text{O}$ , intermediate with  $\text{SnCl}_2$  and lowest with  $\text{ZnCl}_2$  (these will be discussed further later).

(ii) Nmr spectroscopy

An estimate of the concentration of combined phenolic material was obtained by nmr spectroscopy from the area of the peak at  $8.66\tau$  ( $-\text{C}(\text{CH}_3)_3$ ) to one due to IR. For the phenolic material the resonance at  $8.66\tau$  was chosen since, because there are nine contributing protons, its area is sufficient even in the very early stages of reaction where the amount of phenolic material combined is very low. Furthermore, this resonance band is not overlapped by other resonances. In the IR/MP/ $\text{SnCl}_2$ , IR/MP/ $\text{SnCl}_2 \cdot 2\text{H}_2\text{O}$ , IR/E/ $\text{SnCl}_2$  and IR/E/ $\text{SnCl}_2 \cdot 2\text{H}_2\text{O}$  interactions, where the gel content was very high, no satisfactory nmr spectra could be obtained. Results could therefore not be expressed in quantitative terms since the true solution concentration would be lower than the apparent one as prepared. However, there was no gel content in the IR/MP, IR/E, IR/MP/ $\text{ZnCl}_2$  and IR/E/ $\text{ZnCl}_2$  interactions, and quantitative measurements were made with the acetone-extracted rubber using the phenolic peak at  $8.66\tau$  and, as a reference, the IR trialkylethylene  $\text{R}_2\text{C}=\text{CR}-\text{H}$  resonance at  $4.70\tau$ , which is clearly resolved, with no overlapping. Using these two resonances, results for combined phenolic material were obtained as described in Chapter 6, Section 6.3.

In the IR/MP/SnCl<sub>2</sub>·2H<sub>2</sub>O and IR/E/SnCl<sub>2</sub>·2H<sub>2</sub>O interactions combined phenolic contents calculated by this method would be higher than the real ones since some further consumption of the -C=H unsaturation occurs by cyclization. Thus, results as calculated by this method for these interactions are not reliable, both because of gel formation and because of cyclization.

The corrected results for the various interactions are presented in the Experimental Chapter and summarised graphically in Fig. 27. The graph shows changes in moles of phenolic material combined both per mole of rubber and per mole of the total phenolic material, as reaction proceeds. Some kinetic data corresponding to those given for results obtained by acetone extraction above (Table 4) are presented in Table 5. These nmr results show the same general trend as the corresponding ones obtained by acetone extraction with the exception of those for the IR/MP/SnCl<sub>2</sub>·2H<sub>2</sub>O and IR/E/SnCl<sub>2</sub>·2H<sub>2</sub>O interaction products. The latter, as anticipated, gave higher values for combined phenolic matter, presumably for the reasons discussed above. Comparison of the other results with those obtained by acetone extraction show that agreement is generally quite reasonable (see Further Discussion).

(iii) Ir spectroscopy

Ir spectroscopy was used to illustrate the increase of phenolic material combined in the acetone-extracted products

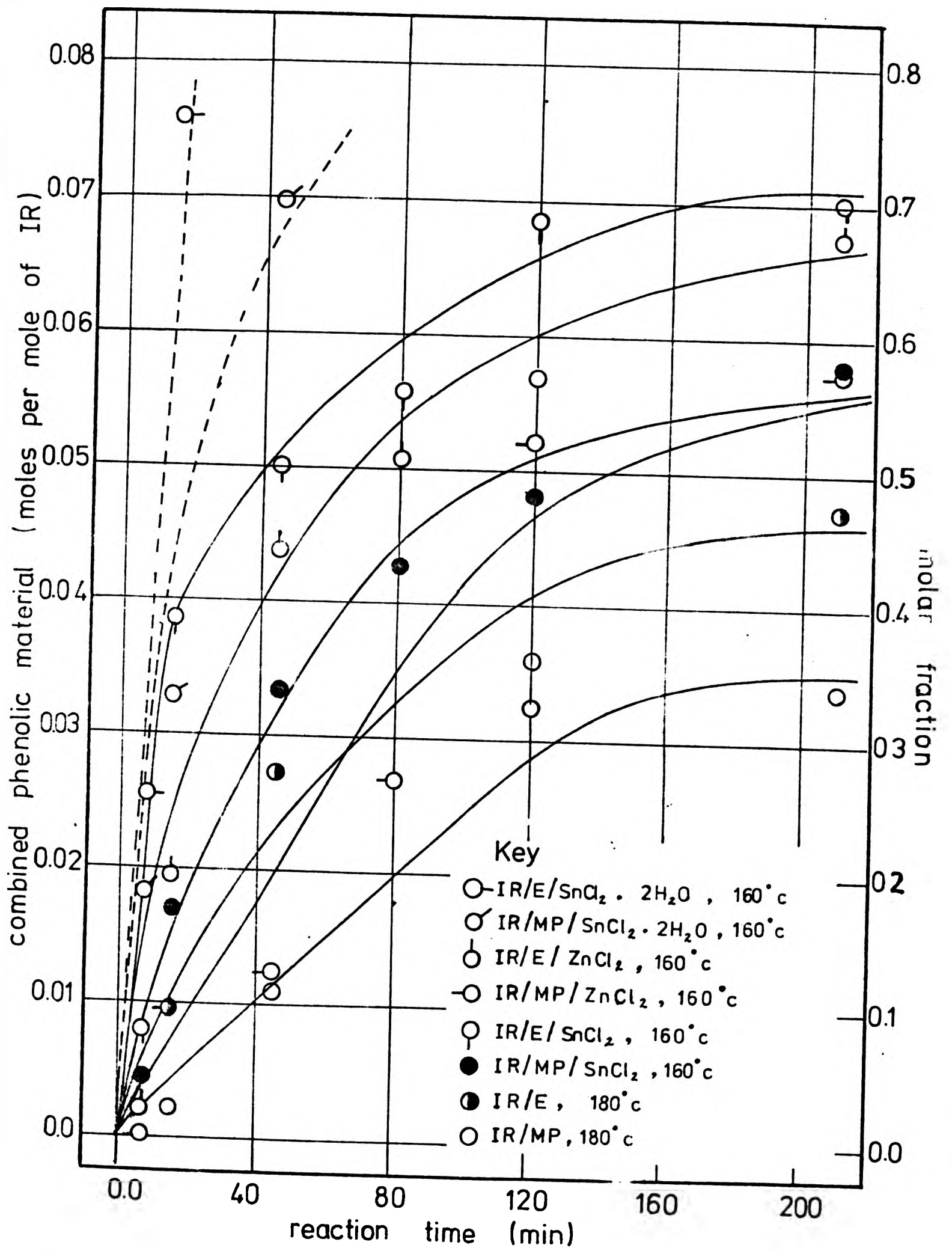


Fig. 27 Kinetics of combination of phenolic material as determined by nmr method.

by a plot of absorbance (A) ratio  $A_{6.7}/A_{7.3}$  against reaction time Fig. 28). The absorption band at  $6.75\mu\text{m}$ , a substituted aromatic ring vibration, was chosen as representative of phenolic material since this band is medium in intensity and is not overlapped (see Section 3.6). The band at  $7.3\mu\text{m}$  is a  $-\text{CH}_3$  deformation vibration and is believed to be little affected by the adduct formation. The results (Fig. 28) follow the same general trend as those obtained by the previous two methods ((i) and (ii) above). An exception is seen in the higher combination rate and ultimate extent of combination in the IR/MP/ $\text{SnCl}_2 \cdot 2\text{H}_2\text{O}$  interaction compared with the IR/E/ $\text{SnCl}_2$  and IR/E/ $\text{ZnCl}_2$  interactions. This might be accounted for by cyclization in the former interaction (see Section 3.6) and/or differences in unextractable phenolic material for which these results were not corrected.

It is emphasised that, due to the absence of known standards for calibration, the ir results are relative to one another and cannot be expressed in absolute terms. It would have been possible to prepare some appropriate standard mixtures for calibration, but this was not done because results would probably have been less reliable than those obtained from the two methods (i) and (ii) above.

(iv) Efficiency of combining of phenolic material

The efficiency (E) of the combination of the phenolic material with rubber is defined as the moles of phenolic material combined per mole of "active" phenolic material consumed

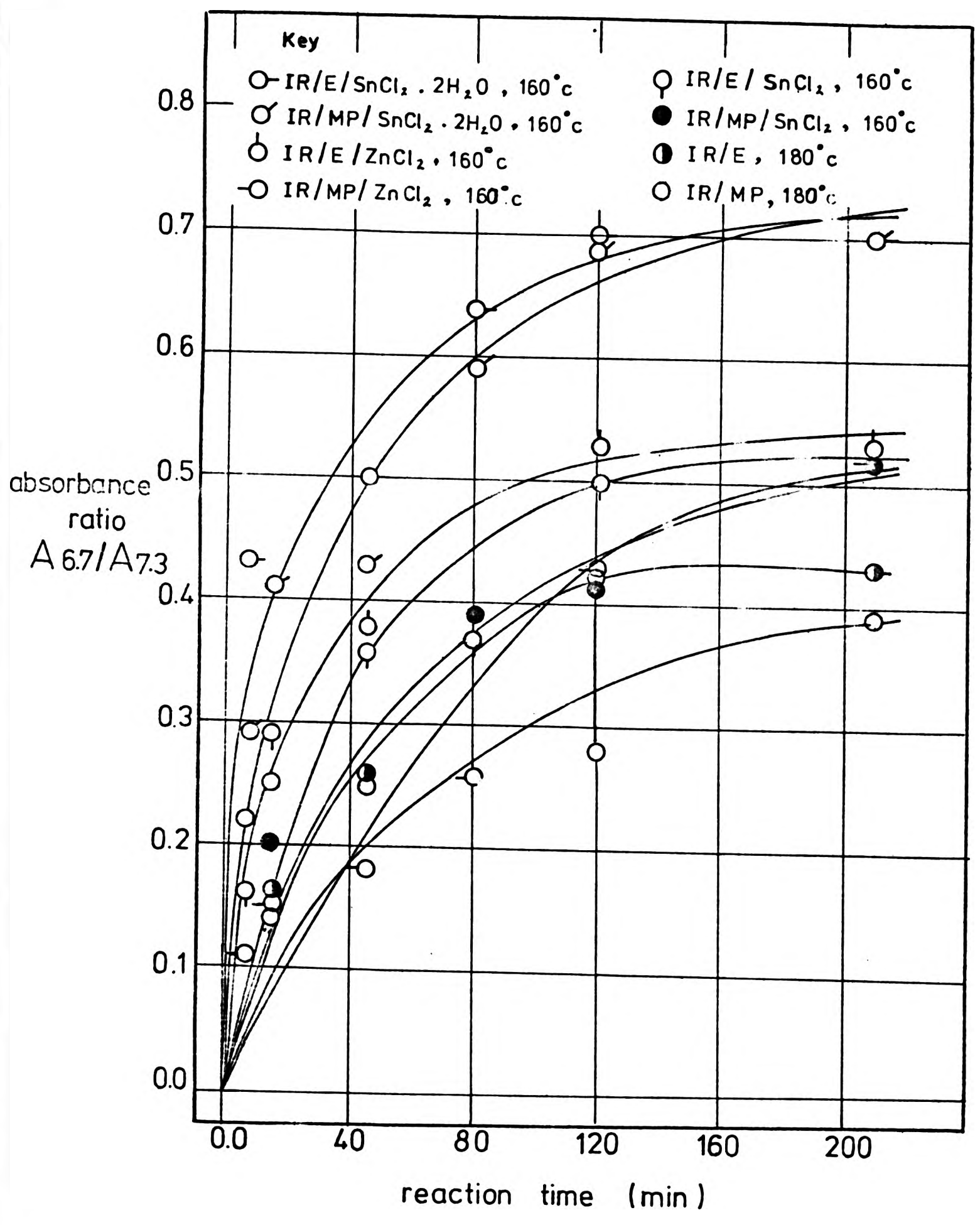


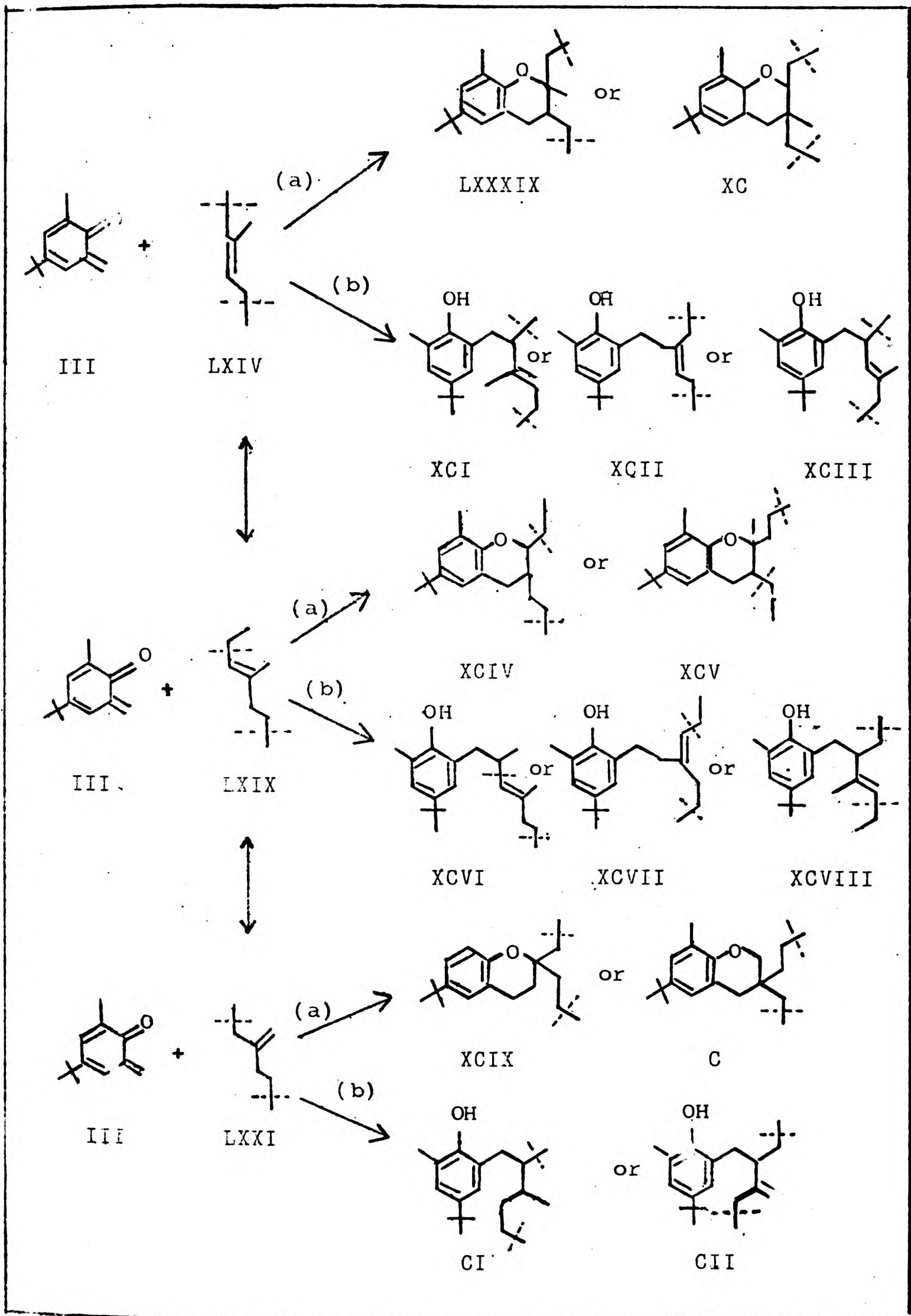
Fig. 28 Illustration of combination of phenolic material with time, using ratio of absorbance (A) of infra-red bands at 6.7 and 7.3  $\mu$ m.

(for this purpose both methylol phenol and dibenzyl ether must be regarded as active material). E will therefore depend not on time but on the extent of side-reactions (e.g., formation of 'inactive' diphenyl methane, trimer, etc.). Clearly, however, if the relative rates of adduct formation and side reactions are dependent upon time then E will be so accordingly.

In this study it was not practicable to estimate the phenolic material consumed and efficiency could not therefore be calculated. However, the values of yield, expressed as the moles of phenolic material combined per mole of "active" starting phenolic material, clearly represent a minimum value of efficiency, the difference between yield and efficiency diminishing as the active phenolic material is gradually consumed. Results for yield were presented in the graphs of Figs. 26 and 27 above.

### 3.6 Nature of the linkage between rubber and phenolic material

As discussed in Chapter 1, two schools of thought have evolved in the literature on the mode of linkage between a phenol-formaldehyde condensate and an alkene. One view considers the linkage to involve a chroman ring, the other a simple methylene bridge. Relating these earlier views to the materials used in the present work, some of the more likely possible structure for the adduct are illustrated in Scheme 3, where routes labelled (a) lead to chroman structure and



Scheme 3 Some possible structures for the adduct formed from methylolphenol and polyisoprene rubber..

routes (b) to methylene bridge structures. There are several feasible chroman adduct isomers from reaction between IR and quinone methide. If reaction between them takes place at the original trialkylethylene double bond LXIV, the isomers conceivable are LXXXIX and XC. If the isoprene reacts in the  $\Delta$ -1,2 isomerised form LXIX structure XCIV or XCV would result. Finally, if the double bond reacts as the 1,1-di-alkylethylene isomer LXXI the isomers XCIX and C could form. The isomer formed in each case would be dependent upon the orientation between reactants, the more likely product being the one with the chroman  $-\text{CH}_2-$  group attached to the least substituted side of the double bond. Since the formation of adducts from a 1-olefin (by analogy with Fitch) is unlikely, formulae XCIX and C (3rd row) are most improbable. This leaves the 2 most likely chroman structures as LXXXIX and XCV. It is possible that methylene bridge formation might be accompanied by double bond shifting resulting in still further possibilities.

It will be noted that several of the formulae in Scheme 3 may display ring conformational and configurational isomerism. Such different stereoisomerism may depend on additions at cis- or trans- double-bonded units but knowledge of these is beyond the scope of the present work.

(a) Earlier studies

Most of the spectroscopic data in the literature relate to the interaction products of p/f condensates with simple

alkenes. In those cases where unsaturated rubbers were vulcanized by bifunctional p/f condensates, because of insolubility of the vulcanizate products, data are restricted to ir spectroscopy. The reported results are discussed exclusively on the basis of the p/f and rubber absorption bands rather than reporting characteristic bands of the chroman ring or methylene bridge structure.

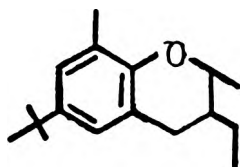
Nmr and ir spectra of some of these earlier interaction products, and those for p/f condensates, are discussed below (nmr and ir spectra of IR have already been discussed in Chapter 2).

(i) Ir spectroscopy

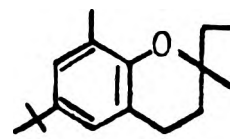
Several investigations<sup>42,100-102</sup> established that, in the spectrum of p/f condensates, the band at  $10\mu\text{m}$  represents a bond-stretching vibration of the C-O bond of the methylol group, the band near  $8.0\mu\text{m}$  is a deformation vibration of OH bonds together with a bond-stretching vibration of C-O bonds, the broad band at  $2.7-3.2\mu\text{m}$  is an O-H bond-stretching vibration of combined hydroxyl groups. Bands of moderate intensity in the 6 to  $7\mu\text{m}$  region and between 11 and  $13.50\mu\text{m}$  have been attributed to substituted benzene nuclei and the band near  $9.6\mu\text{m}$  to the methylene ether bridge.<sup>103</sup> The latter band in the dibenzyl ether of this work has been reported<sup>11</sup> to occur at  $9.4\mu\text{m}$ .

In Fitch's work<sup>11</sup> on the reactions of the methylolphenol with 2-methylpent-2-ene and 2-methylpent-1-ene, there are

clearly various possible chroman and methylene bridge structures which might be produced, analogous to those of the 1st and 3rd rows in Scheme 3, suggested as being possible in this present work. However, Fitch found only the chroman XXXII (analogous to structure LXXXIX of Scheme 3); other structures, if present, were in undetectable quantities.



XXXII



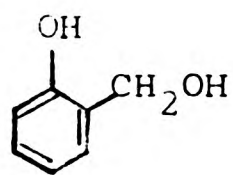
CIV

The characteristic absorption band of this internal chroman ring was reported by Fitch to occur at 10.5  $\mu\text{m}$ ; the hydroxyl (2.3  $\mu\text{m}$ ) or alkenic double bond (12.0  $\mu\text{m}$ ) absorptions were completely absent. Diagnostic peaks for the 'external' chroman CIV (synthesised by another method) were reported<sup>11</sup> to occur at 10.3 and 11.0  $\mu\text{m}$ , again with no hydroxyl or ethenyl double bond (11.2  $\mu\text{m}$ ) absorptions detectable. It would appear that there is very little hope of identifying the type of chroman formed in the present work, in view of the number possible. However, the absence of phenolic OH absorptions and the presence of a band near 10.5  $\mu\text{m}$  may reliably indicate the presence of a chroman. The observation by Fitch that the 1-alkene did not react would appear to make the chromans of the 3rd row in Scheme 3 very unlikely.

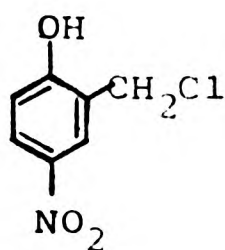
(ii) Nmr spectroscopy

In the spectra of p/f condensates the aryl protons (Ar H's) have been reported as a broad band near  $3.0\tau$ , while the hydroxyl phenolic protons (ArOH) resonance appears near  $3.3\tau$ <sup>104,105</sup>. The latter resonance is very variable in position, depending upon the sample temperature, solvent, and concentration of the solution. Under some circumstances it may not be observed because it falls outside the 0 to  $10\tau$  region. Methylene protons of the methylol group ( $-\overset{*}{\text{C}}\text{H}_2\text{OH}$ ) and those of the methylene ether bridge ( $-\overset{*}{\text{C}}\text{H}_2-\text{O}-\overset{*}{\text{C}}\text{H}_2-$ ) have been reported in the  $5.0$  to  $5.7\tau$  region.<sup>104,105</sup> Assignments for resonance for the methylolphenol and the ether (in  $\text{CDCl}_3$ ) have been reported<sup>11</sup> as follows:  $8.8\tau$  ( $-\text{C}(\text{CH}_3)_3$ ),  $7.8\tau$  (Ar- $\text{CH}_3$ ),  $5.2\tau$  ( $-\overset{*}{\text{C}}\text{H}_2-\text{OH}$ ),  $3.2$  and  $2.9\tau$  (ArH's),  $5.3\tau$  ( $\text{CH}_2-\text{O}-\text{CH}_2$ ),  $4.0\tau$  (ArOH).

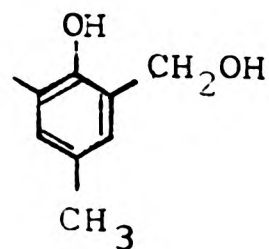
In Fitch's work<sup>11</sup> resonances for the internal chroman XXXII have been listed as follows:  $9$  and  $8.9\tau$  ( $\overset{\text{CH}_3}{\text{C}}-\text{C}-$ ),  $8.78\tau$  ( $\text{C}(\text{CH}_3)_3$ ),  $8.6\tau$  ( $\overset{*}{\text{C}}\text{H}_3-\text{CH}_2$ ),  $8.4\tau$  ( $\text{C}-\overset{\text{CH}_3}{\text{C}}-\text{C}$ ),  $8.3\tau$  ( $\text{C}-\overset{\text{C}}{\text{C}}-\text{C}$ ),  $7.9\tau$  (Ar- $\text{CH}_3$ ),  $7.3\tau$  (Ar- $\text{CH}_2-\text{C}$ ), and  $3.1\tau$  (ArH's). Chroman derivatives have been reported<sup>29</sup> from reaction between 2-methylolphenol (CV) or 2-chloromethyl-4-nitrophenol (CVI) and various simple alkenes i.e., trans-1-methyl-2-phenyl ethylene, cyclohexene, 1-heptene, cis-2-pentene and norbornene. Chromans were represented by the structures CVIII and CIX, where  $\text{R}_1$ ,  $\text{R}_3$  and  $\text{R}_4$  depend on the particular alkene used, but only the OCH proton resonance was reported, occurring as a multiplet between  $5.50$  and  $6.10\tau$ .



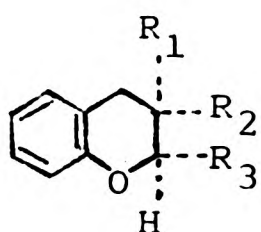
CV



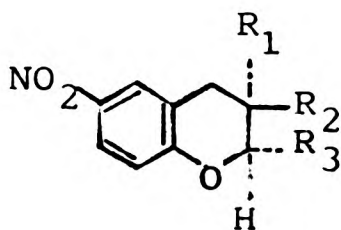
CVI



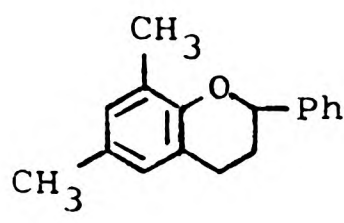
CVII



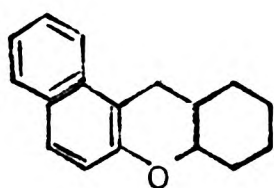
CVIII



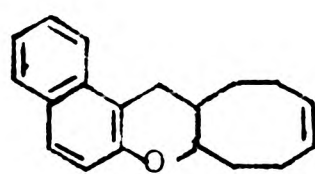
CIX



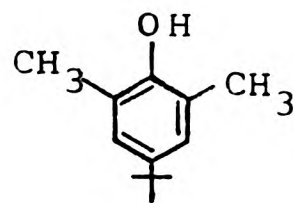
CX



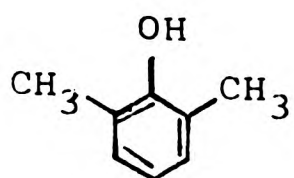
CXI



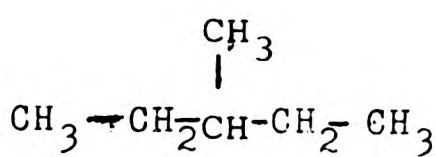
CXII



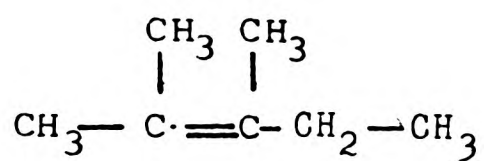
XXIX



CXIII



CXIV



CXV

Resonances (in  $\text{CDCl}_3$ ) assigned for the chroman CX reported<sup>26</sup> as a product from the reaction between 2-hydroxymethyl-4,6-dimethyl phenol CVII and styrene, were: 8.34 $\tau$  (d, J 7 Hz,  $\text{CH}\cdot\text{CH}_3$ ), 8.00 $\tau$  (s, 6- $\text{CH}_3$ ), 7.82 $\tau$  (s, 8- $\text{CH}_3$ ), 7.2-7.9 $\tau$  (m,  $\text{CH}_2\cdot\text{CH}_2$ ), 5.45 $\tau$  (s, J 7 Hz, CHMe), 5.03 $\tau$  (dd, J3 and 10Hz, O.CH. $\text{CH}_2$ ), 3.12 $\tau$  (7-H), and 2.8 $\tau$  (m,  $\text{C}_6\text{H}_5$ ). The synthesis of several chroman derivatives from the reaction between naphthoquinone methides with alkenes has been reported<sup>28</sup>. The resonance assignments suggested for two of these chromans, CXI and CXII, were listed as follows: CXI, 5.80 $\tau$  (m, CHO) and bands corresponding to the methylenic protons of an ABX system at 6.91 $\tau$  (dd, J7 and 17 Hz) and 7.24 $\tau$  (dd, J3 and 17Hz); CXII, 4.4 $\tau$  (m, vinylic protons), 5.61 $\tau$  (td, J 8 and 2Hz, OCH), 6.84 $\tau$  (dd, J15 and 7Hz; one proton of ABX system  $\text{ArCH}_2\cdot\text{CH}$ ), the others being overlaid).

(b) Results of the present study

(i) Ir spectroscopy

(i-a) Uncatalysed interactions

Infrared spectra of IR before and after heating at 180°C for various times with methylol phenol and dibenzyl ether are presented in Figs. 32 and 33, respectively. The more important changes in the spectrum of both the IR/MP and IR/E interaction products as reaction proceeds are (1) the development of new bands at 6.2, 6.7, 8.2, 10.5, 11.5 and

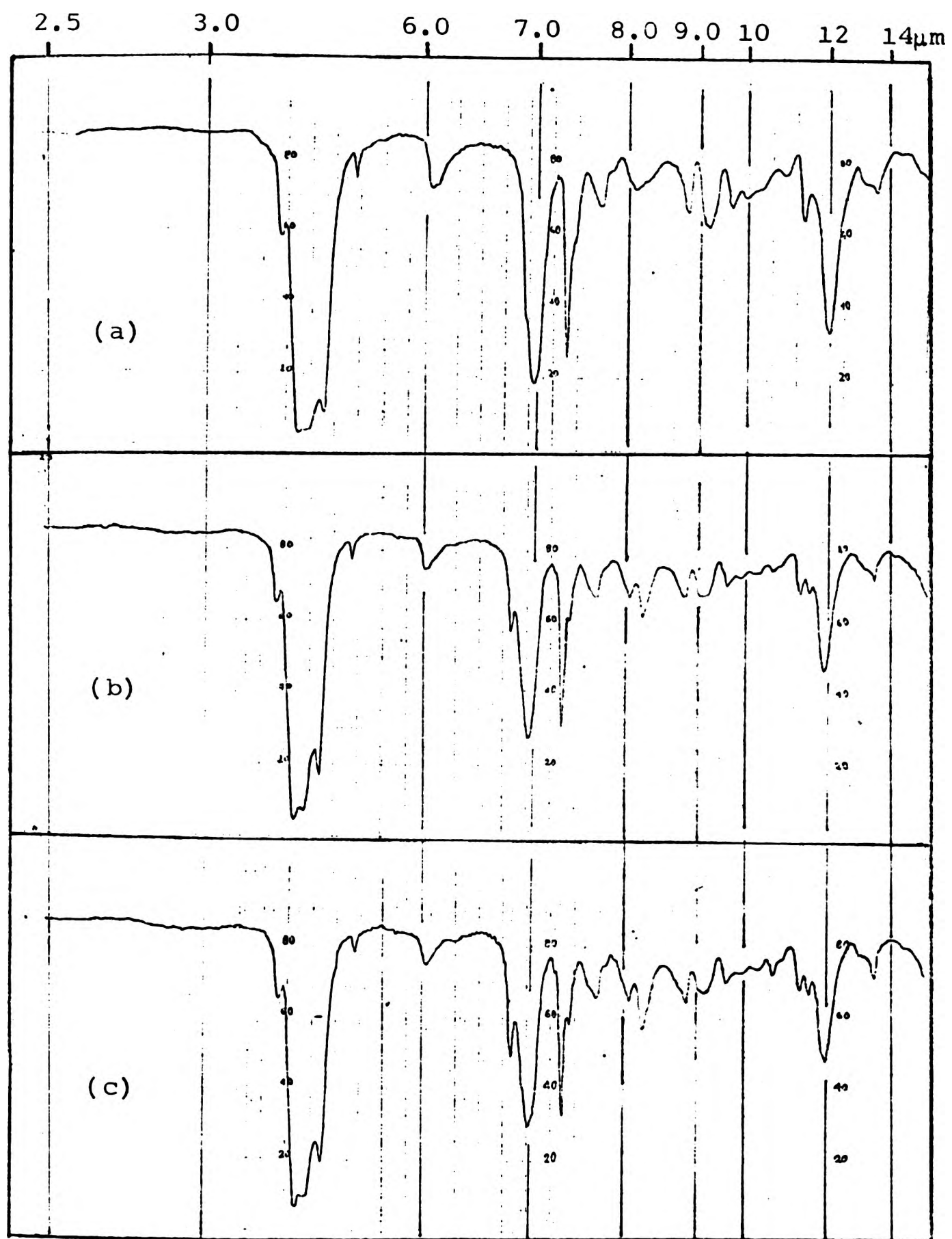


Fig. 32 Infra-red spectra of IR/MP products heated at  $180^{\circ}\text{C}$  for various times: (a) 0 min; (b) 45 min; (c) 210 min.

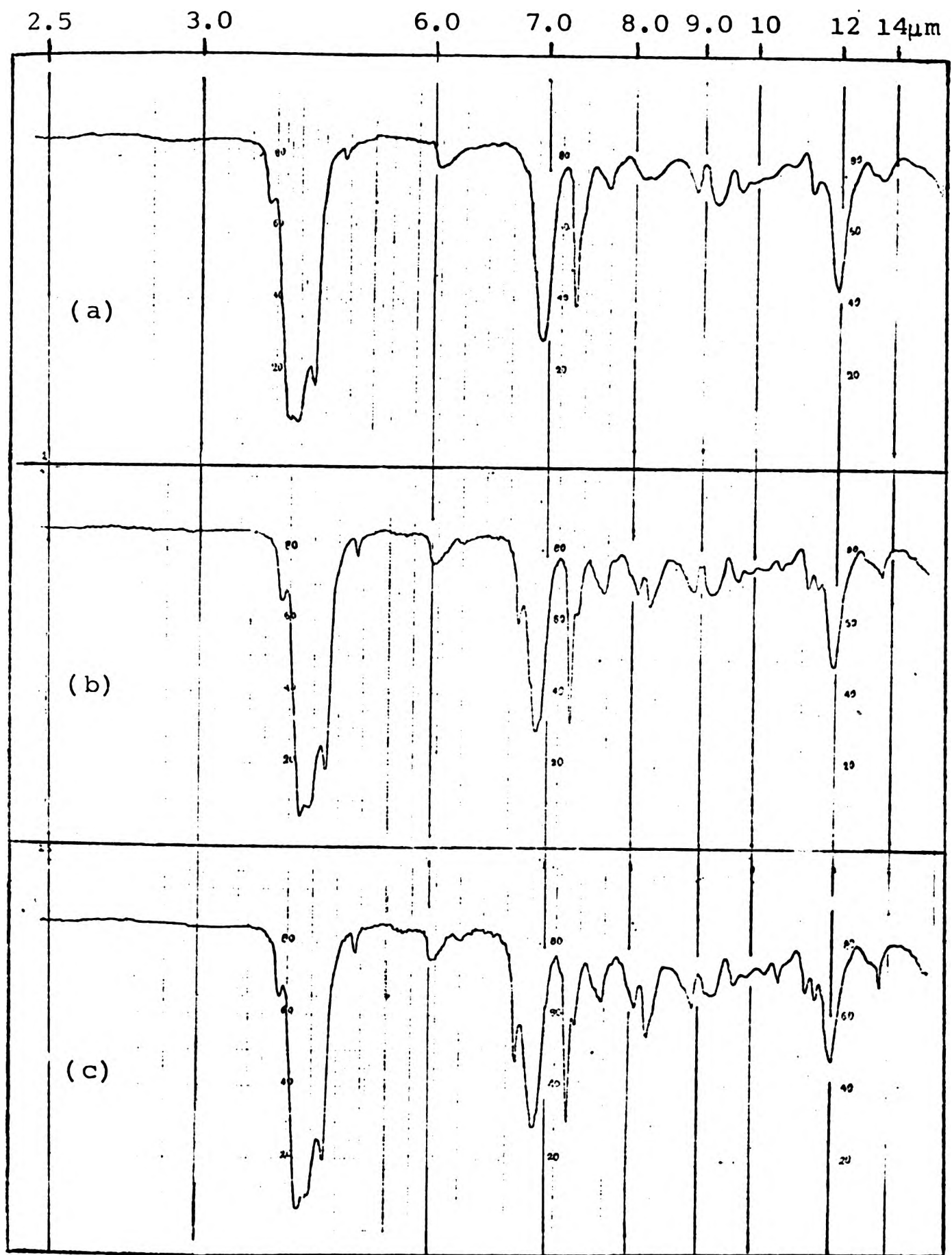


Fig. 33 Infra-red spectra of IR/E products heated at 180°C for various time: (a) 0 min; (b) 45 min; (c) 210 min.

(very weak) at 2.7-3.2 $\mu$ m), (2) a increase in intensity of the 13.5 $\mu$ m band, and (3) a very slight reduction in intensity of the 12.0 $\mu$ m band. The development of bands at 6.25, 6.7 and 11.5 $\mu$ m, and the increase in intensity of the 13.5 $\mu$ m band show the presence of substituted benzene nuclei. The band at 2.7-3.2 $\mu$ m corresponding to combined hydroxyl (OH) is hardly detectable. This band does not increase as reaction proceeds, unlike those bands assigned to aromatic nuclei and it is therefore suggested that traces of -OH compounds are present as impurity. Ir spectra of methylene bridge or closely-similar structures do not appear to have been reported in the literature. However, because of its structural similarity to the various methylene bridge structures (Scheme 3), 2,6-dimethyl-4-tert butyl-phenol XXIX might be expected to show similar absorptions, at least in respect of the OH group and the aromatic substitution pattern. This compound (spectrum in Chapter 6, Fig. 107 shows a weak band at 10.5 $\mu$ m, a position which has also been reported<sup>11</sup> as diagnostic for the chroman ring XXXII. However, despite this uncertainty, the fact that in the present study the hydroxyl band (2.7-3.2 $\mu$ m), suggested to be caused by impurity, is less sharp and in a different peak position to that of the model XXIX, indicates that the band at 10.5 $\mu$ m might with confidence be assigned to the chroman ring, e.g., LXXXIX. Although a band also occurs in this position in the methylolphenol (Fig. 107), Chapter 6), all free methylolphenol has been removed by extraction. The peak thus attributed to chroman is small, but increases noticeably with reaction time. The band at 8.22 $\mu$ m, in the absence of

OH groups, might be assigned to a C-O stretching vibration in a chroman structure. This band may be observed in internal chroman XXXII reported by Fitch<sup>11</sup> (Fig. 108, Chapter 6). The reduction in intensity of the 12 $\mu$ m band is a further indication of chroman formation, since trialkyl-ethylenic double bonds are consumed.

(i-b) Catalysed interactions

Infrared spectra of the extracted products from IR before and after heating at 160<sup>o</sup>C for various times with methylolphenol and dibenzyl ether in the presence of the catalysts ZnCl<sub>2</sub>, SnCl<sub>2</sub> and SnCl<sub>2</sub>.2H<sub>2</sub>O are presented in Figs. 34 to 39. In general, the changes in the spectrum as reaction proceeds are in all cases the same as those described for the uncatalysed interactions above. Some significant new features appear, however: (i) in the SnCl<sub>2</sub>.2H<sub>2</sub>O - catalysed reactions, the reduction in intensity of the 12.0 $\mu$ m band is much greater than observed in the uncatalysed reaction, whereas the other catalysts produce only about the same, slight, reduction; (ii) a band due to -OH at 2.8-3.1 $\mu$ m is now rather more noticeable, being most pronounced in the SnCl<sub>2</sub>.2H<sub>2</sub>O products, less in the SnCl<sub>2</sub> products, and hardly detectable in the ZnCl<sub>2</sub> ones; (iii) in the products with SnCl<sub>2</sub>.2H<sub>2</sub>O as catalyst, the band near 6 $\mu$ m due to unsaturation is very much reduced, and a shoulder at 6.1 $\mu$ m becomes more noticeable. These observations may be interpreted as follows:-

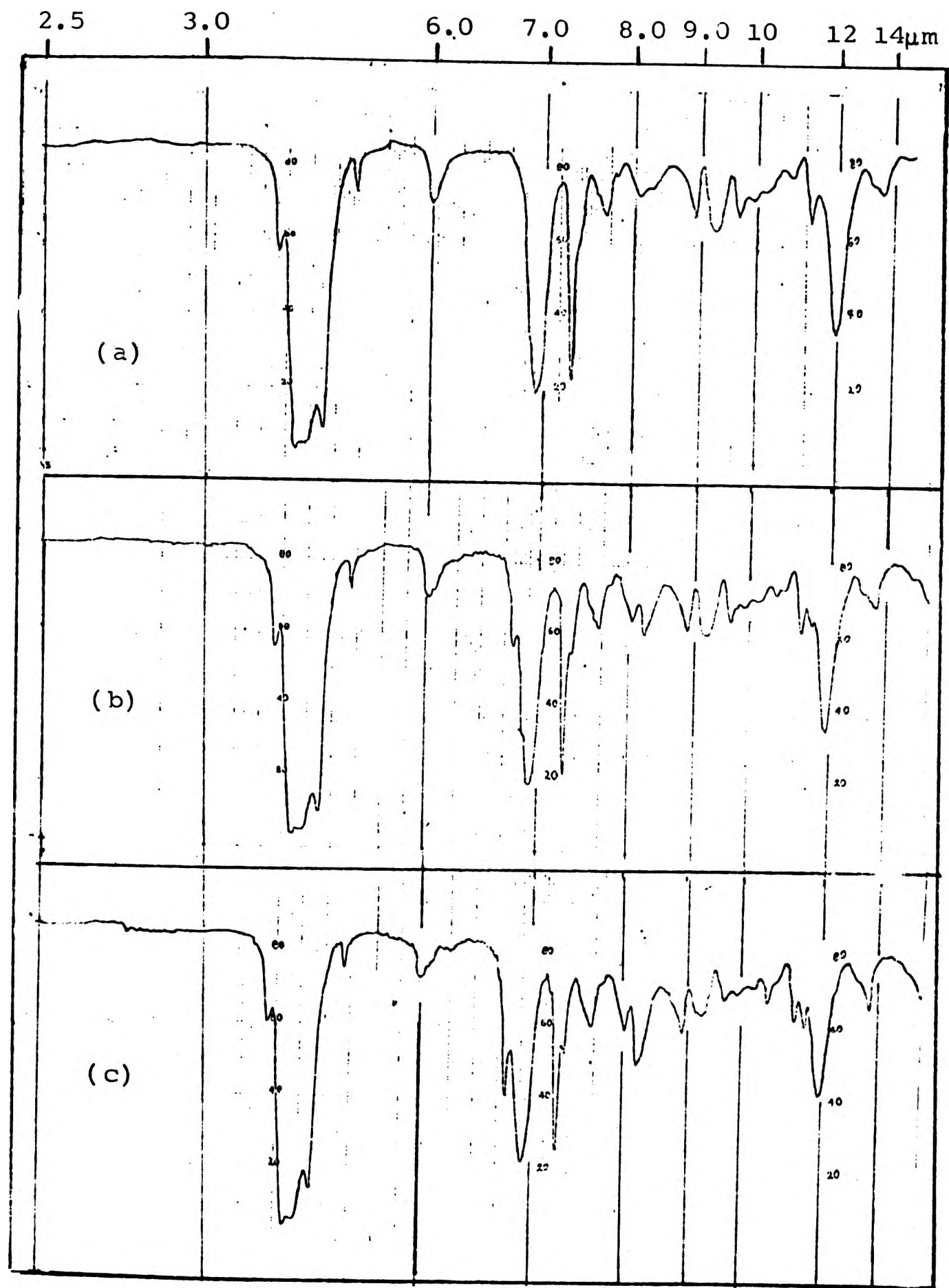


Fig. 34 Infra-red spectra of IR/MP/ZnCl<sub>2</sub> products heated at 150°C for various times: (a) 0 min; (b) 45 min; (c) 210 min.

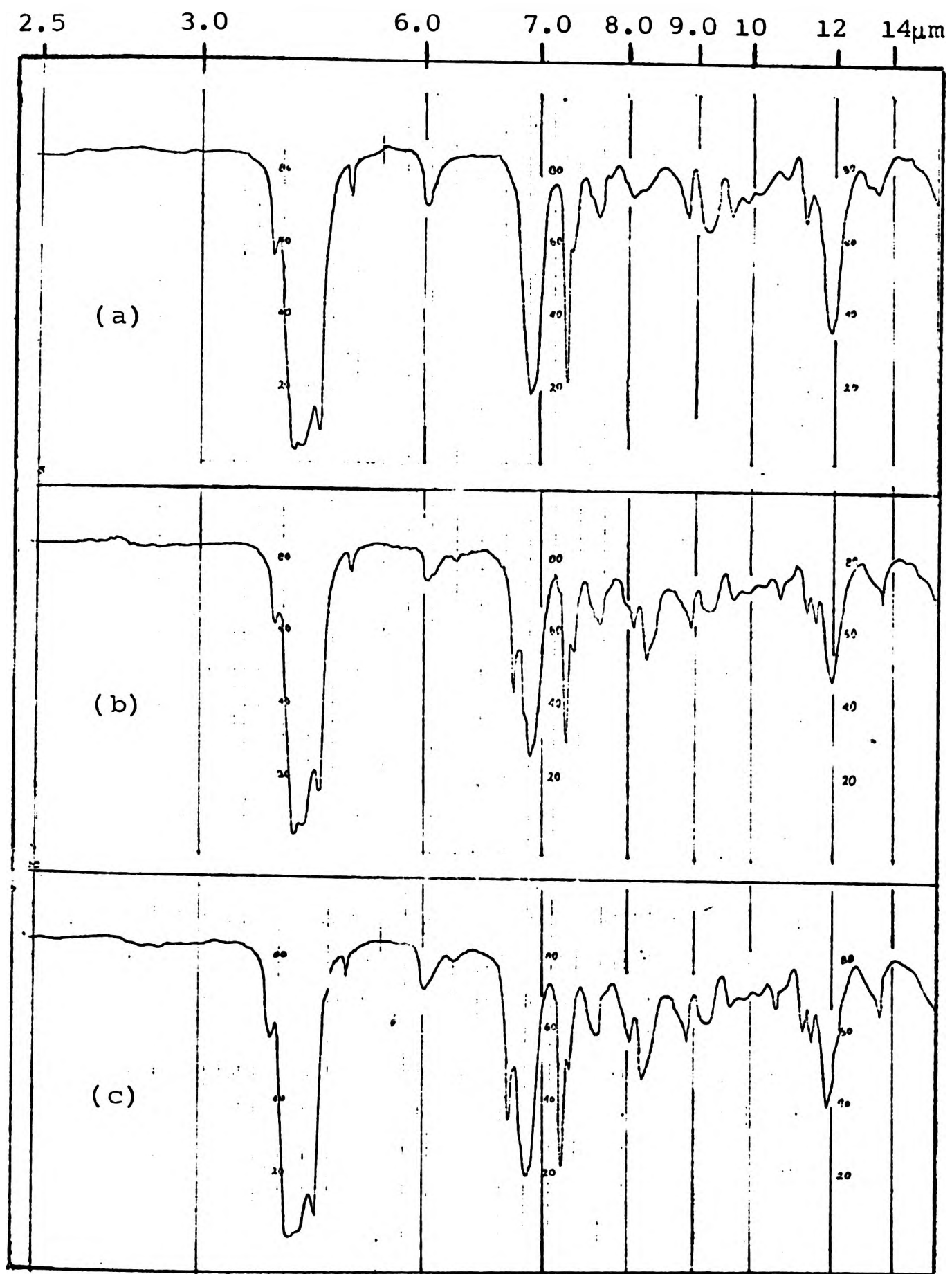


Fig. 35 Infra-red spectra of IR/E/ZnCl<sub>2</sub> products heated at 160°C for various times: (a) 0 min; (b) 45 min; (c) 210 min.

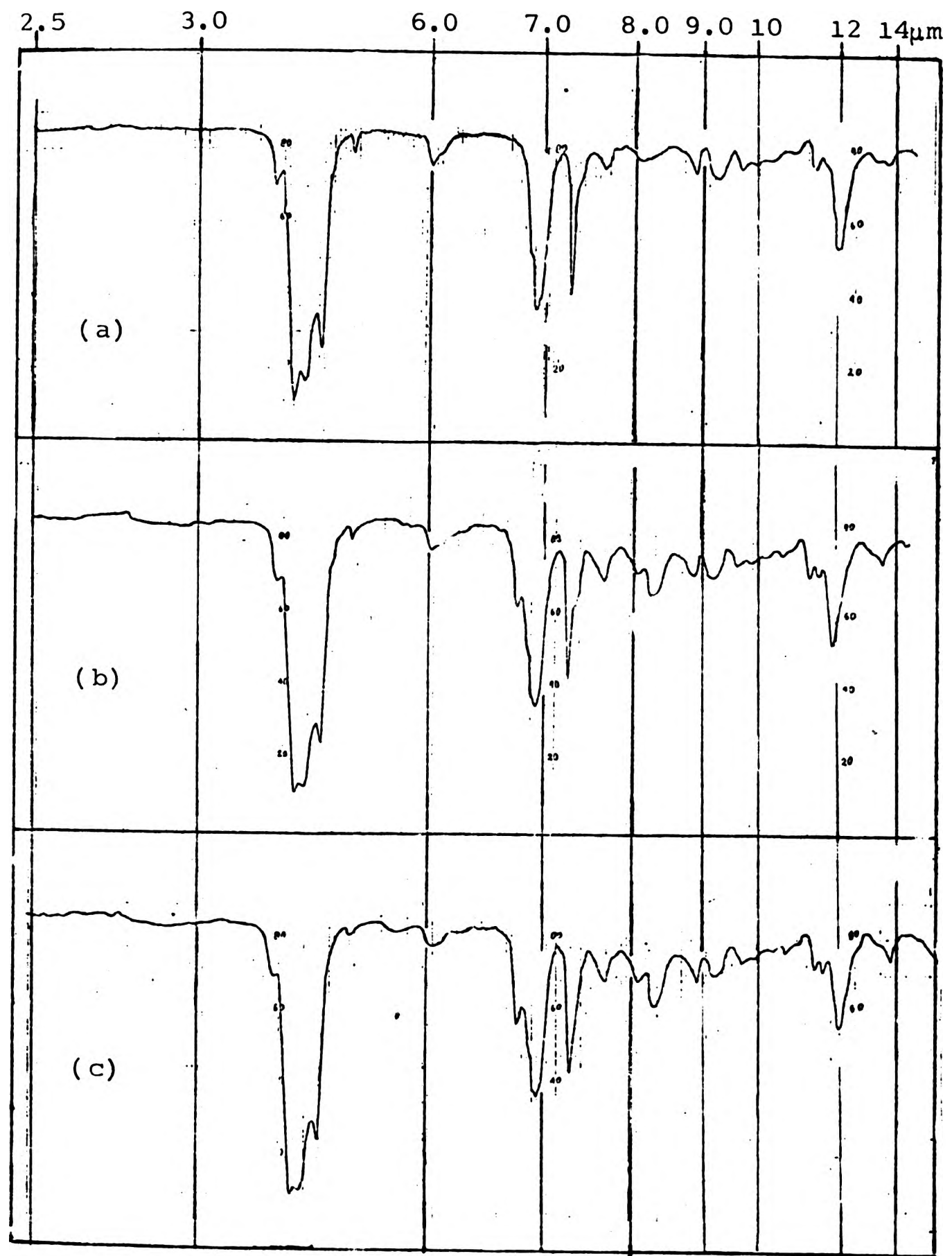


Fig. 36 Infra-red spectra of IR/MP/SnCl<sub>2</sub> products heated 160°C for various times: (a) 0 min; (b) 45 min; (c) 210 min.

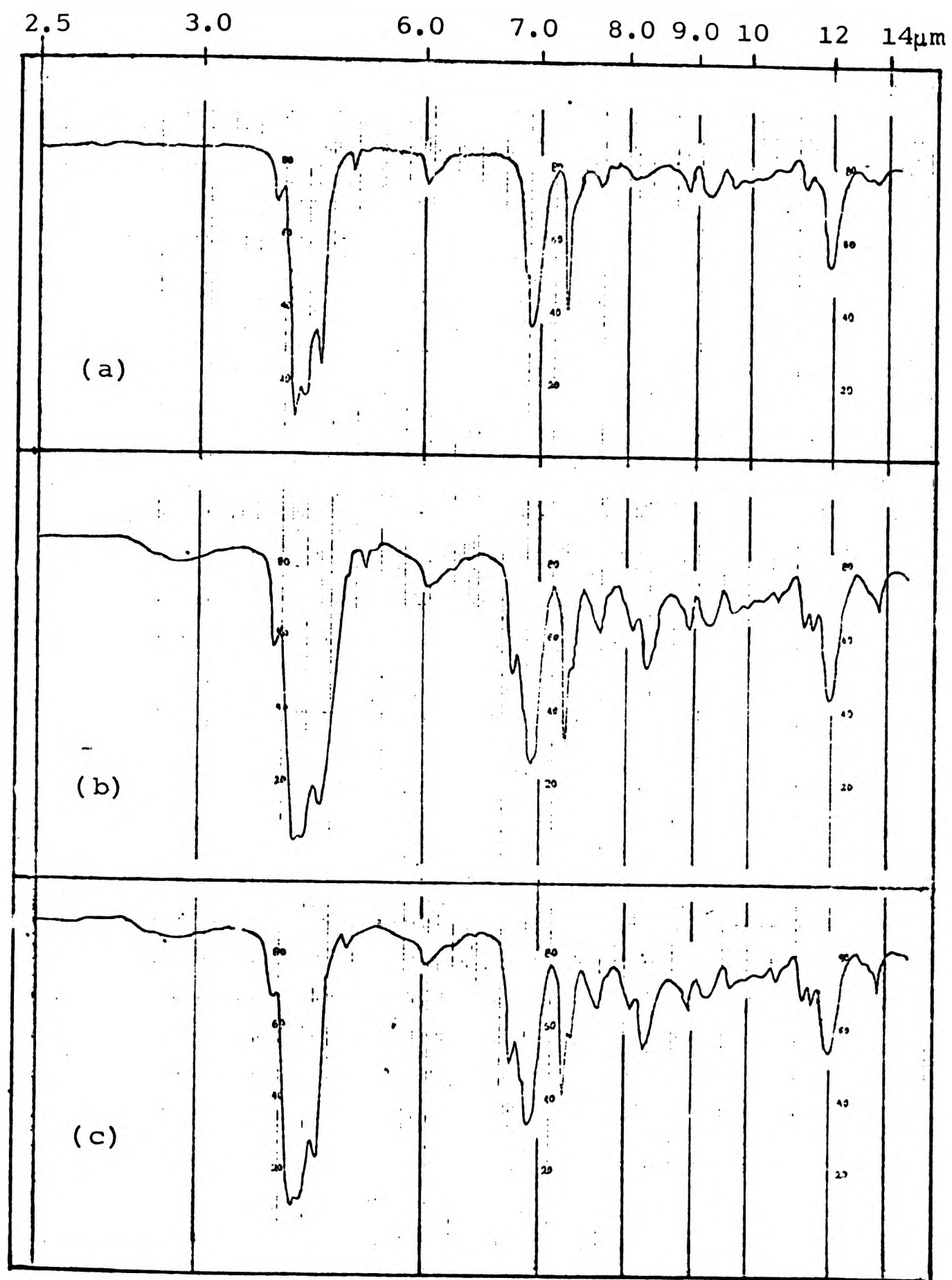


Fig. 37 Infra-red spectra of IR/E/SnCl<sub>2</sub> products heated at 160°C for various times: (a) 0 min; (b) 45 min; (c) 210 min.

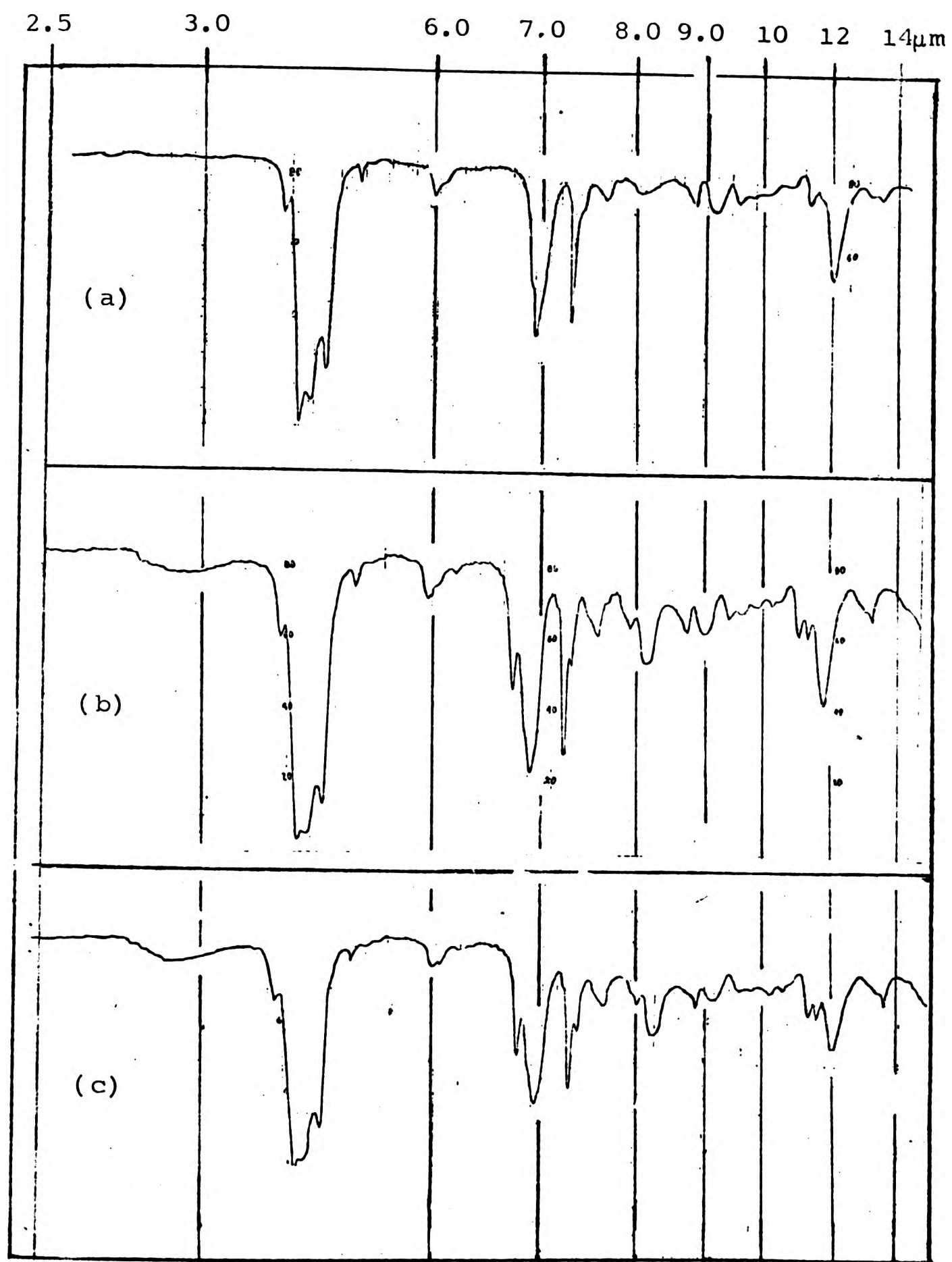


Fig. 38 Infra-red spectra of IR/MP/SnCl<sub>2</sub>·2H<sub>2</sub>O products heated at 160°C for various time: (a) 0 min; (b) 45 min; (c) 210 min.

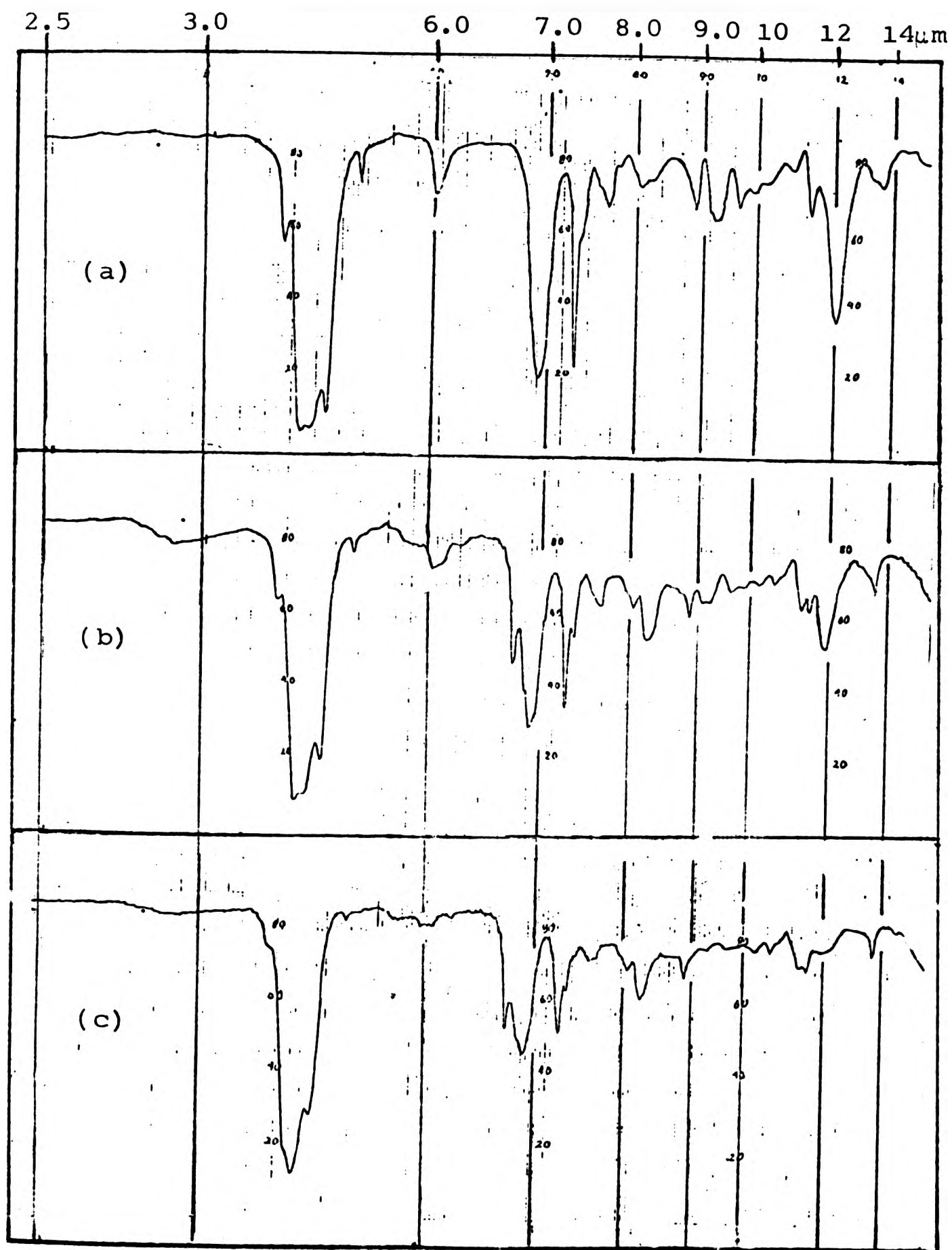


Fig. 39 Infra-red spectra of IR/E/SnCl<sub>2</sub>·2H<sub>2</sub>O products heated at 160°C for various times: (a) 0 min; (b) 45 min; (c) 210 min.

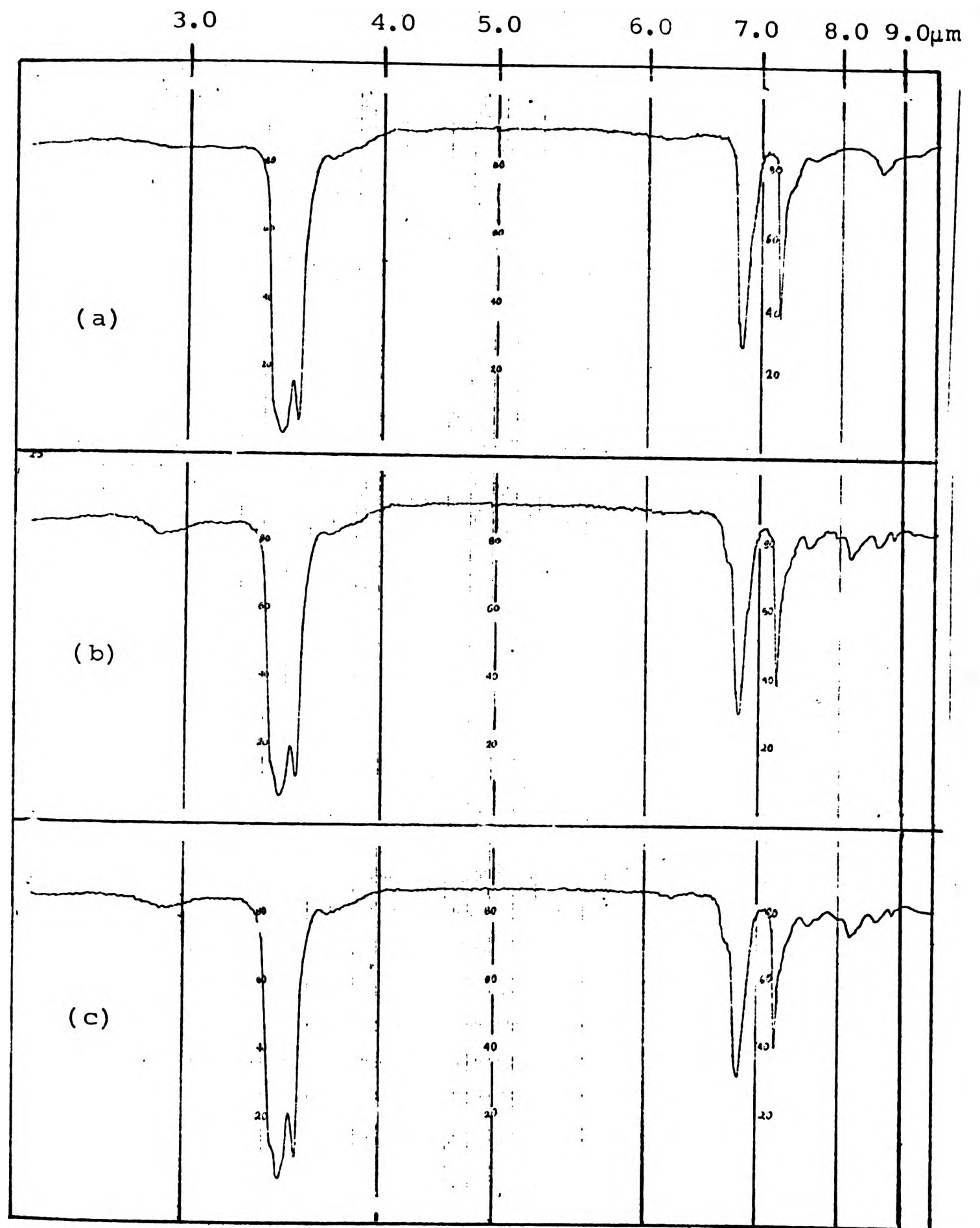


Fig. 40 Infra-red spectra of EPR/MP products heated at  $180^{\circ}\text{C}$  for various times: (a) 0 min; (b) 45 min; (c) 210 min.

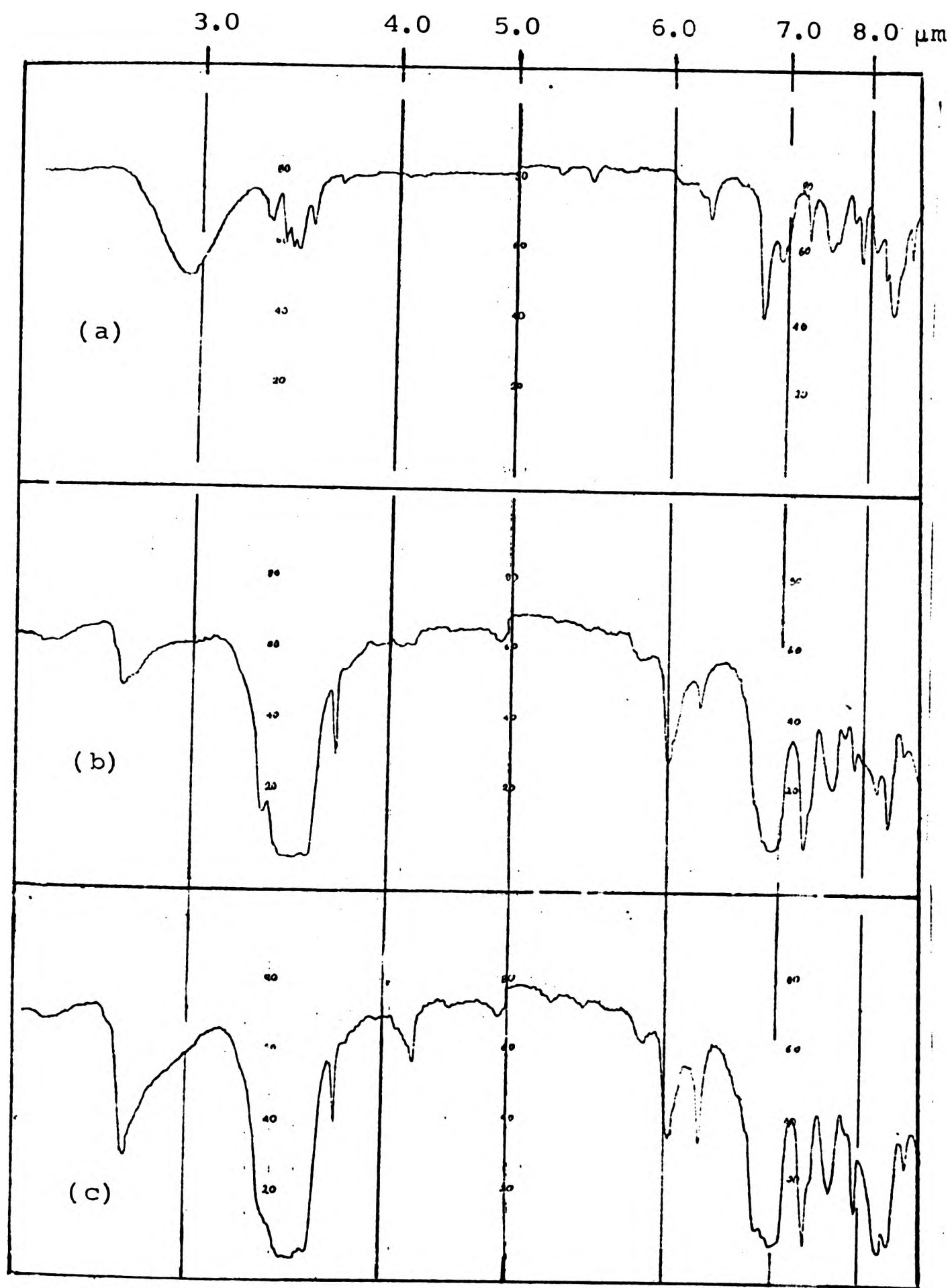


Fig. 41 Infra-red spectra of the hydroxyl calibration IR/2,6 dimethyl phenol for various concentration (% in mols): (a) 2,6 dimethyl phenol; (b) 3.30% (c) 6.0%.

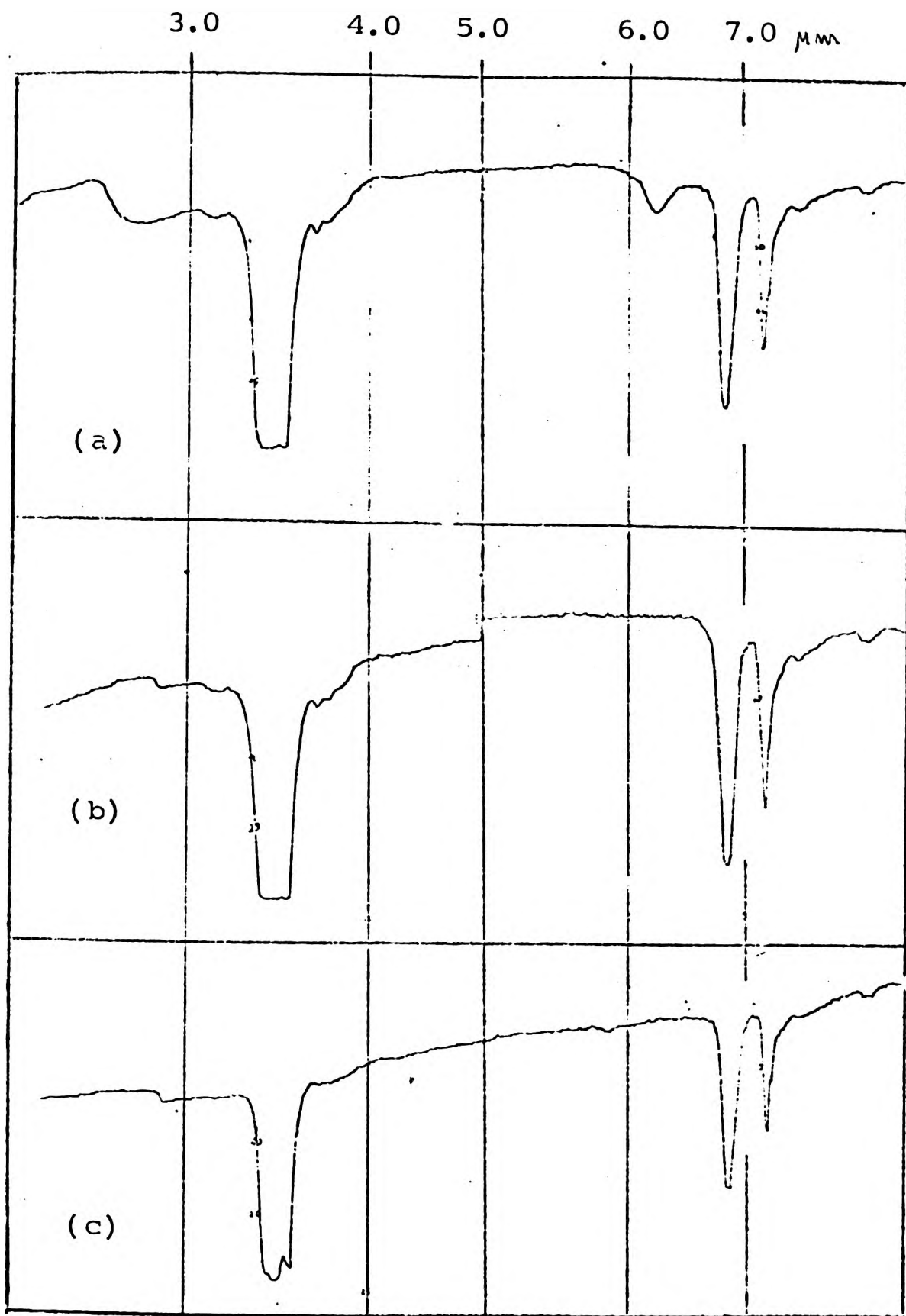


Fig. 41-i Infra-red spectra of: (a)  $\text{SnCl}_2 \cdot 2\text{H}_2\text{O}$ ;  
 (b) hydrolysed product of  $\text{SnCl}_2 \cdot 2\text{H}_2\text{O}$ ;  
 (c) hydrolysed product of  $\text{SnCl}_2$ .  
 (all 3% in liquid paraffin)

Spectral changes in the  $\text{SnCl}_2$ - and  $\text{ZnCl}_2$ - catalysed reactions are virtually the same as in the uncatalysed ones, and the same conclusions regarding chroman formation may therefore be drawn.

The differences in the unsaturation vibration bands for the  $\text{SnCl}_2 \cdot 2\text{H}_2\text{O}$  case, noted under (i) and (iii) above, are fully consistent with the occurrence of isomerization reactions. Thus, the reduction in intensity of unsaturation bands at  $6.0 \mu\text{m}$  and  $12.0 \mu\text{m}$  illustrates the consumption of double bonds by cyclization, as discussed in Chapter 2. The retention of the absorption at  $11.3 \mu\text{m}$  (and, possibly, at  $6.1 \mu\text{m}$ ) would appear to suggest that 1,1-dialkylethylenic double bonds are not consumed in this process.

Closer examination of the spectra in the  $\text{SnCl}_2 \cdot 2\text{H}_2\text{O}$  cases shows that cyclization (as seen by loss of unsaturation) is apparently much higher with the ether than with the methylol phenol. This accords with the greater  $T_g$  increase in the former case (Fig. 58), although the spectral differences are surprisingly large considering the rather modest nature of the  $T_g$  increase. The development of the band at  $10.5 \mu\text{m}$  in all cases suggest chroman formation. Difference (ii), suggesting the presence of hydroxyl groups in some products, might be taken as indicative of the presence of methylene bridge structures, at least for those interactions catalysed by  $\text{SnCl}_2$  and  $\text{SnCl}_2 \cdot 2\text{H}_2\text{O}$ . However, the hydroxyl band in these interactions might alternatively be due to unextractable phenolic or catalyst material. A

critical examination of those spectra showing -OH absorption suggests that there is a maximum in its concentration at some stage during the reaction. This is particularly noticeable in the IR/E/SnCl<sub>2</sub>.2H<sub>2</sub>O case where the maximum is seen at about 15 min. reaction time. This would lead one to suspect that the hydroxyl is due to an intermediate catalyst decomposition or hydrolysis product rather than the formation of a methylene bridge structure (which would not be expected to lose its -OH subsequently).

Ir spectra of the interaction products catalysed by SnCl<sub>2</sub> and ZnCl<sub>2</sub> are very similar, with the exception that the intensity of the hydroxyl bands, though noticeable in the former case is hardly detectable in the latter. These considerations are discussed further in a later section.

(ii) Nmr spectroscopy

(ii-a) Uncatalysed interactions

Nmr spectra of IR before and after heating at 180°C for various times with methylol phenol and dibenzyl ether are presented in Figs. 42 and 43, respectively. The most pronounced change in the spectrum of both products as reaction proceeds is the development of a new peak at 8.66τ (which may be assigned to -C(CH<sub>3</sub>)<sub>3</sub>). Accompanying this change, new peaks also appear at 7.60τ and (very weak) at 8.7τ and near 9τ. No apparent reduction in intensity of the -CH= protons (4.6τ) was observed (this is considered

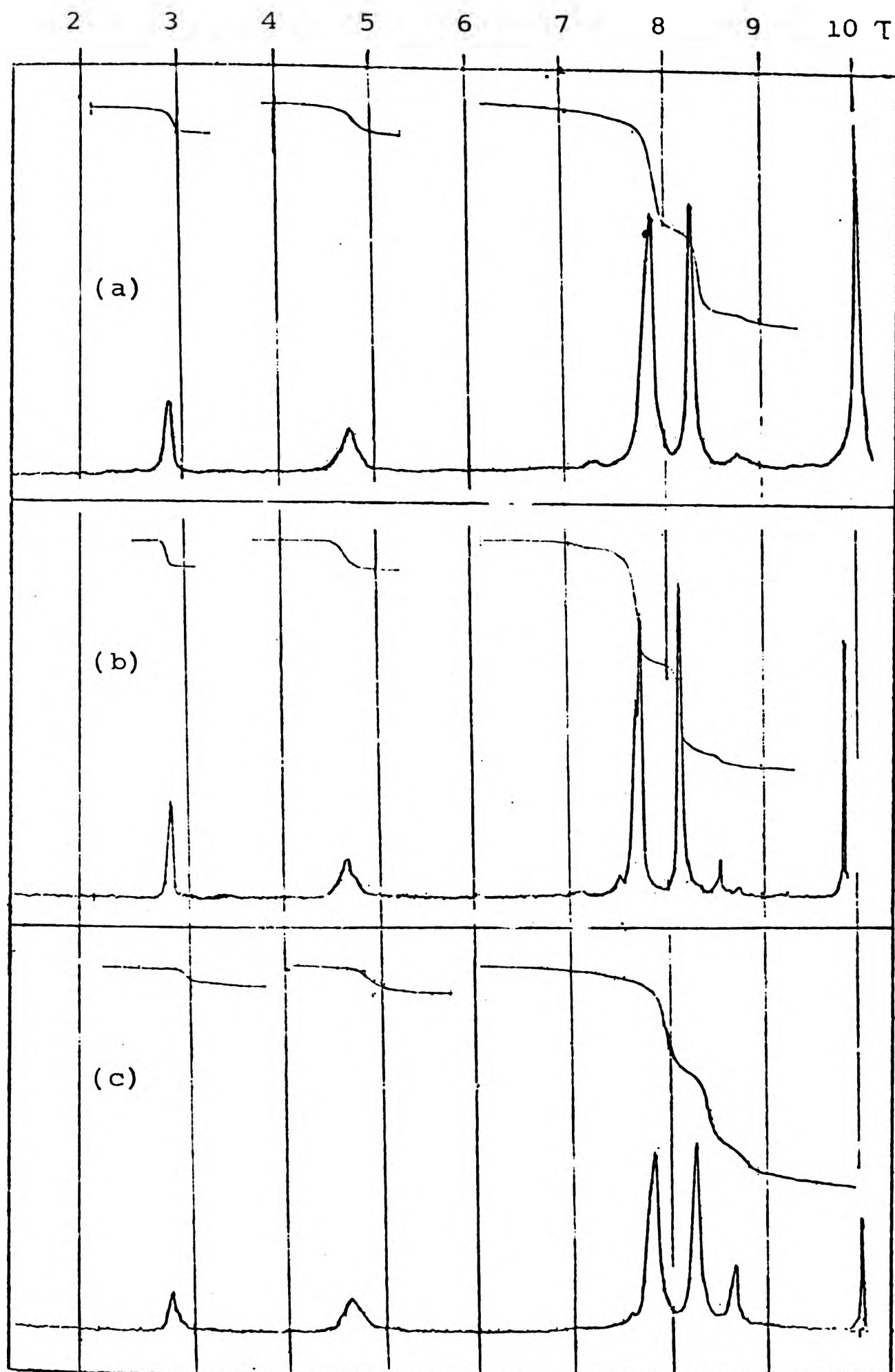


Fig. 42 Nuclear magnetic resonance spectra of IR/MP products heated at 180°C for various times: (a) 0 min; (b) 45 min; (c) 210 min.

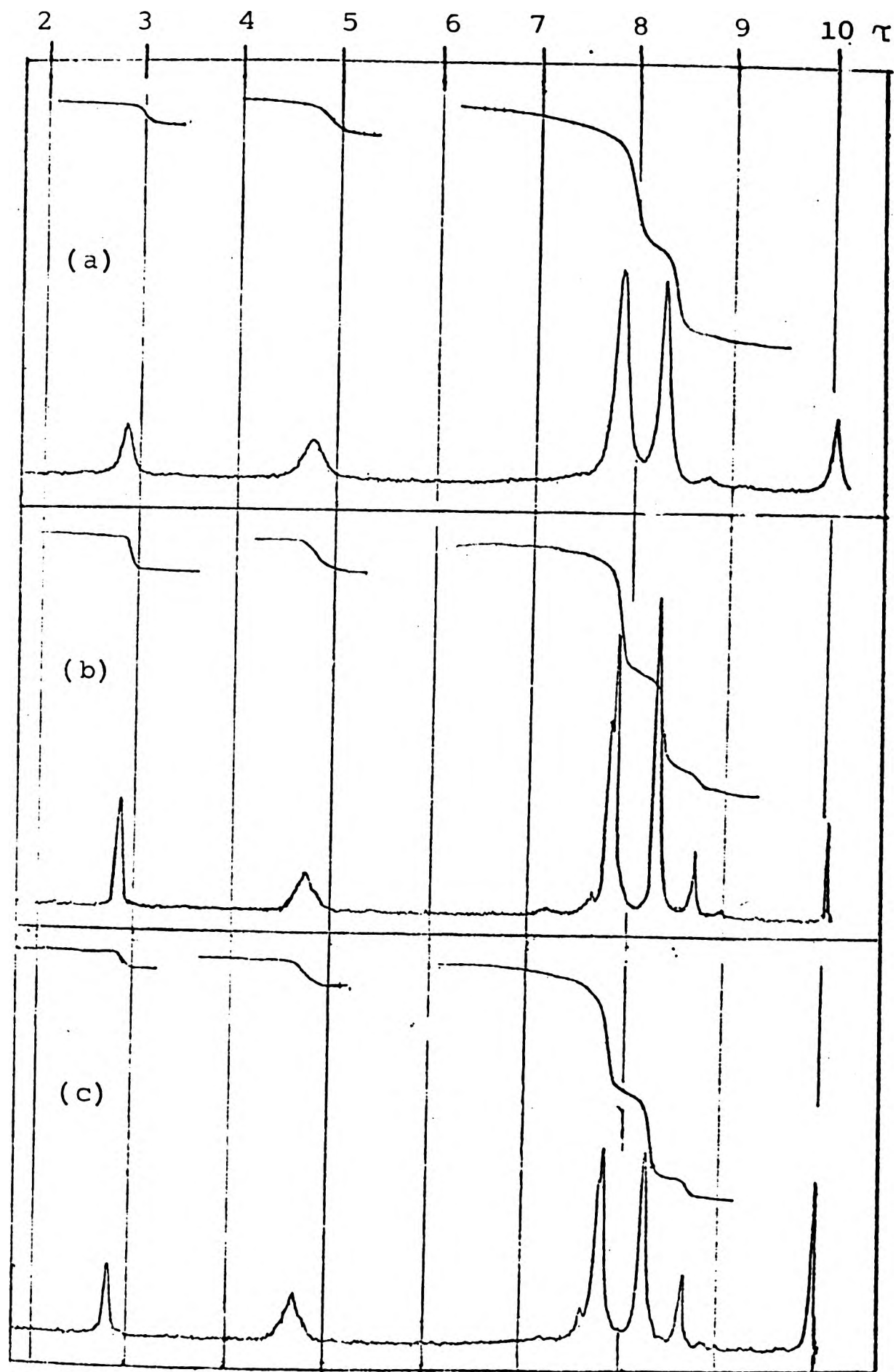


Fig. 43 Nuclear magnetic resonance spectra of IR/E products heated at 180°C for various time: (a) 0 min; (b) 45 min; (c) 210 min.

further in the Discussion Section). The peak at  $7.6\tau$  could reasonably be assigned to  $\text{ArCH}_3$ ; these protons appear at  $7.8\tau$  in the original methylol phenol and dibenzyl ether, as can be seen from their spectra (Fig. 109, Experimental Chapter). The very weak peaks at  $8.7$  and  $9.0\tau$  might be assigned to  $\text{CH}_3\text{-C}$  and/or  $\text{-CH}_2\text{-}$  protons in chroman structures. The  $\text{Ar-CH}_2\text{-C}$  protons in the internal chroman structure XXXII are reported to resonate at  $7.3\tau$ .<sup>11</sup> The peak at  $7.20\tau$  in this work might therefore reasonably be assigned to protons present in chroman structures. The present chromans, as discussed, are most likely to be structures LXXXIX and XCV; this would be supported by the spectra since resonances due to OCH structures, reportedly at  $5.5\text{--}6.1\tau$ <sup>26,28,29</sup>, present in some alternative chromans (XC, XCIV and C) were not observed. The remaining chroman XCIX is unlikely for reasons discussed earlier.

(ii-b) Catalysed interactions

Nmr spectra of IR before and after heating at  $160^\circ\text{C}$  for various times with methylol phenol and dibenzyl ether in the presence of the catalysts  $\text{ZnCl}_2$ ,  $\text{SnCl}_2$  and  $\text{SnCl}_2 \cdot 2\text{H}_2\text{O}$  are presented in Figs 44 to 49. In general, changes in the spectra for the interactions using  $\text{SnCl}_2$  and  $\text{ZnCl}_2$  as catalyst are the same as those for the uncatalysed interactions i.e., new peaks at  $8.66$ ,  $7.6\tau$  and (hardly detectable) at  $8.7$  and  $9.0\tau$ , with no reduction of the intensity of the  $\text{-CH=}$  proton resonances at  $4.6\tau$ . In the case with  $\text{SnCl}_2 \cdot 2\text{H}_2\text{O}$  as catalyst, in addition to the above changes,

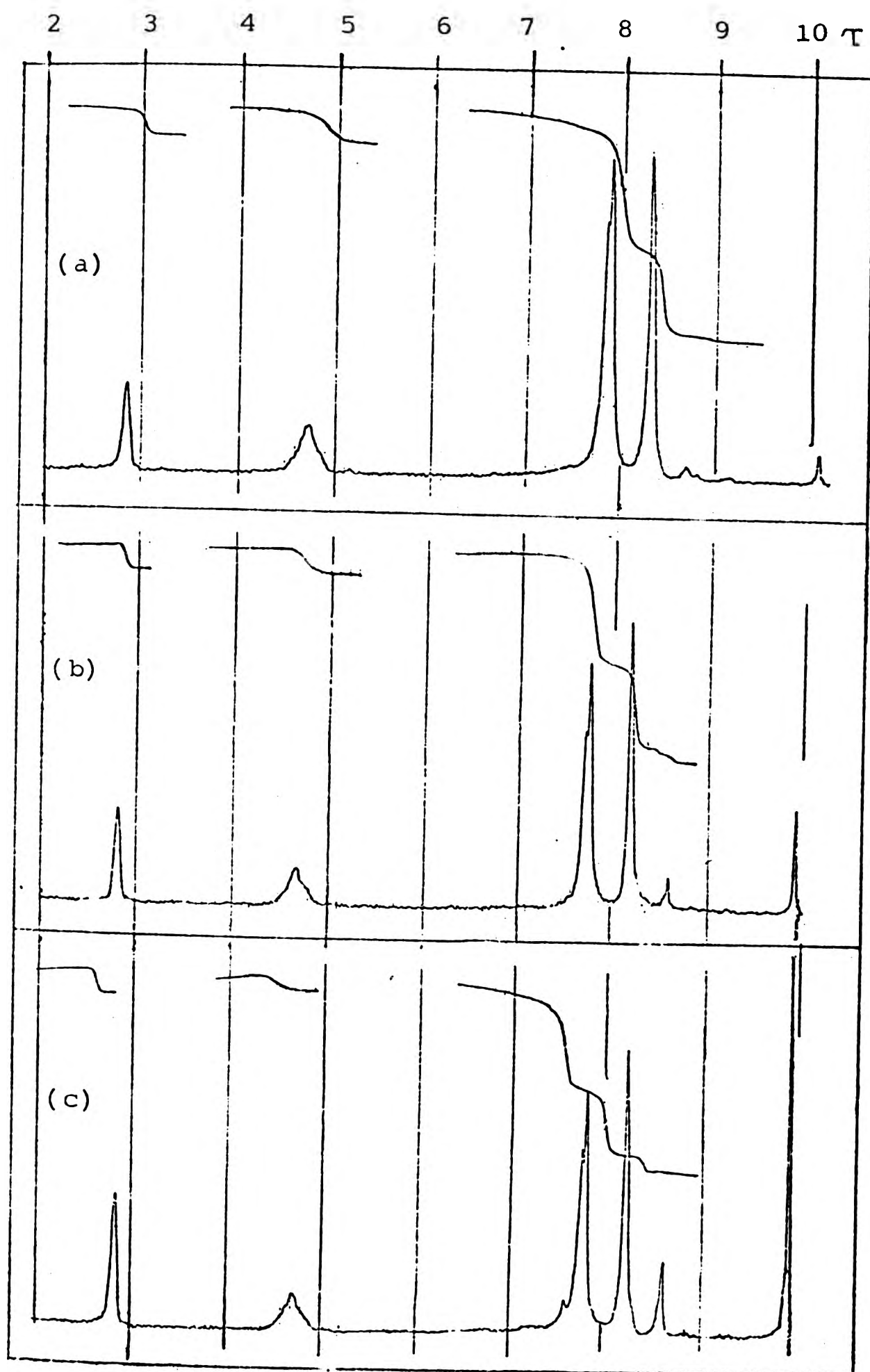


Fig. 44 Nuclear magnetic resonance spectra of IR/MP/ZnCl<sub>2</sub> products heated at 160°C for various times: (a) 0 min; (b) 45 min; (c) 210 min.

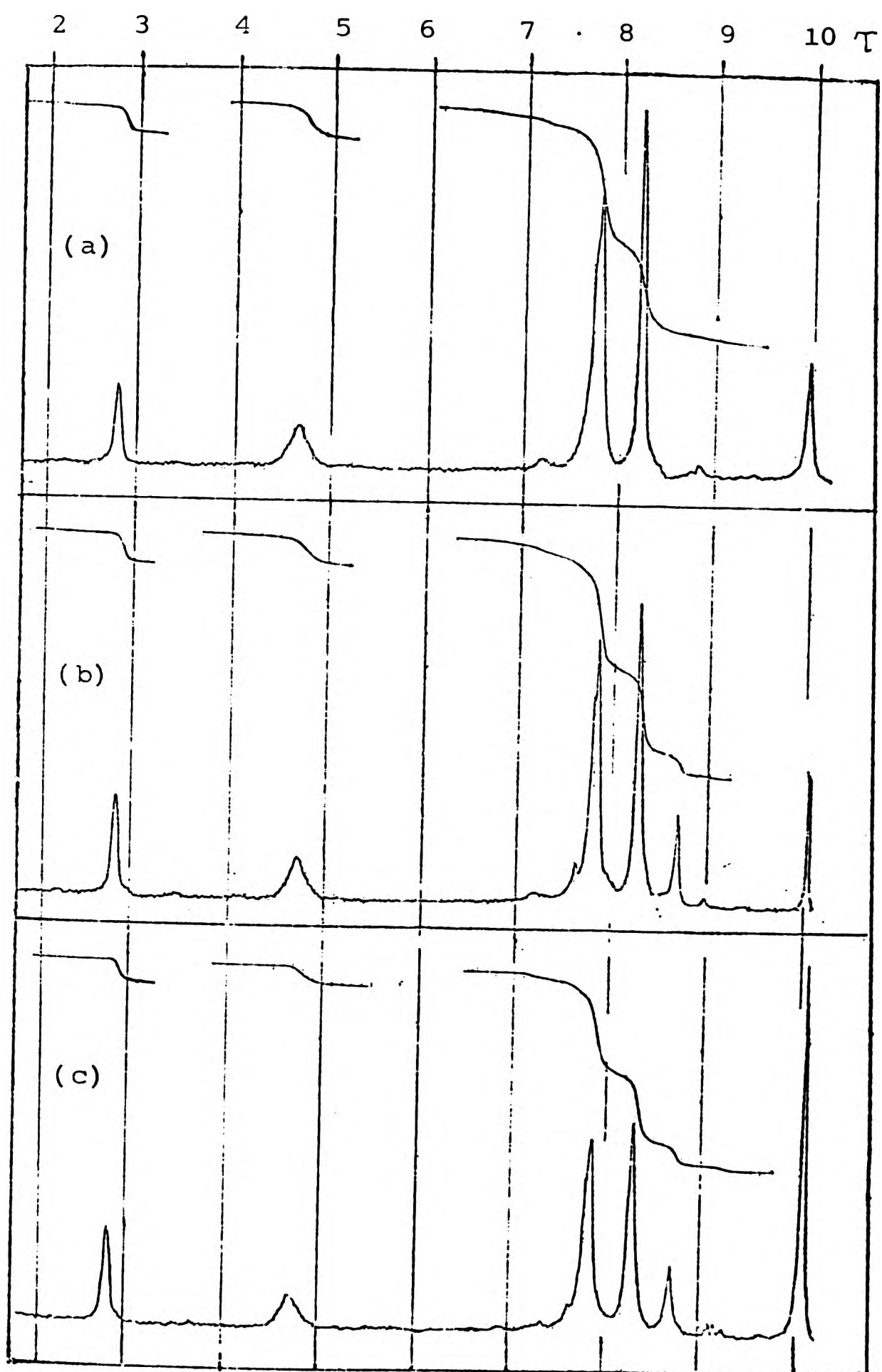


Fig. 45 Nuclear magnetic resonance spectra of IR/E/ZnCl<sub>2</sub> products heated at 160°C for various times: (a) 0 min; (b) 45 min; (c) 210 min.

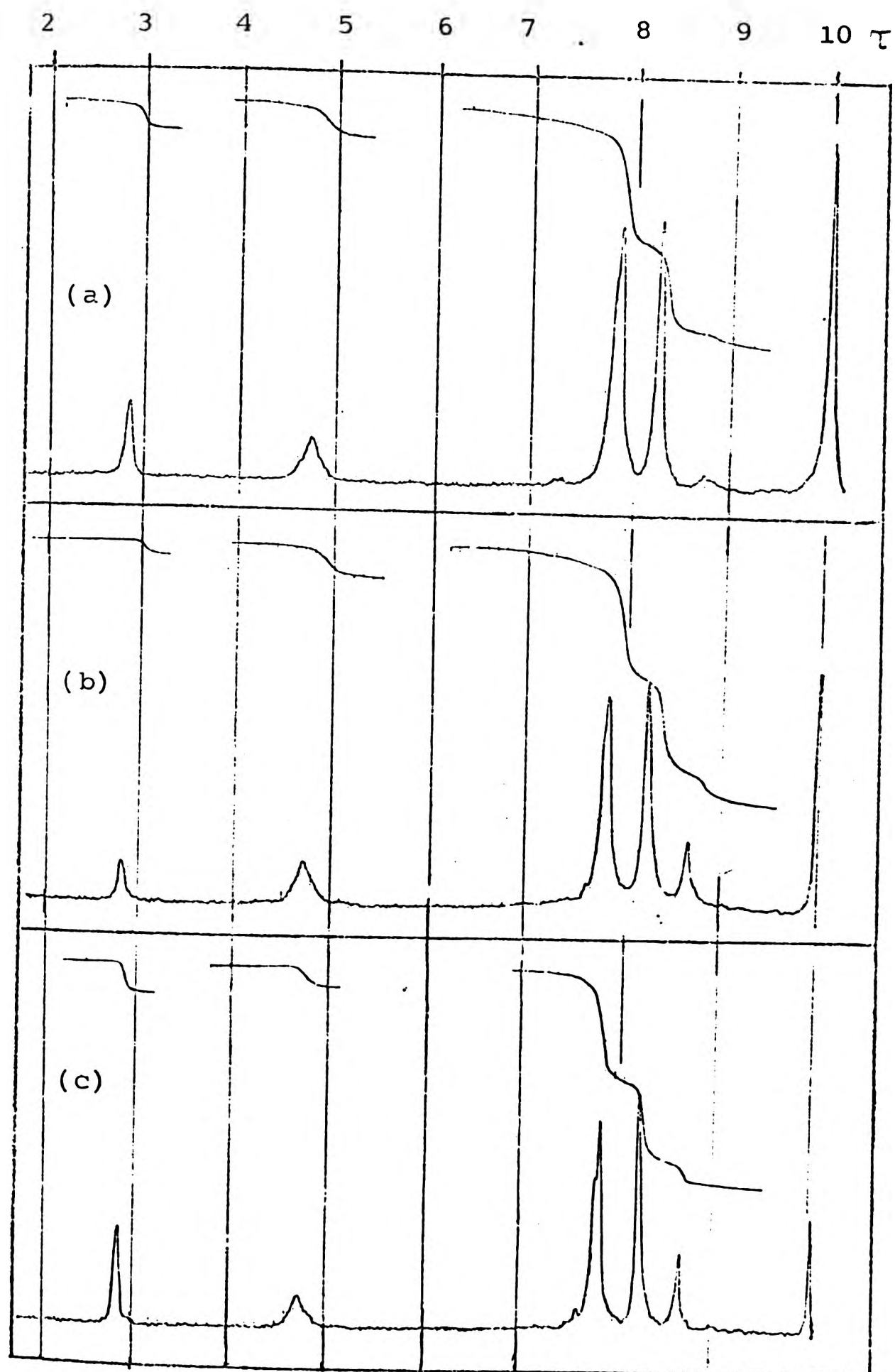


Fig. 46 Nuclear magnetic resonance spectra of IR/MP/SnCl<sub>2</sub> products heated at 160°C for various times: (a) 0 min; (b) 45 min; (c) 210 min.

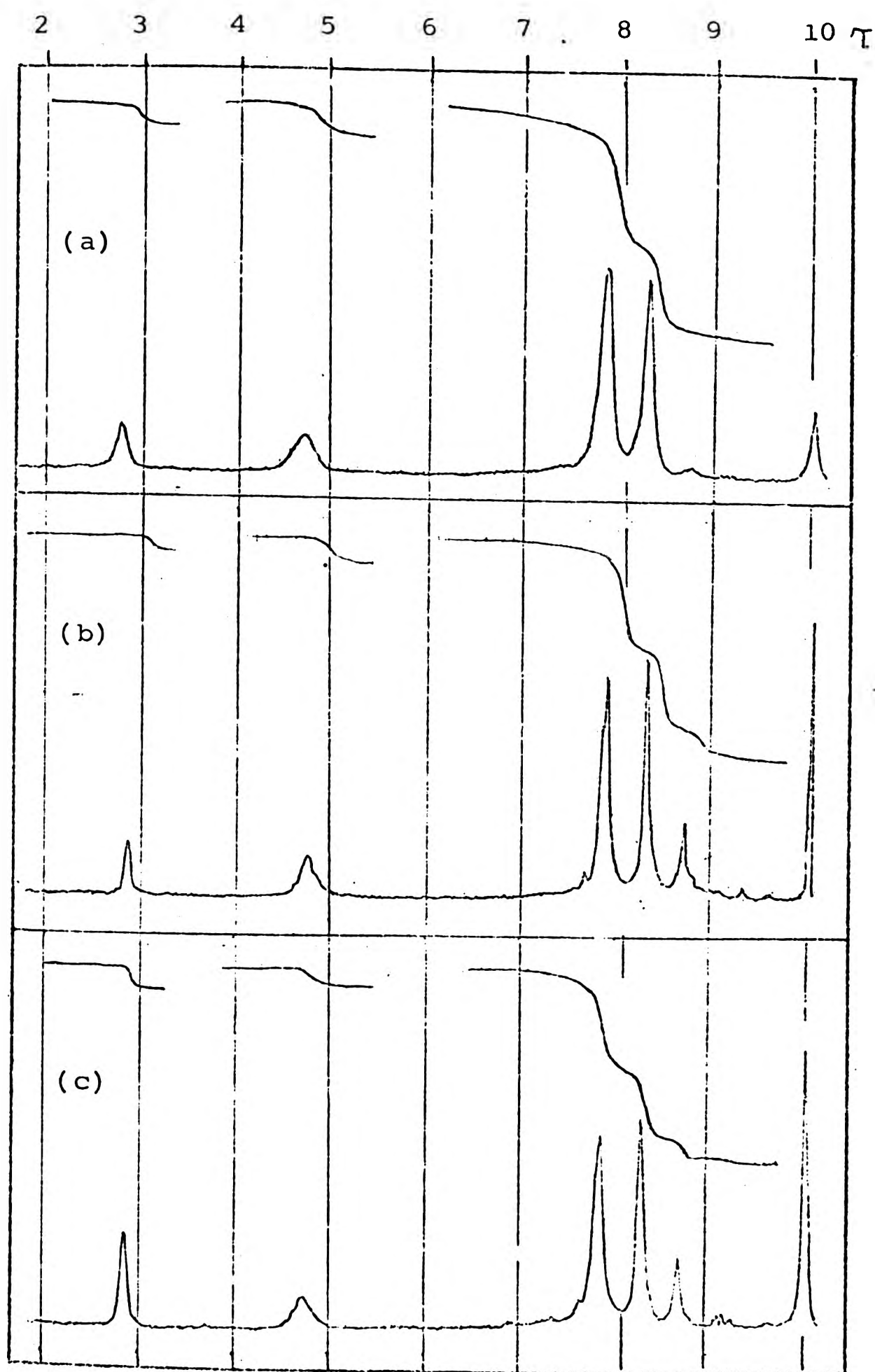


Fig. 47 Nuclear magnetic resonance spectra of IR/E/SnCl<sub>2</sub> products heated at 160°C for various times: (a) 0 min; (b) 45 min; (c) 210 min.

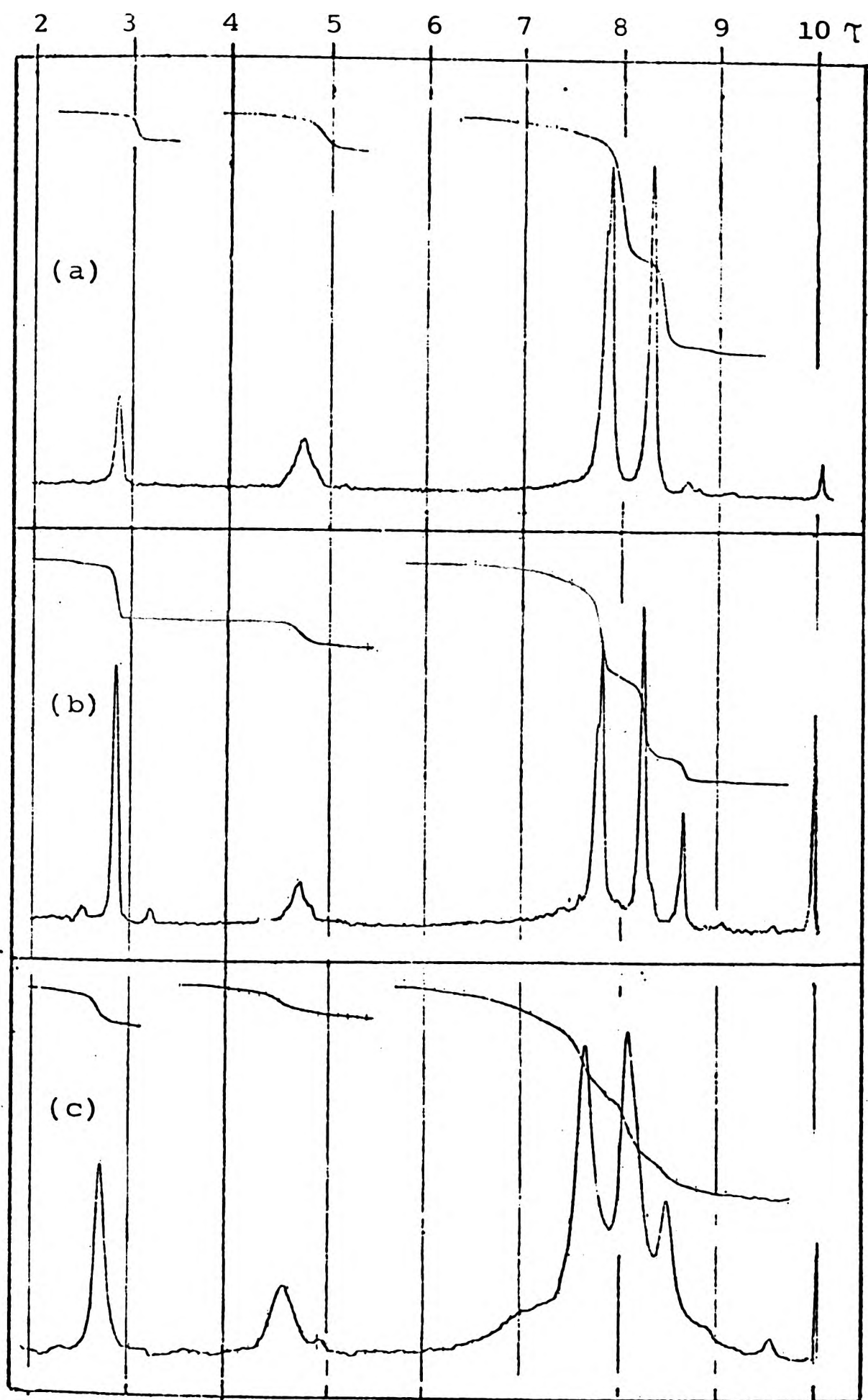


Fig. 48 Nuclear magnetic resonance spectra of IR/MP/SnCl<sub>2</sub>·2H<sub>2</sub>O products heated at 160°C for various times: (a) 0 min; (b) 45 min; (c) 210 min.

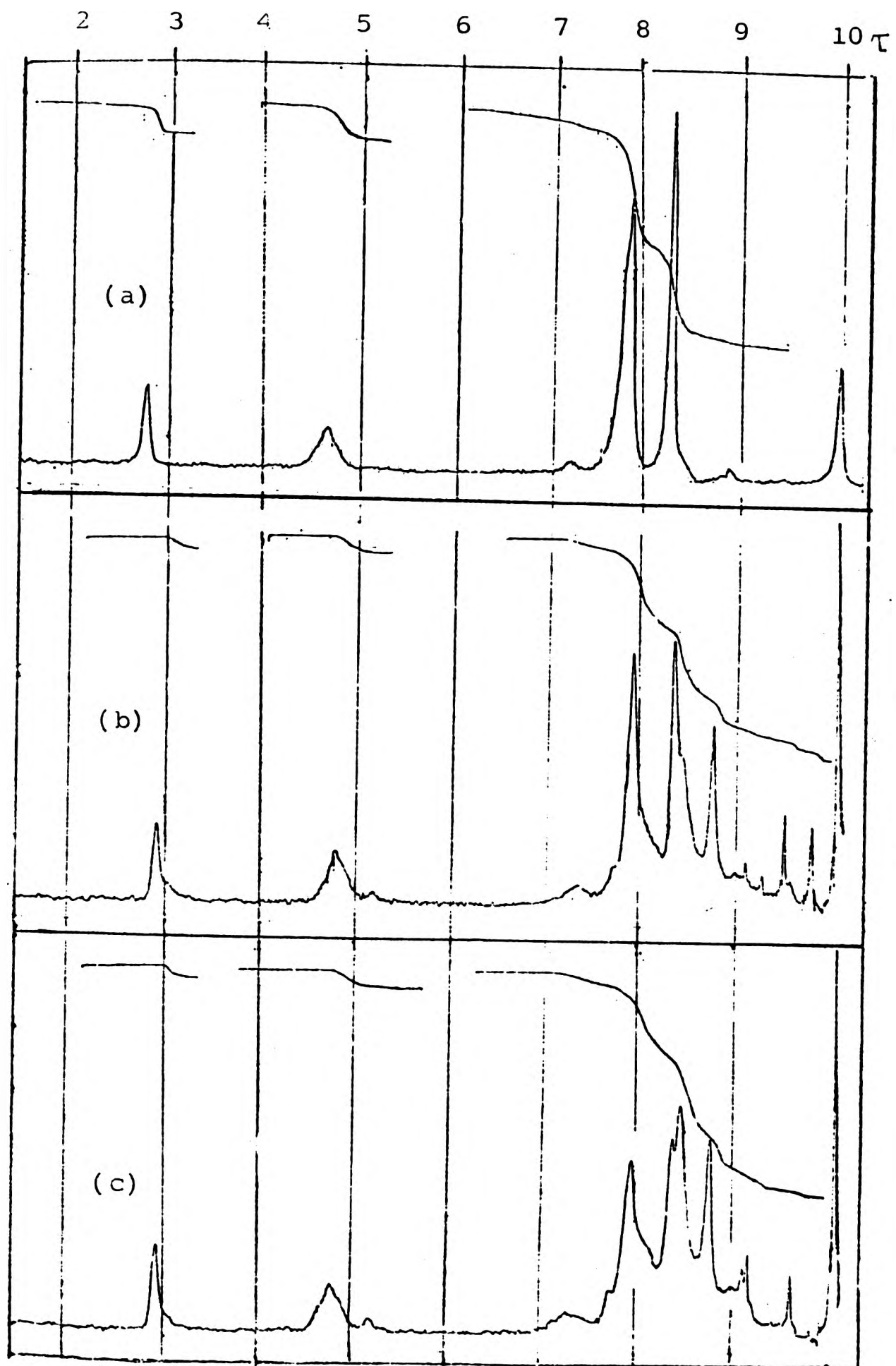


Fig. 49 Nuclear magnetic resonance spectra of IR/E/SnCl<sub>2</sub>·2H<sub>2</sub>O products heated at 160°C for various times: (a) 0 min; (b) 45 min; (c) 210 min.

new peaks appear at 5.10, 8.00, 8.35 and 9.10 $\tau$  which suggest double bond shifts (5.10 $\tau$  , vinylidene protons, e.g., structure LXXI), cis/trans isomerization (8.35 $\tau$  , trans  $\text{CH}_3-\overset{\text{H}}{\underset{\text{H}}{\text{C}}}=\text{C}$  , e.g. structure LXV) and cyclization (8 and 9.10 $\tau$  ,  $\text{CH}_3-\overset{\text{H}}{\underset{\text{H}}{\text{C}}}=\text{C}$  and  $\text{CH}_3-\overset{\text{H}}{\underset{\text{H}}{\text{C}}}-$  respectively, e.g., structures LXXVI and LXXVII). The appreciable reduction in intensity of the peak at 4.60 $\tau$  (-CH=), would also support the occurrence of extensive cyclization. These results show the same general trend as those obtained by ir spectroscopy, i.e., whereas  $\text{SnCl}_2$  (and  $\text{ZnCl}_2$ ) do not cause isomerization of IR in the presence of methylol phenol or dibenzyl ether,  $\text{SnCl}_2 \cdot 2\text{H}_2\text{O}$  does. Therefore, in view of the absence of peaks at 5.50-6.10 $\tau$  (OCH) in all cases, the results support the formation of chromans of the types LXXXIV and XLV. Additional chroman of type XCIX is possible in the  $\text{SnCl}_2 \cdot 2\text{H}_2\text{O}$  case, but is unlikely in view of Fitch's observation that vinylidene alkene did not react to form a chroman.

### 3.7 Hydroxyl concentration

An attempt was made to estimate hydroxyl concentration for the IR/MP/ $\text{SnCl}_2$ , IR/E/ $\text{SnCl}_2$ , IR/MP/ $\text{SnCl}_2 \cdot 2\text{H}_2\text{O}$ , and IR/E/ $\text{SnCl}_2 \cdot 2\text{H}_2\text{O}$  interaction products by quantitative ir analysis. For this purpose it was necessary to use a reference material for calibration purposes. Because of its structural similarity with the various methylene bridge structures (Scheme 3) and also with the expected phenol - containing decomposition products (e.g., the diphenyl

methane), 2,6-dimethyl phenol (Formula CXIII) was used, The -OH group of this compound is in a reasonably similar chemical environment to those in the structures in question. This compound was therefore mixed with IR in various proportions and ir spectra obtained for calibration purposes. However, examination of the ir spectra of the calibration mixtures (Fig. 41) reveals that, although the pure phenol shows a broad peak centred near 3.0  $\mu\text{m}$ , its mixtures with rubber show sharper phenolic -OH peaks, moved down-wavelength to 2.7-2.8  $\mu\text{m}$ . This is undoubtedly due to the fact that the phenolic OH is hydrogen-bonded in the pure phenol but is free and unassociated in dilute solution in the rubber.

Since the -OH absorption observed in the reaction products is broad and centred at about 2.85  $\mu\text{m}$  (Fig.36-39) it would appear from the above observation that it cannot be due to phenolic OH. Although the model chosen may not be ideal, it seems unlikely that such severe discrepancies in wavelength could occur. None of the products of reaction show absorption at 2.7-2.8 $\mu\text{m}$  and it therefore seems that 'methylene bridge' adducts must be absent. Nevertheless, the spectra of the IR/model mixtures were used as an (approximate) -OH calibration by using the area under the total OH absorption as a measure of concentration. Methyl/hydroxyl absorbance ratios ( $A_{7.3}/A_{2.7-3.2}$ ) were plotted against molar phenol concentration to obtain a calibration curve (Fig. 50).

Corresponding absorbance ratios  $A_{(7.3)}/A_{(2.7-3.2)}$  were obtained from spectra of the various interaction products at

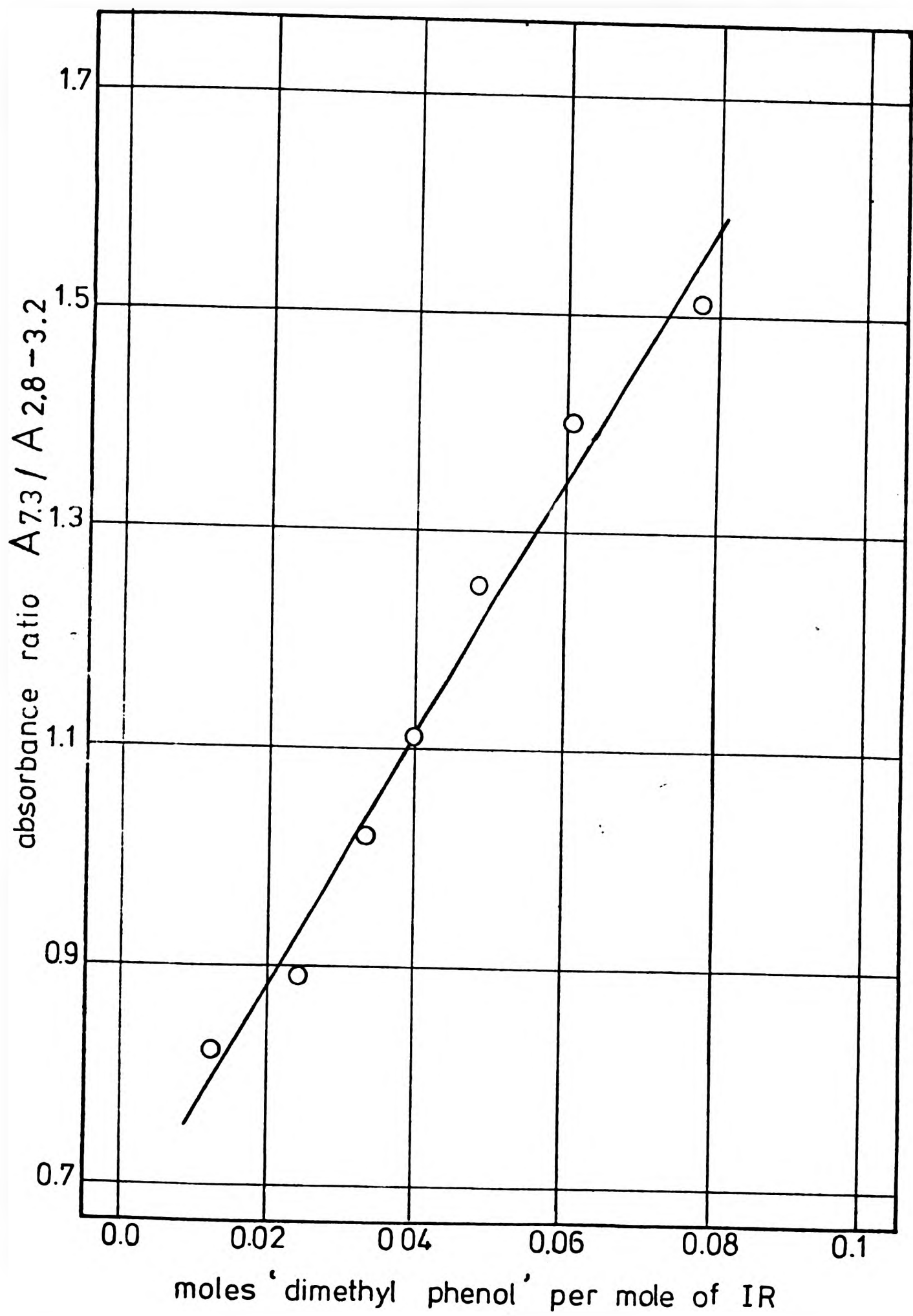


Fig. 50 Methyl/hydroxyl absorbance ratio ( $A_{7.3}/A_{2.8-3.2}$ ) versus concentration in IR of 2,6-dimethyl phenol.

various reaction times, and from the calibration curve, the corresponding hydroxyl concentration was estimated. The changes in hydroxyl concentration are presented in the Experimental Chapter and summarised graphically in Fig. 51. The results show for all 4 interactions examined a sharp increase in hydroxyl concentration in the early stages of reaction. For the IR/MP/SnCl<sub>2</sub>.2H<sub>2</sub>O and IR/E/SnCl<sub>2</sub>.2H<sub>2</sub>O interaction hydroxyl concentration clearly passes through a peak value which it is reached earlier in the latter case. An even earlier, though less distinct, maximum is observed in the SnCl<sub>2</sub>/E case. The SnCl<sub>2</sub>.2H<sub>2</sub>O absorptions show much higher maxima than the SnCl<sub>2</sub> ones, but whereas hydroxyl concentration was greater in the IR/E/SnCl<sub>2</sub> than in the IR/MP/SnCl<sub>2</sub> products, the concentration was higher in the IR/MP/SnCl<sub>2</sub>.2H<sub>2</sub>O than IR/E/SnCl<sub>2</sub>.2H<sub>2</sub>O cases. These results are clearly large compared with the corresponding ones for unextractable material found after acetone extraction (see Chapter 6), an observation which may be taken as a further indication that the hydroxyl absorption is not due to unextractable materials. It is still possible, though unlikely in view of the wavelength discrepancies, that methylene bridge structures are present. It seems much more probable however, in view of all these results, that the hydroxyl absorption bands have a non-phenolic origin, and catalyst decomposition or hydrolysis products appear to be the most likely explanation for them (see also Further Discussion).

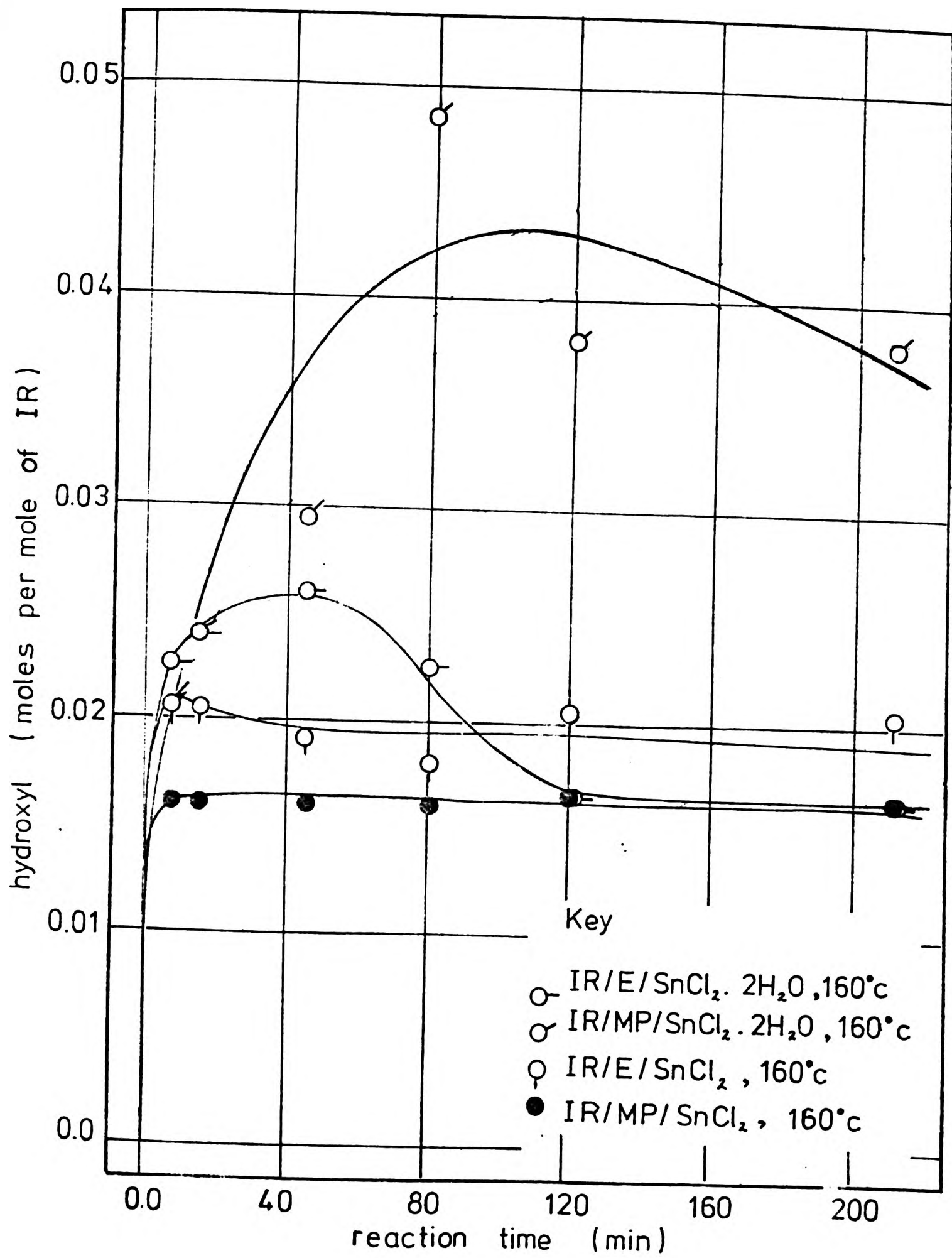


Fig. 51 Change of hydroxyl concentration with reaction time.

### 3.8 Total Unsaturation

#### (i) Tests on 'model' compounds

The iodine chloride and perbenzoic acid reagents were tested with some selected 'models' in order to establish whether or not they react with (a) combined and/or unextractable phenolic material, (b) tertiary hydrogen atoms which might be present in chroman, methylene bridge and polycyclic structures, and (c) tetra-substituted double bonds which are expected to occur in cyclized rubber. The models selected were: (a) 2,6 dimethyl phenol (Formula CXIII) as model for combined phenolic material (for similar reasons to those discussed in the previous section); it was considered that phenolic material combined in the form of chroman rings was unlikely to react with these reagents; (b) 3-methyl pentane (CXIV) as model in respect of possible tertiary hydrogen atom reactivity; (c) 2,3-dimethyl 2-butene (CXV) as suitable model containing tetra-substituted double bonds. The results show that whereas perbenzoic acid does not react with 2,6-dimethyl phenol (Formula CXIII), iodine chloride reacts to an appreciable extent, giving an apparent 'Iodine Value' (IV) of 215.9 (this being the number of gms of iodine equivalent to one hundred grams of sample). This suggests that iodine chloride is capable of extensive substitutive or other side reactions with phenolic materials (see also Further Discussion). Neither iodine chloride nor perbenzoic acid reacts with 3-methyl pentane, an iodine value of 0.0 being obtained by both reagents. This would appear to suggest that

neither iodine chloride nor perbenzoic acid cause substitution of tertiary hydrogen atoms present. However, later work casts some doubt on the suitability of the model for representing cyclised structures; also, Lee et al<sup>93</sup> found substitution to occur with iodine chloride and cyclized rubber. Both reagents reacted with 2,3 dimethyl-2-butene, by giving iodine values corresponding to 98.9% (iodine chloride) and 98.6% (perbenzoic acid) of the theoretical values for the pure model. These values were considered satisfactory since the specified purity of the reagent was 98%. Thus both reagents might be considered reliable for the determination of unsaturation when tetra-substituted double bonds are present. Altogether, it seems that perbenzoic acid is the more reliable reagent for the determination of unsaturation in this study where samples may be contaminated with unextractable and/or combined phenolic material. Nevertheless, both methods were used in assessing unsaturation of the various products of interaction.

(ii) Total unsaturation found for the various interaction products.

In order to express results in terms of total unsaturation of the IR itself after interaction with the phenolic materials, the overall iodine value of the reaction product was 'corrected' to allow for the combined and unextractable phenolic material present. In view of the results obtained with the model compounds (above) a further correction should be necessary in the iodine chloride case because of the

presence of unextractable phenolic material in the samples. Such a correction was not, however, carried out in view of the lack of precise knowledge of the reactions involved. Thus, it might be expected that iodine monochloride should generally give higher iodine values than perbenzoic acid. Results obtained with both reagents for the various interaction products are detailed in the Experimental Chapter, and are summarised in graphical form in Figs. 52 and 53. These figures show changes in total unsaturation of the IR expressed as a fraction of the total original unsaturation, as reaction proceeds. They clearly indicate that reduction of unsaturation occurs in all cases. The values of unsaturation determined by iodine chloride were higher than the corresponding values obtained by perbenzoic acid, as was anticipated. Unsaturation values obtained by perbenzoic acid, which are believed to be the more reliable in view of the foregoing considerations, show that the least reduction in unsaturation arises in the uncatalysed reactions; the  $\text{ZnCl}_2$ - and  $\text{SnCl}_2$ - catalysed products show somewhat greater reduction, and in each case the reduction is greater with the ether than with the methylol phenol. In those interactions catalysed by  $\text{SnCl}_2 \cdot 2\text{H}_2\text{O}$ , however, there is a very marked reduction of unsaturation, probably due to cyclization in addition to chroman formation. This reduction was again greater for the ether than for the methylol phenol case, a result which also accords with that obtained by ir spectroscopy (Section 3.5).

For the uncatalysed interactions and for those catalysed by  $\text{SnCl}_2$  and  $\text{ZnCl}_2$ , the loss of unsaturation calculated by

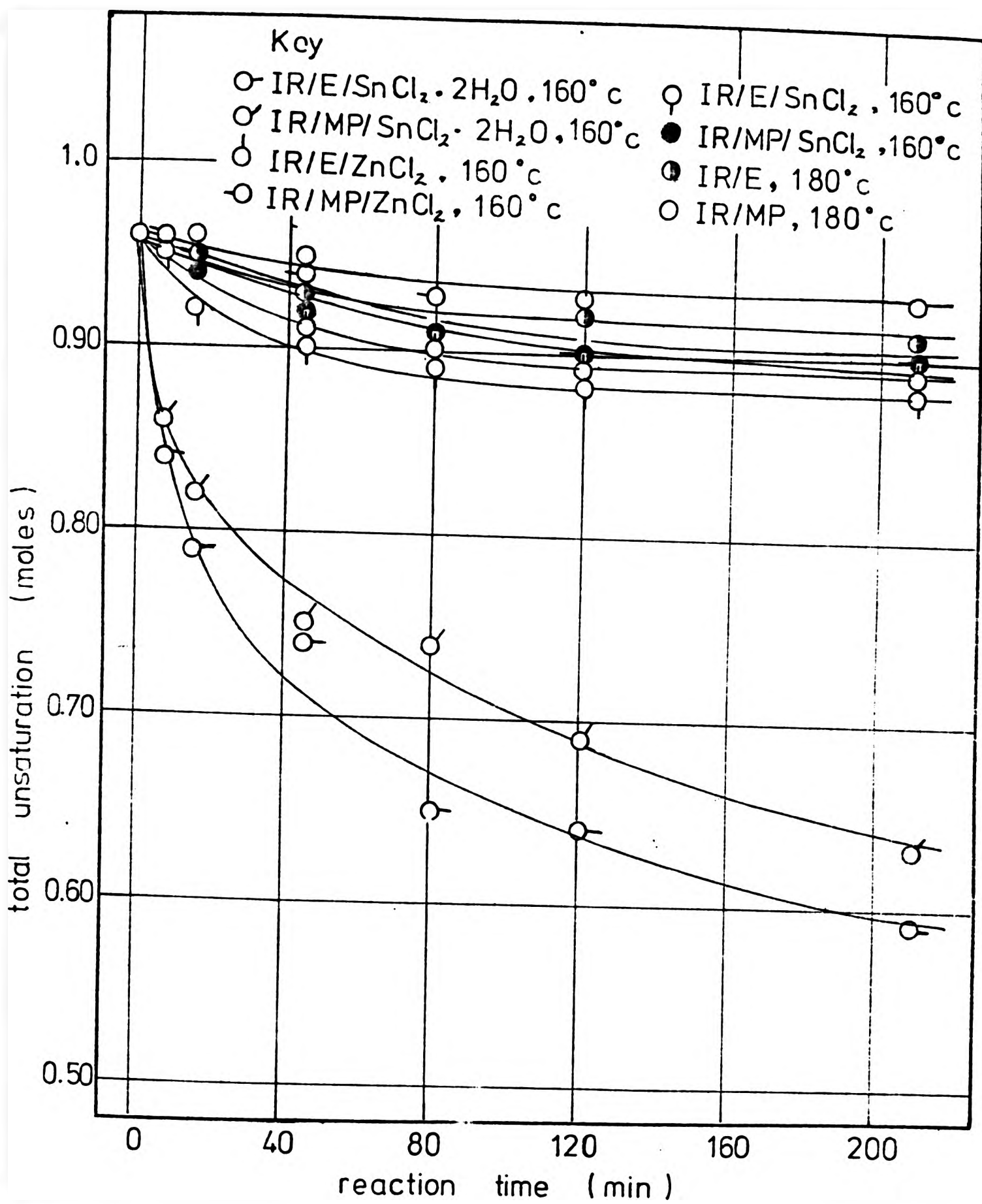


Fig. 52 Changes in total unsaturation with reaction time for IR in the various interactions as calculated from perbenzoic acid consumed.

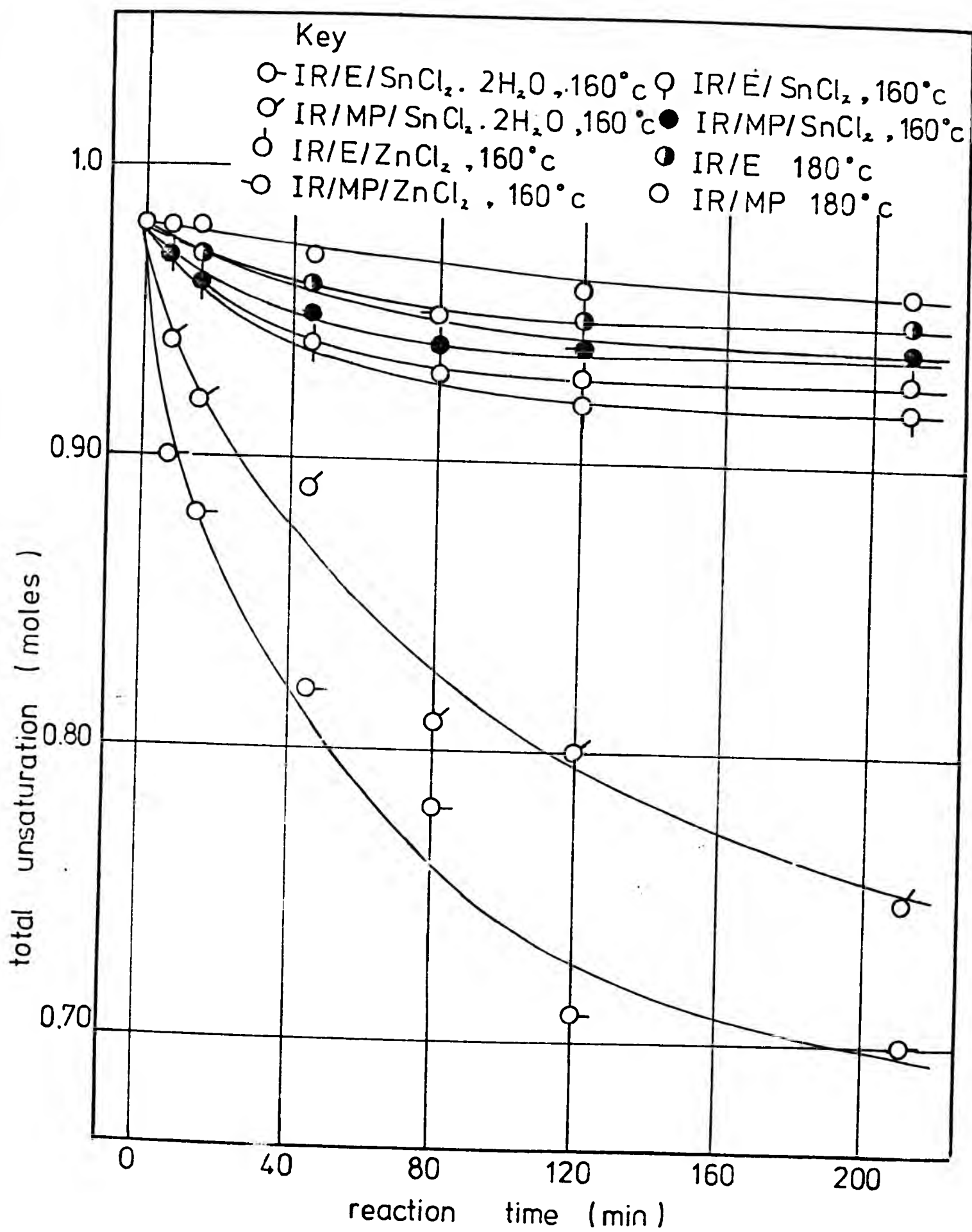


Fig. 53 Changes in total unsaturation with reaction time for IR in the various interactions as calculated from iodine chloride consumed.

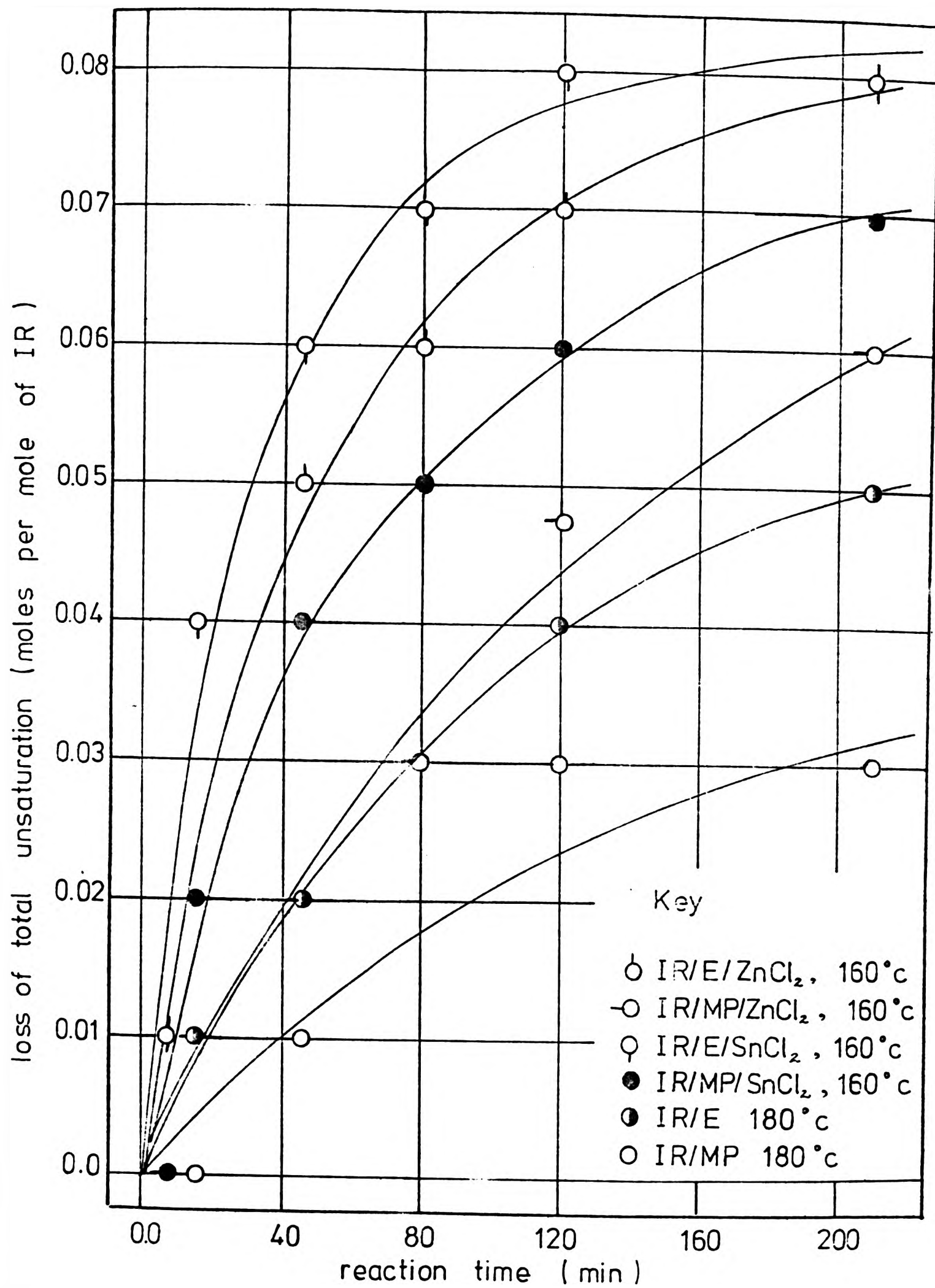


Fig. 52 Loss of unsaturation with reaction time for IR in various interactions, calculated from perbenzoic acid consumed.

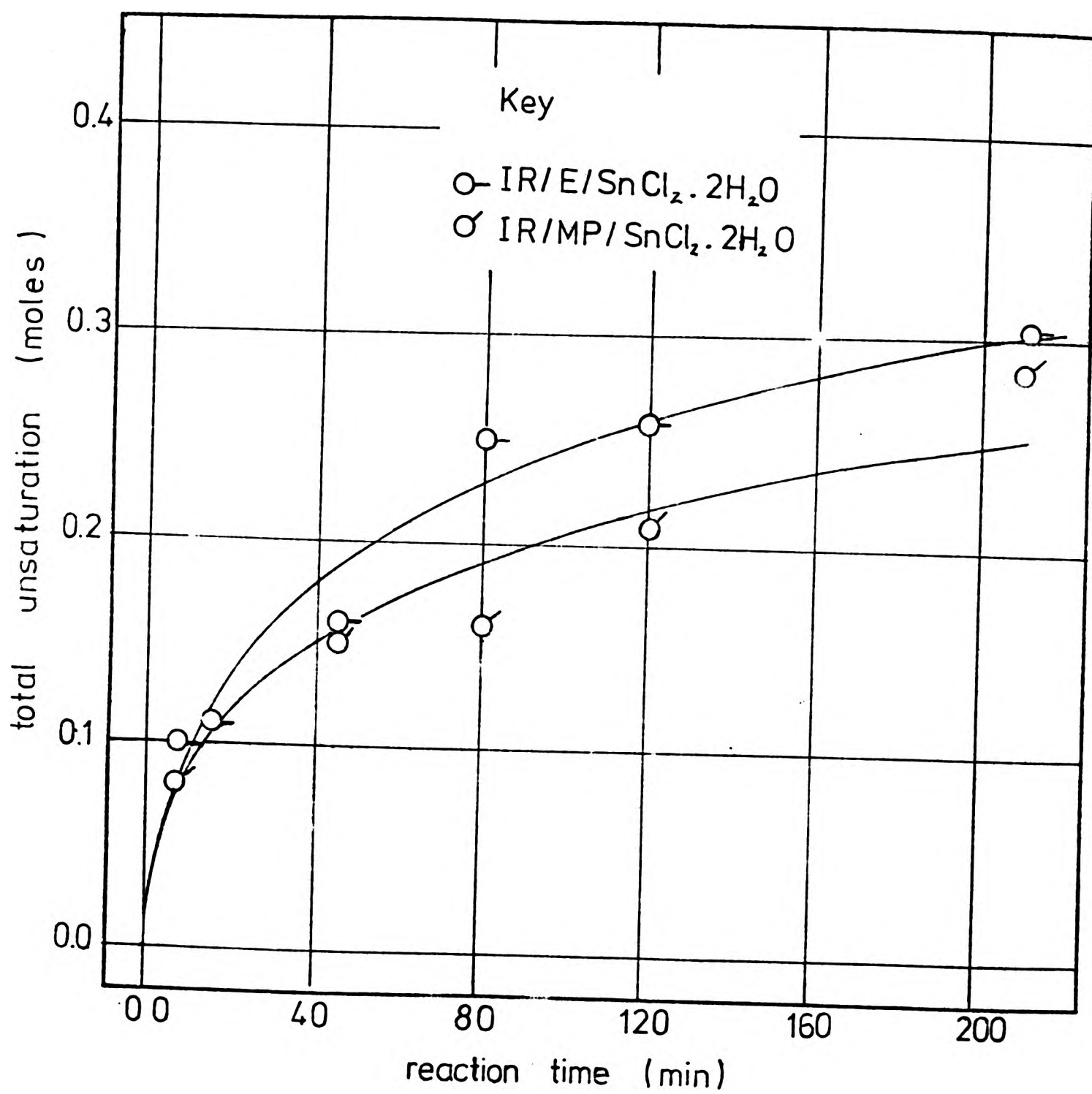


Fig. 55 Unsaturation consumed by cyclization with reaction time in the IR/MP/SnCl<sub>2</sub>·2H<sub>2</sub>O and IR/E/SnCl<sub>2</sub>·2H<sub>2</sub>O interactions.

perbenzoic acid (see Fig. 54) is in reasonable agreement with those values of phenolic material combined as calculated by the other methods of analysis (e.g., Fig. 26). This suggests that the chroman-type adduct is the only one occurring, since the presence of methylene bridge structures would have caused a discrepancy in this comparison. Clearly, if chroman adduct formation is the only reaction, then the fractional reduction of unsaturation should be numerically equivalent to the moles of phenolic material combined per mole of IR (i.e., the ordinates of Fig. 54 is equivalent to that of Fig. 26). If it is supposed that chroman-type adduct formation is the only reaction other than cyclization occurring in the interactions catalysed by  $\text{SnCl}_2 \cdot 2\text{H}_2\text{O}$ , then the difference between the loss of unsaturation (from perbenzoic acid) and phenolic material combined (as calculated from acetone extraction) would give the total unsaturation consumed by cyclization. These values are presented in the Experimental Chapter and they are summarised in graphical form in Fig. 55, which shows total unsaturation consumed by cyclization expressed in molar fraction as reaction proceeds. These results show reasonable agreement with those obtained for the IR/ $\text{SnCl}_2 \cdot 2\text{H}_2\text{O}$  interaction, as will be discussed later.

### 3.9 Isomerization

In the uncatalysed interactions and in those catalysed by  $\text{SnCl}_2$  and  $\text{ZnCl}_2$  reduction of the trialkyl ethylenic unsaturation was observed by ir spectroscopy ( $12 \mu\text{m}$ ) but not by nmr spectroscopy (this will be discussed later). For

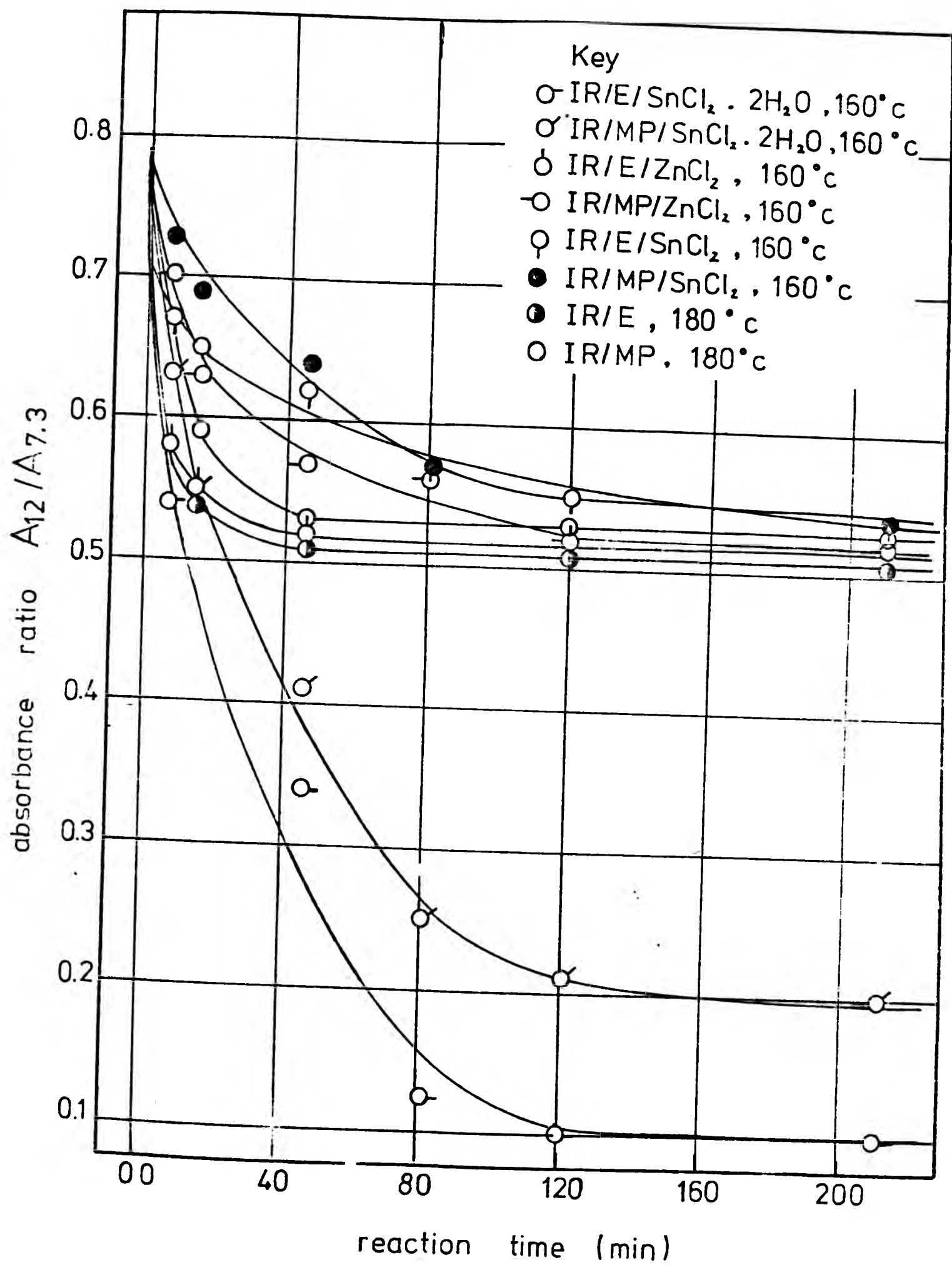


Fig. 56 Illustration of loss of trialkylethylenic unsaturation with time, using ratio of absorbance (A) of infra-red bands at 12 and 7.3  $\mu$ m.

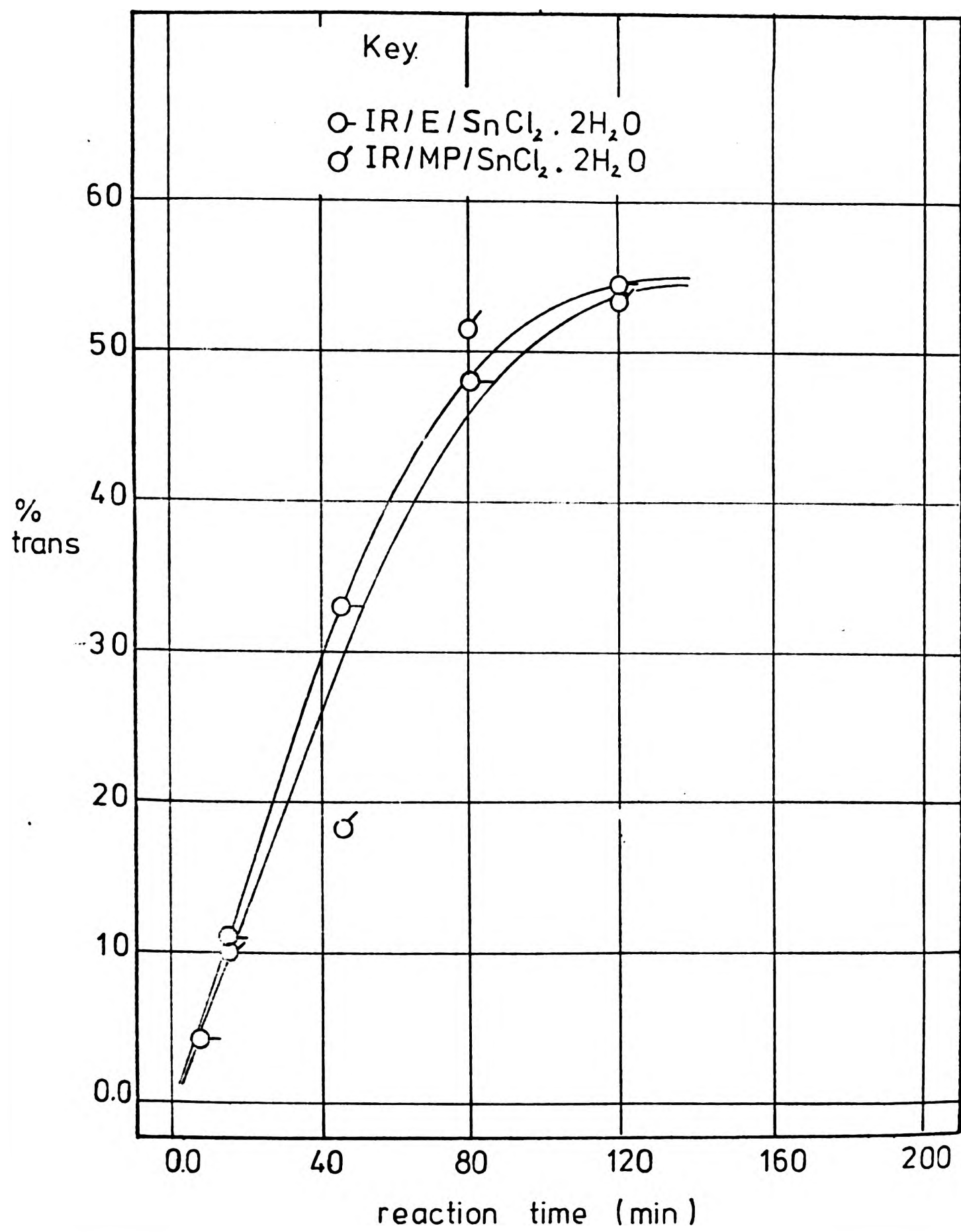


Fig. 57 Cis/trans isomerization in the IR/MP/SnCl<sub>2</sub> · 2H<sub>2</sub>O and IR/E/SnCl<sub>2</sub> · 2H<sub>2</sub>O interactions.

those cases catalysed by  $\text{SnCl}_2 \cdot 2\text{H}_2\text{O}$ , in addition to reduction of the trialkyl ethylenic unsaturation, nmr spectroscopy shows 1,1-dialkyl ethylenic double bonds ( $\text{>C=CH}_2$ , 5.10  $\tau$ ),  $\text{-}\overset{\text{CH}_3}{\underset{\text{CH}_3}{\text{C}}=\text{C}-\text{CH}_2-\overset{\text{CH}_3}{\underset{\text{CH}_3}{\text{C}}}=\text{C}-$  methylene protons (7.15  $\tau$ ), and cis/trans 2,3 unsaturation ( $\text{-}\overset{\text{CH}_3}{\underset{\text{CH}_3}{\text{C}}=\overset{\text{CH}_3}{\underset{\text{CH}_3}{\text{C}}}$  8.25 and 8.35  $\tau$ , respectively). In all cases ir spectroscopy was used to illustrate the relative loss of trialkylethylenic unsaturation by a plot of ratio  $A_{12}/A_{7.3}$  (i.e., trialkylethylenic absorbance/methyl absorbance) against reaction time (Fig. 56). For the  $\text{SnCl}_2 \cdot 2\text{H}_2\text{O}$ -catalysed cases, since gel content was present in considerable amount from the early stages of reaction, nmr spectroscopy could only be used to measure a cis/trans ratio rather than an absolute amount for trialkylethylenic unsaturation (from the ratio of the 8.25 and 8.35  $\tau$  peaks). The % trans present in this trialkylethylenic unsaturation is plotted against reaction time in Fig. 57. The cis/trans ratio after 120 min of reaction time could no longer be measured because of the extensive overlapping of resonance peaks. The results clearly show, however, that an equilibrium cis/trans ratio is being approached.

### 3.10 Glass-transition temperature

Glass transition temperature ( $T_g$ ) values (as measured by differential scanning calorimetry) of the various products of interaction for various times at 160°C (180°C for the uncatalysed interaction) are tabulated in the Experimental Chapter and illustrated graphically in Fig. 58.  $T_g$  values for the interaction products  $\text{IR/SnCl}_2$  and  $\text{IR/SnCl}_2 \cdot 2\text{H}_2\text{O}$

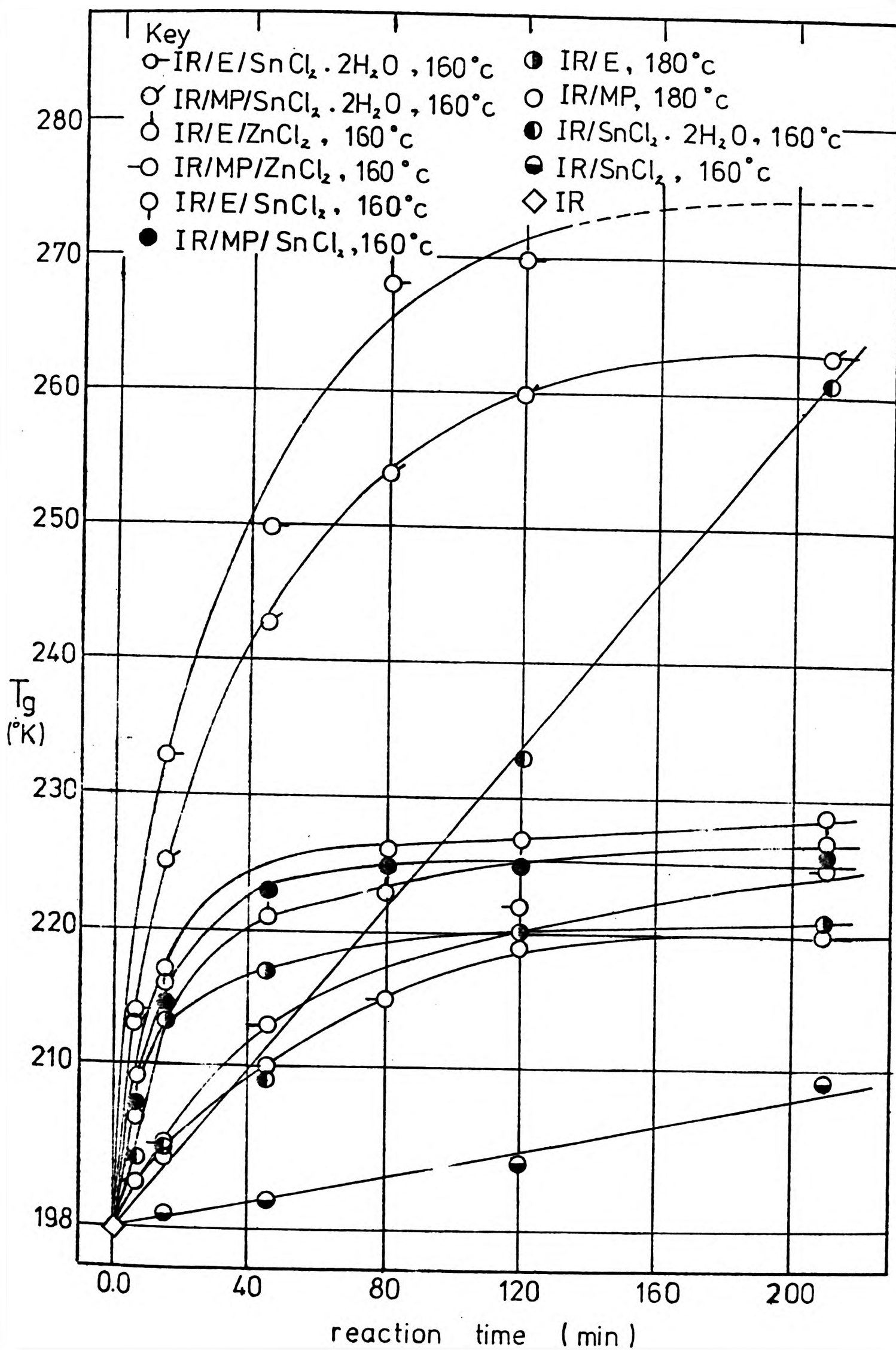


Fig. 58 Kinetics of combination of phenolic material and/or cyclization as reflected in  $T_g$  changes (dsc).

are also plotted in Fig. 58, to enable comparison to be made.  $T_g$  changes follow the same general trend as was observed for other product characteristics, i.e., values for the uncatalysed interaction increase more slowly than those for the catalysed cases.  $T_g$ 's for the  $\text{SnCl}_2 \cdot 2\text{H}_2\text{O}$  cases increase much more quickly and reach much higher maxima than those for the  $\text{SnCl}_2$  and  $\text{ZnCl}_2$  interactions, which do not differ greatly from each other. These results clearly support the view that, whereas cyclization is not occurring to a significant extent in the  $\text{SnCl}_2$  and  $\text{ZnCl}_2$  cases, it is a major process occurring in the  $\text{SnCl}_2 \cdot 2\text{H}_2\text{O}$  case, where a  $T_g$  increase of 62 and 73° for the IR/MP/ $\text{SnCl}_2 \cdot 2\text{H}_2\text{O}$  and IR/E/ $\text{SnCl}_2 \cdot 2\text{H}_2\text{O}$  interactions respectively, is observed after 120 min. of reaction time. These  $T_g$  values are higher than those for the IR/ $\text{SnCl}_2 \cdot 2\text{H}_2\text{O}$  interaction at equivalent times, presumably due to a contribution from the adduct formed towards the  $T_g$ . The increase in  $T_g$  by up to 26° for the catalysed interactions with  $\text{SnCl}_2$  and  $\text{ZnCl}_2$  and by up to 20° for the uncatalysed reactions may be accounted for entirely by adduct formation since no cyclization could be detected by ir and nmr spectroscopy for these interactions. If it is assumed that  $\text{SnCl}_2 \cdot 2\text{H}_2\text{O}$  catalyst can catalyse both adduct formation and cyclization at the same time and independently of each other, the  $T_g$  values due to adduct formation for the  $\text{SnCl}_2 \cdot 2\text{H}_2\text{O}$ -catalysed dibenzyl ether and methylolphenol interactions may be obtained as the difference between the overall  $T_g$  values for these interactions and the corresponding ones for the IR/ $\text{SnCl}_2 \cdot 2\text{H}_2\text{O}$  interaction. These differences are plotted in Fig. 59v reaction time, and show maxima at 80 and

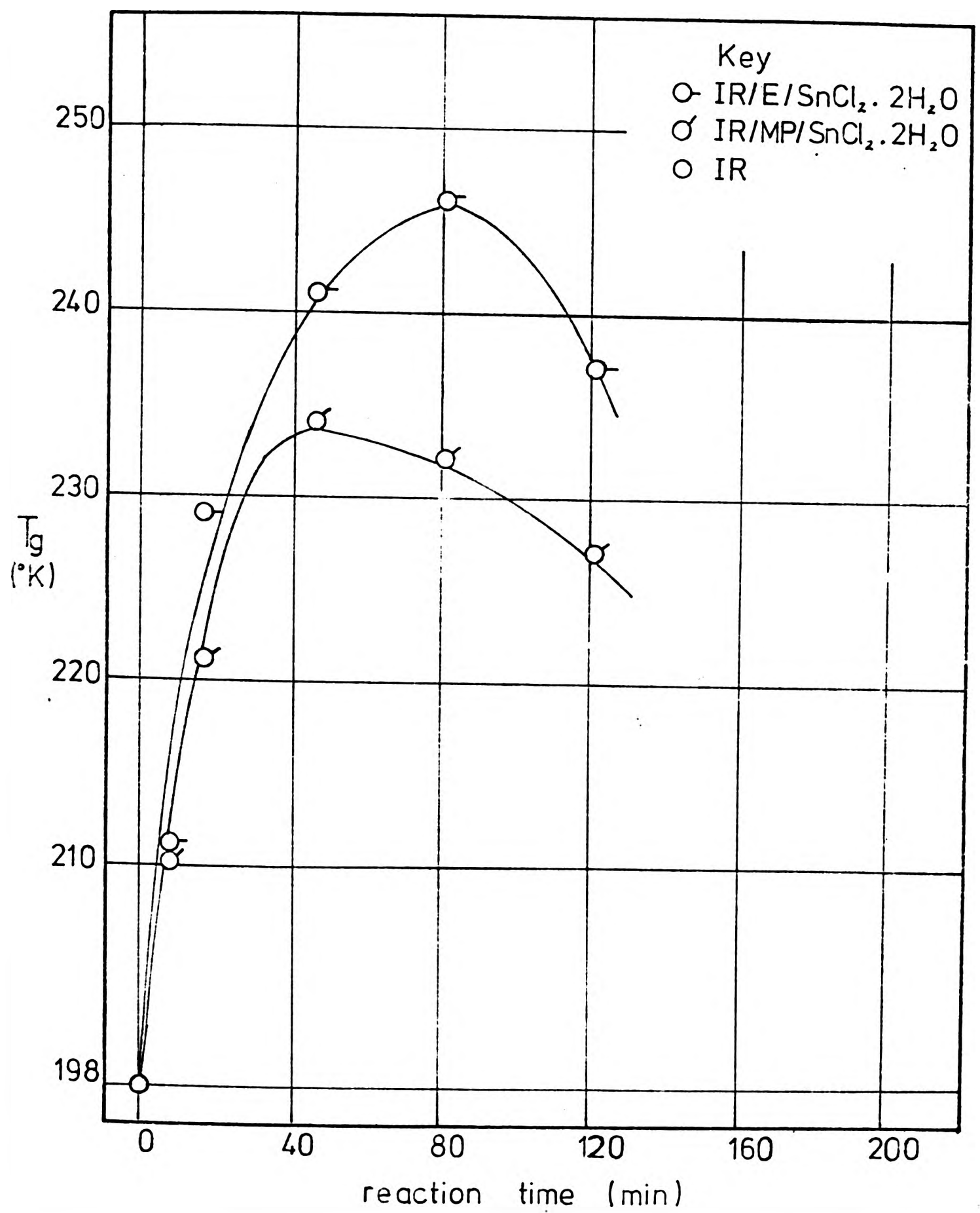


Fig. 59 Kinetics of combination of phenolic material as reflected in  $T_g$  changes (dsc) for the IR/MP/SnCl<sub>2</sub>·2H<sub>2</sub>O and IR/E/SnCl<sub>2</sub>·2H<sub>2</sub>O interactions.

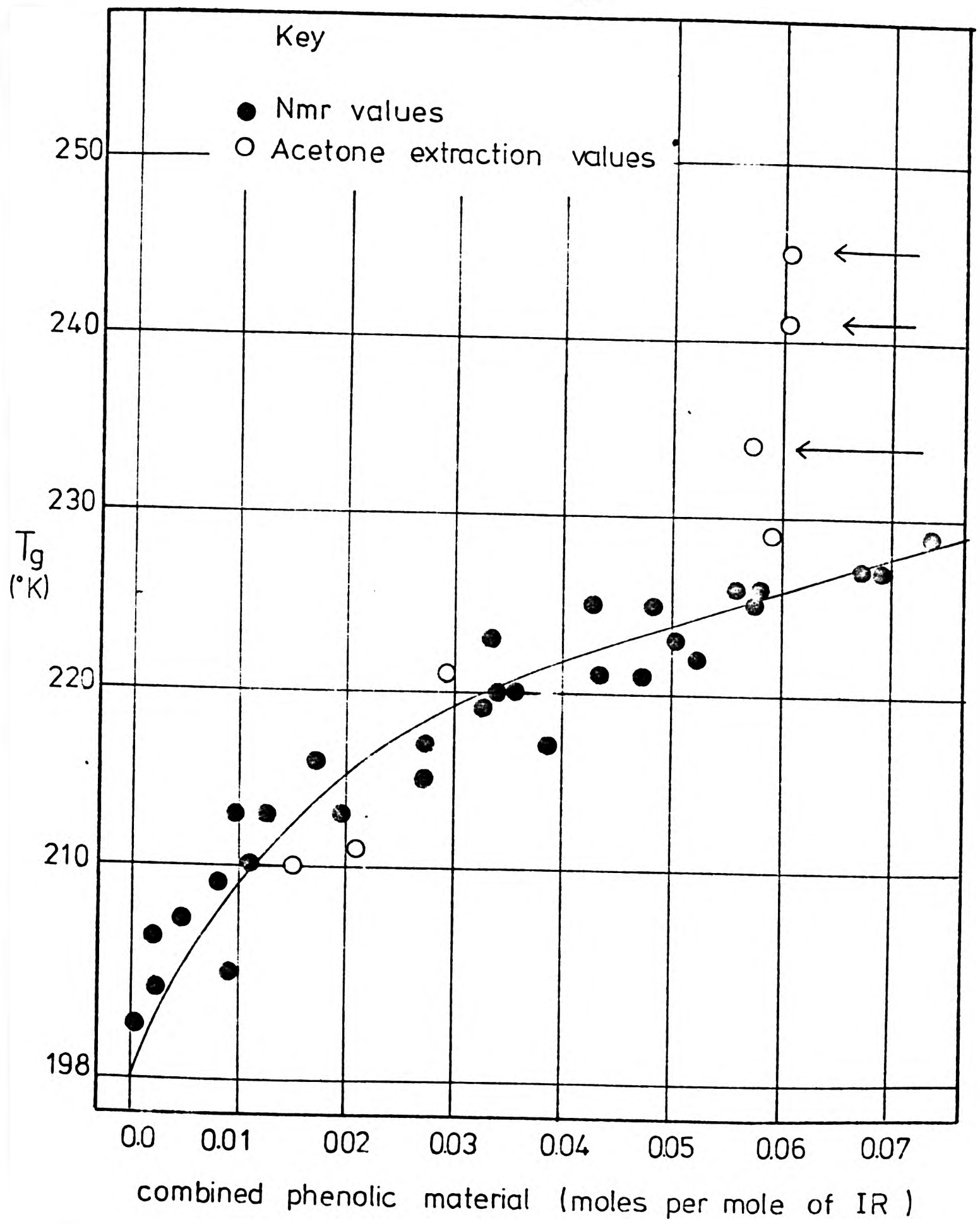


Fig. 60 Increase in  $T_g$  of IR with phenolic material combined.

120 min. of reaction time for the IR/MP/SnCl<sub>2</sub>.2H<sub>2</sub>O and IR/E/SnCl<sub>2</sub>.2H<sub>2</sub>O interactions, respectively. This implies that adduct formation ceases and then reverses, which is clearly not the case from the earlier investigations of the process. It is clear, therefore, that cyclization is slowing down in the later stages of the interactions, compared with its rate in the absence of the phenolic materials. This is presumably due to destruction of catalyst, possibly through hydrolysis from the liberated water of reaction. The higher degree of cyclization apparent from these results (and from earlier results) in the ether case, compared with the methylol phenol case, is in agreement with this hypothesis, since less water is liberated in the former reaction.

Fig. 60 show T<sub>g</sub> values plotted against phenolic material combined (obtained by nmr spectroscopy or acetone extraction) for all interactions at various times. The main deviations to the general trend of this curve (indicated by arrows in Fig. 60) seems to be those data for the IR/MP/SnCl<sub>2</sub>.2H<sub>2</sub>O and IR/E/SnCl<sub>2</sub>.2H<sub>2</sub>O interactions after 80-120 min. of reaction time, thus again clearly showing the onset of appreciable cyclization in these interactions.

### 3.11 Molecular Weight Changes and Gel Content

Intrinsic viscosity  $[\eta]_{c=0}$  values for the uncatalysed and ZnCl<sub>2</sub>-catalysed interaction products (all of which remained completely soluble), and gel content for the SnCl<sub>2</sub>- and SnCl<sub>2</sub>.2H<sub>2</sub>O-catalysed interaction products, are tabulated in the Experimental Chapter and they are plotted

against reaction time in Figs. 61 and 62, respectively. The data of Fig. 61, though very scattered, show that a very small increase in viscosity has occurred in each case. The crosslinking process responsible must be insignificant comparable to the main reaction. The viscosity value for the uncatalysed and  $\text{ZnCl}_2$ -catalysed interaction at zero reaction time ( $1.95(\text{g}/100\text{ml})^{-1}$ ) was smaller than the corresponding value for the IR/ $\text{ZnCl}_2$  interaction (i.e., in the absence of phenolic condensate) ( $2.90(\text{g}/100\text{ml})^{-1}$ ); this is probably due to a somewhat higher degree of rubber breakdown in the longer mixing time required in the former case. Fig. 62 shows that toluene-insoluble gel, which was undetectable in the uncatalysed and  $\text{ZnCl}_2$ -catalysed interactions, was formed in a large amount (40-80%) in the initial stages of the  $\text{SnCl}_2$  and  $\text{SnCl}_2 \cdot 2\text{H}_2\text{O}$ -catalysed interactions and increased very slowly with further reaction time. The high amount of gel formed in the  $\text{SnCl}_2$  and  $\text{SnCl}_2 \cdot 2\text{H}_2\text{O}$  cases indicates the formation of crosslinks in appreciable numbers. The gel in these cases forms at a higher rate than in the corresponding IR/ $\text{SnCl}_2$  and IR/ $\text{SnCl}_2 \cdot 2\text{H}_2\text{O}$  interactions, suggesting that phenolic material-rubber interaction is responsible in some degree for the crosslinking. Despite the high proportion of gel, the degree of swelling observed was very high in all cases, and the swollen gels were very difficult to handle without breaking. This suggests that the number of crosslinks present are not very significant when compared with the number produced during the conventional vulcanization of IR by p/f resins or other reagents.

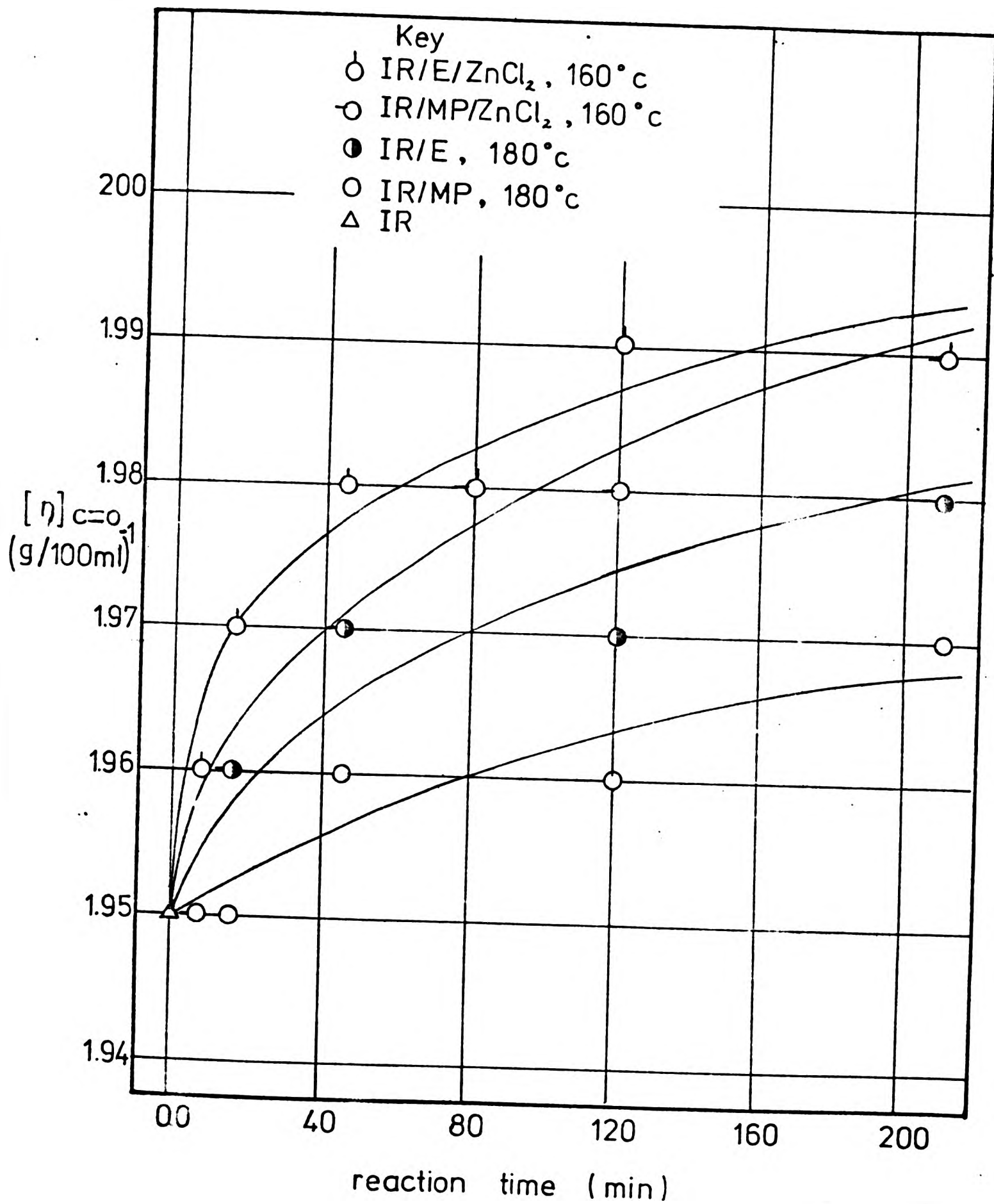


Fig. 61 Intrinsic viscosity ( $[\eta]_{c=0.1}$ ) versus reaction time for the IR/MP, IR/E, IR/MP/ZnCl<sub>2</sub> and IR/E/ZnCl<sub>2</sub> interactions.

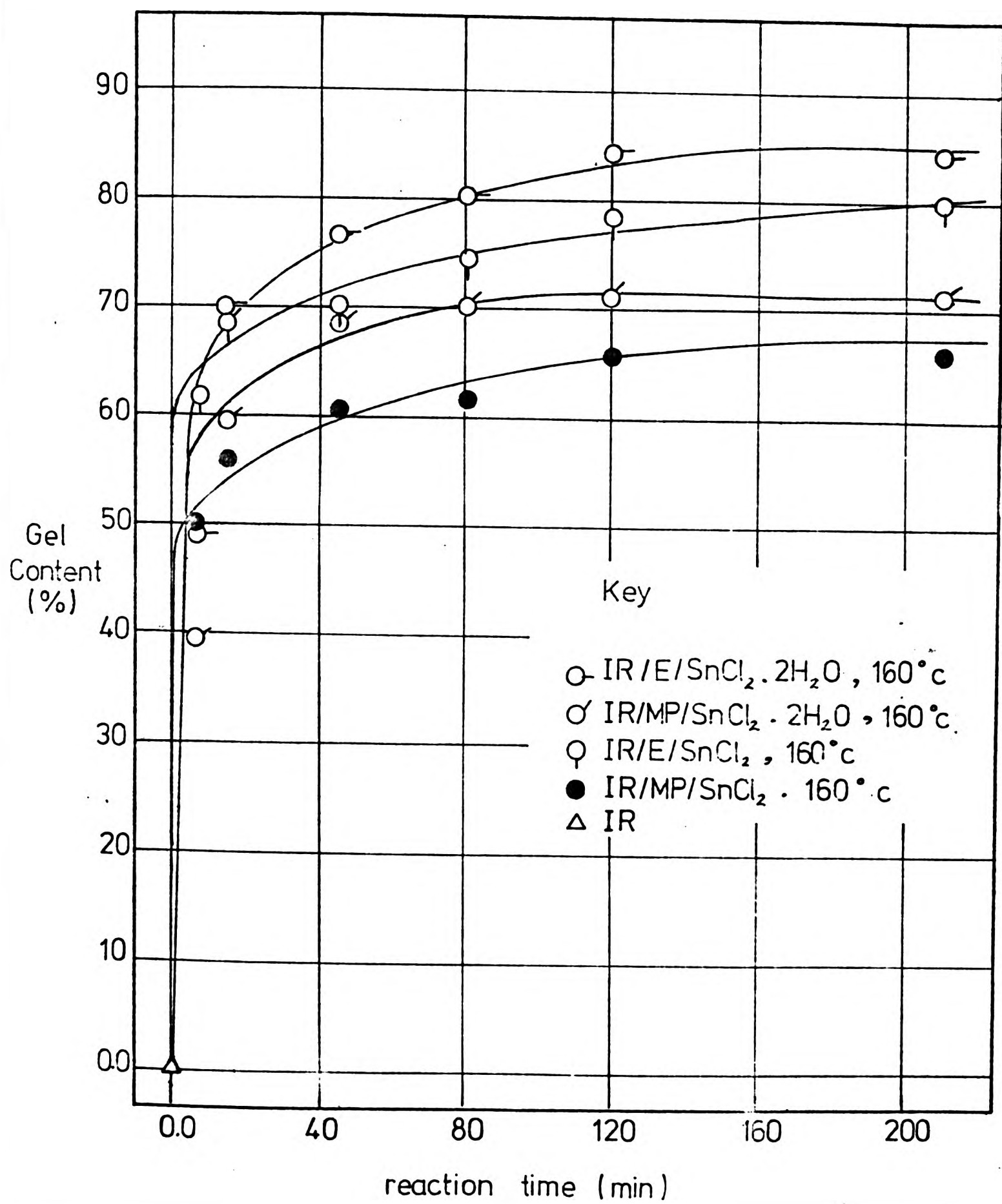


Fig. 62 Gel content versus reaction time for the IR/MP/SnCl<sub>2</sub>, IR/E/SnCl<sub>2</sub>, IR/MP/SnCl<sub>2</sub>·2H<sub>2</sub>O and IR/E/SnCl<sub>2</sub>·2H<sub>2</sub>O interactions.

### 3.12 Discussion

#### (a) Kinetics of adduct formation

##### (i) Bound phenolic material

A comparison of values for 'bound phenolic material' as obtained by acetone extraction and nmr spectroscopy show a reasonable agreement (Figs. 26 and 27) considering the reservations which have been expressed about these methods. Ultimate concentration maxima and rates of combination after 30 min. of reaction time are similar when calculated by the two methods. However, initial rates are different, being in general faster when calculated from nmr spectroscopy than from acetone extraction results for the catalysed interactions. Initial rates as obtained by nmr spectroscopy might be considered more reliable than those by acetone extraction since the small amounts of material combined in these early stages of reaction are expected to be more accurately determined by nmr spectroscopy than by gravimetric analysis.

Comparison of results for the catalysed and uncatalysed interactions show that, in the former, not only were rates of combination of phenolic material higher (as expected) but also, for all catalysts, concentration maxima were much higher. A comparison of results for the dibenzyl ether and the methylphenol interactions reveals that the former always gives higher rates and higher concentration maxima. This can be explained by the

premise that the quinone methide intermediate arises directly from the dibenzyl ether and not from the methylolphenol, and thereby inhibits the consumption of 'active' phenolic material by side-reactions (see Fig. 4).

(ii) Relationship to Fitch's model study

In his study of the interaction between 2-methylpent-2-ene and dibenzyl ether or methylol phenol,<sup>11</sup> Fitch found that although initial rates for the catalysed ( $\text{SnCl}_2 \cdot 2\text{H}_2\text{O}$ ) interactions were higher than those for the uncatalysed ones, the final rates and chroman concentration maxima achieved were similar in level (Fig. 23 and 24). Fitch considered that retardation in the later stages of reaction could be attributed in part to 2 factors: first, hydrolytic instability of the catalyst limited its activity and led to its eventual exhaustion; secondly, catalysed isomerization of the alk-2-ene produced an approximately equimolar mixture of alk-2-ene, and inactive alk-1-ene. However, reactions were faster and chroman concentration maxima increased approximately two-fold for the catalysed interactions when an excess of added methanal was present. This was explained in terms of a suppression of the dissociation of methylol phenol into the phenol and methanal, thereby minimising the formation of the diphenylmethane and possibly other by-products (see Fig. 4). Thus, the concentration of 'active' phenolic material was higher and also therefore the combination efficiency of the phenolic nuclei with the alk-2-ene. In the present study

there is no evidence for isomerization of the IR for the  $\text{ZnCl}_2$  and  $\text{SnCl}_2$ -catalysed reactions but there is for the  $\text{SnCl}_2 \cdot 2\text{H}_2\text{O}$  case (see later Discussion). For all of them rates and bound phenolic concentration maxima (Table 4) were similar to those for the catalysed interaction with added methanal of Fitch's study (Table 1). It would seem that retention of volatiles in the mould under pressure (between the two protective sheets of FEP film) might be responsible for the high rate and degree of combination in the present work, through a mechanism similar to that suggested by Fitch. However, the results might also partly be accounted for by the ( $\sim 4$  fold) higher concentration of catalyst used compared with that used by Fitch and because the model 2-methyl pent-2-ene shows a somewhat lower degree of unsaturation (one double bond per  $\text{C}_6\text{H}_{12}$ ) and therefore reduced reactivity compared with IR (one double bond per  $\text{C}_5\text{H}_8$ ). For the uncatalysed interactions the temperature used ( $180^\circ\text{C}$ ) was higher than that used ( $150^\circ\text{C}$ ) in the corresponding case in Fitch's study. Despite this difference, however, rates and concentration maxima were similar in the two studies (Tables 1 and 4). In the present study volatile reaction products were again presumably retained by the FEP sheets in the uncatalysed interactions, and this, together with the higher temperature and (presumed) higher reactivity of the IR would lead to the expectation of higher rates and concentration maxima in the present study.

There is no obvious explanation for this anomaly,

except possibly to note that traces of a catalyst might be expected to exert a profound effect on reaction rates in comparison with even large changes in temperature. As with cationic mechanisms in general, it is almost impossible to ensure that truly 'uncatalysed' mechanisms are operating, since reactions are extremely sensitive to minute amounts of Lewis acid reagents. The presence of very small amounts of such contaminants in the IR could well account for these differences.

Comparison of the kinetics of combination of phenolic material for the various catalysts shows that rates of combination were higher for  $\text{SnCl}_2 \cdot 2\text{H}_2\text{O}$  than for  $\text{SnCl}_2$  which in turn was faster than for  $\text{ZnCl}_2$ . These differences might best be considered in conjunction with the observation that there is no isomerization of IR by  $\text{SnCl}_2$  or  $\text{ZnCl}_2$  in the presence of methylol phenol or ether whereas cis/trans isomerization, double bond shift and cyclization of the IR occurs in the  $\text{SnCl}_2 \cdot 2\text{H}_2\text{O}$  case (Section b below). If high rates of combination and isomerization are presumed to require appreciable 'proton' concentration e.g.,  $\text{H}_3\text{O}^+$ , the differences might well be associated with the ease of co-ordination of (e.g.) water or phenolic material with  $\text{ZnCl}_2$  and  $\text{SnCl}_2$ , a topic which is discussed more fully later (Section d below).

(iii) Unbound unextractable material

Decomposition of methylol phenol and dibenzyl ether

in a saturated hydrocarbon medium such as EPR would give the same results as in IR under the same conditions, the major difference being that of adduct formation in the latter. In the EPR case adduct formation is not possible and the major final products from the phenolic materials would be trimer (Fig. 4) and possibly more highly condensed by-products. Although trimer is acetone-soluble and therefore extractable, some of the by-products might well be acetone-insoluble and unextractable. Indeed, whereas IR spectroscopy of the 'reacted' EPR after acetone-extraction shows the presence of bands attributable to hydroxyl and substituted benzene nuclei (Fig. 40), carbonyl bands characteristic of the trimer were not observed. Thus, it appears that the unextractable material is likely to be a mixture of phenolic side-reaction products of which the trimer is not a major component. Since it is not known whether or not the formation of chroman in IR will affect the formation of this insoluble phenolic material, it is difficult to decide whether correction of the IR results for unextractable material, using the EPR figures, is justifiable. Fitch<sup>11</sup> also observed that insoluble by-products were formed during his 'model' studies and, although his results are not strictly comparable in magnitude with the present ones, his insoluble material was formed more quickly and in greater final amounts for the catalysed compared with the uncatalysed reactions. These findings agree with those of the present study (Fig. 91 Chapter 6). The amount of unextractable material under consideration is, of course, very small and its estimation is subject to considerable error in view of the methods available for its

determination. Nevertheless, on balance it was considered desirable to correct results in the present work in accordance with the unextractable contents found for the EPR work.

Although the catalysts themselves are soluble in acetone, some of the products of decomposition or hydrolysis of the catalysts are expected to be insoluble and therefore to remain as unextractable matter. However, since they are used in such small proportions their contribution to the unextractable matter is considered negligible. In any case ir spectroscopy (Fig. 41-a) shows that the hydrolysis products of  $\text{SnCl}_2 \cdot 2\text{H}_2\text{O}$  and  $\text{SnCl}_2$ , which are likely to be mainly  $\text{Sn}(\text{OH})_2$ , are not ir active in the organic hydroxyl region. Therefore, although this compound might be present in the unextratable matter in the various interaction, it would not contribute to the unextractable hydroxyl concentration as determined from the spectra of the IR/MP/ $\text{SnCl}_2$ , IR/E/ $\text{SnCl}_2$ , IR/MP/ $\text{SnCl}_2 \cdot 2\text{H}_2\text{O}$  and IR/E/ $\text{SnCl}_2 \cdot 2\text{H}_2\text{O}$  interaction products.

(b) Isomerization and other side-reactions

(i) Cis-trans isomerization and double-bond shifts

In the IR/MP/ $\text{SnCl}_2 \cdot 2\text{H}_2\text{O}$  and IR/E/ $\text{SnCl}_2 \cdot 2\text{H}_2\text{O}$  interactions the occurrence of double bond shifts, cis/trans isomerization, and cyclization is suggested by ir and nmr spectroscopy, whereas it does not occur in the IR/MP/ $\text{ZnCl}_2$ ,

IR/MP/SnCl<sub>2</sub>, IR/E/ZnCl<sub>2</sub>, IR/E/SnCl<sub>2</sub>, IR/MP, and IR/E interactions. Therefore, in all the latter interactions reduction in the intensity of the original trialkylethylenic ir unsaturation band at 12.0μm (Fig. 56) might be interpreted only in terms of chroman formation, whereas in former cases cyclization and double bond shifts would also reduce this absorption. Since both chroman and methylene bridge structures would consume -CH= protons the absence of reduction in this peak in the nmr spectrum (for interactions IR/MP, IR/E, IR/MP/ZnCl<sub>2</sub> and IR/E/ZnCl<sub>2</sub>, where gel was absent) is interpreted in terms of a lack of sufficient precision in the method. For example, accuracy of solution concentration made up at different reaction times would be critical in order to observe this reduction since the loss of total unsaturation as calculated by perbenzoic acid (Fig. 54) is very small. For those cases where gel content was present in high amount from the early stages of reaction (i.e., IR/MP/SnCl<sub>2</sub>, IR/MP/SnCl<sub>2</sub>.2H<sub>2</sub>O and IR/E/SnCl<sub>2</sub>.2H<sub>2</sub>O) no satisfactory spectra could be obtained for the concentration of polymer as made up (5%). In these cases it was necessary to dissolve further amounts of polymer which resulted in different and unknown concentrations of polymer at different times of reaction for the same interaction. In spite of these difficulties, reduction of the nmr peak for the -CH= protons was observed for the IR/MP/SnCl<sub>2</sub>.2H<sub>2</sub>O and IR/E/SnCl<sub>2</sub>.2H<sub>2</sub>O interactions, since more drastic reduction was occurring through cyclization (Section ii below).

(ii) Cyclization

The clearest indications of the occurrence of cyclization are seen in the reduction of total unsaturation further than that required for chroman formation, and an increase in  $T_g$  over and above any increase which might result from adduct formation, these effects have already been considered individually and are now considered in combination.

A plot of total unsaturation v.  $T_g$  (Section 2.9) for rubber and catalyst only enables an estimate of degree of cyclization to be obtained from changes in either unsaturation or  $T_g$ . However, both are complicated by the presence of phenolic adduct, which makes unsaturation measurements somewhat less reliable (Section 3.10) and which also makes a slight positive contribution to  $T_g$  (Section 3.10).

As will be seen in later discussion, the loss of unsaturation in all those interactions involving  $ZnCl_2$  and  $SnCl_2$  catalysts approximately corresponds with the loss required for chroman formation, so that no cyclization can be occurring in these reactions. However, for the reaction catalysed by  $SnCl_2 \cdot 2H_2O$ , an excessive loss of unsaturation indicates the occurrence of cyclization. In these  $SnCl_2 \cdot 2H_2O$ -catalysed interactions, the amounts of unsaturation consumed by cyclization (calculated as described earlier-Fig. 55) are slightly higher for the

IR/E/SnCl<sub>2</sub>.2H<sub>2</sub>O case than for the IR/MP/SnCl<sub>2</sub>.2H<sub>2</sub>O interaction. This is opposite to the expected order if cyclization and chroman formation are competitive reactions, since there is evidence of further adduct formation in the former interaction than in the latter. However, the differences are small and might be due to limitations in the method of analysis. Comparison between unsaturation consumed by cyclization in the IR/MP/SnCl<sub>2</sub>.2H<sub>2</sub>O interaction (as calculated from the difference between moles total unsaturation (perbenzoic acid) and moles phenolic material combined) and that of the IR/SnCl<sub>2</sub>.2H<sub>2</sub>O case is illustrated in Fig. 63. Fig. 63 shows the serious discrepancy which may arise in estimating unsaturation from nmr and from iodine values; it indicates a degree of cyclization for the methylol phenol interaction which is intermediate between those values of 'pure rubber' cyclization as determined by the nmr and iodine value methods. Lower values of cyclization for the IR/MP/SnCl<sub>2</sub>.2H<sub>2</sub>O and IR/E/SnCl<sub>2</sub>.2H<sub>2</sub>O interactions than for the IR/SnCl<sub>2</sub>.2H<sub>2</sub>O case would be expected if adduct formation and cyclization are regarded as competing for the available catalyst.

The value of T<sub>g</sub> for the various reaction products will in theory be influenced by at least 3 factors:

(i) a slight change in T<sub>g</sub> might be expected to arise from cis/trans isomerizations and double-bond shifts, but since

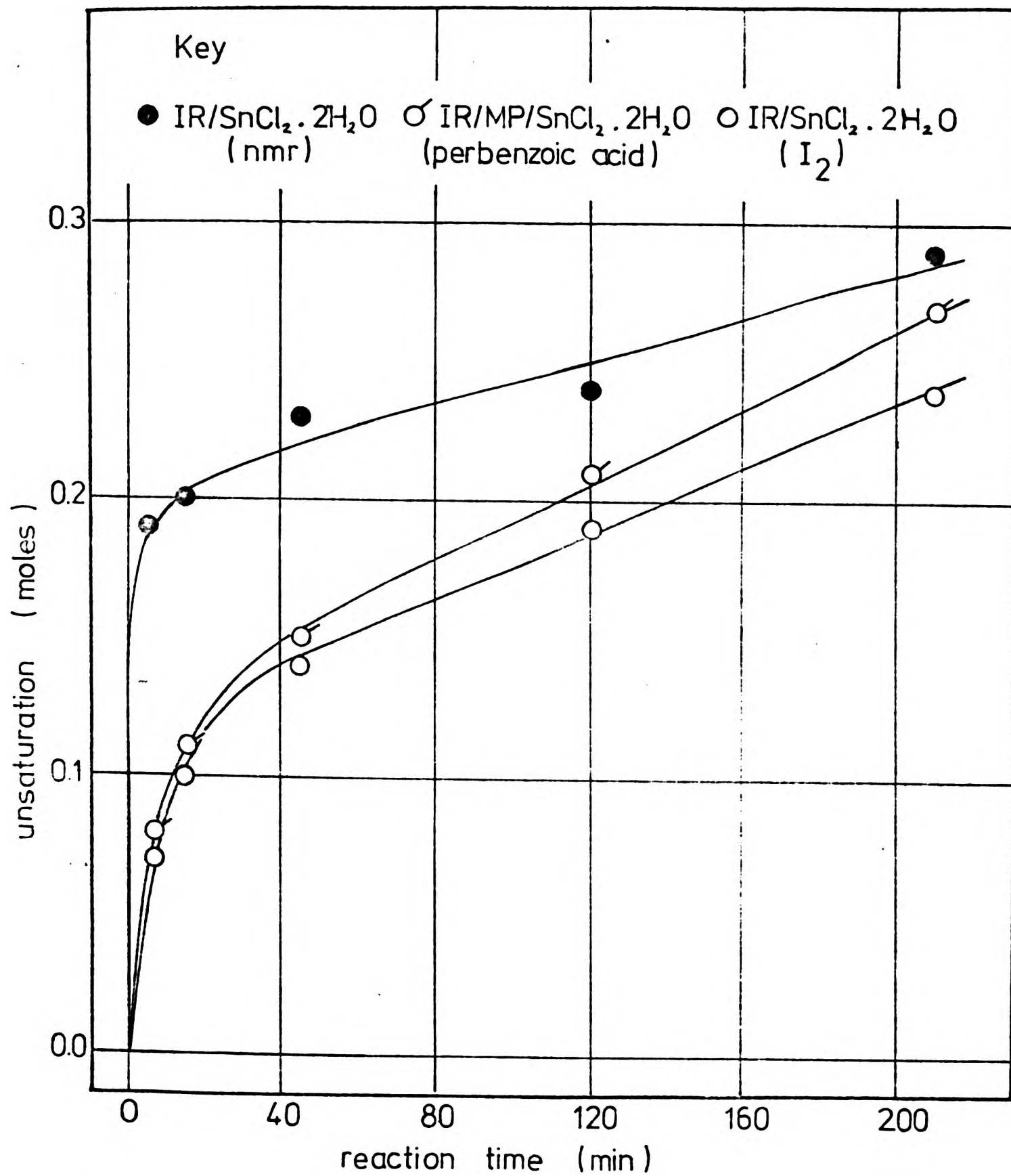


Fig. 63 Comparison between unsaturation consumed by cyclization in the IR/MP/SnCl<sub>2</sub>·2H<sub>2</sub>O and IR/SnCl<sub>2</sub>·2H<sub>2</sub>O interactions.

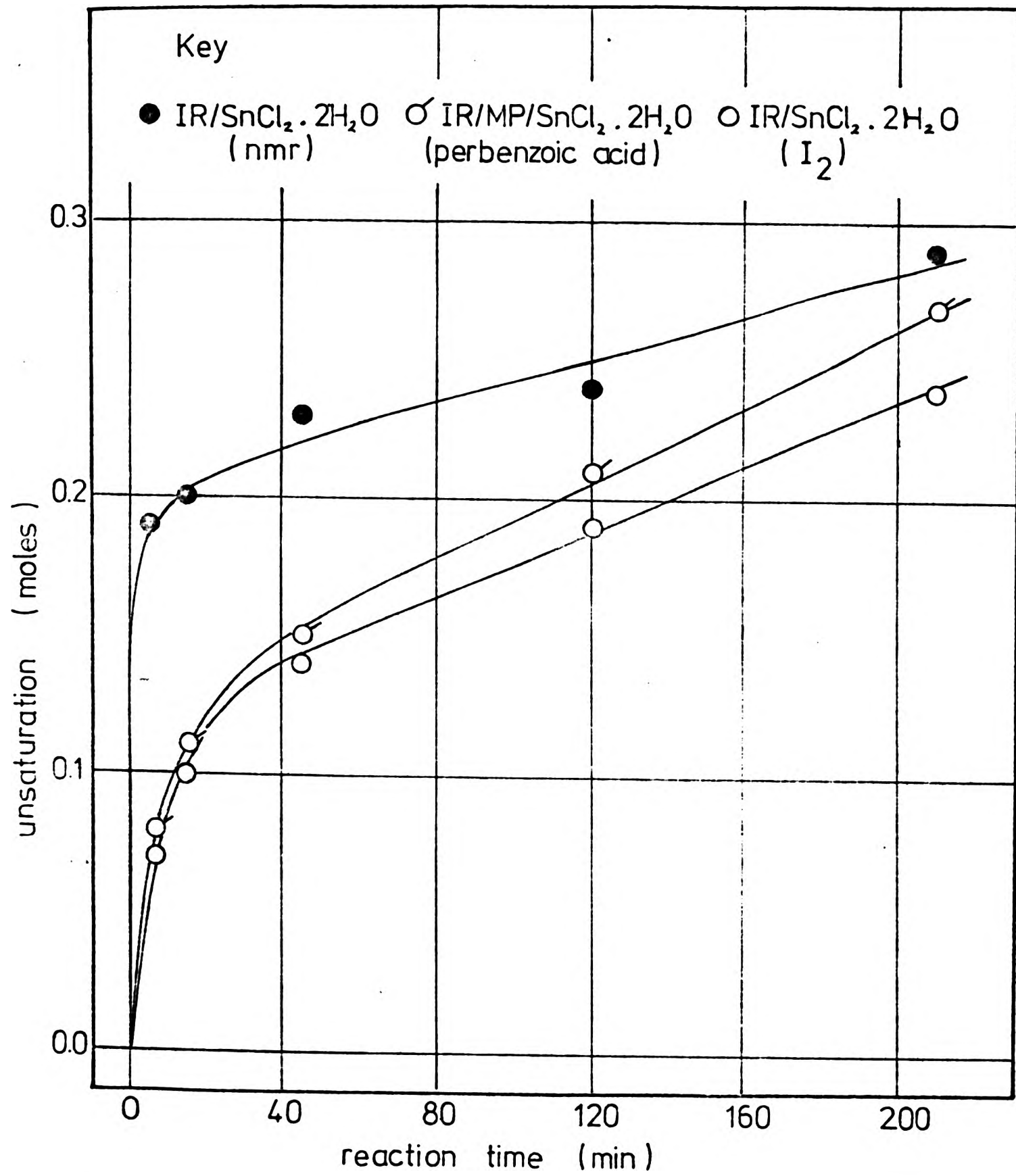


Fig. 63 Comparison between unsaturation consumed by cyclization in the IR/MP/SnCl<sub>2</sub>·2H<sub>2</sub>O and IR/SnCl<sub>2</sub>·2H<sub>2</sub>O interactions.

the  $T_g$  of trans-1,4 polyisoprene is only some  $13^\circ$  higher than cis-1,4 polyisoprene<sup>92</sup> and since some isomerised cis-polyisoprenes of  $\sim 40\%$  trans content have been reported to show  $T_g$ 's undetectably different from the pure cis isomer,<sup>106</sup> it will be assumed that these effects will exert a negligible contribution to  $T_g$ .

(ii) an increase in  $T_g$  would be expected to accompany adduct formation, which inserts cyclic groups showing severe hindrance to chain rotation. The increase in  $T_g$  for all reaction products except the  $\text{SnCl}_2 \cdot 2\text{H}_2\text{O}$  catalysed ones is attributed solely to this effect, and it enables a plot of adduct concentration v.  $T_g$  to be obtained (Fig. 60). This change in  $T_g$ , although not negligible, will be small at those levels of adduct formation involved in vulcanization.

(iii) main-chain cyclization would also be expected to increase  $T_g$  and, since this may occur extensively through a cationic chain reaction, large increase in  $T_g$  would be looked for. Thus, in the  $\text{SnCl}_2 \cdot 2\text{H}_2\text{O}$ -catalysed interactions, where both adduct-formation and cyclization occur simultaneously, it is possible to distinguish between the 2 effects and, assuming additivity, the total rise in  $T_g$  is given by the sum of the rises due to these two individual processes. This is illustrated in Fig. 58, where the more important contribution of cyclization in determining  $T_g$  is clearly revealed.

(iii) Crosslinking and gel content

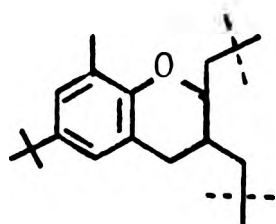
The  $\text{SnCl}_2$  and  $\text{SnCl}_2 \cdot 2\text{H}_2\text{O}$ -catalysed interactions of methylolphenol and dibenzyl ether with IR both showed higher rates of gel formation and higher gel concentration maxima than the corresponding catalysed isomerizations in the absence of phenolic material. In the latter case, light crosslinking appears to accompany cyclization, and has already been discussed (Section 2.10, Chapter 2). The additional crosslinking found in the presence of the phenolic materials would imply that some bifunctional material is formed as a by-product. The amount of crosslinking is very low and only traces of such a material need be formed. In the  $\text{SnCl}_2$ -catalysed cases, where no gel formation is observed in the absence of phenolic material, it must be the sole crosslinking agency. Thus, those mechanisms proposed earlier (Section 2.11, Chapter 2) for the crosslinking, involving Diels-Alder type addition of conjugate double bonds formed by double bond shifts or any mechanism involving cationic modification of the IR are clearly not applicable in this case. These crosslinking mechanisms may operate in the IR/MP/ $\text{SnCl}_2 \cdot 2\text{H}_2\text{O}$  and IR/E/ $\text{SnCl}_2 \cdot 2\text{H}_2\text{O}$  interactions since there is evidence for such modifications of the rubber. However, they cannot be operating at higher levels in the corresponding phenolic interaction, where adduct formation is occurring, than they are in the IR/ $\text{SnCl}_2 \cdot 2\text{H}_2\text{O}$  case, i.e., in the absence of phenolic materials. Thus, the faster rates of gel formation and higher concentration maxima are almost certainly the

result of interaction with phenolic material of higher functionality. The crosslinking agents probably arise from interaction between  $\text{SnCl}_2$  (or  $\text{SnCl}_2 \cdot 2\text{H}_2\text{O}$ ) and phenolic decomposition products, since no crosslinking is observed in the uncatalysed reactions or in the  $\text{ZnCl}_2$ -catalysed ones. It is difficult to account for the absence of gel with the latter catalyst, but it is possibly connected with the more limited ability of Zn to expand its outer shell of electrons, i.e., to accommodate further ligands (see mechanisms of catalysis discussed in Section d below). The crosslinking is most likely to be through the original trialkylethylenic double bonds for the  $\text{SnCl}_2$  case but may involve any of the various double bond types formed in the  $\text{SnCl}_2 \cdot 2\text{H}_2\text{O}$  case. The nature of the crosslinking species is obscure, but it would seem to be necessary to invoke the idea of substitution at one of the 'unreactive' free ring positions. The presence of an additional methylol group in the nucleus would allow crosslinking to occur through a mechanism similar to that discussed for the dimethylol phenol, to be examined in Chapter 4.

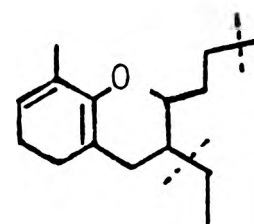
(c) Nature of the adduct

It is clearly much more difficult to identify precisely the types of structures present in the adducts formed in this work than it is in the case of model studies, where products are much more amenable to separation and identification techniques. If the alkenes used by Fitch<sup>11</sup> are considered to be appropriate as models

for the IR used in the work, then it would appear that the only significant product would contain chroman units of one or both of the structures:



LXXXIV



XCV

However, other chromans and methylene bridge structures are, of course, also possible (Scheme 3) and, although the present results can give no information about detailed structures, it is possible to examine them for evidence supporting chroman structures as compared with methylene bridge structures. As pointed out earlier, the most distinguishing features for these would be the retention of phenolic hydroxyl and unsaturation in the methylene bridge structures, whereas both are eliminated by chroman formation. Additionally, the presence of the chroman nucleus might be directly detectable by spectroscopic or other methods. The extent to which the findings of the present work relate to these is now examined.

(i) Evidence from residual phenolic hydroxyl

The presence of hydroxyl absorption bands in the infrared spectra of some of the adducts has already been reported and discussed in terms of concentration (Section 3.7). It seems that it is most unlikely that this

absorption is due to methylene bridge structures for the reasons:

1. The absorption passes through a peak value, then diminishes in the later stages of reaction; however, methylene bridge structures, if formed, would be expected to be stable. There is no scope for further reaction with methanal and loss of phenolic OH via quinone methide intermediates, since both ortho- positions are occupied by alkyl groups.

2. Comparison of the adduct spectra with those of 'model' methylene bridge compounds strongly suggest that the -OH absorption of the adduct is too broad and is at the wrong wavelength to be due to such structures. This same feature would also suggest that it cannot be due to other types of (unextractable) phenolic material.

The most obvious alternative source of hydroxyl is from the catalyst. However, hydrolysis products of the catalysts also failed to absorb in this region when examined by ir. The most likely remaining possibility would appear to be that the hydroxyl absorption is caused by an intermediate product of reaction between catalyst and phenolic material, which is supported by the fact that in the uncatalysed products the hydroxyl absorption is hardly detectable. This could also account for its apparent disappearance in the later reaction stages. However, identification of the hydroxylic species was not

absorption is due to methylene bridge structures for the reasons:

1. The absorption passes through a peak value, then diminishes in the later stages of reaction; however, methylene bridge structures, if formed, would be expected to be stable. There is no scope for further reaction with methanal and loss of phenolic OH via quinone methide intermediates, since both ortho- positions are occupied by alkyl groups.

2. Comparison of the adduct spectra with those of 'model' methylene bridge compounds strongly suggest that the -OH absorption of the adduct is too broad and is at the wrong wavelength to be due to such structures. This same feature would also suggest that it cannot be due to other types of (unextractable) phenolic material.

The most obvious alternative source of hydroxyl is from the catalyst. However, hydrolysis products of the catalysts also failed to absorb in this region when examined by ir. The most likely remaining possibility would appear to be that the hydroxyl absorption is caused by an intermediate product of reaction between catalyst and phenolic material, which is supported by the fact that in the uncatalysed products the hydroxyl absorption is hardly detectable. This could also account for its apparent disappearance in the later reaction stages. However, identification of the hydroxylic species was not

pursued further as it became apparent that it is most unlikely to be due to methylene bridge structures.

3. The nmr spectrum was expected to show a phenolic hydroxyl proton absorption at  $3.3\tau$ . However, this absorption was not observed.

(ii) Evidence from unsaturation

Total residual unsaturation, as estimated from iodine values using perbenzoic acid and iodine chloride, is reduced with adduct formation in all interactions. In the absence of extensive crosslinking, cyclization, and double bond shifting, i.e., in the IR/MP, IR/E, IR/MP/ZnCl<sub>2</sub>, IR/E/ZnCl<sub>2</sub>, IR/MP/SnCl<sub>2</sub> and IR/E/SnCl<sub>2</sub> interactions a reduction in total unsaturation means a loss of trialkylethylenic unsaturation and can be interpreted only in terms of chroman formation. Furthermore, for these interactions, values for this loss calculated from the perbenzoic acid results, are in fairly good agreement with the values of combined phenolic material as obtained by nmr spectroscopy and acetone extraction. This can be seen in Fig. 64, where results of unsaturation by both methods are compared with results for combined material.

These results (Fig. 64) strongly suggest that the chroman adduct is the only one formed. It is unfortunate that the

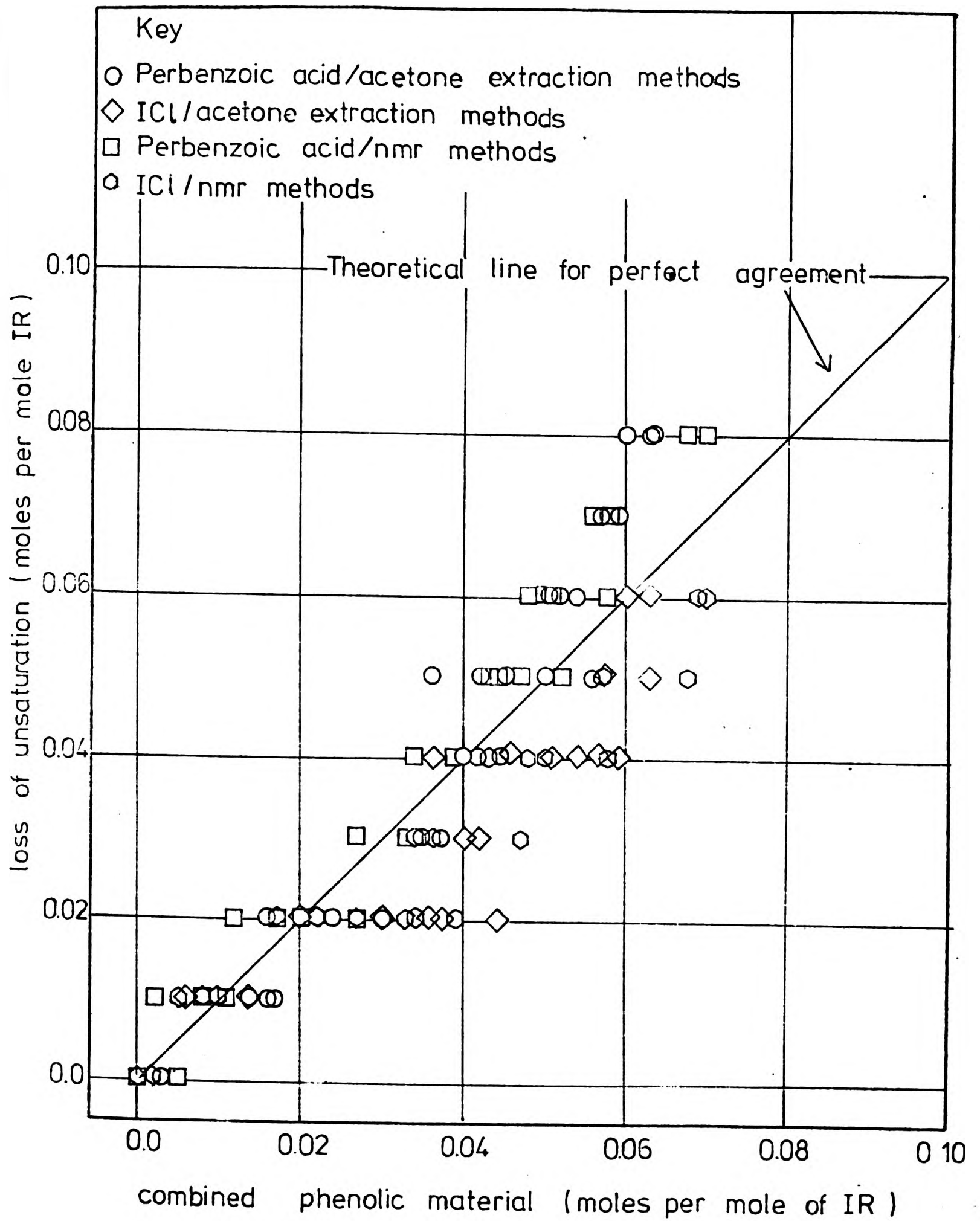


Fig. 64 Comparison of moles of loss unsaturation as determined by iodine monochloride and perbenzoic acid methods with moles combined phenolic material as determined by nmr and acetone extraction methods.

results for unsaturation cannot be confirmed by quantitative analysis of the nmr spectra but, as pointed out earlier, the nmr spectra do not show a clear reduction in -CH= resonances due, it is believed, to the inaccuracies introduced by the presence of gel in the 'solutions' used.

(iii) Additional spectroscopic evidence for chroman structures

Both ir and nmr spectroscopy show peaks which might be attributable to chroman structures. The development of a band at  $10.5 \mu\text{m}$  in the ir spectrum in all cases might with confidence be assigned to the chroman ring in accord with the previous discussion in Section 3.6. Nmr peaks at  $8.7$  and  $9.0\tau$  might be assigned to  $\text{CH}_3\text{-C}$  and/or  $\text{-CH}_2\text{-}$  protons, respectively, in chroman structures. However, in all cases these peaks might also be attributable to the presence of small amounts of 1.2 and 3.4 polyisoprene units (e.g., structures LXVI and LXVII, respectively—see Section 2.8), in the original rubber. In addition, for the IR/MP/ $\text{SnCl}_2 \cdot 2\text{H}_2\text{O}$  and IR/E/ $\text{SnCl}_2 \cdot 2\text{H}_2\text{O}$  interactions where there is evidence of cyclization the above peaks might also be assigned to  $\text{-CH}_2\text{-}\overset{\text{I}}{\underset{\text{I}}{\text{C}}}$  ( $8.65\tau$ ) and  $\text{CH}_3\text{-}\overset{\text{I}}{\underset{\text{I}}{\text{C}}}$  ( $9.00\tau$ ) protons present in cyclized structures such as LXXVI. The additional peak at  $7.20\tau$ , present in all interactions, might with some confidence be assigned to Ar- $\text{CH}_2\text{-C}$  protons in chroman structures, since these protons in the internal chroman structure XXXII are reported to resonate at  $7.3\tau$ <sup>11</sup>. Furthermore, if such

protons were present in methylene bridge structures (see Scheme 3), they might be expected to resonate at a somewhat lower field in view of their proximity to the double bond present in all the possible methylene bridge structures.

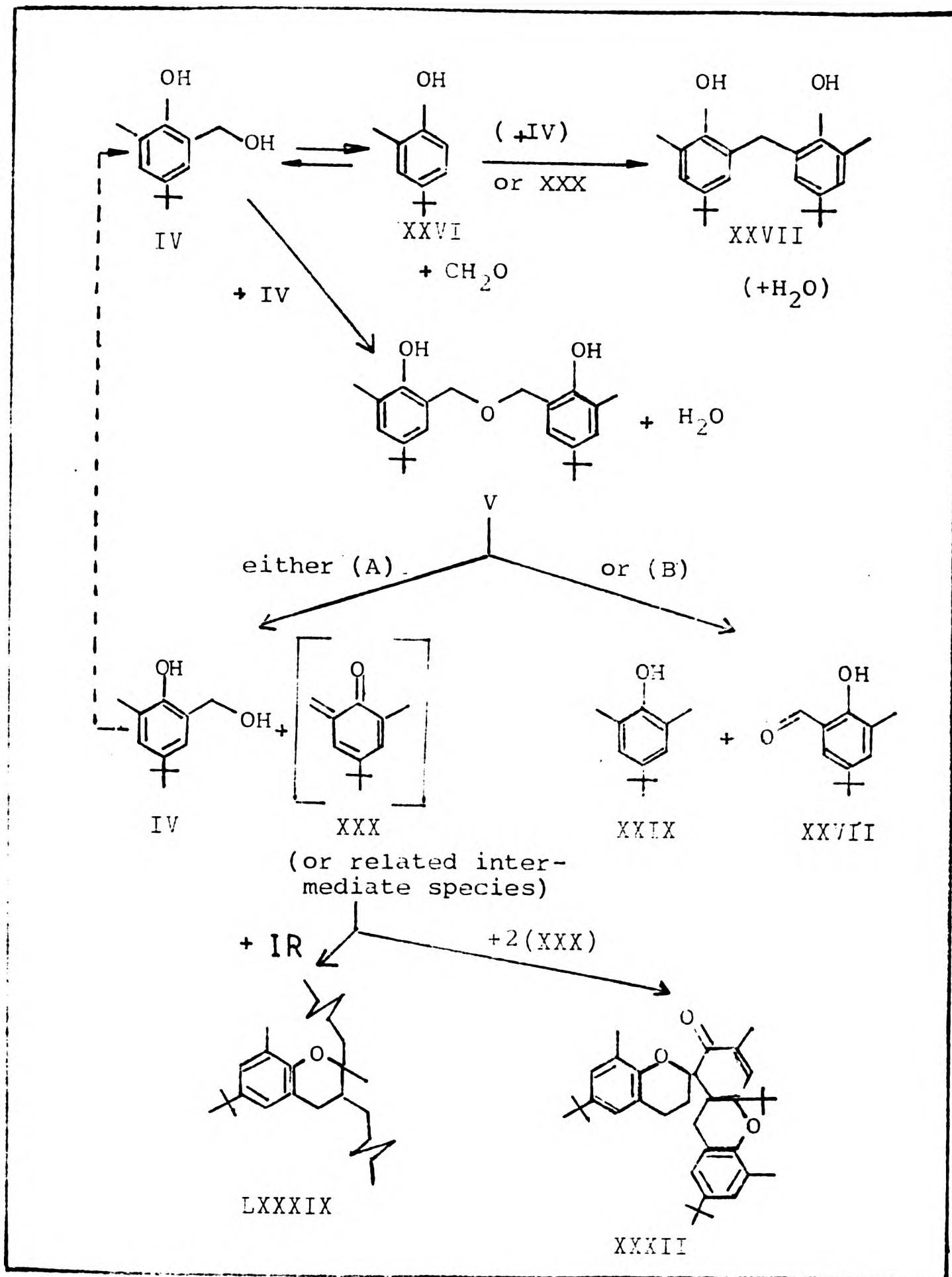
(d) Mechanism and catalysis of adduct formation

(i) Overall scheme

The progress of the interaction between the methylol phenol or dibenzyl ether and IR may be represented by the generalised Scheme 4, which represents an extension of that (Fig. 4) proposed by Fitch<sup>11</sup> for the interaction of the methylol phenol and dibenzyl ether with alk-2-ene. Fitch's conclusions were based on the analysis of products of decomposition of methylol phenol (or dibenzyl ether) in inert hydrocarbon medium (N-pentane) as well as on the interaction of them in a reactive medium (2-methyl-pent-2-ene). In the present study it is assumed that the hydrocarbon medium provided (isoprene rubber) will not cause any serious departure from the course of reaction found, and that the intermediate stages of reaction identified by Fitch will therefore be applicable in this present study.

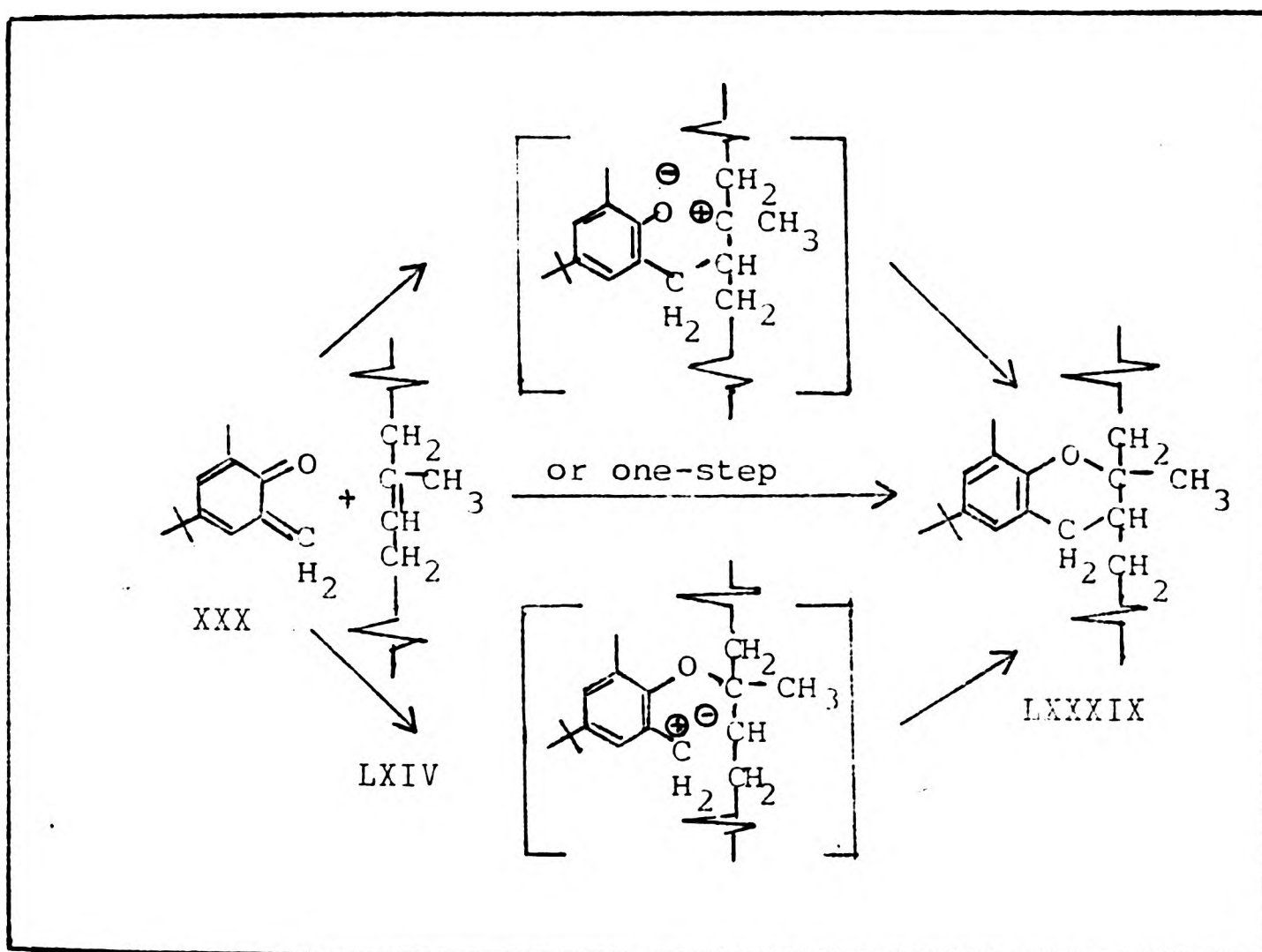
(ii) Uncatalysed mechanism of adduct formation

As discussed in Chapter 1, a Diels-Alder-type addition of the quinone methide to the IR would adequately explain



Scheme 4 Possible reaction scheme for the interaction of the methylolphenol (IV)/dibenzyl ether (V) with IR (LXIV).

the formation of the chroman, with the mechanism envisaged as either a two-step or a one-step process (Scheme 5). The two-stage mechanism has two possibilities for the intermediate ionic species, depending on whether the oxygen or the methylene group is first to add to the double bond of the IR.



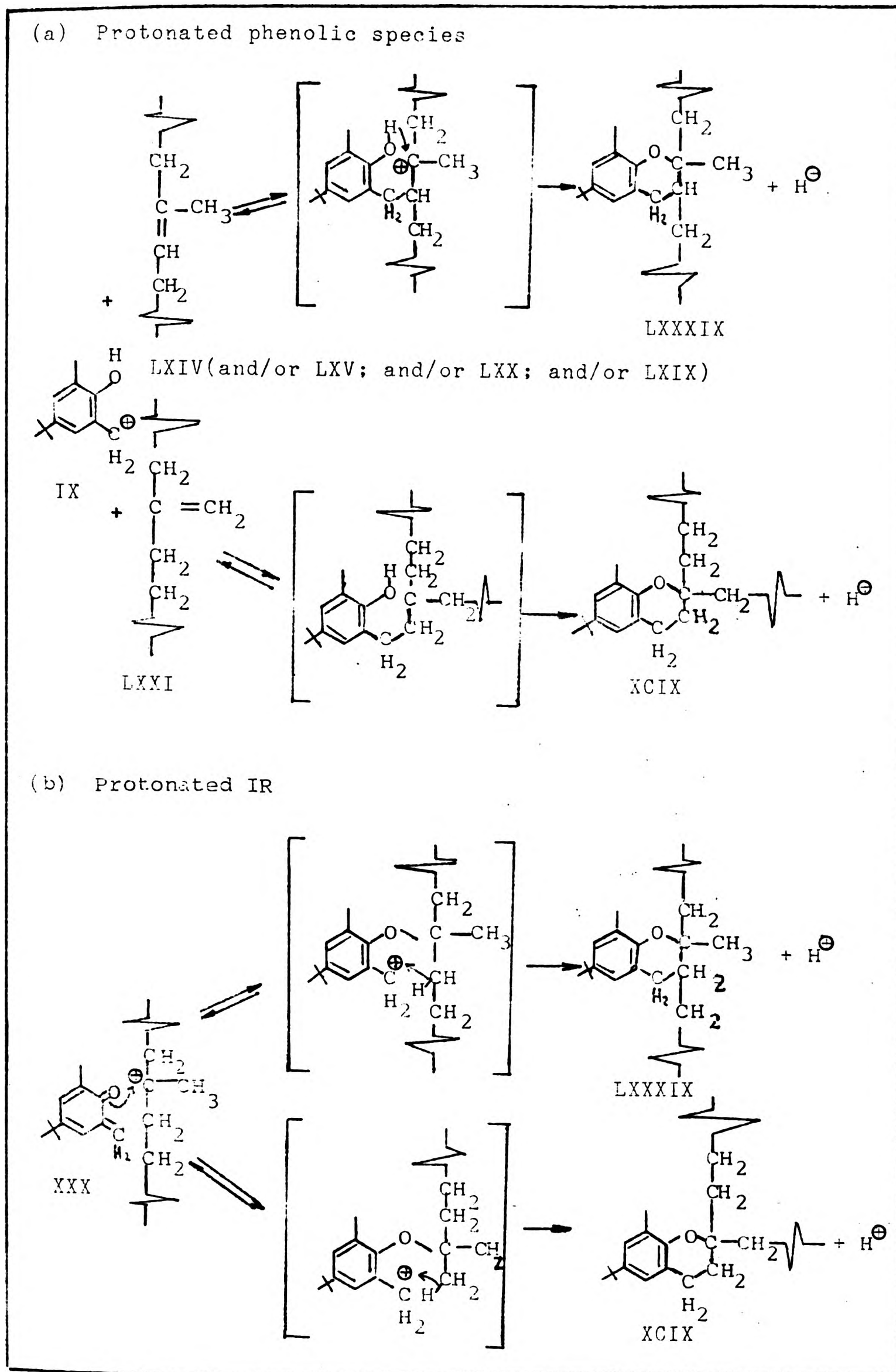
Scheme 5 Possible mechanistic scheme for uncatalysed adduct formation.

(iii) Catalysed mechanism involving  $\text{SnCl}_2 \cdot 2\text{H}_2\text{O}$

The results obtained suggest that a different mechanism is probably operating for those interactions catalysed

by  $\text{SnCl}_2 \cdot 2\text{H}_2\text{O}$  than those by  $\text{ZnCl}_2$  or  $\text{SnCl}_2$ , since for the former case cis/trans isomerization, cyclization, and double bond shifting of the rubber were observed whereas they were not found to occur in the  $\text{ZnCl}_2$  or  $\text{SnCl}_2$  case. This might be the result of a different action by these catalysts, or might be just a rate effect. Further discussion below will show that the former is more likely.

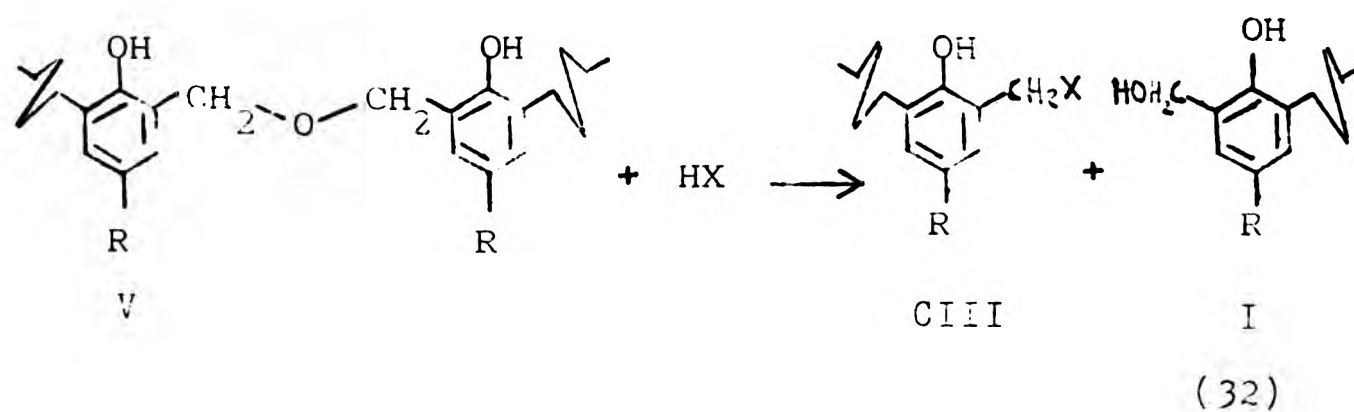
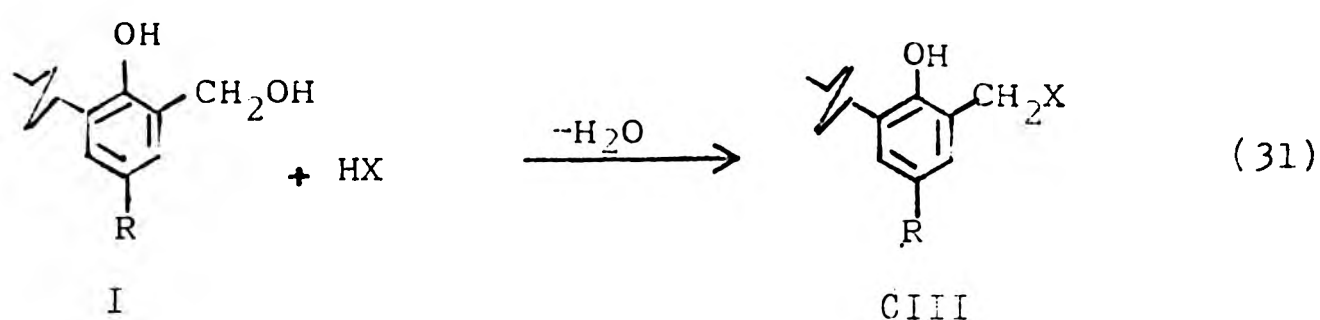
The action and subsequent destruction of the  $\text{SnCl}_2 \cdot 2\text{H}_2\text{O}$  may be envisaged as occurring as proposed by Fitch in reaction (23) to (26) (Chapter 1), leading to reaction (8) (Chapter 1) being the most likely route of formation of the rubber-reactive entity (X). By analogy with Fitch's proposals for the model compounds, the  $\text{SnCl}_2 \cdot 2\text{H}_2\text{O}$ -catalysed mechanism of adduct formation between IR and methylolphenol (or dibenzyl ether) may be envisaged as a modified Diels-Alder mechanism occurring through the two alternative possibilities: (a) protonated phenolic species reacting with uncharged IR, or (b) protonated IR reacting with uncharged phenolic species (Scheme 6). In this scheme, for the case (a) above, possible reactions of the rubber-reactive entity IX are illustrated both with the original trialkyl-ethylenic unsaturation (LXIV) and with the 1,1-dialkyl-ethylenic unsaturation (LXXI) resulting from double bond shift. The additional double-bond-shifted structure LXIX is not illustrated since it would react in the same way as structure LXIV in this scheme.



Scheme 6 Possible mechanistic schemes for  $\text{SnCl}_2 \cdot 2\text{H}_2\text{O}$  catalysed adduct formation.

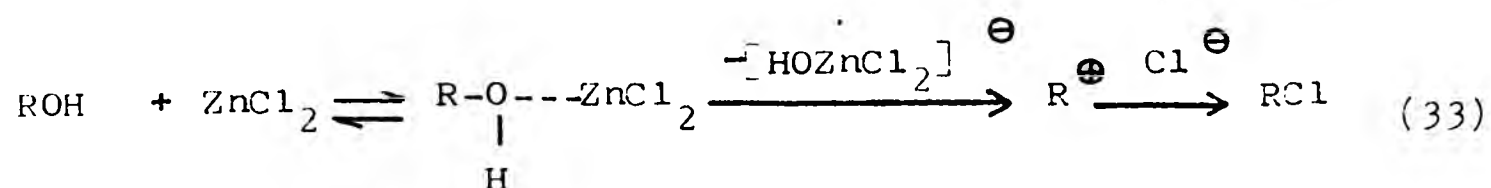
(iv) Mechanism for catalysts other than  $\text{SnCl}_2 \cdot 2\text{H}_2\text{O}$

It has been shown<sup>107</sup> by a comparison of moduli at 100% extension before and after aging that anhydrous  $\text{SnCl}_2$ ,  $\text{ZnCl}_2$  and  $\text{FeCl}_3$  were active catalysts of vulcanization of butyl rubber by phenolic resins.  $\text{SbCl}_3$ ,  $\text{CoCl}_2$  and  $\text{CdCl}_2$  also showed distinct catalyst activity.  $\text{NiCl}_2 \cdot 6\text{H}_2\text{O}$ ,  $\text{NiCl}_2 \cdot 2\text{H}_2\text{O}$  and  $\text{NiCl}_2$  were active, less active and inactive respectively. The catalyst action was suggested to be the result of formation of  $\text{HCl}$  by hydrolysis of the salts, so that only the more readily hydrolyzed salts were effective.<sup>109</sup> Mixtures of  $\text{SnCl}_2$  and carbon black were shown<sup>108</sup> by Mossbauer spectra to be completely converted to  $\text{SnO}_2$  by heating for a sufficient time or at sufficiently high temperature (e.g., 20-60 min. at  $170^\circ\text{C}$ ). When the heated  $\text{SnCl}_2$  was used in vulcanization, vulcanizate properties became increasingly poor, due to undercure, with increasing conversion to  $\text{SnO}_2$  prior to vulcanization<sup>108</sup>. It has been reported<sup>109</sup> that the stress at 100% elongation of unaged resin-vulcanized butyl rubber is highest when the  $\text{ZnCl}_2$  accelerator is added as anhydrous powder, lower when crystallizable  $\text{ZnCl}_2 \cdot 1.5\text{H}_2\text{O}$  is used and lower still for aqueous or alkaline solutions of  $\text{ZnCl}_2$ . On the above grounds it has been proposed<sup>110</sup> that the hydrohalogen acid liberated would react with the methylol group and dimethyl ether units present in the phenolic resin, equations (31) and (32) respectively:



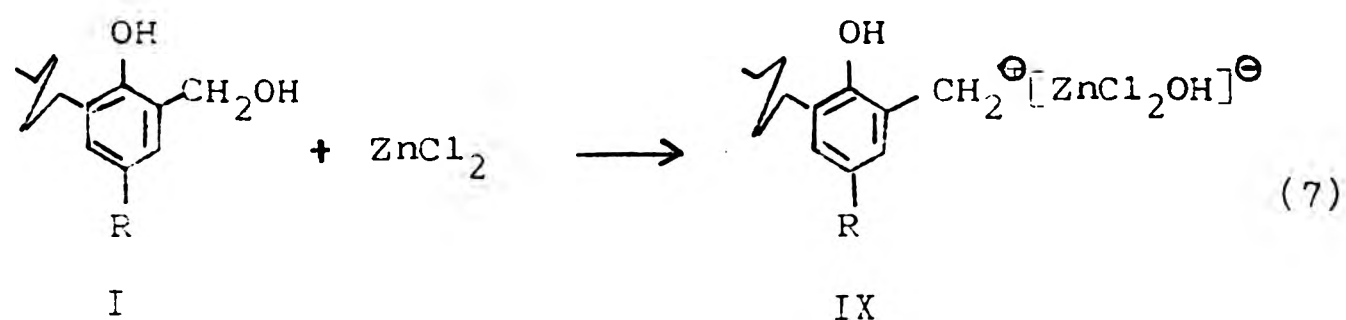
Equations (31) and (32) above may be envisaged as halomethylation of the phenolic resin in situ. As discussed in Chapter 1, such halomethylated materials ('self-reactive resins') lose hydrogen halide very readily to form the active o-quinone methide intermediate (III) ((1), x=Cl) and this would account for the catalytic effect observed. A solution of  $\text{ZnCl}_2$  in concentrated HCl (Lucas reagent) is widely used as a convenient reagent to differentiate between the lower primary, secondary and tertiary alcohols. Tertiary alcohols react very rapidly to give an insoluble layer of alkyl chloride at room temperature. Secondary alcohols react in several min., whereas primary alcohols

form chlorides only on heating. The order of reactivity is typical of S<sub>N</sub>1-type reactions. ZnCl<sub>2</sub> probably assists in the breaking of the C-O bond of the alcohol as follows:<sup>111</sup>

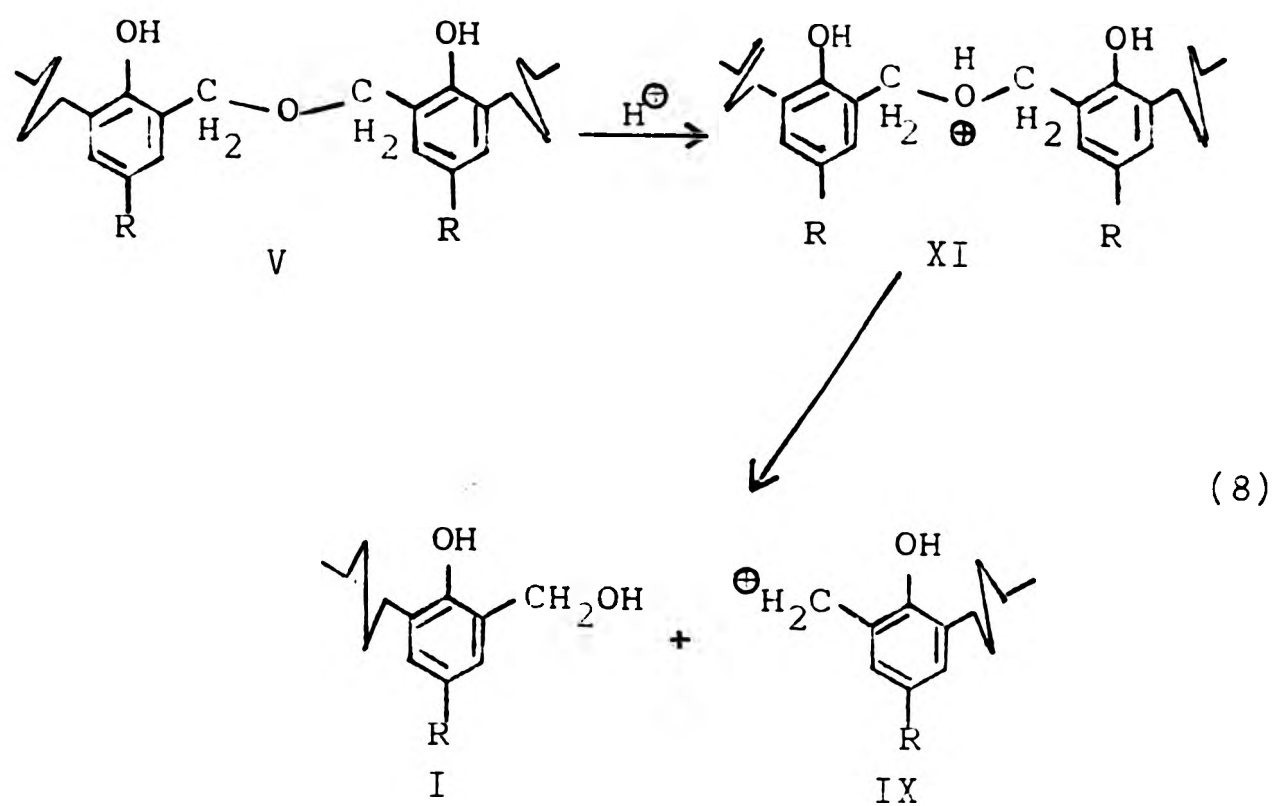


Reaction between Lucas reagent and methylolphenol has also been reported to form chlorides.

It will be noted that the above proposal for catalyst action does not directly require the production of carbonium ion (cationic) species. However, other workers have postulated the carbonium ion IX (see Section 1.2, Chapter 1) as a reactive intermediate<sup>29,30</sup> obtained by interaction of the methylol compounds with ZnCl<sub>2</sub> and SnCl<sub>2</sub>. As was discussed in Chapter 1 the formation of the carbonium ion IX has been represented by a direct complexing of the catalyst with the methylol group of I through reaction (7):

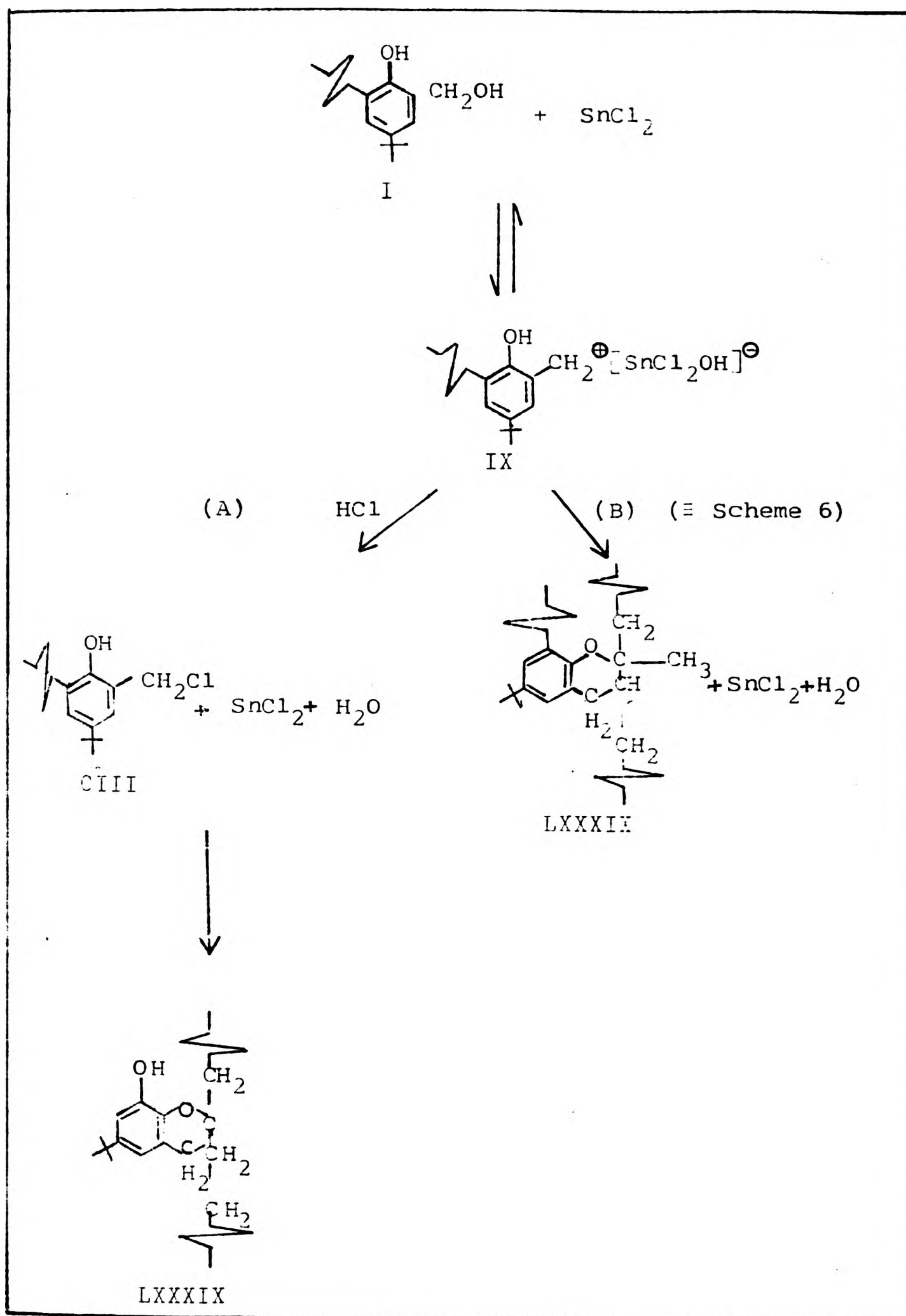


Alternatively, IX or some other protonating species (H<sup>+</sup>) may protonate a methylene ether unit as in reaction (8):



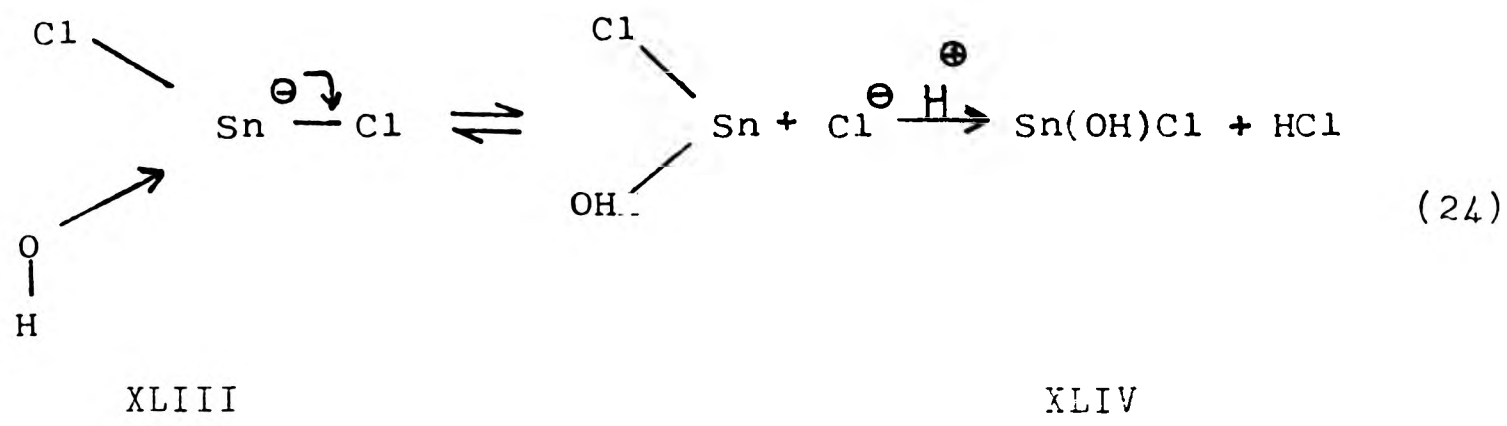
In each case, (7) or (8) show the formation of a carbonium ion intermediate IX which would account for the observed catalytic action.

If halomethylation does indeed occur as proposed in (33), then the intermediate ion IX would still be produced (it is represented as  $\text{R}^{\oplus}$  in (33)). This intermediate ion might then react directly with rubber, as above (Scheme 6), or indirectly after hydrogen halide addition (Scheme 7): The HCl is formed by hydrolysis of  $\text{SnCl}_2$  which may completely destroy its catalytic activity eventually. The ease with which the hydrolysis occurs depends upon the

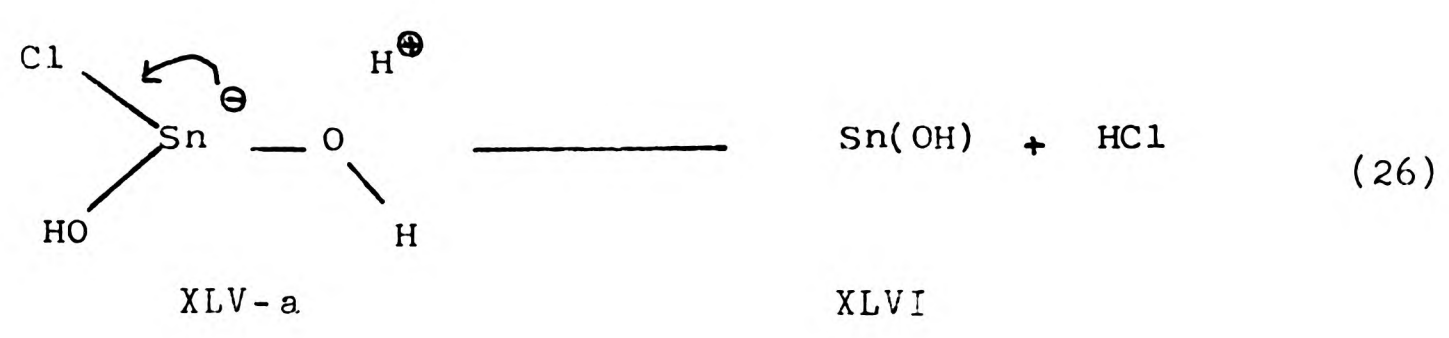
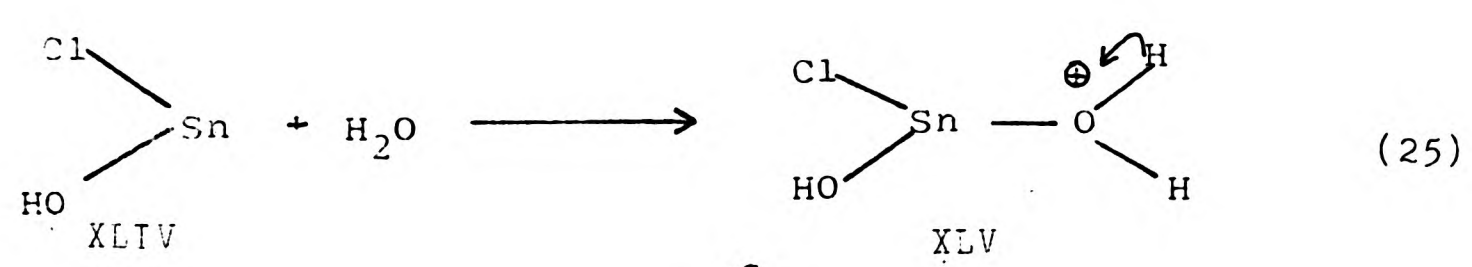


Scheme 7 Possible mechanistic scheme for  $\text{SnCl}_2$ -catalysed adduct formation.

ability of the counterion  $(\text{SnCl}_2\text{OH})^\ominus$  to eject a chloride anion, as discussed earlier in (24):



Co-ordination of a further molecule of water to the non-ionic  $\text{Sn}(\text{OH})\text{Cl}$  formed through (24) will produce further ionic species and eventually, to non-ionic species through a sequence of reactions similar to reaction (24):

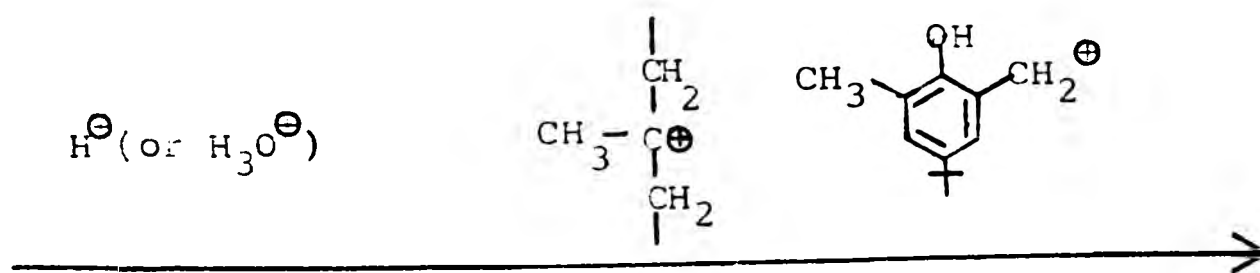




(v) Relative activities of metal halides

The relative activities of different metal halides as catalysts may be rationalised by considering that the concentration of 'active' species present depends upon a balance between rate of formation (expansion of the outer shell by coordination of ligands) and rate of destruction (through a hydrolysis sequence of the kind described).

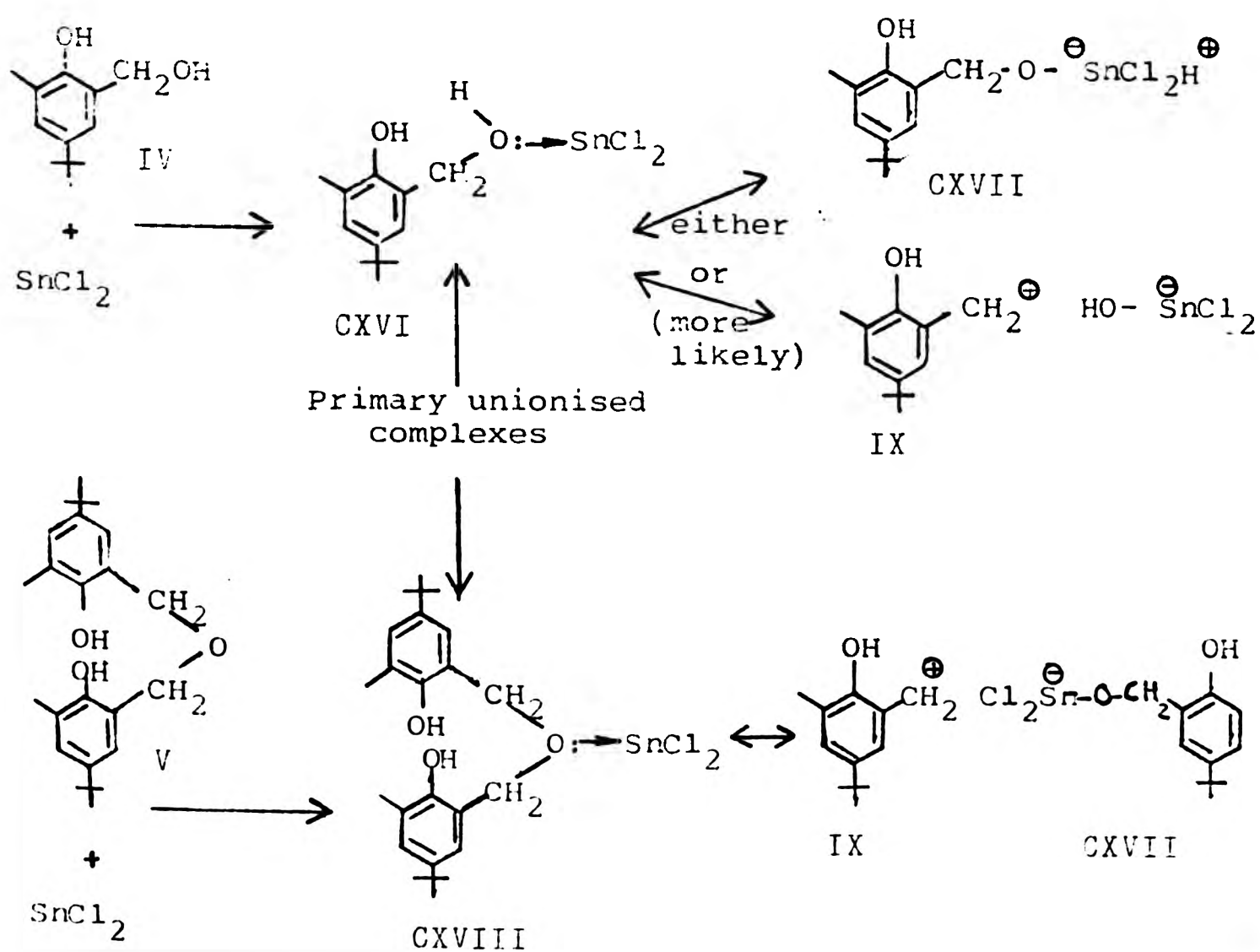
The most active ionised complex to form is probably that obtained with water as the co-catalyst. This has as active cation the proton which, because of its small size and high-reactivity, can very rapidly add to double bonds of the rubber and cause a sequence of isomerization processes to occur. The rubber<sup>⊖</sup> ions will soon interact with the phenolic species (methylolphenol or dibenzyl ether), regenerating the double-bond and forming species of type IX which are rubber-reactive and add back to a double bond. These last 2 processes are described as separate but could in fact be a fast concerted process. The driving force for all of these processes is the increase of stability of the cation, thus:



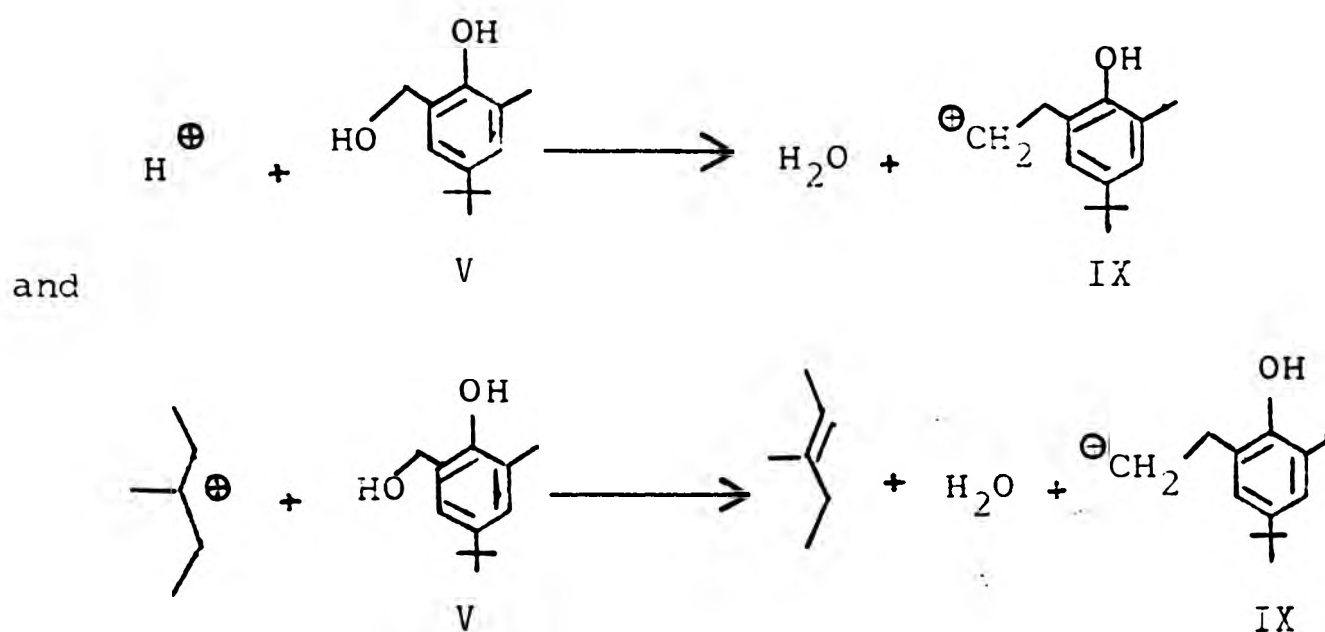
increasing stability with ease of electron delocalisation  
hence reduced reaction rate.

The catalyst  $\text{SnCl}_2 \cdot 2\text{H}_2\text{O}$  is, presumably, already in the form of a stable ionised complex rich in protons and is therefore expected to cause rapid isomerization as well as to produce, quickly, a high concentration of the rubber-reactive carbonium ions of type IX. Thus, both the isomerization processes and the high rate of adduct formation can be accounted for.

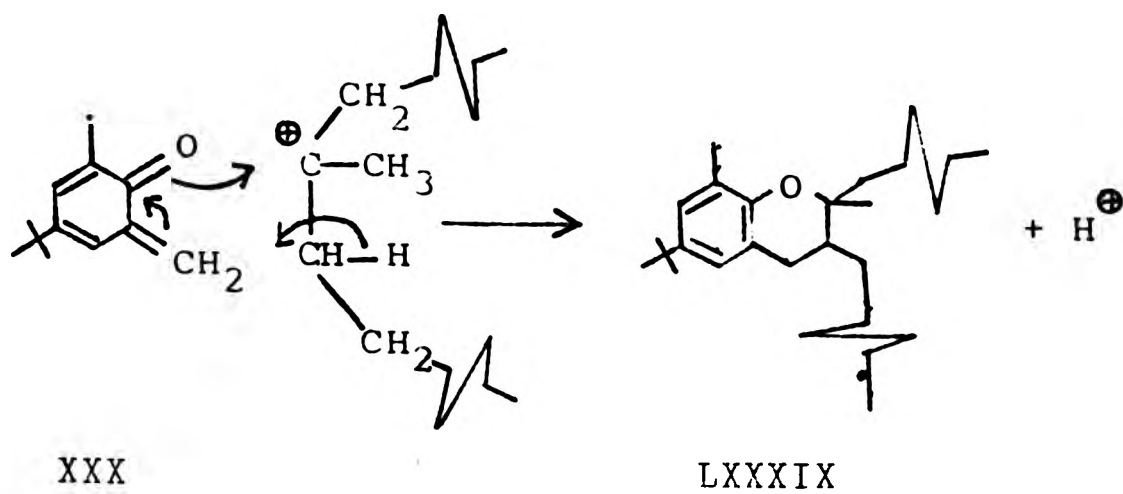
When anhydrous stannous chlorides are used, however, there is (initially) no free water available to generate appreciable quantities of protonic acid species. Since the only other oxygenated species present is methylolphenol (or dibenzyl ether), the first complex to form will be that of type CXVI which can yield protons or carbonium ions of type IX according to the dissociation equilibria:



The proton-forming decomposition probably does not occur in view of the alternative possibility of forming the resonance-stabilised ion of type CXVI. Thus, it is likely that the catalyst, soon after mixing, is converted into phenolic complexes which dissociate slowly as the rubber-reactive ionic species is consumed. The dissociation is considered slow because otherwise the adduct formation rate would be as high as that for the hydrated catalyst. There is no need for any dissociation in the latter case since the rubber-reactive species is formed directly by proton or (substituted) benzyl group abstraction:



Similar interactions with the dibenzyl ether produce the same ion. However, an alternative possibility may allow the assumption of complete dissociation but an enhanced rate of reaction for the hydrated catalyst due to a fast adduct-forming reaction between the rubber<sup>⊖</sup> ions and the quinone methide, thus:



Such a process would be energetically favoured despite the formation of the proton, by the regeneration of resonance energy in the nucleus.

The absence of  $H^{\oplus}$  (protonic) and hence rubber $^{\oplus}$  ions in the anhydrous catalyst interactions accounts for the absence of isomerization in these cases. It might be expected at first sight that some protonic acid would form from interaction of water of reaction and catalyst; however, if all the catalyst is in the form of complexes or ionized products of type IX it is most unlikely that free protons would form. Instead, the water of reaction is more likely to cause hydrolysis and eventual destruction of the catalyst.

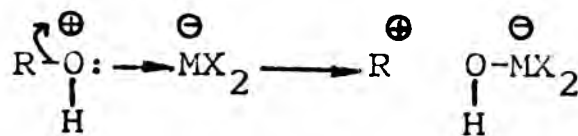
It will be apparent that the different activities noted in this and other work for different anhydrous metal halides (e.g.,  $SnCl_2$ ,  $ZnCl_2$ ,  $FeCl_3$ ,  $NiCl_2$  etc.) may result

from various causes:

1. The ease with which the primary complex forms may differ due to differences in the ease of expansion of the d-electron shell of the different metals.

2. The degree of dissociation of the primary complex into ionized species will vary according to the ease whereby the cation can be transferred from the oxygen to adjacent atoms, thus:

e.g.



This will mainly depend on the stability of the ion  $\text{R}^\oplus$ , but may also depend on other factors such as steric conditions around the metal atom or the intensity of the localisation of the charges (i.e., the degree to which the negative charge is shared between the metal and halogen atoms - see below).

3. The lifetime of the active ionized species will vary according to the ease with which the negative charge on the metal can be transferred to the halogen atom X. This will depend on the metal-halogen bond and the energetics of formation of  $\text{X}^\ominus$ . Thus, hydrolysis will increase in the

order  $F \rightarrow Cl \rightarrow Br \rightarrow I$ . The fluoro- and chloro- derivatives are normally the only ones with sufficient lifetime to be effective. These halogen displacements cause eventual destruction of the catalytic activity.

4. BIFUNCTIONAL PHENOL-FORMALDEHYDE CONDENSATES AS  
VULCANIZING AGENTS FOR IR

4.1 Introduction

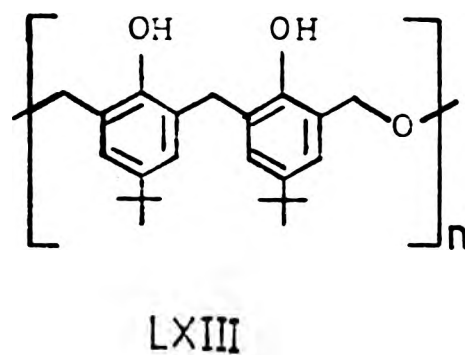
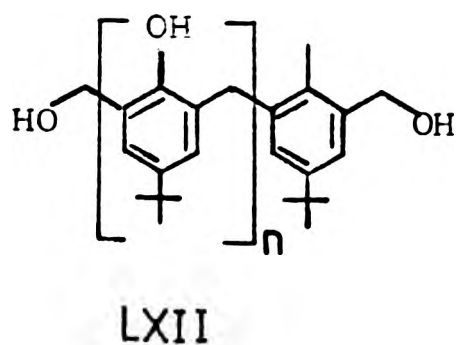
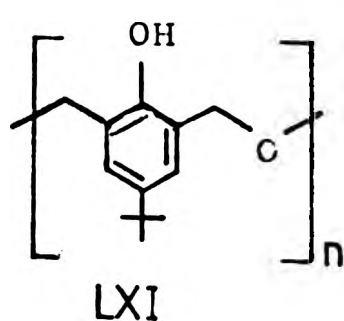
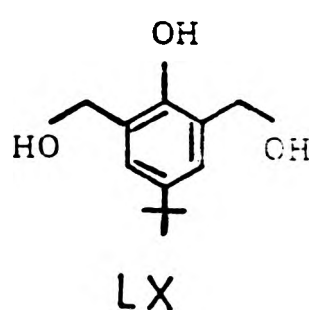
(a) Objectives of this study

The objectives of this part of the work are:

- (i) To establish structural requirements for the p/f condensate and reaction conditions for efficient vulcanization of IR. For this, various bifunctional p/f condensates are prepared and one commercial p/f condensate is obtained for comparison. They are characterised in respect of chemical structure and evaluated as crosslinking agents.
- (ii) To confirm the relevance of the results obtained in the adduct formation between monofunctional p/f 'models' and IR (see previous chapter) to the resin vulcanization of IR. For this the extent of crosslinking, measured by physical methods, is compared with that expected on the basis of the earlier kinetic and mechanistic studies with the models.
- (iii) To examine whether or not phase separation might occur during resin vulcanization of IR. For this, the crosslink concentrations evaluated by equilibrium modulus are compared with those obtained by equilibrium swelling.

(b) Reagents

The rubber used was the same grade of IR as that described in Chapter 2. The catalyst used was  $ZnCl_2$ , since earlier results (Chapter 3) showed that cationic modifications of the IR with resulting detrimental effects on its physical and mechanical properties are minimal with this catalyst. In particular, no gel formation occurs using this catalyst, and allowance for such gelation in measured crosslink concentrations is therefore unnecessary. However, from the results of the earlier kinetic studies with 'models' it may be expected that the vulcanization catalysed by  $ZnCl_2$  will occur at a lower rate than that catalysed by  $SnCl_2$  or  $SnCl_2 \cdot 2H_2O$ . The bifunctional p/f condensates used as crosslinking agents were the dimethylol phenol (LX), its ether derivative the poly benzyl ether (LXI), the dimethylol diphenyl methane (LXII), and its ether derivative (LXIII). These were previously synthesised (as described in the



Experimental Chapter). In addition, the commercial resin Bakelite CK 1634 (BP Chemicals Limited, London) was used. These condensates were chosen because they would have different concentrations of the various reactive groups; thus, in accord with earlier results, they might be expected to give different efficiencies and rates of crosslinking.

The dimethylolphenol (LX) is expected to be unsuitable as a crosslinking agent since, after chroman formation, the second methylol group will be inactive in the absence of an adjacent phenolic OH group. The representation of the formula for the dimethylol diphenyl methane by LXII is an oversimplification since, from its method of preparation, it is expected to be a mixture of bifunctional methylol compounds (further discussed later). Similarly the representation of the formulae of the polybenzylether and the polyether derivative of the dimethylol diphenyl methane as (LXI), and (LXIII), respectively, is also an oversimplification as will be shown later. The effect on crosslinking of adding selected materials such as paraformaldehyde and/or 2-methylol-4-tert. butylphenol (LIX) is also investigated. Each of the p/f condensates was characterised in terms of concentration of dibenzyl ether-type linkages, diphenylmethane-type methylene links, and methylol groups, by a method involving acetylation of the condensates followed by nmr spectroscopy (detailed in Section 4.2, below).

(c) Reaction conditions and procedure

The amount of dimethylolphenol used was 13.52 phr. This concentration is 1/2 the molar concentration used for the monofunctional methylolphenol studies (previous chapter) and was chosen because the dimethylolphenol is potentially twice as reactive as the monomethylol phenol (assuming that the reactivity of each methylol group it is not affected by the presence of the other). The amount used of the poly benzylether, the dimethylol diphenyl methane, its ether derivative, and of the commercial resin was 11.97 phr in each case, so as to contain the same number of 'active moles' (defined in Section 3.3) as that contained by the dimethylolphenol, thereby enabling results to be compared directly. For that interaction with dimethylolphenol where 2-methylol-4-tert butylphenol was added the amounts used were 6.76 and 5.79 phr respectively so as to contain the same number of moles of phenolic nuclei as that contained by the dimethylolphenol alone in an amount of 13.52 phr. For those cases where paraformaldehyde was added its concentration used was 5 phr. The amount of the catalyst  $ZnCl_2$  used was 0.73 phr, the same as that employed for the IR/model interactions (Chapter 3).

In all cases vulcanization was carried out at 160°C in bulk, using the same procedure as that described for the IR/model interactions (Chapter 3).

(d) Characterisation of the products of vulcanization

The products of vulcanization between IR and the various p/f condensates were acetone extracted then stored in the dark in vacuo. They are referred to below by the codings IR/DMP/ZnCl<sub>2</sub>, IR/DMP/MMP/ZnCl<sub>2</sub>, IR/DMP/M<sub>x</sub>/ZnCl<sub>2</sub>, IR/PE/ZnCl<sub>2</sub>, IR/PE/M<sub>x</sub>/ZnCl<sub>2</sub>, IR/DMDPM/ZnCl<sub>2</sub>, IR/PEDPM/ZnCl<sub>2</sub> and IR/CR/ZnCl<sub>2</sub>, where the abbreviation have the following meanings:

<u>Abbreviation</u>	<u>Formula No.</u>	<u>Name</u>
IR	LXIV	Isoprene rubber
DMP	LX	dimethylolphenol
MMP	LIX	monomethylolphenol
M <sub>x</sub>	-	paraformaldehyde
PE	LXI	polybenzylether
DMDPM	LXII	dimethylol diphenyl methane
PEDPM	LXIII	polyether derivative of LXII
CR	-	commercial resin

Each product was examined at various reaction times in respect of the following characteristics:

(i) Bound phenolic material

The total concentration of phenolic material combined was determined by acetone extraction as described earlier (Chapter 3, and detailed in the Experimental Chapter).

(ii) Crosslink concentration

Concentration of physically-effective crosslinks  $[X]_{\text{phys}}$  was determined by equilibrium swelling (all interactions),

using n-decane and benzene as swelling liquids, and by equilibrium modulus (for the IR/DMP/ZnCl<sub>2</sub>, IR/DMP/MMP/ZnCl<sub>2</sub>, IR/DMP/M<sub>x</sub>/ZnCl<sub>2</sub>, and IR/DMDPM\*/ZnCl<sub>2</sub> interactions). For these values the concentration of chemical crosslinks,  $[X]_{\text{chem}}$ , was determined using the correlation between  $[X]_{\text{phys}}$  and  $[X]_{\text{chem}}$  proposed by Mullins for NR.<sup>120</sup> It is assumed for this determination that the correlation applies equally to IR. Crosslink concentrations are expressed in terms of moles crosslinks per gram of total vulcanizate.

\*A slightly impure form of DMDPM used for some early work (see Experimental Chapter).

(iii) Phase separation

Phase separation of the p/f and IR components in the vulcanizates would be expected to produce a dispersed hard phase of p/f component in a continuous rubbery matrix. Such a firmly-bound hard phase would serve to increase the apparent number of physically-effective crosslinks, i.e., it would give the physical effect of crosslinking even if no chemical crosslinks were present. Thus, the values of  $[X]_{\text{phys}}$  (and hence  $[X]_{\text{chem}}$ ) obtained by equilibrium modulus measurements or swelling in n-decane (a solvent for the rubber but probably not for the resin phase) would be higher than the values obtained by swelling in benzene (a solvent for both rubber and resin phases, i.e., one which would homogenise the morphology). Crosslink concentrations obtained from the different methods will therefore be

examined for evidence of possible phase separation.

(iv) Efficiency

From the measurements of phenolic material combined with the rubber, and from the values obtained for  $[X]_{\text{chem}}$ , it is possible to obtain measures of efficiencies for the various processes calculated according to the following definitions:

Efficiency of combination ( $E_c$ ) is defined as the number of moles of phenolic material combined per mole of starting phenolic material used.

Efficiency of crosslinking ( $E_x$ ) is defined as the moles of chemical crosslinks produced per 2 moles of combined phenolic material.

Efficiency of vulcanization ( $E_v$ ) is defined as the moles of chemical crosslinks obtained per 2 moles of starting phenolic material.

From the above definitions, it follows that

$$E_v = E_c E_x$$

The factor 2 arises in these definitions from the binuclear nature of the vulcanizing agents. It will be recalled that the mole is defined in terms of the weight of condensate

containing 1 aromatic nucleus, according to its formula. Each of the above characteristics are considered in more detail and results in the present work are presented in Section 4.2 below.

#### 4.2 Characterisation Methods and Results

##### (a) Characterisation of the vulcanizing agents used

P/f condensates sold commercially are often characterised in terms of their methylol content as a measure of their activity in vulcanization. However, such reactive condensates also contain dibenzyl ether and methylene bridges. In Fitch's work<sup>11</sup> and in the present study it has been shown that the dibenzyl ether is also reactive and may in fact react more directly with the rubber. However, methylene bridge structures are unreactive and therefore wasteful of phenolic material (discussed in Section 4.3). Since groups other than these are negligible in concentration, it would appear that a full characterisation of the resin in terms of the concentrations of these three groups amounts to a complete structural characterisation of the resin (except for molecular weight distribution and the sequence distribution of the groups). A knowledge of the functional group concentration is clearly essential in interpreting results for rates and efficiency of vulcanization.

##### (i) Earlier studies

Chemical methods have been applied to the measurements

of total methylol<sup>112</sup> and ether-bridge<sup>113</sup> content in p/f condensates. Infrared spectroscopy has been one of the few useful methods applicable to the study of structures of insoluble crosslinked p/f resins.<sup>114</sup> However, most of the results from the infrared methods are only qualitative and the type and amount of information obtainable by any of the above single experimental methods is quite limited. Further, most of these methods are not quantitative. Nmr spectroscopy has been used<sup>104</sup> as a method which yields detailed and quantitative number-average structures for any soluble p/f resin. Because of the overlap among chemical shifts for some of the groups, the relative amounts of methylol groups and dibenzyl ether bridges cannot be established on the basis of spectra of the unmodified resins. For resins containing both of these functionalities quantitative analyses were found to be possible on the acetylated materials. Acetylations were carried out in pyridine solutions near 0°C. Such treatment did not cleave the ether bridges in dibenzyl ether model compounds examined and it was accompanied only by conversion of methylol groups to the correspondent acetates. No other modification of the resin was observed by vapour-phase chromatography (vpc) analysis. Nmr spectral assignments for the various groups were based on a number of nonacetylated and acetylated model compounds. The resonances attributed to some of these groups were as follows:

acetoxymethyl,  $\text{ArCH}_2\text{OAc}$ , 4.92-5.10 ; dibenzyl-ether bridges,  $(\text{ArCH}_2)_2\text{O}$ , 5.45-5.73 ; diphenylmethane-type methylene protons,  $\text{ArCH}_2\text{Ar}$ , 5.97-6.58 . From these, quantitative

results for the average number of each of the functional groups were determined for various p/f condensates.

(ii) Results in the present study

The concentration of dibenzyl ether-type bridges, diphenylmethane-type methylene groups, and methylool groups present in the polybenzyl ether, dimethylool diphenylmethane, polyether derivative of the dimethylool diphenylmethane, and in the commercial resin Bakelite CK 1634 were estimated by acetylation of these condensates (detailed in Experimental Chapter), followed by nmr spectroscopy (spectra presented in Fig. 93 in the Experimental Chapter). Spectral assignments for these three functional groups were made by analogy with those reported by Woodbrey et al.<sup>104</sup> and those obtained in the present study by acetylation of dimethyloolphenol, and the 'model' compounds methyloolphenol and dibenzyl ether (spectra presented in Fig. 99 in the Experimental Chapter). The concentration of these groups were measured from the areas A, of the peaks at 5.70 ((ArCH<sub>2</sub>)<sub>2</sub>O), 6.40 (ArCH<sub>2</sub>Ar), and 5.05 (ArCH<sub>2</sub>OAc). The number of moles, N<sub>i</sub>, of the various groups (the mole for (ArCH<sub>2</sub>)<sub>2</sub>O and ArCH<sub>2</sub>Ar is ArCH<sub>2</sub>O<sub>0.5</sub> and Ar(CH<sub>2</sub>)<sub>0.5</sub>, respectively), was then expressed as a fraction F of the total number of moles N<sub>(Ar)</sub> using the relationships (36), (37) and (38) (for which the origin is discussed in the Experimental Chapter):

$$F_{(\text{ArCH}_2\text{OH})} = \frac{N_{(\text{ArCH}_2\text{OH})}}{N_{(\text{Ar})}} = \frac{9}{2} \frac{A_{5.05}}{A_{8.10}} \quad (36)$$

$$F_{((ArCH_2)_2O)} = \frac{N_{((ArCH_2)_2O)}}{N_{(Ar)}} = \frac{9}{2} \frac{A_{5.70}}{A_{8.70}} \quad (37)$$

$$F_{(ArCH_2Ar)} = \frac{N_{(ArCH_2Ar)}}{N_{(Ar)}} = 9 \frac{A_{6.40}}{A_{8.70}} \quad (38)$$

The above equations assume that the methylol groups in the condensate become completely acetylated and other groups remain unaffected by acetylation, i.e., that no other modification of the resin structure occurs during such treatment. If this is the case, then since the condensates have two positions occupied in each aromatic nucleus, the summation (39)

$$\frac{9}{2} \frac{A_{5.05}}{A_{8.10}} + \frac{9}{2} \frac{A_{5.10}}{A_{8.10}} + 9 \frac{A_{6.40}}{A_{8.70}} = 2 \quad (39)$$

should apply. For the monofunctional compounds, methylolphenol and dibenzyl ether, there is only one position occupied in the corresponding functional group in each aromatic ring so that the corresponding summation should be equal to one. Thus for the methylolphenol,  $F_{(ArCH_2OH)}=1$ ,  $F_{((ArCH_2)_2O)}=0$  and  $F_{(ArCH_2Ar)}=0$ , for the dibenzyl ether  $F_{((ArCH_2)_2O)}=1$ ,  $F_{(ArCH_2OH)}=0$  and  $F_{(ArCH_2Ar)}=0$ . Thus equation (39) might be used to assess the validity of the method. Determination of MW(ms) of the acetylated methylolphenol and dibenzyl ether was also used as a check to ensure quantitative acetylation without other modification to the resin structure.

Since the overall reactivity of the p/f condensate depends upon the sum  $F_{(\text{ArCH}_2\text{OH})} + F_{((\text{ArCH}_2)_2\text{O})}$ , is reduced proportionately by  $F_{(\text{ArCH}_2\text{Ar})}$ , it is possible to express the potential reactivity of a particular bifunctional resin  $R_{\text{pot}}$  as a percentage of the maximum possible reactivity (where  $F_{(\text{ArCH}_2\text{Ar})} = 0$ ) by

$$R_{\text{pot}} = 50F_{(\text{ArCH}_2\text{OH})} + F_{((\text{ArCH}_2)_2\text{O})} \quad (40)$$

$$= 50(2 - F_{(\text{ArCH}_2\text{Ar})}) \quad (41)$$

Concentrations obtained for the functional groups of the various p/f condensates expressed as a fraction of the total number of moles are presented in Table 6. These results show that the summation (39) applies reasonable well for all the p/f condensates, indicating a good degree of reliability in the method. This summation is approximately equal to 1 for the 'models' methylolphenol and dibenzyl ether. For these models the MW's found for the corresponding acetylated derivative were exactly those predicted theoretically, assuming quantitative acetylation of methylol groups and no cleavage of dibenzyl ether bridges. All this suggests that the method is quantitative and reliable.

(b) Bound phenolic material

Bound phenolic material was estimated from the weights of acetone extracts as described in Chapter 3 (details in

Table 6: Concentration of dibenzylether, methylene bridges and methylol groups in the various p/f condensates as determined by acetylation of the condensates followed by nmr spectroscopy

Acetylation product of	Methylol ( $F(\text{ArCH}_2\text{OH})$ ) (molar fraction)	Dibenzylether ( $F(\text{ArCH}_2)_2\text{O}$ ) (molar fraction)	Methylene bridges ( $F(\text{ArCH}_2\text{Ar})$ ) (molar fraction)	Check of summation of eq.(39)	Potential reactivity $R_{\text{pot}}$ (%)
Commercial resin (I)	0.41	1.16	0.58	2.15	74.8
Polybenzyl ether(LXI)	0.05	1.24	0.79	2.08	62.5
Dimethylol dibenzyl methane (LXII)	0.82	0.07	1.13	2.02	44.0
Polyether of di-methylol diphenyl methane (LXIII)	0.0	0.53	1.39	1.92	28.5
Dimethylol phenol(LX)	2.07	0.0	0.0	2.07	-
Methylol phenol(IV)	1.09	0.0	0.0	1.09	-
Dibenzyl ether(V)	0.0	1.05	0.0	1.05	-

\* Mean value from equations(40) and (41)

the Experimental Chapter). Vulcanized samples after extraction showed the presence of unextractable and probably uncombined material dispersed randomly in the form of dark spots. Experimental observations suggested this to be a product of interaction between the p/f condensate (and/or its decomposition products) and the  $ZnCl_2$  catalyst since, when the IR and p/f condensates were heated in the absence of  $ZnCl_2$ , such dark spots were not observed. Corrections for unbound unextractable material as obtained by experiments with EPR (Chapter 3, Section 3.3) were not used here since it was considered that the conditions under which such corrections were obtained were not the same as in the present vulcanizate cases. In this present case it was not practicable to estimate the unbound unextractable material, so that the results obtained for bound phenolic matter will be higher than the real ones. However, since the concentration of catalyst used (0.73 phr) is small the error arising from unextractable catalyst-condensate interaction product was considered negligible. Results were expressed as moles of phenolic material combined per gram of vulcanizate and/or per mole of IR, as appropriate for further calculations (the moles of bound phenolic material were obtained as described in Section 3.5, Chapter 3).

For those interactions where paraformaldehyde was added (i.e., IR/DMP/ $M_x$ / $ZnCl_2$  and IR/PE/ $M_x$ / $ZnCl_2$ ) bound phenolic material can be calculated only for prolonged reaction times. This is because paraformaldehyde is not soluble in acetone and its concentration is diminishing with time. The final

vulcanizates were heated in air to eliminate it.

Detailed results for the various interactions are presented in Table 16 and summarised in graphical form in Fig. 84 in the Experimental Chapter, which shows changes in moles of phenolic material combined per mole of IR, and per mole of starting phenolic material (i.e.,  $E_c$ ) as reactions proceed. This method of expression was chosen to enable a direct comparison to be made with the results of the IR-p/f model interactions. These results will be discussed more fully later.

(c) Crosslink concentration

(i) Measurement of crosslink concentration

The macromolecular structure of a vulcanizate network may be specified in terms of basic network elements:

(a) network chains (macromolecular segments bounded at each end by a crosslink, (b) free chain ends (segments bound to a crosslink at one end only) and (c) permanent chain entanglements. In an ideal situation in which the network is free from free chain ends and permanent chain entanglements, the concentration of crosslinks can be determined directly from the 'functionality' of the crosslinks (i.e., the number of network chains terminated by each crosslink) and  $M_c$ , the number-average molecular weight of network chains between crosslinks. In the case of tetrafunctional crosslinks, each crosslink is associated with one half of the four network chains bound to it. Therefore, if  $M_c$  is the number-average

vulcanizates were heated in air to eliminate it.

Detailed results for the various interactions are presented in Table 16 and summarised in graphical form in Fig. 84 in the Experimental Chapter, which shows changes in moles of phenolic material combined per mole of IR, and per mole of starting phenolic material (i.e.,  $E_c$ ) as reactions proceed. This method of expression was chosen to enable a direct comparison to be made with the results of the IR-p/f model interactions. These results will be discussed more fully later.

(c) Crosslink concentration

(i) Measurement of crosslink concentration

The macromolecular structure of a vulcanizate network may be specified in terms of basic network elements:

(a) network chains (macromolecular segments bounded at each end by a crosslink, (b) free chain ends (segments bound to a crosslink at one end only) and (c) permanent chain entanglements. In an ideal situation in which the network is free from free chain ends and permanent chain entanglements, the concentration of crosslinks can be determined directly from the 'functionality' of the crosslinks (i.e., the number of network chains terminated by each crosslink) and  $M_c$ , the number-average molecular weight of network chains between crosslinks. In the case of tetrafunctional crosslinks, each crosslink is associated with one half of the four network chains bound to it. Therefore, if  $M_c$  is the number-average

molecular weight of the network chains between crosslinks and  $N$  is Avogadro's Number, each crosslink will be associated with an average of  $2M_c N^{-1}$  grams of rubber. One gram of rubber will therefore contain  $N(2M_c)^{-1}$  crosslinks; or, more conveniently, one gram of rubber will contain  $(2M_c)^{-1}$  gram-moles of crosslinks.  $(2M_c)^{-1}$  is therefore the concentration of crosslinks expressed as moles per gram of rubber. This is conveniently taken as a measure of the degree of crosslinking, shown as  $[X]$  below.

It is too difficult to determine the concentration of actual crosslinks  $[X]_{\text{chem}}$  by a chemical method. Estimates of crosslink concentration are therefore made from the physical properties of the vulcanizates. The values obtained,  $[X]_{\text{phys}}$ , are strongly affected by free chain ends and chain entanglements, and correction of  $[X]_{\text{phys}}$  for such effects is necessary in order to obtain an estimate of  $[X]_{\text{chem}}$ . The concentration of physically effective crosslinks,  $[X]_{\text{phys}}$ , may be determined experimentally from measurements of elastic properties of the vulcanizate by two methods.

(i-i) Equilibrium modulus

$M_c$  can be determined experimentally from stress-strain measurements using a method which depends upon the statistical theory of rubber elasticity.<sup>115,116</sup> According to the simplest form of theory, the stored energy function per unit of rubber,  $W$ , is given by

$$W = 2^{-1} G(\lambda_1^2 + \lambda_2^2 + \lambda_3^2 - 3) \quad (42)$$

where  $G$  is the elastic constant, and  $\lambda_1, \lambda_2, \lambda_3$  are the ratio of strained to unstrained dimension along the principal axis of  $X, Y$  and  $Z$ . For simple elongation, there is no change in volume and the extension ratios are given by:

$$\lambda_1 = \lambda; \quad \lambda_2 = \lambda_3 = \lambda^{-1/2}$$

Equation (42) then reduces to:

$$W = 2^{-1} G(\lambda^2 + \frac{2}{\lambda} - 3) \quad (43)$$

The equilibrium force per unit area required to extend an ideal network in the direction of  $l$  is therefore given by:

$$F = \frac{dW}{d\lambda} = G(\lambda - \lambda^{-2}) \quad (44)$$

For ideal rubber networks which do not contain chain ends and permanent chain entanglements,  $G$  is related to  $M_c$  by the equation:

$$G = \rho RT/M_c \quad (45)$$

where  $\rho$  is the density of the network,  $R$  is the gas constant and  $T$  is the absolute temperature. Therefore equations (44) and (45) provide the basis of a method whereby stress-strain measurements can be used to obtain estimates of  $M_c$  for real networks. However, in practice, stress-strain relationships

are found to deviate from the ideal form predicted by equation (44). Some of the reasons for such deviations are: (a) no account is taken of the contribution made by chain entanglements to the concentration of elastically-effective network chains, (b) no allowance is made for chain ends which do not contribute to the stress and (c) there is a finite extensibility of the network which is not taken into consideration.

A more satisfactory description of the elastic behaviour of vulcanizate networks was obtained<sup>117-119</sup> by an essentially phenomenological approach, which for simple extension and moderate strains gave the following empirical expression:

$$F = 2(\lambda - \lambda^{-2})(C_1 + \lambda^{-1}C_2) \quad (46)$$

where  $C_1$  and  $C_2$  are constants. A linear relation is obtained when results for simple extension are plotted in the form  $F/2(\lambda - \lambda^{-2})$  against  $\lambda^{-1}$ , this being consistent with the re-written form of equation (46):

$$F/2(\lambda - \lambda^{-2}) = C_1 + \lambda^{-1}C_2 \quad (47)$$

Values of  $C_1$  and  $C_2$  may thus be obtained graphically from the intercept ( $\lambda^{-1}=0$ ) and slope, respectively, of this straight line relationship. It has been established<sup>120,121</sup> for natural rubber vulcanizates that the  $C_2$  term in equation (46) is almost zero for stress-strain obtained using

vulcanizates highly swollen with a liquid. In this case, equation (47) reduces to the form predicted by simple statistical theory (equation 44) provided that

$$C_1 = \frac{G}{2} = \rho RT/2M_c = \rho RT[X]_{\text{phys}} \quad (48)$$

(i-ii) Equilibrium swelling

An alternative method to the use of stress-strain measurements for the determination of  $M_c$  takes advantage of the property of rubber network of becoming swollen to equilibrium when immersed in liquids. The equilibrium volume fraction of rubber,  $V_r$ , in the swollen network is related to  $M_c$ , by the modified Flory-Rehner equation.<sup>122</sup> This equation is as follows:

$$-\ln(1 - V_r) - V_r - \chi V_r^2 = \rho V_o M_c^{-1} V_r^{1/3} \quad (49)$$

where  $V_o$  is the molar volume of the swelling liquid, and  $\chi$  is a rubber-solvent interaction parameter. This relationship, is again restricted to networks which are free from chain entanglements and chain ends. In order to use equation (49) to determine  $M_c$  values, the interaction parameter,  $\chi$  must first be determined. By combining equations (48) and (49) an expression is obtained which relates equilibrium swelling to  $C_1$ :

$$-\ln(1 - V_r) - V_r - \chi V_r^2 = 2C_1 (RT)^{-1} V_o V_r^{1/3} \quad (50)$$

Equation (50) thus represents a method whereby  $\chi$  may be determined from  $C_1$  obtained from stress-strain measurements.

Values of  $M_c$  and the derived concentration of physically-effective crosslinks,  $[X]_{\text{phys}}$ , obtained from swelling (equation (49)) or from stress-strain measurements (equations (47) and (48)) are based upon the assumption that the rubber network is 'ideal' in that there are no network chains possessing free ends. This implies that the primary polymer was of infinite molecular weight. In practice, however, the primary molecular weight is finite. It is therefore necessary to make a 'finite molecular weight' allowance. The correct allowance is in doubt. On theoretical grounds, some workers<sup>1,2,3</sup> have suggested:

$$\frac{1}{M_c^{\text{corr}}} = \frac{1}{M_c} + \frac{\alpha}{\bar{M}_n} \quad (51)$$

where  $\alpha$  is a constant and  $\bar{M}_n$  the number average molecular weight. An experimental investigation<sup>120</sup> of the dependence of  $C_1$  on  $\bar{M}_n$  has revealed  $\alpha$  to be 5.44 and therefore:

$$\frac{1}{M_c^{\text{corr}}} = \frac{1}{M_c} + \frac{5.44}{\bar{M}_n} \quad (52)$$

Values of  $[X]_{\text{phys}}$  and  $[X]_{\text{phys}}^{\text{corr}}$  are calculated from  $M_c$  and  $M_c^{\text{corr}}$  for all of the vulcanizates obtained in the present work. Even after allowance is made for the effect of chain ends, no account is taken of the effect of network entanglements on  $C_1$ . These entanglements, which may be thought to arise as the result of interlooping of network chains, act

as physically effective crosslinks and make a positive contribution to elastic modulus; in terms of  $C_1$ , therefore, they are indistinguishable from chemical crosslinks inserted by vulcanization reactions. To resolve these difficulties, attempts have been made to introduce known quantities of chemical crosslinks into rubber so that an independent assessment of the validity of physical measurements of  $M_c$  could be made. This is considered now in more detail.

(i-iii) Determination of concentration of chemical crosslinks,  $[X]_{\text{chem}}$

The  $C_1$  data have been critically analysed<sup>120</sup> for many natural rubber vulcanizates in which known concentrations of chemical crosslinks,  $[X]_{\text{chem}}$ , had been introduced. The concentrations of chemical crosslinks were accurately estimated from analysis of peroxide decomposition products and knowledge of the chemistry of the crosslinking reaction. It was found that, in general, the concentration of physically-effective crosslinks,  $[X]_{\text{phys}}$ , determined by application of equation (48) to  $C_1$  data, considerably exceeded  $[X]_{\text{chem}}$ . This discrepancy was particularly apparent at low crosslink densities, and was attributed to the effects of permanent chain entanglements. Therefore, in order to derive  $[X]_{\text{chem}}$  for a network from  $[X]_{\text{phys}}$ , a correction must be applied for this effect. In addition, a correction must be made for the free chain ends, as discussed above. To date the most reliable correlation between  $[X]_{\text{phys}}$  and  $[X]_{\text{chem}}$  is the relationship proposed by Mullins.<sup>120</sup> This

relationship, which is used in the present study, is

$$\begin{aligned}
 C_1 &= \rho RT [X]_{\text{phys}} \\
 &= (\rho RT [X]_{\text{chem}} + 0.78 \times 10^6) \left( 1 - \frac{2.3}{2} [X]_{\text{chem}}^{-1} \bar{M}_n^{-1} \right) \quad (53)
 \end{aligned}$$

↑ correction for entanglements
 ↑ correction for free chain ends

where  $\rho$  is the density of the vulcanizate,  $R$  the gas constant per gram-molecule,  $T$  the absolute temperature,  $\bar{M}_n$  the number average molecular weight of the primary rubber molecules, the factor  $0.78 \times 10^6$  is a correction which includes the maximum contribution of entanglements, and the second bracketed term is the correction for free chain ends.

(ii) Results in the present study

(ii-i) Determination of concentration of physically effective crosslinks,  $[X]_{\text{phys}}$  and  $[X]_{\text{phys}}^{\text{corr}}$ .

(ii-ii) Equilibrium modulus

Values of  $C_1$  were obtained from stress-strain measurements (detailed in the Experimental Chapter). The data were analysed according to equation (47):

$$F/2(\lambda - \lambda^{-2}) = C_1 + \lambda^{-1} C_2 \quad (47)$$

The results for the IR/DMP/ZnCl<sub>2</sub>, IR/DMP/MMP/ZnCl<sub>2</sub>, IR/DMP/M<sub>x</sub>/ZnCl<sub>2</sub> and IR/DMDPM\*/ZnCl<sub>2</sub> interactions were plotted

in the form of  $F/2(\lambda-\lambda^{-2})$  against  $\lambda^{-1}$  and the values of  $C_1$  were obtained from the intercept ( $\lambda^{-1}=0$ ) (graphs presented in the Experimental Chapter). The  $C_1$  values were used to derive the  $M_c$  and  $[X]_{\text{phys}}$  values through equation (48):

$$C_1 = \rho RT/2M_c = \rho RT[X]_{\text{phys}} \quad (48)$$

Values of  $M_c^{\text{corr}}$  were obtained by using the allowance for the presence of chain ends given by equation (52)

$$\frac{1}{M_c^{\text{corr}}} = \frac{1}{M_c} + \frac{5.44}{\bar{M}_n} \quad (52)$$

where  $\bar{M}_n$ , the number average molecular weight of the primary rubber molecules, was obtained from the intrinsic viscosity,  $[\eta]_{c=0}$ , of the unvulcanized rubber using the relation<sup>124</sup>

$$[\eta]_{c=0} = 2.29 \times 10^{-7} \bar{M}_n^{1.33} \quad (54)$$

The method is described in detail in the Experimental Chapter. Although the same rubber was used initially in each case, values of  $[\eta]_{c=0}$  and hence,  $\bar{M}_n$  for the various interactions were different since different mixing times for the various compositions were necessary in order to get good dispersion. Some degradation of the rubber occurred during this mixing period. From the  $M_c^{\text{corr}}$  values the  $[X]_{\text{phys}}^{\text{corr}}$  values were evaluated from the relation

$$[X]_{\text{phys}}^{\text{corr}} = [2M_c^{\text{corr}}, \text{phys}]^{-1} \quad (55)$$

i.e., again assuming tetrafunctional crosslinks which are most likely with the bifunctional p/f condensates used.

Equations (51) to (54) have been experimentally determined for NR. In this study it is assumed that the same constants can also be applied to IR.

For the IR/DMP/ZnCl<sub>2</sub>, and IR/DMP/MMP/ZnCl<sub>2</sub> interactions, measurements of crosslink density for reaction products before 25 min. of vulcanization, and for the IR/DMP/M<sub>x</sub>/ZnCl<sub>2</sub> case before 80 min., were not practicable. These products were too soft and weak, presumably due to a very low crosslink concentration.

All of the vulcanized samples after acetone extraction showed localised porosity and presence of dark spots. The porosity is attributed to evolution of water and formaldehyde whereas the dark spots are related to unextractable uncombined phenolic material. Both might have some effect on tensile-strain measurements, and care was taken to avoid porous areas when cutting test-pieces.

The equilibrium modulus method was used only for the DMP and DMDPM\* cases so that the results could be compared with the corresponding ones obtained by swelling, in order to establish whether or not phase separation is likely. The swelling method is most widely used and essentially the standard method for determining the crosslink density, and was used as the main analysis method in the present study.

Detailed results are presented in the Experimental Chapter (Table 12). Results for determination of  $C_1$  values for various interactions are summarised in graphical form in Figs. 95 to 98 (Experimental Chapter), which show  $F/2(\lambda - \lambda^{-2})$  expressed in  $N/cm^2$  against  $\lambda^{-1}$  at various reaction times. These results show that stress-strain measurements at moderate strains conform to the linear relationship of equation (47). Deviations from the linearity are observed at low and high strains. Similar effects have been widely reported with other vulcanization systems. These lines at different reaction times are substantially parallel (Figs. 95-98) showing that  $C_2$  is independent of degree of vulcanization, also widely reported.

Values of  $[X]_{phys}$  and  $[X]_{phys}^{corr}$  calculated from the experimental  $C_1$  values for various interactions at different reactions times are presented in the Experimental Chapter (Tables 12 and 13). From the  $[X]_{phys}$  values, the corresponding  $[X]_{chem}$  values were obtained as described below (Section ii-iv).

(ii-iii) Equilibrium swelling

$M_c$  values were calculated from the Flory-Rehner equation (49)

$$-\ln(1-v_r) - v_r - \chi v_r^2 = \rho v_o M_c^{-1} v_r^{1/3} \quad (49)$$

using samples swollen in n-decane and benzene. The principal

difficulty encountered in attempting to use this relationship is the selection of a value for the interaction parameter  $\chi$ . In the present work there are two main sources of difficulty:

(a) There is good indication that phase separation occurs in the samples swollen in decane (see below), and it is very likely that a 2-phase morphology exists in the unswollen bulk. Such microheterogeneity is likely to increase the number of physically-effective crosslinks over and above those produced by crosslinking and entanglements. Furthermore, the extent of phase separation is likely to change with the extent of reaction. Since the degree of correlation between the bulk and solution morphology is completely unknown, it is almost certainly not justifiable to apply values of  $\chi$  derived using equation (50) from modulus and swelling measurements. Although such  $\chi$  values have not been used in this work, examples of them have been derived for interest from the results of one interaction (IR/DMP/ZnCl<sub>2</sub>), as follows:

Reaction Time: (min)	25	45	80	120	210
$\chi$ (benzene):	0.463	0.470	0.471	0.468	0.507
$\chi$ (decane):	0.514	0.539	0.591	0.582	0.614

These values show no definite trend as cure time increases, but the variability is quite large. They are all extremely high in comparison with values reported for other types of vulcanizate.

(b) Since the Flory-Rehner equation assumes complete homogeneity, and there is no indication of phase separation in samples swollen in benzene, it would appear that this solvent would be the better one to choose for measuring  $[X]_{\text{chem}}$ . However,  $\chi$  still cannot with confidence be derived from  $C_1$  measurements via equation (50) because of the likelihood of a 2-phase structure in the bulk vulcanizate. It was therefore decided to select a value for  $\chi$  from values obtained by other workers using simple vulcanizates of NR which are likely to be homogeneous in their morphology. A difficulty which immediately arises is that the value should increase with the degree of reaction (since combined phenolic material will progressively increase the cohesive energy density of the vulcanizate) in an unpredictable way. When there is very little material combined, it is likely that the value will not differ significantly from that ( $\sim 0.40$ ) for a peroxide vulcanizate, but it is expected to increase as polar material combines with the rubber in the same way as has been demonstrated for a sulphur vulcanizate.<sup>150</sup> In view of the uncertainties involved, it was decided to use a single value for  $\chi$  chosen from values obtained with typical sulphur vulcanizates. The values used for the IR-n-decane and IR-benzene interaction parameters  $\chi$  were 0.443 and 0.422, respectively, which are those reported<sup>121</sup> as average values for NR vulcanizates with these solvents. Most of the published values for  $\chi$  are for swelling in n-decane. A correlation between  $V_r$  values for n-decane and benzene has been provided by Bristow,<sup>151</sup> from which it may be deduced

that a reasonable value for  $\chi_{(\text{benzene})}$  for a peroxide vulcanizate (containing no polar combined material) would be 0.40-0.42. Inefficient sulphur vulcanizates, containing appreciable proportion of polar main-chain modification, give values of  $\chi_{(\text{decane})}$  of 0.43<sup>150</sup> or 0.45,<sup>152</sup> which would appear from general observations to correspond to  $\chi_{(\text{benzene})}$  values of 0.41 to 0.43. In those studies the value for  $\chi$  did not change appreciably with degree of cure. It seems, therefore, that the value of 0.422 selected for this present study is reasonable. Values of  $V_r$  were calculated from equation (59) (procedure described in the Experimental Chapter)

$$V_r = \frac{W_1/\rho}{W_1/\rho + (W_e - W_1)\rho_1} \quad (59)$$

where  $W_1$  is the weight of the vulcanizate prior to swelling,  $W_e$  the equilibrium weight of the vulcanizate after swelling,  $\rho$  the density of the vulcanizate and  $\rho_1$  the density of the swelling liquid.

Values of  $M_c$  and hence  $[X]_{\text{phys}}$  were calculated as described above from equation (49). It was not found practicable to correct values for unextractable uncombined phenolic material and for porosity. However, since both these phenomena were observed to occur to very low extent, results would not be drastically affected. Again for the IR/DMP/ZnCl<sub>2</sub>, IR/DMP/M<sub>x</sub>/ZnCl<sub>2</sub> and IR/DMP/MMP/ZnCl<sub>2</sub> interactions, products before 25 min. of reaction time were too

soft and weak to handle after swelling, so that crosslink measurements were not practicable. In all cases, samples swollen in n-decane appeared 'cloudy' whereas the benzene-swollen samples were clear. The possible significance of this is discussed later.

Values of  $[X]_{\text{phys}}$  and the corrected values  $[X]_{\text{phys}}^{\text{corr}}$  for the various interactions at different times and using both n-decane and benzene as swelling liquids are presented in the Experimental Chapter (Tables 12 and 13). From the  $[X]_{\text{phys}}$  values the corresponding  $[X]_{\text{chem}}$  values were calculated as detailed below.

(ii-iv) Determination of concentration of chemical crosslinks,  $[X]_{\text{chem}}$

The concentration of chemical crosslinks  $[X]_{\text{chem}}$  was calculated from the  $[X]_{\text{phys}}$  values by making use of equation (53). Thus, the values obtained will be subject to the same reservations as expressed above for the  $[X]_{\text{phys}}$  values.

Results for the various interactions obtained from  $[X]_{\text{phys}}$  (swelling) for all cases and from  $[X]_{\text{phys}}$  (modulus) for the IR/DMP/ZnCl<sub>2</sub>, IR/DMP/M<sub>x</sub>/ZnCl<sub>2</sub>, IR/DMP/MMP/ZnCl<sub>2</sub>, and IR/DMDPM\*/ZnCl<sub>2</sub> interactions, are summarised in graphical form in Figs. 65 to 70, which show crosslinking in terms of chemical crosslinks per gram of vulcanizate as reaction proceeds and they are presented in the Experimental Chapter (Table 14).

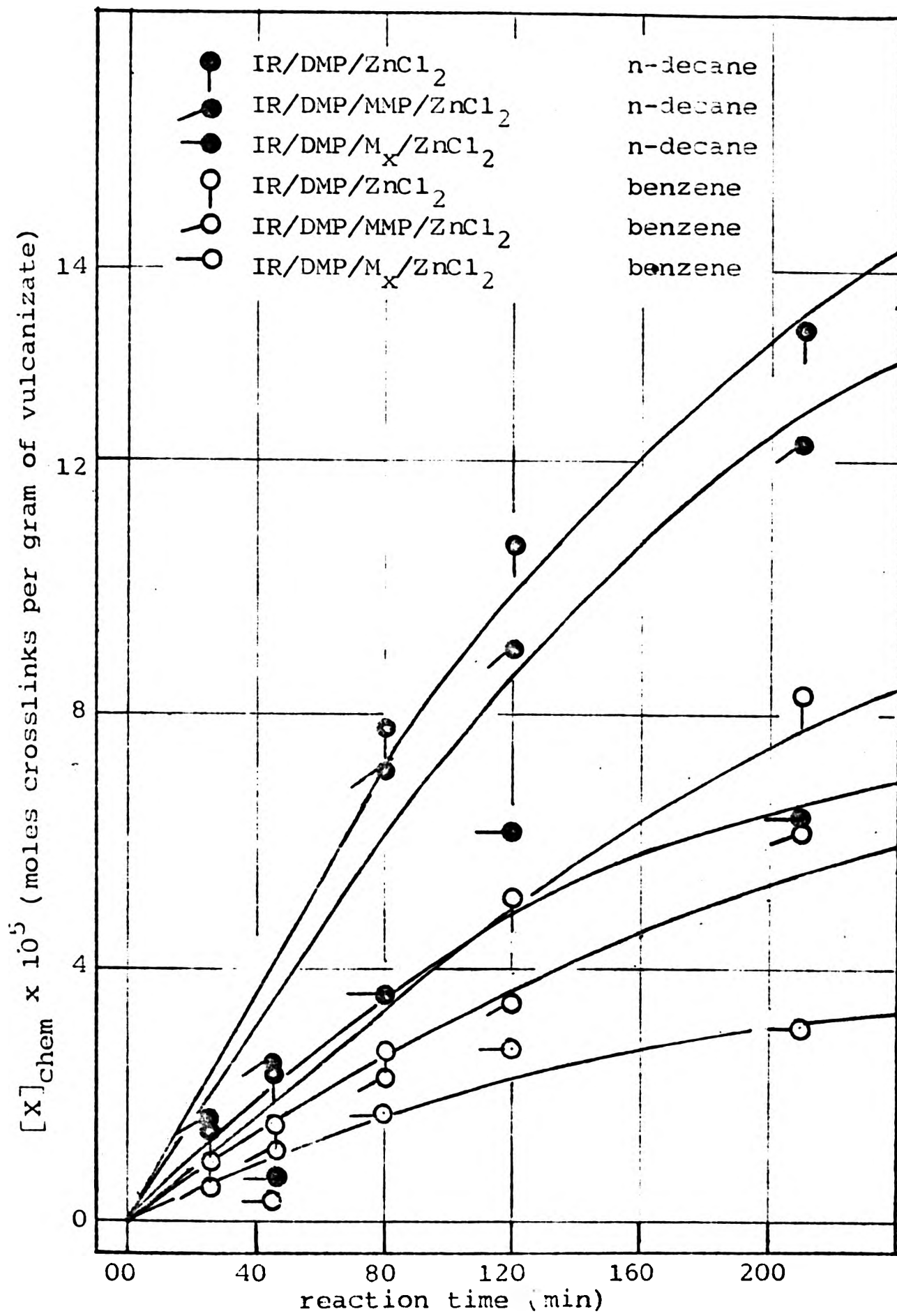


Fig. 65 Changes in concentration of chemical crosslinks,  $[X]_{chem}$ , with reaction time for the DMP as calculated from the physically effective crosslinks determined by swelling in n-decane and benzene.

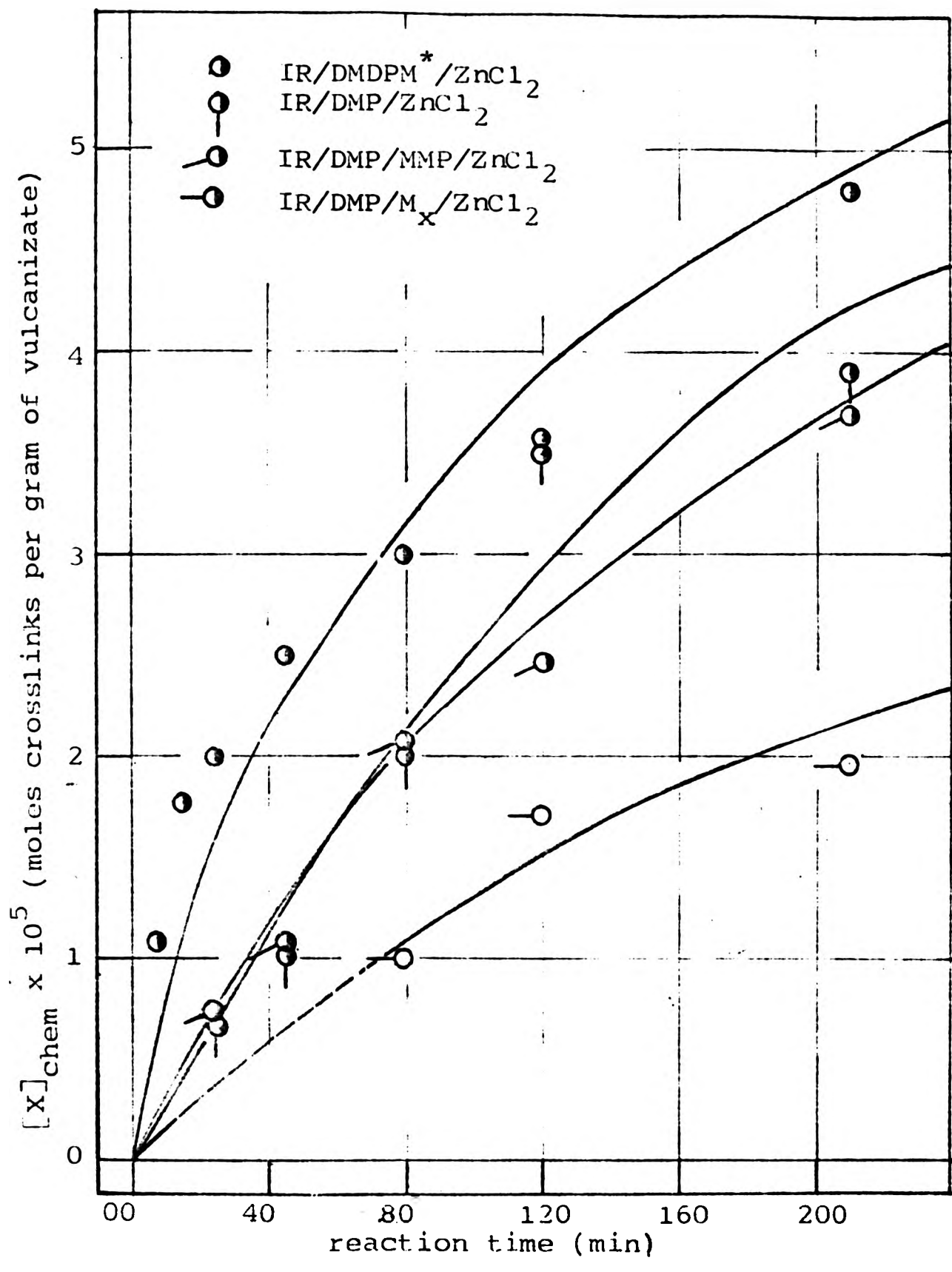


Fig. 66 Changes in concentration of chemical crosslinks,  $[X]_{chem}$ , with reaction time for the DMP and DMDPM\* as calculated from the physically effective crosslinks determined by equilibrium modulus.

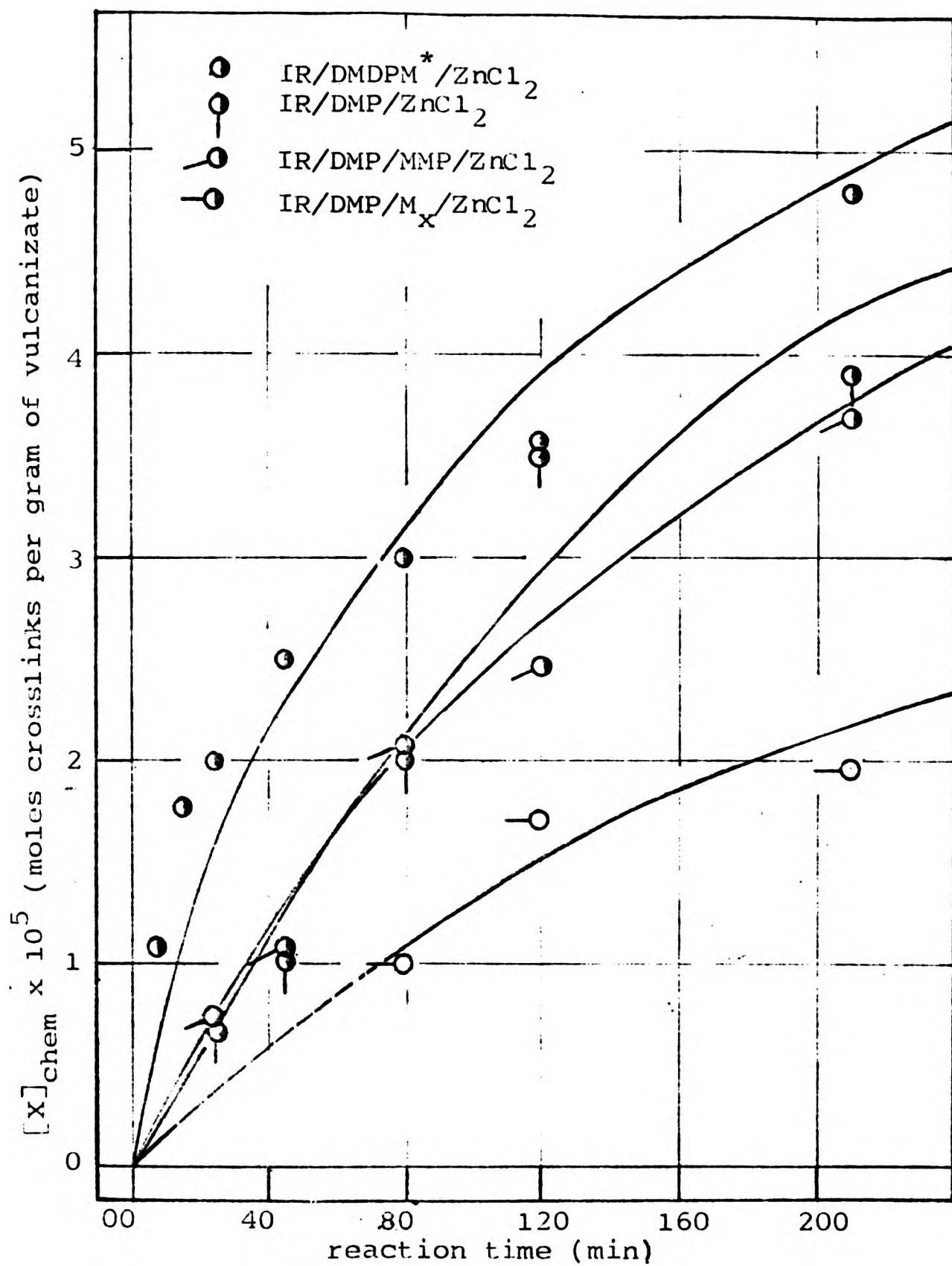


Fig. 66 Changes in concentration of chemical crosslinks,  $[X]_{\text{chem}}$ , with reaction time for the DMP and DMDPM\* as calculated from the physically effective crosslinks determined by equilibrium modulus.

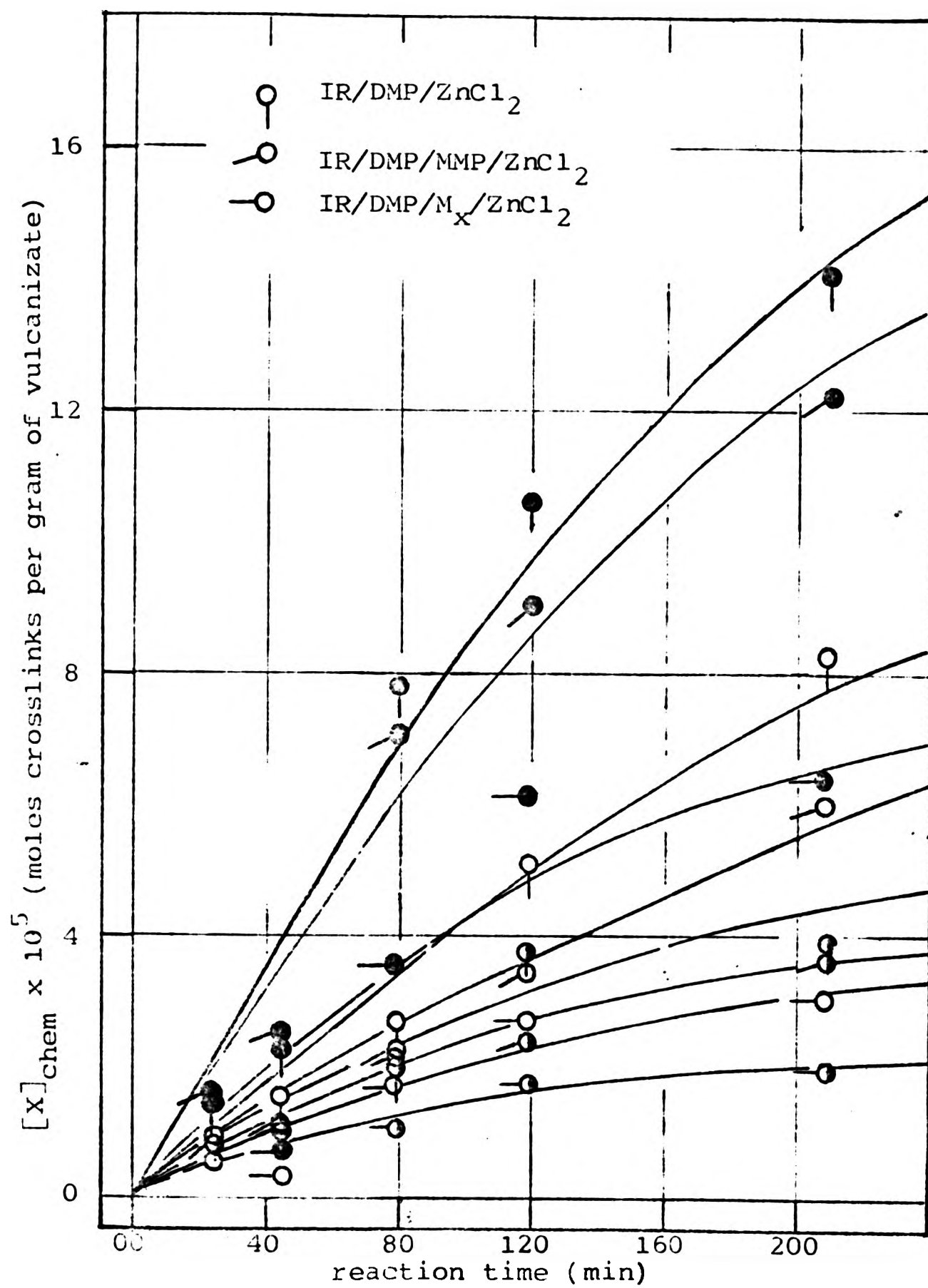


Fig. 67 Comparison of changes in concentration of chemical crosslinks,  $[X]_{chem}$ , with reaction time for the DMP as calculated from the physically effective crosslinks determined by equilibrium modulus ( $\circ$ ) and equilibrium swelling in n-decane ( $\bullet$ ) and in benzene ( $\circ$ ).

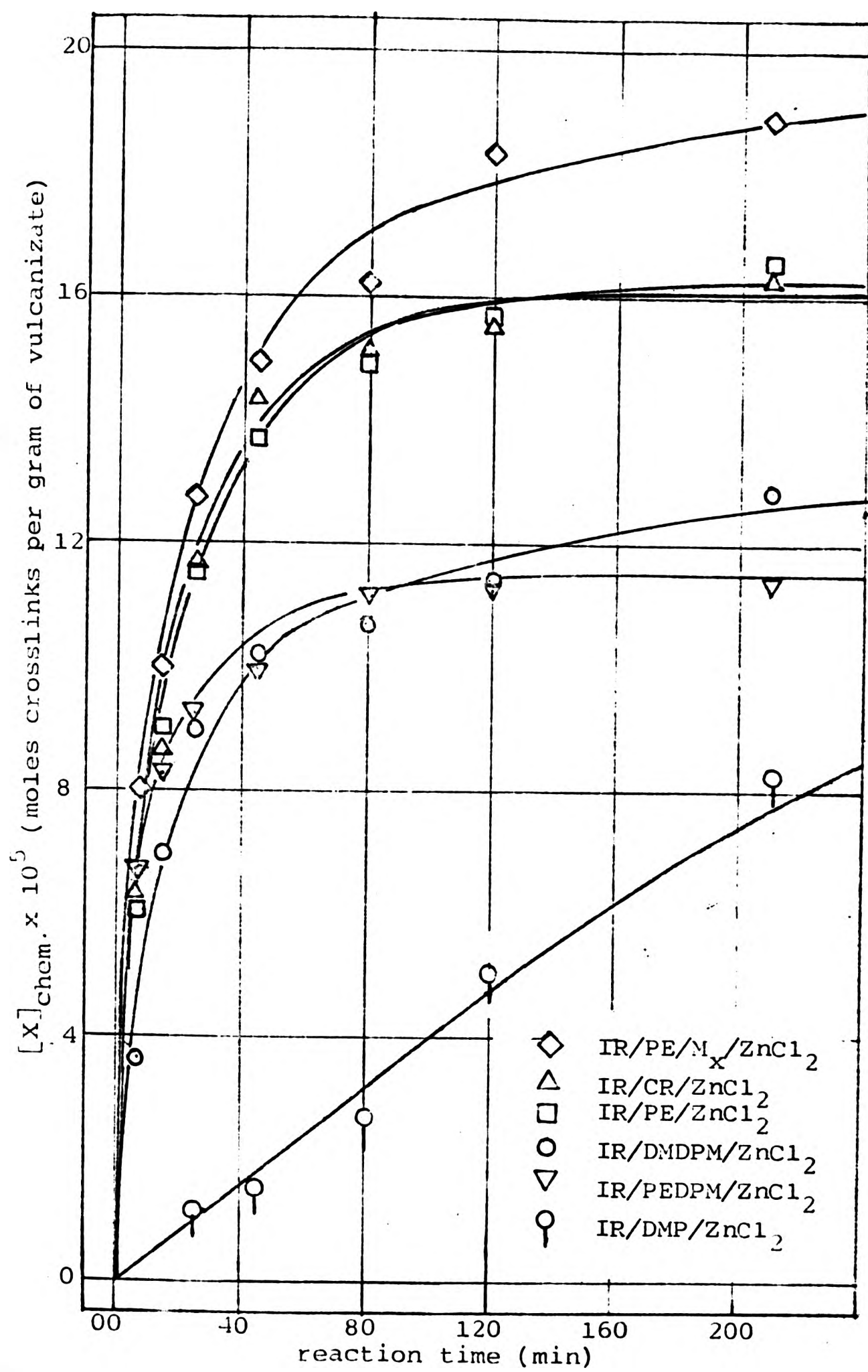


Fig. 68 Changes in concentration of chemical crosslinks,  $[X]_{chem}$ , with reaction time for the DMP, DMDPM, PEDPM, PE and CR calculated from the physically effective crosslinks determined by equilibrium swelling in benzene.

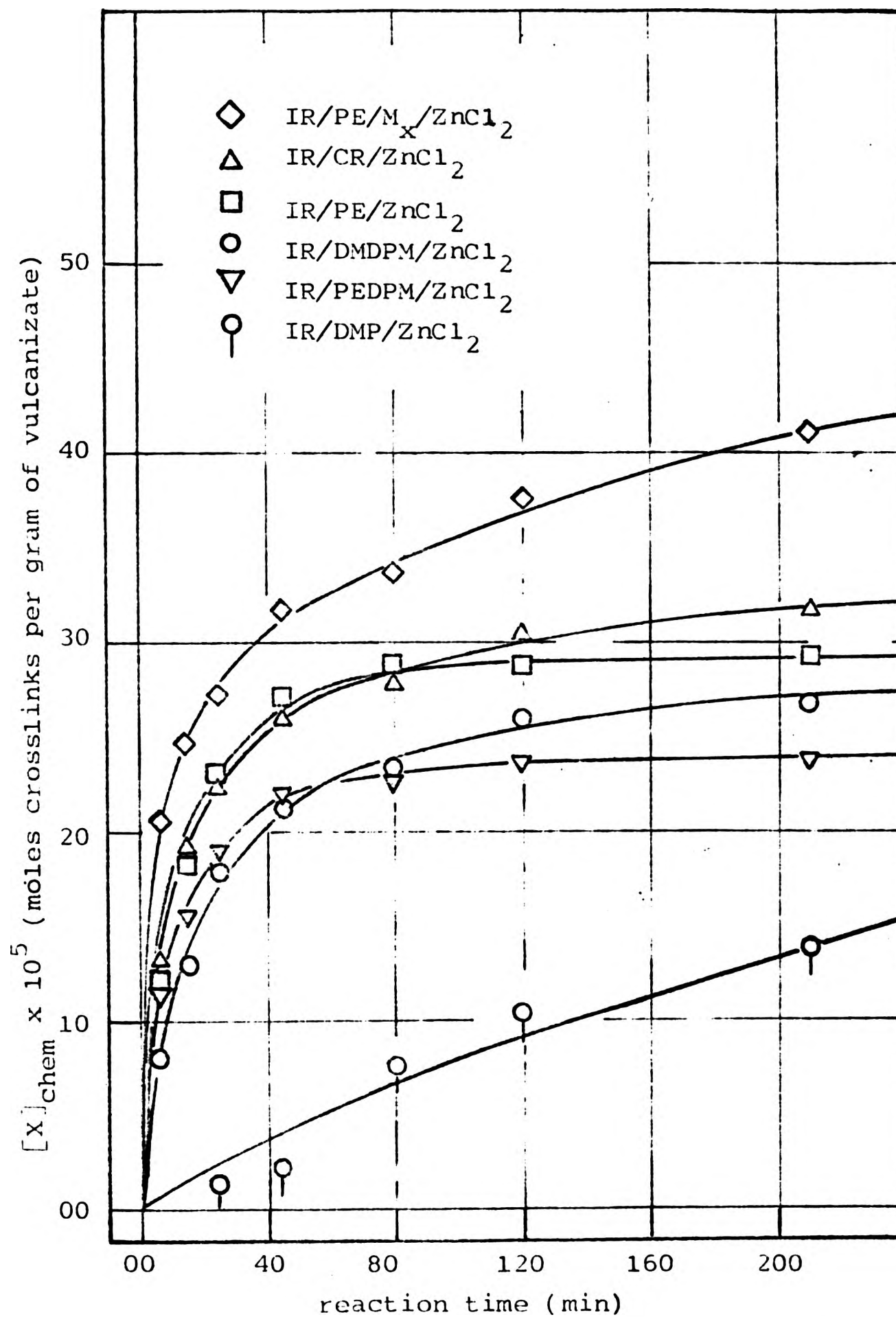


Fig. 69 Changes in concentration of chemical crosslinks,  $[X]_{\text{chem}}$ , with reaction time for DMP, DMDPM, PEDPM, PE and CR as calculated from the physically effective crosslinks determined by equilibrium swelling in *n*-decane.

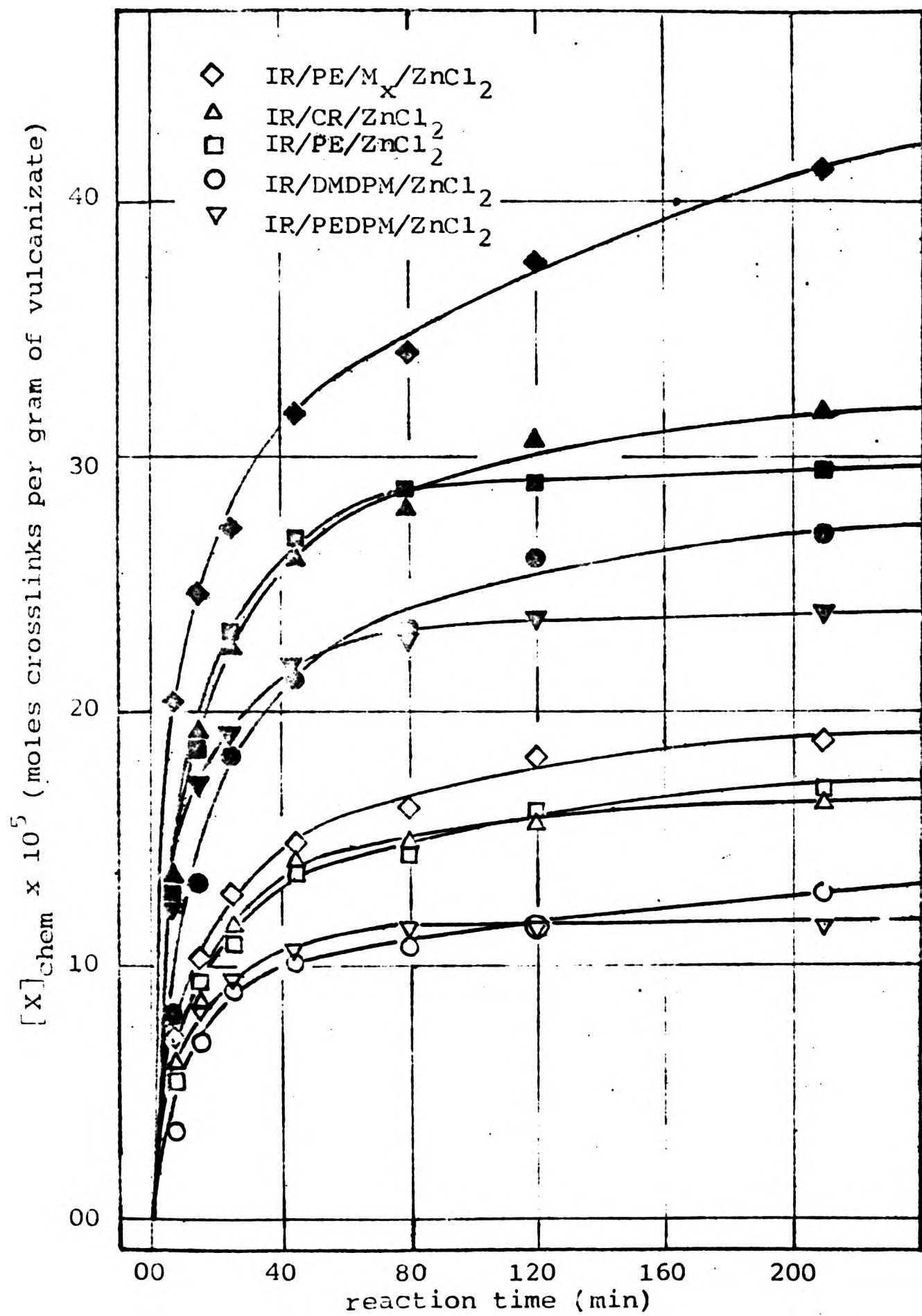


Fig. 70 Comparison of changes in concentration of chemical crosslinks,  $[X]_{\text{chem}}$ , with reaction time for the DMDPM, PEDPM, PE and CR as calculated from the physically effective crosslinks determined by equilibrium swelling in benzene (o) and in n-decane (•).

(ii-v)  $[X]_{\text{chem}}$  from  $[X]_{\text{phys}}$  measured by swelling in benzene

Examination of the results for the DMP interaction show (Fig. 65) that addition of  $M_x$  (i.e., IR/DMP/ $M_x$ /ZnCl<sub>2</sub> interaction) decreases the rate of crosslink insertion whereas addition of MMP (i.e., IR/DMP/MMP/ZnCl<sub>2</sub> interaction) gives about the same rate of insertion. This latter observation means an effective increase in the efficiency of crosslinking since the amount of DMP used was only  $\frac{1}{2}$  that used for the case of DMP alone. Comparison of results for DMP alone with those for CR, PE, DMDPM and PEDPM (Fig. 70) shows that all the latter condensates show an appreciably higher rate of crosslink insertion than DMP. Rates of crosslink formation, and  $[X]_{\text{chem}}$  maxima were approximately equal for the CR and PE cases, which in turn were higher than those for DMDPM and PEDPM (Fig. 68). Comparison of the DMDPM and PEDPM cases shows a similar level of reactivity. However, in the early stages of reaction, rates for the PEDPM case were higher than for DMDPM. The fastest rates and the highest  $[X]_{\text{chem}}$  maxima were obtained in the IR/PE/ $M_x$ /ZnCl<sub>2</sub> interaction, a result which was expected on the basis of the IR/pf 'model' studies (this will be discussed further later).

(ii-vi)  $[X]_{\text{chem}}$  from  $[X]_{\text{phys}}$  measured by swelling in n-decane

These values are presented in Fig. 69 and they are compared with those obtained from swelling in benzene in Fig. 70. They show the same general trend as the corresponding ones obtained from swelling in benzene but  $[X]_{\text{chem}}$

values are ~2 times higher. This difference possibly arises from a phase-separation effect. The p/f phase in the vulcanizates is not expected to dissolve completely in n-decane, an effect which will increase the apparent number of crosslinks. Further evidence for phase inhomogeneity is seen in the cloudiness of the decane-swollen samples. It therefore seems likely that phase inhomogeneity is present on a microscopic scale in the decane-swollen vulcanizates.

(ii-vii)  $[X]_{\text{chem}}$  from  $[X]_{\text{phys}}$  measured by equilibrium modulus

These values are presented in Fig. 66 and they are compared with those obtained from swelling in both solvents used in Fig. 67. They show again the same general trend as the corresponding ones obtained from swelling. Values for  $[X]_{\text{chem}}$  are in all cases lower than the corresponding ones from swelling in either of the solvents used. However, they were closer to those obtained from swelling in benzene, being especially similar in the early stages of reaction.

All the above would appear to suggest that phase separation is not likely in the dry vulcanizate. It seems possible that phase separation is assisted by the solvent action of n-decane, and does not arise in the dry state or in benzene. This suggests that the values obtained from swelling in benzene or by equilibrium modulus are more reliable than those obtained by swelling in n-decane.

Further support for the greater reliability of the former is seen in a better correspondence of results with those from acetone extraction. In some cases the n-decane results for  $[X]_{\text{chem}}$  would require >100%, i.e.,  $E_c$  values >1 which is clearly not the case from the acetone extraction values (Fig. 94, Experimental Chapter). The values chosen for further discussion (below) are therefore those from equilibrium swelling in benzene.

(d) Efficiency

For the purpose of the discussion which follows, it is convenient to express results in terms of efficiencies of the various processes. The efficiency of combination  $E_c$ , efficiency of crosslinking by combined material  $E_x$ , and the overall efficiency  $E_v$ , as defined in Section 4.1 were calculated from the phenolic material combined and the  $[X]_{\text{chem}}$  values.  $E_x$  and  $E_v$  were calculated from  $[X]_{\text{chem}}$  derived from swelling in benzene. Typical  $E_x$  and  $E_v$  values from  $[X]_{\text{chem}}$  derived from equilibrium modulus measurements were also calculated for comparison purposes. Values of  $E_x$  calculated from  $[X]_{\text{chem}}$  derived from swelling in n-decane for the DPM case were ~1 and for PE, CR, DMDPM and PEDPM ~1.6. These efficiencies are improbably high as has been discussed above. Therefore, these and the  $E_v$  values for n-decane swelling figure were not plotted.

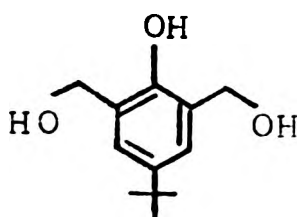
Results are summarised in graphical form in Figs. 72 to 88 in the next section where they will be discussed and they are presented in the Experimental Chapter (Table 15).

### 4.3 Discussion

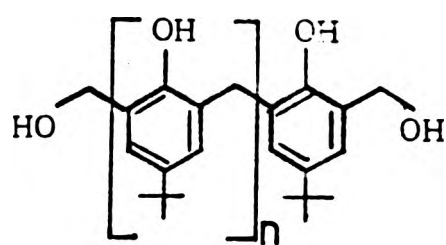
(a) Vulcanization with bifunctional methylol derivatives

(i) Structure, functionality and expected efficiency of reaction

The preparation of the dimethylolphenol (LX) and of the dimethylol diphenyl methane (LXII) are described in the Experimental Chapter. The dimethylolphenol was obtained as a pure crystalline solid whereas the dimethylol diphenyl methane did not appear to crystallise and is likely to be a mixture of dimethylol diphenyl methanes which might be represented by the formula (LXII) with an average  $n=1$ . This was supported by the  $M_n$  of 397 obtained (theory=372) and by nmr spectroscopy which showed (Table 6) that values of  $F_{(\text{ArCH}_2\text{OH})}$  and  $F_{(\text{ArCH}_2\text{Ar})}$  were 0.82 and 1.13, instead of the value 1 for each group which would be consistent with the pure material (LXII) for which  $n=1$ . Furthermore, nmr spectroscopy also shows the presence of a very small dibenzyl ether content ( $F_{((\text{ArCH}_2)_2\text{O})}=0.07$ ), which could have been



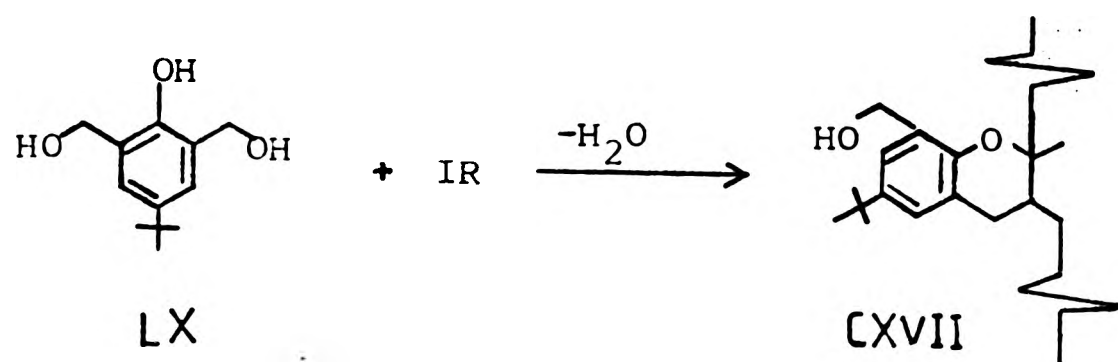
LX



average  $n=1$

LXII

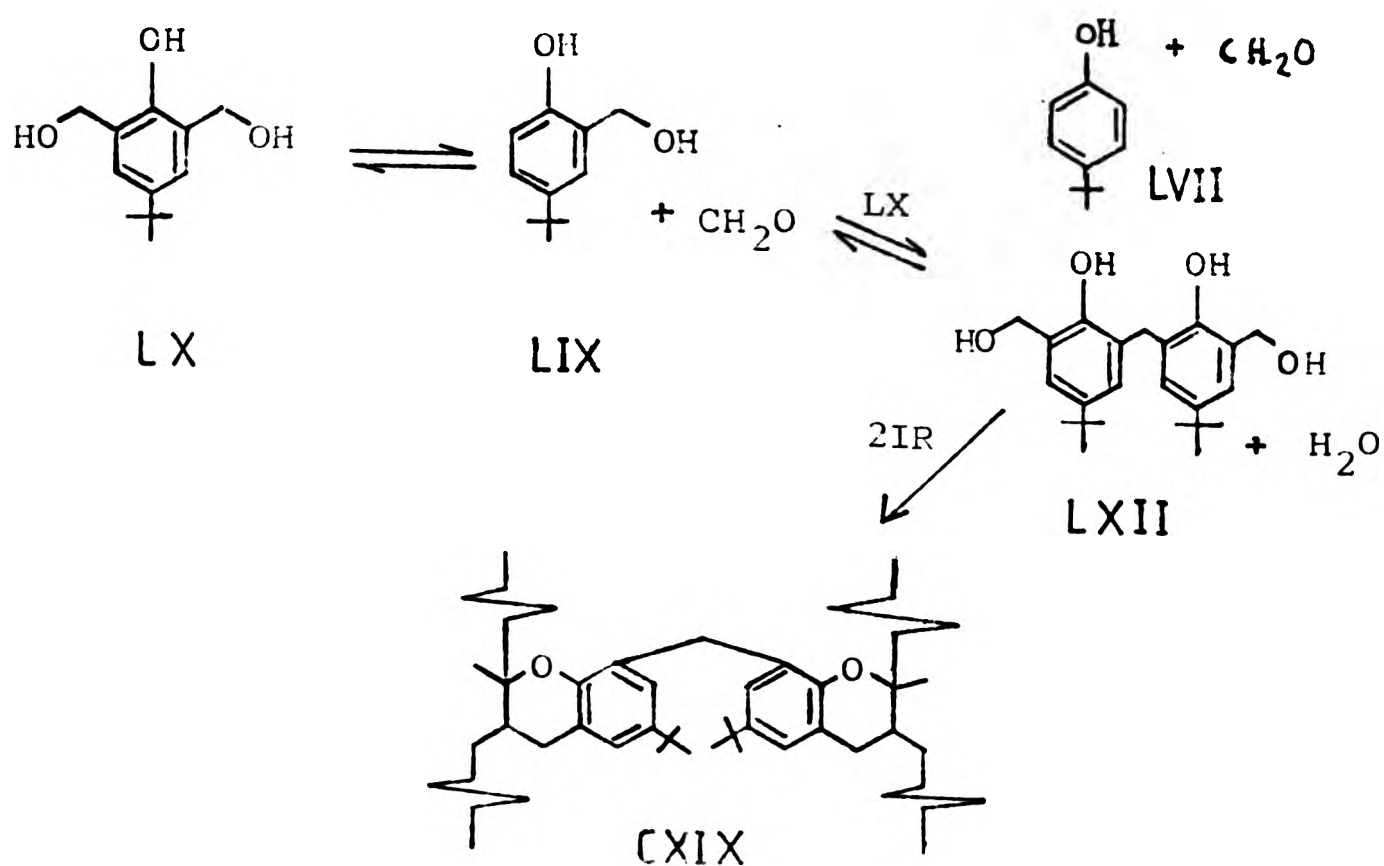
formed during its preparation and/or by self-condensation of the methylol groups when the material was dried at 50°C. The latter is considered the more likely since dibenzyl ether formation under the conditions used in the preparation of this material is most improbable.



The dimethylolphenol (LX) itself can be regarded as mono-functional from the point of view of the 'chroman theory' since, after chroman formation, the second methylol group is inactive. Thus, this material should react mainly with the rubber to form main chain modifications (Formula CXVIII) rather than crosslinks. Any crosslinks produced must arise from side-reactions and there are two kinds of side reaction which might well contribute to this.

First from the generalised Scheme 4 (Chapter 2), this material can undergo side-reactions producing the dimethylol diphenyl methane (LXII, n=1) which can provide crosslinks. This sequence of reactions may be envisaged as in Scheme 8. Scheme 8 might be tested by adding excess methanal to the reaction, when the increase in partial pressure of CH<sub>2</sub>O would

suppress the formation of (LIX) and hence the formation of

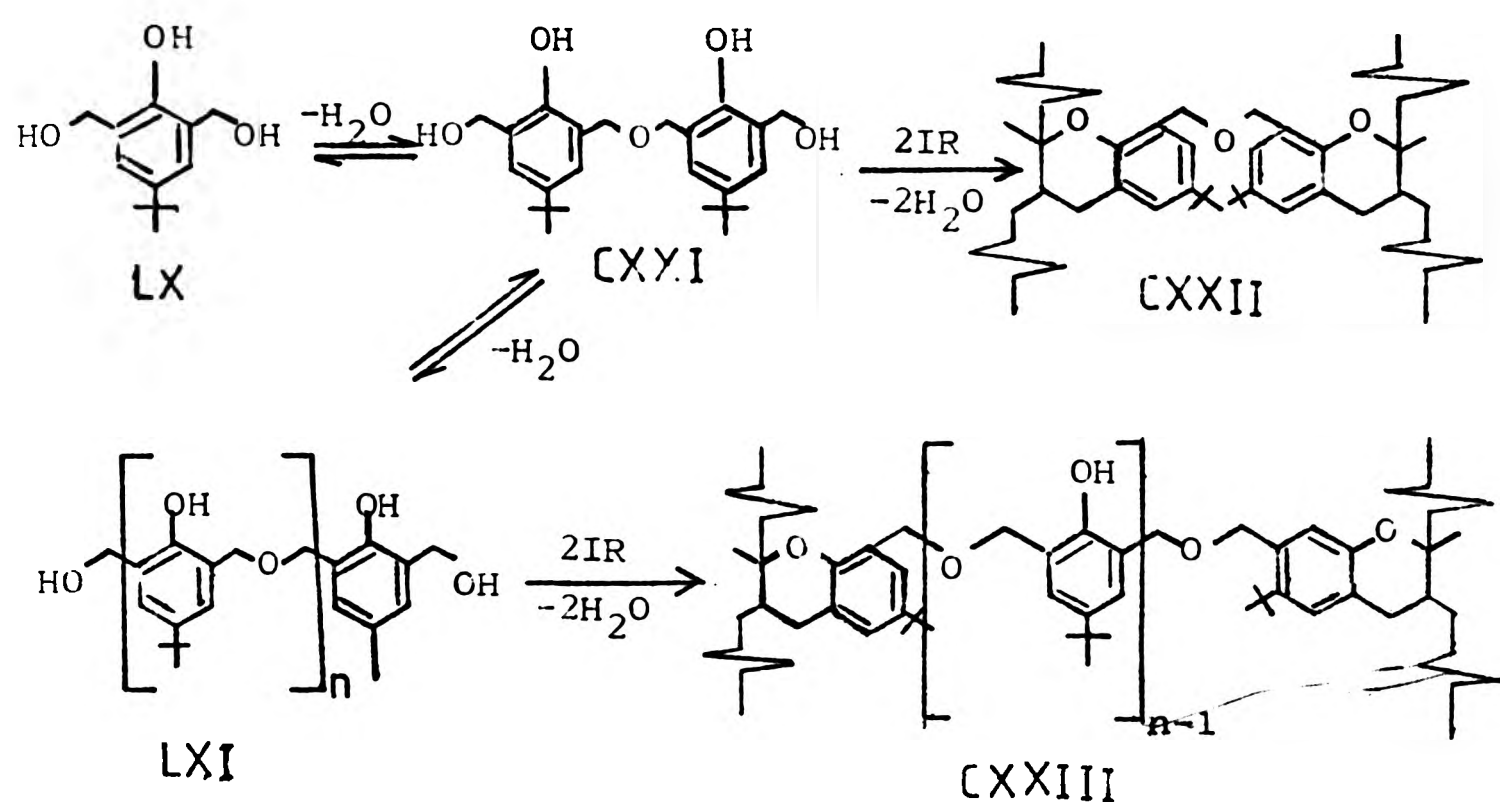


Scheme 8 Side reactions of dimethylol phenol (LX) giving crosslinking (alternative 1).

the crosslinking agent (LXII). On the other hand, the addition of 2-methylol-4-tert.butyl phenol (LIX) would favour its formation. Thus, the former addition would be expected to decrease the concentration of crosslinks and the latter to increase them. The results of such tests are presented and discussed later.

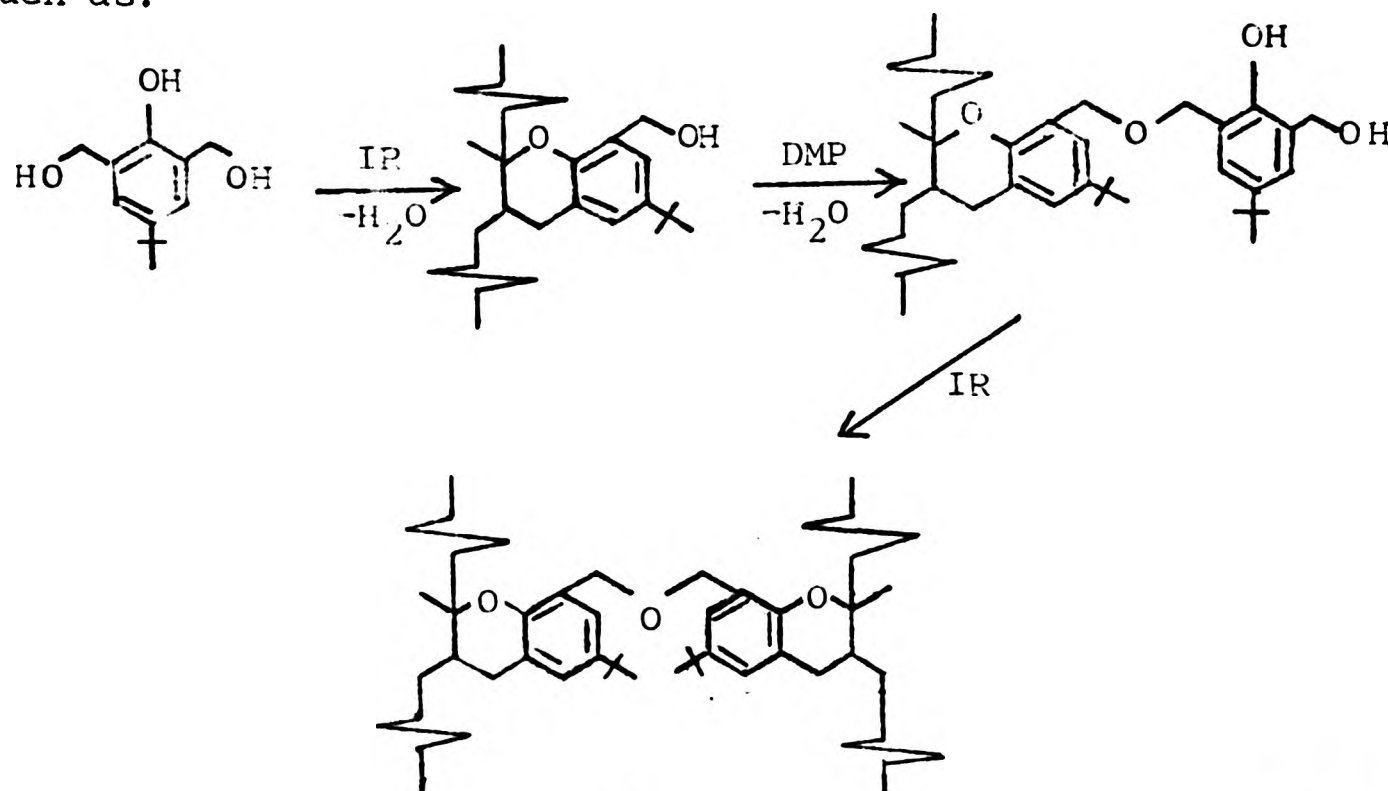
A second kind of side-reaction sequence which might produce crosslinking is that shown in Scheme 9, in which the dimethylolphenol undergoes self-condensation to form the dimethylol dibenzyl (CXXI) or polybenzyl ether (LXI). These materials are truly bifunctional in their potentiality to form chroman links with rubber, and will therefore form

crosslinks. The crosslinks (CXXII) from the dimeric ether



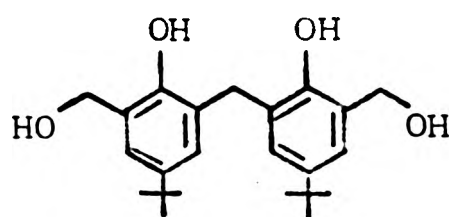
Scheme 9 Side reactions of dimethylol phenol (LX) giving crosslinking (alternative 2)

would be expected to show high stability since the dibenzyl ether link is not activated by the presence of phenolic hydroxyls. The crosslinks (CXXIII) from the polymeric ether, on the other hand, might be expected to undergo cleavage followed by further rearrangements. It will be appreciated that the sequence of reactions is not necessarily fixed as shown in Scheme 9, and might follow an alternative pattern such as:

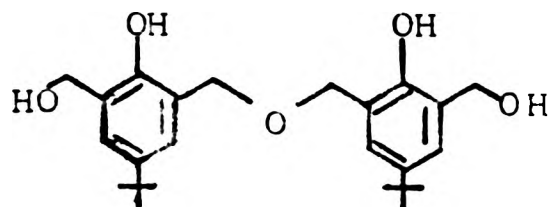


whichever sequence is applicable, the Scheme 9 would be expected to be insensitive to the presence of excess methanal. Excess moisture might be expected to suppress the ether formation, but it would also suppress quinone methide formation. The only test which would distinguish these reactions from those in Scheme 8 would be one which establishes the presence of an ether linkage in the crosslink. It has not been possible to do this so far.

It will be evident from these considerations that the simplest materials which are potentially bifunctional chroman-forming (and hence crosslink-forming) reagents are:



For methylene bridge crosslinks according to Scheme 8



For ether crosslinks according to Scheme 9

Unfortunately, it has not been found possible to prepare either of these in pure form. As pointed out above, attempts to prepare the methylene-linked material (LXII,  $n=1$ ) resulted in a mixture of homologues of the general formula (LXII). It will be clear that, in such a mixture, if average  $n=1$  there must be some material of  $n=0$  (i.e., the dimethylol phenol) which we have already seen is not expected to be an efficient vulcanizing agent. On the other hand, the

components having  $n > 1$  are also expected to be inefficient, since the crosslinks will now contain more methylene-linked phenolic nuclei than necessary and hence some of the phenolic material is wasted (Fig. 71). It is clear from Fig. 71 that for materials of  $n > 1$ ,  $E_x = 2/n+1$ .

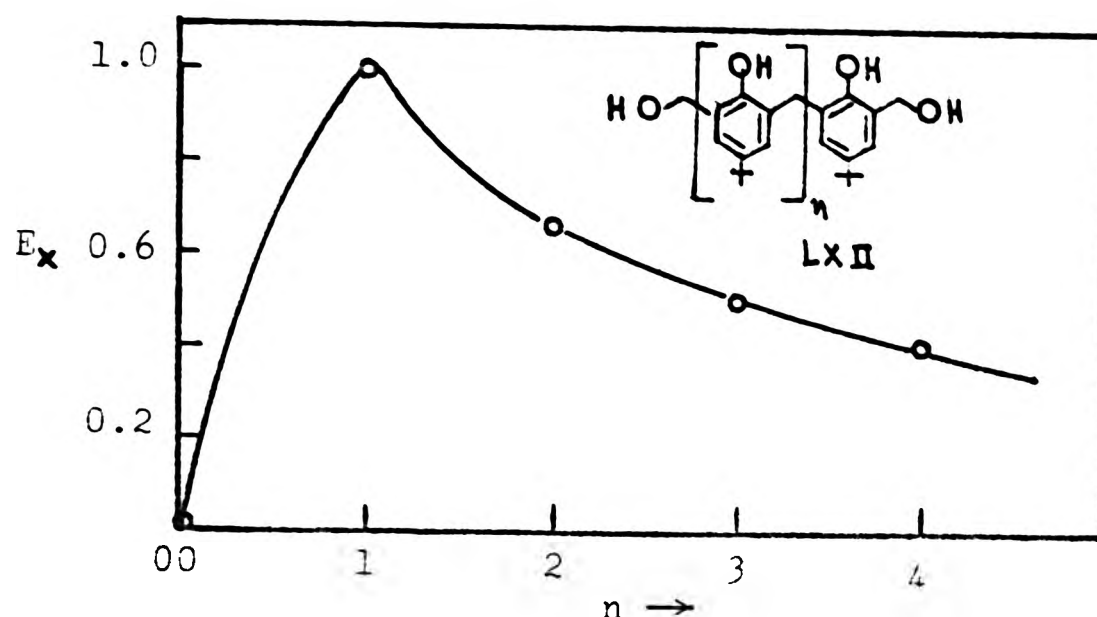
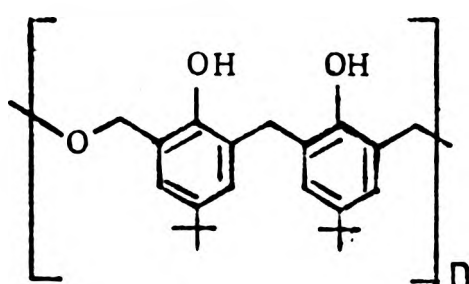


Fig. 71 Theoretical crosslinking efficiency of homologues of Formula (LXII).

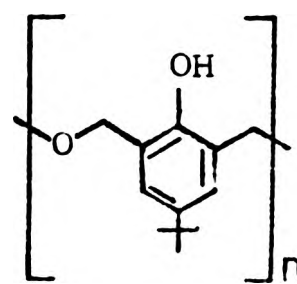
Attempts to prepare the ether-linked material (CXXI) also produce a mixture of homologues, this time of formula LXI (in Scheme 9). However, the crosslinking efficiency for values of  $n > 1$  is not now reduced, since the ether links are still active (each ether link reacting ultimately as 2 methylols). These polyethers, as well as the polyether derived from the dimethylol diphenyl methane (LXIII), are discussed more fully in the next section.

If, for the present purpose, we assume that each ether link has the same chroman-forming potential as 2 methylol groups, then there is expected to be some correlation between

values of  $R_{pot}$  (equations 40-41) and theoretical ultimate value of  $E_c$  for a material. However, it should be noted that the presence of some methylene links, whilst detracting from  $R_{pot}$ , does not reduce theoretical ultimate  $E_c$  unless methylene links occur in adjacent positions (as in formula LXII where  $n > 1$ ). Thus, the polyether (LXIII) from the pure dimethylol diphenyl methane (LXII,  $n=1$ ) will have the same ultimate crosslinking efficiency  $E_c$  as the polyethers (LXI) from the dimethylol phenol.



LXIII



LXI

These considerations are all based on the assumption that there is no mechanism for forming a crosslink containing only 1 phenolic nucleus. As will be seen later, this appears to be borne out in practice.

From the above, the main structural features which are ultimately present in the fully-reacted vulcanizates and which represent inefficient use of phenolic material are:

- (i) main chain modification (Formula CXVIII),
- (ii) adjacent diphenyl methane groups in crosslinks (Formula LXII,  $n > 1$ ). Additionally, from the earlier studies by Fitch, we might expect:

- (iii) products of trimerisation of quinone methides,
- (iv) inactive aldehyde and methyl phenol groups from scission of the polyether links.

The aim of this work is to eliminate these as far as possible, so as to maximise the efficiency of use of the phenolic material.

It is of some interest to calculate the amount of phenolic material required to give a 'typical' vulcanizate (of, say,  $\bar{M}_c$  values 5,000), assuming the reaction to be 100% efficient, and complete. For the product (LXIII) giving methylene crosslinks this would be 3.30 phr; for the product (LXI) giving ether crosslinks it would be 3.70 phr. Since some 10-15 phr are used in practice, this gives an indication of the advantages to be gained by efficient vulcanization.

Note that the above considerations are all concerned with the efficiency of utilisation of phenolic material rather than purely with rate of vulcanization. The latter will depend strongly upon the type and amount of catalyst, and on the reaction temperature. It will depend only slightly on the type of phenolic material employed, in that the ether groups appear to react slightly more quickly than methylol ones. However, this difference will have no technological significance since the reaction rate can readily be changed by adjustment of catalyst concentration or temperature.

The efficiencies  $E_c$ ,  $E_x$  and  $E_v$ , as defined in Section 4.1, do however vary with time since they depend upon the degree of completion of the reaction. Thus,  $E_c$  will gradually increase as the starting material is used up, even though the starting material may pass through several chemical changes before combining with the rubber. Similarly,  $E_x$  may be low initially since combined material may be in the form of potentially-reactive pendent groups which later react to form crosslinks. This latter efficiency value ( $E_x$ ) is analogous to the corresponding term used by Moore et al. in describing efficiency  $E$  of crosslinking by sulphur systems (although the definitions are different, so that improved efficiency in Moore's work is revealed in reducing values of  $E$ ).

(ii) Results and discussion

The results obtained in the present work (expressed in their original form in the Experimental Chapter) are presented here in the form of combination efficiency  $E_c$  versus time (Fig. 72), crosslinking efficiency  $E_x$  versus time (Fig. 73), and overall vulcanization efficiency  $E_v$  versus time (Fig. 74). In addition, some kinetic data are listed for comparison with other bifunctional phenolic starting materials in Tables 7, 8 and 9.

(a) Efficiency of combination,  $E_c$

Values of  $E_c$  at various reaction times for the methylol

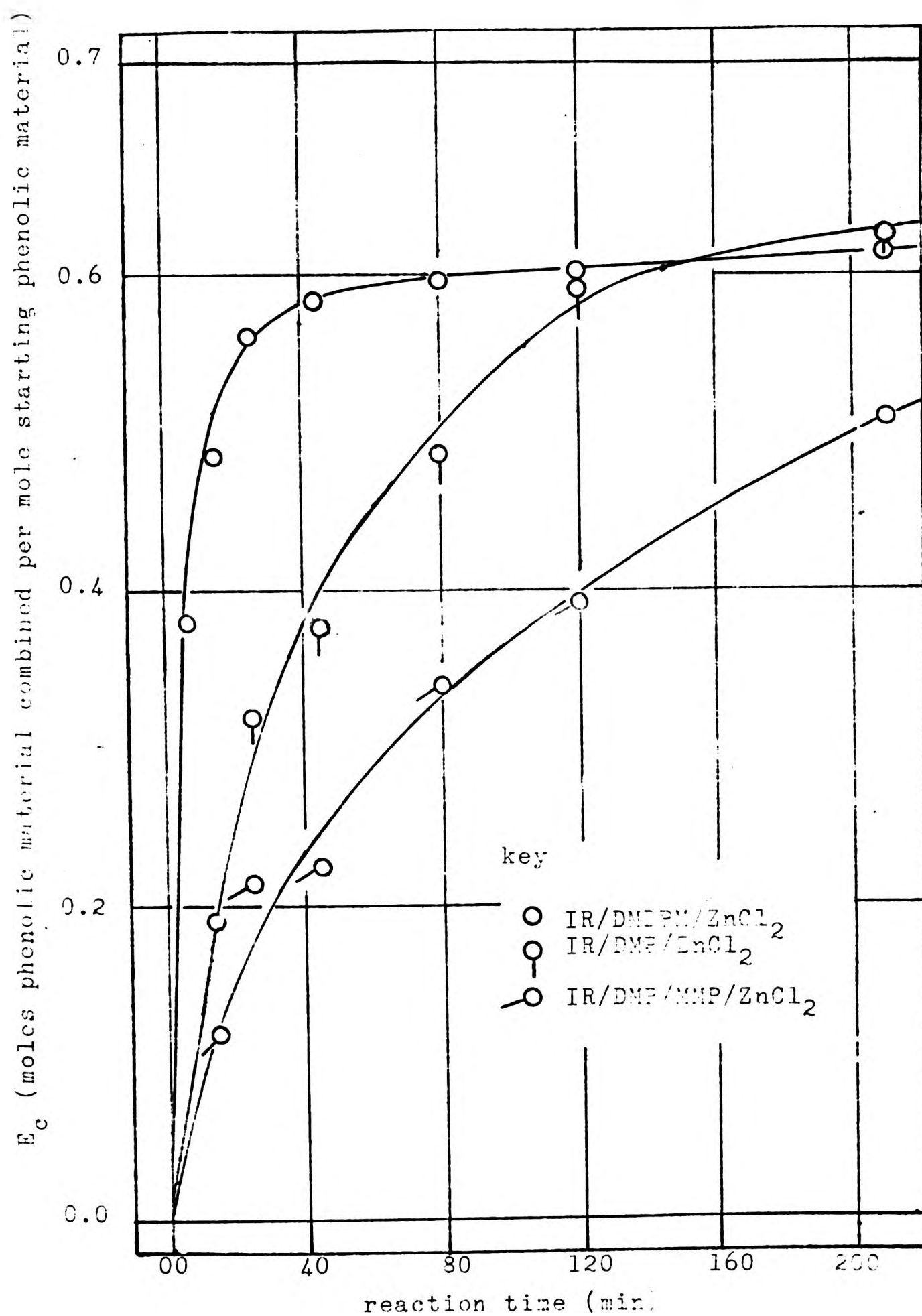


Fig. 72 Kinetics of the efficiency of combination,  $E_c$ , for the bifunctional methylol derivatives as calculated from the amount of acetone extract.

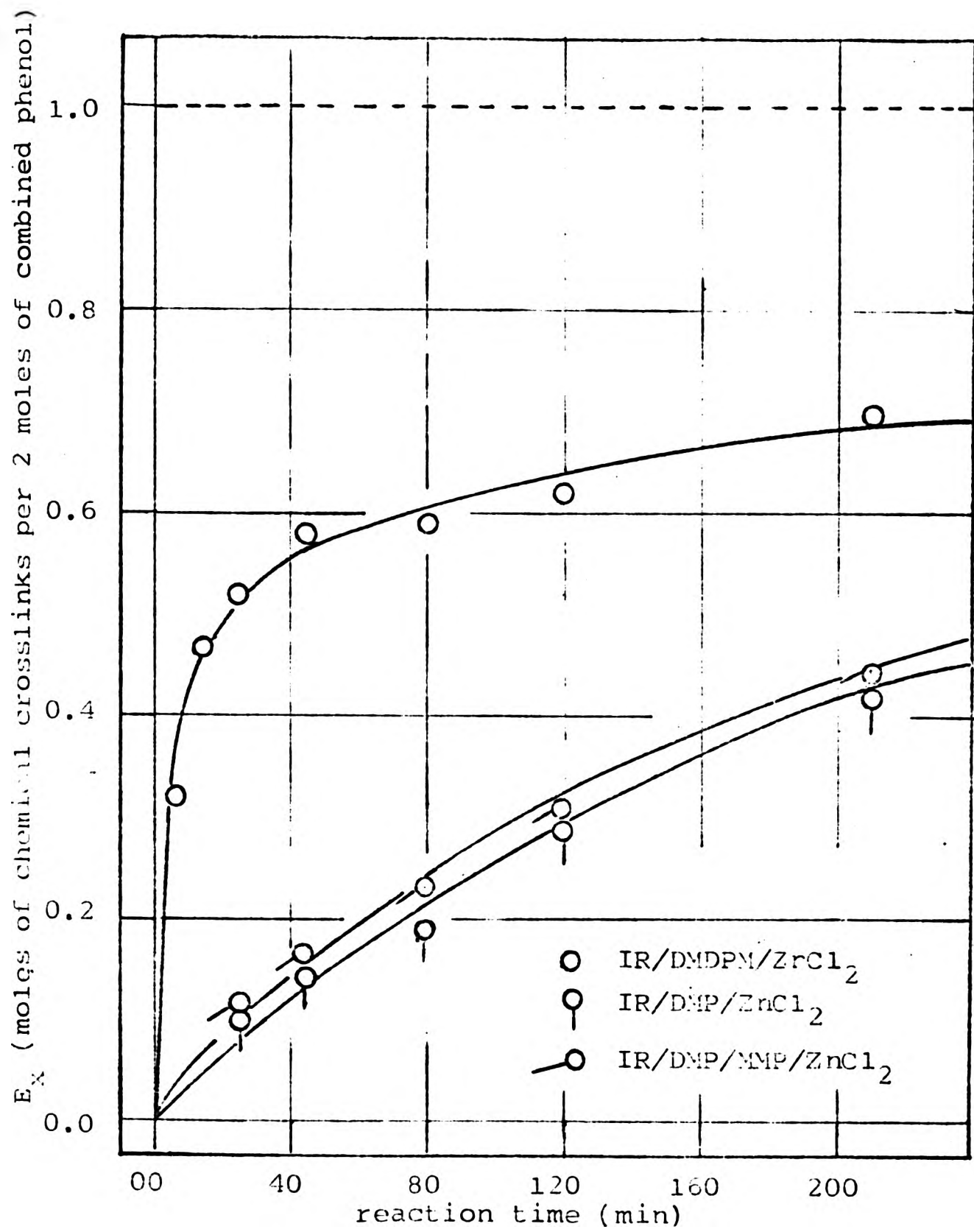


Fig. 73 Kinetics of the efficiency of crosslink formation,  $E_x$ , for the bifunctional methylol derivatives as obtained from values derived from swelling in benzene.

E<sub>v</sub> (moles of chemical crosslinks per 2 moles of starting phenolic material)

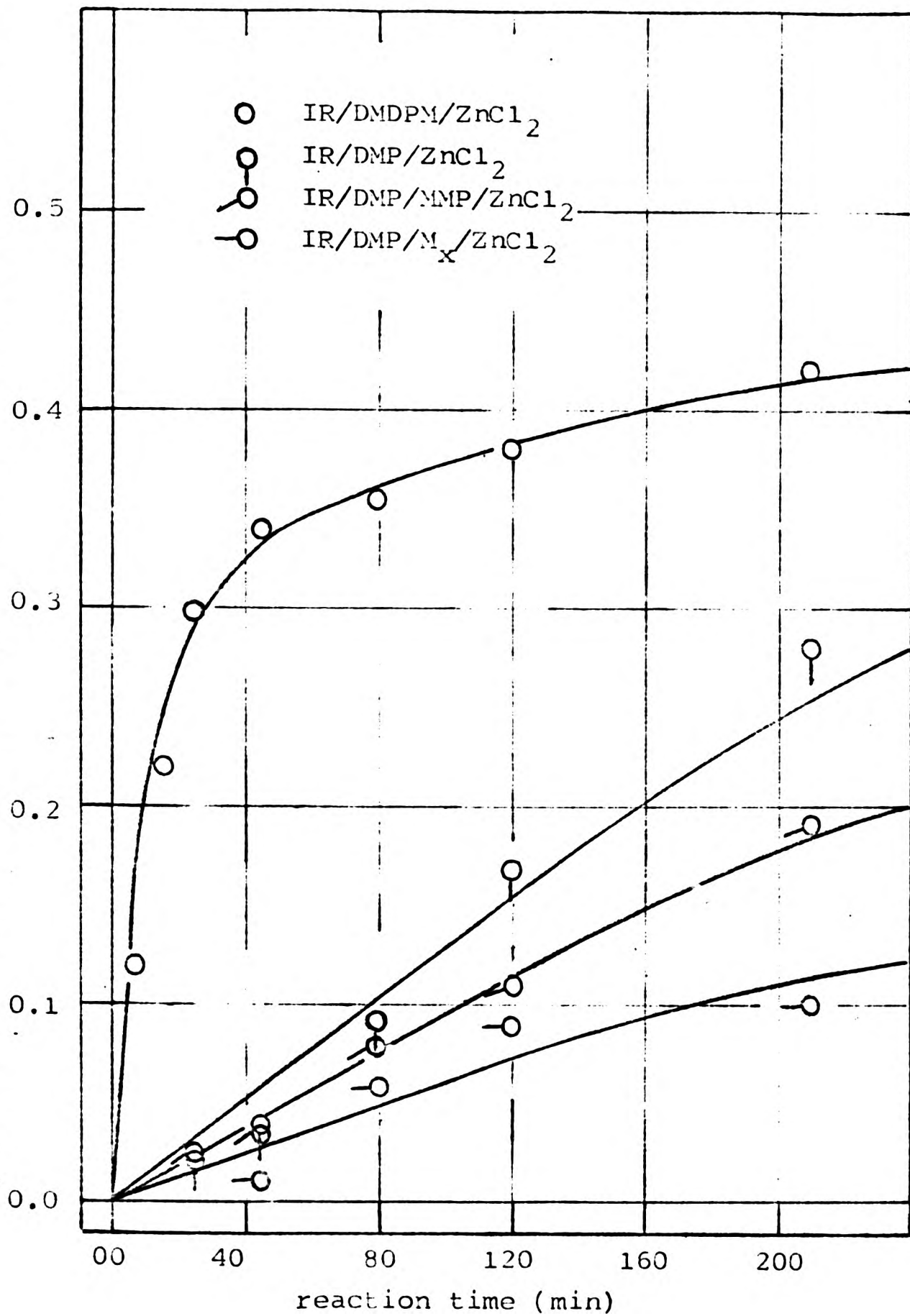


Fig. 74 Kinetics of the vulcanization efficiency, E<sub>v</sub>, for the bifunctional methylol derivatives as obtained from values derived from swelling in benzene.

Table 7: Kinetic data for phenolic material combined in the various interactions, as calculated from the amount of acetone extract

Interaction	Moles phenolic material combined/mole rubber $\times 10^2$		
	after 10 min reaction	after 35 min reaction	after 210 min reaction
IR/CR/ZnCl <sub>2</sub>	2.51	2.86	3.13
IR/PE/ZnCl <sub>2</sub>	1.89	2.61	3.00
IR/DMDPM/ZnCl <sub>2</sub>	2.33	2.84	3.07
IR/PEDPM/ZnCl <sub>2</sub>	2.39	2.90	3.11
IR/DMP/ZnCl <sub>2</sub>	0.67	1.78	3.11
IR/DMP/MMP/ZnCl <sub>2</sub>	0.44	1.11	2.56

Table 8: Kinetic data for chemicals crosslinks (swelling in benzene) per combined 2 moles phenolic material in the various interactions

Interaction	Moles crosslinks/2 moles combined phenolic material		
	after 10 min reaction	after 35 min reaction	after 210 min reaction
IR/CR/ZnCl <sub>2</sub>	0.47	0.67	0.83
IR/PE/ZnCl <sub>2</sub>	0.65	0.81	0.86
IR/DMDPM/ZnCl <sub>2</sub>	0.42	0.55	0.69
IR/PEDPM/ZnCl <sub>2</sub>	0.46	0.49	0.60
IR/DMP/ZnCl <sub>2</sub>	0.03	0.11	0.43
IR/DMP/MMP/ZnCl <sub>2</sub>	0.05	0.13	0.45

Table 9: Kinetic data for chemicals crosslinks (swelling in benzene) per 2 moles starting phenolic material in the various interactions

Interaction	Moles crosslinks/2 moles starting phenolic material		
	after 10 min reaction	after 35 min reaction	after 210 min reaction
IR/CR/ZnCl <sub>2</sub>	0.28	0.43	0.53
IR/PE/ZnCl <sub>2</sub>	0.24	0.41	0.55
IR/PE/M <sub>x</sub> /ZnCl <sub>2</sub>	0.27	0.46	0.62
IR/DMDPM/ZnCl <sub>2</sub>	0.21	0.31	0.42
IR/PEDPM/ZnCl <sub>2</sub>	0.24	0.33	0.37
IR/DMP/ZnCl <sub>2</sub>	0.02	0.05	0.28
IR/DMP/MMP/ZnCl <sub>2</sub>	0.01	0.03	0.19
IR/DMP/M <sub>x</sub> /ZnCl <sub>2</sub>	0.01	0.02	0.12

compounds DMP and DMDPM are plotted in Fig. 72. From this figure, it can be seen that DMDPM (Formula LXII) shows a high rate of combination initially but a levelling off after about 40 min. to a value for  $E_c$  of about 0.6. On the other hand, DMP and its mixture with MMP both show a much lower combination rate, with  $E_c$  still increasing after 200 min., to a value (in the DMP case) of  $> 0.6$ .

These rates of combination should be comparable to the combination rate of the monofunctional compound, MP, discussed in Chapter 3, bearing in mind that the concentrations used are different. Such a comparison may be made by reference to Tables 4 (monofunctional methylol compound) and 7 (bifunctional compounds), from which the following values may be selected as examples:

	Moles/mole rubber combined after 10 min reaction	Moles/mole rubber combined after 35 min reaction	Mole/mole rubber combined after 210 min reaction
IR/MP/ZnCl <sub>2</sub>	0.60	1.80	5.90
IR/DMP/ZnCl <sub>2</sub>	0.67	1.78	3.11

It will be recalled that the concentration of DMP used was  $\frac{1}{2}$  that of the MP, in order to obtain equivalence in concentration of methylol groups. If the assumption is justifiable that the reactivity of DMP is twice that of MP, it would be expected that the amount combined should initially be the same, but with gradual divergence to an ultimate ratio of 2/1 for MP/DMP. The figures shown above, however, suggest that

DMP is rather more than twice as reactive as MP, which in turn indicates that the reactivity of a quinone methide moiety is increased by the presence of a methylol substituent.

Differences of combination rates up to 35 min. between the IR/DMP/ZnCl<sub>2</sub> and IR/DMP/MMP/ZnCl<sub>2</sub> interactions (Table 7) which are ~2 times higher for the former interaction might be attributable to the initial concentration differences. Since the DMP/MMP ratio was 1/1, but the total number of moles used was the same, it follows that the methylol concentration of the mixture is 3/4 that of the pure DMP. An initial rate ratio of 4:3 for DMP:mixture would therefore be expected, and the observed ratio of 1.78:1.11 (after 35 min) seems in reasonable agreement with this bearing in mind the uncertainties of the analysis.

Comparison of the kinetic data for the IR/DMP/ZnCl<sub>2</sub> and IR/DMDPM/ZnCl<sub>2</sub> interactions (Fig. 72, Table 7) show that, whereas E<sub>c</sub> maxima were about equal for both interactions, initial rates were much higher for the IR/DMDPM/ZnCl<sub>2</sub> interaction than for the IR/DMP/ZnCl<sub>2</sub> case.

Since the DMDPM molecule is about twice as large as the DMP molecule, each quinone methide-rubber addition will combine about twice as much material in the former case. However, since the methylol concentration of DMDPM is only ½ that of DMP, it might be expected that this would restore the rate of combination to about the same in each case. There is, however, another factor to consider which increases

the reactivity of DMDPM compared with DMP. Whereas the reaction of one methylo1 group of DMP leaves the second one unable to react further, this is not true for DMDPM where the second group remains reactive. Thus, there is a much more rapid loss of 'active' methylo1 groups in DMP compared with DMDPM, and consequently a more rapid combination rate is expected in the latter case. A further factor which is expected to increase combination rate in DMDPM is the presence of some ether links (see nmr analysis). This will cause more material to be combined in each reaction step as discussed in the case of the ethers generally (Section b, below).

(b) Efficiency of crosslinking by combined material,  $E_x$

Values of  $E_x$  derived from swelling in benzene are plotted against reaction time in Fig. 73. Some data selected from the results are also presented in Table 8 (based on benzene swelling results) for comparison with other systems.

Examination of Fig. 73 shows reducing efficiency of crosslinking by combined material in the order DMDPM >> DMP/MMP > DMP. A very large difference in crosslink insertion rate is seen in the early stages of reaction for DMDPM, compared with the other materials.

Comparing first the curves (Fig. 73) and kinetic values (Table 8) for DMP/MMP with those for DMP alone, it can be

seen that the former is generally the more efficient crosslinking agent. Thus, although the DMP/MMP mixture is less efficient than DMP alone in combining with the rubber (Fig. 72), the material which combines is more efficient in crosslinking the rubber (Fig. 73). This would appear to support the expected reaction scheme (Scheme 8) where it was suggested that the incorporation of the monofunctional MMP would encourage the formation of methylene-bridged crosslinks. The final crosslinks, in fact, will have the same structure (Formula CXIX) as those from DMDPM, although they will have been formed by a different and less efficient sequence of events.

Comparison of the data for DMP with those for DMDPM show that crosslinking rates were faster and ultimate maxima higher (~40%) for the DMDPM case. This is in accord with the expectations discussed earlier, since DMDPM is truly bifunctional in respect of crosslinking, whereas DMP is essentially monofunctional and depends upon side-reactions for its crosslinking action. DMDPM appears to be a fairly efficient crosslinking agent, with crosslink concentrations approaching 70% of theoretical, and still increasing, at the end of the reaction time. It cannot be said with certainty that the DMDPM crosslinking efficiency would not eventually reach 1, but there appears to be a levelling out process occurring. Deviations from this maximum theoretical value of  $E_x=1$  for the DMDPM case might be accounted for by its value of  $F_{(ArCH_2Ar)}=1.13$  as well as by the presence of

'pendent' phenolic material which has combined only at one side as a consequence of side reactions of one of the methylol groups. Alternatively, the levelling off towards  $E_x \sim 0.7$  after 30-40 min. reaction time could be a consequence of the catalyst having been 'used up', probably hydrolysed. It is noticeable that there is a similar change in shape at this time in the DMP and DMP/MMP curves.

(c) Overall efficiency of vulcanization,  $E_v$

The overall efficiency of the materials as vulcanizing agents may be judged from Fig. 74, which is effectively the product of Figs. 72 and 73. It is seen that DMDPM is clearly the most efficient vulcanizing agent, giving almost 45% of the theoretical maximum number of crosslinks after the reaction time allowed. DMP alone is next most efficient at up to 30% theoretical and DMP/MMP is least efficient at up to 20% theoretical (although it is clear from (a) and (b) above that the reduced efficiency of DMP/MMP is due only to its lower rate of reaction caused by the lower methylol content). In each case the crosslinking is still progressing after the maximum reaction time allowed of 200 min., although such lengthy cure times would be impracticable for industrial use. Also included in Fig. 74 are  $E_v$  values calculated for the system IR/DMP/ $M_x$ /ZnCl<sub>2</sub>, for which the  $E_c$  and  $E_x$  values could not be obtained due to uncontrollable volatilisation of paraformaldehyde during the reaction and extraction procedures. These  $E_v$  values were calculated directly from the amount of phenolic material used and the number of

crosslinks obtained. It is clear from Fig. 74 that the efficiency as a vulcanizing agent is markedly lower than that of DMP alone. Since there is no reason why its combination efficiency  $E_c$  should be lower than that of DMP (there are the same number of methylol groups), the loss of vulcanizing efficiency must be due to a lower  $E_x$  value (i.e., the material which combines is less able to undergo the side reactions which produce crosslinks). This is in accord with the discussion in Section 4.3.

Some figures illustrating this trend of results compared with results from other vulcanizing systems are presented in Table 9, and will be referred to again later. The values of  $E_v$  after 35 min. of reaction time (a reasonable time for vulcanization) were 0.05 (DMP) and 0.31 (DMDPM) which represent 18 and 74% respectively of the  $E_v$  maxima. Thus, whereas DMDPM might be considered a practically-useful vulcanizing agent, DMP is much too slow in its action for consideration for practical purposes. Clearly, all reagents would benefit from increased rates of the various reactions, but this might not be a simple matter, since it is suspected that catalyst is consumed during the early stages of reaction. A further catalyst addition would no doubt increase the reaction rate in the early stages, but this might well cause problems of premature vulcanization ('scorch'), a severe disadvantage for practical processing.

(b) Vulcanization with products of polyetherification of bifunctional methylol derivatives

(i) Structure and characterisation

The preparation of the polyether derivatives from the dimethylolphenol and from the dimethylol diphenyl methane (Formulae LXI and LXIII respectively) are described in the Experimental Chapter. The nmr characterisation of these condensates (Table 6) show that, in these polyetherifications, in addition to the formation of dibenzyl ether groups, methylene bridges were also formed. The concentration of methylene bridges,  $F_{(\text{ArCH}_2\text{Ar})}$ , in the polybenzyl ether was 0.79 (theory=0), and in the polyether derivative of the dimethylol diphenyl methane was 1.34 (theory=1). Analyses relevant to the present considerations are summarised in Table 10.

Table 10: Analysis of the derived ethers

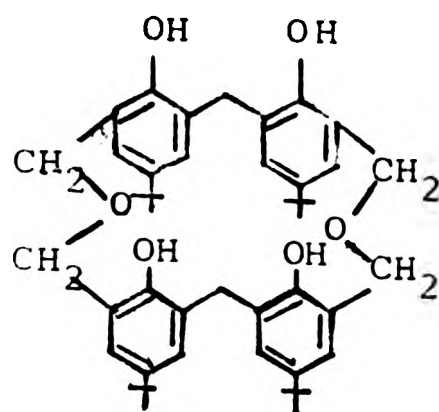
	No.	$F_{(\text{ArCH}_2\text{OH})}$	$F_{((\text{ArCH}_2)_2\text{O})}$	$F_{(\text{ArCH}_2\text{Ar})}$	Total
PE	LXI	0.05	1.24	0.79	2.08
PEDPM	LXIII	0.0	0.53	1.39	1.92

Several attempts were made to refine the method so as to reduce the number of methylene groups, but no method was found to produce the pure ether. It appears from the  $F_{(\text{ArCH}_2\text{Ar})}$  values referred to above that formation of these groups occurs faster in the condensation of dimethylolphenol

than in the condensation of dimethylol diphenyl methane. Addition of paraformaldehyde during the polyetherifications to suppress methylene bridge formation (in accord with the generalised Scheme 4) was not as effective as expected. This is probably because the paraformaldehyde was added before condensation started and was soon lost by volatilisation at the temperature of reaction. This suggests that the continuous addition of paraformaldehyde during might show benefit, but this has not yet been attempted.

From the concentration values  $F_{(\text{ArCH}_2\text{Ar})}$  and  $F_{((\text{ArCH}_2)_2\text{O})}$  obtained for these polyetherification products (Table 10) it is clear that Formulae (LXI) and (LXIII) are idealised, and clearly deviate from the theoretical values of  $F_{((\text{ArCH}_2)_2\text{O})} = 2$  and  $F_{(\text{ArCH}_2\text{Ar})} = 0$  for the former and  $F_{((\text{ArCH}_2)_2\text{O})} = 0.5$  and  $F_{(\text{ArCH}_2\text{Ar})} = 1$  for the latter.

The value of the concentration  $F_{(\text{ArCH}_2\text{OH})}$  for the polybenzyl ether was 0.05. This low concentration would be expected from the presence of the group as chain ends. The corresponding value for the ether derivative of the dimethylol diphenyl methane was unmeasurably low (zero), presumably because the  $M_n$  of this compound was higher (828) than for the polybenzyl ether (615) and hence the proportion of chain end groups was too low to be measured by nmr. Polyetherification including cyclic structures such as (CXXV) might also explain zero methylol concentration, but its MW (708) is rather too low and also  $F_{(\text{ArCH}_2\text{Ar})} + F_{((\text{ArCH}_2)_2\text{O})}$  should = 2,



CXXV

which was not the case (see Table 6 for analysis). Nevertheless, a mixture of rings and chains is a distinct possibility.

(ii) Functionality and reactivity

The polybenzyl ether PE and probably the ether derivative of the dimethylol diphenyl methane PEDPM can be regarded as bifunctional crosslinking agents in accord with the previous discussion.

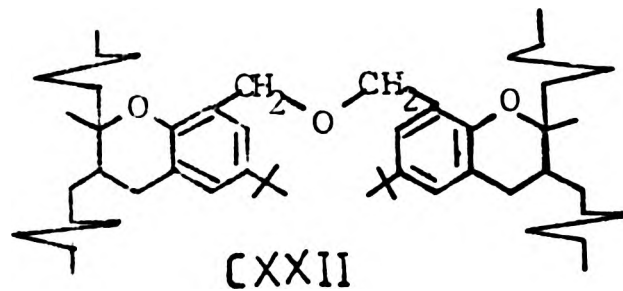
The polybenzyl ether clearly has an appreciable proportion of methylene-bridged nuclei (Table 10) as well as a small amount of methylol substitution. Since the methylene links are 'inactive', i.e., are incapable of scission to produce rubber-reactive entities, they are likely to reduce the rate of reaction with the rubber compared with the 'pure' ether (Formula LXI), since the concentration of active groups is lower. However, the methylene links are not likely to reduce the crosslinking efficiency of the material which combines, except where the methylene links occur in adjacent

chain positions. Assuming that the methylene and ether links are randomly distributed, the probability of finding adjacent methylene links will increase according to their concentration. Since there are 1.57 ether links to every methylene link in the dibenzyl ether used, the probability of adjacent methylene links occurring will be low. On the assumption of an infinite random chain, the probability that any 2 adjacent groups will both be methylenes is given by

$$P = \left(\frac{0.79}{2.03}\right)^2 = 0.15$$

The reasons for the above conclusions concerning crosslinking efficiency may be better understood by considering the minimum lengths of crosslinks which may be obtained, as follows:

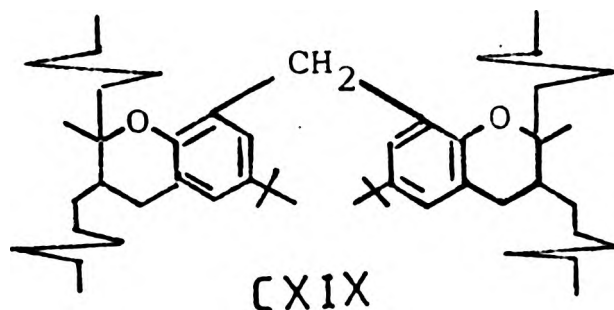
The pure polybenzyl ether may initially form polyether crosslinks of various lengths, but these will shorten as scission of the ether links occurs, ultimately to the monoether:



This cannot react further since the ether link is not now activated by adjacent phenolic OH groups.

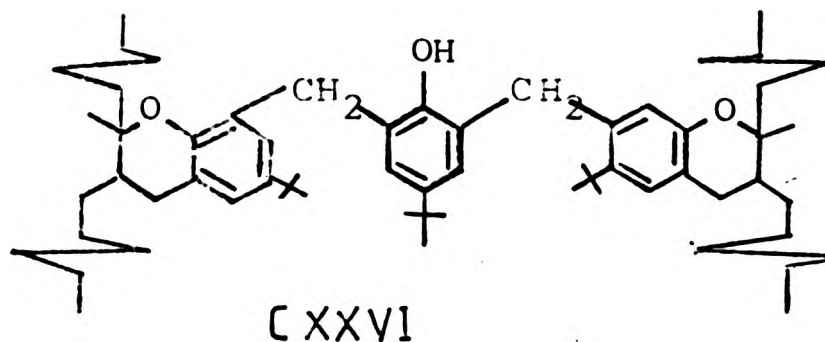
A polybenzyl ether containing some non-adjacent

methylene bridges will react to form the same crosslinks (CXXII) but where the methylene bridges occurs, the ultimate structure will be:



Clearly, this will have no effect on  $E_x$  since there are still 2 phenolic nuclei per crosslink, i.e., no phenolic material has been wasted.

A polybenzyl ether containing adjacent methylene groups will react similarly, but where 2 adjacent methylene groups occur the crosslink structure will be:



Clearly, this involves a loss of efficiency since 3 nuclei are now required to form the crosslink, and there is no obvious mechanism for shortening it. If >2 adjacent methylene links occur the efficiency will clearly reduce further.

The ether derivative of the dimethylol diphenyl methane clearly represents an extension of these considerations.

The 'pure' ether (Formula LXIII) which has alternating ether and methylene links will not suffer any loss of crosslinking efficiency since there are no adjacent methylene links. It will however, be slower to react than the dibenzyl ether since the concentration of active ether groups is lower.

An ether of DMDPM which also has equal numbers of ether and methylene links, but arranged in a more random way, will cause a loss of crosslinking efficiency since adjacent methylene links will now arise. The ether used in this present work will have such a random arrangement since the DMDPM used consists of a mixture of homologues rather than the pure binuclear material (Formula LXII,  $n=1$ ). In addition, the ether used has more methylene than ether links (due to side reactions in the etherification process), as shown by the analysis in Table 10 above. This will clearly further increase the probability of finding adjacent methylene groups and therefore reduce  $E_x$  still further. The probability of any 2 adjacent groups being both methylenes, assuming a random infinite chain, is now  $P=0.52$ . Both of the above products might be expected to react more quickly than the corresponding methylol compounds (discussed in the previous section), since ether links are somewhat more active than methylol in forming quinone methides.

The above discussion refers to rates of reaction of the different products with rubber. It is not to be expected, however, that the rate of reaction will correlate with the

rate of combination, the latter determining the efficiency of combination,  $E_c$ .  $E_c$  will be strongly dependent on the MW of the polyether since, in the initial stages, the scission of only one ether link (to form a quinone methide which then adds to rubber) will cause a pendent chain of the polyether to be attached to the rubber. Clearly, on the average, the length of this pendent chain will increase with the MW of the original polyether. Thus, a polyether product of higher MW is expected to show higher initial  $E_c$  values than a product of lower MW. (In the extreme case, for infinite MW, the scission of only one ether link will cause a pendent chain of infinite MW to be attached to the rubber). A further expectation from these considerations is that although the presence of methylene links reduces the rate of reaction with rubber, it may actually increase  $E_c$  values since the pendent chains attached will be less prone to scission.

The results of the present work will now be examined in the light of these considerations.

### (iii) Results and discussion

Results for the IR/PE/ $ZnCl_2$ , and the IR/PEDPM/ $ZnCl_2$  interactions showing changes of  $E_c$ ,  $E_x$  and  $E_v$  (the two latter derived from measurements of swelling in benzene) as reaction proceeds are summarised in graphical form in Figs. 75, 76 and 77, respectively. A comparison of these results with the

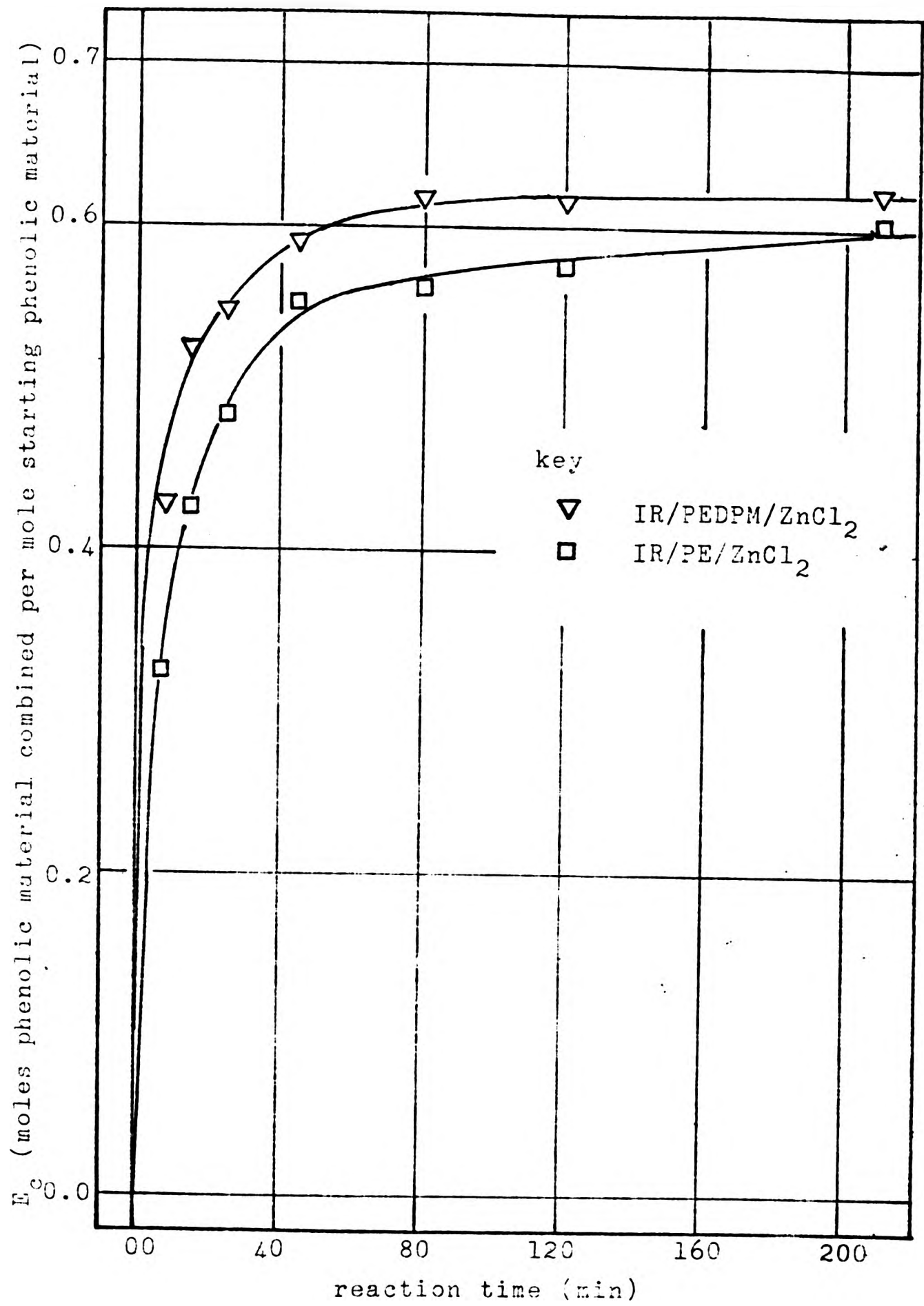


Fig. 75 Kinetics of the efficiency of combination  $E_c$ , for the polyetherification products as calculated from the amount of acetone extract.

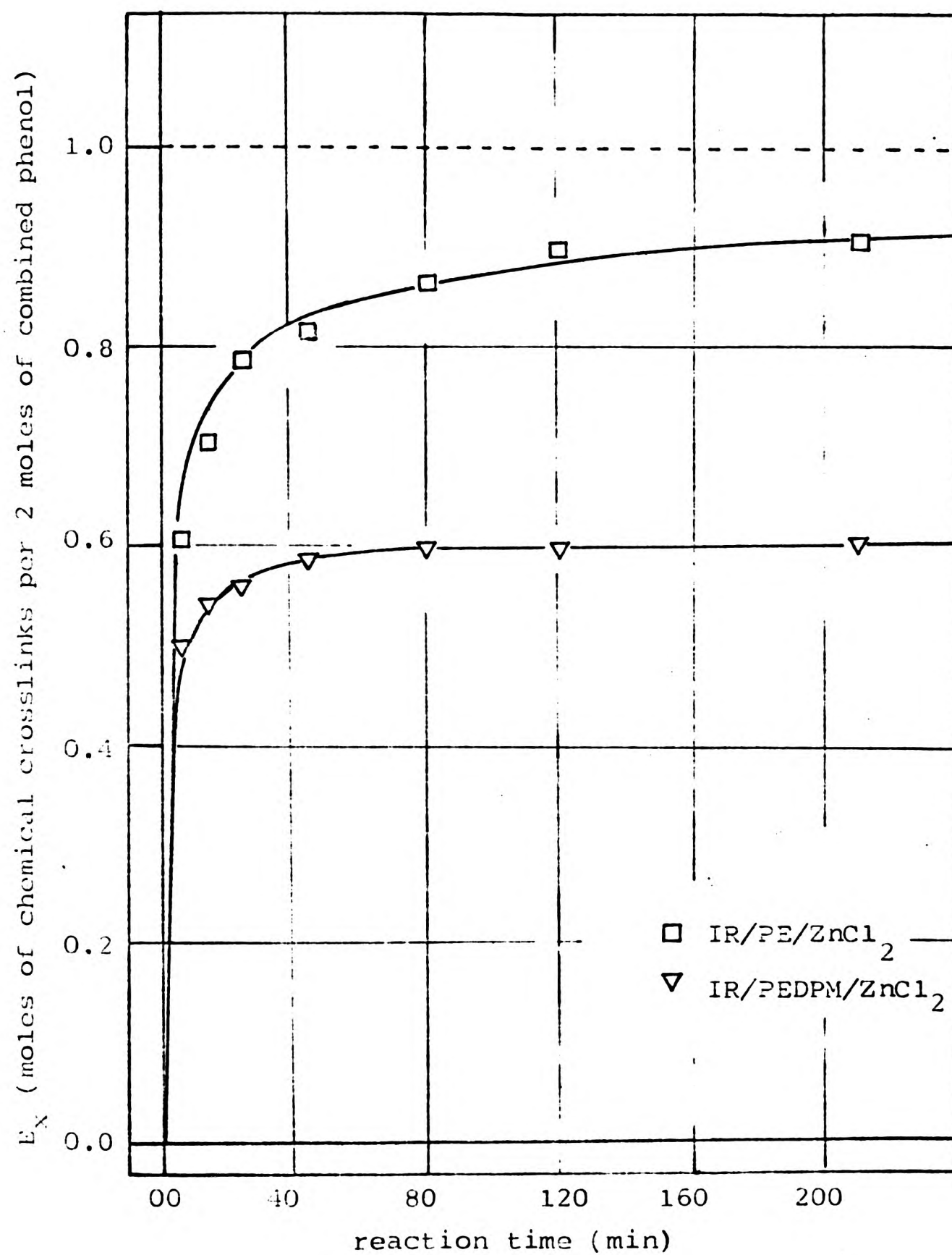


Fig. 76 Kinetics of the efficiency of crosslink formation  $E_x$ , for the polyetherification products as obtained from values derived from swelling in benzene.

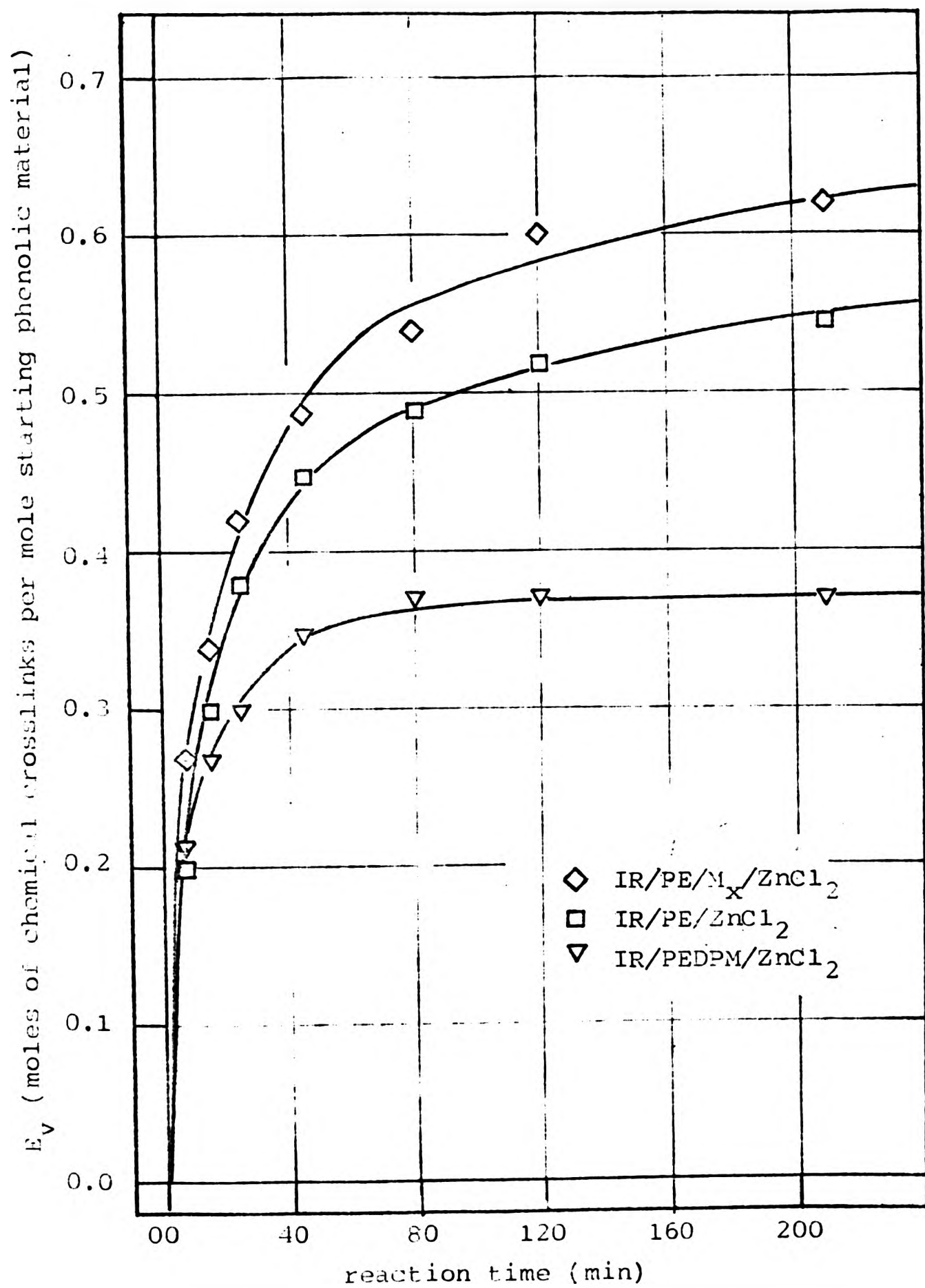


Fig. 77 Kinetics of the vulcanization efficiency,  $E_v$ , for the polyetherification products as obtained from values derived from swelling in benzene.

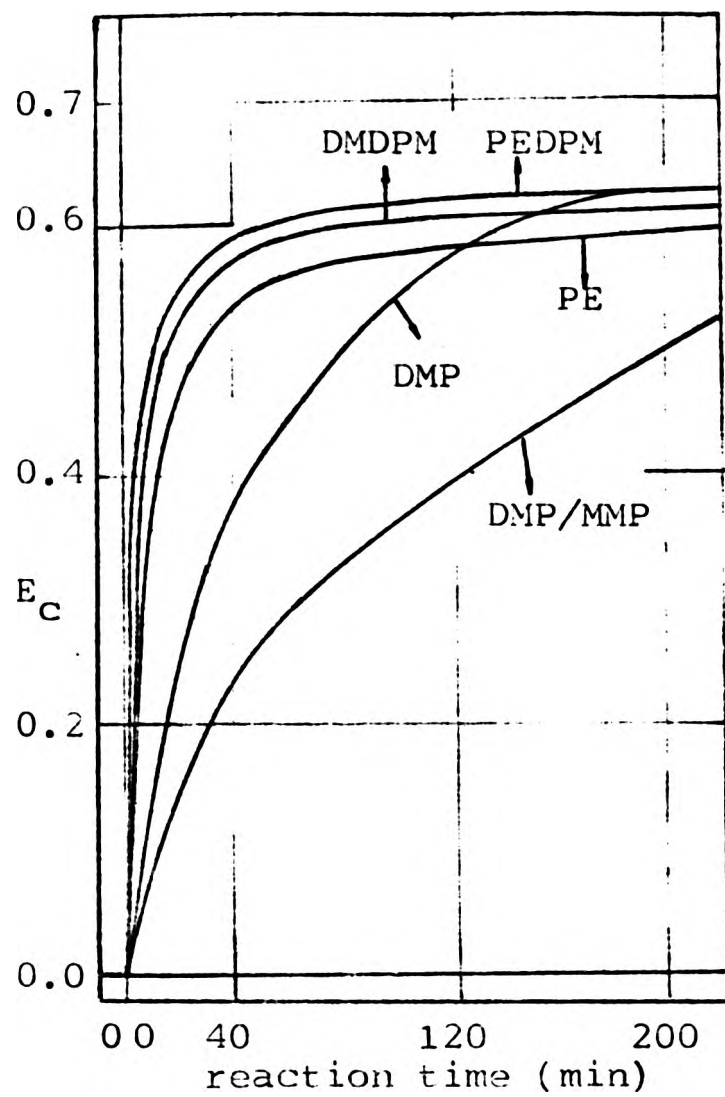
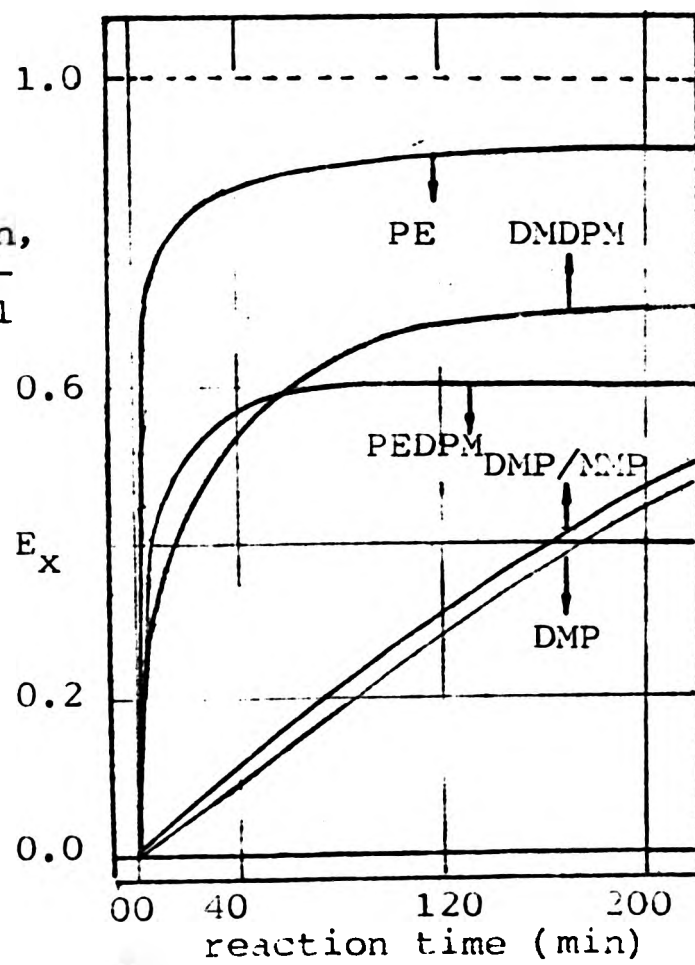


Fig. 78 Comparison of the kinetics of efficiency of combination,  $E_c$ , between the bi-functional methylol derivatives and their polyetherification products.

Fig. 79 Comparison of the kinetics of efficiency of crosslink formation,  $E_x$ , between the bi-functional methylol derivatives and their polyetherification products.



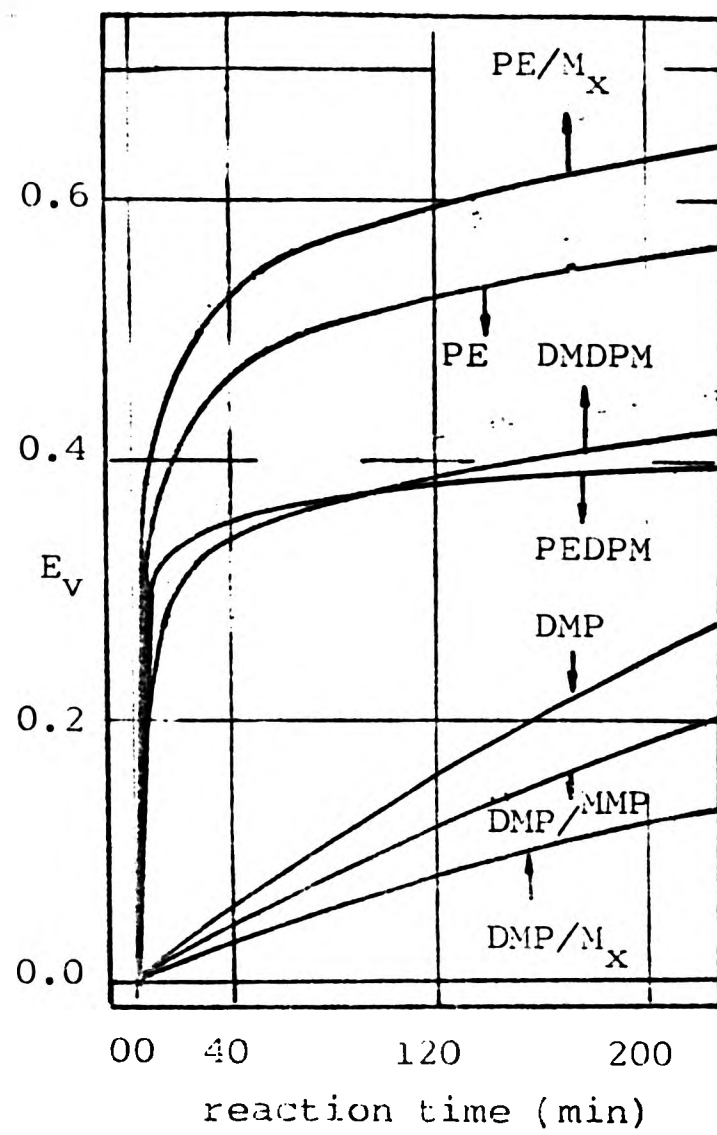


Fig. 80 Comparison of the efficiency of vulcanization,  $E_v$ , between the bifunctional methylol derivatives and their polyetherification products.

corresponding ones for the bifunctional methylol derivatives is illustrated in Figs. 78, 79 and 80 respectively. In addition, some kinetic parameters enabling comparisons to be made have been presented in Tables 7, 8 and 9 (Section ii).

(a) Efficiency of combination,  $E_c$

Examination of Fig. 75, which compares the efficiency of combination,  $E_c$ , of PE with that of PEDPM, clearly shows that the latter combines more rapidly with the rubber. This is particularly marked in the early stages of reaction, but becomes less so towards the end of the time allowed. The figures presented in Table 7 also illustrated the same trend.

The trend is exactly what might be expected in the light of the foregoing discussion. Since the PEDPM has a higher molecular weight (828) than the PE (615), it is expected that each reaction step will cause combination of more material in the former case, despite its (assumed) lower rate of reaction. Additionally, the pendent groups which become attached to the rubber will be shortened more slowly in the PEDPM case, since there are fewer ether links in them to undergo scission. Thus, we have the situation where the lower active ether content of the PEDPM is tending to reduce combination rate, whereas the higher MW and higher methylene content are tending to increase combination rate. The latter factors are clearly the more important generally, but as pendent groups and crosslinks shorten the combination

efficiencies of the 2 reagents become more similar.

Comparing the combination efficiencies of these polyethers with those of the corresponding methylol compounds (e.g., using Table 7 or Fig. 78) reveals that the polyethers combine much more efficiently with the rubber, at least in the early stages of reaction. Again, this is to be expected for 2 reasons: first, the ether links are more reactive generally than the methylol ones, as has been shown in earlier work, and are therefore expected to add more rapidly to the rubber; secondly, for each reaction step the polyethers cause more material to be combined with the rubber, as has been discussed in the previous section. Again, it is expected that the differences become less pronounced as pendent groups and crosslinks shorten in the later reaction stages.

(b) Efficiency of crosslinking,  $E_x$

Examination of the kinetic data presented in Fig. 76 and Table 8 reveals that the rubber-combined product from the polybenzyl ether (PE) is much more efficient in crosslinking than that from the polyether derivative of the dimethylol diphenyl methane (PEDPM). This is in contrast to higher rate combination of the latter, seen in the previous section.

The PE material is, in fact, quite efficient and

efficiencies of the 2 reagents become more similar.

Comparing the combination efficiencies of these polyethers with those of the corresponding methylol compounds (e.g., using Table 7 or Fig. 78) reveals that the polyethers combine much more efficiently with the rubber, at least in the early stages of reaction. Again, this is to be expected for 2 reasons: first, the ether links are more reactive generally than the methylol ones, as has been shown in earlier work, and are therefore expected to add more rapidly to the rubber; secondly, for each reaction step the polyethers cause more material to be combined with the rubber, as has been discussed in the previous section. Again, it is expected that the differences become less pronounced as pendent groups and crosslinks shorten in the later reaction stages.

(b) Efficiency of crosslinking,  $E_x$

Examination of the kinetic data presented in Fig. 76 and Table 8 reveals that the rubber-combined product from the polybenzyl ether (PE) is much more efficient in crosslinking than that from the polyether derivative of the dimethylol diphenyl methane (PEDPM). This is in contrast to higher rate combination of the latter, seen in the previous section.

The PE material is, in fact, quite efficient and

approaches an  $E_x$  value of  $\sim 0.9$  at long times (although the precision of this may be somewhat suspect in view of the uncertainties and assumptions involved in measuring crosslink densities). The PEDPM material is not so efficient, and seems to be levelling off at some 60% of its maximum theoretical crosslinking capacity.

Since the PE reagent contains some methylene links (see analysis, Table 10), it would appear from these results that a negligible number of these are in adjacent chain positions, otherwise a reduced  $E_x$  value would have been observed. From this point of view it would appear that there is no point in purifying the ether further.

The PEDPM reagent, on the other hand, contains 2.6 methylene groups for each ether link (analysis, Table 10), so it is clear that some adjacent methylenes must be present. The  $E_x$  value of 0.6 suggests that each crosslink is associated with  $1/0.30=3.3$  phenolic nuclei, which amounts to a wastage rate of 39.4% of the phenolic material.

Examination of Fig. 79 shows that whereas a very large difference of efficiency exists between the PE and its corresponding methylol compound DMP, there is relatively little difference between PEDPM and its methylol compound, DMDPM. These differences are expected, and are explained on the same grounds as discussed earlier for the methylol compounds, viz. the DMP is effectively monofunctional with

respect to crosslinking, whereas the other reagents are genuinely bifunctional.

A further important feature visible in the comparative curves of Fig. 79 is that the ultimate efficiency is approached much more quickly in the case of the ethers, the curves tending to flatten out after a sharp initial rise. The curves for the methylol compounds, on the other hand, show a much more gradual increase in  $E_x$ , and are still increasing after 210 min. reaction time. This difference in shape is readily noticed in the curves for PEDPM and DMDPM, where a crossover point is seen at about 70 min. reaction time. The difference is attributed to the higher rate of reaction of ether links compared with methylol groups.

(c) Overall efficiency of vulcanization,  $E_v$

Values of the overall efficiency,  $E_v$ , for the PE and PEDPM reagents are compared in Fig. 77, which shows that the vulcanizing efficiency of PE is appreciably higher than that of PEDPM. The overall efficiency  $E_v$  of these materials may be further compared with their corresponding methylol compounds by reference to Fig. 86 and Table 9.

If 35 min. can be taken as a reasonable vulcanization time, it can be seen (Table 9) that the efficiency values at this stage (0.41 for PE, 0.33 for PEDPM) represent 74.5% and 89.2% of the respective final states at 210 min. Such values are appreciably higher than those for the corresponding

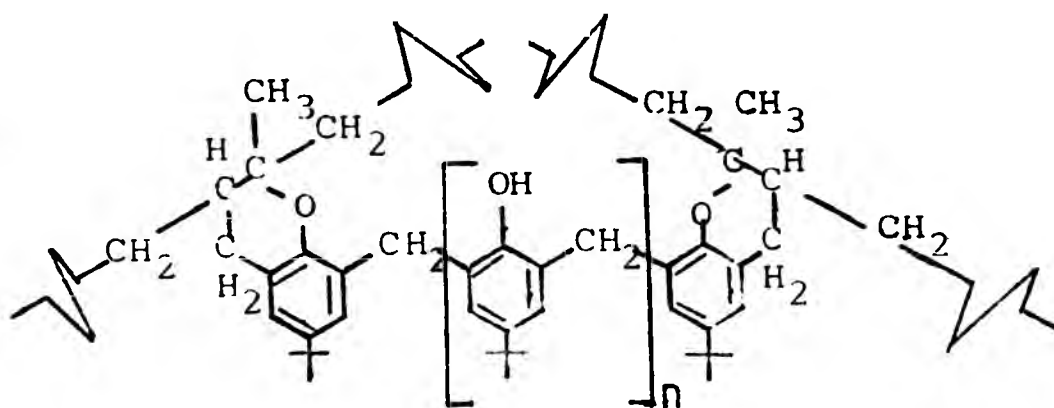
methylol compounds (Table 9), and illustrate the greater suitability of the ethers as vulcanizing agents for conventional curing schedules.

The ethers are clearly, therefore, both faster and more efficient than the methylol compounds as vulcanizing agents. The best polyether appears to be the polybenzyl ether (PE) which gives up to 56% of the theoretical maximum number of crosslinks after a 210 min. cure. It would appear that the other 44% of potential crosslinks is lost in the inability of the ether to combine efficiently with the rubber (Fig. 75). It is presumed that this is caused by side reactions producing trimers, methyl phenols, aldehydes and possibly other by-products as discussed by Fitch,<sup>11</sup> and/or by loss of formaldehyde to produce inactive nuclei. The latter possibility was tested by increasing the partial pressure of formaldehyde during the reaction (e.g., by incorporation of paraformaldehyde,  $M_x$ ). As predicted, the vulcanization efficiency is higher (Fig. 77), but is increased only to 62%. Thus, there is still an important loss of active material, presumably from other side reactions.

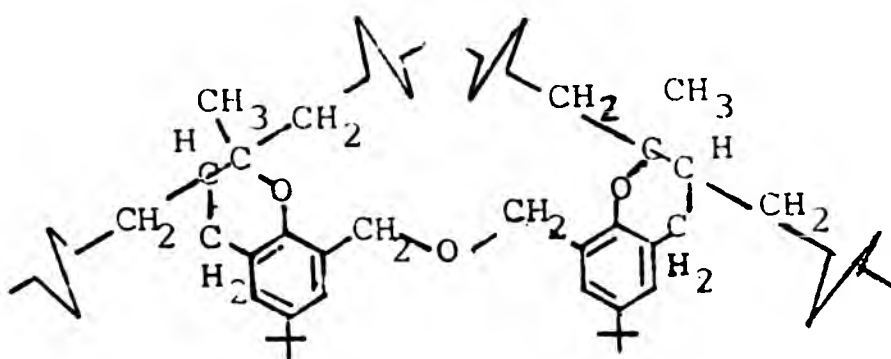
#### (iv) Nature of the crosslink

It will be evident from the foregoing considerations that stable crosslinks of two kinds may be produced during vulcanization with both the methylol compounds and their derived ethers. These crosslinks differ in having either a methylene bridge or a dimethylene ether linkage between

phenolic nuclei and are illustrated in Formulae (XXI) and (CXVII), respectively. Of course, as has already been discussed, the crosslinks may be longer and contain both such linkages in a single crosslink, but then they are likely to be unstable and to breakdown further. However, if we consider only the most efficient cures the crosslinks will be one or other of the simple types XXI ( $n=0$ ) or CXVIII.



XXI



CXVIII

It is emphasised that, whereas crosslinks of the type XXI have been suggested to arise by other workers,<sup>5</sup> the possibility of the ether-containing crosslink CXVIII appears to have been overlooked. The present work, however, shows that it will be the main structure present in the most efficient cures (using the PE reagent). The structure will clearly be stable against scission of the type occurring in

the original PE (Scheme 4), since there are no adjacent phenolic OH groups to enable quinone methides to be formed. The crosslinks are expected to have the same kind of stability as simple dibenzyl ethers, e.g., 1,2-bis(phenyl methyl)ether.

In common with other ethers, dibenzyl ethers are expected to be relatively inert to high temperatures and to chemical oxidising agents. Ethers do show a slow peroxidation on prolonged exposure to air, and dibenzyl ethers might show this to an enhanced degree. However, this does not appear to affect the oxidative stability of vulcanizates.

Ether links between alkyl groups may, however, be split rather easily by a variety of reagents. Thus, acid-catalysed cleavage may be accomplished by heating with HI (e.g., the well-known Zeisel procedure) or HBr, and benzyl ethers are reported to respond particularly readily to such treatment.<sup>128</sup> Alternatively, traces of  $H_2SO_4$  may be sufficient to cause scission of dibenzyl ether in the presence of acetic anhydride.<sup>129</sup> Base-catalysed cleavage of ethers is more difficult, but again benzyl ethers are reported to react more readily. For example, they may be split by treatment with potassium amide in alcohol<sup>130</sup> or by potassium tert-butoxide.<sup>131</sup> Finally, ether links are attacked by Lewis acid halides; treatment with  $BCl_3$  produces alkoxy borons which undergo scission on hydrolysis,<sup>132</sup> and treatment with  $BF_3$  etherate in acetic anhydride is reported to give easy room-temperature cleavage of ethers in the presence of lithium bromide.<sup>133</sup>

Evidence for the presence of ether linkages in the crosslinks may be sought either from their characteristic ir frequencies or by making use of their chemical reactivity. With regard to the former, comparison of an ir spectrum of an extracted vulcanizate with that of the original IR (Fig. 110, Experimental Chapter) shows no definitive difference in the region between 9.0 and 10.0  $\mu\text{m}$ , where dibenzyl ethers are expected to absorb. IR does, however, absorb in this region, and it may well be that an absorption band due to the low concentration of ether linkages in the crosslinks escapes detection because of overlapping. There is some indication in the spectra of an underlying absorption at  $\sim 9.0\mu$ , but it is largely masked by the overlying IR absorptions. The most pronounced difference between the two spectra is the presence in the vulcanizate spectrum of a band at 8.3 $\mu\text{m}$ , believed to be due to a C-O stretching vibration in a chroman structure (Chapter 3, Section 3.6(b)). It seems likely, therefore, that infrared spectroscopy is insufficiently sensitive a method to detect the small concentration of benzyl ether believed to be present. With regard to the chemical reactivity of the crosslinks, a reagent is required which unambiguously causes scission of the ether-type but not the methylene-type crosslinks. This would enable an estimate to be made of the number of each type present, and is analogous to some of the 'chemical probe' studies previously used with sulphur vulcanizates.<sup>134-138</sup> Attempts were made in the present study to demonstrate the presence of ether linkages by treatment of the IR/PE/ZnCl<sub>2</sub>

interaction product with some of the reagents mentioned above. It was hoped that, by measuring the crosslink density before and after the ether-scission treatment, an estimate of the proportion of ether to methylene links could be obtained. However, it was found that treatment with dilute acetic anhydride solutions of either sulphuric acid or  $\text{BF}_3$  etherate (without lithium chloride) caused severe blackening, hardening and eventual disintegration of the rubber. Clearly, the rubber molecule itself is suffering attack.  $\text{BF}_3$  etherate in the presence of lithium chloride produced no blackening or disintegration, but the crosslink density was unchanged by the treatment, indicating no scission of ether linkages.

It is clear from these observations that the development of a suitable method of treatment will require a lengthy and probably difficult study. For this reason it was not pursued further in this work, but it could well form an important basis for a future study.

Although such ether-containing crosslinks must be present in vulcanizates prepared from the laboratory-prepared PE reagent, it is still not certain whether they are present in vulcanizates prepared from a commercial reagent. The difficulty is that commercial condensates are merely described as 'resin based on p-tert-butyl phenol' and no details of structure are disclosed. For this reason it was decided to characterise a typical commercial resin (Bakelite

Resin CK 1634) intended for rubber vulcanization and to compare its vulcanization activity with the laboratory-prepared products described above.

(c) Vulcanization with the commercial resin

(i) Analysis

The commercial resin, Bakelite CK 1634, is described by the manufacturer as being 'based on p-alkyl phenol' (although it is understood to be p-tert-butyl phenol), with 'a softening point of 96° and soluble in ketones, esters and aromatic hydrocarbons'. No information is available concerning its analysis, although it is said to be a highly-reactive resin.

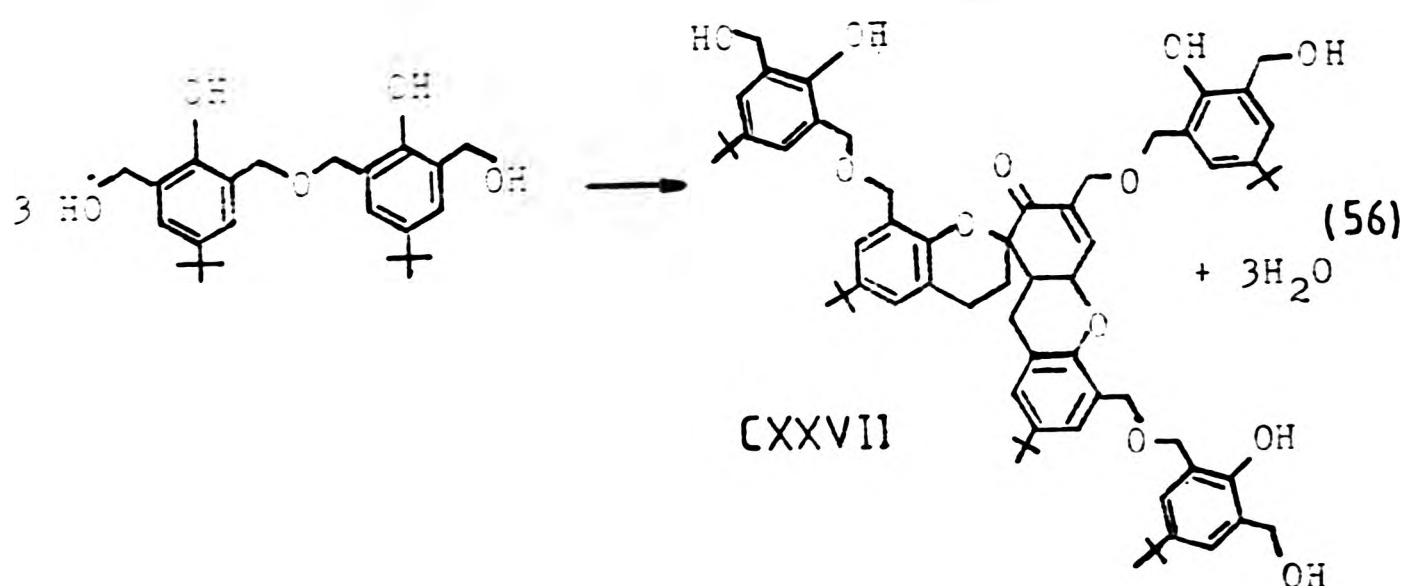
Characterisation by the acetylation/nmr method used in this present study showed the resin to contain a relatively high concentration of dibenzyl ether, with moderate amounts of methylene bridge groups and methylol groups. In this analysis it is reasonably close to the laboratory-prepared PE product, the characteristics of each being compared in Table 11.

Table 11: Comparison of characteristics of PE and commercial resin

	$F_{(ArCH_2OH)}$	$F_{((ArCH_2)_2O)}$	$F_{(Ar_2CH_2)}$	$F_{total}$	MW(gpc)
PE	0.05	1.24	0.79	2.08	615
Commercial resin	0.41	1.16	0.58	2.15	599

The main difference between the two products is the higher methylol content of the commercial product. This, together with its lower MW, indicates that the commercial resin has been less completely etherified. A further difference between these two materials is the presence in the ir spectrum of the commercial resin of an absorption band at  $6\mu\text{m}$ , of moderate intensity. This band remains after shaking the resin with aqueous  $\text{NaCO}_3$  solution, which suggests that it is not attributable to acetic acid present in the resin as impurity. This, and the fact that vulcanization results for the commercial resin (discussed below) were similar to those for the polybenzyl ether, suggested that a similar material to the commercial resin might be obtained from condensation of the methylol phenol. Since the uncatalysed condensation of the latter material needed long reaction times and, therefore, is presumably an impracticable process for industry, it was decided to undertake a series of catalysed condensation of the dimethylol phenol. For these, the dimethylol phenol was dissolved in toluene or benzene, as appropriate, in the same proportions that were used in the preparation of the polybenzyl ether (described in the Experimental Chapter). The catalyst  $\text{SnCl}_2 \cdot 2\text{H}_2\text{O}$  was added (1% based on dimethylol phenol) and the mixture was refluxed with a Dean and Stark head for various times. Infrared spectra showing the progress of reaction, together with those for the uncatalysed process, are presented in Figs. 101 to 104 (Experimental Chapter). The spectra for the catalysed interactions in toluene (Fig. 101) show a rapid reduction in the intensity of the band at  $9.9\mu\text{m}$ , attributable

to methylol groups. This change was accompanied by a fast development of a strong band at  $9.4\mu\text{m}$ , attributable to dibenzyl ether groups, and a new band similar to that in the commercial resin at  $6\mu\text{m}$ . After 5 min. of reaction time the band at  $9.9\mu\text{m}$  has completely gone and the band at  $10.4\mu\text{m}$  reached its maximum intensity. Further increase of reaction time is accompanied by an increase of the band at  $6\mu\text{m}$ . This band is most likely to be due to a carbonyl group of low bond order, and is possibly attributable to a trimer of the type shown in Formula CXXVII. The ir spectrum of the simpler trimer (VI) reported by Fitch<sup>11</sup> is presented in the Experimental Chapter Fig. 106, and shows a similar  $6\mu\text{m}$  absorption band. These structures might arise from the  $\text{SnCl}_2 \cdot 2\text{H}_2\text{O}$ -catalysed decomposition of the polybenzyl ether as it is formed (56). The catalysed condensation in benzene (Fig. 102) yields the same results as those described above for toluene, but at lower rate because of the lower reflux temperature.



Comparison of the ir spectra of the catalysed condensate (Figs. 101 and 102) with those of the uncatalysed one

(Fig. 104) shows that the main difference is the absence of the 6.0 $\mu$ m band in the uncatalysed case. This presumably means that trimer formation (or possibly other side reactions) is not occurring in the uncatalysed condition, and the purity of the ether is therefore higher.

The ir spectrum of the commercial resin (Fig. 105) shows the same general characteristics as those for the catalysed condensation of the dimethylol phenol. Indeed, the spectrum seems identical to that for the catalysed condensation of dimethylol phenol in benzene after 70 min. of reaction time. This suggests that the commercial resin has probably been made by a catalysed process, and has therefore suffered a little undesirable decomposition.

The ir analysis above does not give information about formation of methylene bridges in the catalysed condensation of dimethylol phenol which, as has been pointed out, would have a pronounced effect on the efficiency of vulcanization. However, an nmr analysis after acetylation of the various catalysed condensation products could be carried out to establish the structures more precisely. In the present study this has not been done due to the lengthy nature of the analysis. Such intensive characterisation might, however, be important in any future work designed to prepare resins of maximum vulcanization efficiency and commercial practicability.

(ii) Results and discussion

Results for the IR/CR/ZnCl<sub>2</sub> interaction showing changes of E<sub>C</sub>, E<sub>X</sub> and E<sub>V</sub> (the two latter derived from measurements of swelling in benzene) as reaction proceeds are summarised in graphical form in Figs. 81, 82 and 83 respectively. Comparison of the above results with the corresponding ones for the methylol derivatives and their polyetherification products are presented in Figs. 84, 85 and 86, respectively. Some kinetic data for the commercial resin are also presented in Tables 7, 8 and 9 for comparison against the laboratory-prepared materials.

Figs. 84, 85 and 86 show that, not only is the commercial resin chemically similar to the PE reagent, its vulcanizing power is also quite similar. Thus, Fig. 86 shows the 2 materials to be almost indistinguishable in their overall vulcanizing efficiency. However, inspection of Figs. 84 and 85 reveals that this similarity is somewhat fortuitous, and depends upon the balance of faster combination with the rubber (Fig. 84) and lower crosslinking efficiency (Fig. 85) of the commercial resin compared with the laboratory-prepared one. The most significant curves are probably those of Fig. 85 which show lower crosslinking efficiency by the commercial resin as it combines with the rubber. This is probably to be expected in view of the higher methylol content of the commercial resin, which can allow side reactions to reduce efficiency as has already been

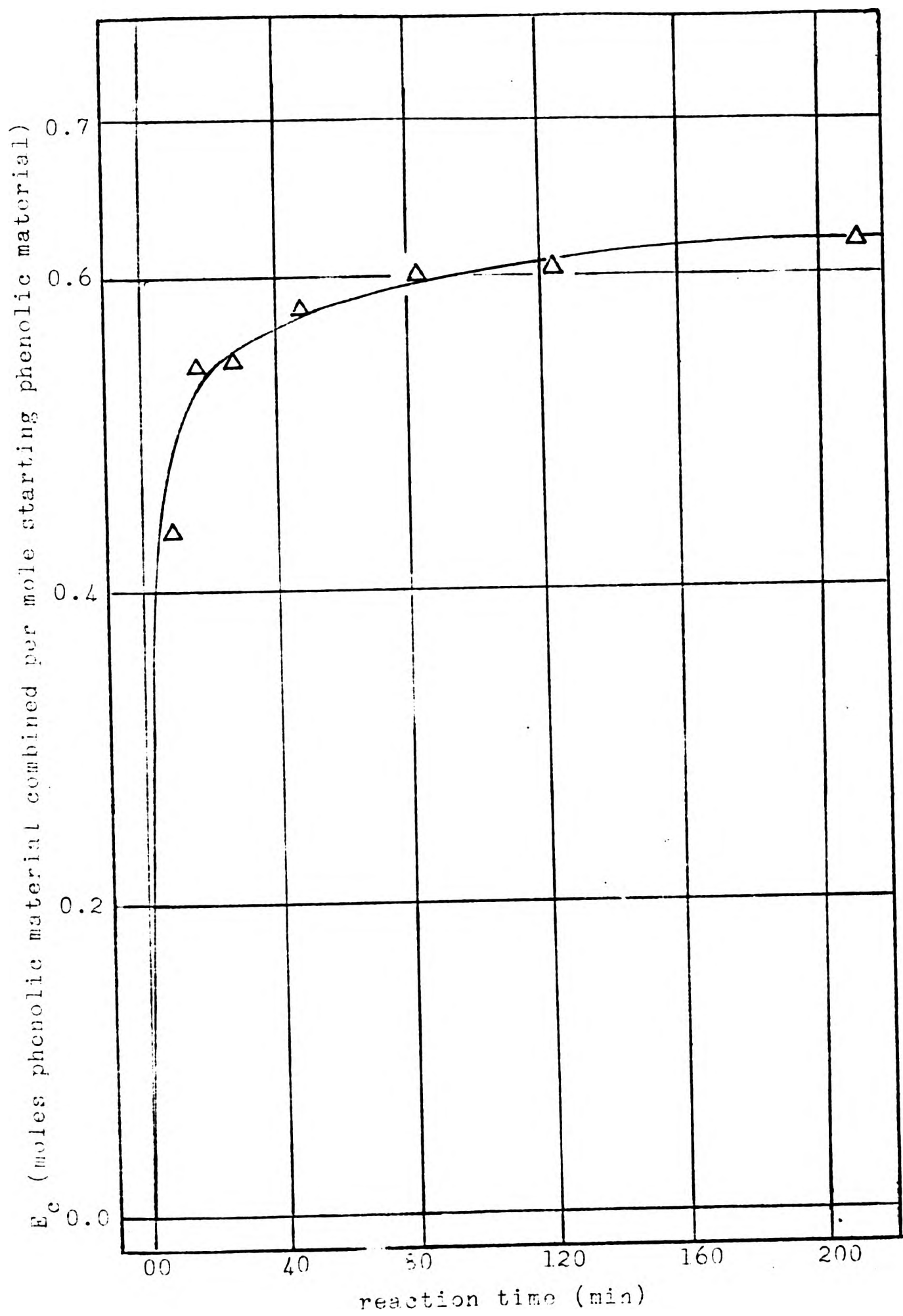


Fig. 81 Kinetics of the efficiency of combination,  $E_c$ , for the commercial resin (CR) as calculated from amount of acetone extract.

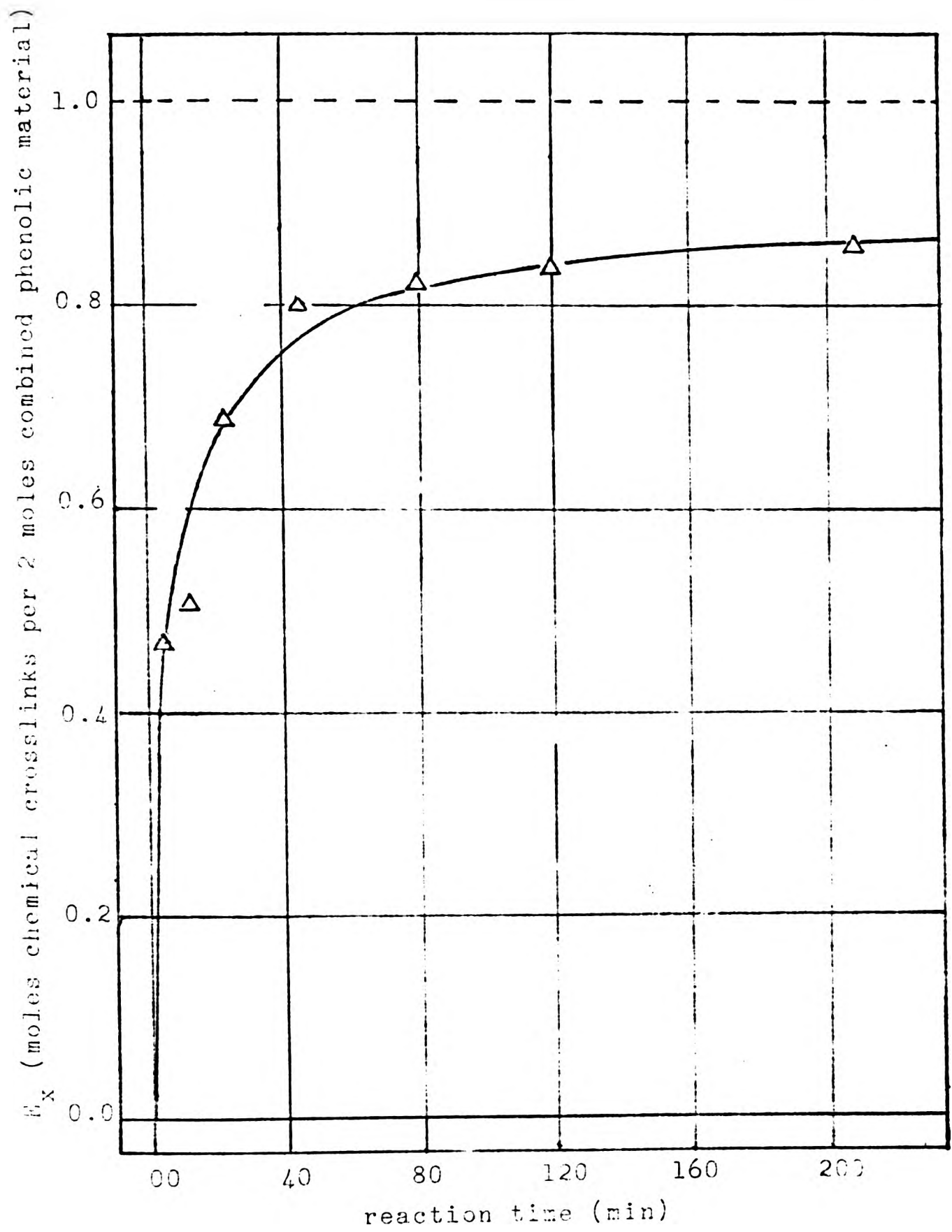


Fig. 82 Kinetics of the efficiency of crosslink formation,  $E_x$ , for the commercial resin (CR) as obtained from values derived from swelling in benzene.

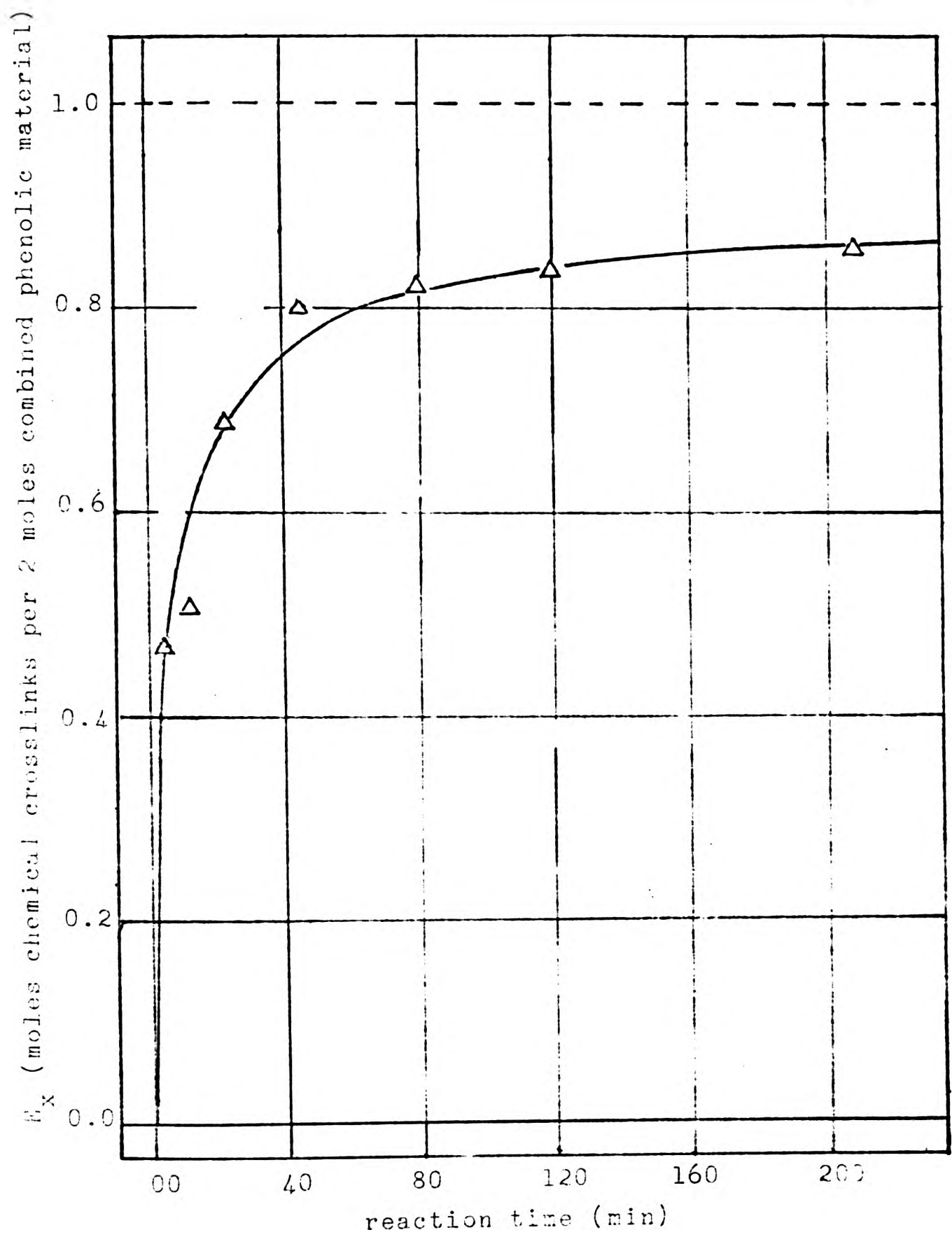


Fig. 82 Kinetics of the efficiency of crosslink formation,  $E_x$ , for the commercial resin (CR) as obtained from values derived from swelling in benzene.

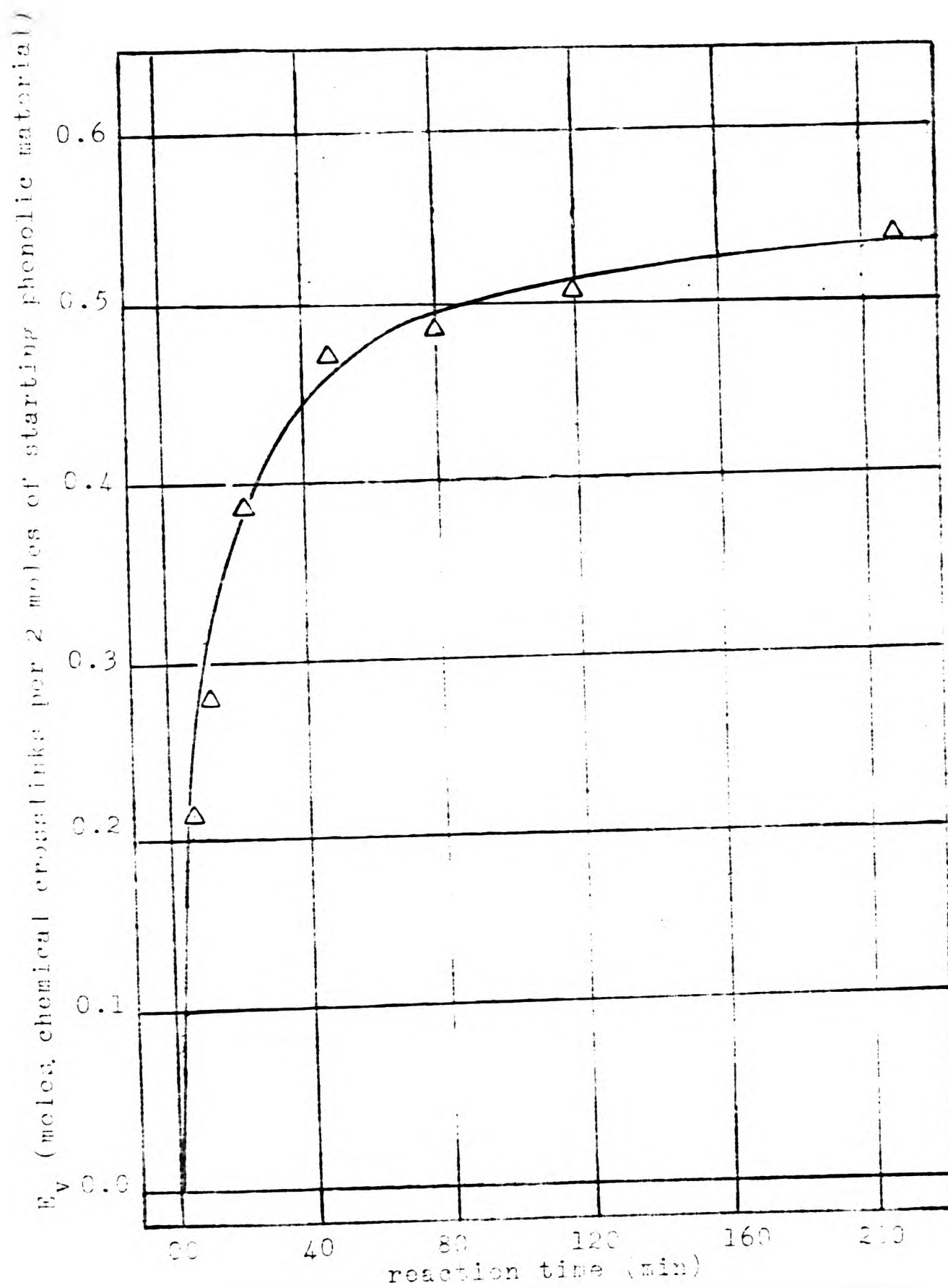


Fig. 83 Kinetics of the vulcanization efficiency,  $E_v$ , for the commercial resin (CP) as obtained from values derived from swelling in benzene.

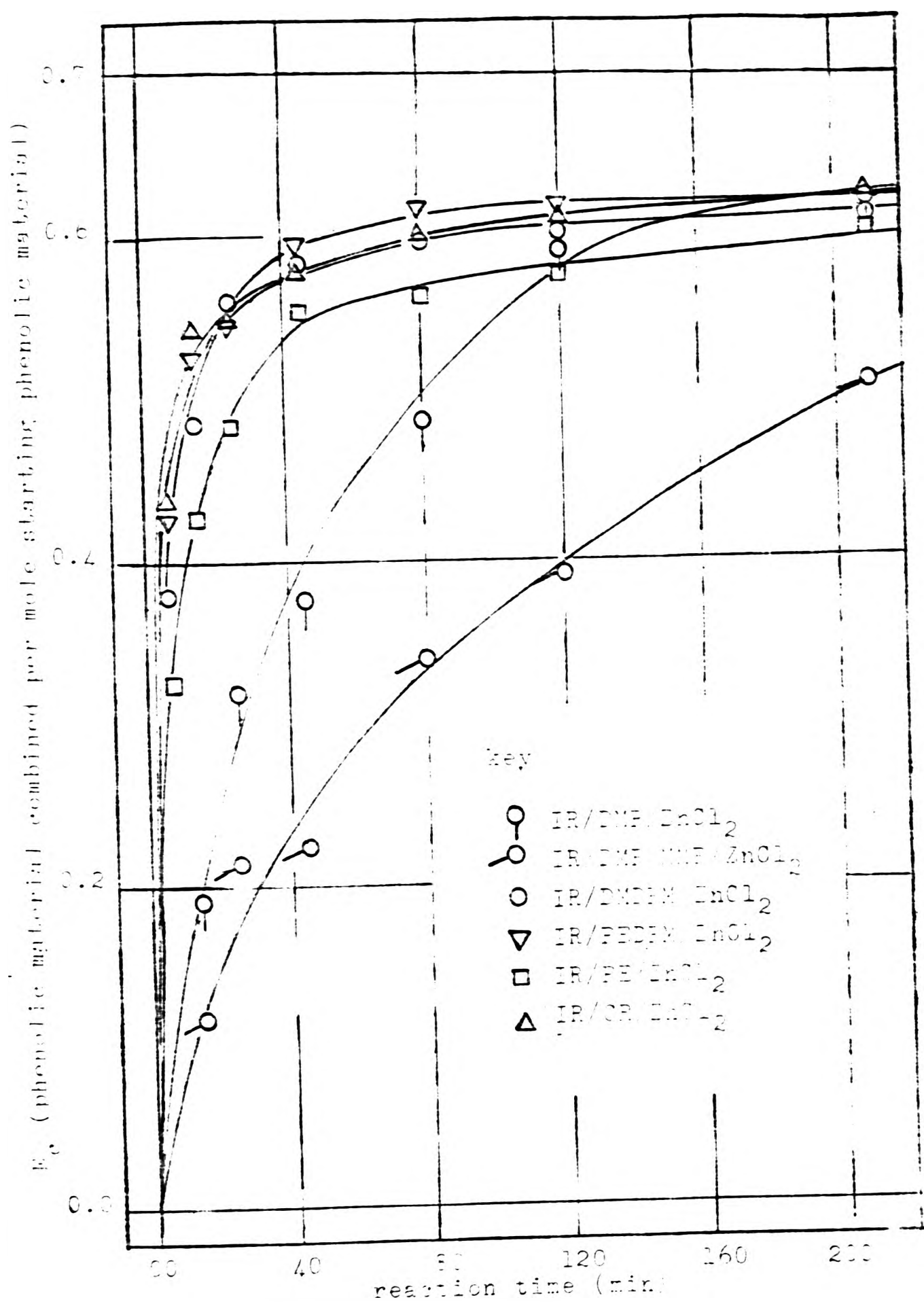


Fig. 8-1 Comparison of the kinetics of efficiency of combination,  $E_c$ , for the commercial resin, the methylol derivatives and their polyetherification products.

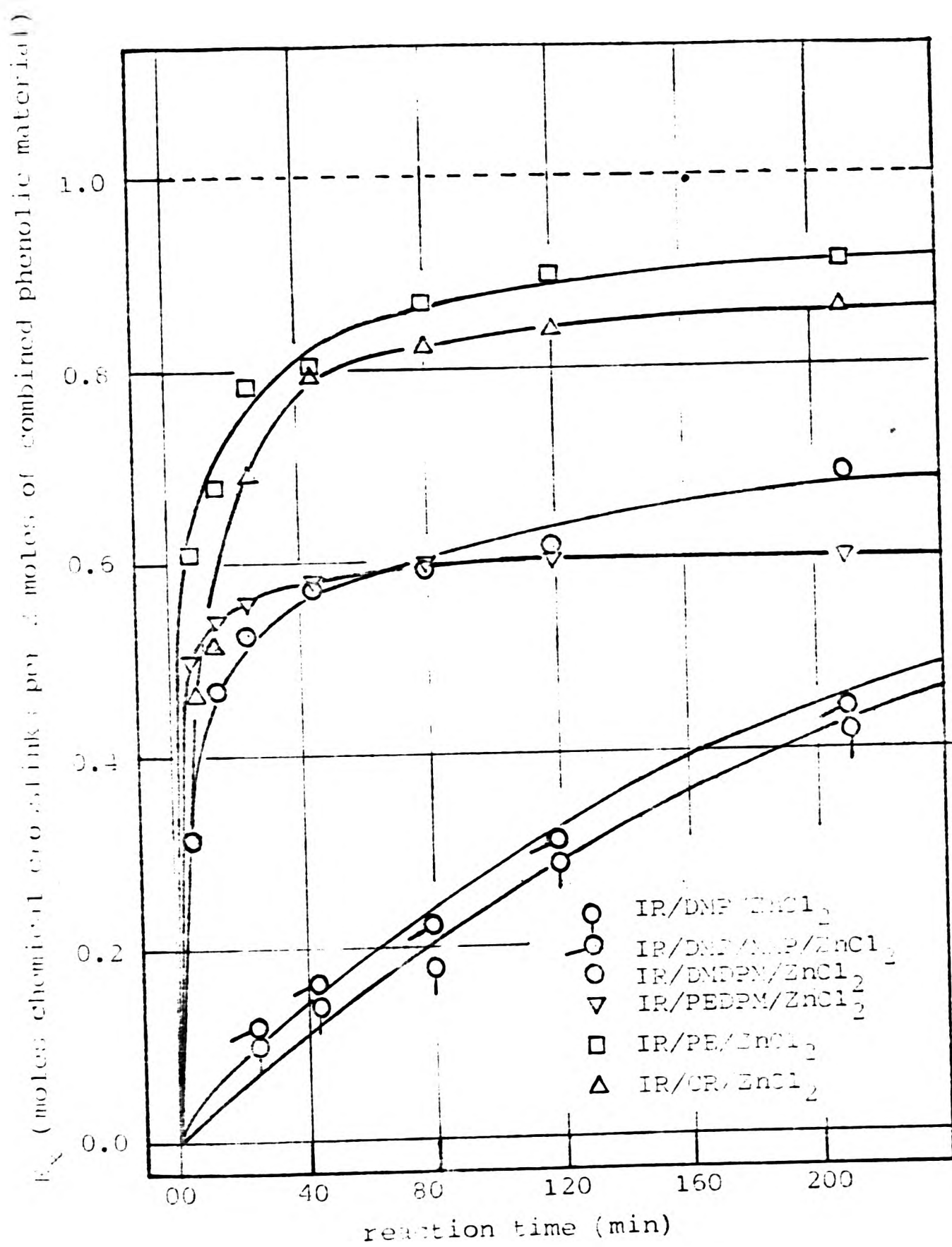


Fig. 85 Comparison of the kinetics of the efficiency of crosslink formation,  $E_x$ , for the commercial resin, the methylol derivatives and their polyetherification products.

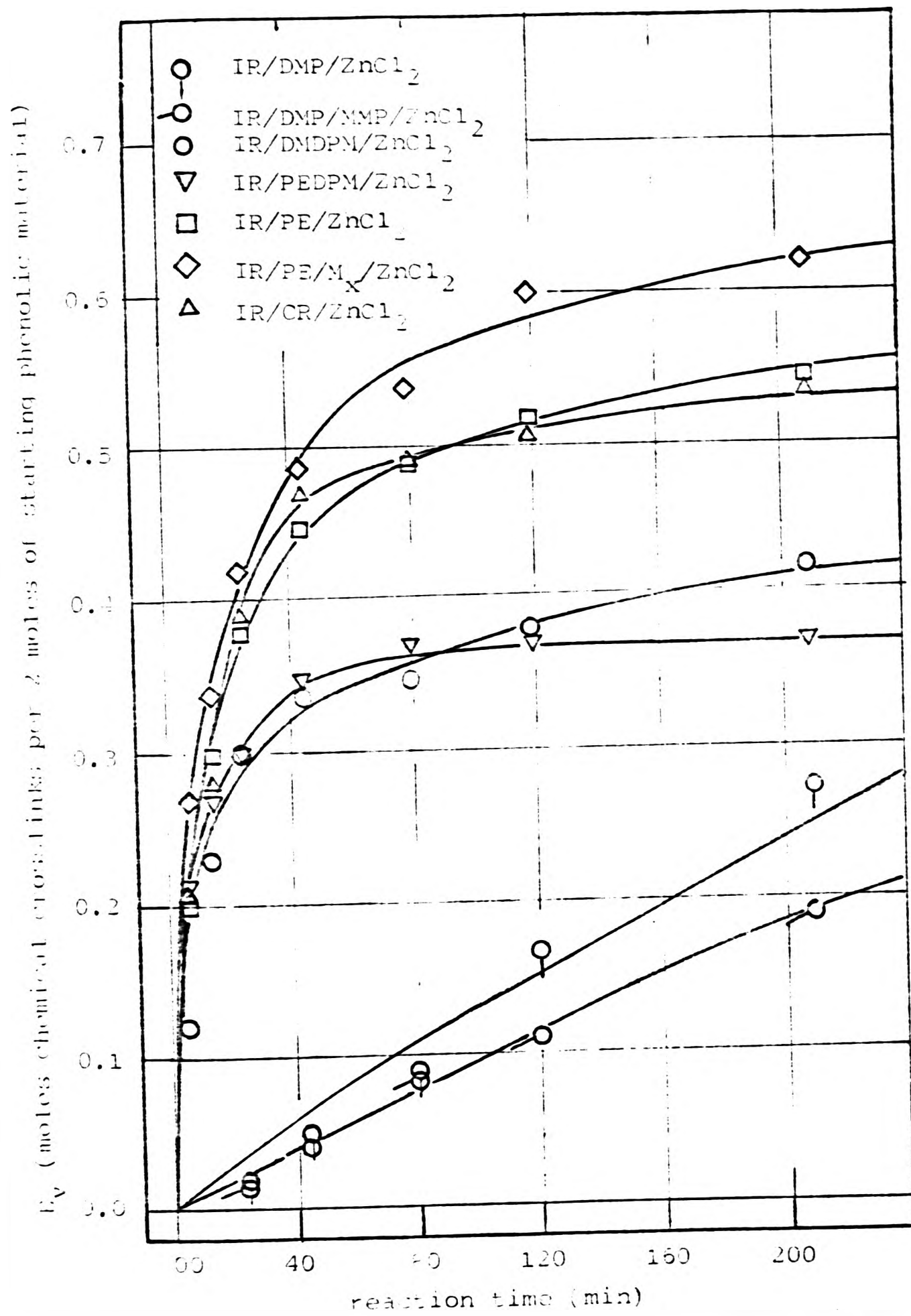


Fig. 86 Comparison of the kinetics of the vulcanization efficiency,  $E_v$ , for the commercial resin, the methylol derivatives and their polyetherification products.

discussed for the resins of high methylol content. The combination efficiency curves of Fig. 84 are probably less significant since they depend strongly on rate of reaction. It is quite possible that the commercial resin contains traces of catalyst, remaining after its manufacture, which can cause the increased rate of combination. An alternative possible explanation for the higher rate of combination in the commercial resin is that the presence of trimer will increase the NW, and therefore the amount combined in a single reaction step. This would also reduce the crosslinking efficiency, as has been observed, since there will now be  $1\frac{1}{2}$  crosslinks per 6 moles of phenol, at each trimer position. Despite these differences, however, it is clear that the laboratory PE resin and the commercial resin are quite similar in both structure and performance.

#### (b) Technological considerations

##### (i) Requirements for high efficiency

The requirements for high efficiency of crosslinking in vulcanization with p/f condensates, based on this work, is best considered under the two headings; (ii) structural requirements of the vulcanizing condensate and (iii) presence of ancillary materials.

##### (ii) Structural requirements of vulcanizing condensate

The minimum structural requirements of a condensate is

a true functionality of two in respect of chroman formation, i.e., chroman formation by the 1st group should leave the second group still active. The active groups studied in this present project are methylol and dimethylene ether links, and the structural requirement for high efficiency is therefore the smallest possible molecule containing two, independently-active, such groups.

The dimethylene ether linkages appear to be more important in raising efficiency than the methylol groups. The latter may well be transformed into the former by polyetherification during the reaction, but this is accompanied by methylene bridge formation which decreases the 'active' content and therefore the efficiency. However, a practical way of suppressing such side reaction might eliminate this disadvantage. It is difficult to see how the methylol compound itself can be modified so as to stabilise it, but the addition of ancillary materials might offer possibilities, as discussed below.

(iii) Addition of ancillary materials

The addition of further amounts of catalyst will clearly increase the amount of crosslinking achieved in a certain time, merely by speeding up the reactions. This will exert its effect primarily via the  $E_c$  value, in increasing the rate of combination. It is unlikely to change significantly the  $E_x$  values, i.e., it will probably not

reduce the extent of side reactions, and may even increase them. Thus, whilst the addition of more catalyst might be beneficial in increasing the rate of vulcanization, it will not increase the ultimate efficiency of cures obtained after long times, when the reactions are substantially complete.

The addition of a source of formaldehyde is, however, expected to influence the ultimate efficiency, not through a rate effect but through a mass action effect in suppressing side reactions (this was discussed in Section a). Thus, whilst the  $E_c$  values should be unaffected, the  $E_x$  and hence the  $E_v$  values should be increased, even after prolonged reaction times. In the present study, the addition of polymethanal (paraformaldehyde) has been clearly shown to improve the efficiency  $E_v$ .

From Scheme 4 it can be seen that the increase in efficiency by addition of methanal might be expected to be more pronounced in those cases where the p/f condensate has a high content of methylol groups. Further, it is likely that paraformaldehyde may not be the best source of methanal since, as was discussed earlier, evolution of the methanal at the temperature of vulcanization is probably too fast. However, retention of the methanal in the mould by pressure could be occurring so as to mitigate this high volatility. The present work gives no quantitative information about this, but there was little indication of gas evolution or foaming when the mould was opened, although there was a powerful odour of formaldehyde.

Since chroman (and hence crosslink) formation involves loss of water, it might be anticipated that the presence of a desiccant (e.g., CaO) might improve crosslinking efficiency by a mass action effect. However, methylene bridge formation (Scheme 4) also involves loss of water and might therefore be promoted.

Practical vulcanizates will contain resins, oils and fillers (e.g., clays) which can show reactivities, catalytic action, water evolution, etc. to varying degrees and it is clear that somewhat complicated effects on curing rates and efficiencies may be expected. A study of such practical technological considerations might well form a logical extension to this present study.

(iv) Comparison of rates and efficiencies with conventional systems

A typical plot of chemical crosslinks as a function of cure time for MET-accelerated sulphur vulcanization of NR<sup>126</sup> at 140°C has been re-drawn in Fig. 87, for comparison against a similar plot for the polyether (PE) used in this present work. Corresponding plots for all of the other phenolic materials were presented in the Section 4.2 (Figs. 65-70). Although the comparison shown in Fig. 87 is rather crude, in view of the differences in rubber, curing system and temperature, it does show that a comparable level of cure may be obtained by sulphur/accelerator and p/f curing systems.

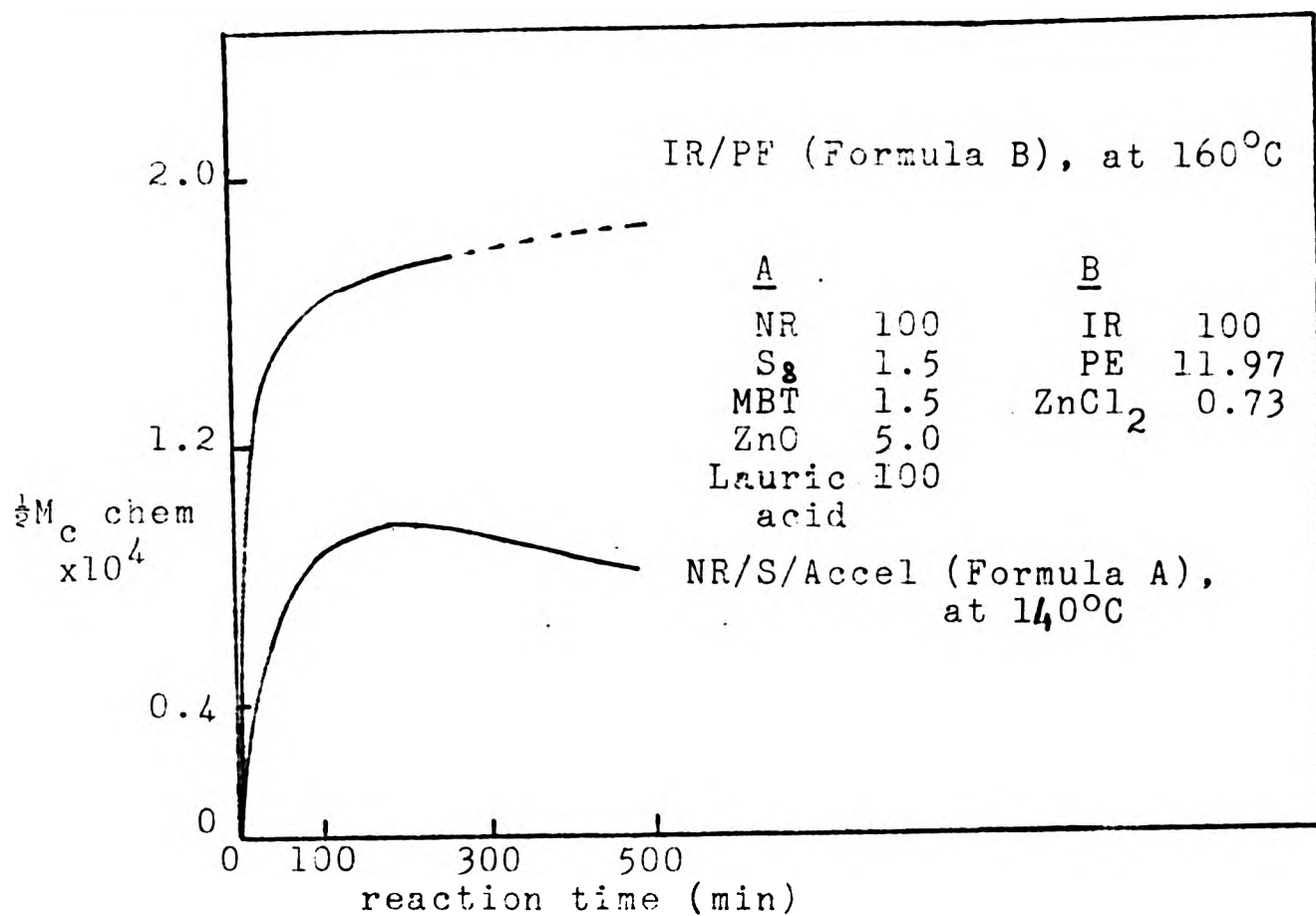


Fig. 87 Comparison of the degree of chemical crosslinking as function of cure time for MBT-accelerated NR-sulphur vulcanizate and ZnCl<sub>2</sub>-accelerate IR-resin vulcanizate.

Of course, the number of crosslinks may be changed merely by adjustment of the concentrations of curatives, and the rates may be changed by altering catalyst or accelerator levels, or cure temperature. The only feature of importance shown by Fig. 87 is the presence of a maximum in the S/accelerator curve, caused by 'reversion', or thermal destruction of crosslinks. The p/f cure shows no such instability and the number of crosslinks is still, in fact, increasing after 200 min., despite the higher temperature used. This reflects the higher thermal stability of p/f resin vulcanizates, discussed further below.

IR rather than NR has been used in this present work, for reasons discussed earlier. It is very likely that NR will react in a very similar way, but at a lower rate since it contains natural amines and other materials which can destroy the Lewis acid catalyst used. In fact, a concurrent study<sup>139</sup> shows that the cure rate for NR/CR/ZnCl<sub>2</sub> is about one-third of that for IR/CR/ZnCl<sub>2</sub>, resin and catalyst concentrations being the same. Of course, this is not technologically significant since a further catalyst addition in the NR case will no doubt restore a reasonable cure time.

The conclusion which may be reached from this comparison is that the same levels and rates of cures as in typical NR/S systems may be obtained using an IR/PE or NR/PE system. The main possible disadvantage of this latter method would appear to be the larger amount of curative required. However, further advantages or disadvantages might arise in respect of cure safety or vulcanizate stability, as discussed below.

(v) Cure safety

A indication of processing safety for any vulcanization system may be obtained by the time to cure initiation or scorch time. A scorch time between 3 and 8 min. may be considered adequate in conventional cures of, say, 20-30 min. at 140°C. Rheometer cure curves for the IR/CR/ZnCl<sub>2</sub> and NR/CR/ZnCl<sub>2</sub> interactions for the same mix composition (i.e., IR or NR 11.93 phr and ZnCl<sub>2</sub> 0.73 phr) show values of 0.5 and 4 min. of scorch time respectively.<sup>139</sup> Thus, whereas

the vulcanization of IR by p/f condensates might be regarded as scorchy at the rates used, that for NR might be considered a safe process. However, this is only a rate effect and there is no indication of a 'delayed-action' effect as is observed in CBS cures.

(vi) Properties of vulcanizates

The use of p/f condensates as curing agents is particularly important in butyl rubber, where it enhances the inherent high resistance to thermal degradation. Such vulcanizates may be used in applications requiring continuous service at 170 to 200°C. Unlike sulphur vulcanizates, they show no tendency towards devulcanization, ('reversion' of cure) and their exceptional thermal resistance is utilised in articles such as curing blankets, seals, gaskets, tapes, many mechanical goods and in tyre curing 'bags'. It has been reported<sup>140</sup> that by curing of NR with p/f condensates at temperatures up to 240°C the vulcanizates maintained a good surface finish with satisfactory strength and hardness, whereas 220°C was the upper limit for an NR-sulphur system. This thermal stability, as well as improved oxidation resistance, and chemical inertness of the p/f vulcanizates compared with other types of crosslink is explained by the polymer chains bound via linkages which involve the heat stable C-C and C-O linkages.

Comparison of sulphur-, dicumyl peroxide-, and resin-

cured systems in the gum, black-filled, and silica-filled state has shown that reinforced p/f vulcanizates have, on average, similar tensile strengths to the peroxide vulcanizates, but somewhat lower than the sulphur-cured systems. Typical values for p/f vulcanizates have been reported as 1.5 to 8 MNm<sup>-2</sup> which are more typical of that given by non-crystallizing rubbers. The higher strength of sulphur-vulcanizates compared with peroxide and other systems is well-known, and is usually attributed to the lability of the crosslink in sulphur vulcanizates, which allows the dissipation of stress concentrations within the rubber.

Compression set for the p/f vulcanizates at 70°C has been reported<sup>141</sup> to be very low and the hysteresis of samples stretched to 75% of their breaking elongation was lower than that of either sulphur- or peroxide-cured rubbers. The black-filled p/f vulcanizates accelerated by ZnCl<sub>2</sub> or SnCl<sub>2</sub>·2H<sub>2</sub>O have been reported<sup>142</sup> to exhibit lower heat build-up than those of ordinary sulphur systems.

In general, therefore, it may be said that p/f-cured vulcanizates possess properties comparable with those obtained from other systems, and in some ways, especially in heat resistance, they are better. Since heat-resistance is one of the important requirements in many of the newer technological applications, it is very probable that the use of p/f resins as curatives will increase. It is hoped therefore, that the results of this present work may be put to good use in such future developments.

## 5. CONCLUSIONS

1. The results of this present work, taken as a whole clearly vindicate the 'chroman' theory rather than the 'methylene bridge' theory for the interaction of isoprene rubber with phenol-formaldehyde condensates based on p-tert.butyl phenol.
2. The rate of interaction is greatly increased by the presence of small amounts of Lewis acid catalysts, with activity increasing in the order  $\text{ZnCl}_2 < \text{SnCl}_2 < \text{SnCl}_2 \cdot 2\text{H}_2\text{O}$  in the present study.
3. Cationically-induced isomerization of IR occurs on heating at  $160^\circ\text{C}$  in the presence of  $\text{SnCl}_2 \cdot 2\text{H}_2\text{O}$ , resulting in cis/trans interconversions, double-bond shifts, cyclisation and crosslinking. The changes occur to a less pronounced extent when phenolic condensates are also present. Anhydrous  $\text{SnCl}_2$  causes the same changes to occur but much more slowly (possibly due to a small extent of hydration), but isomerisation is undetectable in the presence of phenolic material. Anhydrous  $\text{ZnCl}_2$  produces no detectable isomerisation irrespective of whether or not phenolic material is present.
4. Adduct formation between a monomethylol compound (the methylolphenol) or its derived ether (the dibenzyl ether) and isoprene rubber is not quantitative owing to the occurrence of side reactions which produce inactive

## 5. CONCLUSIONS

1. The results of this present work, taken as a whole clearly vindicate the 'chroman' theory rather than the 'methylene bridge' theory for the interaction of isoprene rubber with phenol-formaldehyde condensates based on p-tert.butyl phenol.
2. The rate of interaction is greatly increased by the presence of small amounts of Lewis acid catalysts, with activity increasing in the order  $\text{ZnCl}_2 < \text{SnCl}_2 < \text{SnCl}_2 \cdot 2\text{H}_2\text{O}$  in the present study.
3. Cationically-induced isomerization of IR occurs on heating at  $160^\circ\text{C}$  in the presence of  $\text{SnCl}_2 \cdot 2\text{H}_2\text{O}$ , resulting in cis/trans interconversions, double-bond shifts, cyclisation and crosslinking. The changes occur to a less pronounced extent when phenolic condensates are also present. Anhydrous  $\text{SnCl}_2$  causes the same changes to occur but much more slowly (possibly due to a small extent of hydration), but isomerisation is undetectable in the presence of phenolic material. Anhydrous  $\text{ZnCl}_2$  produces no detectable isomerisation irrespective of whether or not phenolic material is present.
4. Adduct formation between a monomethylol compound (the methylolphenol) or its derived ether (the dibenzyl ether) and isoprene rubber is not quantitative owing to the occurrence of side reactions which produce inactive

phenolic material. The side reactions occur to a greater extent with the methylol compound than with the ether. The maximum efficiency of adduct formation achieved in this work was 63% of the theoretical (after 210 min at 160°C).

5. The interaction between dimethylol compounds (DMP and DMDPM) or their derived ethers (PE and PEDPM) and isoprene rubber produce adducts which are crosslinked (vulcanized). Since polynuclear reactive phenolic entities are necessary to effect crosslinking, the crosslinking efficiency achieved by DMP is lower than that observed with the other three reagents, and crosslinking arises only through side reactions which produce polynuclear material. Of the polynuclear crosslinking agents (DMDPM, PE and PEDPM), vulcanizing activity is reduced in the order PE > PEDPM  $\approx$  DMDPM.
  
6. The preferred vulcanizing agent on the grounds of both speed and efficiency is the polyether PE. This produces an initial inefficiently-crosslinked structure containing polynuclear crosslinks and pendent groups. As reaction proceeds the number of crosslinks increases, their length reduces to a binuclear minimum, and pendent groups are eliminated. The presence of some methylene links between phenolic nuclei reduces vulcanization rate but does not reduce ultimate efficiency unless they occur in adjacent positions in the molecule.

7. The crosslinks ultimately produced by the above reagents and by a commercially-available vulcanizing resin are mainly of two types - binuclear crosslinks containing an ether linkage and binuclear crosslinks containing a methylene linkage. Additionally, a smaller number of polynuclear crosslinks containing multiple methylene linkages may be present.
8. The efficiency of crosslinking, in addition to depending on the structure of the condensate (6 above), is also subject to reduction through side-reactions which produce inactive phenolic material. These side-reactions may be reduced by the addition of paraformaldehyde. The case of DMP this reduces the number of crosslinks obtained (in accordance with 5 above), but in the other 3 cases (PE, PEDPM and DMDPM) it increased the crosslinking efficiency. The highest value for efficiency of vulcanization ( $E_v$ ) achieved in the present work was some 62% of that theoretically possible.

## 6. EXPERIMENTAL

### 6.1 Reagents

(a) Monomethylolphenols and their derived ethers

(i) The methylolphenol (IV)

This compound was prepared following Hultzsch's procedure<sup>16</sup>; a technical grade (Aldrich Co.) of the original phenol (XXVI) (164g, 1.0 mole) was added dropwise to aqueous sodium hydroxide (40g, 1.0 mole, as 10% w/v) with constant stirring. A pink precipitate, presumed to be the sodium salt of the original phenol, was formed then dissolved by gentle heating. The solution was cooled, and aqueous methanal added (30g, 1.0 mole, as 40% w/v).

After storing for 1 week at 20°C, the solution was just acidified with dilute acetic acid, when a brown oil precipitated. The oil was washed thoroughly with distilled water, and on standing formed a yellow crystalline precipitate.

The product was repeatedly re-crystallised from hexane fraction (b.p. 65-70°C), and the methylolphenol was obtained as a colourless crystalline solid, (100g, 52%): mp 63-64.5°C (lit.<sup>16</sup> mp 64°C); ir (CHCl<sub>3</sub>) 10.0μ (methylol); nmr (CDCl<sub>3</sub>) 8.8τ (ArC(CH<sub>3</sub>)<sub>3</sub>), 7.8τ (ArCH<sub>3</sub>), 5.2τ (ArCH<sub>2</sub>OH), 3.1 and 2.9τ

(ArH's), (the hydroxy protons were not assigned).

Anal. Calcd. for  $C_{12}H_{18}O_2$  : C, 74.2; H, 9.3; molecular weight (M); 194.

Found : C, 74.3; H, 9.3; M(ms); 194.

(ii) The dibenzylether (V)

This compound was prepared following the procedure described by Fitch,<sup>11</sup> except that paraformaldehyde was added in order to suppress side reactions. Paraformaldehyde (1g) was added to a solution of the methylolphenol (IV) (97g, 0.5 mole) in toluene (500ml). This mixture was refluxed with a Dean and Stark head until 95% of the theoretical amount of water (4.3ml) had been collected (approx. 24 hr). The toluene was removed in a rotary film evaporator leaving a yellow solid. This was then re-crystallised from hexane fraction (b.p. 65-70°C) to give the dibenzylether as a colourless crystalline solid, (70g, 76%): mp 129-130.5°C (lit.<sup>11</sup> 129-130°C); ir ( $CHCl_3$ ) 9.4 $\mu$  (ether); nmr ( $CDCl_3$ ) 5.3 $\tau$  ( $(ArCH_2)_2O$ ), 4.0 $\tau$  (ArOH).

Anal. Calcd. for  $C_{24}H_{34}O_3$  : C, 77.8; H, 9.2; M, 370.

Found : C, 77.5; H, 9.4; M(ms); 370.

(iii) 2-methylol-4-tert.butylphenol (5(-1,1-dimethyl-ether)-2-hydroxy phenyl)methanol (LIX)

This compound was prepared following the procedure

described by S. Van der Meer<sup>12</sup>: a technical grade (Aldrich Co.) of 4-tert.butylphenol (LV) (150g, 1.0 mole) was dissolved in a mixture of ethanol (AR grade) (200ml) and aqueous methanal (60g, 2.0 mole, as 40% w/v) after which aqueous sodium hydroxide (40g, 1.0 mole; as 42% w/v) was added.

After 1 week at 20°C, the crystallised sodium salt of the methylol compound was separated, washed with aqueous sodium chloride (10% w/v) and dissolved in water (4l). Aqueous sodium hydroxide (17g, 0.42 mole, as 32% w/v) was added, and the solution was filtered and just acidified with dilute ethanoic acid.

The precipitated methylol compound was washed with water, dried, and recrystallised from petroleum ether (b.p. 100-130°C), to give the 2-methylol-4-tert.butyl phenol as colourless crystals, (60g, 34%); mp 91-92°C (lit.<sup>12</sup>. 90-91°C);  $\nu$  (CHCl<sub>3</sub>) 10.0 $\mu$  (methylol); nmr (CDCl<sub>3</sub>) 8.8 $\tau$  (ArC(CH<sub>3</sub>)<sub>3</sub>), 5.2 $\tau$  (ArCH<sub>2</sub><sup>\*</sup>OH), 3.0 and 2.8 $\tau$  (ArH's).

Anal. Calcd. for C<sub>11</sub>H<sub>16</sub>O<sub>2</sub> : C, 73.3; H, 8.9; M 179.

Found : C, 73.6; H, 9.0; M(ms); 179.

(b) Dimethylolphenols and their derived ethers

(i) The dimethylolphenol (LX)

This compound was prepared by the base-catalysed

addition of methanal to 4-tert.butylphenol (LV) following the same procedure described above for the synthesis of the methylolphenol, but using an excess of methanal.

A technical grade (Aldrich Co.) of 4-tert.butylphenol (LV) (150g, 1.0 mole) was dissolved in aqueous sodium hydroxide (40g, 1.0 mole, as 10% w/v) by gentle heating. The solution was mixed with aqueous methanal (75g, 2.5 mole, as 40% w/v) at 20°C and allowed to stand for one week at room temperature. After this period the solution was just acidified with dilute acetic acid when a brown oil precipitated. The oil was washed with water, and on standing formed a crystalline precipitate. After repeated recrystallization from hexane fraction (b.p. 65-70°C), the dimethylolphenol was obtained as colourless crystalline solid, (151g, 72%): mp 62-63°C (lit.<sup>143</sup> 61°C); ir(CHCl<sub>3</sub>); 10.0 $\mu$ (methylol); nmr(CD<sub>3</sub>OH); 8.8 $\tau$  (Ar(CH<sub>3</sub>)<sub>3</sub>), 5.1 $\tau$  (ArCH<sub>2</sub>OH); 2.9 $\tau$  (ArH's)

Anal. Calcd. for C<sub>12</sub>H<sub>18</sub>O<sub>3</sub> : C, 68.6; H, 8.6; M 209.

Found : C, 68.4; H, 8.3; M(ms); 209.

(ii) The polybenzylether (LXI)

This compound, apparently not previously reported in the literature, was prepared by self-condensation of the dimethylolphenol (LX) in toluene following the same general procedure described above for the synthesis of the dibenzylether (V).

The dimethylolphenol (LX) (105g, 0.5 mole) was dissolved in toluene (AR grade) (500ml). Paraformaldehyde (1g) was added and the mixture was refluxed with a Dean and Stark head for 47 hr. The toluene was removed in a rotary film evaporator leaving a yellow resinous solid. This solid was reprecipitated several times by cooling its hot solution in hexane, but it did not appear to crystallize. The polybenzyl-ether was obtained as white resinous powder (70g): mp 97-100°C; ir (CHCl<sub>3</sub>) 9.4μ(ether); nmr(CCl<sub>4</sub>) 8.8 (ArC(CH<sub>3</sub>)<sub>3</sub>), 5.3-5.6τ (ArCH<sub>2</sub>\*OH), ((ArCH<sub>2</sub>)<sub>2</sub>O), 6.2τ (Ar-CH<sub>2</sub>-Ar), 2.9τ (ArH's); M<sub>n</sub>(gel permeation chromatography, gpc); 615.

(iii) Methylene bis(2-hydroxy 3-methylol 5-tert.butyl phenol) (4,4'-bis(1,1-dimethylethyl)-6,6'-dimethylol-2,2'-methylenediphenol) (LXII)

This compound was prepared by acid-catalysed condensation of 4-tert.butylphenol (2 mol) with methanal (1 mol) under conditions reported by Ambelang and Binder,<sup>75</sup> followed by base-catalysed addition of the product with methanal (2 mol).

A technical grade (Aldrich Co.) of 4-tert.butylphenol (LV) (150g, 1.0 mole) was mixed with methanal (15g, 0.5 mole, as 40% w/v) and conc. hydrochloric acid (15ml, 1.18sg). The mixture was stirred at 70°C (bath) for 4h, then the insoluble resinous precipitate was washed with distilled water. On standing the resinous material gradually crystallized.

This product was dissolved in a mixture of aqueous sodium hydroxide (40g, 1.0 mole, as 10% w/v) and methanol (AR grade) (200ml) by gentle heating, then cooled to room temperature and mixed with aqueous methanal (75g, 2.5 mole, as 40% w/v). After 2 weeks standing at room temperature the solution was just acidified with dilute acetic acid, when a brown oil precipitated. The oil was washed with distilled water, and on standing formed a pale brown precipitate. This product, referred to earlier as \*DMDPM, was found to show less than the expected reactivity. Tests indicated that this was probably due to traces of residual NaOH, which interfered with the Lewis acid catalysts subsequently used. It is found that the reactivity could be greatly improved by washing in toluene solution with dilute acetic acid. This product (referred to as DMPDM) was obtained as an apparently amorphous powder by cooling its hot solution in hexane fraction (b.p. 65-70°C), to give the dimethylol product (90g) as a pale brown solid:  $\text{ir}(\text{CHCl}_3)$ ; 10.0 $\mu$ (methylol);  $\text{nmr}(\text{CCl}_4)$  8.8 $\tau$  ( $\text{ArC}(\text{CH}_3)_3$ ), 5.4 $\tau$  ( $\text{ArCH}_2^*\text{OH}$ ), 6.1 $\tau$  ( $\text{Ar-CH}_2\text{-Ar}$ ), 2.9 $\tau$  ( $\text{ArH}'\text{s}$ );  $M_n(\text{gpc})$ , 397. theory for LXII; 372.

(iv) Derived polyether from methylene bis(2-hydroxy 3-methyl 5-tert.butylphenol) (LXIII)

This compound was prepared by self-condensation of the dimethylol compound (LXII) in toluene.

The dimethylol compound (60g) was dissolved in toluene (AR grade) (250ml) and paraformaldehyde (0.5g) was added.

This mixture was refluxed for 60hr with a Dean and Stark head.

The toluene was removed on a film evaporator leaving a brown solid. This was then re-precipitated several times by cooling its hot hexane solution to give the product (52g) as a brown resinous material: mp 100-104°C; ir 9.4 $\mu$ (ether); nmr (CCl<sub>4</sub>), 8.8 $\tau$  (ArC(CH<sub>3</sub>)<sub>3</sub>), 5.2-5.4 $\tau$  (ArCH<sub>2</sub>\*OH), ((ArCH<sub>2</sub>)<sub>2</sub>O), 6.0-6.3 $\tau$  (Ar-CH<sub>2</sub>-Ar), 2.9 $\tau$  (ArH's); M<sub>n</sub>(gpc); 828.

(c) Perbenzoic acid

Perbenzoic acid reagent was prepared following the procedure of Kolthoff<sup>144</sup> which represents a modification of the Braun procedure.<sup>145</sup>

Sodium methoxide solution was prepared by reacting sodium metal (23g, 1 mole) with molar excess of methanol (AR grade) (100ml). A solution of benzoyl peroxide (242g, 1 mole, in chloroform) (AR) (200ml) was added dropwise (15-20ml per minute) to the sodium methoxide solution, maintaining the temperature below 0°C during addition and swirling vigorously. 550ml of water containing chopped ice was added to the mixture and the aqueous phase (containing the sodium perbenzoate) was washed with two 100ml portions of carbon tetrachloride to remove chloroform, discarding any emulsion collected at the interface. The aqueous solution was acidified with sulphuric acid, and extracted with benzene (AR grade) (300ml). The benzene solution of perbenzoic acid

was washed with water, dried with powdered, anhydrous sodium sulphate and stored in the dark at 10°C.

### 6.2 Interaction of Phenolic Condensates and/or Catalysts with IR

In all cases the interactions of the IR with the p/f condensates and/or with the catalysts were carried out in bulk.

#### (a) Mixing procedures

Both p/f condensates and catalysts, previously finely divided in a mortar, were mixed with the IR on a two-roll mill at room temperature. When mixing IR with catalyst alone a short mixing cycle of about seven minutes appeared to give good dispersion (judged by visual inspection) without over-fragmentation of the rubber. In those cases where p/f condensate was mixed with the IR, the compound tended to adhere to the back roll and the p/f condensate adhered to both rolls of the mill. This necessitated an increase in the mixing time to twelve minutes. The loss in weight during mixing was found to be less than 1% of the total in all cases.

#### (b) Reaction

The mixed samples were placed between two thin sheets (0.1mm) of inert film of low surface energy (FEP) and pressed

(1 atm/inch<sup>2</sup>) into a thin sheet (5 x 5 x 0.02 cm) in a pre-heated metal mould for various times at 160°C (or 180°C). The inert film prevents possible catalytic effects from the metal plates and, furthermore, facilitates easy removal of the reacted product. The latter is especially important in those interactions involving adduct formation since these products show strong adhesive tendencies to most surfaces.

The sample edges (approx. 1 mm), which had been exposed to air during the reaction, were cut off and discarded.

(c) Isolation of adducts or modified rubbers

It is well known that uncured samples, although they may be finely comminuted, tend to join together during extraction. The fused lump of rubber so formed extracts much less quickly and extraction may be inefficient unless very prolonged times are used. In the present study the IR/catalysts and IR/monofunctional p/f condensate interaction products were uncured and, in addition, in the latter case the adduct showed a high self-adhesion tendency. A modified acetone-extraction procedure was therefore used for these products, as follows: a thin sheet (~0.2 mm) of the sample was rolled up over a glass cylinder (diameter 2 cm, length 6 cm). Care was taken to ensure that no two portions of the surface of the sheet came into contact with each other, so as to maintain a maximum ratio of surface area to volume. The rolled sample was wrapped in a porous aluminium 'thimble', and placed in the Soxhlet extractor cup. Samples were

continuously extracted with hot acetone over sixteen hours. This modified extraction procedure was effective in preventing excessive coalescence of the uncured samples of rubber, and a test showed that all the p/f condensate present in an unheated sample could be efficiently extracted by this method.

In those interactions where samples became crosslinked (i.e., IR/bifunctional p/f condensates), an unsupported thin sheet of sample was directly extracted in the Soxhlet extractor so that subsequent physical tests could be carried out on acetone-extracted samples. Acetone-extract values also formed part of the product characterisation procedure (6.3(e) below).

### 6.3 Analyses and Characterisation Methods

#### (a) Determination of total unsaturation

##### (i) Wijs-Kemp method

A finely comminuted sample (~0.05g) was accurately weighed (to the nearest 0.1mg) and dissolved in a mixture of chloroform (50ml) and o-dichlorobenzene (50ml) in a 250ml iodine flask. The time for dissolution depended upon the particular interaction product and varied between about 1 and 5h. For those samples which contained gel the mixture was left overnight in order to ensure maximum swelling.

0.2N Wijs solution (iodine monochloride in acetic acid)

(20ml) was quantitatively added. Previous experiments had shown that, for the soluble samples, Wijs reagent reacted completely after 1 hour, whereas for samples containing gel complete reaction was obtained only after 4 to 8 hours, depending upon the proportion of gel in the particular sample and also, presumably, on the degree of crosslinking of the gel.

At the end of this reaction time, freshly prepared aqueous potassium iodide solution (about 15ml of 5% solution) was added, causing the contents of the flask to separate into two dark red layers. The liberated (excess) iodine was immediately titrated against standard 0.1N sodium thiosulphate, with continuous shaking. Starch indicator was added near the end-point, which was taken as the point at which both layers remained colourless for one minute. Blank titration were carried out on mixtures of an identical composition but with no sample being used.

The procedure was carried out in duplicate for each sample and the results were averaged. The 'Iodine Value' of the sample, defined as the number of grams of iodine absorbed by one hundred grams of sample, was calculated. The fraction of the total original unsaturation was then calculated from:

$$\text{Fractional residual unsaturation} = \frac{\text{Iodine Value}}{372.8} \quad (57)$$

where the constant 372.8 represents the theoretical Iodine Value for pure IR.

(ii) Perbenzoic acid method

This method is similar to that described by Lee, Scanlan and Watson.<sup>60</sup>

A finely-comminuted sample (0.1 to 0.3g), the quantity depending on the degree of unsaturation expected, was accurately weighed (to the nearest 0.1mg) and mixed with 25ml of benzene (AR grade). Uncrosslinked samples soon dissolved, but insoluble samples containing gel were allowed to swell for 5h at room temperature. 20ml of perbenzoic acid solution in benzene (0.3M, determined iodometrically at the time it was used) was added and the mixture allowed to stand in a dark cupboard at 20°C for 1hr (soluble samples) or 4hr (gelled samples). Reaction times were determined in preliminary experiments. After the reaction, freshly prepared aqueous potassium iodide solution (about 15ml, 3% solution) was added and the iodine liberated titrated with standard 0.1N thiosulphate solution as described in Section (i) above. Parallel blank titrations were always carried out and the procedure was carried out in duplicate for each sample.

Mean values for Iodine Value and hence fractional residual unsaturation were calculated as described in (i) above.

(b) Glass transition temperature ( $T_g$ )

A differential scanning calorimetric (dsc) technique was used for measuring the  $T_g$ . However, the accuracy of  $T_g$  determination by this technique has been questioned because of the dependence of  $T_g$  on heating rate. The rates of heating used in the dsc are relatively high compared to those used in other methods (e.g., the dilatometric method) and therefore the samples may not have enough time to reach thermal equilibrium.

A linear relationship has been demonstrated<sup>146</sup> between logarithm of heating rate and reciprocal absolute temperature at which the transition occurs, over a range of heating rates between  $0.06^\circ/\text{min}$  and  $64^\circ/\text{min}$ , thus, results obtained from a range of high heating rates may be extrapolated to lower heating rates in order to obtain a good approximation to the true value of the  $T_g$ . Values of  $T_g$  for poly(n-butyl-acrylate) using the above technique agree<sup>146</sup> with the value found by using a special refractometer method.<sup>147</sup>

For this study, the sample (~12mg) was cooled to about  $25^\circ$  below its expected  $T_g$  and the linear heating programme was commenced. Differential thermograms were recorded at heating rates of  $1^\circ$ ,  $2^\circ$ ,  $4^\circ$ ,  $6^\circ$ ,  $16^\circ$  and  $32^\circ$  per minute for the same sample. The  $T_g$  at each heating rate was taken as the point of intersection of the extrapolations of the linear parts of the trace before and after the transition. The

(b) Glass transition temperature ( $T_g$ )

A differential scanning calorimetric (dsc) technique was used for measuring the  $T_g$ . However, the accuracy of  $T_g$  determination by this technique has been questioned because of the dependence of  $T_g$  on heating rate. The rates of heating used in the dsc are relatively high compared to those used in other methods (e.g., the dilatometric method) and therefore the samples may not have enough time to reach thermal equilibrium.

A linear relationship has been demonstrated<sup>146</sup> between logarithm of heating rate and reciprocal absolute temperature at which the transition occurs, over a range of heating rates between  $0.06^\circ/\text{min}$  and  $64^\circ/\text{min}$ , thus, results obtained from a range of high heating rates may be extrapolated to lower heating rates in order to obtain a good approximation to the true value of the  $T_g$ . Values of  $T_g$  for poly(n-butyl-acrylate) using the above technique agree<sup>146</sup> with the value found by using a special refractometer method.<sup>147</sup>

For this study, the sample (~12mg) was cooled to about  $25^\circ$  below its expected  $T_g$  and the linear heating programme was commenced. Differential thermograms were recorded at heating rates of  $1^\circ$ ,  $2^\circ$ ,  $4^\circ$ ,  $6^\circ$ ,  $16^\circ$  and  $32^\circ$  per minute for the same sample. The  $T_g$  at each heating rate was taken as the point of intersection of the extrapolations of the linear parts of the trace before and after the transition. The

logarithm of the heating rates were plotted against the reciprocals of the  $T_g$ 's ( $^{\circ}\text{K}$ ). The best straight line through the individual  $T_g$  points was extrapolated to a heating rate of  $4^{\circ}$  an hour ( $0.066^{\circ}$  per min.), and the  $T_g$  value then read off from the graph (e.g., Fig. 88).

(c) Intrinsic viscosity  $[\eta]_{c=0}$

Intrinsic viscosity was measured in a 'suspended level dilution viscometer' (Fig. 89) as follows: 10ml of a toluene solution of the sample of accurately-known concentration (about 1%) was placed in the viscometer via tube 1, and the viscometer was placed in a constant temperature bath at  $25^{\circ}\text{C}$ . After allowing 20 min. for the viscometer and its contents to reach thermal equilibrium, tube 2 of the viscometer was closed and by applying pressure to tube 1 the liquid was blown into tube 3 until the level was above the upper timing mark. Tubes 1 and 2 were then opened and the time for the liquid meniscus to fall from the upper to the lower timing mark was measured. The process was repeated until consecutive readings agreed to within 0.2 sec.

A measured quantity of toluene was added to the solution in the viscometer and a gentle stream of air was blown through the solution until it was homogeneous. The above procedure was repeated for five dilutions, covering between 0.25% and 1% polymer concentration, and for pure solvent.

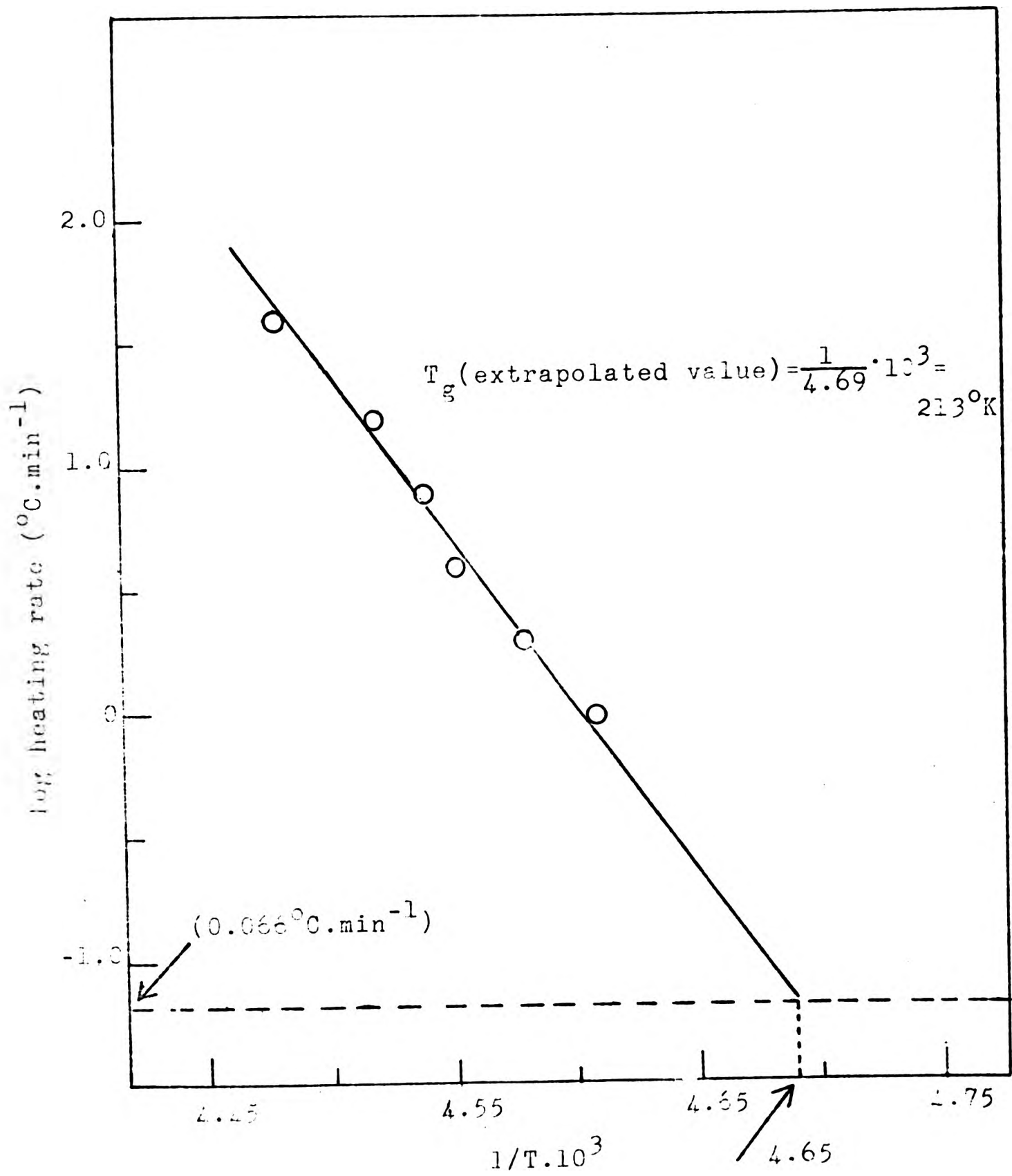


Fig. 88 Determination of the  $T_g$  by extrapolation from dsc results of log heating rate vs  $1/T$  values for the IR/MP/ $\text{ZnCl}_2$  interaction product (heated at  $160^{\circ}\text{C}$  for 45 min).

The measured flow times  $t$ , were converted into viscosities by:

$$\eta = A dt - \frac{Bd}{t} \quad (58)$$

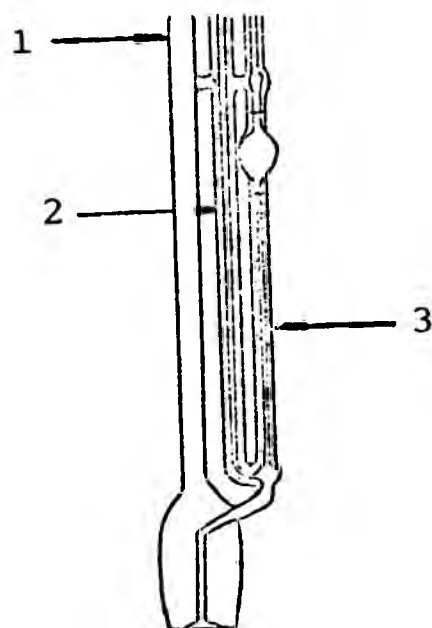


Fig. 89 Suspended level dilution viscometer.

From the measured viscosities  $\eta$  and  $\eta_T$  for the solutions and for pure toluene, values of specific viscosity ( $\eta_{sp} = \frac{\eta - \eta_T}{T}$ ) were calculated for each of the different polymer concentrations ( $c$ ).

The intrinsic viscosity  $[\eta]_{c=0}$  was then obtained by straight line extrapolation of a plot of  $\eta_{sp}/c$  against  $c$  to infinite dilution. The method of least squares was used to obtain the best intercept, and a typical plot is shown in Fig. 90.

(d) Gel content

A test-portion ( $\sim 1g$ ) was accurately weighed (to the nearest 0.1mg) and allowed to stand in a large excess of

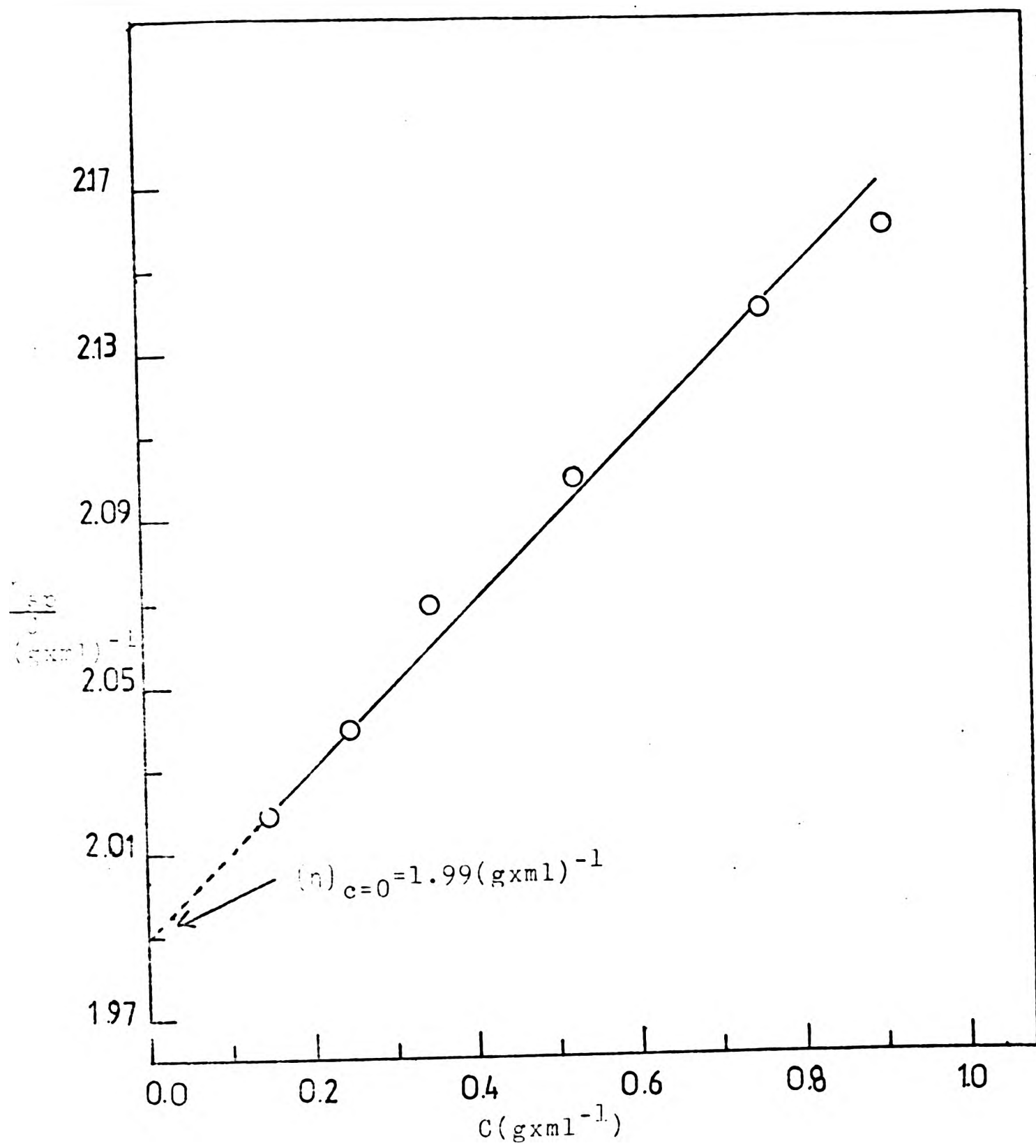


Fig. 90 Determination of the intrinsic viscosity  $(\eta)_{c=0}$  for the IR/E/ZnCl<sub>2</sub> interaction product heated at 160°C for 210 min.

toluene in a screw-cap bottle for 48 hours. The swollen gel was then filtered into a weighed crucible (1-mesh) and dried in a vacuum oven to constant weight. The gel content was expressed as a percentage of the weight of the original test-portion.

(e) Unextractable uncombined phenolic material (Ph)<sub>u</sub>

Unextractable material from the mixes of EPR with methylol phenol and dibenzyl ether with and without catalysts after heating at 160°C (180°C for those mixes without catalyst) for the same times and under the same conditions as those used for interactions with IR, was calculated from the results of acetone extraction (see (f) below). Amounts of extractable matter were corrected to allow for the extractable matter from the original rubber, and it was assumed that no chemical combination with the rubber had occurred. Thus, differences between the amounts used and the amount extracted correspond to uncombined, unextractable material. Results were expressed as moles of unextractable material per mole of IR (i.e., 68g) moles being calculated as weight divided by 176 (MW of quinone methide XXX). This expression of results does not take into account the possible presence of decomposition products of the catalyst in the unextractable material. However, since the proportion catalyst : starting phenolic material is very small (~1:25), catalyst residues are considered to have negligible effect on the above results.

These results are summarised in Fig. 91, showing changes in concentration, expressed in moles per mole of IR, as reaction proceeds.

In all cases, an increase in unextractable matter with heating time is observed, ranging in ultimate values from  $0.64 \times 10^{-2}$  to  $1.70 \times 10^{-2}$  moles per mole of IR, depending on the particular case. Concentrations are higher in those cases where catalyst was present, and follow the order  $\text{SnCl}_2 \cdot 2\text{H}_2\text{O} > \text{SnCl}_2 > \text{ZnCl}_2$ .

(f) Rubber-combined phenolic material,  $(\text{Ph})_c$

(i) as acetone-insoluble matter

A sample (~5g) was accurately weighed (to the nearest 0.1mg) and quantitatively extracted with hot acetone as described above. The acetone extract was dried in an air oven at  $55^\circ\text{C}$  to constant weight. Weighed samples of the IR only and of the unheated mix were also extracted and the corresponding extracts dried to a constant weight.

The amount of phenolic material not combined was obtained from these results by subtracting from the weight of the acetone extract of the sample, the sum of the weights of acetone extract of the IR only and the catalyst. The amount of phenolic material combined,  $(\text{Ph})_c$ , was then obtained by difference from the corresponding value for the acetone extract of the unheated mixture. These results were

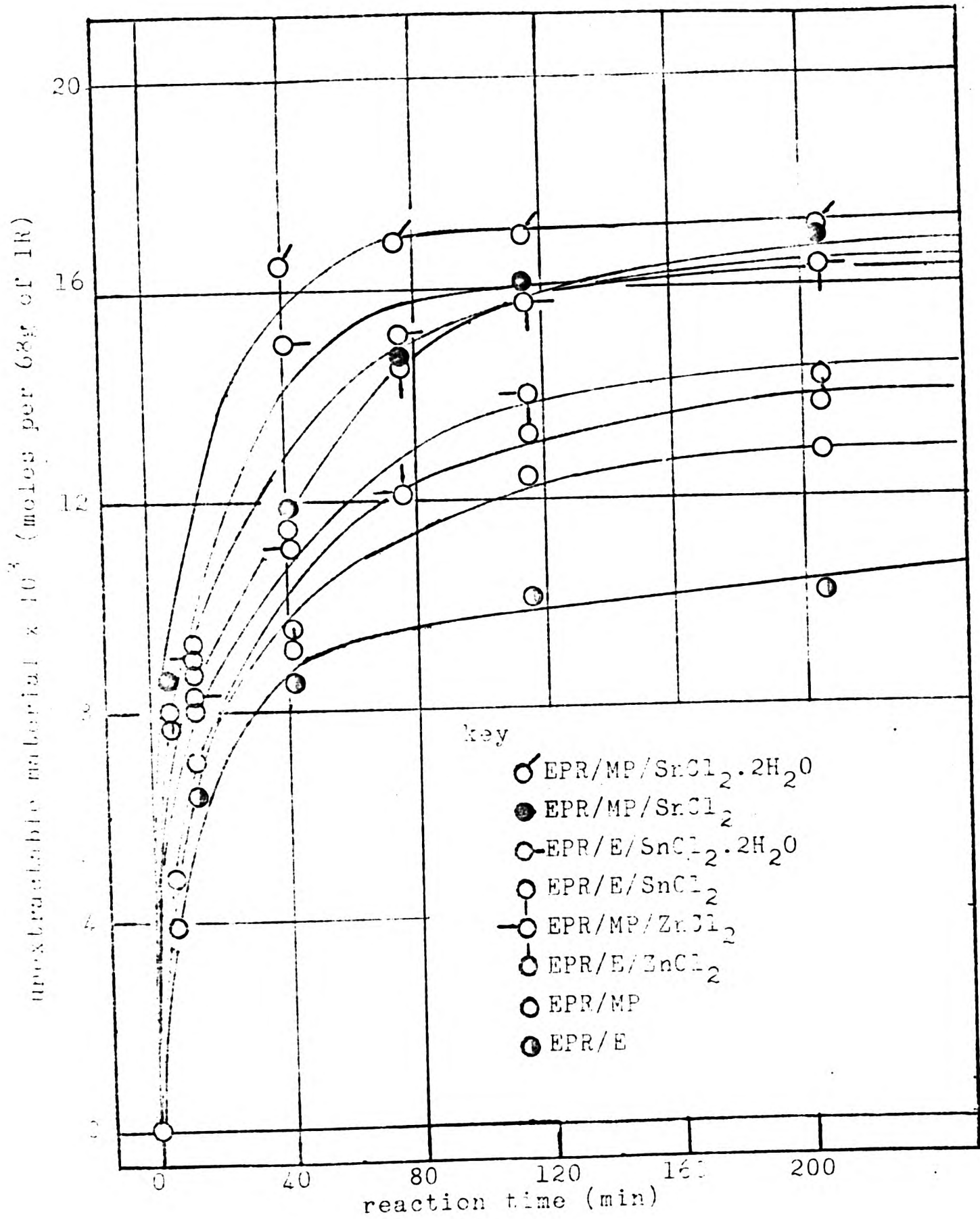


Fig. 91 Kinetics of formation of unextractable material as calculated from acetone extraction results.

corrected for unextractable uncombined phenolic material  $(\text{Ph})_u$ . The unheated extracts, after correction, gave zero value for  $(\text{Ph})_c$ .

(ii) By nmr spectroscopy

The concentration of combined phenolic material in the acetone-extracted rubbers was estimated from the nmr spectrum by comparing the area of the peak at  $8.66\tau$ , attributable to  $\text{Ar-C}(\text{CH}_3)_3$  in phenolic material, with the resonance peak at  $4.70\tau$ , attributable to  $\text{R}_2\text{C}=\text{CRH}$  in IR.

Let  $N(\text{Ph})_t$  = moles of phenolic material not extracted by acetone

$N(\text{Ph})_c$  = moles of phenolic material chemically combined with IR

$N(\text{Ph})_u$  = moles of phenolic material not combined but no extractable with acetone

$N(\text{IR})_o$  = moles of original IR

$A_{8.66}$  = Area of the resonance at  $8.66\tau$  ( $\text{C}(\text{CH}_3)_3$ )

$A_{4.70}$  = Area of the resonance at  $4.70\tau$  ( $-\text{CH}=\text{}$ )

then

$$9N(\text{Ph})_t = K A_{8.66}$$

Since phenolic material contains 9 tert-butyl protons

contributing to the  $8.66\tau$  area ( $A_{8.66}$ ) then

$$N(\text{Ph})_t = \frac{K A_{8.66}}{9}$$

$$\frac{N(\text{Ph})_t}{N(\text{IR})_0} = \frac{K A_{8.66}}{9N(\text{IR})_0}$$

Assuming that negligible reduction of the 4.70 resonance occurs during reaction, i.e., that  $N(\text{IR})_0 \approx K A_{4.70}$  at all reaction times,  $t$ , then:

$$\frac{N(\text{Ph})_t}{N(\text{IR})_0} = \frac{K A_{8.66}}{9K A_{4.70}}$$

since  $N(\text{Ph})_t = N(\text{Ph})_c + N(\text{Ph})_u$ , it follows that:

$$\frac{N(\text{Ph})_c}{N(\text{IR})_0} = \frac{A_{8.66}}{9A_{4.70}} - \frac{N(\text{Ph})_u}{N(\text{IR})_0} \quad (3)$$

The quantity  $\frac{N(\text{Ph})_u}{N(\text{IR})_0}$  was obtained by acetone extraction of an unreactive rubber, as described in Section (e) above.

(g) Characterization of the p/f condensates used as vulcanizing agents

The concentration of dibenzyl ether-type bridges, methylene bridges and methylol groups present in the p/f condensates used as vulcanizing agents, were estimated by acetylation followed by nmr spectroscopy.

(i) Acetylation

The condensates were acetylated using an adaptation of

Woodbrey's procedure.<sup>104</sup>

A molar excess of acetic anhydride was added slowly to an ice-cooled stirred solution of the p/f condensate (2.5g) in pyridine (50ml) and stirring was continued for 24h at 4°C. Water (50ml) was added and the mixture was extracted with 2 x 50ml portions of ether. The organic phase containing the acetylated material was washed with 2 x 50ml portions of dilute HCl, 2 x 50ml portions of dilute aqueous NaHCO<sub>3</sub> solution and 2 x 50ml portions of water. The ether was removed in a rotary film evaporator, leaving the acetylated product.

(ii) Determination of the various groups present in the acetylated p/f condensates by nmr spectroscopy

This is adapted from the method described by Woodbrey<sup>104</sup>:

The concentration of acetoxymethyl groups (ArCH<sub>2</sub>OAc) dibenzylether bridges ((ArCH<sub>2</sub>)<sub>2</sub>O) and methylene bridges (ArCH<sub>2</sub>Ar), were estimated from the nmr spectrum by comparing the area of the peaks at 5.05 (ArCH<sub>2</sub>OAc), 5.70 ((ArCH<sub>2</sub>)<sub>2</sub>O) and 6.40 (ArCH<sub>2</sub>Ar), with the resonance peak at 8.70 (C(CH<sub>3</sub>)<sub>3</sub>).

If it is assumed that the methylol groups in the condensate become completely acetylated and other groups remain unaffected, then the number of moles, N, of the various

groups may be obtained from the peak areas,  $A$ , as follows:

$$N(\text{ArCH}_2\text{OH}) = N(\text{ArCH}_2\text{OAc}) = \frac{K}{2} A_{5.05}$$

$$N(\text{ArCH}_2\text{OCH}_2\text{Ar}) = \frac{K}{2} A_{5.70}$$

$$N(\text{ArCH}_2\text{Ar}) = K A_{6.40}$$

The total number of moles,  $N(\text{Ar})$ , is given by:

$$N(\text{Ar}) = N(\text{Bu}^t) = \frac{K}{9} A_{8.70}$$

The number of moles of each may then be expressed as a fraction of the total number of moles as follows:

$$\frac{N(\text{ArCH}_2\text{OH})}{N(\text{Ar})} = \frac{9}{2} \frac{A_{5.05}}{A_{8.70}}$$

$$\frac{N(\text{ArCH}_2\text{OCH}_2\text{Ar})}{N(\text{Ar})} = \frac{9}{2} \frac{A_{5.70}}{A_{8.70}}$$

$$\frac{N(\text{ArCH}_2\text{Ar})}{N(\text{Ar})} = 9 \frac{A_{6.40}}{A_{8.70}}$$

Since there are two positions occupied in each aromatic nucleus, the summation

$$\frac{9}{2} \frac{A_{5.05}}{A_{8.70}} + \frac{9}{2} \frac{A_{5.70}}{A_{8.70}} + 9 \frac{A_{6.40}}{A_{8.70}} = 2$$

should apply.

(h) Determination of concentration of physically-effective crosslink,  $[X]_{\text{phys}}$

(i) Swelling method

A test-piece of approximate dimensions 2 x 5 x 20mm, cut from the acetone-extracted vulcanizate, was accurately weighed (to the nearest 0.1mg) ( $W_1$ ) and placed in a wide-neck screw-cap bottle. It was covered with the swelling liquid, either benzene or n-decane, as appropriate (20ml), and the bottle was capped and set aside in a dark cupboard.

After eight hours, the swollen specimen was carefully removed with tweezers and transferred immediately and rapidly to a glass specimen tube (1" diam.) lined with filter paper. The tube was tightly capped. The time of removal of the specimen from the liquid was noted. The specimen tube was shaken several times so as to facilitate the absorption by the filter paper of any excess of liquid on the surface of the swollen rubber specimen. The specimen tube with its contents were accurately weighed (to the nearest 0.1mg) ( $W_2$ ). The swollen specimen was removed from the tube with tweezers, and immediately the cap was replaced. The swollen specimen was replaced in the swelling liquid for a further period of time noting the time of replacement. The 'empty' specimen tube was accurately weighed (to the nearest 0.1mg) ( $W_3$ ). The weight ( $W_s$ ) of the swollen rubber specimen was determined by:

$$W_s = W_2 - W_3$$

After further periods of time the above procedure was repeated, noting the times at which the swollen specimen was removed from and replaced in the swelling liquid. The procedure was repeated until sufficient data were obtained to make allowance for network oxidative-degradation (incremental swelling). A graphical method of allowance was used based upon the above values. A typical graph is illustrated in Fig. 92. From this plot the swollen weight at equilibrium ( $W_e$ ) was calculated as the intercept on the  $W_s$  axis obtained by extrapolating the linear portion of the curve back to zero time of immersion.

From the equilibrium swollen weight ( $W_e$ ), the volume fraction of vulcanizate in the swollen system ( $V_r$ ) was calculated by:

$$V_r = \frac{\text{Volume of vulcanizate}}{\text{Volume of vulcanizate} + \text{Volume of the swollen liquid}}$$

$$= \frac{W_1/\rho_v}{W_1/\rho_v + (W_e - W_1)\rho_{liq}} \quad (59)$$

where

$$\rho_v = \text{density of unswollen vulcanizate (0.90}^* \text{g/cc)}$$

$$\rho_{liq} = \text{density of the swelling liquid ( benzene} = 0.88 \text{g/cc;}$$

$$\text{n-decane} = 0.73 \text{g/cc at } 22^\circ\text{C)}$$

\*Determined by the standard procedure using a density bottle.

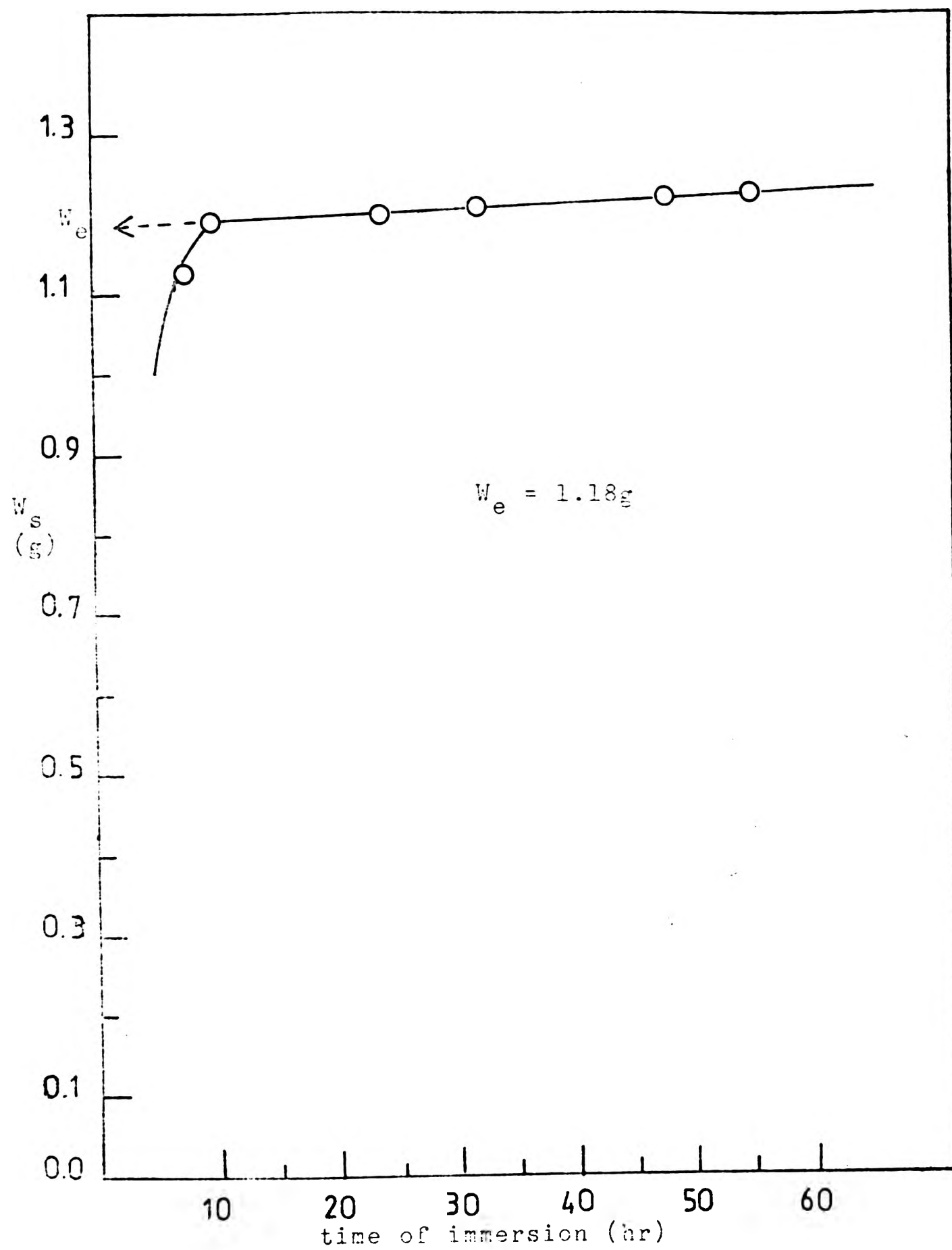


Fig. 92 Determination of swollen weight of equilibrium ( $W_e$ ) for the IR/PE/ $ZnCl_2$  interaction product heated at  $160^\circ C$  for 80 min.

$v_r$  values were obtained in duplicate for each sample, and the average value obtained. With this value and by using the Flory-Rehner equation (49):

$$-\ln(1-v_r) - v_r - \chi v_r^2 = \rho v_o M_c^{-1} v_r^{1/3} \quad (49)$$

the average molecular weight of the network chains between crosslinks ( $M_c$ ) was calculated. These values were corrected ( $M_c^{\text{corr}}$ ) by using the Mullins "finite molecular weight" allowance (52):

$$M_c^{\text{corr}} = M_c^{-1} (1 - 5.44 M_c M_n^{-1}) \quad (52)$$

where the number average molecular weight of the primary rubber molecules ( $M_n$ ) was obtained from measures of intrinsic viscosities (see above) using the relation (54):

$$[\eta]_{c=0} = 2.29 \times 10^{-7} M_n^{1.33} \quad (54)$$

The corrected concentration of physically-effective crosslinks was then calculated from:

$$[X]_{\text{phys}}^{\text{corr}} = [2M_c^{\text{corr}}, \text{phys}]^{-1} \quad (55)$$

(ii) Stress-strain measurements

This is adapted from the method of Gumbrell et al.<sup>121</sup>

The rubber samples were parallel strips approximately 50 x 4 x 2mm and were cut from flat sheets of acetone-extracted samples. Two reference lines A, A' (Fig. 93), approximately 2cm apart and equidistant from the ends, were marked on the samples. The width and thickness of the test samples were first measured at several points and the average cross-sectional area ( $A_0$ ) calculated. The width was measured by means of a travelling microscope, and the thickness by a dial gauge. This measurement of the cross-sectional area was subject to considerable inaccuracy because of experimental difficulties. Much of the difficulty in obtaining very accurate estimates of the cross-sectional area was due to the high deformability of the rubber, the rubber yielding slightly under the action of the cutting tool. As a result of this, their cross-sections were slightly wedge-shaped.

Small clamps B, B' were then fastened to the two ends of the sample. The sample was suspended in the apparatus by the end B and weights were added to the end B'. To minimize the effects of hysteresis, which is present in all vulcanized rubbers, the test samples were initially stretched for 15 min. to the maximum extension they were to receive subsequently and then allowed to recover for a similar period before the actual measurements were made. Then load increments ( $F$ ) were added and after 4 min. for each, the distance between the reference lines measured by means of a cathetometer, the experiment being carried out at room temperature. This distance was measured in the load

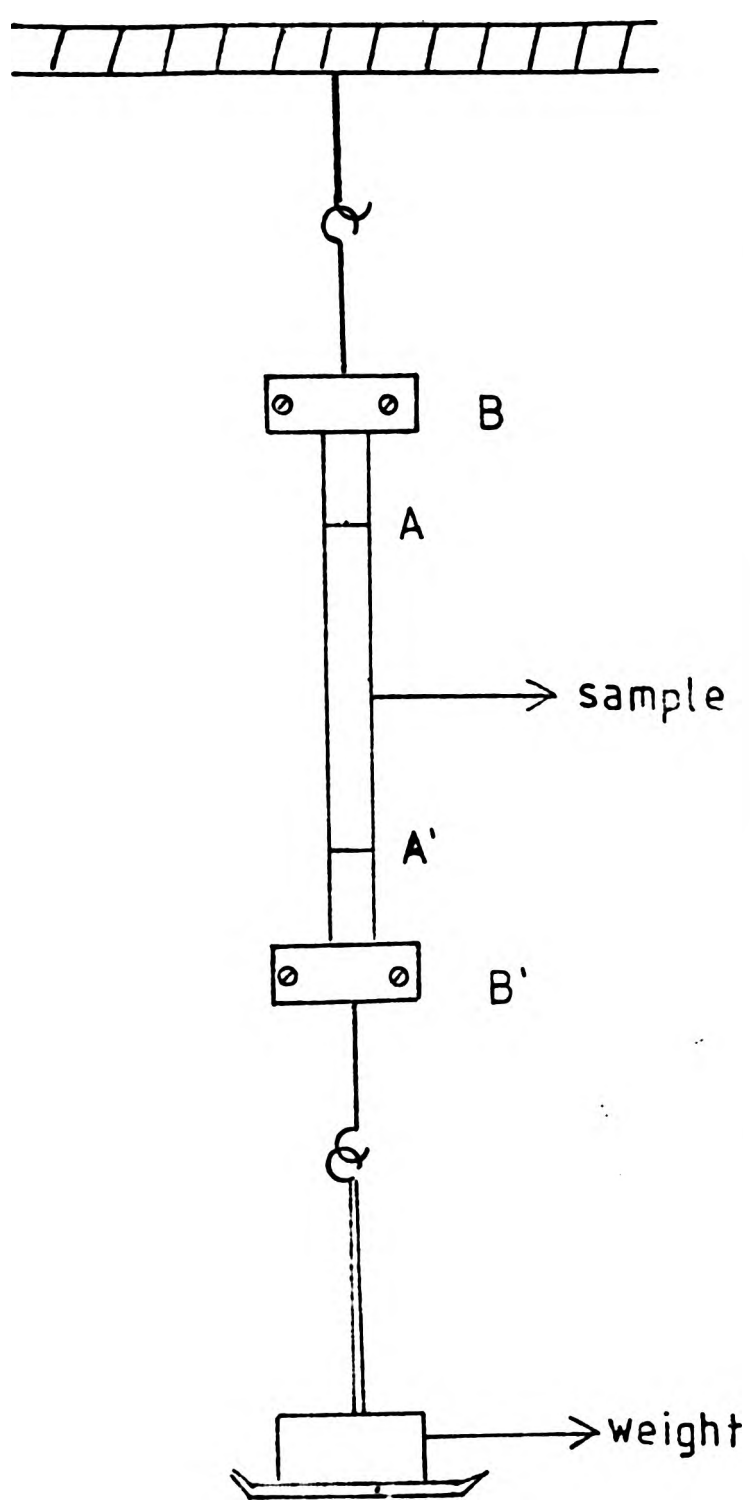


Fig. 93 Apparatus used for stress-strain measurements

increasing and load decreasing direction for each weight, and the average value determined ( $l_a$ ). The initial distance ( $l_0$ ) between the reference lines was found by extrapolating the load-distance curve to zero load. The extension ratio ( $\lambda$ ) corresponding to various loads then calculated by:

$$\lambda = \frac{l_a}{l_0} \quad (60)$$

Results were plotted in the form of  $f/2A_0(\lambda - \lambda^{-2})$  against  $\lambda^{-1}$  and the value of  $C_1$  of the Mooney-Rivlin function (47) obtained from the intercept ( $\lambda^{-1}=0$ ). Then  $M_c$  values were obtained from equation (48):

$$C_1 = 2^{-1} RT M_c^{-1} = \rho RT [X]_{\text{phys}} \quad (48)$$

The  $M_c^{\text{corr}}$ ,  $[X]_{\text{phys}}$  and  $[X]_{\text{phys}}^{\text{corr}}$  were then calculated from equations (52), (48) and (55), respectively.

(i) Determination of concentration of chemical crosslinks,  $[X]_{\text{chem}}$

The concentration of chemical crosslinks,  $[X]_{\text{chem}}$ , was calculated using the relationship between this and the concentration of physically-effective crosslinks,  $[X]_{\text{phys}}$ , proposed by Mullins<sup>120</sup>:

$$\begin{aligned} C_1 \text{ (in dynes cm}^{-2}\text{)} &= \rho RT [X]_{\text{phys}} \\ &= (\rho RT [X]_{\text{chem}} + 0.78 \times 10^6) \left(1 - \frac{2.3}{2} [X]_{\text{chem}}^{-1} \bar{M}_n^{-1}\right) \end{aligned} \quad (53)$$

where  $\rho$  is the density of the unswollen-vulcanizate,  $R$  the gas constant per gram-molecule,  $T$  the absolute temperature and  $M_n$  the number average molecular weight of the primary rubber molecules which was obtained as described in Section (g) above. Note that the uncorrected values,  $[X]_{\text{phys}}$ , are used in equation (53).

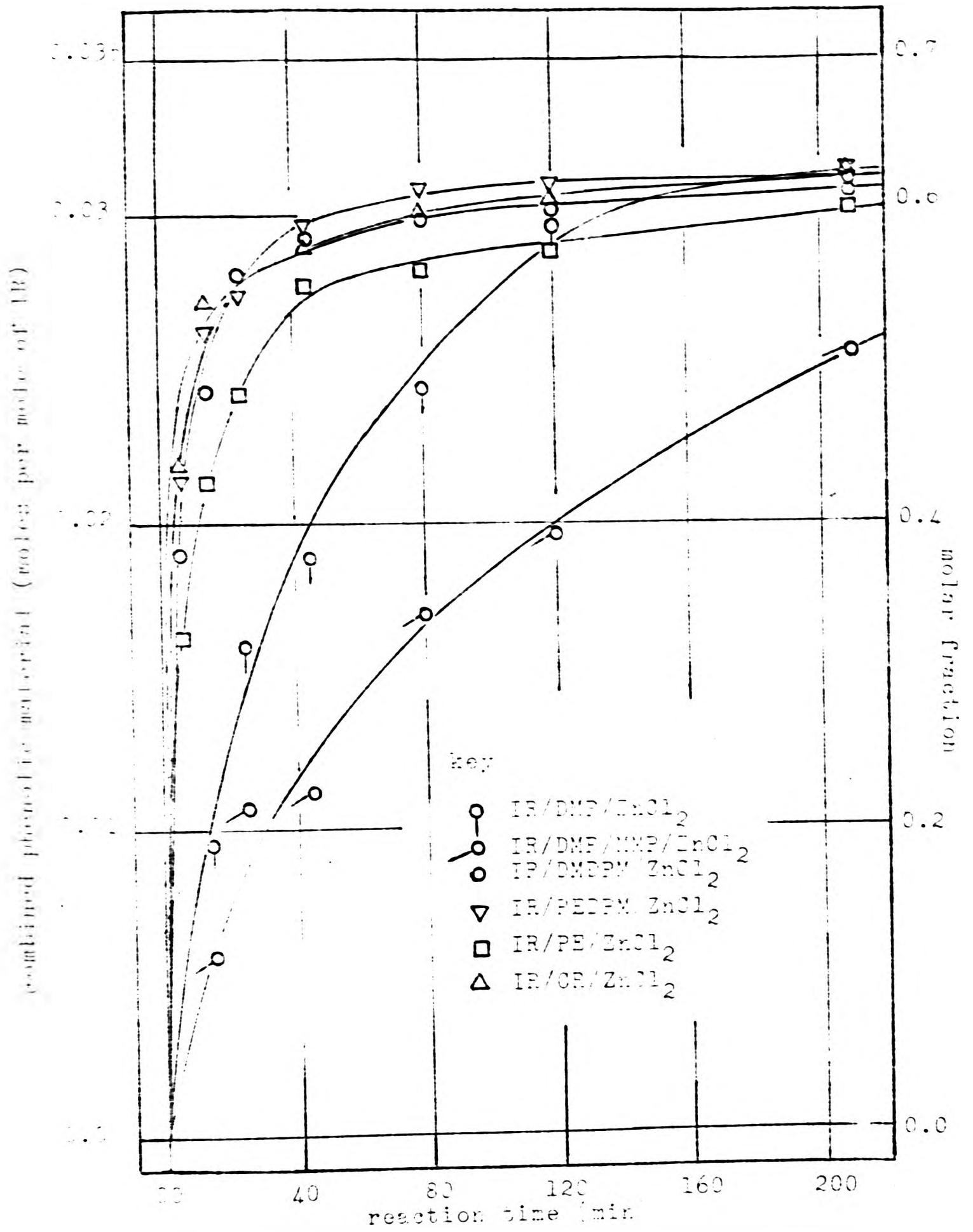


Fig. 91 Kinetics of combination of phenolic material as calculated from the amount of acetone extract.

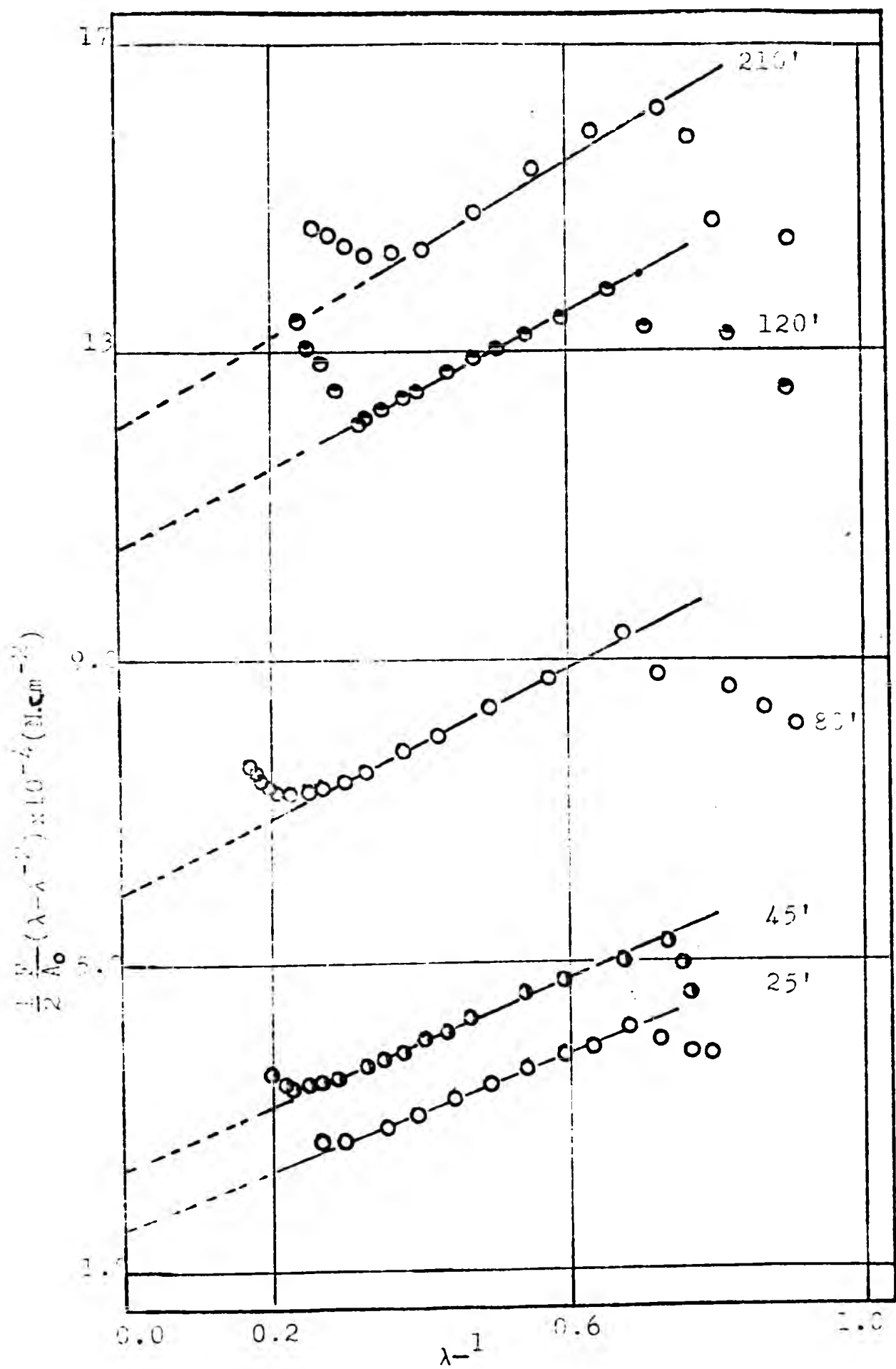


Fig. 95 Determination of the elastic constant  $C_1$  for the IP/DMP/ $ZnCl_2$  interaction at various reaction times as obtained from the intercept ( $\lambda^{-1}=0$ ).

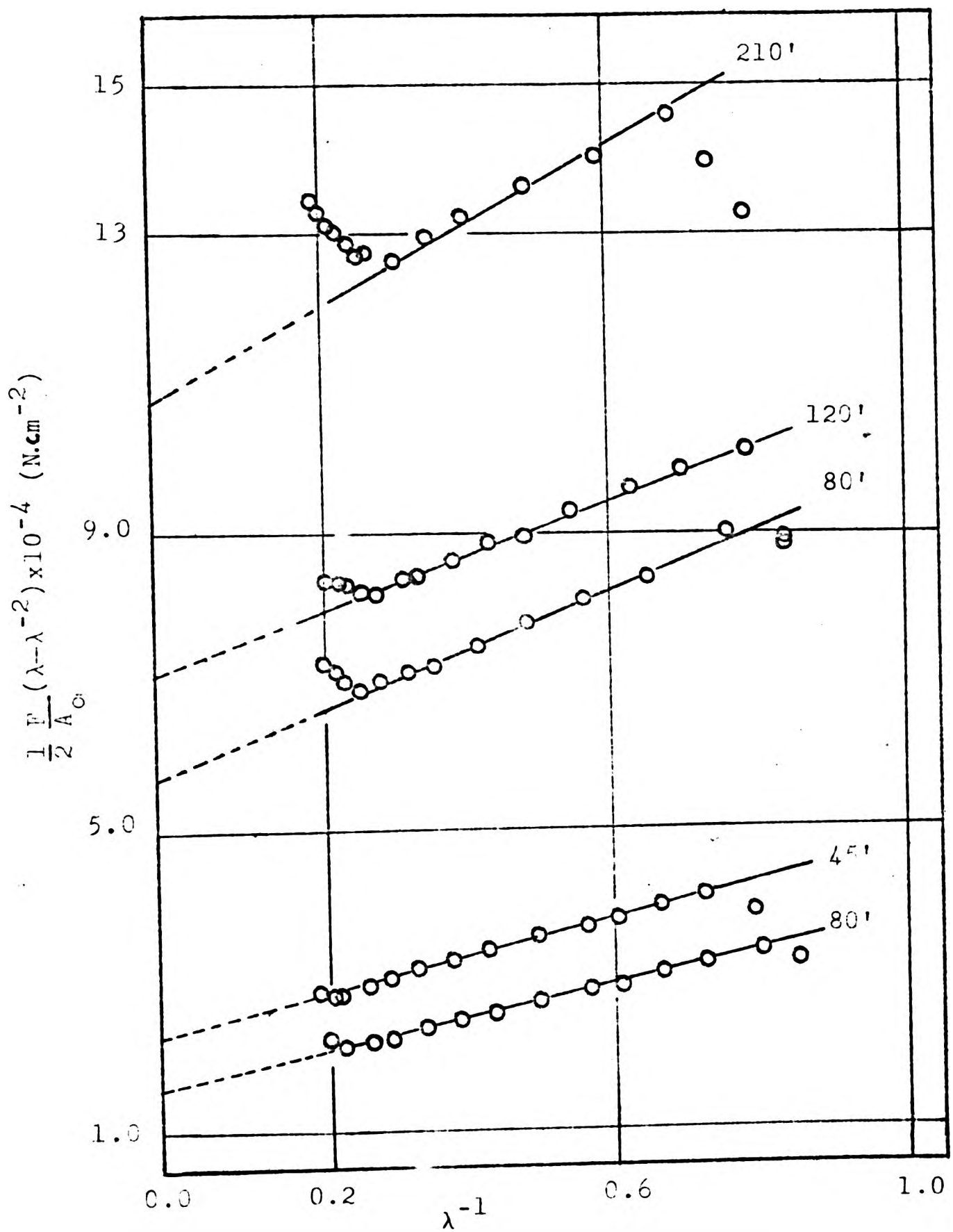


Fig. 96 Determination of the elastic constant  $C_1$  for the IR/DMP/MMP/ZnCl<sub>2</sub> interaction at various reaction times as obtained from the intercept ( $\lambda^{-1}=0$ ).

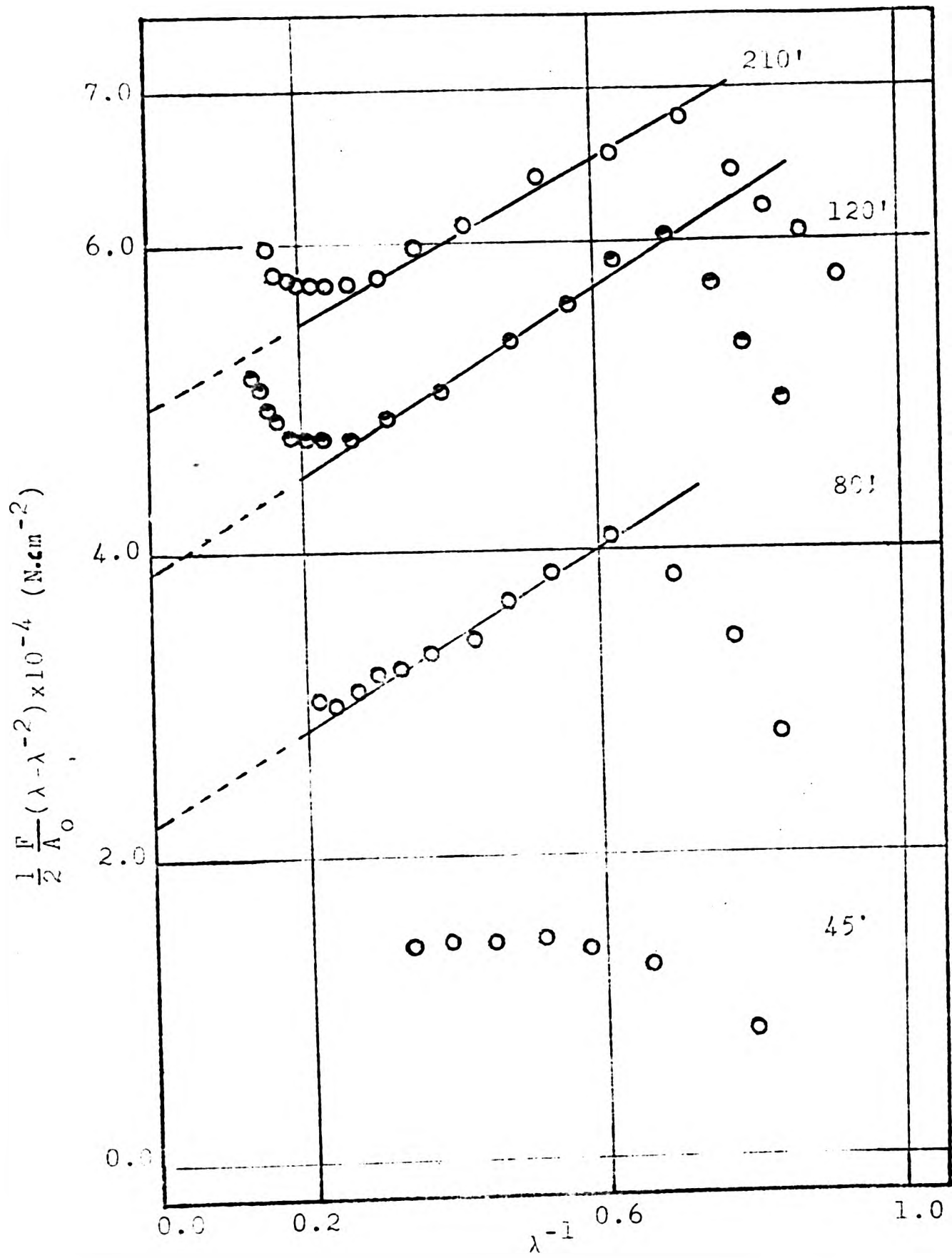


Fig. 97 Determination of the elastic constant  $C_1$  for the IR/DMP/ $M_x$ /ZnCl<sub>2</sub> interaction at various reaction times as obtained from the intercept ( $\lambda^{-1}=0$ ).

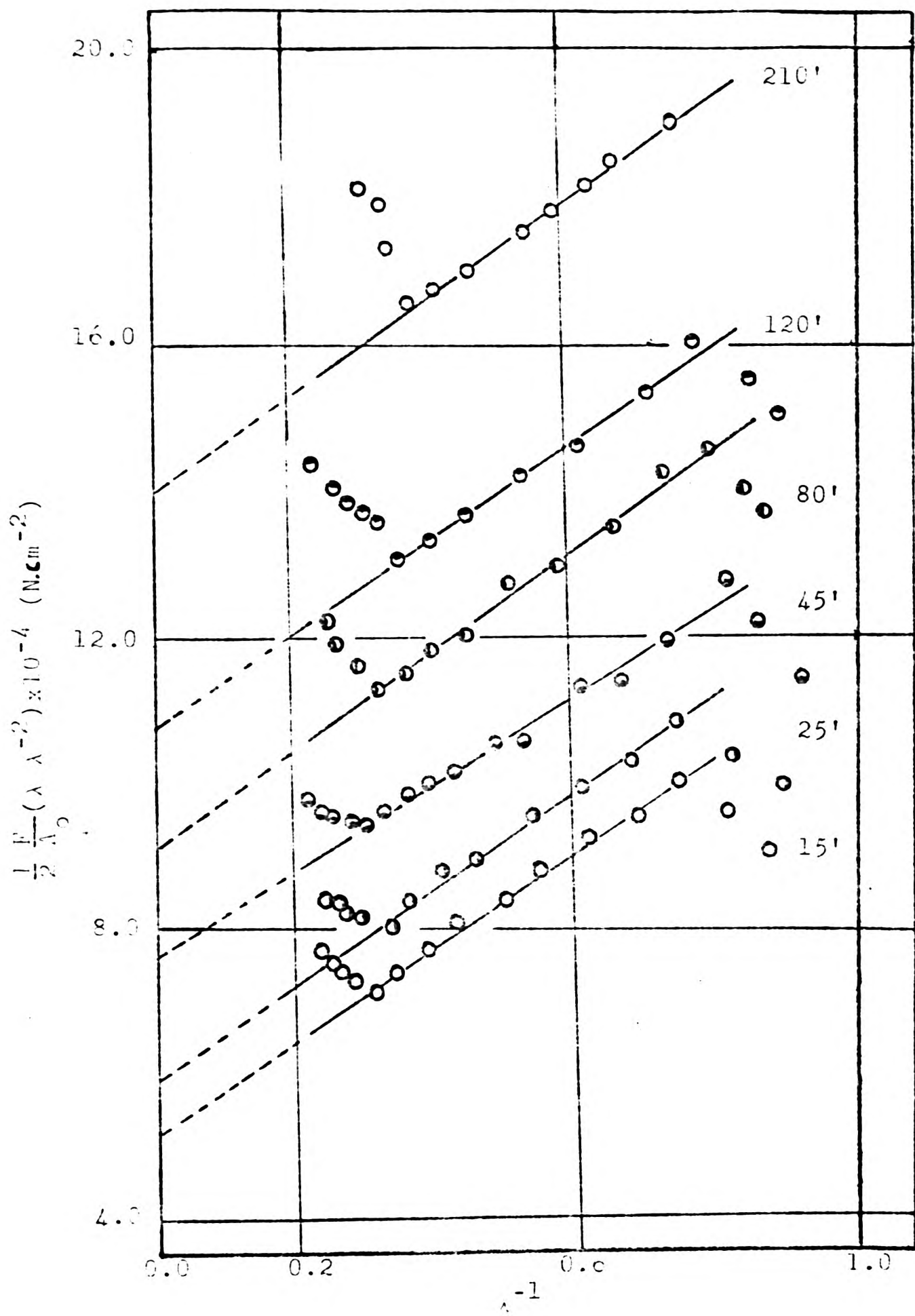


Fig. 98 Determination of the elastic constant  $G_1$  for the IR/DMDPM\*/ZnCl<sub>2</sub> interaction at various reaction times as obtained from the intercept ( $\lambda - \lambda^{-1} = 0$ ).

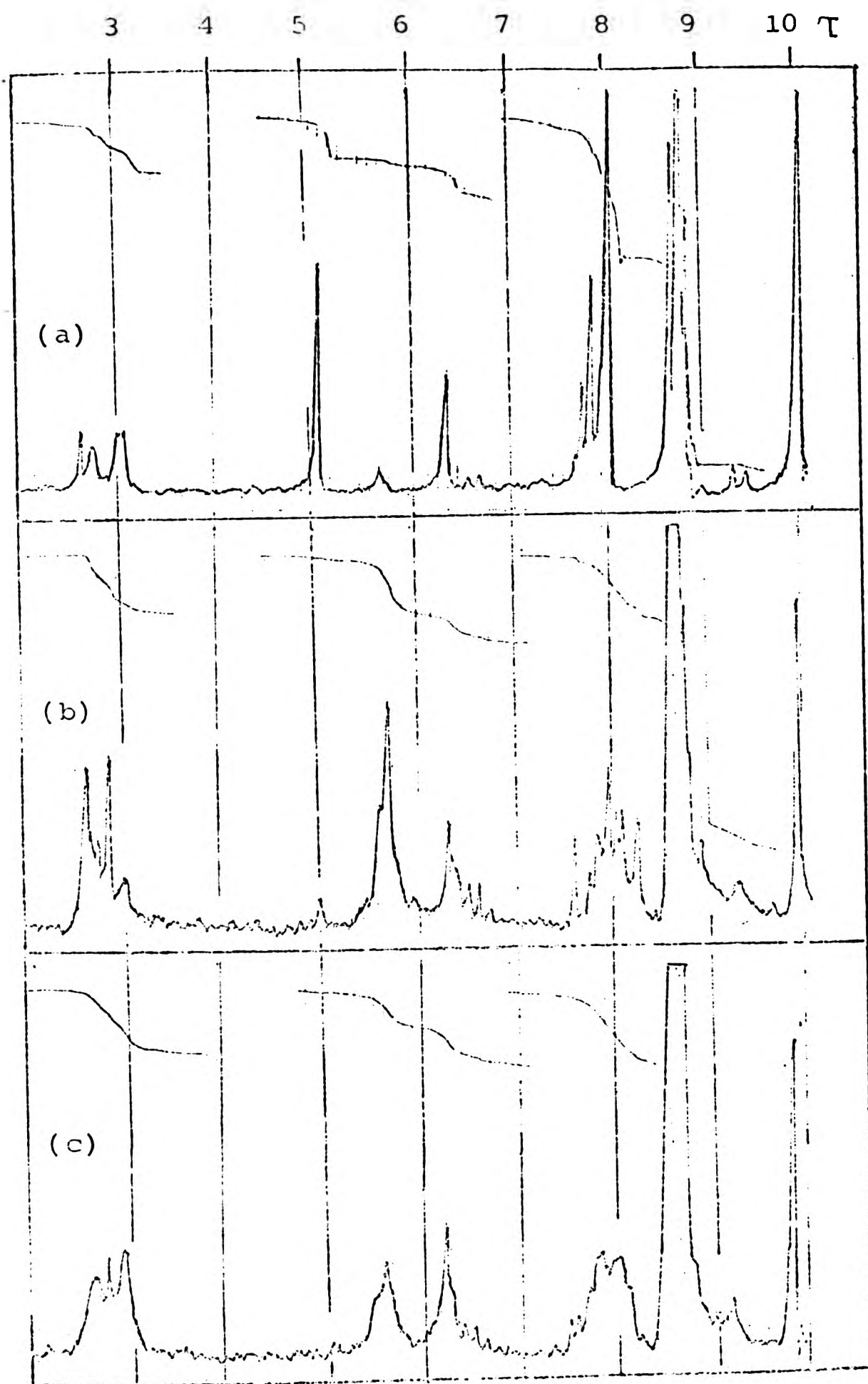


Fig. 99 Nuclear magnetic resonance spectra of the acetylated materials: (a) dimethylol diphenyl methane; (b) polybenzyl ether; (c) ether derivative of the dimethylol diphenyl methane; (d) commercial resin; (e) dimethylolphenol (f) dibenzyl ether; (g) methylolphenol.

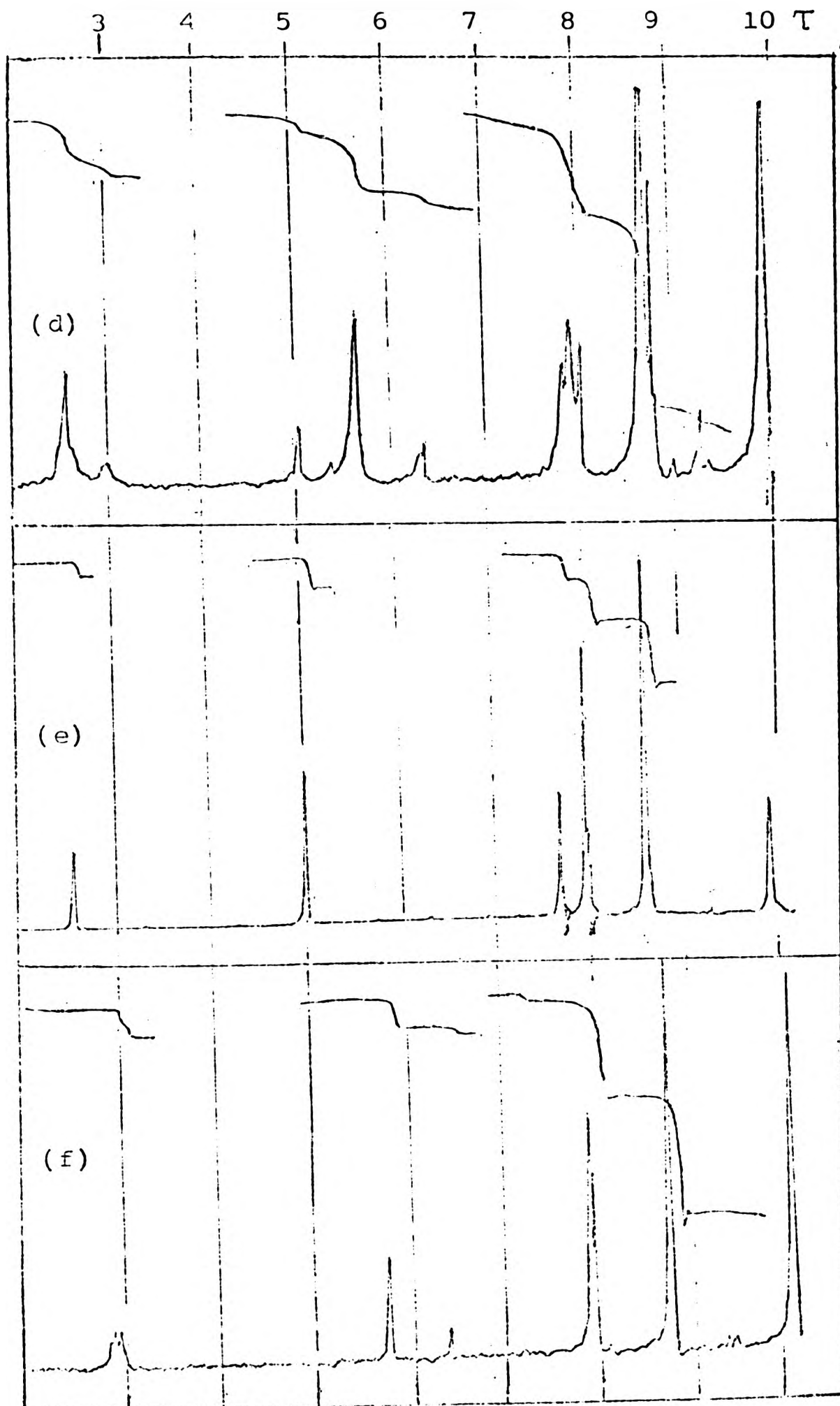


Fig. 99 (continued)

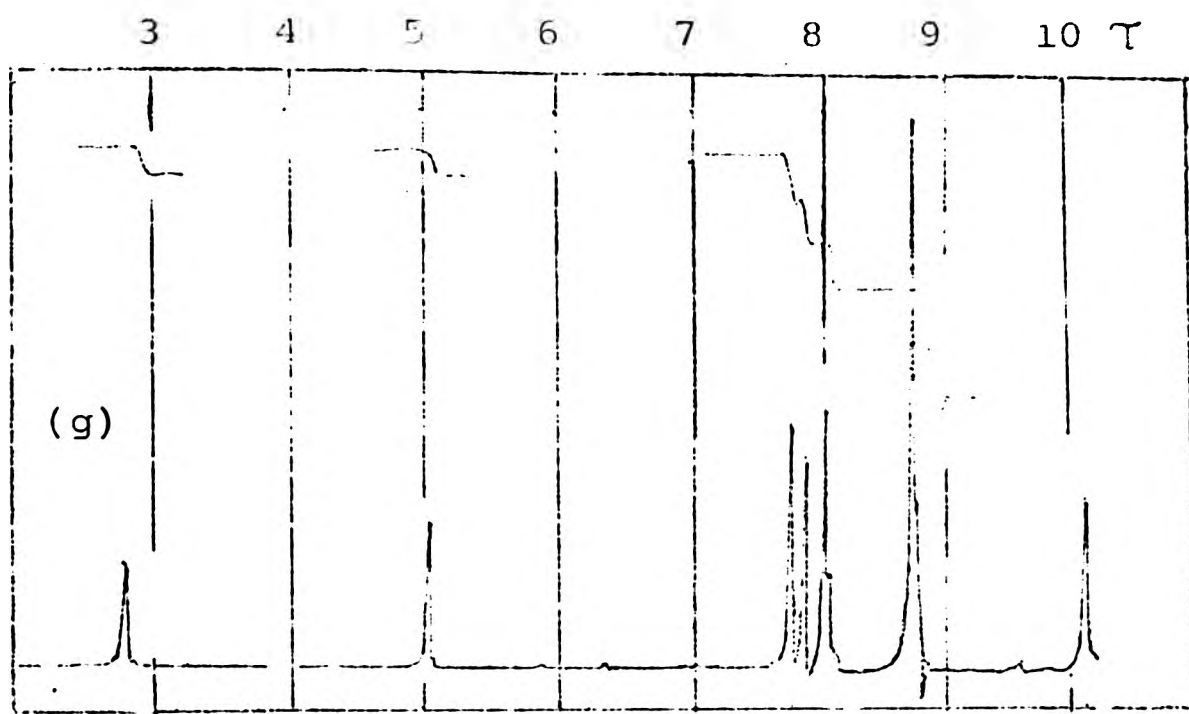


Fig. 99 (continued)

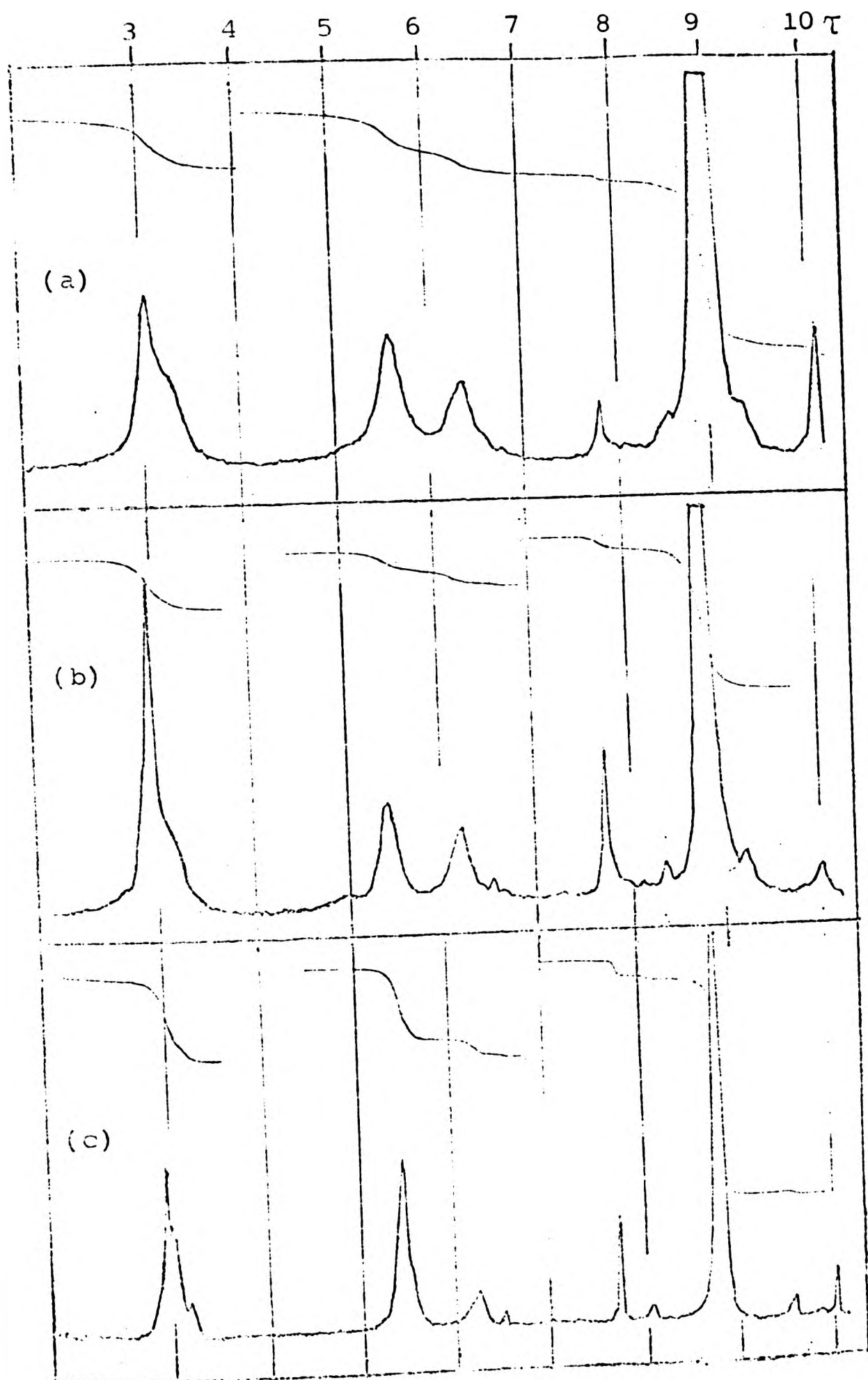


Fig. 100 Nuclear magnetic resonance spectra of (a) dimethylol diphenyl methane; (b) ether derivative of the dimethylol diphenyl methane; (c) polybenzyl ether; (d) commercial resin.

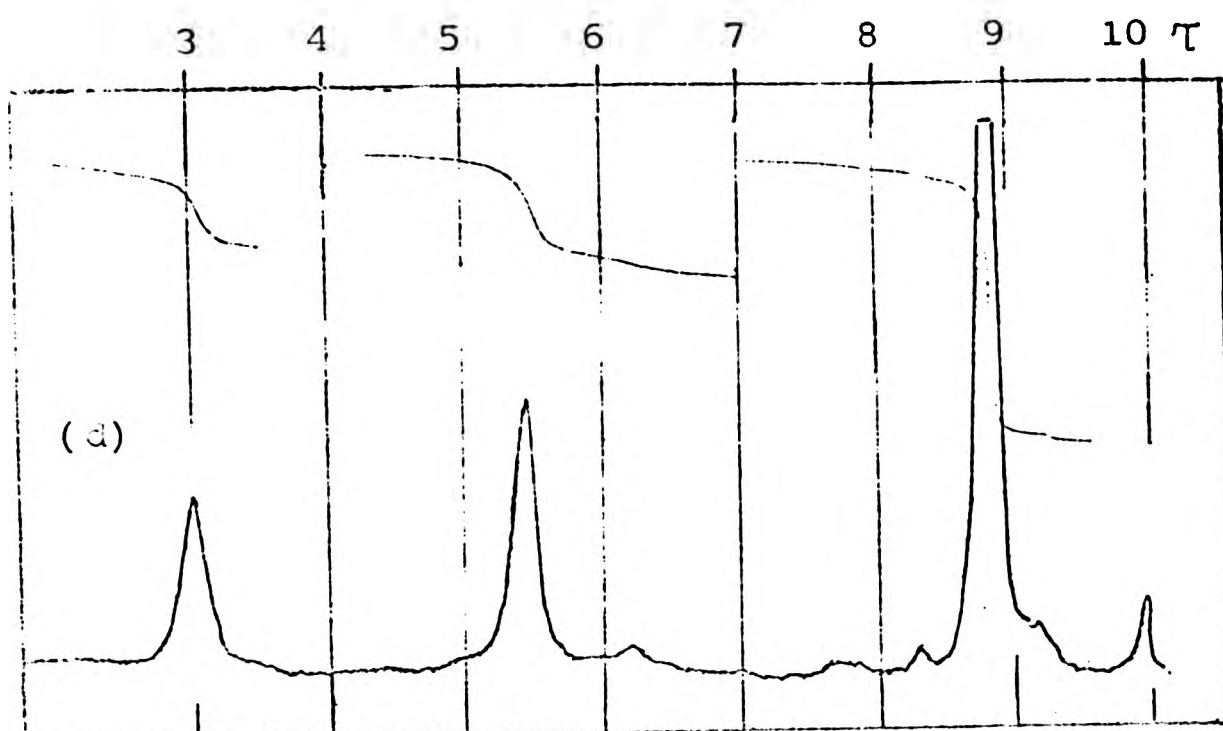


Fig. 100 (continued)

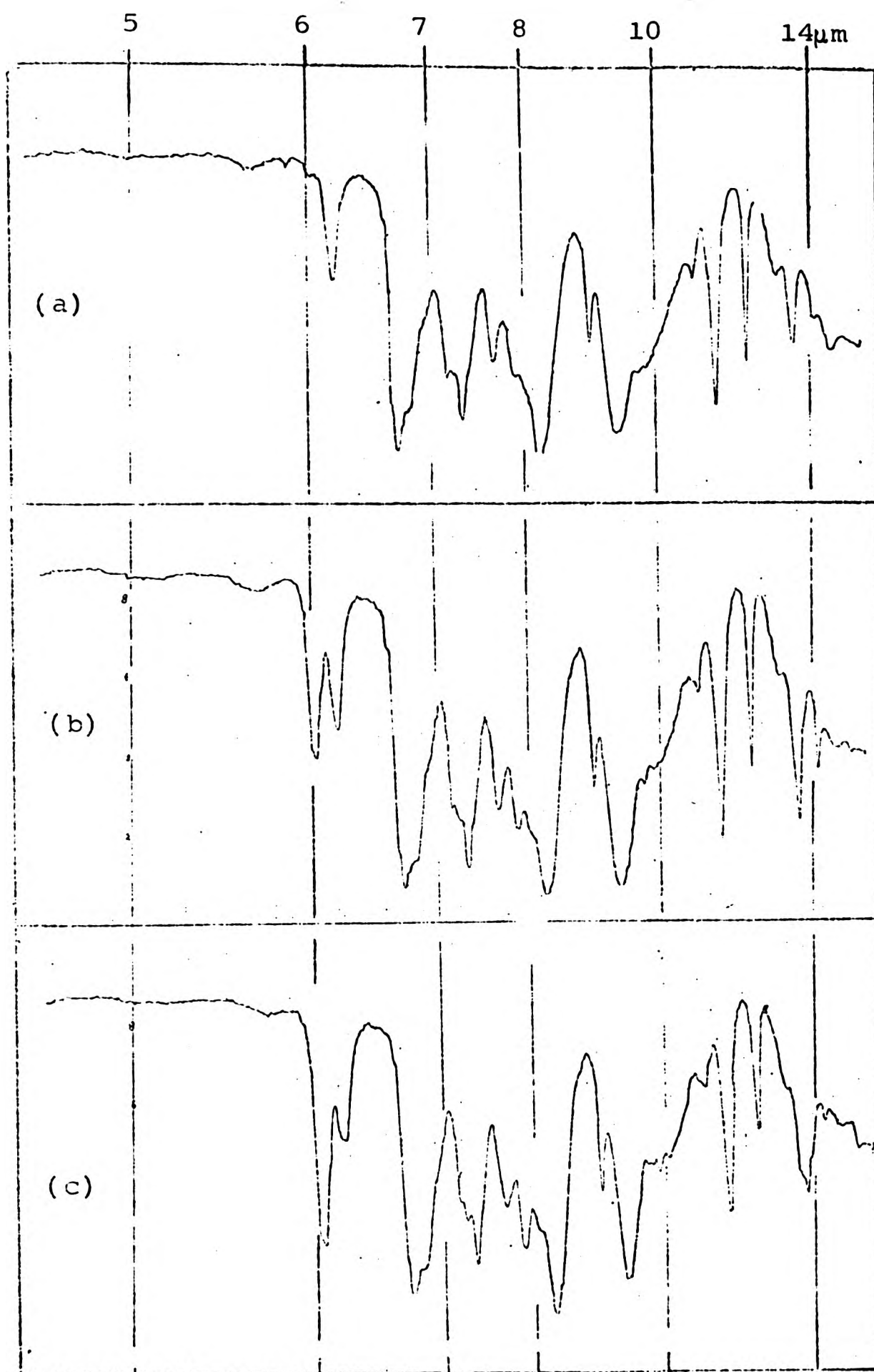


Fig. 101 Infra-red spectra of DMP/ $\text{SnCl}_2 \cdot 2\text{H}_2\text{O}$  products refluxed in toluene for various times: (a) 2 min; (b) 10 min; (c) 20 min.

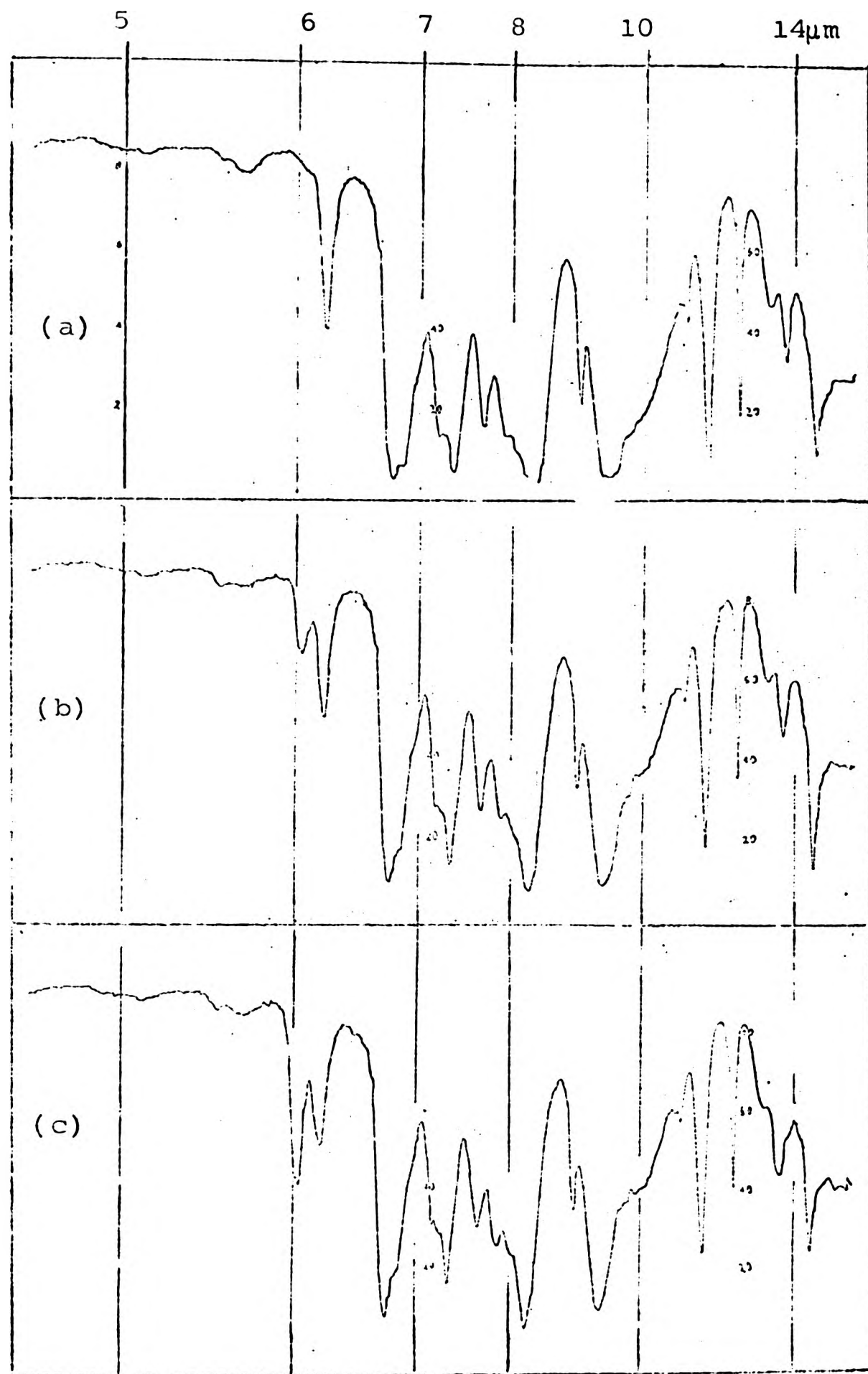


Fig. 102 Infra-red spectra of  $\text{DMP}/\text{SnCl}_2 \cdot 2\text{H}_2\text{O}$  products refluxed in benzene for various times: (a) 30 min; (b) 70 min; (c) 120 min.

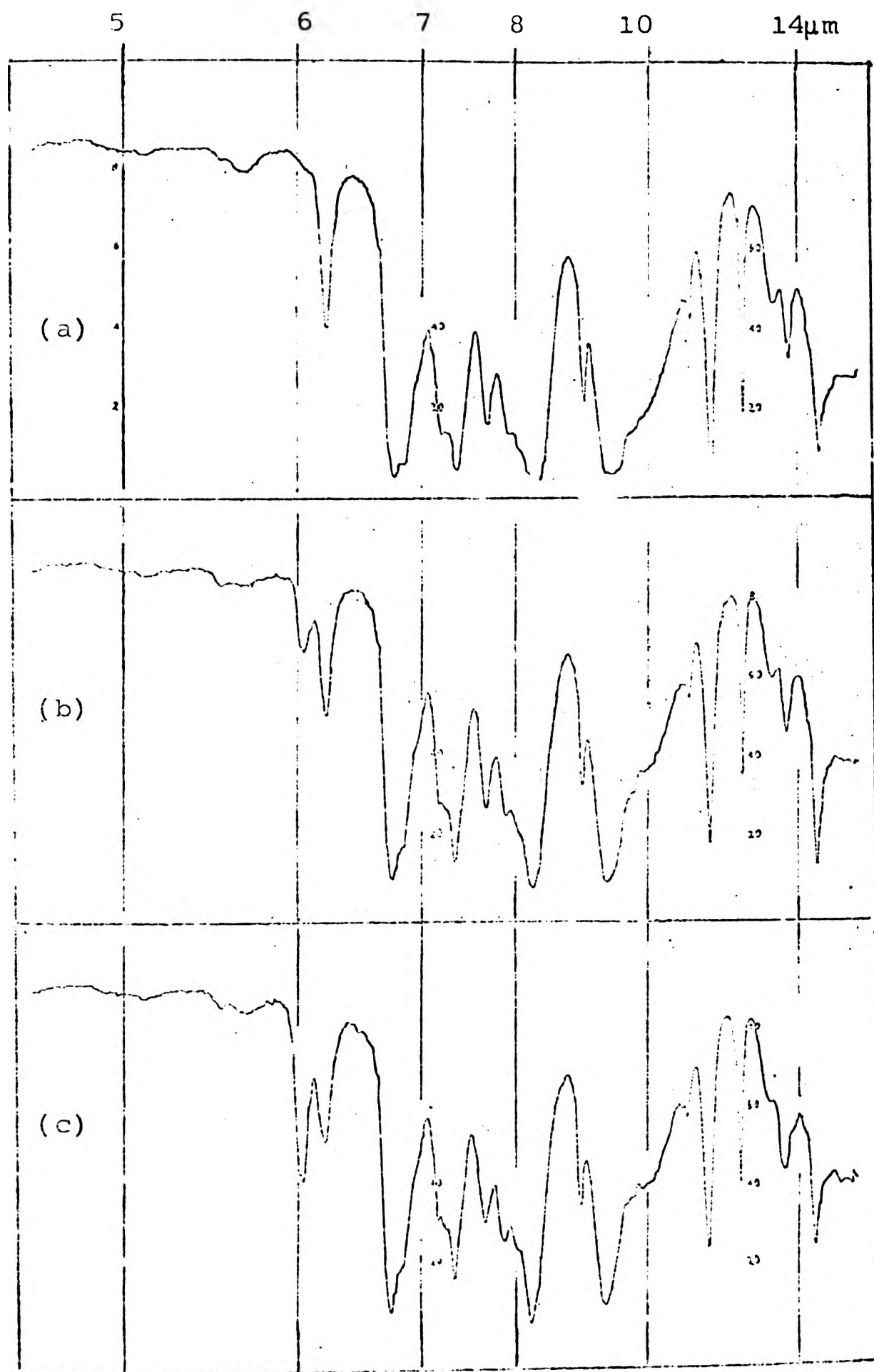


Fig. 102 Infra-red spectra of DMP/SnCl<sub>2</sub>·2H<sub>2</sub>O products refluxed in benzene for various times: (a) 30 min; (b) 70 min; (c) 120 min.

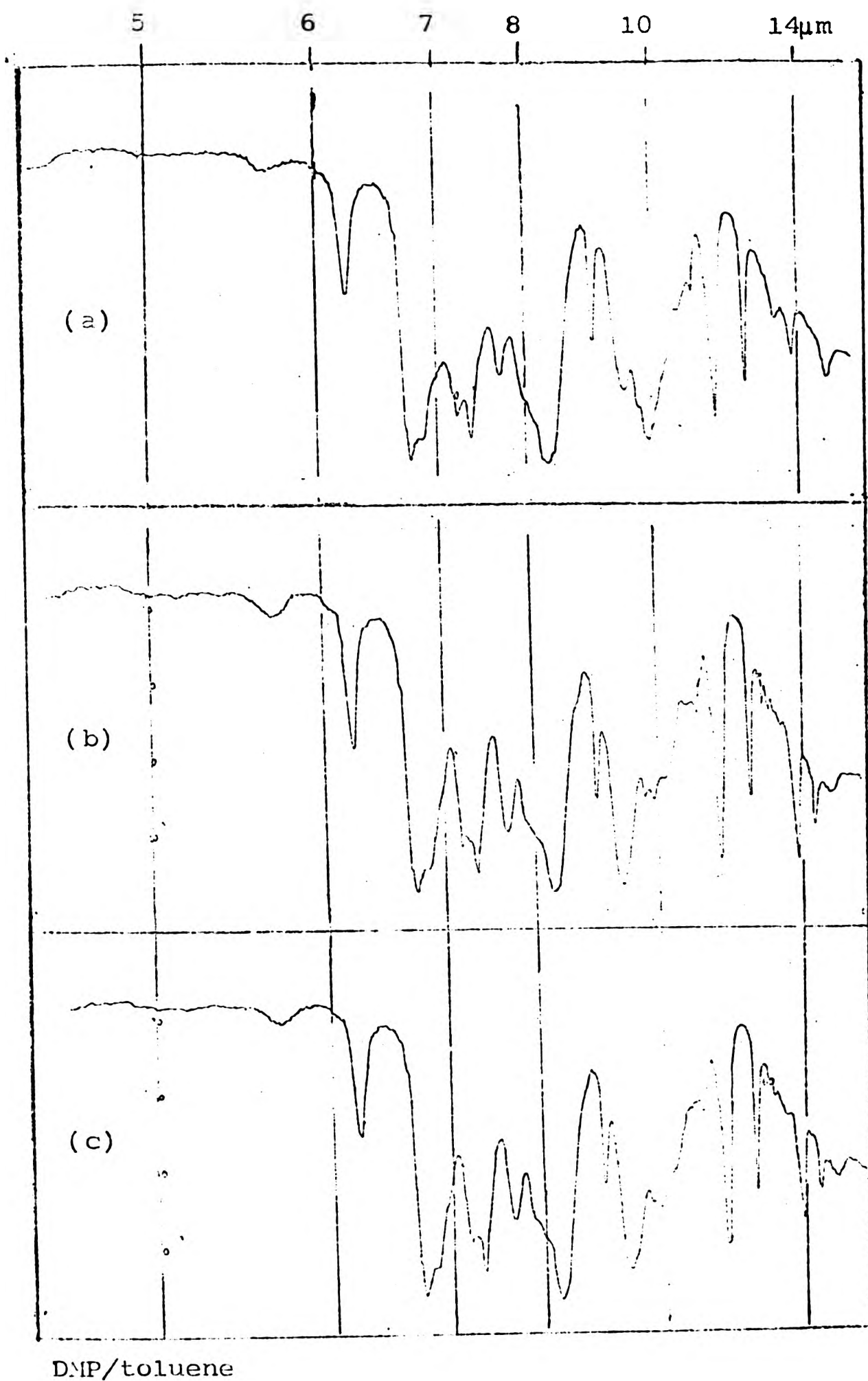


Fig. 104 Infra-red spectra of DMP refluxed in toluene for various times: (a) 1h; (b) 27h; (c) 47h.

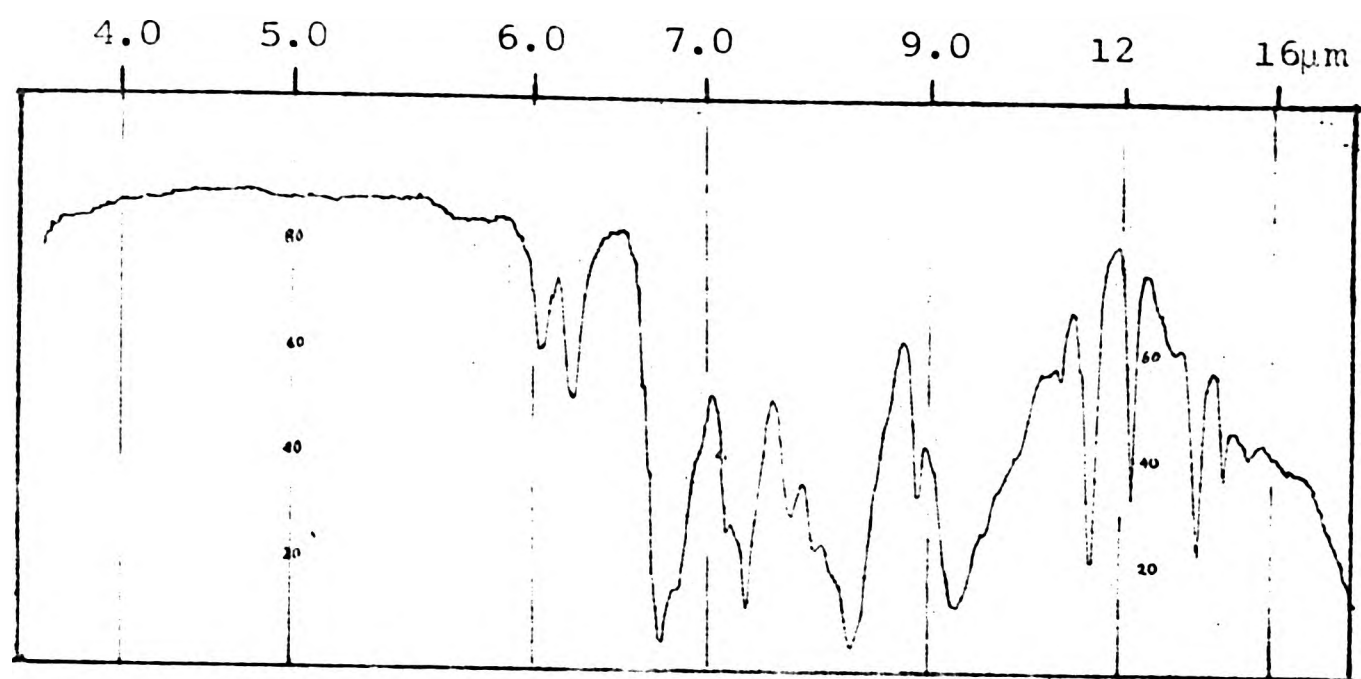


Fig. 105 Infra-red spectrum of the commercial resin

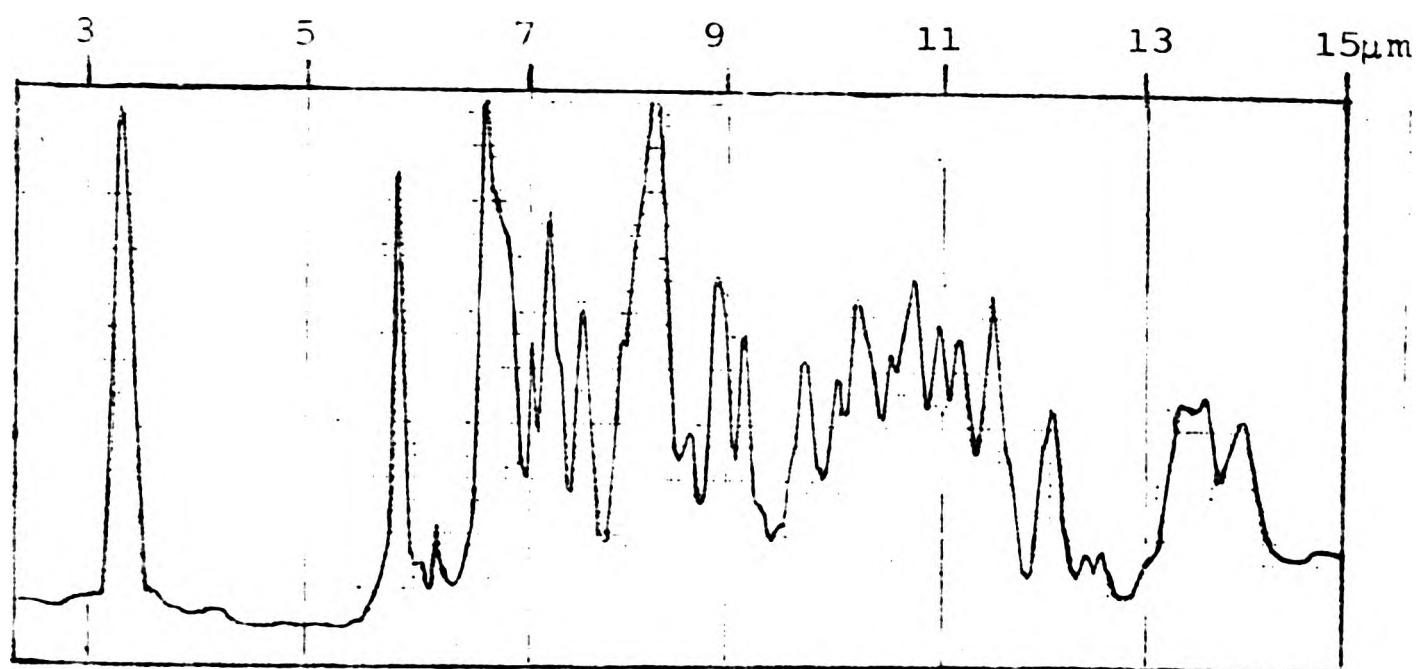


Fig. 106 Infra-red spectrum of the trimer VI<sup>11</sup>

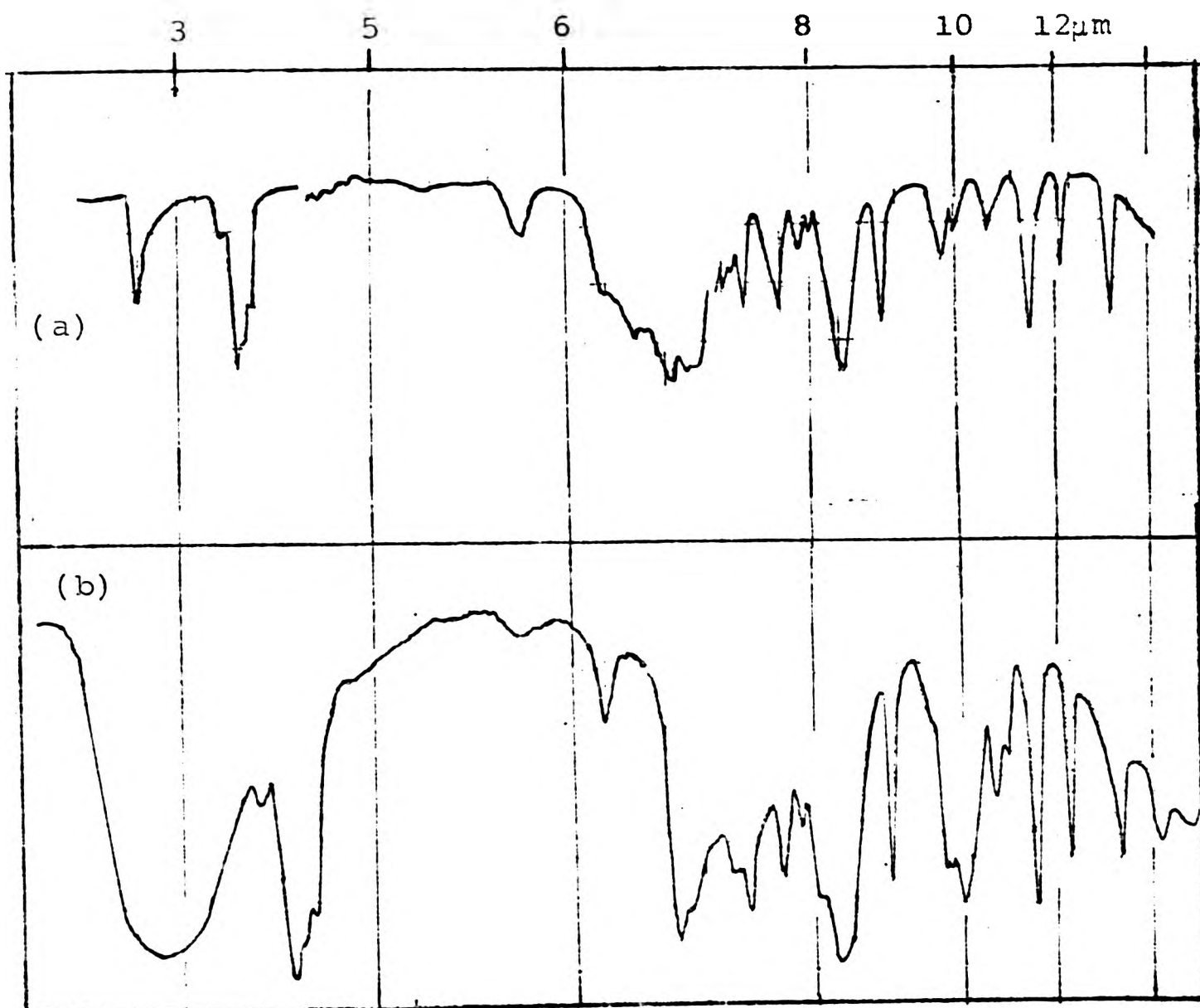


Fig. 107 Infra-red spectra of: (a) 2,6-dimethyl-4-tert-butyl-phenol; (b) methylolphenol.

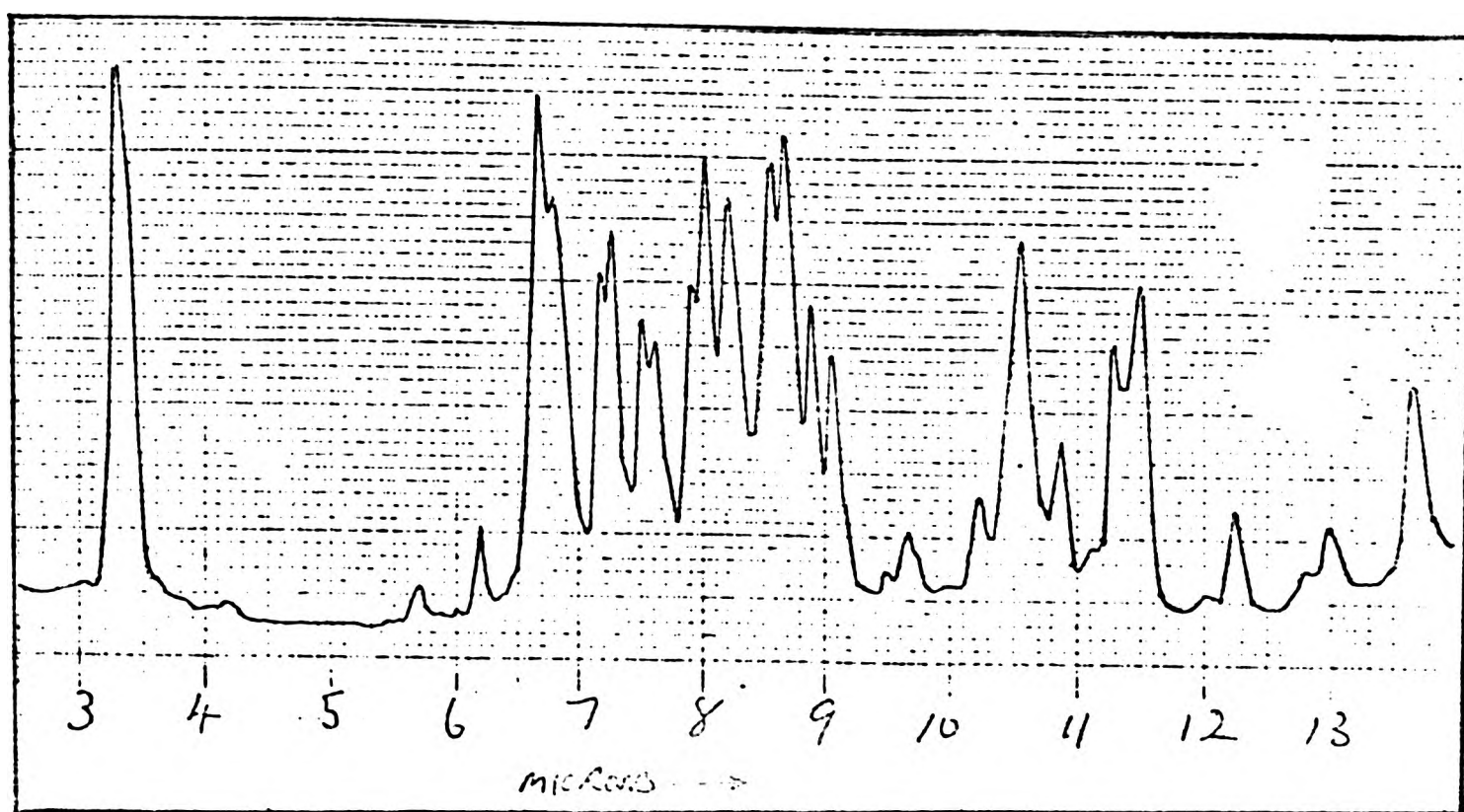


Fig. 108 Infra-red spectrum of the internal chroman XXXIII.<sup>11</sup>

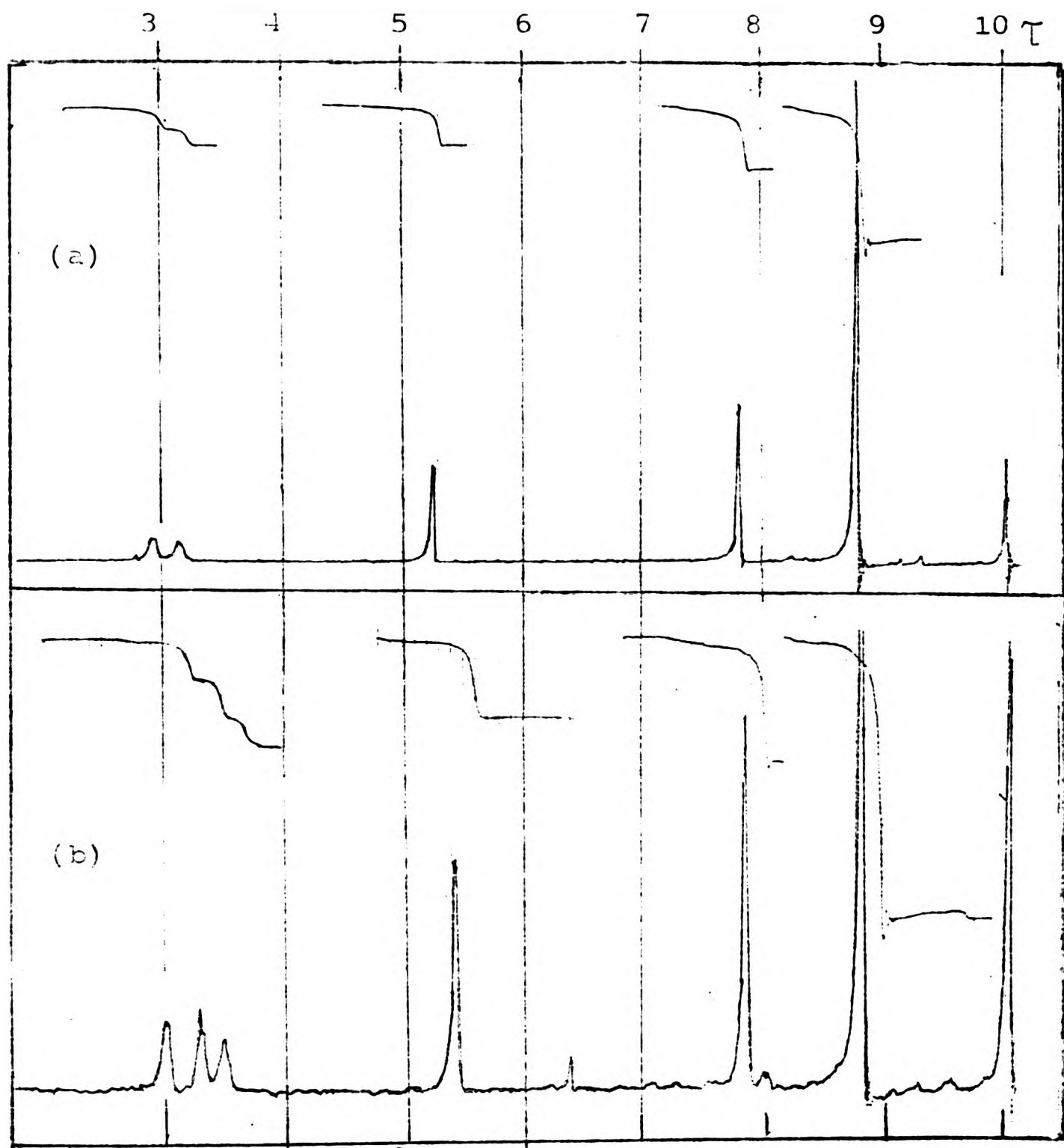


Fig. 109 Nuclear magnetic resonance spectra of: (a) methylphenol; (b) dibenzyl ether.

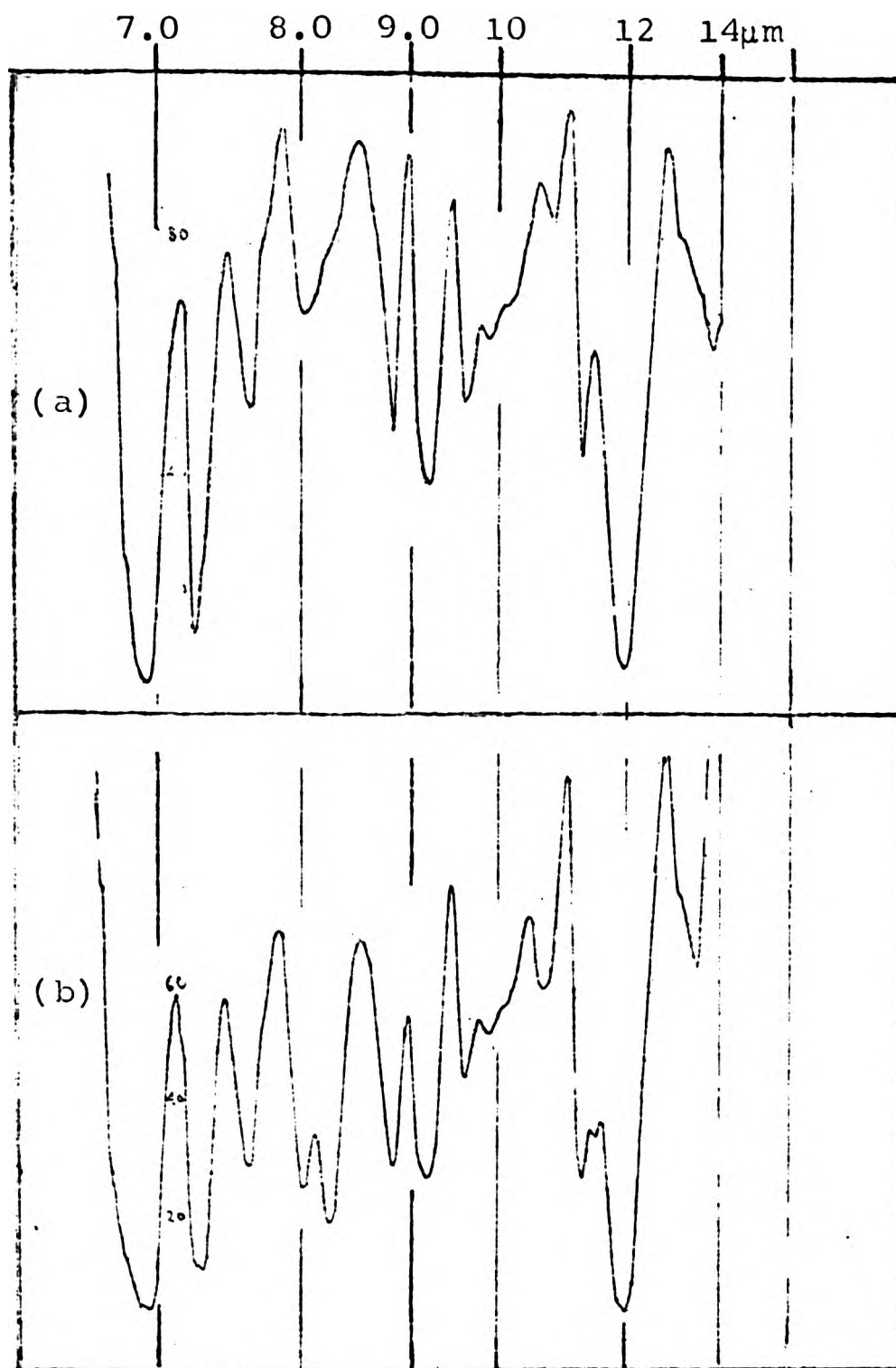


Fig. 110 Infra-red spectra of:  
(a) Isoprene rubber; (b) IR/PE/ZnCl<sub>2</sub>  
interaction product heated at 160°C  
for 210 min.

Table 12 Determination of concentration of physically effective crosslinks  $[X]_{\text{phys}}^{\text{corr}}$  for various interactions at different reaction times as obtained from measurements of swelling in n-decane and benzene and from equilibrium modulus.

Interaction	Reaction time (min)	$[X]_{\text{phys}}^{\text{corr}}$ (moles crosslinks / g vulcanizate) $\times 10^5$		
		a	b	c
IR/DMP/ZnCl <sub>2</sub>	25	2.78	3.46	2.48
	45	3.62	4.93	2.84
	80	5.53	11.28	4.49
	120	8.44	14.20	6.53
	210	10.83	17.72	7.00
IR/DMP/MMP/ZnCl <sub>2</sub>	25	2.39	3.42	2.58
	45	3.03	4.91	2.90
	80	5.03	10.53	4.49
	120	6.47	12.51	5.13
	210	9.04	15.88	6.77
IR/DMP/Mx/ZnCl <sub>2</sub>	45	2.39	2.63	-
	80	3.85	6.58	3.07
	120	5.52	9.47	3.82
	210	5.94	9.66	4.31
IR/DMDPM/ZnCl <sub>2</sub>	7	6.74	11.75	-
	15	10.36	16.84	-
	25	12.50	21.87	-
	45	13.77	25.00	-
	80	14.27	27.10	-
	120	14.95	29.83	-
	210	16.46	30.71	-
IR/DMDPM* /ZnCl <sub>2</sub>	7	3.60	6.10	2.80
	15	5.78	9.93	4.09
	25	7.50	12.99	4.43
	45	8.87	15.36	5.20
	80	10.62	17.50	5.88
	120	11.75	20.43	6.61
	210	12.77	21.84	8.07
IR/PEDPM/ZnCl <sub>2</sub>	7	9.76	15.83	-
	15	11.82	20.90	-
	25	12.71	22.81	-
	45	14.04	25.41	-
	80	14.81	26.46	-
	120	14.83	27.40	-
	210	14.86	27.41	-

Table 12 (continued)

Interaction	Reaction time (min)	$[X]_{\text{phys}}^{\text{corr}} \left( \frac{\text{moles crosslinks}}{\text{g vulcanizate}} \right) \times 10^5$		
		a	b	c
IR/PE/ZnCl <sub>2</sub>	7	9.41	16.94	-
	15	12.50	22.50	-
	25	15.10	26.29	-
	45	17.32	30.40	-
	80	18.51	32.13	-
	120	19.28	32.60	-
	210	20.24	33.11	-
IR/PE/Mx/ZnCl <sub>2</sub>	7	11.51	24.39	-
	15	13.85	28.49	-
	25	16.46	31.06	-
	45	18.57	35.61	-
	80	19.89	37.43	-
	120	22.00	41.39	-
	210	22.55	45.00	-
IR/CR/ZnCl <sub>2</sub>	7	9.61	17.04	-
	15	12.12	23.00	-
	25	15.28	26.16	-
	45	17.98	29.50	-
	80	18.63	31.59	-
	120	19.19	34.41	-
	210	19.99	35.46	-

a = Determined from swelling in benzene

b = Determined from swelling in n-decane

c = Determined from equilibrium modulus

Table 13 Concentration of physically crosslinks  $[X]_{\text{phys}}$  for various interactions at different reaction times as obtained from measurements of swelling in n-decane and benzene and from equilibrium modulus.

Interaction	Reaction time (min)	$[X]_{\text{phys}}$ ( $\frac{\text{moles crosslinks}}{\text{g vulcanizate}}$ ) $\times 10^5$		
		a	b	c
IR/DMP/ZnCl <sub>2</sub>	25	1.01	1.68	0.70
	45	1.85	3.16	1.06
	80	3.75	9.57	2.72
	120	6.67	12.42	4.76
	210	10.06	15.95	5.23
IR/DMP/MMP/ZnCl <sub>2</sub>	25	0.56	1.59	0.75
	45	1.21	3.09	1.07
	80	3.21	8.70	2.67
	120	4.65	10.70	3.31
	210	7.21	14.05	4.95
IR/DMP/M <sub>x</sub> /ZnCl <sub>2</sub>	45	0.36	0.60	-
	80	1.82	4.55	1.04
	120	3.49	7.44	1.79
	210	3.91	7.63	2.27
IR/DMDPM/ZnCl <sub>2</sub>	7	4.96	9.96	-
	15	8.58	10.06	-
	25	10.72	20.10	-
	45	11.99	23.23	-
	80	12.48	25.32	-
	120	13.17	28.06	-
	210	14.68	28.94	-
IR/DMDPM*/ZnCl <sub>2</sub>	7	1.84	4.34	1.13
	15	4.12	8.17	2.33
	25	5.74	11.23	2.67
	45	7.11	13.60	3.44
	80	8.86	15.74	4.12
	120	9.99	18.66	4.85
	210	11.01	20.08	6.31
IR/PEDPM/ZnCl <sub>2</sub>	7	7.94	14.00	-
	15	9.99	19.08	-
	25	10.88	20.99	-
	45	12.21	23.58	-
	80	12.98	24.63	-
	120	13.01	25.58	-
	210	13.03	25.59	-

Table 13 (continued)

Interaction	Reaction time (min)	$[X]_{\text{phys}}$ ( $\frac{\text{moles crosslinks}}{\text{g vulcanizate}}$ ) $\times 10^5$		
		a	b	c
IR/PE/ZnCl <sub>2</sub>	7	7.77	15.30	-
	15	10.87	20.87	-
	25	13.46	24.65	-
	45	15.68	28.86	-
	80	16.87	30.49	-
	120	17.64	30.95	-
	210	18.60	31.47	-
IR/PE/M <sub>x</sub> /ZnCl <sub>2</sub>	7	9.69	22.56	-
	15	12.03	26.67	-
	25	14.63	29.22	-
	45	16.75	33.88	-
	80	18.06	35.61	-
	120	20.18	39.56	-
	210	20.73	43.17	-
IR/CR/ZnCl <sub>2</sub>	7	7.83	15.26	-
	15	10.34	21.22	-
	25	13.50	24.39	-
	45	16.20	27.89	-
	80	16.85	29.80	-
	120	17.41	32.64	-
	210	18.21	33.67	-

a = Determined from swelling in benzene

b = Determined from swelling in n-decane

c = Determined from equilibrium modulus

Table 14 Determination of concentration of chemical crosslinks,  $[X]_{\text{chem}}$ , for various interactions at different reaction times as obtained from the physically effective crosslinks  $[X]_{\text{phys}}$  determined by swelling in benzene, and n-decane and from equilibrium modulus

Interaction	Reaction time (min)	$[X]_{\text{chem}}$ ( $\frac{\text{moles crosslinks}}{\text{g vulcanizate}} \times 10^5$ )		
		a	b	c
IR/DMP/ZnCl <sub>2</sub>	25	1.20	1.47	0.96
	45	1.55	2.30	1.21
	80	2.72	8.85	2.02
	120	5.18	10.67	3.51
	210	8.37	14.13	3.90
IR/DMP/MMP/ZnCl <sub>2</sub>	25	0.80	1.47	1.15
	45	1.11	2.31	1.26
	80	2.39	7.12	2.04
	120	3.70	9.04	2.45
	210	7.00	12.31	3.72
IR/DMP/M <sub>x</sub> /ZnCl <sub>2</sub>	45	0.35	0.59	-
	80	1.75	3.60	1.40
	120	2.79	6.15	1.74
	210	3.10	6.32	1.99
IR/DMDPM/ZnCl <sub>2</sub>	7	3.68	8.29	-
	15	6.96	13.26	-
	25	9.02	18.25	-
	45	10.25	21.36	-
	80	10.73	23.44	-
	120	11.41	26.17	-
	210	12.89	28.04	-
IR/DMDPM*	7	1.53	3.15	1.23
	15	2.98	6.56	1.8
	25	4.33	9.49	1.98
	45	5.57	11.81	2.48
	80	7.21	13.92	2.98
	120	8.29	16.80	3.57
	210	9.28	18.21	4.84
IR/PEDPM/ZnCl <sub>2</sub>	7	6.41	12.26	-
	15	8.36	1.28	-
	25	9.22	19.17	-
	45	10.51	21.75	-
	80	11.26	22.79	-
	120	11.29	23.74	-
	210	11.31	23.75	-

Table 14 (continued)

Interaction	Reaction time (min)	$[X]_{\text{chem}} \left( \frac{\text{moles crosslinks}}{\text{g vulcanizate}} \right) \times 10^5$		
		a	b	c
IR/PE/ZnCl <sub>2</sub>	7	6.06	13.37	-
	15	9.02	18.84	-
	25	11.56	22.64	-
	45	13.74	26.74	-
	80	14.92	28.46	-
	120	15.68	28.92	-
	210	16.63	29.44	-
IR/PE/M <sub>x</sub> /ZnCl <sub>2</sub>	7	8.07	20.73	-
	15	10.34	24.82	-
	25	12.88	27.36	-
	45	14.97	31.90	-
	80	16.27	33.83	-
	120	18.37	37.68	-
	210	18.92	41.28	-
IR/CR/ZnCl <sub>2</sub>	7	6.26	13.46	-
	15	8.65	19.36	-
	25	11.73	22.51	-
	45	14.39	26.00	-
	80	15.03	27.90	-
	120	15.59	30.73	-
	210	16.38	31.76	-

a =  $[X]_{\text{chem}}$  determined from swelling in benzene

b =  $[X]_{\text{chem}}$  determined from swelling in n-decane

c =  $[X]_{\text{chem}}$  determined from equilibrium modulus

Table 15 Efficiencies  $E_C$ ,  $E_X$  and  $E_V$  for various interactions at different reaction times as obtained from the amount of acetone extract (phenolic combined) and/or from values derived from swelling in benzene ( $[X_{phys}]$ ).

Interaction	Reaction time (min)	$E_C$	$E_X$	$E_V$
IR/DMP/ZnCl <sub>2</sub>	15	0.20	-	-
	25	0.32	0.10	0.02
	45	0.37	0.14	0.05
	80	0.48	0.18	0.09
	120	0.59	0.29	0.17
	210	0.63	0.44	0.28
IR/DMP/MMP/ZnCl <sub>2</sub>	15	0.12	-	-
	25	0.21	0.12	0.02
	45	0.22	0.16	0.04
	80	0.34	0.23	0.08
	120	0.39	0.31	0.11
	210	0.51	0.45	0.19
IR/DMP/M <sub>X</sub> /ZnCl <sub>2</sub>	45	-	-	0.01
	80	-	-	0.06
	120	-	-	0.09
	210	-	-	0.10
IR/DMDPM/ZnCl <sub>2</sub>	7	0.38	0.32	0.12
	15	0.48	0.47	0.23
	25	0.56	0.53	0.30
	45	0.58	0.58	0.34
	80	0.59	0.59	0.35
	120	0.60	0.62	0.38
	210	0.61	0.70	0.42
IR/DMDPM <sup>*</sup> /ZnCl <sub>2</sub>	7	0.28	0.18	0.05
	15	0.39	0.25	0.10
	25	0.41	0.34	0.14
	45	0.44	0.41	0.18
	80	0.45	0.53	0.24
	120	0.45	0.60	0.27
	210	0.48	0.64	0.31
IR/PEDPM/ZnCl <sub>2</sub>	7	0.42	0.50	0.21
	15	0.51	0.54	0.27
	25	0.54	0.56	0.30
	45	0.59	0.59	0.35
	80	0.62	0.60	0.37
	120	0.62	0.60	0.37
	210	0.62	0.60	0.37

Table 15 (continued)

Interaction	Reaction time (min)	$E_C$	$E_X$	$E_V$
IR/PE/ZnCl <sub>2</sub>	7	0.33	0.61	0.20
	15	0.43	0.69	0.30
	25	0.48	0.79	0.38
	45	0.55	0.81	0.45
	80	0.56	0.87	0.49
	120	0.58	0.90	0.52
	210	0.61	0.91	0.55
IR/PE/M <sub>x</sub> /ZnCl <sub>2</sub>	7	-	-	0.27
	15	-	-	0.34
	25	-	-	0.42
	45	-	-	0.49
	80	-	-	0.54
	120	-	-	0.60
	210	-	-	0.62
IR/CR/ZnCl <sub>2</sub>	7	0.44	0.47	0.21
	15	0.55	0.51	0.28
	25	0.56	0.69	0.39
	45	0.59	0.80	0.47
	80	0.60	0.82	0.49
	120	0.61	0.84	0.51
	210	0.63	0.86	0.54

Table 16 Combined phenolic material in the various interactions, as calculated from the corrected amount of acetone extract (a) and from nmr method (b).

Interaction	Reaction time (min)	Combined phenolic material $\times 10^2$ (moles per mole of IR)	
		a	b
IR/MP	15	0.43	0.22
	45	1.61	1.09
	120	3.54	3.26
	210	3.66	3.39
IR/E	15	1.43	0.97
	45	3.13	2.74
	120	4.16	3.57
	210	4.20	4.74
IR/MP/SnCl <sub>2</sub>	7	0.34	0.46
	15	1.63	1.71
	45	4.01	3.35
	80	5.03	4.28
	120	5.38	4.83
	210	5.91	5.82
IR/E/SnCl <sub>2</sub>	7	1.23	0.78
	15	4.42	3.88
	45	5.11	5.01
	80	5.73	5.58
	120	5.96	6.89
	210	6.27	7.02
IR/MP/ZnCl <sub>2</sub>	7	0.09	0.02
	15	0.63	0.93
	45	2.05	1.24
	80	3.56	2.70
	120	4.53	5.22
	210	5.69	5.75
IR/E/ZnCl <sub>2</sub>	7	0.92	0.20
	15	2.37	1.96
	45	3.55	4.39
	80	5.28	5.07
	120	5.66	5.68
	210	6.31	6.75

Table 16 (continued)

Interaction	Reaction time (min)	Combined phenolic material $\times 10^2$ (moles per mole of IR)	
		a	b
IR/E/SnCl <sub>2</sub> ·2H <sub>2</sub> O	7	2.11	2.56
	15	5.89	7.60
	45	6.07	20.47
	80	6.08	-
	120	6.17	-
	210	6.33	-
	IR/DMP/ZnCl <sub>2</sub>	15	0.82
25		1.33	-
45		1.44	-
80		2.01	-
120		2.45	-
210		2.58	-
IR/DMP/MMP/ZnCl <sub>2</sub>		15	0.48
	25	0.88	-
	45	0.92	-
	80	1.41	-
	120	1.62	-
	210	2.10	-
	IR/DMDPM/ZnCl <sub>2</sub>	7	1.57
15		2.01	-
25		2.32	-
45		2.40	-
80		2.47	-
120		2.49	-
210		2.51	-
IR/DMDPM*/ZnCl <sub>2</sub>	7	1.16	-
	15	1.60	-
	25	1.71	-
	45	1.81	-
	80	1.84	-
	120	1.86	-
	210	1.97	-
IR/PEDPN/ZnCl <sub>2</sub>	7	1.75	-
	15	2.11	-
	25	2.25	-
	45	2.43	-
	80	2.56	-
	120	2.56	-
	210	2.56	-

Table 16 (continued)

Interaction	Reaction time (min)	Combined phenolic material $\times 10^2$ (moles per mole of IR)	
		a	b
IR/PE/ZnCl <sub>2</sub>	7	1.34	-
	15	1.77	-
	25	1.99	-
	45	2.29	-
	80	2.32	-
	120	2.38	-
	210	2.50	-
IR/CR/ZnCl <sub>2</sub>	7	1.81	-
	15	2.29	-
	25	2.30	-
	45	2.43	-
	80	2.48	-
	120	2.52	-
	210	2.58	-

Table 17 Changes in type and amount of unsaturation with reaction time for the IR/SnCl<sub>2</sub> and IR/SnCl<sub>2</sub>·2H<sub>2</sub>O interactions, as determined from nmr spectroscopy.

Interaction	Reaction time (min)	CHR=CR <sub>2</sub> (moles)	CHR=CR <sub>2</sub> trans (moles)	CH=CR <sub>2</sub> cis (moles)	=C-CH <sub>2</sub> -C= (moles)	CH <sub>2</sub> =CR <sub>2</sub> (moles)
IR/SnCl <sub>2</sub>	0	1	0	1	0	0
	4	-	-	-	-	-
	7	-	-	-	-	-
	15	0.96	0.14	0.78	0.16	0.03
	45	0.85	0.21	0.59	0.17	0.03
	120	0.74	0.27	0.47	0.17	0.04
	210	0.73	0.31	0.42	0.18	0.05
360	0.51	0.32	0.24	0.11	0.05	
IR/SnCl <sub>2</sub> ·2H <sub>2</sub> O	0	1	0	1	0	0
	4	0.60	0.16	0.43	0.10	0.03
	7	0.57	0.24	0.32	0.15	0.05
	15	0.57	0.28	0.29	0.26	0.03
	45	0.51	0.30	0.21	0.17	0.03
	120	0.49	0.31	0.18	0.11	0.03
	210	0.41	-	-	0.06	0.0
360	0.25	-	-	0.04	0.0	

Table 18 Cis/trans ratios for the IR/SnCl<sub>2</sub> and IR/SnCl<sub>2</sub>·2H<sub>2</sub>O interactions, as determined from nmr spectroscopy.

Interaction	Reaction time (min)	Trans-2,3 unsaturation (%)
IR	0	0
	4	•
	7	-
	15	9
	45	24
	120	39
	210	47
	360	56
IR/SnCl <sub>2</sub> ·2H <sub>2</sub> O	0	0
	4	14
	7	32
	15	49
	45	54
	120	55
	210	-
	360	-

Table 19 Changes in hydroxyl concentration for various interactions

Interaction	Reaction time (min)	Hydroxyl concentration (moles per mole of IR)
IR/MP/SnCl <sub>2</sub>	7	0.016
	15	0.016
	45	0.016
	80	0.016
	120	0.017
	210	0.017
IR/E/SnCl <sub>2</sub>	7	0.021
	15	0.021
	45	0.019
	80	0.018
	120	0.021
	210	0.021
IR/MP/SnCl <sub>2</sub> ·2H <sub>2</sub> O	7	0.021
	15	0.024
	45	0.029
	80	0.048
	120	0.038
	210	0.038
IR/E/SnCl <sub>2</sub> ·2H <sub>2</sub> O	7	0.022
	15	0.024
	45	0.026
	80	0.025
	120	0.016
	210	0.016

Table 20 Unsaturation consumed by cyclization with reaction time in the IR/MP/SnCl<sub>2</sub>·2H<sub>2</sub>O and IR/E/SnCl<sub>2</sub>·2H<sub>2</sub>O interactions.

Interaction	Reaction time (min)	Unsaturation consumed by cyclization (moles)
IR/MP/SnCl <sub>2</sub> ·2H <sub>2</sub> O	0	0
	7	0.08
	15	0.11
	45	0.15
	80	0.16
	120	0.21
	210	0.27
IR/E/SnCl <sub>2</sub> ·2H <sub>2</sub> O	0	0
	7	0.10
	15	0.11
	45	0.16
	80	0.25
	120	0.26
	210	0.31

Table 21 Total unsaturation with reaction time for IR in the various interactions as calculated from perbenzoic acid consumed (a) and from iodine chloride consumed (b).

Interaction	Reaction time (min)	Total unsaturation (moles)	
		(a)	(b)
IR/SnCl <sub>2</sub>	0	-	0.98
	4	-	-
	7	-	-
	15	-	0.97
	45	-	0.94
	120	-	0.91
	210	-	0.86
	360	-	0.83
IR/SnCl <sub>2</sub> ·2H <sub>2</sub> O	0	-	0.98
	4	-	0.92
	7	-	0.91
	15	-	0.88
	45	-	0.84
	120	-	0.79
	210	-	0.74
	360	-	0.70
IR/ZnCl <sub>2</sub>	0	-	0.98
	4	-	-
	7	-	0.98
	15	-	0.98
	45	-	0.97
	120	-	0.98
	210	-	0.97
	360	-	0.97
IR/MP	0	0.96	0.98
	4	-	-
	7	-	-
	15	0.96	0.98
	45	0.95	0.97
	80	-	-
	120	0.93	0.96
	210	0.93	0.96
IR/E	0	0.96	0.98
	4	-	-
	7	-	-
	15	0.95	0.97
	45	0.94	0.96
	80	-	-
	120	0.92	0.95
	210	0.91	0.95

Table 21 (continued)

Interaction	Reaction time (min)	Total unsaturation (moles)	
		(a)	(b)
IR/MP/ZnCl <sub>2</sub>	0	0.96	0.98
	4	-	-
	7	0.96	0.98
	15	0.93	0.97
	45	0.94	0.96
	80	0.93	0.95
	120	0.91	0.94
	210	0.90	0.94
IR/E/ZnCl <sub>2</sub>	0	0.96	0.98
	4	-	-
	7	0.95	0.97
	15	0.94	0.96
	45	0.91	0.94
	80	0.90	0.94
	120	0.89	0.93
	210	0.88	0.93
IR/MP/SnCl <sub>2</sub>	0	0.96	0.98
	7	0.96	0.97
	15	0.94	0.96
	45	0.92	0.95
	80	0.91	0.94
	120	0.90	0.94
	210	0.89	0.94
IR/E/SnCl <sub>2</sub>	0	0.96	0.98
	7	0.95	0.97
	15	0.92	0.96
	45	0.90	0.94
	80	0.89	0.93
	120	0.88	0.92
	210	0.88	0.92

Table 21 (continued)

Interaction	Reaction time (min)	Total unsaturation (moles)	
		(a)	(b)
IR/MP/SnCl <sub>2</sub> ·2H <sub>2</sub> O	0	0.96	0.98
	7	0.86	0.94
	15	0.82	0.92
	45	0.75	0.89
	80	0.4	0.81
	120	0.69	0.80
	210	0.63	0.75
IR/E/SnCl <sub>2</sub> ·2H <sub>2</sub> O	0	0.96	0.98
	7	0.84	0.90
	15	0.74	0.88
	45	0.65	0.82
	80	0.64	0.78
	120	0.62	0.71
	210	0.59	0.70

Table 22 Glass transition temperature,  $T_g$ , of IR with reaction time in the various interactions.

Interaction	Reaction time (min)	$T_g$ ( $^{\circ}\text{K}$ )
IR/SnCl <sub>2</sub>	0	198
	4	-
	7	-
	15	199
	45	200
	120	203
	210	209
	360	215
IR/SnCl <sub>2</sub> ·2H <sub>2</sub> O	0	198
	4	202
	7	203
	15	204
	45	209
	120	233
	210	261
	360	-
IR/MP	0	198
	7	-
	15	203
	45	210
	80	-
	120	219
	210	220
IR/E	0	198
	7	-
	15	213
	45	217
	80	-
	210	221
IR/MP/SnCl <sub>2</sub>	0	198
	7	207
	15	216
	45	223
	80	225
	120	225
	210	226

Table 22 (continued)

Interaction	Reaction time (min)	T <sub>g</sub> (°K)
IR/E/SnCl <sub>2</sub>	0	198
	7	209
	15	217
	45	223
	80	226
	120	227
	210	229
IR/MP/ZnCl <sub>2</sub>	0	198
	7	201
	15	204
	45	213
	80	215
	120	222
	210	225
IR/E/ZnCl <sub>2</sub>	0	198
	7	206
	15	213
	45	221
	80	223
	120	225
	210	227
IR/MP/SnCl <sub>2</sub> ·2H <sub>2</sub> O	0	198
	7	213
	15	225
	45	248
	80	254
	120	260
	210	263
IR/E/SnCl <sub>2</sub> ·2H <sub>2</sub> O	0	198
	7	214
	15	233
	45	250
	80	268
	120	270
	210	-

Table 23 Intrinsic viscosity ( $[\eta]_{c=0}$ ) and gel content with reaction time in the various interactions.

Interaction	Reaction time (min)	$[\eta]_{c=0}$ (g/100 ml) <sup>-1</sup>	Gel content (%)
IR/SnCl <sub>2</sub>	0	2.90	0
	4	-	-
	7	-	-
	15	3.72	1.04
	45	4.20	2.54
	120	4.42	5.21
	210	4.65	7.30
	360	4.86	7.30
IR/SnCl <sub>2</sub> ·2H <sub>2</sub> O	0	2.90	0
	4	3.35	0.29
	7	4.00	0.87
	15	4.25	2.22
	45	5.04	3.31
	120	-	-
	210	-	-
	360	-	-
IR/ZnCl <sub>2</sub>	0	2.89	0
	4	-	-
	7	2.89	0
	15	2.88	0
	45	2.87	0
	120	2.70	0
	210	2.52	0
	360	2.33	0
IR/NP	0	1.95	-
	15	1.95	-
	45	1.96	-
	120	1.96	-
	210	1.97	-
IR/E	0	1.95	-
	15	1.96	-
	45	1.97	-
	120	1.97	-
	210	1.98	-

Table 23 (continued)

Interaction	Reaction time (min)	$[\eta]_{c=0}^{-1}$ (g/100 ml) <sup>-1</sup>	Gel content (%)
IR/MP/ZnCl <sub>2</sub>	0	1.95	-
	7	1.95	-
	15	1.96	-
	45	1.97	-
	80	1.98	-
	120	1.98	-
	210	1.99	-
IR/E/ZnCl <sub>2</sub>	0	1.95	-
	7	1.96	-
	15	1.97	-
	45	1.98	-
	80	1.98	-
	120	1.99	-
	210	1.99	-
IR/MP/SnCl <sub>2</sub>	0	-	0
	7	-	50.12
	15	-	56.01
	45	-	60.40
	80	-	61.60
	120	-	65.80
	210	-	66.30
IR/E/SnCl <sub>2</sub>	0	-	0
	7	-	61.41
	15	-	68.40
	45	-	70.10
	80	-	74.60
	120	-	78.40
	210	-	80.01
IR/MP/SnCl <sub>2</sub> ·2H <sub>2</sub> O	0	-	0
	7	-	39.52
	15	-	59.54
	45	-	68.80
	80	-	70.10
	120	-	71.40
	210	-	71.60
IR/E/SnCl <sub>2</sub> ·2H <sub>2</sub> O	0	-	0
	7	-	49.00
	15	-	70.04
	45	-	76.80
	80	-	80.60
	120	-	84.80
	210	-	84.90

#### REFERENCES

1. D.J. Elliot, B.K. Tidd; J. IRI. Prog. Rubb. Technol., 37, 83, (1973).
2. N.J.L. Megson; Phenolic Resin Chemistry, Academic Press, New York, 1958, p125.
3. H.E. Rooney; Polysar Butyl Handbook, The Ryerson Press, Toronto, 1966, p23, 117.
4. H.F. Payne; Organic Coating Technology, John Wiley & Sons, Inc., New York, 1961, I, p176.
5. P.O. Tawney, J.R. Little, P. Viohl; Rubber Age, 83, 101, (1958).
6. Enjay Chemical Company Booklet; Butyl Rubber, Enjay Polymer Lab., New Jersey, 1969; p23.
7. U.S. Patent 2,734,877.
8. U.S. Patent 2,734,039.
9. U.S. Patent 2,727,874.
10. U.S. Patent 2,857,357.
11. A. Fitch, Ph.D. Thesis, C.N.A.A., (1978).
12. S. Van der Meer; Rubber Chem and Technol, 18, 853, (1945).
13. S. Van der Meer; Kunststoffe, 37, 41, (1947).
14. S. Van der Meer; Rec. trav. Chim, 63, 157, (1944).
15. S. Van der Meer, Rec. trav. Chim, 63, 147, (1944).
16. K. Hultsch; J. Prakt. chem, 158(2), 275, (1941).
17. J.I. Cunneen; E.H. Farmer and H.P. Koch, J. Chem. Soc.; 472, (1943).
18. K. Hultsch; Ber, 748, 898, (1941).

19. A.B. Turner; Quart. rev, 18, 347, (1964).
20. A.J. Wildschut; Rubber Chem. and Technol, 19, 86, (1946).
21. L.M. Kurachenkova, A.C. Shwarts, L.A. Igonin; Soviet Rubb. Technol, 26(7), 21, (1967).
22. V.P. Bugrov; Vysokomol. Soedin, Ser B, 12(7), 497, (1970).
23. S.B. Cavitt, H. Sarrafizodeh, and P.D. Gardener; J. Org. Chem, 28, 2148, (1963).
24. D.A. Bolon; J. Org. Chem, 35(3), 715, (1970).
25. A. Merijan, B.A. Shoulders, P.D. Gardener; J. Org. Chem, 28, 2148, (1963).
26. M.S. Chauhan, F.M. Dean, S. McDonald, M.S. Robinson; J. Chem. Soc, Perkin I, 359, (1973).
27. D.A. Bolon; J. Org. Chem, 35(11), 3666, (1970).
28. M.S. Chauhan, F.M. Dean, D. Matkin, M.L. Robinson; J. Chem. Soc, Perkin I, 120, (1973).
29. R.R. Schmidt; Tetrahedron letters, 60, 5279, (1969).
30. M. Wakeschman, M. Vilkas; Compt. Rend, 258, 1526, (1964).
31. W. Hofman; Vulcanization and Vulcanizing Agents, Maclaren & Sons, London, 1967, p300.
32. O.C. Elmer, A.E. Schmucker; Rubb. Age, 94, 438, (1963).
33. H.U. Wagner, R. Gompper; Quinone methides, Chemistry of Quinoid Compounds, edited by S. Patai, Academic Press, New York, 1974, II, p1145.
34. K. Hultzsch; Ber. Dtsch. Chem. Ges, 74, 275, (1941).
35. A. Greth; Kunststoffe, 31, 345, (1941).

19. A.B. Turner; Quart. rev, 18, 347, (1964).
20. A.J. Wildschut; Rubber Chem. and Technol, 19, 86, (1946).
21. L.M. Kurachenkova, A.C. Shwarts, L.A. Igonin; Soviet Rubb. Technol, 26(7), 21, (1967).
22. V.P. Bugrov; Vysokomol. Soedin, Ser B, 12(7), 497, (1970).
23. S.B. Cavitt, H. Sarrafizodeh, and P.D. Gardener; J. Org. Chem, 28, 2148, (1963).
24. D.A. Bolon; J. Org. Chem, 35(3), 715, (1970).
25. A. Merijan, B.A. Shoulders, P.D. Gardener; J. Org. Chem, 28, 2148, (1963).
26. M.S. Chauhan, F.M. Dean, S. McDonald, M.S. Robinson; J. Chem. Soc, Perkin I, 359, (1973).
27. D.A. Bolon; J. Org. Chem, 35(11), 3666, (1970).
28. M.S. Chauhan, F.M. Dean, D. Matkin, M.L. Robinson; J. Chem. Soc, Perkin I, 120, (1973).
29. R.R. Schmidt; Tetrahedron letters, 60, 5279, (1969).
30. M. Wakeschman, M. Vilkas; Compt. Rend, 258, 1526, (1964).
31. W. Hofman; Vulcanization and Vulcanizing Agents, Maclaren & Sons, London, 1967, p300.
32. O.C. Elmer, A.E. Schmucker; Rubb. Age, 94, 438, (1963).
33. H.U. Wagner, R. Gompper; Quinone methides, Chemistry of Quinoid Compounds, edited by S. Patai, Academic Press, New York, 1974, II, p1145.
34. K. Hultsch; Ber. Dtsch. Chem. Ges, 74, 275, (1941).
35. A. Greth; Kunststoffe, 31, 345, (1941).

36. J. Sauer; *Angew. Chem. Internat. Edit*, 5(2), 211, (1966).
37. R. Zapp, J. Peery; *J. Appl. Polym. Sci*, 13, 2102, (1969).
38. C.R. Sprengling; *J. Amer. Chem. Soc*, 74, 2937, (1952).
39. J.C. Martin, R.K. Hill; *Chem. Rev*, 61, 537, (1961).
40. J. Sauer; *Angew. Chem. Internat. Edit*, 6(1), 16, (1967).
41. Yu.N. Nikitin, V.C. Epshtein, M.A. Polyak; *Russ. Chem. Technol*, 41, 621, (1968).
42. L.V. Ginzburg, V.A. Shershneu, V.P. Pshemtsyna, B.A. Dogadkin; *Polym. Sci. USSR*, 7(1), 57, (1965).
43. L.V. Ginzburg, V.A. Shershneu, A.C. Shvarts; T.N. Nerotova, B.A. Dogadkin; *Polym. Sci., USSR*, 8(2), 389, (1966).
44. V.P. Bugrov, N.M. Pashchenko, E.P. Kopylov; *Nouch-Issled. Inst. Monomer*, 11(8), 1742, (1969).
45. A.C. Shvarts, B.Z. Kamenskii; *Soviet Russ. Technol*, 22(2), 8, (1963).
46. D. Crdenic, B. Kameuar; *Proc. Chem. Soc*, 312, (1960).
47. R.F. Heck, D.S. Breslow; *J. Amer. Chem. Soc*, 83, 4023, (1961).
48. B. Fell, P. Krinys, F. Asinger; *Chem. Ber*, 99, 3688, (1966).
49. M.A. Golub; *J. Polym. Sci*, 25, 337, (1957).
50. M.A. Golub; *Russ. Chem. Technol*, 30, 1142, (1957).
51. M.A. Golub; *High Polymers*, edited by Kennedy and Törquist, 1969, p969.

52. J.I. Cunneen, C.M. Higgins, and W.F. Watson; *J. Polym. Sci*, 40, 1, (1959).
53. J.I. Cunneen; *Rubb. Chem. Tech*, 33, 445, (1960).
54. J.D. D'Ianni, F.J. Naples, J.W. March and J.L. Zarney; *Indust. Engng. Chem. (Industr)*, 38, 1171, (1946).
55. M. Gordon; *Industr. Engng. Chem*, 43, 386, (1951).
56. M. Gordon; *Proc. Roy. Soc. A*, 204, 569, (1951).
57. P.J. Flory; *J. Amer. Chem. Soc*, 61, 1518, (1939).
58. C.J. Van Veersen; *Rec. Trav. Chim. Pays-Bas*, 69, 1965, (1950).
59. J.R. Shelton, H.L. Lee; *Rubb. Chem. Technol*, 31, 415, (1958).
60. D.F. Lee, J. Scanlan, W.F. Watson; *Proc. Roy. Soc*, A273, 345, (1963).
61. A.A. Yehia, E.M. Abdel-Barry; *Evr. Polym. J*, 9, 1417, (1973).
62. V.P. Bugrov, E.P. Kopylov; *Soviet Rubb. Technol*, 22(7), 22, (1970).
63. C.M. Ronkin, I.R. Levitin, A.C. Shvarts; *Soviet Rubb. Technol*, 23(4), 17, (1964).
64. K.C. Petersen; *Rubb. Chem. Technol*, 44, 914, (1971).
65. T. Novikova; *Kouch. Rezina.*, 9, 13, (1978).
66. A.C. Shvarts, U.K. Sodykhova, I.I. Eitingon; *Azerb. Khim. Zh*, 4, 58, (1965).
67. M.S. Fel'dshtein, V.A. Zhukova; *Soviet Rubb. Technol*, 23(6), 19, (1964).
68. D.B. Boguslavsku, E.E. Collteuzen, V.A. Soprouov, S.A. Uvarova; *Soviet Rubb. Technol*, 26(3), 23, (1967).

69. Idem. Spektrosk. At. Mol, 1969, 396.
70. B.A. Dogadkin; Polym. Sci. USSR, 7(1), 57, (1965).
71. C. Sprengling, S. Betty, K.B. Adams; J. Amer. Chem. Soc, 72, 4314, (1950).
72. O. Manasse; Ber, 27, 2109, (1894).
73. L. Lederer; J. Prakt. Chem, 2, 50, (1894).
74. K. Hultzsch; J. Prakt. Chem, 159(5-7), 155, (1941).
75. J.C. Ambelang, J.L. Binder; J. Amer. Chem. Soc, 75, 947, (1953).
76. N. Grassie; Chemistry of High Polymer Degradation Processes, Butterworth Scientific Publications, London, 1956, pp315-319.
77. M.A. Golub, J. Heller; Can. J. Chem, 41, 937, (1963).
78. M. Stolka; J. Vodehnal. I. Kossler; J. Polym. Sci, 2(A), 3987, (1964).
79. M.A. Golub, J. Heller; J. Polym. Sci. (Polym. Letters), 4, 469, (1966).
80. M.A. Golub, G.L. Stephens; J. Polym. Sci, 6(A), 763, (1968).
81. M.A. Golub. J. Danon; Can. J. Chem, 43, 2772, (1965).
82. B.A. Dolgoplosk, E.N. Kropacheva, K.V. Nelson; Rubb. Chem. Technol, 32, 1036, (1959).
83. I.I. Boldyreva, B.A. Dolgoplosk, E.N. Kropacheva, K.N. Nelson; Rubber Chem. Technol, 33, 985, (1960).
84. B.A. Dolgoplosk, G.B. Belonouskaya, I.T. Boldyreva; J. Polym. Sci, 53, 209, (1961).
85. H.Y. Chen; Analyt. Chem, 34, 1793, (1962).
86. F.A. Bovey; High Resolution NMR of Macromoleculars, Academic Press, London, 1972, p220.

87. H.Y. Chen; J. Polym. Sci, 4(B), 891, (1966).
88. J.L. Binder; J. Polym. Sci, (Polymer Letters), 4, 19, (1966).
89. M.A. Golub; J. Polym. Sci. (Polymer Letters), 4, 227, (1966).
90. C.J. Van Veersen; Rubber Chem. Technol, 24, 957, (1966).
91. M.A. Golub; J. Heller, Tetrahedron Letters, 30, 2137, (1963).
92. J.M. Barton; Polymer, 10, 319, (1969).
93. D.E. Lee, J. Scanlan, W.F. Watson; Chem. and Eng. News, June 17, 44 (1963).
94. C.J. Pouchert, J.R. Campbell; "The Aldrich Library of nmr Spectra", Aldrich Chemical Company, Inc. Milwaukee, 1924-1975, vol. 1, p.320.
95. Varian Spectrum Catalogue, volume 1, Cpd No. 337.
96. F.A. Bovey; NMR Data Tables for Organic Compounds; volume 1, pp228, John Wiley and Sons, Inc. USA.
97. J.C. Bailar; Comprehensive Inorganic Chemistry, Pergamon Press, (1973).
98. R.J.H. Clark; The Chemistry of Titanium and Vanadium, Elsevier, Amsterdam, (1968).
99. A.G. Evans, C.W. Meadows; Trans. Faraday Soc, 46, 327, (1950).
100. R.I. Grisentwaite, R.F. Hunter; J. Appl. Chem, 6, 324, (1956).
101. D. Hummel; Kunststoff, Lack- und Gummi- Analyse, Hanser Munken, (1958).

102. L.A. Igonin, M.M. Mirakhmedow, K.I. Turchaminova, A.N. Shabadash; Dokl. Akad. Nauk. SSSR, 141, 1366, (1961).
103. J. Haslam, H.A. Willis, D.C.M. Squirrell; Identification and Analysis of Plastics, Second Edition, Butterworth & Co., London, pp496.
104. J.C. Woodbrey, H.P. Higginbottom, H.M. Culberton; J. Polym. Sci, Pt. A, 3, 1079, (1965).
105. R.C. Hirst, D.M. Grant, R.E. Roff, W.J. Burke; J. Polym. Sci, Pt. A, 3, 2091, (1965).
106. K. Subramanian, M.Sc. Thesis, C.N.A.A., (1978).
107. D. Khristow, T. Boncher, N. Nerow; Kautsch. Gummi. Kunstst, 28(4), 201, (1975).
108. Idem, 29(3), 116, (1976).
109. Idem, Die. Angewandte. Makromolekulare. Chemie, 30(7), 431, (1977).
110. Idem, 65, 49, (1977).
111. J.D. Roberts, M.C. Caserio; Basic Principles of Organic Chemistry, W.M. Benjamin, Inc., New York, pp392.
112. R.W. Martin; Anal. Chem, 23, 883, (1951).
113. H.S. Lilley, D.W.J. Osmond; J. Soc. Chem. Ind. (London), 66, 425, (1947).
114. R.T. Conley, J.P. Bieron; J. Appl. Polymer Sci, 7, 103, (1963).
115. P.J. Flory, Principles of Polymer Chemistry, Cornell University Press, (1953), pp464-494.
116. L.R.C. Treolar; The Physics of Rubber Elasticity, 3rd Ed., Clarendon Press, Oxford, (1975).

117. M. Mooney; J. Appl. Phys, 11, 582, (1940).
118. R.S. Rivlin; Philos. Trans, A241, 379, (1948).
119. R.S. Rivlin, D.W. Saunders; Philos. Trans, A243, 251, (1951).
120. L. Mullins; J. Appl. Polym. Sci, 2, 1, (1959).
121. S.M. Cumbrell, L. Mullins, R.S. Rivlin; Trans. Faraday Soc, 49, 1495, (1953).
122. P.J. Flory; J. Chem. Phys, 18, 108, (1950).
123. B. Ellis, G.N. Welding; Rubb. Chem. Technol, 37, 563, (1964).
124. L. Mullins, W.F. Watson; J. Appl. Polymer Sci, 1, 245, (1959).
125. J. Reese; Kunststoffe, 45, 137, (1955).
126. L. Bateman; Chemistry and Physics of Rubber-like Substances, Applied Science, 1963, p498.
128. B.V. Tronow, L.V. Ladigina; Chem. Ber, B62, 2844, (1929).
129. K. Kratzl, G.E. Mischke; Momatsh, Chem, 94, 715, (1936).
130. C.H. Hauser, S.W. Kantor; J. Am. Chem. Soc, 73, 1437, (1951).
131. D.Y. Curtin, S. Leskowitz; J. Am. Chem. Soc, 73, 2630, (1951).
132. W. Gerrard; Chem. Rev, 58, 1081, (1958).
133. R.D. Youssefyeh, Y. Mazur; Tetrahedron Letters, 1287, (1962).
134. K.H. Meyer, W. Hohenemser; Rubb. Chem. Technol, 9, 201, (1936).

135. B.A. Dogadkin, Z.N. Tarasova; *Rubb. Chem. Technol*, 27, 883, (1954).
136. M.L. Studebaker, L.G. Nabors; *Rubb. Chem. Technol*, 32, 941, (1959).
137. C.G. Moore, B.R. Trego; *J. Appl. Polymer Sci*, 8, 1957, (1964).
138. M. Porter, B. Saville, A.A. Watson; *J. Chem. Soc*, 346, (1963).
139. H. Ghazaly, B.Sc. Thesis, C.N.A.A., (1983).
140. J.R. Pyne; *J. IRI*, 7, No.2, February 1973, pp22-6.
141. C. Thelamon; *Rubb. Chem. Technol*, 36, 268, (1963).
142. A.G. Shuarts, B.Z. Kamenskii, I.I. Eitingon; *Soviet Rubb. Technol*, 19, No.8, August 1960, pp5-9.
143. W. Charlton, L.E. Perrins; *J. Oil and Colour Chemist's Assoc*, 30, No.324, 185, (1947).
144. I.M. Kolthoff, T.S. Lee and M.A. Mairs; *J. Polym. Science*, 2, No.2, p199, (1947).
145. C. Braun; *Organic Syntheses, Coll.*, Vol.I, 2nd ed., Wiley, New York, 1941, p431.
146. J.M. Barton; *Polymer*, 10, 319, (1969).
147. S. Ginosatis; M.Sc. Thesis, C.N.A.A., (1977).
148. T.K. Wong, Ph.D. Thesis, C.N.A.A., (1970).
149. R.H. Wiley, C.M. and A.R. Bennett; *J. Polymer Sci*, 5, 609, (1949).
150. R.B. Redding, Ph.D. Thesis, C.N.A.A., (1969).
151. G.M. Bristow; Private Communication.
152. C.G. Moore, M. Porter; *J. Appl. Polym. Sci*, 2, 2227, (1967).

Attention is drawn to the fact that the copyright of this thesis rests with its author.

This copy of the thesis has been supplied on condition that anyone who consults it is understood to recognise that its copyright rests with its author and that no quotation from the thesis and no information derived from it may be published without the author's prior written consent.

**IV**

D48820 84

END